Systems analysis of Lrp family expansions in an extreme halophile

Fang Yin Lo

A dissertation

submitted in partial fulfillment of the

requirements for the degree of

Doctor of Philosophy

University of Washington

2013

Reading Committee:

John Aitchison, Chair

Nitin Baliga, Adviser

John Leigh

Program Authorized to Offer Degree:

Molecular and Cellular Biology

©Copyright 2013

Fang Yin Lo

University of Washington

Abstract

Systems analysis of Lrp family expansions in an extreme halophile

Fang Yin Lo

Chair of the Supervisory Committee:

John Aitchinson

Molecular and Cellular Biology

Lineage-specific expansions of transcription factors (TF) play an important role in increasing the repertoire of regulatory programs for dealing with complex environmental change. Here, we have investigated how an expanded family of Leucine Responsive Protein (Lrp) --one of the most widespread families of TFs in prokaryotes-- equips an organism with strategies for adapting to a dynamically changing environment. We have used a systems approach to study the entire family of 8 Lrps in *Halobacterium salinarum NRC-1* by (i) mapping genome-wide binding locations for each Lrp; (ii) discovering co-location of binding sites for multiple Lrps; (iii) identifying conditional activities of Lrps by analyzing a compendium of 1018 transcriptome measurements in diverse environments; (iv) correlating mRNA level changes of Lrps and their targets across different environments to discover conditional regulatory targets of each Lrp; and (v) analyzing global transcriptional consequences of Lrp deletions. By integrating all of these data, we have reconstructed a systems scale transcriptional regulatory network (TRN) that has provided mechanistic insights into how the expanded family of 8 Lrps encodes complex environment-dependent global coordination of disparate metabolic pathways. A surprising Lrp-mediated coordination of copper efflux and glutamate metabolism was validated by performing global metabolomic analysis on three Lrp deletion strains.

Table of Contents

Table of Contents i
List of Figures v
List of Tables vi
Acknowledgments vii
Chapter 1 : Introduction 1
1.1 Archaeal transcriptional machinery 1
1.1.1 Overview 1
1.1.2 Basal transcription 1
1.1.3 Regulated transcription 6
1.1.4 Archaea use some unique transcriptional mechanisms different from both bacteria and eukaryotes 8
1.1.5 Relative to bacteria, archaeal genomes encode relatively fewer TFs 9
1.1.6 Archaeal TFs are significantly smaller than bacterial TFs 9
1.1.7 Expansions of TF family contribute to complexity of gene regulatory networks 10
1.2 The Leucine Responsive Protein (Lrp) family 10
Chapter 2 : Comparative Genomics and Sequence Analysis 15
2.1 Overview 15
2.2 Results 16
2.2.1 Phylogenetic analysis reveals that the Lrp family has ancient origin 16
2.2.2 Protein domain analysis reveals functional insights 20
2.3 Summary and discussion 20
Chapter 3 : Genome wide DNA-binding locations for all Lrps reveals that their regulatory networks are highly intertwined 22
3.1 Overview 22
3.2 Results 22
3.2.1 The predicted target genes of Lrps revealed by genome-wide Lrp-binding locations 22
3.3 Summary and discussion 26
3.3.1 Environmental context is critical to the functions of Lrps 26

3.3.2 Five Lrps in *H. salinarum NRC-1* putatively regulate more than 100 genes each 29
3.3.3 Co-location of Lrp binding sites in many promoters suggests cooperative or competitive regulatory mechanisms 29
3.3.4 The regulatory influence of Lrps is expanded through their binding to promoters of nearly a quarter of all TFs encoded in the genome 32
3.3.5 Lrps regulate genes in diverse pathways, including ribosome biogenesis and amino acid metabolism 34
3.3.6 Lrp-mediated conditional coordination of metabolic pathways 36
Chapter 4 : Analysis of transcriptional consequences of knocking out Lrps reveals genes they regulate directly and indirectly 38
4.1 Overview 38
4.2 Results 38
4.2.1 Transcriptomic analysis of Lrp deletion strains 38
4.3 Summary and discussion 41
4.3.1 Despite extensive buffering in the Lrp network, transcriptome analysis of Lrp deletion strains verifies direct regulation and reveals indirect causal influences 41
Chapter 5 : Correlation analysis identifies conditional regulation by Lrps 43
5.1 Overview 43
5.2 Results 43
5.2.1 Integration of genome wide Lrp binding targets with transcriptional changes across 1018 conditions reveals conditional regulation by Lrps 43
5.2.2 Lrp regulons defined by integration of evidence from protein-DNA interaction maps, conditional correlation in expression, and dysregulation upon deletion of each Lrp 47
5.3 Summary and discussion 47
Chapter 6 : Coordination of metabolic pathways by specific Lrps 49
6.1 AsnC regulates the siderophore biosynthesis pathway under high paraquat conditions 49
6.2 Trh3 regulates glutamate metabolism 53
6.3 Coordination of key enzymes by Lrps for amino acid metabolism 53
6.3.1 Aspartic acid metabolism 53
6.3.2 Three Lrps coordinate regulation of glutamate metabolism and copper trafficking 54
Chapter 7 : Conclusions 59
Chapter 8 : Materials and Methods 62
8.1 Strain construction and culturing conditions 62

8.2 Phylogenetic analysis and tree reconstruction 65
8.3 Genome wide Lrp binding site analysis (ChIP-chip) 66
8.3.1 Predictions of DNA-binding locations and target genes of Lrps 66
8.3.2 Calculation of relationships of DNA-binding specificities among Lrps 67
8.4 Microarray analysis of Lrp knockouts 67
8.5 Correlation analysis for the conditional regulations by Lrp 68
8.6 Functional enrichment analysis 72
8.7 DNA-binding motif searching through iterative refining structural homology-based prediction of Lrp-like DNA binding 72
8.8 Metabolomic analysis 73
Bibliography 74
Appendices 80
Appendix A. Phylogenetic tree of archaeal Lrp family 80
Appendix B. Clustal X color scheme 82
Appendix C. The numbers of Lrps in some archaeal genomes 83
Appendix D. All binding targets of the 8 Lrps 86
Appendix E. Lrp binding sites within each promoter 116
Appendix F. Lrp targets genes with putative feed-forward regulatory structure 133
Appendix G. Growth measurements of the eight Lrp knockout strains 137
Appendix H. p-values and fold changes of genes differentially expressed in Δ*asnC* 139
Appendix I. p-values and fold changes of genes differentially expressed in Δ*vng1179C* 144
Appendix J. p-values and fold changes of genes differentially expressed in Δ*vng1237C* 145
Appendix K. p-values and fold changes of genes differentially expressed in Δ*trh2* 152
Appendix L. p-values and fold changes of genes differentially expressed in Δ*trh3* 155
Appendix M. p-values and fold changes of genes differentially expressed in Δ*trh4* 157
Appendix N. p-values and fold changes of genes differentially expressed in Δ*trh6* 160
Appendix O. p-values and fold changes of genes differentially expressed in Δ*trh7* 161
Appendix P. Genes with evidence from both ChIP-chip and microarray of deletion strains 162
Appendix Q. Detailed list of 66 condition sets and corresponding experiments 163
Appendix R. Experimental details of each experiment 302
Appendix S. List of Lrp binding targets whose expression correlated with the Lrp 394

Appendix T. List of genes whose expression correlated with the Lrp, and were also dysregulated in Lrp knockout strains 414

Appendix U. List of Lrp binding targets whose expression correlated with the Lrp and were dyregulated upon the deletion of Lrp 424

Appendix V. Condition sets tested for each Lrp 425

Appendix W. List of sequences for phylogenetic analysis 429

List of Figures

Figure 1-1 Comparison of the PIC among all three domains of life 3
Figure 1-2 Comparison of the compositions of RNAPs in all three domains of life 4
Figure 1-3 Examples of repressor mechanisms used by some archaeal TRs 7
Figure 2-1 Distribution of the Lrp family in Archaea and its expansion in *H. salinarum NRC-1* 17
Figure 2-2 Multiple sequence alignment of 9 Lrps in *H. salinarum NRC-1* 18
Figure 3-1 Genome-wide binding co-locations among Lrps 24
Figure 3-2 Distribution of protein-DNA interactions of Lrps during early and late phases of growth 27
Figure 3-3 Hierarchical clustering of DNA-binding specificities among 8 Lrps in early and late phases of growth 28
Figure 3-4 Co-location of Lrp binding events among three Lrps in different phases of growth . 31
Figure 3-5 Protein-DNA interaction map of Lrps and other TFs 33
Figure 4-1 Growth phase specific regulation by AsnC 40
Figure 5-1 Flow chart of the correlation analysis 45
Figure 6-1 Correlation analysis of AsnC under high paraquat conditions 51
Figure 6-2 Multiple Lrp coordinately regulate two of the amino acid metabolism 57

List of Tables

Table 3-1 *p*-values of the significance of overlap target genes between all Lrp pairs..... 25
Table 3-2 Number of Lrp target genes involved in amino acid metabolic pathway..... 35
Table 5-1 Condition sets over which expression levels of three Lrps were positively or negatively correlated with variance in gene expression changes in target genes within each of their protein-DNA interaction maps 46
Table 5-2 Number of genes from genome wide Lrp-binding location, transcriptomic analysis in Lrp deletion strains, and correlation analysis 48
Table 8-1 Complete defined medium (CDM) recipe..... 62
Table 8-2 Oligonucleotides used to construct Lrp deletion strains..... 63
Table 8-3 Description and summary of 117 condition sets 70

Acknowledgments

Completing the PhD has been a long learning journey and I would not have been able to finish this without countless support and help. I cannot overstate my gratitude to my adviser, Dr. Nitin Baliga, for giving me the opportunity to carry out my dissertation research in his laboratory and for his support and mentorship. I would also like to thank my committee members – John Aitchison, John Leigh, Leroy Hood, and Beth Traxler for their support, feedback and direction. I would particularly like to thank Dr. John Aitchison and Dr. John Leigh for reading my dissertation. I would like to thank all the current and former members of the Baliga Laboratory for discussions, input and friendship over the years. I would particularly like to thank Chris Plaisier for his numerous suggestions, contributions and help. I would also like to thank Justin Ashworth for his contributions on this project. I wish to thank David Reiss, Serdar Turkarslan, and Min Pan for their help and contributions, Marc Facciotti for being my mentor during my first year in the lab, and all the administrators in the MCB graduate program, especially MaryEllin Robinson and Michele Karantsavelos for their support of graduate students. Lastly, I would like to thank my friends and family, especially my parents, for their support and encouragements. Without all this help I would not have been able to make it to this point. Thank you.

Chapter 1 : Introduction

1.1 Archaeal transcriptional machinery

1.1.1 Overview

Adjustment of cellular physiology in response to stressful and routine environmental changes is critical for the survival of all organisms. This process is manifested at varying levels of genetic information processing, from receptor-mediated sensing of environmental factors to transcriptional, post-transcriptional, translational, post-translational and metabolic mechanisms. Regulation of transcription is a critical step that directly influences gene expression by modulating various aspects of RNA polymerase recruitment and function. With the advancement of tools for global analysis of cellular responses at a molecular level it has become possible to explore the evolution of transcriptional regulatory networks in the context of environmental adaptation. This is especially powerful in the context of studying regulatory mechanisms in archaea, a relatively understudied group of organisms that make use of a hybrid transcriptional apparatus that is assembled from homologs of eukaryotic and bacterial components[1,2] (**Figure 1-1**). Therefore, archaea present an interesting model to study the evolution of transcriptional regulation mediated by proteins with complex mixed ancestry. Further, many archaea have adapted to habitats with extremes in temperature, pressure, salinity and acidity; in addition, they are also omnipresent in "normal" habitats and even as part of the human microbiome. Some of these habitats, such as hypersaline lakes, are characterized by routine and stressful changes in many environmental factors. Organisms adapted to such environments are useful for investigation of key aspects of a transcriptional regulatory network and its evolution to deal with complex and dynamic environmental changes.

1.1.2 Basal transcription

While necessary for basal transcription, RNA polymerase (RNAP) is unable to directly recognize promoter regions. Basal transcription factors are necessary for recruiting an RNAP to a promoter and formation of the preinitiation complex (PIC) that is primed to initiate transcription

upon opening of the DNA helix. Although archaea resemble bacteria in many respects (e.g. they are both prokaryotes with circular genomes in which genes are organized into operons and transcribed by a single RNAP) their basal transcription apparatus shares ancestry with core components of the eukaryotic RNAPII apparatus [3,4,5]. Archaeal RNAP has at least 10 subunits that are similar in sequence to eukaryotic RNAPII[5] (**Figure 1-2**). Recruitment of the archaeal RNAP is not mediated by the bacterial-type sigma factors; instead archaea require orthologs of eukaryotic general transcription factors (GTFs), TATA binding protein (TBP) and transcription factor B (TFIIB, called TFB in archaea) for promoter recognition and transcription initiation[1,6,7,8,9].

Accordingly, a typical gene promoter in archaea consists of an AT-rich TATA-like element recognized by TBP; TFB binds to the TBP–DNA complex to form the PIC. Interaction of TFB with the asymmetrically located purine-rich B recognition element (BRE) element gives directionality to PIC for initiating transcription at an initiator element located 25 bp downstream of the TATA element. In several archaea species, TBPs and TFBs are present in multiple copies. With a relatively simple genome (2.6Mb)[10] that encodes six TBPs and seven TFBs[11,12], *Halobacterium salinarum NRC-1* has served as an excellent tractable model for investigating the role of GTF expansion in archaeal transcription.

By mapping protein interactions among TBPs and TFBs, their DNA binding locations across the entire genome, and assaying transcriptional consequences of deleting or overexpressing these GTFs, previous work in the Baliga lab has demonstrated that at least seven of the possible 42 TBP-TFB pairs function in a scheme similar to sigma factors in bacteria to globally partition transcription of large subsets of genes across the entire genome[13]. Further work has demonstrated that the combinatorial scheme in which the TBPs and TFBs function drives rapid adaptation to new environments, because simple mutations in any of these factors has dramatic effects of global transcriptional regulation and fitness[14].

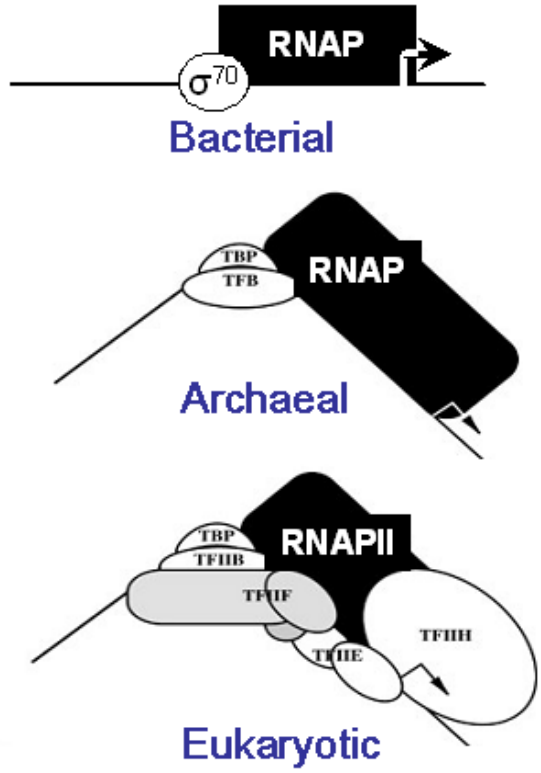

Figure 1-1 Comparison of the PIC among all three domains of life

Top: bacteria have a single RNAP. This core apoenzyme requires a dissociable sigma (σ) factor for promoter recognition and to form a holoenzyme. Middle: archaeal basal transcription machinery is an orthologous albeit simplified version of the eukaryotic RNAPII system, requiring a TBP (an ortholog of eukaryotic TBP) and TFB (an ortholog of eukaryotic TFIIB) to bind to promoters. Bottom: eukaryotic RNAPII machinery consists of RNAPII and a large number of general transcription factors (GTFs), including TFIIA, TFIIB, TFIID, TFIIE, TFIIF, and TFIIH.

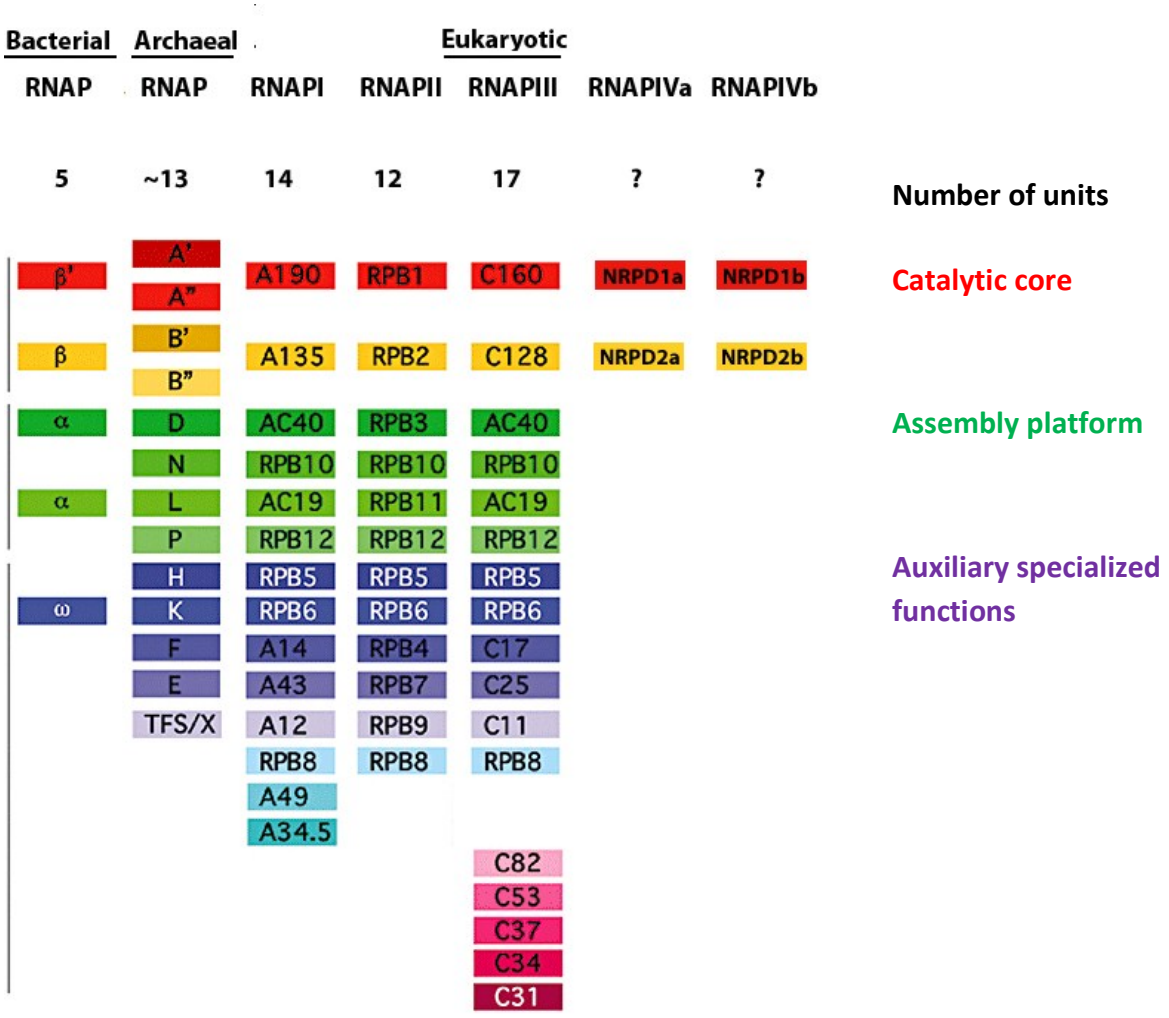

Figure 1-2 Comparison of the compositions of RNAPs in all three domains of life

Each column represents the composition of the corresponding RNAP at the subunit level. Colors indicate the homology among RNAP subunits across bacterial, archaeal and eukaryotic RNAPs (e.g. red boxes represent the subunits that are homologous to the β' subunit of bacterial RNAP). Bacterial RNAP have five subunits - ββ'$\alpha_2\omega$, all have homologs in archaeal and eukaryotic RNAPs. Eukaryotes have five RNA polymerases (RNAPI, RNAPII, RNAPIII, RNAPIVa and RNAPIVb) that transcribe distinct and non-overlapping sets of genes. RNAPI has 14 subunits; it is specialized for the constitutive transcription of the precursor rRNA, which is further processed into 18S, 5.8S and 28S rRNAs. RNAPII consists of 12 subunits; it drives the transcription of all protein coding mRNAs and many non-protein coding RNAs (ncRNAs), e.g. snRNAs and microRNAs. RNAPIII is composed of 17 subunits, and is exclusively dedicated to the transcription of tRNAs, 5S rRNA, and U6 snRNA. In addition, higher plants possess two

additional RNA polymerases, RNAPIVa and RNAPIVb. Although these plant-specific RNAPs appear to be nonessential to viability, they are responsible for the production of siRNA involved in RNA-directed DNA methylation and transcriptional silencing. The exact subunit composition, the templates and enzymatic products of RNAPIV remain poorly characterized[15,16]. Archaeal RNAP is more similar to eukaryotic RNAPII in terms of subunit complexity and homology; it has at least 10 subunits that are homologous to the subunits of eukaryotic RNAPII[5] (figure adapted from [17]).

1.1.3 Regulated transcription

In addition to the basal apparatus, activators and repressors play crucial roles to appropriately tune up or down the transcription of genes as dictated by challenges and opportunities in their environment. Surprisingly, in spite of the similarity of archaeal and eukaryotic basal transcriptional components, analyses of archaeal genome sequences revealed that gene induction and repression in archaea are mostly mediated by TFs that more closely resemble those in bacteria. It follows that most archaeal TFs are homologues of bacteria[18,19]. Several archaeal TFs have been characterized, and in the following sections I will use a few of these TFs as examples of negative and positive regulators of archaeal transcription.

1.1.3.1 Negative regulation

Mechanisms used by archaeal repressors are often similar to those by bacterial repressors, e.g. they occlude the TATA box and/or BRE by binding to DNA sites that overlap with a promoter, thus blocking the binding of TBP (and/or TFB) or inhibit the recruitment of the RNAP. One of the earliest insights into the transcriptional repression in archaea was obtained through the study of the metal dependent repressor 1 (MDR1) from *Archaeoglobus fulgidus*. As a homolog of bacterial metal-dependent transcription regulators MDR1 binds to multiple DNA sites that are just downstream of, and overlapping with, the start site of *mdr1* (**Figure 1-3**), blocking the recruitment of the RNAP[20]. Other archaeal TFs that use a similar mechanism include the *Pyrococcus furiosus* Phr[21] and a homologue of the *E. coli* leucine responsive regulatory protein (Lrp), LrpA[22]. Another commonly used mechanism for transcriptional repression in archaea is through blocking the access to the TATA box and BRE - e.g. the *Sulfolobus solfataricus* Lrs14, a homologue of the *E.coli* Lrp, has been shown by EMSA and DNaseI footprinting to bind to at least two operator sites that overlap the TATA box and BRE, and it represses transcription by competing for binding sites with TFB and TBP[23] (**Figure 1-3**).

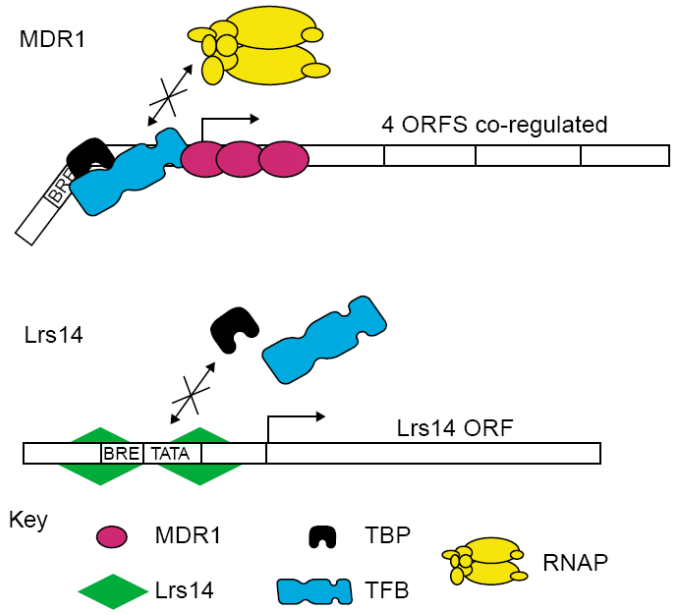

Figure 1-3 Examples of repressor mechanisms used by some archaeal TRs

Top: MDR1 binds to downstream operator sequences. MDR1 does not prevent TBP and TFB from binding to the core promoter region; however, the binding of MDR1 blocks recruitment of the RNAP by the TBP and TFB. Bottom: Lrs14 blocks access to the BRE and TATA-box and prevents GTFs from binding to the core promoter region (figure adapted from [24]).

1.1.3.2 Positive regulation

Although most archaeal TFs characterized thus far are repressors, two homologues of the Lrp family protein, *Sulfolobus solfataricus* LysM and *Methanococcus jannaschii* Ptr2, have been proposed as positive regulators of transcription. *Sulfolobus solfataricus lysM* is part of a large gene cluster, *lysWSJK*, which encodes the lysine biosynthetic enzymes. LysM binds to DNA sites immediately upstream of the TATA box and BRE of the *lysWSJK* transcription unit as an activator[25]. *Methanococcus jannaschii* Ptr2 was also shown to convey its stimulatory effects by facilitating the recruitment of TBP to the promoter region of the rubredoxin 2 (*rb2*)[26,27].

1.1.4 Archaea use some unique transcriptional mechanisms different from both bacteria and eukaryotes

In addition to the fact that archaea possess a hybrid transcriptional mechanism, little is known about the nuances that enable cooperation among families of eukaryotic-like GTFs and bacterial-like TFs within these organisms. Notably paralogous TBPs and TFBs also exist in eukaryotes and they potentially play functional roles in driving tissue-specific or developmental stage-specific gene expression; however, in archaea all homologs of the two TBPs and TFBs are functional in the same cell-type. In that regard archaeal TBPs and TFBs are functionally analogous to bacterial σ factors. Furthermore, *in vitro* experiments showed that three of the paralogous TBPs among methanogenic archaea (*Methanocaldococcus jannaschii* TBP, *Methanothermococcus thermolithotrophicus* TBP, and *Methanococcus maripaludis* TBP) differ widely in their ability to support transcriptional activation by both *M. jannaschii* Ptr2 and its homologue *M. thermolithotrophicus* Lrp[26]: among the three TBPs, *M. jannaschii* TBP is the most effective in supporting both *M. jannaschii* Ptr2 and *M. thermolithotrophicus* Lrp mediated transcription activation. These data suggest that despite their shared ancestry, the archaeal transcription regulatory mechanisms are bound to have some significant differences to enable cooperation between eukaryotic-like GTFs and bacterial-like TFs.

1.1.5 Relative to bacteria, archaeal genomes encode relatively fewer TFs

The numbers of TFs in archaea and bacteria positively correlate with the sizes of the genomes[28,29]. It has been suggested that the abundance of TFs usually correlates with the complexity of habitats, and that organisms with complex life styles may require relatively larger genomes and higher proportion of TFs to better adjust to changing environements[29,30]. Thus, archaea like *H. salinarum* that thrive in complex environments would be predicted to carry a comparatively large number of TFs. Interestingly, relative to bacteria, the proportion of TFs is generally lower in archaeal genomes[28]. While TFs represent about 8%-10% of all genes in bacterial genomes, less than 5% of genes in most archaeal genomes encode TFs –similar to the fraction observed in genomes of some bacteria with very specific, non-complex environments such as intracellular pathogens and bacterial parasites[31,32]. What can explain this discrepancy? Besides the possibility that some lineage or organism-specific TFs have not yet been identified, another explanation could be the existence of archaeal-specific regulatory mechanisms that expand the regulatory purview of only a few TFs.

1.1.6 Archaeal TFs are significantly smaller than bacterial TFs

Archaea tend to encode a larger proportion of short TFs (100-200 amino acids) than bacteria[29]. This tendency is the same even after taking the genome size into consideration. Calculations based on randomly sampled collections show that the length of archaeal TFs is significantly shorter than that of their overall proteome; in contrast, bacteria TFs do not show this trend. More studies show that most archaeal TFs are significantly smaller than bacterial ones. On average archaeal TFs have fewer functional domains than bacterial TFs[29].

The high proportion of short TFs together with the underrepresentation of TFs in archaea genomes suggests that archaea might have alternate strategies for generating complex regulatory programs[29,33]. In addition to the functional similarity between different TBP-TFB complexes and bacterial σ factors within the eukaryotic-like basal transcriptional machinery[13,34], some archaeal TFs can form different oligomeric assembly forms in different environments, e.g. one of the Lrp-like proteins, *Pyrococcus* sp. *OT3* FL11, assemble higher order oligomers upon interaction with glutamine and disassemble to dimers upon interaction with leucine[35]. *In vitro* experiments

showed that the formation of hetero-octamer of FL11 and another Lrp-like protein DM1 in *Pyrococcus* sp. *OT3* is facilitated by Arginine while the assembly of homo-octamer of FL11 is facilitated by lysine[36]. Archaeal TFs may also assemble into different combinations through protein-protein interactions and regulate different sets of genes or bind to a spectrum of different ligands to regulate cell physiology under different conditions[35]. In summary, archaea may use a dense combinatorial interplay among TFs to mediate transcriptional regulation upon sensing dynamically changing environments[29,33].

1.1.7 Expansions of TF family contribute to complexity of gene regulatory networks

One of the mechanisms for enhancing the TF repertoire is through gene duplication of transcriptional factors (TFs), which leads to new topology in gene regulatory networks (GRNs) and enables complex behavior[37,38]. Ninety percent of all regulatory interactions in *E. coli* and yeast are believed to have arisen through duplication of either TFs or their target genes[39]. Lineage-specific expansions of TF families across all domains of life underscore the universally important role of this process in the evolution of nearly all organisms[37]. Simple mutations that alter the functions of duplicated TFs give an organism an exponentially larger landscape of combinatorial interactions from which to explore effective strategies to deal with complex environmental changes[14]. Selection in a structured environment results in a GRN architecture that mimics coupled changes in concentrations of small molecules that can directly or indirectly modulate activity of over half of all TFs in bacteria[40,41,42]. This dissertation focus on the study of one of the largest families of archaeal TFs, the Leucine Responsive Protein (Lrp) family, with a special emphasis on understanding the roles of this expanded gene family on the structure of TRNs.

1.2 The Leucine Responsive Protein (Lrp) family

Lrp-like proteins[43] - also called Lrp/AsnC family (PF01037, AsnC_trans_reg) protein or feast/famine regulatory proteins (FFRPs)[44] - represent one of the largest families of prokaryotic transcriptional regulators that have evolved through numerous expansions. These exclusively prokaryotic regulators have been implicated in the regulation of a wide range of physiological

processes including amino acid biosynthesis and degradation, pili synthesis, metabolite transport[25,45,46], DNA bending and chromosome organization[47]. Although the amino acid sequences of these proteins have limited similarity (<30%)[48], their domain architecture and secondary structure are similar. A typical Lrp[a] is a small protein (~15 kDa) with an N-terminal Helix-turn-Helix (HTH) DNA-binding domain connected by a hinge to the C-terminal Regulation of Amino acid Metabolism (RAM) domain[48], which modulates functions through effector-binding and oligomeric interactions[49]. Lrps exist in solution as dimers, tetramers, hexadecamers and octamers[35,49,50,51,52,53,54]. Different ligands have been found for different Lrps, including Leu[49,54,55], Ile[36], Val[56], Arg[36], Asn[57], Glu[58], Gln[35], Lys[25], and Pro[59]. While the binding of ligand is not an absolute requirement for multimer formation it has been shown that ligand-binding is likely to alter the regulated targets of Lrps by inducing conformational change of the multimer structure[50,52,60]. Bcause Lrps assemble into functional heterogeneous multimer assemblies[35,36] it is feasible that in the same organism combinations of regulators could encode a spectrum of complex regulatory programs that efficiently coordinate physiology in response to combinatorial changes in the availability of ligands[36].

Crystal structures have been determined for eight full length Lrp family proteins, including *Pyrococcus furiosus* LrpA, *Pyrococcus* sp. FL11, *E. coli* AsnC, *Bacillus subtilis* LrpC, *E. coli* Lrp, *Neisseria meningtidis* NMB0573, *Mycobacterium tuberculosis* LrpA, and *Sulfolobus tokodaii* strain 7 Grp[35,50,51,52,60,61,62,63]. Lrp members share similar secondary structure in spite of limited similarity in their amino acid sequences. Full length Lrp consists of an N-terminal Helix-turn-Helix (HTH) DNA binding domain connected by a hinge to the C-terminal Regulation of Amino acid Metabolism (RAM) domain which has a βαββαβ fold[64]. Some proteins bearing only the RAM domain and lacking the HTH DNA binding domain have also been found, such as *Pyrococcus* sp. DM1[61] and *Thermus thermophilus* HB8[65]. These proteins are classified as "stand alone RAM domain proteins (SARD)"[64], also called headless Lrp proteins[61] or demi-FFRPs[35]. Their three dimensional structures are similar to the C-terminal RAM domain of the full length Lrp proteins.

The basic structural units of the Lrp family proteins are dimers[66,67]. These dimers are formed mainly through interactions between the anti-parallel β sheets of the C-terminal RAM domain.

[a] In order to simplify the naming, for the rest of this dissertation Lrp-like protein is simplified to Lrp.

Besides FL11, all the above solved three-dimensional structures of full length Lrp proteins revealed an octameric disc assembled by four dimers, with their RAM domains contacting in the center and their N-terminal HTH domains facing outward[52,60]. In the case of the FL11 protein, the dimers form a six fold helix, also with the RAM domains facing toward the center and the N-terminal domains facing outward[35]. Lrps across diverse organisms (*E. coli*, *Agrobacterium tumefaciens*, *Pseudomonas aeruginosa* and *Pyrococcus furiosus*) have been observed in multimeric forms ranging from dimers, tetramers, octamers and hexadecamers[49,53,54], as well as heterooligomers[36]. In addition, the RAM domain of the Lrp family proteins may also be involved in their effector-dependent regulatory role[49]. In fact, bound asparagine molecules were found in the RAM domain of *E. coli* AsnC[52], and bound leucine or methionine were found in that of *Neisseria meningtidis* NMB0573[62]. However, although the bound amino acid in *N. meningtidis* NMB0573 did stabilize the octamer, both the assembly of multimer and the auto-regulatory role of NMB0573 and AsnC do not require the binding of amino acid ligands[52,62], which indicates diverse physiological roles of this family of regulators.

The *Escherichia coli* Lrp is one of the best studied members of the Lrp family. It is a global regulator affecting the expression of about 10% of genes in *E. coli*. These include genes involved in amino acid biosynthesis, amino acid degradation, pili synthesis and metabolite transport[46]. *E. coli* Lrp senses the nutrition status by leucine concentration to either act as a positive regulator or a negative regulator and can also regulate target genes independent of leucine, i.e., its auto-regulatory role of the expression Lrp itself[49]. It has also been shown independently that *E. coli* Lrp may regulate many genes related to the transition to stationary phase independent of the presence of leucine[46]. However, besides *E. coli* Lrp, most of the other Lrp family members characterized to date have more specific rather than global regulatory roles. For instance, *E. coli* AsnC, another Lrp homologue which shares 25% amino acid sequence identity with *E. coli* Lrp, is a specific TF that activates the expression of its adjacent gene, asparagine synthase (*asnA*)[45]. In archaea, in addition to *Pyrococcus sp*. FL11 and *Sulfolobus solfataricus* LysM[25], which are known to regulate lysine biosynthesis in response to lysine, most of the other characterized Lrp proteins have only been shown to exert a negative autoregulatory role independent of any amino acid ligand, such as *S. solfataricus* Lrs14 and *Pyrococcus furiosus* LrpA[23]. In summary, of the hundreds of Lrp homologues that have been identified in prokaryotic genomes so far, only a small number have been functionally characterized. While some of them have diverse

physiological roles (*E. coli* Lrp shows global control and the paralogue AsnC exerts specific control on AsnC), some have cooperative functions (*Pyrococcus sp.* FL11 and DM1 can associate to exert gene regulation).

Relatively little is known about the roles of Lrp family of regulators in archaea. It is difficult to predict their function based on sequence homology with their amino acid sequence similarity usually below 30%. Archaea typically inhabit extreme environments unsuitable for most bacteria and eukaryotes, e.g., *H. salinarum NRC-1* thrives in 4.5 M high salt environment. With a total of 9 Lrp homologues in this organism, what are the functional roles of the members of this protein family? Does each Lrp have a distinct function or do they control overlapping sets of functions? What are the consequences of Lrp family expansions on regulation of cell physiology in dynamically changing environmental conditions? How does the expansion help with evolution of transcriptional regulation?

Here, we have applied a systems approach to elucidate the architecture of the GRNs encoded by interactions of all the eight full length Lrp family regulators in *Halobacterium salinarum NRC-1*. We have mapped the genome-wide DNA binding locations of all Lrps under nutrient repleted and depleted conditions; integrated the various protein-DNA binding maps to discover co-location of binding sites for multiple Lrps; correlated binding with global transcriptional responses during complex growth-associated physiological changes[68]; integrated Lrp genome-wide binding locations, correlation of global mRNA expression of Lrps and their targets across 1018 experiments, and the gene expression profile in the wild-type and Lrp-deletion strains to discover conditional regulation by Lrps; identified putative *cis*-regulatory Lrp motifs by refining *de novo* motif predictions based on Lrp structure with genome-wide binding data; reconstructed coordination of metabolic pathways by multiple Lrps. These analyses have recapitulated known biology of Lrps such as their putative ligand-dependent regulation of amino acid metabolism and their genome-wide impact on regulation of at least one third of all genes in the genome. In addition to conferring robustness through extensive buffering, the complex GRN architecture that emerges through the conditional, combinatorial and competitive action of these eight Lrps can potentially encode a complex set of dynamically changing regulatory relationships among different metabolic pathways. We have performed comparative metabolomic analysis to demonstrate the network-predicted direct and indirect regulation of glutamate metabolism by

three Lrps. Remarkably, one of these Lrps also regulates Cu trafficking and thereby encodes an interesting coupling between two distinct physiological processes. This is a general theme throughout the Lrp network wherein their combinatorial and conditional activities dynamically encode a different set of operational relationships among the various physiological processes of the cell to best deal with multifactorial environmental changes. Thus, our studies have provided insights into how expansions in the Lrp family have played an important role in generating regulatory programs for conditionally coordinating diverse metabolic processes.

Chapter 2 : Comparative Genomics and Sequence Analysis

2.1 Overview

Despite low sequence similarity (usually below 30%) across family members, presence of the RAM domain signature (defined by the Pfam family PF01037, AsnC_trans_reg[69]) identified 9 Lrps in *Halobacterium salinarum NRC-1* -- AsnC (VNG1377G), VNG1179C, VNG1237C, Trh2 (VNG1285G), Trh3 (VNG1816G), Trh4 (VNG2094G), Trh6 (VNG1351G), Trh7 (VNG1123G), and Trh5 (VNG1922G)[a]. With the exception of Trh5, all of the other eight TFs are full length Lrp regulators with both the N-terminal DNA binding HTH domain and the C-terminal RAM domain (**Figure 2-1A**). Trh5 is a standalone protein that only has the RAM domain. We focus just on the 8 full length Lrps in this study.

Lrps exist in multiple copies in prokaryotic genomes. We discovered that over two-thirds of archaeal genomes have at least two Lrp copies, and nearly 10% possess more than 10 Lrps (**Figure 2-1B**). The number of Lrps in genomes seems to be proportional to the adaptability of organisms to changes in environmental conditions[29,30], suggesting that the repertoire of these TFs in an organism may be related to the unique characteristics of its habitat[30]. For example, *Sinorhizobium fredii NGR234*, a member of a group of α-proteobacteria that can nodulate more than 112 genera of legumes[70], possesses over 30 Lrps; on the other hand, organisms confined to habitats with very specific nutritional requirements such as the symbiotic *Nanoarchaeum equitans* and the methanogen *Methanocaldococcus jannaschii DSM 2661* have only 2 Lrps each. In other words, the 9 Lrps in *H. salinarum NRC-1* may play important roles in adaptation to a

[a] VNG1179C, VNG1237C and Trh2 possessed significant matches to the PF01037 region in the earlier version of Pfam. The newer version of Pfam has a much larger and diverse set of members in the PF01037 family. As a result the PF01037 signature has become degenerated. Even though the overall coverage of sequences was increased during the version update, some families have lost members. This was observed in several protein families that are highly diverged[69]

Punta, M. *et al.* The Pfam protein families database. *Nucleic Acids Res* **40**, D290-301

.

dynamically changing hypersaline environment that is characterized by a wide spectrum of routine and stressful changes in sunlight, salinity, oxygen and nutrients.

2.2 Results

2.2.1 Phylogenetic analysis reveals that the Lrp family has ancient origin

Multiple sequence alighment showed low sequence similarity (<30%)[64] across members of the Lrps (**Figure 2-2**). Further phylogenetic analysis did not show any striking correlations between the expansions of Lrps and evolutionary splits in different phylogenetic lineages (**Appendix A**). For instance, the multiple Lrps across all Halobacteria within the Euryarcheoata group did not cluster into a single clade, suggesting that the similar number of Lrps across the halophilic archaea might have resulted from convergent evolution or through horizontal gene transfers. Irrespective of an evolutionary explanation for how the Lrp family might have expanded within each lineage, sequence-based phylogenetic analysis did not provide any further clue into functions for the Lrps in *H. salinarum NRC*-1 beyond what is already known about this family of regulators.

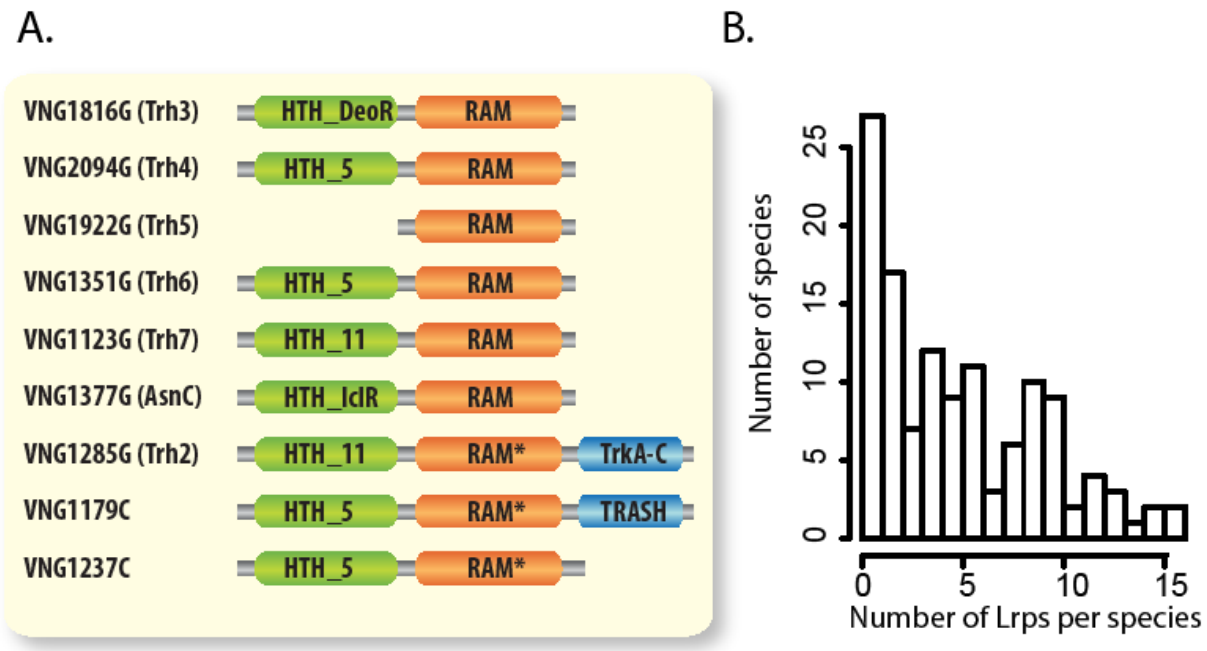

Figure 2-1 Distribution of the Lrp family in Archaea and its expansion in *H. salinarum NRC-1*

A. The Lrp family is expanded in *H. salinarum NRC-1*. Eight of the nine Lrps are full length Lrps with both the RAM domain and a HTH DNA binding domain[a]. Trh2 and VNG1179C have additional protein domains at the C terminus, thus providing clues into their possible functional roles. See the footnote (a) on page 15 for more detailed information about the * on the RAM domain of Trh2, VNG1179C and VNG1237C. **B.** The frequency of distribution of 676 Lrp regulators in 125 sequenced archaeal genomes reveals that over 75 % of the archaea possessing the Lrp/AsnC protein have two or more Lrp regulators.

[a] Trh5 is truncated in this respect as it has just the RAM domain.

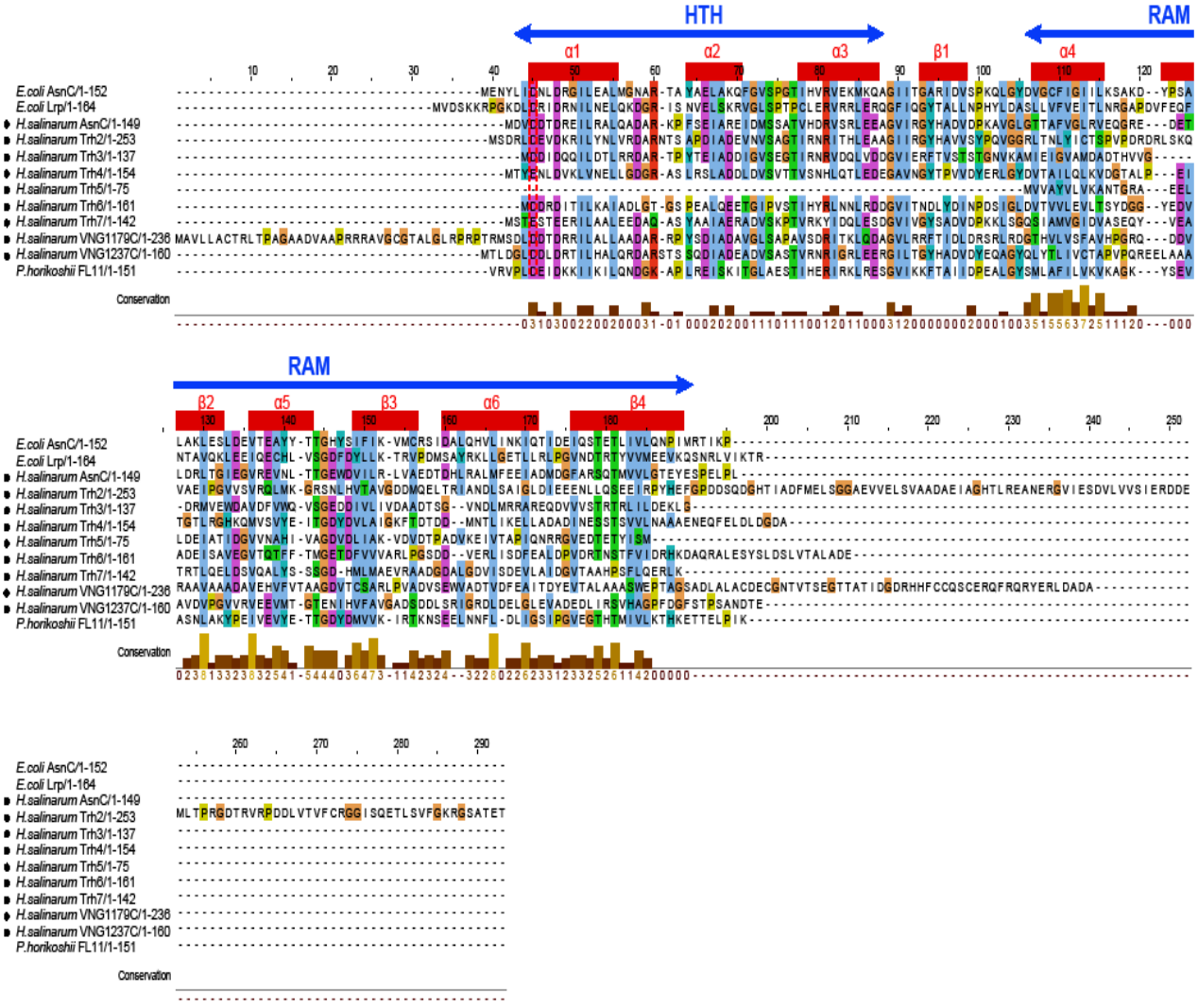

Figure 2-2 Multiple sequence alignment of 9 Lrps in *H. salinarum NRC-1*

Multiple sequence alignment of all 9 Lrps in *H. salinarum NRC-1* together with three Lrps with solved crystal structures - *E. coli* Lrp, *E. coli* AsnC, and *P. horikoshii OT3* FL11. ClustalW[71] was used for multiple sequence alignment and JalView[72] was used for visualization. If an amino acid residue at a particular position meets certain minimum criteria, a certain color based on the ClustalX color scheme[a] is then assigned to the residue. The 9 Lrps from *H. salinarum* are labled with black dots on the left of the sequences. The HTH and RAM domains are indicated by blue arrows above the multiple sequence alighment. The brown histogram labled as conservation below the sequence alignments represents the conservation score, a quantitative numerical index that measures the number of conserved physico-chemical properties conserved for each column of the alignment[73]. Columns with calculated scores above

11 using the default amino acid property grouping are typically categorized as conserved residues and indicated by '*'; however, no positions here pass this threshold, showing the diversity among the sequences of these Lrp-like proteins. Trh5 lacks the HTH DNA binding domain at the N-terminus; Trh2 and VNG1179C has TrkA-C and TRASH domain at the C-terminus respectively. Although the average sequence similarity among Lrps is less than 30%, some amino acid residues are conserved among all shown Lrps.

---

[a] Details of criteria for color assignment of the ClustalX color scheme shown in **Appendix B**.

2.2.2 Protein domain analysis reveals functional insights

Detailed investigation of protein domains in each Lrp gave some clues into putative physiological roles for two of the eight Lrps [Trh2 (VNG1285G), and VNG1179C]. The TrkA-C domain[69] in Trh2 and the TRASH domain[48] in VNG1179C implicated these Lrps in the regulation of potassium transport and metal trafficking, respectively. Consistent with this predicted function, and the systems analysis of *H. salinarum* response to six transition metals, it was discovered that deletion of VNG1179C results in dysregulation of the copper efflux system making the mutant hypersensitive to small increases in extracellular copper (Cu)[74]. Similarly, physical mapping of binding locations (described in **Chapter 3**) supported the likely role of Trh2 in regulating potassium transport. Other than the two special cases described here, none of the other Lrps possessed any additional protein domains that could serve as clues for their physiological functions.

2.3 Summary and discussion

In summary, protein sequence and domain analysis provided limited albeit valuable clues into evolution of the Lrp family and putative functions for two of the eight Lrps. Although there is low sequence similarity across the nine Lrp family members, sequence alignments to three previously characterized Lrps- two from *E. coli* and one from *P. horikoshi OT3* – revealed that some key amino acid residues are conserved among all Lrps in *H. salinarum*, suggesting the existence of evolutionary pressure on these amino acid residues. However, phylogenetic analysis showed no significant correlation between the sequence-predicted Lrp duplication events and evolutionary splits in phylogenetic lineages. Because of the low sequence similarity, the phylogenetic analysis could be considered to have been inconclusive. However, the results do support an ancient origin for the Lrp family, which is consistenet with the presence of this family of TFs in both archaea and bacteria. It has been suggested that the last universal common ancestor already possessed a prototype of Lrps because of the potential ancestral nature of Lrps[49,67].

Lrps usually exist in multiple copies. Over 75% of the sequenced archaeal genomes possess two or more copies of Lrps. Interestingly, some phylogenetically-related organisms possess

similar numbers of Lrps. For example, while there are 13 Lrps in *Pyrococcus sp. NA2*, 11 in *Pyrococcus horikoshii OT3* and 9 in *Pyrococcus abyssi GE5*, several methanogens have only one or two Lrps (**Appendix C**). Our phylogenetic analysis suggests that this is most likely an outcome of horizontal gene tranfers or convergent evolution. As the expansion or contraction of the repertoire of TFs can be a consequence of adapting to particular life styles ot habitats[29], the 9 Lrps in *H. salinarum NRC-1* are likely to have functional roles that assist the organism in adapting to its specific hypersaline habitat and the dynamic environmental changes associated with this particular life style.

Chapter 3 : Genome wide DNA-binding locations for all Lrps reveals that their regulatory networks are highly intertwined

3.1 Overview

We reconstructed the regulatory network for each Lrp by mapping their binding locations across the entire genome. Lrp functions are known to be modulated through direct binding to effector molecules such as amino acids and other nutrients[43,67]. However, for most of the Lrps we lack knowledge of the possible co-factors or effector molecules. In order to overcome this challenge and comprehensively map all of the binding locations for each Lrp we devised a two-pronged strategy. First, we mapped binding locations of Lrps in batch culture over two different phases of growth which are known to be associated with complex physiological readjustments in response to wide fluctuations in environmental and nutritional conditions[68]. Our rationale for selecting these two conditions was influenced by our knowledge that these two phases of growth are associated with a shift from nutrient repleted to depleted conditions. This experimental design provides the opportunity to identify Lrp regulatory networks by spanning a large range of metabolic and transcriptional states within which co-factors and effector molecules may vary. Second, we over-expressed each Lrp in order to reveal all of its potential binding locations across the entire genome. In subsequent sections we integrate the Lrp binding sites with other data including environment-dependent transcriptional changes to identify functional Lrp binding locations.

3.2 Results

3.2.1 The predicted target genes of Lrps revealed by genome-wide Lrp-binding locations

We performed chromatin immunoprecipitation of C-terminally c-Myc-tagged Lrps and localized the enriched DNA fragments by hybridization to a genomic tiling microarray chip (ChIP-chip). We then used the machine learning algorithm MeDiChI to learn a joint model of

binding events in the ChIP-chip data and accurately locate statistically significant genomic binding sites for each Lrp (p-value <=0.01)[75] . The approximate length of promoter regions was determined based on the calculated average length of intergenic regions (~200nt) in *H. salinarum NRC-1* genome and a buffer of 50nt was added to account for the resolution of MeDiChI. We then assigned each Lrp binding site to the promoter(s) of one or more gene(s) within 250nt upstream or 50nt downstream of the start codon. Genes in an operon downstream of a gene with a Lrp binding site were also considered targets of that Lrp. A complete list of targets genes in the Lrp regulatory network determined by the genome wide Lrp binding locations is shown in **Appendix D**.

Overall, nearly 30% of all genes (712 out of 2,400 genes) in *H. salinarum NRC-1* are putatively regulated by one or more Lrps, and 37.5% (267, permuted p-value < 10^{-5}) of these genes have binding sites in their promoters for two or more Lrps (**Figure 3-1A**), suggesting that the regulatory networks governed by the eight Lrps are highly intertwined – an observation that was further supported by the significant overlap across sets of genes regulated by the eight Lrps (**Figure 3-1B**). The extensive overlapping target genes among Lrps might be a consequence of the known ability of Lrps to assemble into heterogeneous multimers[35,36]. On the other hand, one could argue that this is an outcome of overexpressing the Lrps, which might have resulted in perturbed stoichiometry of the multimeric complexes. However, there were clear differences in the overall binding patterns of most Lrps, suggesting that there are differences in their binding preferences. For instance, clustering based on the similarity between target gene sets shows that AsnC, Trh4 and Trh6 have the most similar binding profiles (**Figure 3-1B,C**), with corrected hypergeometric p-values of association 1.78×10^{-59}, 1.14×10^{-46}, and 3.92×10^{-63} between AsnC and Trh4, AsnC and Trh6, and Trh4 and Trh6 respectively. In **Chapter 5** we present evidence from expression analysis across multiple environmental conditions that each of these three Lrps has different conditional relationships with their binding targets, suggesting that their binding to the same target genes might happen in different environmental conditions.

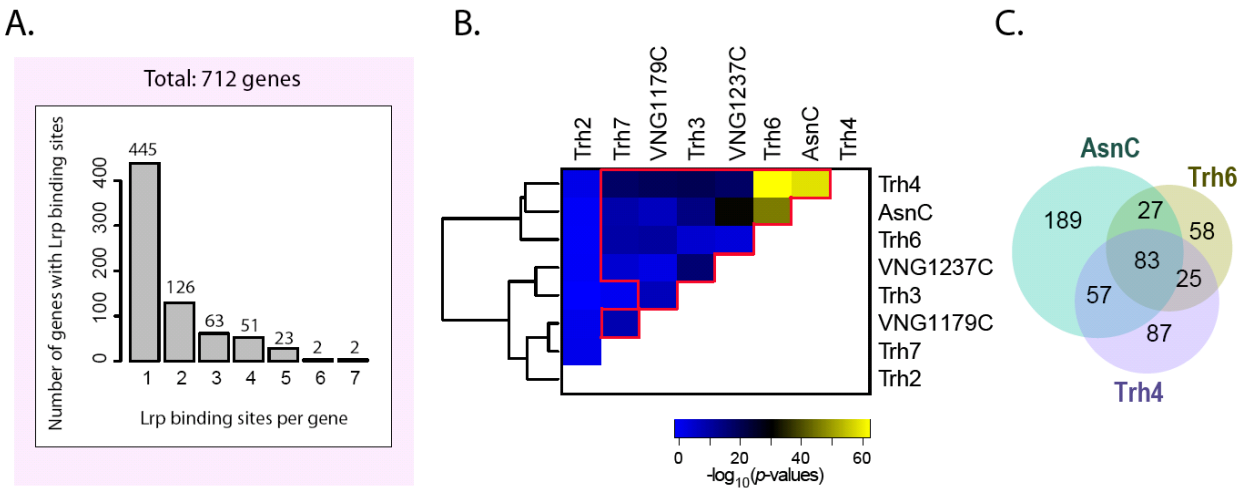

Figure 3-1 Genome-wide binding co-locations among Lrps

Analysis of Lrp binding locations reveals a highly interconnected Protein-DNA interaction map. The promoter regions of 712 genes were bound by at least one Lrp. **A.** Genome wide distribution of ChIP-Chip interactions. This histogram summarizes the number of genes that have been associated with one, two, or multiple Lrps. The number of promoters in each category is written above each bar. **B.** The heatmap of the hypergeometric overlap corrected enrichment *p*-values of each Lrp pair. Areas included in the highlighted red box represents overlap between the two corresponding Lrps is significant (corrected *p*-values <=0.05) **C.** Venn diagram of the target genes of AsnC, Trh4, and Trh6.

Table 3-1 *p*-values of the significance of overlap target genes between all Lrp pairs

	AsnC	VNG1179C	VNG1237C	Trh2	Trh3	Trh4	Trh6	Trh7
AsnC		7.02E-09	1.96E-33	0.127	1.62E-16	6.37E-61	4.06E-48	3.22E-11
VNG1179C			0.0004042	0.005	3.71E-09	1.61E-21	9.54E-13	1.54E-10
VNG1237C				0.125	2.33E-18	4.57E-20	2.69E-05	2.32E-06
Trh2					1	0.00198	0.214912	0.00214
Trh3						2.81E-22	1.06E-06	0.017954
Trh4							1.40E-64	9.01E-20
Trh6								6.46E-12
Trh7								

3.3 Summary and discussion

3.3.1 Environmental context is critical to the functions of Lrps

When we examined the Lrp binding results from each growth phase, we observed largest DNA binding by most Lrps occurred at late growth phase, implicating these proteins in stress- or nutrition-responsive gene regulation (**Figure 3-2A**). There was also a significantly higher degree of overlap among the Lrp regulatory networks in the later phase of growth. Going from early to late growth phase, the number of promoters bound by two or more Lrps went up from 20% to 33% (**Figure 3-2B**). This is consistent with a previous study that suggested *E. coli* Lrp played a major role in the transition of the cell from exponential to stationary phase[46]. In addition, regulation of very different sets of genes across the two growth phases by most Lrps (**Figure 3-3**) underscores the importance of growth environments and potentially the ligand-dependent activities.

A.

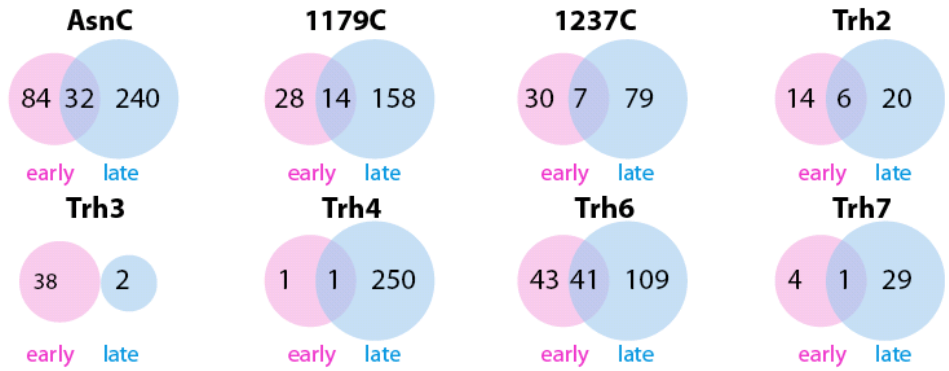

B.

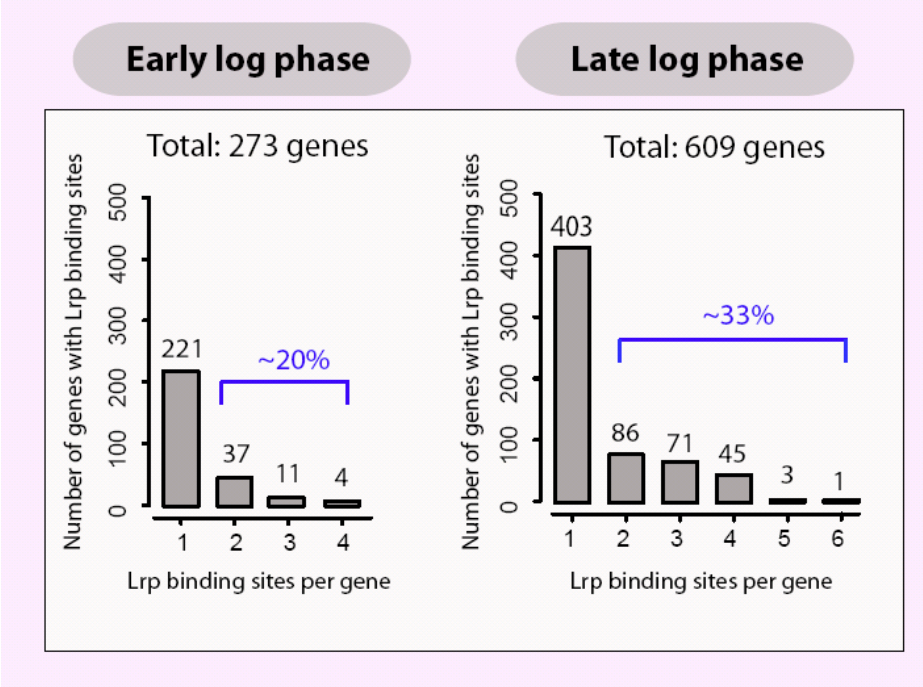

Figure 3-2 Distribution of protein-DNA interactions of Lrps during early and late phases of growth

A. Venn diagram of the genes regulated by these 8 Lrps based on the ChIP-Chip results. Each shows the number of genes putatively controlled by the Lrp in early and late log phase individually and also the number of genes controlled by the Lrp in both phases of growth. This shows the binding of all these 8 Lrp proteins are condition dependant. **B.** Growth phase-dependent distribution of Lrp protein binding. During early log phase, 20% of all genes that have Lrp binding sites are bound by two or more Lrps; this percentage is increased to 33% during late log phase.

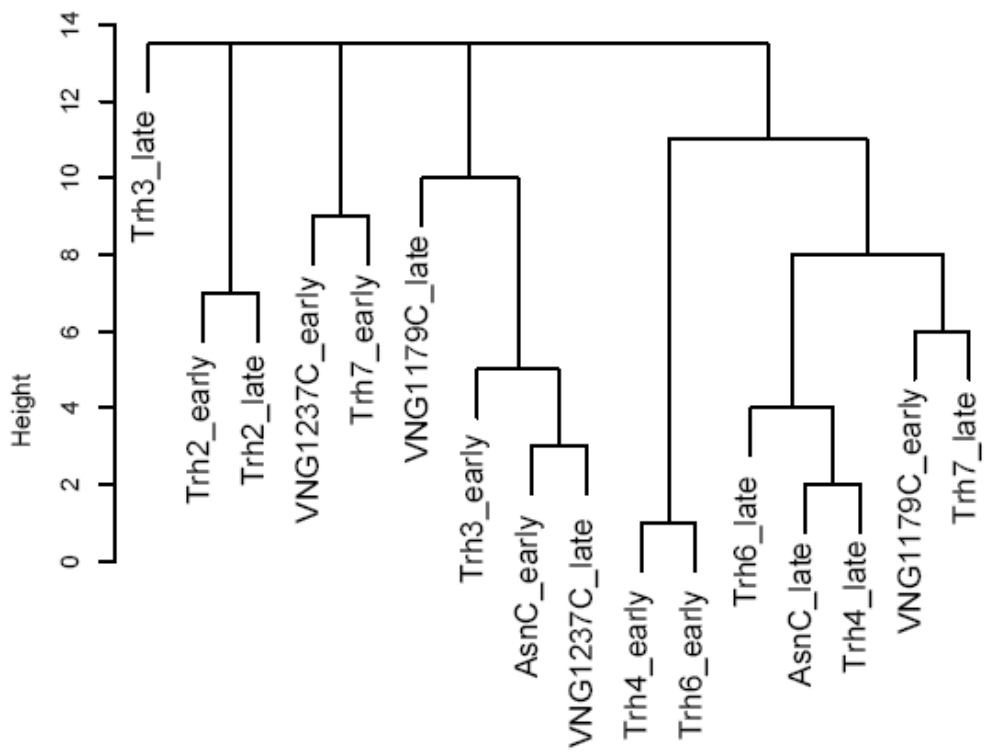

Figure 3-3 Hierarchical clustering of DNA-binding specificities among 8 Lrps in early and late phases of growth

Hierarchic clustering was based on the hypergeometric enrichment *p*-values of shared binding locations between each Lrp pair. This shows that the same Lrp does not necessarily regulate the same set of genes during both phases of growth, indicating environmental context is critical to the regulatory function of Lrps.

3.3.2 Five Lrps in *H. salinarum NRC-1* putatively regulate more than 100 genes each

Relative to what is known from studies conducted in other organisms the Lrps in *H. salinarum NRC-1* regulate a significantly larger repertoire of physiological functions. Five of the eight Lrps (AsnC, VNG1179C, VNG1237C, Trh4, and Trh6) potentially regulated over 100 genes (**Figure 3-2**). By contrast, Trh2, Trh3 and Trh7 have fewer binding sites, which suggests that they either have specific functions, or that they do not function optimally under growth conditions in which the genomic binding locations were mapped. These results recapitulated what is known in other organisms, wherein some Lrps have very specific functions, e.g. AsnC in *E. coli* and Ptr2 in *M. jannaschii*, and others have a larger number of targets, e.g. Lrp in *E.coli*. While at least 10% of genes in *E. coli* were shown to be affected by Lrp[46], *E. coli* AsnC was only shown to regulate the transcription of *asnC* itself and *asnA*, which is transcribed divergently from *asnC*. The global analysis that we have performed here provides an opportunity to understand whether and how there is functional interplay to coordinate across Lrps with specific regulatory functions and those with a wider spectrum of regulatory roles. For instance, the significance of the number of overlapping target genes among Lrps (permuted p-value $< 10^{-5}$) showed that the regulatory networks governed by the eight Lrps are highly intertwined. We hypothesized that this interconnectedness may aid in expanding the repertoire of regulatory programs for adjusting physiology in response to complex environmental changes, while lending robustness through redundant and complementary mechanisms[29,30].

3.3.3 Co-location of Lrp binding sites in many promoters suggests cooperative or competitive regulatory mechanisms

We investigated the putative mechanisms by which multiple Lrps regulated the same promoters by analyzing in a pairwise manner distances between the genome-wide binding locations of all Lrps. As mentioned earlier and in **Figure 3-1B**, a significant number of binding locations for many Lrps were discovered to be indistinguishable and consistent with the known ability of the Lrps to heteromultimerize[36]. While the co-location of binding sites might predict cooperative regulation by two or more Lrps, we cannot rule out the possibility that some Lrps might also compete for regulation of the same promoter. As mentioned in **3.3.1**, we observed that environmental context is critical to the function of Lrps. Remarkably, there was at least one

instance in which a large number of genes under the control of one Lrp (AsnC) during early growth phase shifted to the regulatory network of a different Lrp (VNG1237C) at the later growth phase (**Figure 3-3** and **Figure 3-4**). Based on this broader view of Lrp function we propose that from the expansion of this family of regulators emerges a scheme of heteromultimerization and cooperative/competitive promoter-binding to encode complex and robust (i.e. buffered) regulatory relationships among different physiological processes in various environmental contexts. Further, because the binding locations were mapped through overexpresion of the Lrps, with these data alone we cannot rule out the possibility that some or a significant fraction of these interactions may occur in different environmental conditions. Further details on the conditional regulaiton by Lrps are described in **4.3**.

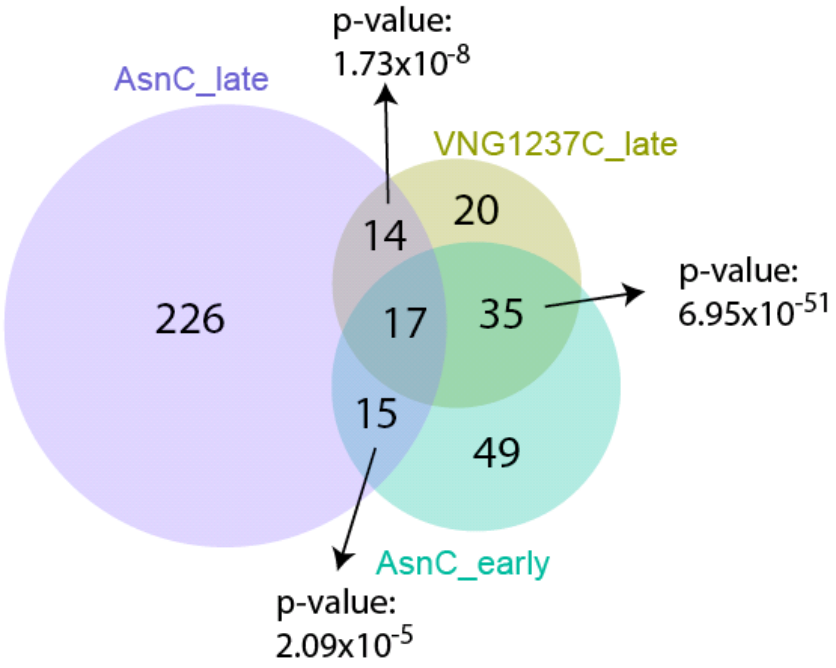

Figure 3-4 Co-location of Lrp binding events among three Lrps in different phases of growth

The Venn diagram illustrates unique and shared targets of AsnC and VNG1237C across different phases of growth (early and late). AsnC potentially regulates more than twice (272) as many genes in late as opposed to early log phase (116 genes). AsnC regulates only about 10% of its targets in both growth phases (Bonferroni corrected hypergeometric *p-value* 2.09×10^{-5}). Remarkably, many genes under the control of AsnC in early phase (about 50% of which) shift to a VNG1237C regulatory program in late log phase (Bonferroni corrected hypergeometric *p-value* 6.95×10^{-51}).

3.3.4 The regulatory influence of Lrps is expanded through their binding to promoters of nearly a quarter of all TFs encoded in the genome

Promoter regions of 1/5 of all TFs in *H. salinarum NRC-1* (25 out of 125) were bound by at least one Lrp, and seven of those TFs were bound by two or more Lrps (**Appendix E**). The integrated protein-DNA interaction data of Lrps and 13 other TFs - KaiC, Idr1, Idr2[76], ArcR, VNG1451C[42], and 8 GTFs[13], together representing nearly 15% of known and predicted TFs in *H. salinarum NRC-1* revealed a highly interconnected network (**Figure 3-5**). This suggests that the global impact of Lrp might be further extended through the direct regulation of other TFs.

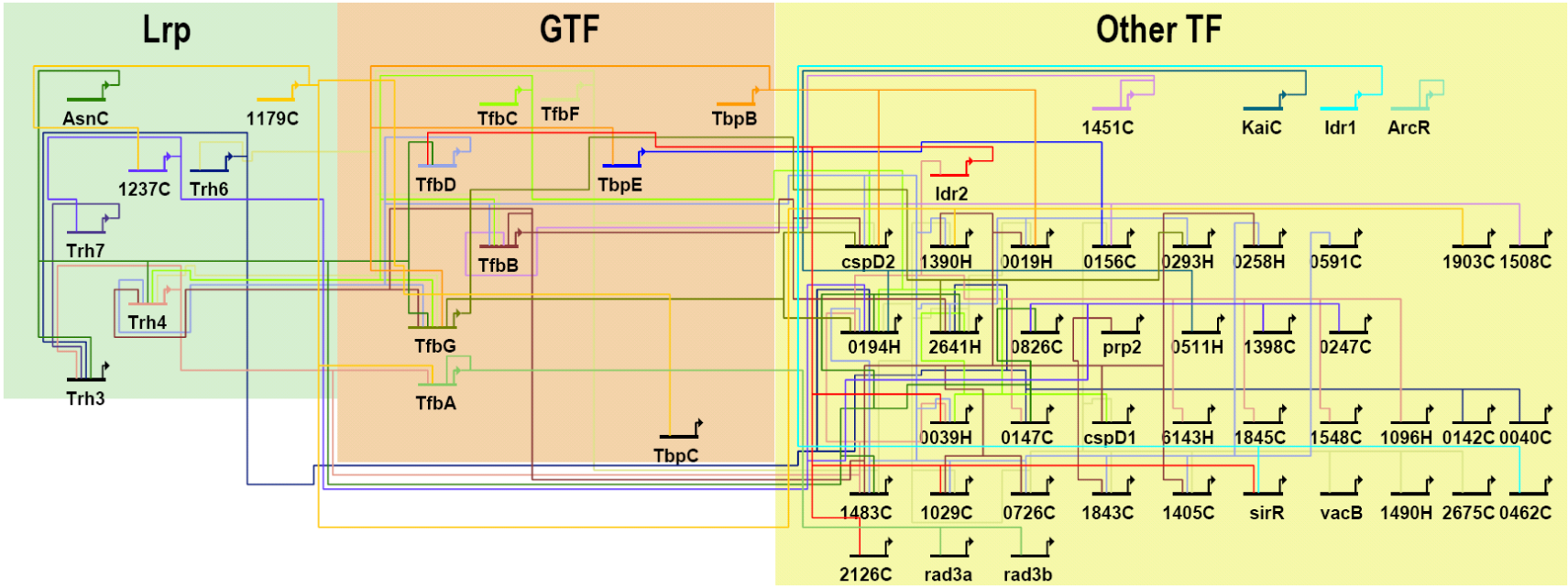

Figure 3-5 Protein-DNA interaction map of Lrps and other TFs

The promoter regions of 1/5 of all TFs in *H. salinarum NRC-1* were bound by at least one Lrp, and seven of those TFs were bound by two or more Lrps. Integrating the genome-wide DNA binding location data of Lrps with that of 13 other TFs - KaiC, Idr1, Idr2[76], ArcR, VNG1451C[42], and 8 GTFs[13], together representing nearly 15% of all of the known transcriptional regulators in *H. salinarum NRC-1* revealed a highly interconnected protein-DNA interaction map. This suggests that Lrps not only bind to the promoter regions of a large set of genes, but that they are also likely to have additional regulatory influences through other TFs.

3.3.5 Lrps regulate genes in diverse pathways, including ribosome biogenesis and amino acid metabolism

As implied by the RAM domain, the functions of Lrps were originally discovered and presumed to be associated with amino acid metabolism[49]. However, by mapping the genome-wide Lrp binding locations we found that the eight Lrps in *H. salinarum NRC-1* bound to the promoter regions of genes widely distributed across different cellular processes (**Appendix D, Appendix E**). This is consistent with some characterized archaeal Lrps that appear to regulate genes of broader functions including those involved in transport, central metabolism and energy[26,77]. Yet, given the historic precedent, we investigated whether there was any evidence for regulation of specific physiological functions by any of the eight Lrps, especially vis-à-vis amino acid metabolism. Not surprisingly, the interconnected nature of the Lrp TRN made it difficult to exclusively associate each Lrp to regulation of any specific physiological function(s). Functional enrichment analysis shows that binding targets of three of the 8 Lrps - AsnC, VNG1237C, and Trh3 - were enriched in "translation"(GO: 0006412, multiple hypothesis correction *p*-value <=0.05), with most genes involved in ribosome biogenesis — 32 genes encoding ribosomal proteins were binding targets of AsnC, 25 were targets of VNG1237C, and 16 were targets of Trh3. While many binding locations for Lrps were indistinguishable, the 445 targets that were bound by a single Lrp were discovered to be associated with few amino acid metabolism pathways, e.g., Trh3 regulates *carB* (*vng1814G*) in the glutamine family amino acid metabolic process (GO:0009064), and Trh4 regulates *carA* (*vng1815G*), *vng1999H*, and *arcC* (*vng6316G*) in the glutamine family amino acid metabolic process. Consistent with their reported roles in other organisms[49], our data implicate all 8 Lrps in the regulation of genes involved in amino acid metabolism (**Table 3-2**). However, our analysis overwhelmingly demonstrated that the Lrps are potentially involved in the regulation of many additional metabolic functions.

Table 3-2 Number of Lrp target genes involved in amino acid metabolic pathway

Amino Acid Metabolic pathway[a]	AsnC	Vng1179C	Vng1237C	Trh2	Trh3	Trh4	Trh6	Trh7
Alanine, aspartate and glutamate metabolism	5				1	3	2	1
Arginine and proline metabolism	2	1				3		
Cysteine and methionine metabolism	2	3	1		2	3	1	
Glycine, serine and threonine metabolism	5	1	3			6	5	
Histidine metabolism	4	1	1			1	2	
Lysine biosynthesis	1		1					
Phenylalanine, tyrosine and tryptophan biosynthesis	5		3			3	3	
Phenylanaline metabolism	2	2	1					
Thiamine metabolism	1					1	1	
Tryptophan metabolism	1	1					1	
Tyrosine metabolism	2		1					
Valine, leucine and isoleucine biosynthesis	0							
Valine, leucine and isoleucine degradation	3	1				2	2	
Total number of genes involved in AA metabolic pathways (non-overlap)	21	8	4	0	3	18	14	1

[a] Categories of amino acid pathways and the genes involved are absed on the Kyoto Encyclopedia of Genes and Genomes (KEGG)[78] Kanehisa, M., Goto, S., Sato, Y., Furumichi, M. & Tanabe, M. KEGG for integration and interpretation of large-scale molecular data sets. *Nucleic Acids Res* **40**, D109-114, doi:gkr988 [pii]
10.1093/nar/gkr988.

3.3.6 Lrp-mediated conditional coordination of metabolic pathways

We analyzed the topology of protein-DNA interactions of all Lrp TFs in order to discover network motifs within the TRN. This analysis revealed three primary modes of regulation by Lrps:

a. *Multiple Lrps regulate the same gene*: 37.5% of all genes in the Lrp TRN are potentially regulated by more than one Lrp (**Figure 3-1, Appendix E**). Specifically, 4 or more Lrps bound to the promoter regions of 78 genes including tryptophan synthase (*vng0307G*, *vng0308G*) and Glu-tRNA amidotransferase (*gatA*, *vng0872G*), both bound by AsnC, VNG1237C, Trh4 and Trh6; and *trh3* bound by AsnC, Trh4, Trh6 and Trh7.
b. *A single Lrp regulates multiple genes involved in the same or multiple metabolic pathways*: Among the five Lrps that regulate in excess of 100 genes each, AsnC regulates the largest number of genes (356 total). It regulates at least two different genes of the asparagine biosynthesis pathway including asparagine synthetases (*asnA*, *vng0867G*), and *aspB2* (*vng0629G*), which encodes aspartate aminotransferase. In addition, AsnC also regulates other Lrps (e.g., *trh3*, *trh4*) and multiple enzymes in other amino acid metabolism pathways (**Appendix E**).
c. *Putative Feed Forward (FFL) Loops*: Among all 712 Lrp binding targets, 153 of the target genes were organized in putative FFL motifs (**Appendix F**). For example, Trh3 regulates AsnC, and both are putative regulators of *cheR* (VNG0966G), which is a methyltransferase involved in the signal transduction pathway for chemotaxis. The predicted regulation of *cheR* by both of these Lrps, was supported by the differential expression in both Δ*asnC* (corrected *p*-value 8.38×10^{-3}) and Δ*trh3* (corrected *p*-value 6.76×10^{-3}). The expression of *cheR* was downregulated in both Δ*asnC* and Δ*trh3*, suggesting that AsnC and Trh3 may regulate chemotaxis through induction of *cheR*.

In summary, protein-DNA interactions for each of the eight Lrps in *H. salinarum NRC-1* changed significantly over two growth phases, underscoring the importance of environmental context in understanding Lrp function. The overall Lrp TRN included nearly one-third of all genes in the genome with five Lrps regulating >100 target genes each. The impact of the Lrp

family is further broadened through their regulation of 20% of all TFs encoded in the genome. The shared binding locations of several Lrps suggested a competitive or cooperative system of interactions that is consistent with a heteromultimeric scheme of action that has been observed for Lrps in other organisms. In addition, as Lrps play a central role by regulating nearly all aspects of physiology, we can expect that they are likely to be functional under various conditions other than the standard growth conditions. We expand on this hypothesis and identify the conditional regulation by Lrps in **4.3**.

Chapter 4 : Analysis of transcriptional consequences of knocking out Lrps reveals genes they regulate directly and indirectly

4.1 Overview

Although protein-DNA interactions are valuable for mapping TF-target gene relationships, perturbation studies are another method commonly conducted to deduce causal roles played by TFs in regulation[79]. In this chapter, we focus on perturbation studies in which the gene encoding a Lrp was deleted and the functional consequences of deletion of the Lrps were analyzed. We performed transcriptomic analyses of Lrp deletion strains, and compared these data to the protein-DNA interaction network in an effort to find orthogonal evidence for functional Lrp-promoter interactions. While the redundancy in action of the eight Lrps might explain why deletion of the eight Lrps did not have significant phenotypic consequences, systematic analysis of transcriptional changes upon deleting each Lrp did in fact validate several of the protein-DNA network predictions.

4.2 Results

4.2.1 Transcriptomic analysis of Lrp deletion strains

Using a two-step gene replacement strategy with selection and counter-selection[80], we constructed in-frame deletions of each of the eight Lrps. We performed whole genome microarray analyses at four different phases of growth of each Lrp deletion strain as well as the parent *Δura3* strain in batch culture in complete defined medium (CDM, recipe see **8.1**). No growth defect was observed in any of the eight Lrp knockout strains (**Appendix G**), perhaps because the duplicated Lrps have some functional redundancy. For the same reasons, we expected that evidence for direct regulation would be difficult to obtain; yet, careful inspection of transcriptome profiles revealed significant dysregulation of a number of genes that was consistent with the physical protein-DNA interaction map thereby validating direct regulation by several Lrps. Specifically, we performed paired t-tests to identify genes with significantly

different expression levels between the Lrp knockout strains and the parent. After multiple hypothesis testing (Benjamini-Hochberg) corrections and fold-change filtering (>1.25 fold), we discovered that relative to the parent strain, over 300 genes were differentially expressed in Δ*asnC* (**Appendix A**) and Δ*vng1237c* (**Appendix J**), and over 100 genes were differentially expressed in Δ*trh2* (**Appendix K**), Δ*trh3* (**Appendix L**), and Δ*trh4* (**Appendix M**). There was also evidence for growth-stage specific regulation of some genes, e.g. stationary phase regulation of *gvpO2* by AsnC (**Figure 4-1**).

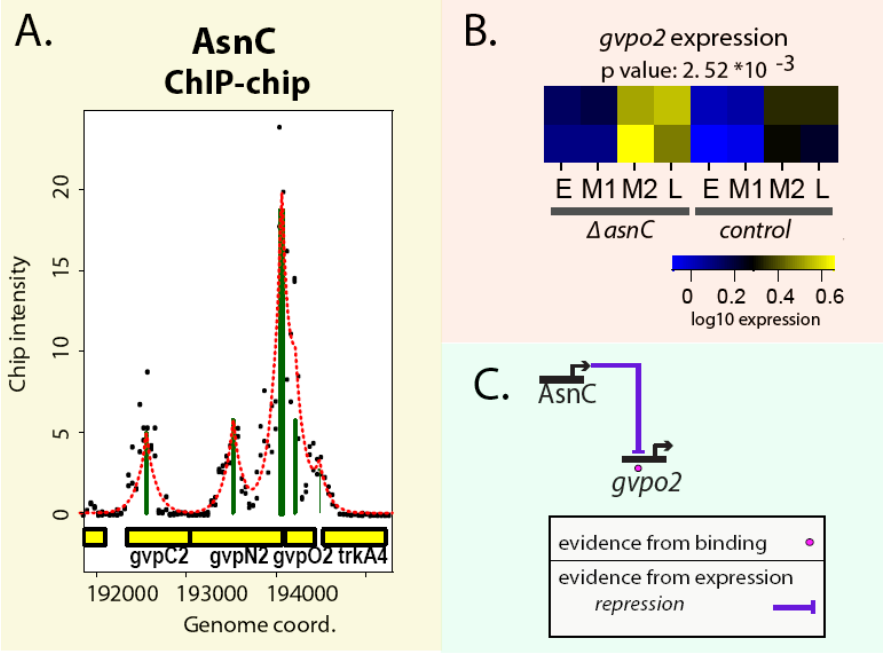

Figure 4-1 Growth phase specific regulation by AsnC

Shown here is an example of the growth phase specific regulation by AsnC based on integration of the Lrp protein-DNA interaction data and gene expression data of Lrp knockout strains. **A.** MeDiChI output of the ChIP-chip data identified significant AsnC binding locations near the start codon of *gvpO2* in late log phase but not in early log phase. **B.** The heatmap shows relative gene expression changes in *gvpO2* in the wild type and the AsnC knockout strains (experiments were performed in duplicates, each sampled at four ime points – early(E), early mid log(M1), late mid log(M2), late/ stationary (L) - along the growth curve). The color scheme of the heatmap represents the expression level in $\log_{10}$ ratios. The two rows represent the biological replicates. **C.** A regulatory network diagram to illustrate the regulation of *gvpO2* by AsnC is supported by both protein-DNA interaction and gene expression analysis.

4.3 Summary and discussion

4.3.1 Despite extensive buffering in the Lrp network, transcriptome analysis of Lrp deletion strains verifies direct regulation and reveals indirect causal influences

In **Chapter 3** we have shown extensive crosstalk and functional overlap among the eight Lrps based on protein-DNA interaction data, suggesting that these eight Lrps may combinatorially regulate their target genes or regulates the same set of genes under different conditions. Despite their large number of potential target genes, there was no obvious growth defect upon deleting any of the 8 Lrps. This result suggested that the Lrps might have retained redundant functions that lend robustness against loss of function mutations in other family members. For example, a null mutation in one Lrp can potentially be buffered by another Lrp with related or similar function[81]. This hypothesis is consistent with our findings that some Lrps physically bind to significantly similar set of promoters. This might also explain why only a subset of target genes for each Lrp was dysregulated upon its deletion (**Appendix P**). An alternate hypothesis is that the overexpression of Lrps recovered all of their potential binding locations throughout the genome, only a subset of which are functional under specific environmental conditions.

In addition to significant consequences on the regulation of some target genes (**Appendix P**), we also observed that deletion of Lrps resulted in differential expression genes that were not part of their protein-DNA interaction network. These genes are potentially regulated indirectly by the Lrp through the regulation of other TFs (**Appendix A - Appendix O**). Again, we cannot rule out that the binding locations in the promoters of these genes are conditional and do not occur in the two growth conditions in which the ChIP-chp experiments were performed. In **4.3**, I present results from further investigation of transcriptional changes across a wide array of environmental conditions as evidence in support of this hypothesis. Whatever the mechanism, direct or indirect, the causual influence of the Lrp on regulation of these genes suggests that integration of different streams of evidence is necessary to comprehensively undrstand the global physiological consequences of Lrp regulatory network. Therefore, in the Chapter 5 we describe a strategy to expand the Lrp regulatory network to include all of the potential target genes that were

discovered through protein-DNA interaction mapping, Lrp deletion analysis, and gene expression correlation analysis.

Chapter 5 : Correlation analysis identifies conditional regulation by Lrps

5.1 Overview

The protein-DNA interaction map suggested that regulatory network governed by the eight Lrps potentially includes nearly 30% all genes in *H. salinarum NRC-1* (**Chapter 3**). Analysis of this physical interaction map in context of global transcriptional changes of Lrp knockout strains further suggested that differing subsets of this network is active across environmental conditions (**Chapter 4**). In this chapter, we describe how we used the protein-DNA interaction data and a compendium of global transcriptional profiles collated from experiments that were performed across a wide spectrum of environments to discover conditional regulation by four of the eight Lrps.

5.2 Results

5.2.1 Integration of genome wide Lrp binding targets with transcriptional changes across 1018 conditions reveals conditional regulation by Lrps

To find specific environments in which each Lrp has a potential regulatory role, we used the protein-DNA interaction map to select target genes that had correlated expression changes with each Lrp in a subset of 1489 transcriptome measurements, which were collated from 246 different genetic and environmental perturbation experiments (**Appendix Q**). Our rationale was that the expression of an active Lrp is likely to correlate with that of its binding targets in the set of condition(s) where it is functional (**Figure 5-1**).

First, we selected 1018 from the 1489 transcriptome measurements where no genetic perturbations (over-expression or knock-out) were used. These 1018 transcriptome profiles were then categorized into 66 conditions sets, based on the type of environmental (high temperature, copper, high H_2O_2, etc) perturbation (**Appendix Q**). Next, we selected the condition sets in which the transcript level of a given Lrp had changed at least 1.25-fold higher or lower across the experiments. This analysis identified 61, 60, 56, 56, 55, 53, 61, and 57 condition sets for *asnC,*

vng1179C, vng1237C, trh2, trh3, trh4, trh6, and *trh7*, respectively (**Appendix V**). By analyzing these datasets in context of their protein-DNA interaction maps for 6 of the 8 Lrps (*asnC*, *trh2, trh3, trh4, vng1179C,* and *vng1237C*) we discovered at least one condition where the Lrp was significantly correlated with its binding targets (corrected permuted *p*-value <=0.05). We then applied another filter to select only the condition sets in which the variance of the transcription level among the Lrp targets inversely correlated with the transcription level of the Lrp. This resulted in at least one condition in which 3 of the Lrps – *asnC, trh3* and *trh4* – significantly correlated with a subset of their binding targets, and the variance among the transcription level of these binding targets also inversely correlated with the transcription level of the Lrp (**Table 5-1**). The rationale for doing this was that higher expression of a regulator would lead to lower variation between the target genes of the regulator and conversely when the regulator is down the variance between targets would be higher. Importantly, this effect should be observable for both activators and repressors. One of several discoveries from this analysis was that in presence of paraquat the transcript level changes of *trh3* were correlated with 21 of 40 putative Trh3 target genes, including 14 ribosomal proteins, one protein translocase (*secY*), two hypothetical proteins, and a key metabolic enzyme (*carB*, carbamoyl-phosphate synthase). Further, the *trh3* promoter was bound by Trh4, whose expression is repressed by VNG1179C (*trh4* was significantly up-regulated in Δ*vng1179C*; **Appendix I**). VNG1179C is known to have a key role in regulating copper trafficking and efflux[74]. Interestingly, the transcription level of *trh4* was significantly correlated with its target genes in the presence of copper, suggesting functional and causal associations across the regulatory networks of VNG1179C, Trh3, and Trh4, which was subsequently validated with additional experiments that are described in the following chapter.

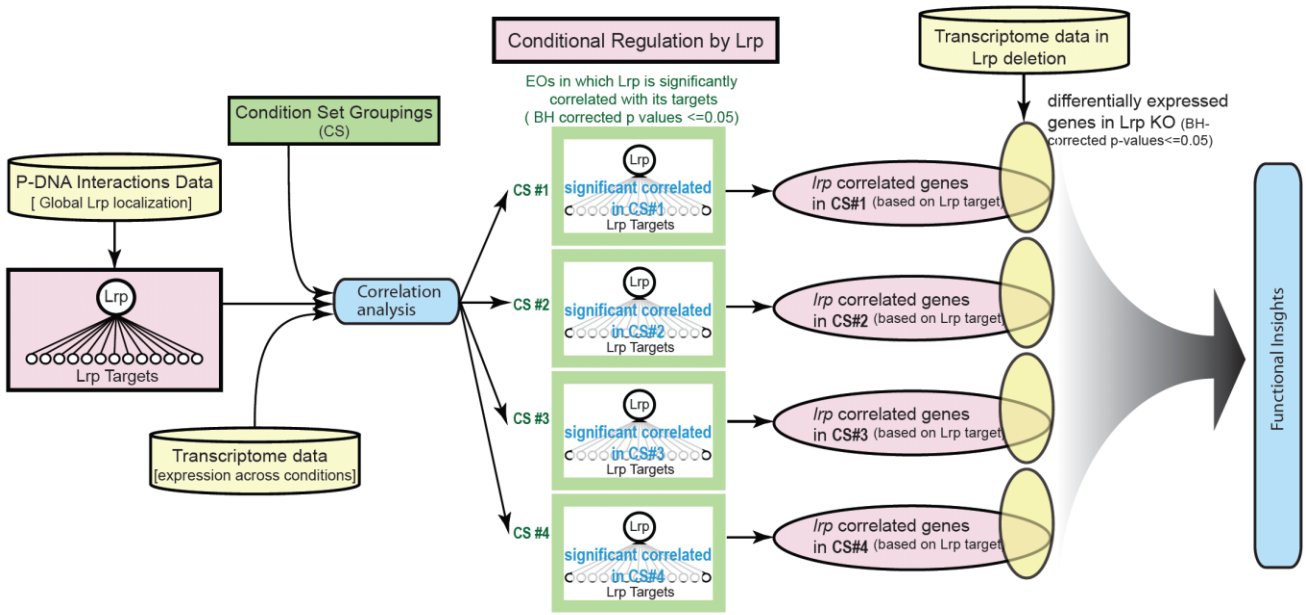

Figure 5-1 Flow chart of the correlation analysis

This figure illustrates the methods that were used for correlation analysis. Changes in the expression of experimentally verified Lrp binding targets were tested for correlation with corresponding changes in expression of the Lrp in different sets of conditions. We then used a permutation test to assess whether the correlation was statistically significant. The regulatory network for each Lrp was further expanded to include genes that were *both* correlated with expression changes of the Lrp *and* differentially expressed in the Lrp knockout strain.

Table 5-1 Condition sets over which expression levels of three Lrps were positively or negatively correlated with variance in gene expression changes in target genes within each of their protein-DNA interaction maps

Lrp	Condition Set	Fold Change	Positive Correlation				Negative Correlation			
			median correlation coefficients	BH.corrected permuted p value	correlation coefficients between variance and Lrp expression	p.value	median correlation coefficients	BH.corrected permuted p value	correlation coefficients between variance and Lrp expression	p.value
AsnC	**high paraquat constant**	1.78E+00	7.05E-01	**1.22E-02**	-6.72E-01	3.23E-04				
AsnC	**high paraquat**	1.78E+00	4.63E-01	**1.22E-02**	-3.53E-01	2.19E-02				
AsnC	**low h202 constant**	1.50E+00	5.16E-01	**3.25E-02**	-4.86E-01	1.62E-02				
AsnC	**ros constant**	1.78E+00	4.69E-01	**1.22E-02**	-5.66E-01	4.46E-06				
Trh3	**high paraquat**	1.51E+00	4.53E-01	**1.83E-02**	-3.79E-01	1.34E-02				
Trh3	**low h202 constant**	1.40E+00	8.52E-01	**2.75E-04**	-6.80E-01	2.55E-04				
Trh4	**Copper**	1.37E+00	3.91E-01				-5.73E-01	**1.06E-03**	-2.40E-01	3.78E-02
Trh4	**high copper**	1.37E+00	3.87E-01				-5.74E-01	**3.98E-03**	-4.26E-01	6.80E-04

This table shows the result of correlation analysis based on ChIP-chip targets of Lrps. The expression of *asnC* and *trh3* were found to positively correlate with the expression of their target genes under four and three condition sets respectively. The expression of *trh4* was found to negatively correlate with their target genes in the presence of copper.

5.2.2 Lrp regulons defined by integration of evidence from protein-DNA interaction maps, conditional correlation in expression, and dysregulation upon deletion of each Lrp

The correlation analyses identified specific conditions in which each Lrp putatively performs its regulatory role. This suggested that the protein-DNA interactions that were mapped in a limited number of standard growth conditions might have not identified Lrp binding locations for target genes that are typically regulated under specific conditions. To overcome this limitation, we used a two-step approach to expand the Lrp regulatory network to include additional target genes that were conditionally regulated: (i) we pruned the protein-DNA interaction network to a subset of genes that were also significantly correlated with expression changes of each Lrp (**Appendix S**); (ii) we added to this network additional genes that were both correlated with expression changes of a given Lrp and also differentially regulated upon deletion of that Lrp (**Appendix T**, **Figure 5-1**). Our rationale was that the Lrp protein-DNA interaction map and evidence for dysregulation upon deletion of the Lrp provide orthogonal streams of evidence for Lrp regulation of genes that are conditionally correlated with its expression. This two-step approach expanded the original regulatory networks based on protein-DNA interaction maps.

5.3 Summary and discussion

It is not practical to map protein-DNA interactions across a diverse array of environmental conditions, especially given that we cannot *a priori* predict the context in which a TF might function. Instead, what we have shown is that by overexpressing a TF we can map its potential binding locations across the entire genome and, subsequently, by using gene expression data from diverse environments and from TF-knockout backgrounds we can identify the context in which a subset of binding events are functional and responsible for mediating regulation of specific genes. While the analysis of gene expression data from 66 environmental conditions revealed the context for regulation by 3 of the 8 Lrps, this strategy is not designed to uncover weak protein-DNA interactions; and likely misses target genes whose transcription is regulated in a ligand dependent manner and therefore not expression-correlated with the Lrp.

Table 5-2 Number of genes from genome wide Lrp-binding location, transcriptomic analysis in Lrp deletion strains, and correlation analysis

Lrps	ChIP-chip target genes	Differentially expressed genes in Lrp knockouts	Overlap between binding targets and genes whose expression correlated with Lrp[a]	
			Positive	Negative
AsnC	356	157	232	
VNG1179C	200	13		
VNG1237C	116	251		
Trh2	40	104		
Trh3	40	53	22	
Trh4	252	76		82
Trh6	193	20		
Trh7	34	11		

[a] The total number of correlated targets in EOs where the expression of Lrp ChIP-chip targets significantly correlated with that of Lrp itself (corrected p-values <=0.05).

Chapter 6 : Coordination of metabolic pathways by specific Lrps

Conclusive evidence for transcriptional regulation comes from a combination of physical interaction of a TF with a promoter, demonstration of dysregulation of the downstream gene upon deleting the TF, and the coexpression between the regulated gene and the TF. Thus, by integrating genome-wide binding locations, correlation of gene expression, protein-DNA interactions, and the global gene expression consequences of deleting each Lrp, we have generated a comprehensive Lrp transcriptional regulatory network. In this chapter, we demonstrate how analysis of this network from the perspective of metabolism provides insights into the physiological consequences of conditional gene regulation by the expanded Lrp family.

6.1 AsnC regulates the siderophore biosynthesis pathway under high paraquat conditions

By integrating across protein-DNA interactions, gene expression correlations, and dysregulation in knockout strains we discovered that the integrated Lrp regulatory network coordinates conditional regulation of interconnected metabolic processes. For instance, many AsnC targets were significantly correlated with its expression changes in 42 experiments in which *H. salinarum* was either recovering from, or grown for up to 4 hours with, a sub-lethal dose of the superoxide-generating agent paraquat (4mM) that resulted in 20%-30% loss of survival[82]. Expression level changes in 147 of all 356 AsnC bound genes (hypergeometric enrichment *p*-value 0.02) were highly correlated with transcriptional changes of *asnC* across these time series experiments (**Figure 6-1A**). Of these, seventy one genes were significantly dysregulated in the *ΔasnC* background (out of a total of 91 genes, **Figure 6-1B, C**). Included in this set were all seven genes known to be associated with siderophore biosynthesis (GO: 0009237) (**Figure 6-1D, E**)[82] strongly suggesting that AsnC directly regulates siderophore biosynthesis under high levels of superoxide. In the subsequent section we provide one more example of how we could bootstrap across the different streams of evidence to discover conditional regulation of specific genes and pathways. Further, we will also demonstrate how

multiple Lrps act in concert to coordinate the regulation of genes across many metabolic pathways.

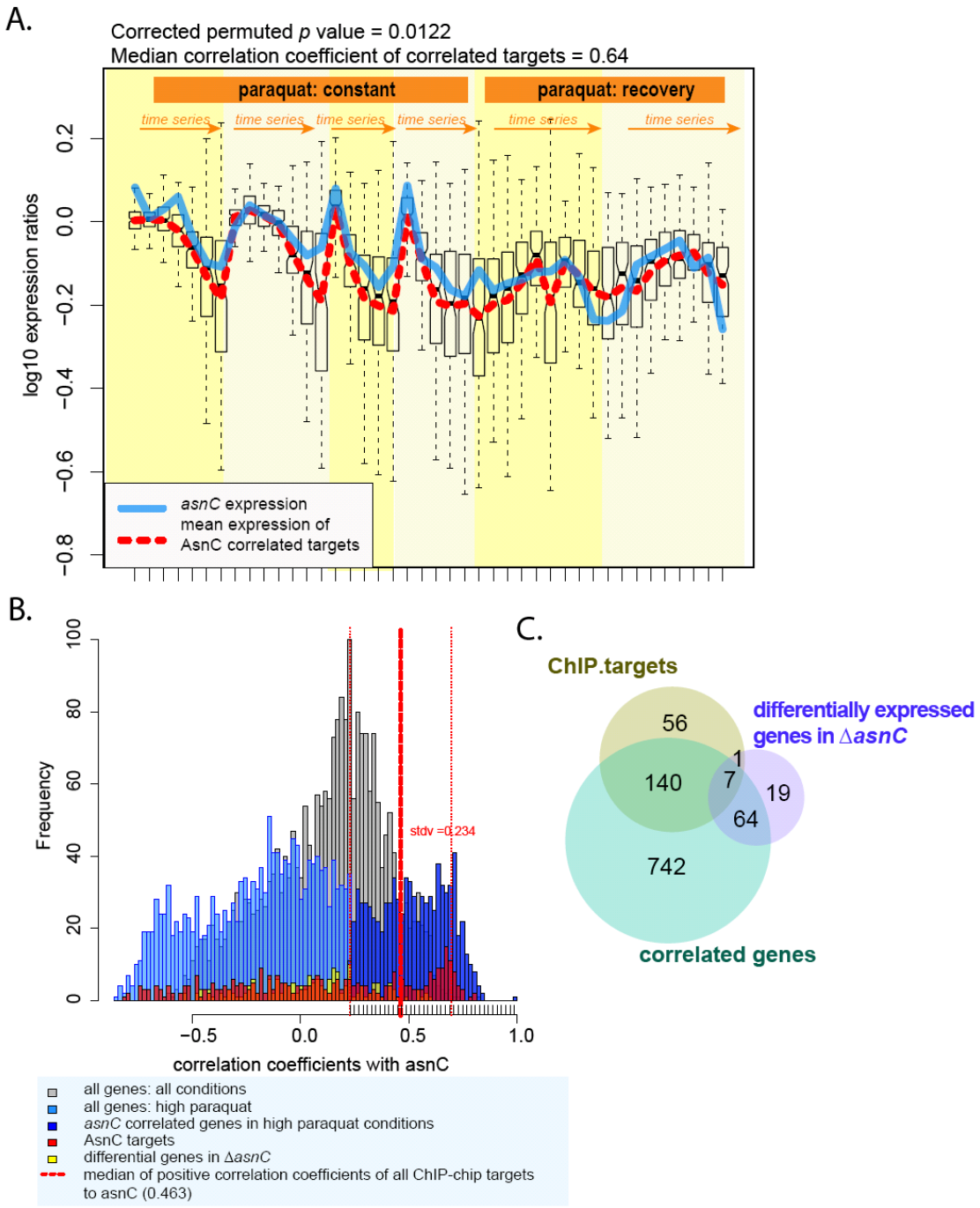

Figure 6-1 Correlation analysis of AsnC under high paraquat conditions

A. Expression profiles of *asnC* and a subset of AsnC binding targets whose expression correlated with that of *asnC* in the presence of or during recovery from a sub lethal dose of paraquat ('paraquat study'). **B.** Distribution of coefficients of correlation between the expression of *asnC* and the expression of other genes in the paraquat study. **C.** In the paraquat study, 204 out of the 356 AsnC targets were positively

correlated with transcript level changes in *asnC*, and 147 out of these 204 target genes were significantly correlated with *asnC*. Based on the distribution of the correlation coefficients of these 147 genes, a total of 953 genes were identified as highly correlated with *asnC*. Transcriptome measurements in Δ*asnC* background shows that deletion of *asnC* resulted in differential regulation of 91 genes, of which 71 were also expression correlated with *asnC* in the paraquat study.

6.2 Trh3 regulates glutamate metabolism

Carbamoyl-phosphaste synthase is one of the key enzymes in glutamate metabolism, catalyzing the synthesis of carbamoyl-phosphate from glutamine, the first committed enzymatic step of the arginine and pyrimidine biosynthesis pathways[83]. In *H. salinarum NRC-1*, carbamoyl-phosphaste synthase consists of two subunits, encoded by *carA* and *carB*. *carA* is divergently transcribed relative to *trh3*, an arrangement that is typically observed for many TF-regulated gene pairs[84] and at the very least suggests a functional association between Trh3 and CarA. Among all eight Lrps, Trh3 was the only Lrp that bound to the promoter of *carB*. Moreover, *carB* was differentially expressed in Δ*trh3* (Benjamini-Hochberg corrected *p*-value 6.76×10^{-3}; fold change 3.57), and the expression of *carB* was significantly correlated with that of *trh3* under oxidative stress conditions (i.e. paraquat and H_2O_2, **Appendix T**). In addition, we identified a putative *cis*-regulatory–binding motif for Trh3 in the promoter region of *carB* through *de novo* motif predictions based on structure modeling[a]. These disparate sources of evidence collectively support the conclusion that Trh3 directly regulates the transcription of *carB*.

6.3 Coordination of key enzymes by Lrps for amino acid metabolism

Integration across the eight regulatory networks uncovered how members of the expanded family of Lrps act in varied combinations to regulate functionaly-coupled genes across metabolic pathways. We performed in depth analysis of pathways for metabolism of two amino acids (i.e. aspartic acid and glutamatic acid) and demonstrated with phenotypic validation for coordination of glutamate metabolism with Cu trafficking by a regulatory network governed by three Lrps.

6.3.1 Aspartic acid metabolism

In addition to regulating its own transcription, AsnC in *E. coli* also regulates *asnA* (asparagine synthetase A), which is transcribed divergently relative to *asnC*, a prototypical

[a] Motif predictions conducted by Justin Ashworth.

prokaryotic genome organization for many TFs and their regulated target gene(s). AsnA catalyzes the synthesis of asparagine from aspartate and ammonia. The reconstructed Lrp regulatory network for asparagine biosynthesis pathway revealed that AsnC-mediated regulation of AsnA is also conserved in *H. salinarum NRC-1*, even though the two genes -- *asnA* (*vng0867g*) and *asnC* (*vng1776g*) -- are not genomically co-located as in *E. coli* (**Figure 6-2A**). In addition to *asnA*, AsnC in *H. salinarum NRC-1* also regulates *aspB2* (aspartate aminotransferase), which catalyzes the preceding enzymatic step. Interestingly, five additional Lrps, Trh3, Trh4, Trh6, VNG1179C and VNG1237C, regulate the *gatCAB* operon (subunits of a tRNA-dependent amidotransferase). *gatCAB* encodes a heterotrimeric aminoacyl-tRNA amidotransferase, essential for the formation of Asn-tRNA^{Asn} in *H. salinarum NRC-1*. Asparaginyl-tRNA synthetase is absent in most prokaryotes, including *H. salinarum NRC-1*. Asn-tRNA^{Asn} is therefore formed through an indirect pathway in these organisms. Using a nondiscriminate aspartyl-tRNA synthtase first forms Asp-tRNA^{Asn} and the mischarged Asp-tRNA^{Asn} is converted to Asn-tRNA^{Asn} by GatCAB a heterotrimeric aminoacyl-tRNA amidotransferase[10,85,86]. It has been proposed that this tRNA-dependant amino acid biosynthetic pathway is carried out by a nondiscriminated aspartyl-tRNA synthetase and GatCAB is an essential route for asparagine biosynthesis in *D. radiodurans* and many other bacteria that do not possess asparagine synthetase, an enzyme that catalyzes the ATP-dependent biosynthesis of asparagine from aspartate[85,87]. In fact, it has been shown that there is evolutionary interrelationship between the tRNA-independent and tRNA-dependant Asn synthesis pathways - studies in *Pyrococcus abyssi* showed that asparagine synthetase A (AsnA) evolved from ancestral Aspartyl-tRNA synthetase[88,89]. The integrated regulatory network assembled from influences of 6 Lrps including AsnC coordinates synthesis of Asn and Asn-tRNA via two alternate pathways.

6.3.2 Three Lrps coordinate regulation of glutamate metabolism and copper trafficking

Seven of the eight Lrps regulate genes of glutamate metabolism including glutamine synthase (*glnA*), carbamoyl-phosphaste synthase (*carA*, *carB*), and glucosamine-fructose-6-

phosphate aminotransferase (*glmS*) (**Figure 6-2B**). AsnC, Trh4, and Trh6 regulate all three enzymes by controlling *glnA*, *carA* and *glmS.* Interestingly, the two subunits of carbamoyl-phosphaste synthase are regulated by different sets of Lrps – whereas *carA* is directly regulated by Trh4, AsnC, Trh6 and Trh7, *carB* is directly regulated by just Trh3. Regulation of subunits of ATP synthase by AsnC, VNG1179C and VNG1237C might coordinate production of ATP cofactor for both glutamine synthase and carbamoyl-phosphaste synthase (**Appendix S**). The complex coordination of these pathways is potentially accomplished by Lrps regulating each other –e.g. *trh3* is directly controlled by four other Lrps, and *trh4* is dysregulated in Δ*vng1179C* (Benjamini-Hochberg corrected *p*- value 3.37×10^{-2}; fold change 2.81).

While our previous studies demonstrated a role for VNG1179C in regulating copper trafficking and efflux[74] our new data suggests an indirect role for this regulator in amino acid metabolism. The reconstructed regulatory and metabolic network suggests that VNG1179C is an upstream regulator of glutamate metabolism acting through Trh4, VNG1237C, Trh7 and Trh3 – each exerting control in a different environmental context (see Figure 6-2). This network also explains significant copper-dependent co-expression of *trh4* with its target-genes. The physiological explanation for the inter-coordination of copper metabolism and amino acid metabolism is not immediately obvious although there is some evidence in the literature that provides a link between decreased activity of glutamine synthetase in fungi or plants with copper exposure[90,91] or copper deficiency[92]. We performed experiments to investigate this network-predicted role of VNG1179C in regulation of glutamate/glutamine metabolism. Our hypothesis was that deletion of VNG1179C would have an indirect effect on intracellular glutamate levels based on its putative roles in the glutamine/glutamate metabolic pathway. We performed unbiased quantitative comparisons of metabolite levels across three Lrp knockout strains, Δ*vng1179C*, Δ*trh3* and Δ*trh4* and two control strains (the parent genetic background Δ*ura3* and Δ*vng0314G*, which is not predicted to affect glutamic acid metabolism). Relative difference in abundance of intracellular metabolites in each of the five strains were evaluated by metaXCMS2 analysis of mass spectrometry-based measurements[93]. Relative to the parent strain the abundance of 34 metabolites was altered in Δ*vng1179C*, Δ*trh3* and Δ*trh4*, but not in the control strain. As predicted, glutamate levels

were dysregulated in all three Lrp deletion strains (fold change of glutamate in Δ*vng1179C*, Δ*trh3* and Δ*trh4* were 1.9 (p-value 0.01), 2.2 (p-value 0.03) and 1.6 (p-value 0.01), respectively)[93]. Thus, these experiments validated the predicted effect of deleting VNG1179C on intracellular glutamate levels.

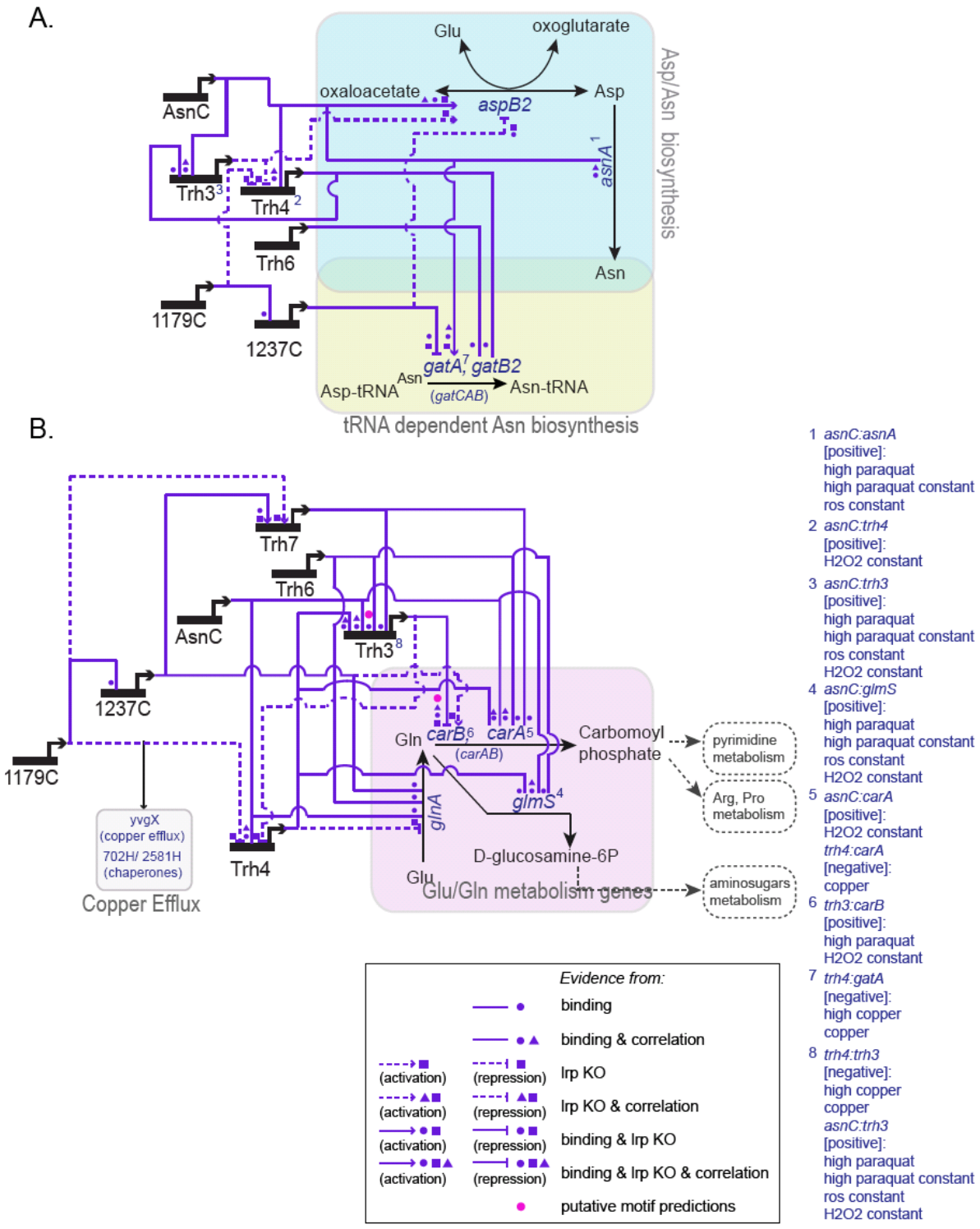

Figure 6-2 Multiple Lrp coordinately regulate two of the amino acid metabolism

Multilayer control of Lrps on metabolic pathways acts as a potential link among different cellular processes. Here the interplay of various Lrps in two amino acid metablic pathways is shown. **A.** Based on the location of binding sites and/or the expression profile in Lrp knockout strains, six of the eight Lrps

regulate the asparagine biosynthesis pathway under various environmental contexts. In addition to regulating *asnA* (asparagine synthetase) and *aspB2* (aspartate aminotransferase), responsible for two adjacent enzymetic steps in the asparagine biosynthesis pathway, AsnC also regulates two other Lrps, *trh3* and *trh4*. Moreover, AsnC regulates both direct asparagine biosynthesis and tRNA-dependent asparagine biosynthesis. **B.** AsnC, Trh6, Trh7, and Trh4 all regulate Trh3, which regulates *carB* (the large subunit of the carbamoyl-phosphate synthase). In addition to their indirect roles, AsnC also directly regulates *carA* (the small subunit of the carbamoyl-phosphate synthase) and *glmS* (glucosamine-fructose-6-phosphate aminotransferase), and Trh4 directly regulates *trh3*, *glmS*, and *glnA* (glutamine synthetase). VNG1179C is an upstream regulator of the glutamate metabolic pathway; indirectly regulating this pathway through other Lrps. ChIP- chip data showed that VNG1179C directly binds to the promoter region of *vng1237C*, which directly regulates *glnA* and indirectly (through Trh7 and Trh3) regulates *carA* and *carB*. Whole genome mRNA expression data of Δ*vng1179C* showed that Trh4 is repressed by VNG1179C. In addition, VNG1179C is also essential for the copper efflux system[74]

Chapter 7 : Conclusions

Previous work in the Baliga Laboratory demonstrated that expansions of the TBP and TFB families in *H. salinarum NRC-1* enable adaptation to changing environments[13,14]. Work presented in this dissertation demonstrates that a similar strategy has evolved at the level of transcriptional regulation through expansions in the Lrp family. The idea that archaea might utilize the eukaryotic strategy of combinatorial interplay among TFs for mediating environmental regulation had been proposed previously because archaeal genomes encode disproportionely fewer TFs, and most of these TFs are smaller and without ligand-binding domains[29].

Our study is the first to systematically investigate consequences of expansions in the Lrp family in archaea. Analyses of protein-DNA interactions of 8 Lrps over two phases of batch culture growth of *H. salinarum NRC-1*, as well as their conditional expression correlations with target genes, showed that the active regulatory network of each Lrp changes dramatically with environmental context. The Lrp regulatory network included nearly one-third of all genes in the genome with five Lrps regulating >100 target genes each based solely on the Lrp binding sites. The overall impact of transcriptional regulation by the Lrp family is further broadened through their regulation of ~20% of all TFs encoded in the genome. The integrated Lrp TRN revealed that Lrps play a central role in regulating nearly all aspects of physiology. Further, binding of multiple Lrps to the same locations suggests a redundant, competitive, and collaborative system of interactions that is consistent with a heteromultimeric scheme of action that has been observed for Lrps in other organisms[35,36]. The systems view of the Lrp TRN has provided insights into how expansions in this family provides *H. salinarum NRC-1* with strategies for adaptation to complex environmental changes by generating robustness through redundancy and introducing capability for complex environment-dependent coordination of disparate physiological processes.

By integrating and statistically analyzing the ChIP-chip data and transcriptome data from a compendium of ~1000 transcriptomes, we identified conditional regulation for 3 of the 8 Lrps. Consistent with previous studies on Lrps in other organisms[27,30,77], these analyses also

demonstrated that some Lrps are transcriptional activators (e.g. AsnC and Trh3), whereas others are repressors (e.g. Trh4) (**Table 5-1**).

It is striking that the same sets of metabolic pathways are regulated by different combinations of Lrps in the two phases of growth. Our data suggest that the system of interactions among Lrps encodes context-dependent regulatory interrelationships among the various physiological processes. This is consistent with the results of our correlation analysis (**4.3**), and the reconstruction of two amino acid metabolic pathways (**Figure 6-2**). We validated one such previously undocumented regulatory coordination of copper trafficking and glutamate transport by VNG1179C. In prior work, we demonstrated that deletion of VNG1179C results in failure to transcriptionally upregulate a copper effluxing P1-type ATPase that results in hypersensitivity to small increases in copper. The new data revealed that VNG1179C also acts indirectly on glutamate metabolism through regulation of Trh4 – an influence that was validated experimentally upon observing differential regulation of Trh4 and increased glutamate levels upon knocking out VNG1179C. The increased glutamate levels in the copper efflux defective background of Δ*vng1179C* are consistent with the known ability of glutamate to scavenge toxic copper(II) ions into non-toxic complexes[94]. In other words, the upregulation of glutamate levels through indirect regulation by VNG1179C might act to minimize copper toxicity.

The mechanistic insights into how Lrps function will have important implications into how TRNs are modeled. For instance, the hetermomultimeric and conditional nature of interactions among Lrps underscores the importance of incorporating interaction terms and dynamics in the modeling of TRNs. The multiple layers of complexity generated through combinatorial control of the expanded basal (TBPs and TFBs) as well as regulatory (Lrps) TFs could only be explored and characterized by a systems approach, as we have done in this study. Admittedly, it is logistically infeasible to generate all of the global molecular measurements that are needed for such a systems analysis. However, we have shown that it is possible to overcome such logistical challenges through data integration. For instance, by overexpressing each Lrp and by making measuremments over two of the most distinct physiological states (exponential growth vs. stationary phase) we ensured that we would detect all of possible Lrp binding locations in the genome. Further, by integrating all of these possible protein-DNA interactions with gene expression data measured over a wide array of environmental conditions we were able to identify

the contexts in which each of these interactions were functional. We also teased apart direct and indirect regulation and expanded the Lrp TRN by investigating global transcriptional changes in each of the eight Lrp deletion strains. Finally, we interpreted the physiological implications of conditional and combinatorial regulation by the expanded family of Lrps by analyzing the TRN in the context of metabolism. None of the individual datasets could by themselves have revealed these complex regulatory schemes. The data integration was necessary and able to overcome issues with data incompleteness and noise by joining evidence across multiple datasets to find statistically significant patterns of gene regulation by the expanded family of Lrps.

Chapter 8 : Materials and Methods

8.1 Strain construction and culturing conditions

All Lrp knockout strains were derived from *H. salinarum NRC-1* Δ*ura3* strain via a two step gene replacement strategy[74]. cMmyc tagged strains for ChIP-Chip were constructed as previously described[13]. Details of oligonucleotides used for strain construction are listed in **Table 8-2**. All *H. salinarum NRC-1* strains were cultured in standard growth conditions in complete medium[95] (CM, 250g NaCl, 20 g/L $MgSO_4$-7H2O, 3 g/L sodium citrate, 2 g/l KCl, 10 g/L peptone) or complete defined medium (**Table 8-1**) with 20 amino acids. All knockout strains and the control parental strains *(*Δ*ura3*) of knockouts were grown in CM or CDM added with 0.05 mg/ml uracil to compensate for their uracil deficiency.

Table 8-1 Complete defined medium (CDM) recipe

Halobacterium defined medium		
(adapted from Shand and Perez, 1999. pp. 414-424 in Seckbach (ed) Enigmatic Organisms…., Kluwer.)		
Salts (per L)		
	mass (g)	mM
NaCl	250.00	4.02M
MgSO4.7H2O	20.00	40.00
MOPS	8.37	40.00
KCl	2.00	27.00
NaH2PO4	0.02	0.167*
*0.167mM PO4 is sufficient, up to 2mM is ok, but more than 2mM results		
in rapid decrease in OD over time.		
Vitamins (per L)		
	mass (mg)	
Folic Acid	5.00	11.33uM
Thiamine HCl	5.00	14.82uM
Biotin	0.50	2.05uM
Amino Acids (per L)	per 1L	
Total amino acids : 9g/L		
	mg	mM

L-ala	628.04	7.05
L-arg-HCl	672.06	3.19
L-asn	429.95	3.25
L-asp	429.95	3.23
L-glu	759.37	5.16
L-gln	759.37	5.20
L-gly	1137.22	15.15
L-his-HCl	68.04	0.32
L-ile	149.67	1.14
L-leu	535.60	4.08
L-lys-HCl	592.82	3.25
L-met	186.35	1.25
L-phe	393.26	2.38
L-pro	917.12	7.97
L-ser	258.26	2.46
L-thre	215.70	1.81
L-trp	130.59	0.64
L-tyr	48.42	0.27
L-val	564.95	4.82
L-cys	123.26	1.02
carbon source		
glycerol	1mL/L	0.5ml
	(13.68mM)	
Trace metals (Add right before the experiment, not in stock)		
Mn		1.1μM
Fe		13.24μM
(0.0109g $MnCl_2$ & 0.179g $FeCl_2$ in 50ml d_2H_2O -> 1000X stock soln.)		
pH		6.80

Table 8-2 Oligonucleotides used to construct Lrp deletion strains

Name	Sequence (5'-> 3')
VNG1377G.a	CGGTCGCGGCGTGTAATCGGT
VNG1377G.b	GTCCGTGTCGTCTACATCCAT
VNG1377G.c	GATGTAGACGACACGGACTGAACGCACGCCCGGCGGCAA
VNG1377G.d	GCGACCTCGACTTCGAGGACA
VNG1377G.e	GACGTCGAAACGAAATCCGGG
VNG1377G.f	GCGATCCAGGAGGTCGTCACG
VNG1377G.g	TCGCCCGCGAGATAGACATGT
VNG1377G.h	TCAGCGATCTCCTCGAACATG

VNG1179C.a	CCTTCGAGACCTTCGGCGCGA
VNG1179C.b	ACAGGCCAACAGCACAGCCAT
VNG1179C.c	GCTGTGCTGTTGGCCTGTTGATGCAGCGCCACCGCTTCG
VNG1179C.d	GCGTGGACGCCATCGTGCAGG
VNG1179C.e	CGCAGCCACCAGGATCATCGC
VNG1179C.f	GGACGCAGTGCTGTATTTGG
VNG1179C.g	TCTCCGACCGGATCACGAAG
VNG1179C.h	CTCGAAATCGACGGTGTCTG
VNG1237C.a	GTCGAGGTGCCCGCCGTGCAG
VNG1237C.b	GTCGAGCCCGTCGAGTGTCAT
VNG1237C.c	ACACTCGACGGGCTCGACTAATATACCTCCTCTTTGGG
VNG1237C.d	GTGATGATGTCGGCGTCGAG
VNG1237C.e	CGTGTTGGCGTGCTCGGTGCT
VNG1237C.f	GGTCGCCATCTCGGATTTCGA
VNG1237C.g	GACGAAGCCGACGTATCGGCG
VNG1237C.h	CCAACTCGTCGAGATCGCGGC
VNG1285G.a	GTACGCCGCCATCATGAGTGA
VNG1285G.b	CTCGTCCAGTCGGTCGCTCAT
VNG1285G.c	AGCGACCGACTGGACGAGTAGTAGTACGCAATTCAGGTG
VNG1285G.d	CCGTGCCGGTGAACCCGCTCA
VNG1285G.e	AATCGGATGCCATGAGCTTCG
VNG1285G.f	AGGAGCAGGATCGAGAAGAAC
VNG1285G.g	CCGTGCCCGACCGGGATCGGC
VNG1285G.h	GACAGCTCCACGACCTCAGCA
VNG1816G.a	GGGCGCGGGCGGTGGCGGGGC
VNG1816G.b	CTGCTGGTCGATGTCGTCCAT
VNG1816G.c	GACGACATCGACCAGCAGTGAGTCGAAGCGCTATTAGGC
VNG1816G.d	AAGCTGGTGTCGTGCAGCGTC
VNG1816G.e	GGGTCGCCGGGGCCGTTGGAG
VNG1816G.f	CTGAGTCATAGCCCTCCCTCG
VNG1816G.g	CCTACACGGAGATCGCCGACG
VNG1816G.h	TCGCGGGCTCGCCGCATCAGA
VNG2094G.a	CACGTTCTTCAGGACCTGCCG

VNG2094G.b	GTCGAGGTTCTCGTAGGTCAT
VNG2094G.c	ACCTACGAGAACCTCGACTAACCACCCCTCCGGGAACGC
VNG2094G.d	CAGCTCGCCGTCGAGGCGTTC
VNG2094G.e	TGAAGTTGATCTCGTGTTGGC
VNG2094G.f	GGTCACGCGCGACAGCGACGA
VNG2094G.g	CGACCTCGACGTGTCGGTCAC
VNG2094G.h	GTCGGCGTCCGCCAGCAGCTC
VNG1123G.a	GACCGTGCTGACCGGCCGGTA
VNG1123G.b	GGCCACGTCGATCCCGACCAT
VNG1123G.c	GTCGGGATCGACGTGGCCTGAGCGTCGTGGCGCTGGCGA
VNG1123G.d	GTACACCGACGACGCGTTCGT
VNG1351G.a	TCGCGAACCCTGCGGTCAGGA
VNG1351G.b	CGTGATGTCTCGGTCGTCCAT
VNG1351G.c	GACGACCGAGACATCACGTAACGCGCCGCTAGGACCGCT
VNG1351G.d	CTTCGATCTGGACGCCGGACT
VNG1351G.e	AGGGCCAGCGACCCGATGAGC
VNG1351G.f	TCGTGGCCGACGACCCCGAGA
VNG1351G.g	TATCCACCATCCACTATCGGC
VNG1351G.h	TTCGTTCTGTCCACGGGGTCG

8.2 Phylogenetic analysis and tree reconstruction

Phylogenetic analysis was done within 676 archaeal Lrps in 125 sequenced archaeal genomes (**Appendix W**). Multiple sequence alignment was done with the MUSCLE multiple sequence alignment method using the Geneious Software Package[96]. The resulting alignment sequences were further processed to include only the PF01037 domain[69] using MUSCLE and JALVIEW[72]. The neighbored joining method in Geneious Software Package was used for constructing the phylogenetic tree. We further used iTOL [97] for visualization and coloring the tree.

8.3 Genome wide Lrp binding site analysis (ChIP-chip)

8.3.1 Predictions of DNA-binding locations and target genes of Lrps

ChIP-Chip experiments were carried out for all 8 Lrps in *H. salinarum NRC-1* as previously described[98]. To study the Lrp localization in both nutrient repleted and depleted conditions, c-Myc-tagged Lrp strains were grown in 250mL of CDM, and about 45mL of each culture was harvested in both early log phase (OD ~0.2) and late log phase (OD ~0.5). 1.4mL of formaldehyde (37% w/w) was added to each of the above 45ml harvested culture for cross-linking of TF-DNA complexes. Cross-linking was performed at room temperature for 15 minutes then 4°C for 4 hours, and terminated by adding 5mLs of 1.2M glycine. Cells were collected by centrifuged, washed (by basal salt solution, CDM without amino acids), and sonicated. Sonicated lysates were checked for appropriate DNA fragment sizes on a 1.5% agarose gel (range between 300 – 700bp with an average of 400bp). Lysates were subjected to another round of sonication if the sizes of DNA fragments were too large. ChIP of c-Myc-tagged protein complexes were conducted as described[13,42,98]. The DNA fragments cross-linked to the Lrp were enriched by immunoprecipitation (IP) with the anti-c-Myc antibodies (9E10 Monoclonal Antibody, Covance) bound to magnetic beads (Dynabeads M-450 pre-coated with pan anti-mouse IgG, Carlsbad, CA) overnight at 4°C; then an aliquot was checked for the integrity of the immunoprecipitated-TF by western blotting. Samples were washed and eluted from magnetic beads, and the reversal of crosslinking between TF and DNA was conducted overnight at 65°C. Proteinase K digestion was performed for 2 hours at 37°C, followed by DNA extraction by phenol-chloroform extraction (phenol:chloroform:alcohol, Sigma P2069). RNAse digestion was then performed for an hour at 37°C. DNA purification was done by phenol-chloroform extraction and precipitated by ethanol at -80°C for at least 30 minutes. PCR-amplified DNA from both ChIP complexes and non-IP DNA were each labeled by Dyomics-547 and -647 (Kreatech, Leiden, The Netherlands) and hybridized to the whole genome tiling array (HaloSpan array, as previously described[13]). This array includes ORFs and intergenic regions tiled at 500bp resolution, each tile spotted four times on the array. Dye-swapping was conducted to reduce dye bias, yielding total of 8 technical replicates in each 500np tile on the array. Two independent biological replicates were conducted for each c-Myc-tagged Lrp strain at each time point, yielding 16 data points for each 500bp

region on the genome. Hybridization, washing, scanning, and spot-finding on microarrays were conducted as previously described[99].

Resulting localization data was median normalized and further analyzed for statistically significant enrichment of features in the IP sample using MeDiChI, a regression-model that learns a generative model of joint binding events[75]. We used MeDiChI to learn a joint model of binding events in the ChIP-chip data and accurately locate the genome wide binding locations of each Lrp. We only considered enrichment peaks with MeDiChI *p*-value <= 0.01 (based on peaks detected in bootstrap-resampled data that statistically seem to contain only noise). If a MeDiChI binding peak was within upstream 250nt to downstream 50nt of the start codon of a gene, this gene was considered a target of the Lrp. The above window was determined by the average length of intergenic region in *H. salinarum NRC-1* and the resolution of the MeDiChI algorithm (~50nt)[75]. The average length of intergenic region in *H. salinarum NRC-1* is ~200nt. The R code used to perform this calculation exists at: https://github.com/fangylo/Lrp_analysis/blob/master/get.all.intergenic.fragment.length. Genes within operons that are downstream to the binding site were also considered to be under the control of that Lrp.

8.3.2 Calculation of relationships of DNA-binding specificities among Lrps

For calculations of the relationships between DNA-binding specificity among Lrps, the distribution of the genome wide binding locations of Lrps were analyzed to calculate statistical significance (hypergeometric distribution) of shared-binding targets for each Lrp pair. The matrices of hypergeometric *p*-values for shared-binding across all Lrp pairs were then hierarchically clustered using Euclidean distance and complete linkage method.

8.4 Microarray analysis of Lrp knockouts

The Δ*ura3* parental strain and all 8 Lrp knockout strains (Δ*asnC*, Δ*1179C,* Δ*1237C*, Δ*trh2*, Δ*trh3,* Δ*trh4,* Δ*trh6, and* Δ*trh7*) were grown in CDM. Cultures were sampled four times along the growth curve to capture the dynamics (lag phase, early log phase, mid log phase, and stationary phase). At each time point, samples were removed from the culture, immediately

pelleted at 8000 r.p.m for 4 minutes and snap-frozen in liquid nitrogen. Pellets were stored at -80°C overnight and RNA was prepared using an Absolutely RNA kit (Stratagene) according to manufacturer instructions. RNA quality was checked using Bioanalyzer 2100 (Agilent Technologies, CA). PCR amplification of 200ng of the resultant RNA sample was performed to confirm absence of DNA contamination. 5µg of RNA was labeled with dyes and hybridized against the *H. salinarum NRC-1* reference RNA, which has been used across all *H. salinarum NRC-1* microarray data as previously described[12,100]. Samples were hybridized to a 70-mer oligonucleotide array which contains the 2400 non-redundant open reading frames (ORF) of *H. salinarum NRC-1*. Each ORF was spotted on the array in quadruplicate. Dye-flip was conducted to reduce dye incorporation bias, yielding 8 measurements per gene. Microarray fabrication, RNA preparation, dye labeling (Alexa 594 and 660, Invitrogen,CA), slide hybridization and washing were conducted as previously described[11]. At least two independent biological replicates were examined for each strain at each time point. Raw intensity signals from each array was processed by the SBEAMS-microarray pipeline[101], where data were median normalized. The resultant data were $\log_{10}$ based expression ratios. Paired t-tests were used to test the statistical significance of the differences in gene expression between each Lrp knockout strain and the parent strain Δ*ura3* (Benjamini-Hochberg multiple hypothesis test corrected p-value ≤ 0.05).

8.5 Correlation analysis for the conditional regulations by Lrp

66 condition sets[a] related to environmental perturbations were selected for the analysis (**Table 8-3, Appendix Q**) for details in condition sets and the number of experiments associated with each term). These condition sets were further separately filtered for each Lrp, to include only terms that each Lrp had at least twofold change in mRNA expression among the experiments associated. This resulted in 61, 60, 56, 56, 55, 53, 61, and 57 condition sets for *asnC, vng1179C, vng1237C, trh2, trh3, trh4, trh6*, and trh7 (**Appendix V**). Correlation between the expression of each Lrp and its direct ChIP-chip targets were calculated within the experiments associated with the filtered condition sets. Positive and negative correlations were calculated separately. Median correlation coefficients between Lrp and its ChIP-chip targets under each EO were compared with that of randomly sampled genes. The number of genes

sampled is equal to the number of ChIP-chip target genes. Permutations were performed for 100,000 times, and significance of the correlation between Lrp and its target genes under each EO was calculated based on the resulting permuted p-values (Benjamini-Hochberg multiple hypothesis correction, α =0.05). For each EO in which Lrp significantly correlated with its direct ChIP-chip targets, genes correlated with Lrp were selected based on the distribution of correlation coefficients of Lrp ChIP-chip targets. In cases of positive correlation, genes that had correlation coefficients(r) which satisfy the following were defined as correlated with Lrp under that condition set:

$r_{Lrp,geneX} \geq median\left(r_{Lrp,Lrp\ ChIPchip\ targets}\right) - stdv(r_{Lrp,Lrp\ ChIPchip\ targets})$

In cases of negative correlation, genes correlated with Lrp under one particular condition set satisfy: $r_{Lrp,geneX} \leq median\left(r_{Lrp,Lrp\ ChIPchip\ targets}\right) + stdv(r_{Lrp,Lrp\ ChIPchip\ targets})$

---

[a] The groupings of condition sets were adapted from the Environmental Ontology by Aaron N. Brooks.

Table 8-3 Description and summary of 117 condition sets

Name of Condition Sets	Number of Arrays	Description
circadian	475	light:dark changes on a 12:12 hour cyclic schedule
cobalt	8	2e-3<=mol/L=<5.0e-3.
copper	75	1e-4<=mol/L=<1.0e-3.
dark	258	= 0umol/m2/s.
early-exponential phase	149	0.2 >= OD < 0.4.
edta	8	1e-3 mol/L.
ems	8	0.1 mol/L.
expects dark	127	= 50umol/m2/s.
expects high light	71	> 100 mol/m2/s.
expects low light	11	0 < mol/m2/s < 100.
exponential phase	442	0.2 > OD < 0.8.
gamma	37	2500 gy.
glucose perturbation	8	7% w/v.
h202 recovery	26	cells received perturbation then washed off. Samples were collected when cells were in revocovery
h202	50	2.5e-2<=mol/L=<5.0e-2.
high atp level	4	atp (mol/L) > 1.5.
high copper	60	mol/L>0.8e-3.
high h202 recovery	8	5e-2 mol/L.
high iron	14	>=4e-3 mol/L.
high light	72	> 100 mol/m2/s.
high manganese	5	1.5e-3 mol/L.
high oxygen	34	>75 pct
high oxygen shift	10	high oxygen (chemostat) 90.3%-94.7%
high paraquat constant	24	constant perturbation
high paraquat recovery	18	cells received perturbation then washed off. Samples were collected when cells were in revocovery
high paraquat	42	4e-3 mol/L.
high temperature	238	> 40 C
high zinc	5	> 2 mol/L.
high2low	4	oxygen shift from high to low(86%->4.8%)
iron	16	1e-5<=mol/L=<7.0e-3.
irradiation	41	including gamma(2500 gy) and uv (200 J/m2)

lag phase	21	OD < 0.2.
low atp level	8	atp (mol/L) < 1.0.
low copper	16	mol/L<1e-4.
h202 constant	24	2.5e-2 mol/L.
low h202 recovery	18	2.5e-2 mol/L.
low h202	42	2.5e-2 mol/L.
low iron	11	<4e-3 mol/L.
low light	145	0 < mol/m2/s < 100.
low manganese	5	8.0e-4 mol/L.
low oxygen	28	< 25 pct.
low oxygen shift	9	low oxygen(chemostat) 1.1%-4.1%
low paraquat constant	8	2.5e-4 mol/L.
low salt	20	200 g/L NaCl.
low temperature	18	<= 30C.
low zinc	10	<=.1e-5 mol/L zinc.
low2high	7	oxygen shift from low to high(0.5%->84.7%)
manganese	15	8e-4 mol/L
medium atp level	6	1.0 > atp (mol/L) < 1.5.
medium copper	11	1e-4>mol/L<0.8e-3.
medium manganese	5	1.0e-3 mol/L.
medium zinc	29	1.5e-5<mol/L<-2e-5.
medium-high oxygen	36	50 < pct < 75.
medium-low oxygen	10	25 < pct < 50.
metal chelation	12	dip (2.5e-5<=mol/L<=2.5e-4)or edta(1e-3 mol/L)
mid-exponential phase	293	0.4 >= OD < 0.6.
nickel	8	5e-4<=mol/L<=1.5e-3.
oxygen shift	28	high oxygen shift, low oxygen shift, high oxygen shift to low oxygen, or low oxygen shift to high oxygen
paraquat constant	32	constant perturbation
paraquat	50	2.5e-5<=mol/L<=4e-3.
ros constant	57	constant perturbation
ros recovery	44	cells received perturbation then washed off. Samples were collected when cells were in revocovery
ros	101	h2o2 and paraquat
saturation phase	276	optical density > 0.8.
uv	5	200 J/m2.
zinc	44	5e-6<=mol/L<=5e-5.

8.6 Functional enrichment analysis

We used the bioconductor package topGO[102] to analyze GO terms enriched in our gene sets of interest.

8.7 DNA-binding motif searching through iterative refining structural homology-based prediction of Lrp-like DNA binding[a]

The amino acid sequences of all Lrp-like DNA binding domains were collected using BLAST[103,104] and aligned using MUSCLE[96] and Jalview[72]. The amino acids from each Lrp sequence were threaded onto the protein backbone from the crystal structure of FL11[66] and side-chain energy minimized using the macromolecular modeling software Rosetta[105]. Random bound DNA sequences were simulated in the presence of flexible amino acid side-chains and hydrated nucleotide base atoms[106,107]. The DNA sequence preferences for each Lrp were derived as a position specific weight matrix (PWM) calculated from an ensemble of the 100 lowest-energy DNA sequences resulting from structural simulations. These PWMs were compared to the experimentally derived (SELEX) motifs for Lrp orthologs in other archaeal species[108].

The predicted PWMs for each Lrp were adapted to more closely reflect possible transcription factor binding sites in the upstream regions of its putatively regulated target genes (as identified by genome–wide Lrp binding locations, differentially expressed genes in Lrp deletion strains, and genes whose expression highly correlated with each Lrp). Each predicted PWM was mixed with a new PWM resulting from an alignment of matches to the starting PWM within the regions (-300 to +100 basepairs) around the transcriptional start site for each target gene. The MAST tool from the MEME suite[109] was used to identify, score and filter PWM matches. This was iterated for each resulting PWM until convergence, or the failure to identify a PWM that was consistent with the other existing evidence of regulation.

[a] This section was conducted by Justin Ashworth.

8.8 Metabolomic analysis

Three Lrp knockout strains - Δ*trh3*, Δ*trh4* and Δ*vng1179C*, one enzymatic knockout strain Δ*vng0314G*, and the parent strain Δ*ura3*, were cultured in CDM (**Table 8-1**). Culture aliquots were harvested at mid log growth phase by centrifugation, and samples were pelleted and lyophilized. Δ*vng0314G* strain was served as a non-Lrp knockout negative control as *vng0314G* encodes an enzyme in the shikimate biosynthesis pathway, and it does not have functional role in the glutamine/glutamate metabolic pathway. The samples were subjected to mass spectrometry based unbiased metabolomics analysis. metaXCMS was used to identify shared dysregulated features, and dysregulated metabolites were further identified by mapping databases based on accurate mass and the comparison of retention time and tadem mass spectrometry as previously described[93]. .

Bibliography

[1] Geiduschek, E. P. & Ouhammouch, M. Archaeal transcription and its regulators. *Mol Microbiol* **56**, 1397-1407(2005).

[2] Bell, S. D., Magill, C. P. & Jackson, S. P. Basal and regulated transcription in Archaea. *Biochem Soc Trans* **29**, 392-395 (2001).

[3] Zillig, W., Stetter, K. O. & Janekovic, D. DNA-dependent RNA polymerase from the archaebacterium Sulfolobus acidocaldarius. *Eur J Biochem* **96**, 597-604 (1979).

[4] Kyrpides, N. C. & Ouzounis, C. A. Transcription in archaea. *Proc Natl Acad Sci U S A* **96**, 8545-8550 (1999).

[5] Langer, D., Hain, J., Thuriaux, P. & Zillig, W. Transcription in archaea: similarity to that in eucarya. *Proc Natl Acad Sci U S A* **92**, 5768-5772 (1995).

[6] Hethke, C., Geerling, A. C., Hausner, W., de Vos, W. M. & Thomm, M. A cell-free transcription system for the hyperthermophilic archaeon Pyrococcus furiosus. *Nucleic Acids Res* **24**, 2369-2376 (1996).

[7] Qureshi, S. A., Bell, S. D. & Jackson, S. P. Factor requirements for transcription in the Archaeon Sulfolobus shibatae. *Embo J* **16**, 2927-2936. (1997).

[8] Bell, S. D., Jaxel, C., Nadal, M., Kosa, P. F. & Jackson, S. P. Temperature, template topology, and factor requirements of archaeal transcription. *Proc Natl Acad Sci U S A* **95**, 15218-15222. (1998).

[9] Brinkman, A. B. *et al.* An Lrp-like transcriptional regulator from the archaeon Pyrococcus furiosus is negatively autoregulated. *J Biol Chem* **275**, 38160-38169 (2000).

[10] Ng, W. V. *et al.* Genome sequence of Halobacterium species NRC-1. *Proc Natl Acad Sci U S A* **97**, 12176-12181 (2000).

[11] Baliga, N. S. *et al.* Coordinate regulation of energy transduction modules in Halobacterium sp. analyzed by a global systems approach. *Proc Natl Acad Sci U S A* **99**, 14913-14918. (2002).

[12] Bonneau, R. *et al.* A predictive model for transcriptional control of physiology in a free living cell. *Cell* **131**, 1354-1365, doi:10.1016/j.cell.2007.10.053 (2007).

[13] Facciotti, M. T. *et al.* General transcription factor specified global gene regulation in archaea. *Proc Natl Acad Sci U S A* **104**, 4630-4635 (2007).

[14] Turkarslan, S. *et al.* Niche adaptation by expansion and reprogramming of general transcription factors. *Molecular Systems Biology* **7**, 554, doi:10.1038/msb.2011.87 (2011).

[15] Pikaard, C. S., Haag, J. R., Ream, T. & Wierzbicki, A. T. Roles of RNA polymerase IV in gene silencing. *Trends Plant Sci* **13**, 390-397 (2008).

[16] Herr, A. J., Jensen, M. B., Dalmay, T. & Baulcombe, D. C. RNA polymerase IV directs silencing of endogenous DNA. *Science* **308**, 118-120 (2005).

[17] Werner, F. Structure and function of archaeal RNA polymerases. *Mol Microbiol* **65**, 1395-1404, (2007).

[18] Ouhammouch, M. Transcriptional regulation in Archaea. *Curr Opin Genet Dev* **14**, 133-138, (2004).

[19] Aravind, L. & Koonin, E. V. DNA-binding proteins and evolution of transcription regulation in the archaea. *Nucleic Acids Res* **27**, 4658-4670 (1999).

[20] Bell, S. D., Cairns, S. S., Robson, R. L. & Jackson, S. P. Transcriptional regulation of an archaeal operon in vivo and in vitro. *Mol Cell* **4**, 971-982 (1999).

[21] Vierke, G., Engelmann, A., Hebbeln, C. & Thomm, M. A novel archaeal transcriptional regulator of heat shock response. *J Biol Chem* **278**, 18-26 (2003).

[22] Dahlke, I. & Thomm, M. A Pyrococcus homolog of the leucine-responsive regulatory protein, LrpA, inhibits transcription by abrogating RNA polymerase recruitment. *Nucleic Acids Res* **30**, 701-710 (2002).

[23] Bell, S. D. & Jackson, S. P. Mechanism of autoregulation by an archaeal transcriptional repressor. *J Biol Chem* **275**, 31624-31629. (2000).

[24] Bell, S. D. & Jackson, S. P. Mechanism and regulation of transcription in archaea. *Curr Opin Microbiol* **4**, 208-213. (2001).

[25] Brinkman, A. B., Bell, S. D., Lebbink, R. J., de Vos, W. M. & van der Oost, J. The Sulfolobus solfataricus Lrp-like protein LysM regulates lysine biosynthesis in response to lysine availability. *J Biol Chem* **277**, 29537-29549 (2002).

[26] Ouhammouch, M. & Geiduschek, E. P. An expanding family of archaeal transcriptional activators. *Proc Natl Acad Sci U S A* **102**, 15423-15428 (2005).

[27] Ouhammouch, M., Dewhurst, R. E., Hausner, W., Thomm, M. & Geiduschek, E. P. Activation of archaeal transcription by recruitment of the TATA-binding protein. *Proc Natl Acad Sci U S A* **100**, 5097-5102 (2003).

[28] Perez-Rueda, E., Collado-Vides, J. & Segovia, L. Phylogenetic distribution of DNA-binding transcription factors in bacteria and archaea. *Comput Biol Chem* **28**, 341-350 (2004).

[29] Perez-Rueda, E. & Janga, S. C. Identification and genomic analysis of transcription factors in archaeal genomes exemplifies their functional architecture and evolutionary origin. *Mol Biol Evol* **27**, 1449-1459

[30] Peeters, E. & Charlier, D. The Lrp family of transcription regulators in archaea. *Archaea* **2010**, 750457

[31] Perez-Rueda, E. & Collado-Vides, J. Common history at the origin of the position-function correlation in transcriptional regulators in archaea and bacteria. *J Mol Evol* **53**, 172-179 (2001).

[32] Perez-Rueda, E. & Collado-Vides, J. The repertoire of DNA-binding transcriptional regulators in Escherichia coli K-12. *Nucleic Acids Res* **28**, 1838-1847 (2000).

[33] Tenorio-Salgado, S., Huerta-Saquero, A. & Perez-Rueda, E. New insights on gene regulation in archaea. *Comput Biol Chem* **35**, 341-346.

[34] Baliga, N. S. *et al.* Is gene expression in Halobacterium NRC-1 regulated by multiple TBP and TFB transcription factors? *Mol Microbiol* **36**, 1184-1185 (2000).

[35] Koike, H., Ishijima, S. A., Clowney, L. & Suzuki, M. The archaeal feast/famine regulatory protein: potential roles of its assembly forms for regulating transcription. *Proc Natl Acad Sci U S A* **101**, 2840-2845 (2004).

[36] Okamura, H. *et al.* A structural code for discriminating between transcription signals revealed by the feast/famine regulatory protein DM1 in complex with ligands. *Structure* **15**, 1325-1338, (2007).

[37] Nowick, K. & Stubbs, L. Lineage-specific transcription factors and the evolution of gene regulatory networks. *Brief Funct Genomics* **9**, 65-78 (2010).

[38] van Nimwegen, E. Scaling laws in the functional content of genomes. *Trends in Genetics* **19**, 479-484 (2003).

[39] Teichmann, S. A. & Babu, M. M. Gene regulatory network growth by duplication. *Nat Genet* **36**, 492-496 (2004).

[40] Tagkopoulos, I., Liu, Y.-C. & Tavazoie, S. Predictive behavior within microbial genetic networks. *Science* **320**, 1313-1317 (2008).

[41] Babu, M. M., Luscombe, N. M., Aravind, L., Gerstein, M. & Teichmann, S. A. Structure and evolution of transcriptional regulatory networks. *Current opinion in structural biology* **14**, 283-291 (2004).

[42] Schmid, A. K., Reiss, D. J., Pan, M., Koide, T. & Baliga, N. S. A single transcription factor regulates evolutionarily diverse but functionally linked metabolic pathways in response to nutrient availability. *Molecular systems biology* **5**, 282 (2009).

[43] Calvo, J. M. & Matthews, R. G. The leucine-responsive regulatory protein, a global regulator of metabolism in Escherichia coli. *Microbiol Rev* **58**, 466-490 (1994).

[44] Yokoyama, K. *et al.* Feast/famine regulatory proteins (FFRPs): Escherichia coli Lrp, AsnC and related archaeal transcription factors. *FEMS Microbiol Rev* **30**, 89-108 (2006).

[45] de Wind, N., de Jong, M., Meijer, M. & Stuitje, A. R. Site-directed mutagenesis of the Escherichia coli chromosome near oriC: identification and characterization of asnC, a regulatory element in E. coli asparagine metabolism. *Nucleic Acids Res* **13**, 8797-8811 (1985).

[46] Tani, T. H., Khodursky, A., Blumenthal, R. M., Brown, P. O. & Matthews, R. G. Adaptation to famine: a family of stationary-phase genes revealed by microarray analysis. *Proc Natl Acad Sci U S A* **99**, 13471-13476 (2002).

[47] Wang, Q. & Calvo, J. M. Lrp, a major regulatory protein in Escherichia coli, bends DNA and can organize the assembly of a higher-order nucleoprotein structure. *EMBO J* **12**, 2495-2501 (1993).

[48] Ettema, T. J., Huynen, M. A., de Vos, W. M. & van der Oost, J. TRASH: a novel metal-binding domain predicted to be involved in heavy-metal sensing, trafficking and resistance. *Trends Biochem Sci* **28**, 170-173 (2003).

[49] Brinkman, A. B., Ettema, T. J., de Vos, W. M. & van der Oost, J. The Lrp family of transcriptional regulators. *Mol Microbiol* **48**, 287-294 (2003).

[50] Kumarevel, T. *et al.* Crystal structure of glutamine receptor protein from Sulfolobus tokodaii strain 7 in complex with its effector L-glutamine: implications of effector binding in molecular association and DNA binding. *Nucleic Acids Res* **36**, 4808-4820 (2008).

[51] de los Rios, S. & Perona, J. J. Structure of the Escherichia coli leucine-responsive regulatory protein Lrp reveals a novel octameric assembly. *J Mol Biol* **366**, 1589-1602 (2007).

[52] Thaw, P. *et al.* Structural insight into gene transcriptional regulation and effector binding by the Lrp/AsnC family. *Nucleic Acids Res* **34**, 1439-1449 (2006).

[53] Willins, D. A., Ryan, C. W., Platko, J. V. & Calvo, J. M. Characterization of Lrp, and Escherichia coli regulatory protein that mediates a global response to leucine. *J Biol Chem* **266**, 10768-10774 (1991).

[54] Chen, S., Rosner, M. H. & Calvo, J. M. Leucine-regulated self-association of leucine-responsive regulatory protein (Lrp) from Escherichia coli. *J Mol Biol* **312**, 625-635, (2001).

[55] Marasco, R. *et al.* In vivo footprinting analysis of Lrp binding to the ilvIH promoter region of Escherichia coli. *J Bacteriol* **176**, 5197-5201 (1994).

[56] Madhusudhan, K. T., Luo, J. & Sokatch, J. R. In vitro transcriptional studies of the bkd operon of Pseudomonas putida: L-branched-chain amino acids and D-leucine are the inducers. *J Bacteriol* **181**, 2889-2894 (1999).

[57] Kolling, R. & Lother, H. AsnC: an autogenously regulated activator of asparagine synthetase A transcription in Escherichia coli. *J Bacteriol* **164**, 310-315 (1985).

[58] Peekhaus, N., Tolner, B., Poolman, B. & Kramer, R. The glutamate uptake regulatory protein (Grp) of Zymomonas mobilis and its relation to the global regulator Lrp of Escherichia coli. *J Bacteriol* **177**, 5140-5147 (1995).

[59] Cho, K. & Winans, S. C. The putA gene of Agrobacterium tumefaciens is transcriptionally activated in response to proline by an Lrp-like protein and is not autoregulated. *Mol Microbiol* **22**, 1025-1033 (1996).

[60] Leonard, P. M. *et al.* Crystal structure of the Lrp-like transcriptional regulator from the archaeon Pyrococcus furiosus. *EMBO J* **20**, 990-997 (2001).

[61] Kudo, N., Allen, M. D., Koike, H., Katsuya, Y. & Suzuki, M. Crystallization and secondary-structure determination of a protein of the Lrp/AsnC family from a hyperthermophilic archaeon. *Acta Crystallogr D Biol Crystallogr* **57**, 469-471 (2001).

[62] Ren, J. *et al.* The structure and transcriptional analysis of a global regulator from Neisseria meningitidis. *J Biol Chem* **282**, 14655-14664 (2007).

[63] Reddy, M. C., Gokulan, K., Jacobs, W. R., Jr., Ioerger, T. R. & Sacchettini, J. C. Crystal structure of Mycobacterium tuberculosis LrpA, a leucine-responsive global regulator associated with starvation response. *Protein Sci* **17**, 159-170 (2008).

[64] Ettema, T. J., Brinkman, A. B., Tani, T. H., Rafferty, J. B. & Van Der Oost, J. A novel ligand-binding domain involved in regulation of amino acid metabolism in prokaryotes. *J Biol Chem* **277**, 37464-37468 (2002).

[65] Nakano, N. *et al.* Structure of the stand-alone RAM-domain protein from Thermus thermophilus HB8. *Acta Crystallogr Sect F Struct Biol Cryst Commun* **62**, 855-860 (2006).

[66] Yokoyama, K. *et al.* Feast/famine regulation by transcription factor FL11 for the survival of the hyperthermophilic archaeon Pyrococcus OT3. *Structure* **15**, 1542-1554 (2007).

[67] Kawashima, T. *et al.* Transcription regulation by feast/famine regulatory proteins, FFRPs, in archaea and eubacteria. *Biol Pharm Bull* **31**, 173-186 (2008).

[68] Facciotti, M. T. *et al.* Large scale physiological readjustment during growth enables rapid, comprehensive and inexpensive systems analysis. *BMC Syst Biol* **4**, 64 (2010).

[69] Punta, M. *et al.* The Pfam protein families database. *Nucleic Acids Res* **40**, D290-301

[70] Streit, W. R. *et al.* An evolutionary hot spot: the pNGR234b replicon of Rhizobium sp. strain NGR234. *J Bacteriol* **186**, 535-542 (2004).

[71] Goujon, M. *et al.* A new bioinformatics analysis tools framework at EMBL-EBI. *Nucleic Acids Res* **38**, W695-699

[72] Waterhouse, A. M., Procter, J. B., Martin, D. M., Clamp, M. & Barton, G. J. Jalview Version 2--a multiple sequence alignment editor and analysis workbench. *Bioinformatics* **25**, 1189-1191, (2009).

[73] Livingstone, C. D. & Barton, G. J. Protein sequence alignments: a strategy for the hierarchical analysis of residue conservation. *Comput Appl Biosci* **9**, 745-756 (1993).

[74] Kaur, A. *et al.* A systems view of haloarchaeal strategies to withstand stress from transition metals. *Genome Res* **16**, 841-854 (2006).

[75] Reiss, D. J., Facciotti, M. T. & Baliga, N. S. Model-based deconvolution of genome-wide DNA binding. *Bioinformatics* **24**, 396-403 (2008).

[76] Schmid, A. K., Pan, M., Sharma, K. & Baliga, N. S. Two transcription factors are necessary for iron homeostasis in a salt-dwelling archaeon. *Nucleic Acids Res* **39**, 2519-2533

[77] Peeters, E., Willaert, R., Maes, D. & Charlier, D. Ss-LrpB from Sulfolobus solfataricus condenses about 100 base pairs of its own operator DNA into globular nucleoprotein complexes. *J Biol Chem* **281**, 11721-11728 (2006).

[78] Kanehisa, M., Goto, S., Sato, Y., Furumichi, M. & Tanabe, M. KEGG for integration and interpretation of large-scale molecular data sets. *Nucleic Acids Res* **40**, D109-114

[79] Yosef, N., Kaufman, A. & Ruppin, E. Inferring functional pathways from multi-perturbation data. *Bioinformatics* **22**, e539-546 (2006).

[80] Peck, R. F., DasSarma, S. & Krebs, M. P. Homologous gene knockout in the archaeon Halobacterium salinarum with ura3 as a counterselectable marker. *Mol Microbiol* **35**, 667-676, (2000).

[81] Brookfield, J. Can genes be truly redundant? *Curr Biol* **2**, 553-554 (1992).

[82] Kaur, A. *et al.* Coordination of frontline defense mechanisms under severe oxidative stress. *Mol Syst Biol* **6**, 393

[83] Holden, H. M., Thoden, J. B. & Raushel, F. M. Carbamoyl phosphate synthetase: an amazing biochemical odyssey from substrate to product. *Cell Mol Life Sci* **56**, 507-522 (1999).

[84] Korbel, J. O., Jensen, L. J., von Mering, C. & Bork, P. Analysis of genomic context: prediction of functional associations from conserved bidirectionally transcribed gene pairs. *Nat Biotechnol* **22**, 911-917 (2004).

[85] Liang Feng, D. T.-H., Bokkee Min, Suk Namgoog, Juan Salazar, omar orellana and Dieter Soll. in *Eurekah Bioscience* Vol. 1 Ch. 86, (Landes Bioscience, 2005).

[86] Cardoso, A. M., Polycarpo, C., Martins, O. B. & Soll, D. A non-discriminating aspartyl-tRNA synthetase from Halobacterium salinarum. *RNA Biol* **3**, 110-114 (2006).

[87] Min, B., Pelaschier, J. T., Graham, D. E., Tumbula-Hansen, D. & Soll, D. Transfer RNA-dependent amino acid biosynthesis: an essential route to asparagine formation. *Proc Natl Acad Sci U S A* **99**, 2678-2683 (2002).

[88] Roy, H., Becker, H. D., Reinbolt, J. & Kern, D. When contemporary aminoacyl-tRNA synthetases invent their cognate amino acid metabolism. *Proc Natl Acad Sci U S A* **100**, 9837-9842, (2003).

[89] Blaise, M. *et al.* Crystal structure of the archaeal asparagine synthetase: interrelation with aspartyl-tRNA and asparaginyl-tRNA synthetases. *J Mol Biol* **412**, 437-452

[90] Llorens, N., Arola, L., Blade, C. & Mas, A. Effects of copper exposure upon nitrogen metabolism in tissue cultured Vitis vinifera. *Plant Sci* **160**, 159-163 (2000).

[91] Subramanyam, C., Venkateswerlu, G. & Rao, S. L. Cell Wall Composition of Neurospora crassa Under Conditions of Copper Toxicity. *Appl Environ Microbiol* **46**, 585-590 (1983).

[92] Harper, J. E. & Paulsen, G. M. Nitrogen Assimilation and Protein Synthesis in Wheat Seedlings as Affected by Mineral Nutrition. II. Micronutrients. *Plant Physiol* **44**, 636-640 (1969).

[93] Tautenhahn, R. *et al.* metaXCMS: second-order analysis of untargeted metabolomics data. *Anal Chem* **83**, 696-700

[94] M Goto, T. H., T Kyuda, M Nakajima. Induction of copper resistance in plant-pathogenic bacteria exposed to glutamate, plant extracts, phosphate buffer, and some antibiotics. *Phytopathology* **83**, 1449-1453 (1993).

[95] Baliga, N. S. & DasSarma, S. Saturation mutagenesis of the TATA box and upstream activator sequence in the haloarchaeal bop gene promoter. *Journal of bacteriology* **181**, 2513-2518 (1999).

[96] Edgar, R. C. MUSCLE: multiple sequence alignment with high accuracy and high throughput. *Nucleic Acids Res* **32**, 1792-1797 (2004).

[97] Letunic, I. & Bork, P. Interactive Tree Of Life v2: online annotation and display of phylogenetic trees made easy. *Nucleic Acids Res* **39**, W475-478

[98] Ren, B. *et al.* Genome-wide location and function of DNA binding proteins. *Science* **290**, 2306-2309, doi:10.1126/science.290.5500.2306
290/5500/2306 [pii] (2000).

[99] Baliga, N. S. *et al.* Systems level insights into the stress response to UV radiation in the halophilic archaeon Halobacterium NRC-1. *Genome Res* **14**, 1025-1035 (2004).

[100] Schmid, A. K. *et al.* The anatomy of microbial cell state transitions in response to oxygen. *Genome Res* **17**, 1399-1413 (2007).

[101] Marzolf, B. *et al.* SBEAMS-Microarray: database software supporting genomic expression analyses for systems biology. *BMC Bioinformatics* **7**, 286 (2006).

[102] Rahnenfuhrer, A. A. a. J. (2010).

[103] Altschul, S. F. *et al.* Gapped BLAST and PSI-BLAST: a new generation of protein database search programs. *Nucleic Acids Res* **25**, 3389-3402 (1997).

[104] Altschul, S. F., Gish, W., Miller, W., Myers, E. W. & Lipman, D. J. Basic local alignment search tool. *J Mol Biol* **215**, 403-410 (1990).

[105] Leaver-Fay, A. *et al.* ROSETTA3: an object-oriented software suite for the simulation and design of macromolecules. *Methods Enzymol* **487**, 545-574

[106] Havranek, J. J., Duarte, C. M. & Baker, D. A simple physical model for the prediction and design of protein-DNA interactions. *J Mol Biol* **344**, 59-70 (2004).

[107] Ashworth, J. & Baker, D. Assessment of the optimization of affinity and specificity at protein-DNA interfaces. *Nucleic Acids Res* **37**, e73 (2009).

[108] Yokoyama, K. *et al.* The DNA-recognition mode shared by archaeal feast/famine-regulatory proteins revealed by the DNA-binding specificities of TvFL3, FL10, FL11 and Ss-LrpB. *Nucleic Acids Res* **37**, 4407-4419 (2009).

[109] Bailey, T. L., Williams, N., Misleh, C. & Li, W. W. MEME: discovering and analyzing DNA and protein sequence motifs. *Nucleic Acids Res* **34**, W369-373 (2006).

Appendices

Appendix A. Phylogenetic tree of archaeal Lrp family

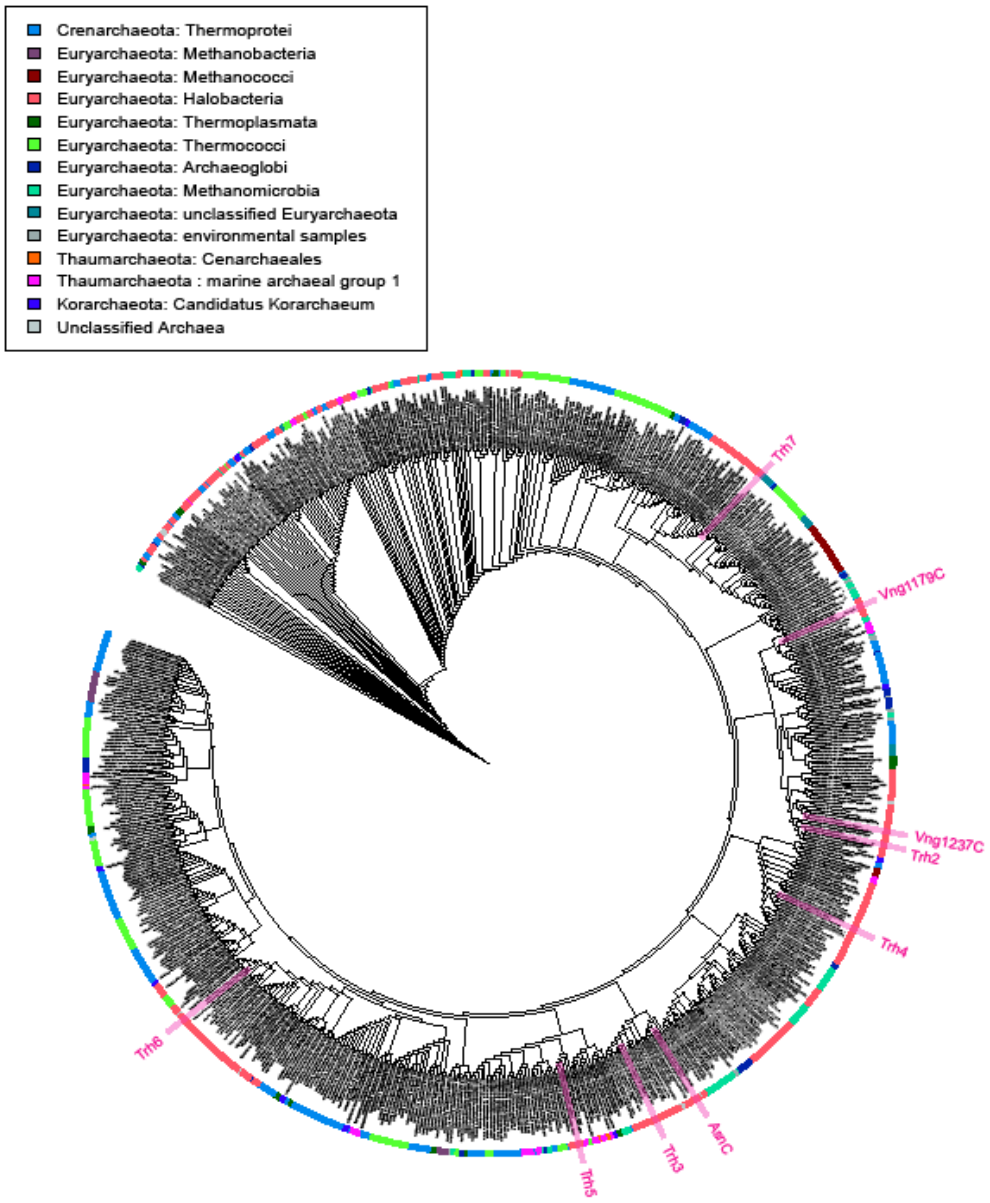

Phylogenetic tree of archaeal Lrps based on the sequence alignment of the PF01037 (RAM) domain. Colored stripes at the outer circle represent different taxonomy lineages as detailed at the upper left part of the figure. The eight Lrps in *H. salinarum NRC-1* are highlighted in pink.

Note to committee: while the font is too small to read in this lo-res image, vector graphics in the original image allows detailed exploration of this dendogram by text searching and zooming in (the original image is provided electronically as a PDF attachment).

Appendix B. Clustal X color scheme[a]

Each residue in the alignment is assigned a colour if the amino acid profile of the alignment at that position meets some minimum criteria specific for the residue type. The table below gives these criteria as clauses: {+X%,xx,y}, where X is the minimum percentage presence for any of the xx (or y) residue types.

Clustal X Default Colouring		
Residue at position	**Applied Colour**	**{ Threshhold, Residue group }**
A,I,L,M,F,W,V	BLUE	{+60%, WLVIMAFCHP}
R,K	RED	{+60%,KR},{+80%, K,R,Q}
N	GREEN	{+50%, N}, {+85%, N,Y}
C	BLUE	{+60%, WLVIMAFCHP}
C	PINK	{100%, C}
Q	GREEN	{+60%,KR},{+50%,QE},{+85%,Q,E,K,R}
E	MAGENTA	{+60%,KR},{+50%,QE},{+85%,E,Q,D}
D	MAGENTA	{+60%,KR}, {+85%, K,R,Q}, {+50%,ED}
G	ORANGE	{+0%, G}
H,Y	CYAN	{+60%, WLVIMAFCHP}, {+85%, W,Y,A,C,P,Q,F,H,I,L,M,V}
P	YELLOW	{+0%, P}
S,T	GREEN	{+60%, WLVIMAFCHP}, {+50%, TS}, {+85%,S,T}

[a] From http://www.jalview.org/help/html/colourSchemes/clustal.html

Appendix C. The numbers of Lrps in some archaeal genomes

Lineage	*organisms*	Number of Lrps
euyarchaeotoes: 401 entried from 72 species	*Haloferax volcanii DS2*	15
	Natrialba magadii ATCC 43099	14
	Halorubrum lacusprofundi ATCC 49239	14
	Pyrococcus sp. NA2	13
	Halomicrobium mukohataei DSM 12286	13
	Haloterrigena turkmenica DSM 5511	13
	Thermococcus gammatolerans EJ3	12
	Halorhabdus utahensis DSM 12940	12
	Pyrococcus horikoshii OT3	11
	Thermococcus onnurineus NA1	10
	Thermococcus sibiricus MM 739	10
	Halogeometricum borinquense DSM 11551	10
	Haloquadratum walsbyi DSM 16790	10
	Haladaptatus paucihalophilus DX253	10
	Aciduliprofundum boonei T469	10
	Pyrococcus abyssi GE5	9
	Thermococcus kodakarensis KOD1	9
	Natronomonas pharaonis DSM 2160	9
	Halobacterium sp. NRC-1	9
	Halobacterium salinarum R1	9
	Halopiger xanaduensis SH-6	9
	Archaeoglobus fulgidus DSM 4304	9
	uncultured methanogenic archaeon RC-I	9
	Pyrococcus furiosus DSM 3638	8
	Thermococcus barophilus MP	8
	Halalkalicoccus jeotgali B3	8
	Ferroglobus placidus DSM 10642	8
	Haloarcula marismortui ATCC 43049	7
	Archaeoglobus profundus DSM 5631	7
	Thermococcus sp. AM4	6
	Methanocella paludicola SANAE	6
	Ferroplasma acidarmanus fer1	6
	Halorhabdus tiamatea SARL4B	6
	Methanosaeta thermophila PT	5
	Picrophilus torridus DSM 9790	5
	Methanosaeta concilii GP6	4

	Methanoculleus marisnigri JR1	4
	Methanosphaerula palustris E1-9c	4
	Methanoregula boonei 6A8	4
	Thermoplasma volcanium GSS1	4
	Thermoplasma acidophilum DSM 1728	4
	Methanosarcina mazei Go1	3
	Methanosalsum zhilinae DSM 4017	3
	Archaeoglobus veneficus SNP6	3
	Methanosphaera stadtmanae DSM 3091	2
	Methanobacterium sp. AL-21	2
	Methanocaldococcus jannaschii DSM 2661	2
	Methanocaldococcus vulcanius M7	2
	Methanosarcina barkeri str. Fusaro	2
	Methanosarcina acetivorans C2A	2
	Methanohalophilus mahii DSM 5219	2
	Methanococcoides burtonii DSM 6242	2
	Methanohalobium evestigatum Z-7303	2
	Methanospirillum hungatei JF-1	2
	Methanoplanus petrolearius DSM 11571	2
	Methanothermus fervidus DSM 2088	1
	Methanobrevibacter ruminantium M1	1
	Methanobrevibacter smithii ATCC 35061	1
	Methanobrevibacter smithii DSM 2375	1
	Methanobrevibacter smithii DSM 2374	1
	Methanococcus maripaludis C5	1
	Methanococcus maripaludis S2	1
	Methanococcus maripaludis C7	1
	Methanococcus maripaludis C6	1
	Methanococcus voltae A3	1
	Methanococcus aeolicus Nankai-3	1
	Methanococcus vannielii SB	1
	Methanothermococcus okinawensis IH1	1
	Methanocaldococcus fervens AG86	1
	Methanocaldococcus sp. FS406-22	1
	Methanocaldococcus infernus ME	1
	Methanocorpusculum labreanum Z	1
crenarchaetoes: 150 entries from 34 species	*Metallosphaera sedula DSM 5348*	10
	Ignicoccus hospitalis KIN4/I	9
	Sulfolobus solfataricus P2	7
	Sulfolobus tokodaii str. 7	7
	Thermofilum pendens Hrk 5	7

	Sulfolobus solfataricus 98/2	6
	Sulfolobus islandicus Y.N.15.51	6
	Sulfolobus islandicus L.D.8.5	6
	Sulfolobus islandicus Y.G.57.14	6
	Sulfolobus islandicus M.16.27	6
	Sulfolobus islandicus M.14.25	6
	Sulfolobus islandicus M.16.4	5
	Sulfolobus islandicus L.S.2.15	5
	Pyrobaculum islandicum DSM 4184	5
	Pyrobaculum calidifontis JCM 11548	5
	Pyrobaculum arsenaticum DSM 13514	5
	Thermoproteus neutrophilus V24Sta	5
	Staphylothermus marinus F1	5
	Vulcanisaeta distributa DSM 14429	4
	Vulcanisaeta moutnovskia 768-28	4
	Aeropyrum pernix K1	4
	Caldivirga maquilingensis IC-167	4
	Desulfurococcus mucosus DSM 2162	3
	Acidianus hospitalis W1	3
	Metallosphaera cuprina Ar-4	3
	Thermosphaera aggregans DSM 11486	2
	Pyrobaculum aerophilum str. IM2	2
	Thermoproteus uzoniensis 768-20	2
	Sulfolobus acidocaldarius DSM 639	2
	Acidilobus saccharovorans 345-15	2
	Desulfurococcus kamchatkensis 1221n	1
	Ignisphaera aggregans DSM 17230	1
	Staphylothermus hellenicus DSM 12710	1
	Hyperthermus butylicus DSM 5456	1
nitrosopumilales	*Nitrosopumilus*	16
	Candidatus Nitrosoarchaeum	5
	Candidatus Korarchaeum	9
	Cenarchaeales	4

Appendix D. All binding targets of the 8 Lrps

Lrp	Lrp Binding targets	
	canonical name	gene name
AsnC	*VNG0110C*	*VNG0110C*
AsnC	*VNG0255C*	*VNG0255C*
AsnC	*VNG0256H*	*VNG0256H*
AsnC	*VNG0361C*	*VNG0361C*
AsnC	*VNG0363G*	*nfi*
AsnC	*VNG0405C*	*VNG0405C*
AsnC	*VNG0421C*	*VNG0421C*
AsnC	*VNG0553C*	*VNG0553C*
AsnC	*VNG0631C*	*VNG0631C*
AsnC	*VNG0826C*	*VNG0826C*
AsnC	*VNG0865C*	*VNG0865C*
AsnC	*VNG0867G*	*asnA*
AsnC	*VNG1069C*	*VNG1069C*
AsnC	*VNG1296C*	*VNG1296C*
AsnC	*VNG1297C*	*VNG1297C*
AsnC	*VNG1323C*	*VNG1323C*
AsnC	*VNG1608C*	*VNG1608C*
AsnC	*VNG1688C*	*VNG1688C*
AsnC	*VNG1689G*	*rpl13p*
AsnC	*VNG1690G*	*rpl4e*
AsnC	*VNG1691G*	*rpl23p*
AsnC	*VNG1692G*	*rpl2p*
AsnC	*VNG1693G*	*rps19p*
AsnC	*VNG1695G*	*rpl22p*
AsnC	*VNG1697G*	*rps3p*
AsnC	*VNG1698G*	*rpl29p*
AsnC	*VNG1699C*	*VNG1699C*
AsnC	*VNG1700G*	*rps17p*
AsnC	*VNG1701G*	*rpl14p*
AsnC	*VNG1702G*	*rpl24p*
AsnC	*VNG1703G*	*rps4e*
AsnC	*VNG1705G*	*rpl5p*
AsnC	*VNG1706G*	*rps14p*
AsnC	*VNG1707G*	*rps8p*
AsnC	*VNG1709G*	*rpl6p*
AsnC	*VNG1711G*	*rpl32e*
AsnC	*VNG1713G*	*rpl19e*
AsnC	*VNG1714G*	*rpl18p*

AsnC	*VNG1715G*	*rps5p*
AsnC	*VNG1716G*	*rpl30p*
AsnC	*VNG1718G*	*rpl15p*
AsnC	*VNG1719G*	*secY*
AsnC	*VNG1735C*	*VNG1735C*
AsnC	*VNG1779C*	*VNG1779C*
AsnC	*VNG1941C*	*VNG1941C*
AsnC	*VNG2296C*	*VNG2296C*
AsnC	*VNG2307C*	*VNG2307C*
AsnC	*VNG2329C*	*VNG2329C*
AsnC	*VNG2369C*	*VNG2369C*
AsnC	*VNG2466C*	*VNG2466C*
AsnC	*VNG2474C*	*VNG2474C*
AsnC	*VNG2475C*	*VNG2475C*
AsnC	*VNG2610C*	*VNG2610C*
AsnC	*VNG0045C*	*VNG0045C*
AsnC	*VNG0124C*	*VNG0124C*
AsnC	*VNG0271C*	*VNG0271C*
AsnC	*VNG0505C*	*VNG0505C*
AsnC	*VNG0713C*	*VNG0713C*
AsnC	*VNG1583C*	*VNG1583C*
AsnC	*VNG1874C*	*VNG1874C*
AsnC	*VNG2488C*	*VNG2488C*
AsnC	*VNG2490H*	*VNG2490H*
AsnC	*VNG2555C*	*VNG2555C*
AsnC	*VNG0002G*	*yvrO*
AsnC	*VNG0003C*	*VNG0003C*
AsnC	*VNG0123G*	*trp1*
AsnC	*VNG0133G*	*rpa*
AsnC	*VNG0134G*	*hpyA*
AsnC	*VNG0136G*	*aup*
AsnC	*VNG0149G*	*zntA*
AsnC	*VNG0166G*	*psmA2*
AsnC	*VNG0181G*	*lpl*
AsnC	*VNG0226G*	*htrA*
AsnC	*VNG0277G*	*crtI3*
AsnC	*VNG0307G*	*trpB*
AsnC	*VNG0308G*	*trpA*
AsnC	*VNG0309C*	*VNG0309C*
AsnC	*VNG0349G*	*topA*
AsnC	*VNG0364G*	*yusZ3*
AsnC	*VNG0387G*	*ilvE1*

AsnC	*VNG0556G*	*sgb*
AsnC	*VNG0627G*	*citE*
AsnC	*VNG0647G*	*nuoM*
AsnC	*VNG0648G*	*ndhG3*
AsnC	*VNG0673G*	*mcmA2*
AsnC	*VNG0674C*	*VNG0674C*
AsnC	*VNG0795G*	*hcpC*
AsnC	*VNG0870G*	*gatC*
AsnC	*VNG0872G*	*gatA*
AsnC	*VNG1143G*	*rps2p*
AsnC	*VNG1145G*	*mvk*
AsnC	*VNG1148G*	*argB*
AsnC	*VNG1150G*	*idsA*
AsnC	*VNG1160G*	*ndk*
AsnC	*VNG1341G*	*fabG*
AsnC	*VNG1435G*	*asd*
AsnC	*VNG1467G*	*bop*
AsnC	*VNG1528G*	*nac*
AsnC	*VNG1553G*	*cbiF*
AsnC	*VNG1554G*	*cbiG*
AsnC	*VNG1555G*	*cobH*
AsnC	*VNG1557G*	*cbiH*
AsnC	*VNG1568G*	*cbiJ*
AsnC	*VNG1816G*	*trh3*
AsnC	*VNG1818G*	*idi*
AsnC	*VNG1822G*	*moaB*
AsnC	*VNG1823C*	*VNG1823C*
AsnC	*VNG1932G*	*nolA*
AsnC	*VNG1939G*	*purC*
AsnC	*VNG1992G*	*pgi*
AsnC	*VNG1993H*	*VNG1993H*
AsnC	*VNG2094G*	*trh4*
AsnC	*VNG2150G*	*etfB*
AsnC	*VNG2151G*	*etfA*
AsnC	*VNG2220G*	*lpdA*
AsnC	*VNG2290G*	*maoC1*
AsnC	*VNG2291G*	*cat*
AsnC	*VNG2294G*	*hisA*
AsnC	*VNG2295G*	*hisB*
AsnC	*VNG2322G*	*hem2*
AsnC	*VNG2326G*	*hemL*
AsnC	*VNG2359G*	*appB*

AsnC	*VNG2361G*	*appC*
AsnC	*VNG2363G*	*oppD1*
AsnC	*VNG2365G*	*appF*
AsnC	*VNG2397G*	*cysA*
AsnC	*VNG2418G*	*aspC1*
AsnC	*VNG2526G*	*dppF*
AsnC	*VNG2527G*	*dppD*
AsnC	*VNG2529G*	*dppB2*
AsnC	*VNG2531G*	*dppC1*
AsnC	*VNG2604G*	*thi1*
AsnC	*VNG2606G*	*thiD*
AsnC	*VNG2617G*	*adh2*
AsnC	*VNG0386G*	*trpG2*
AsnC	*VNG1159G*	*rpl24e*
AsnC	*VNG1433G*	*rps17e*
AsnC	*VNG0022H*	*VNG0022H*
AsnC	*VNG0055H*	*VNG0055H*
AsnC	*VNG0113H*	*VNG0113H*
AsnC	*VNG0138H*	*VNG0138H*
AsnC	*VNG0146H*	*VNG0146H*
AsnC	*VNG0184H*	*VNG0184H*
AsnC	*VNG0217H*	*VNG0217H*
AsnC	*VNG0219H*	*VNG0219H*
AsnC	*VNG0244H*	*VNG0244H*
AsnC	*VNG0296H*	*VNG0296H*
AsnC	*VNG0367H*	*VNG0367H*
AsnC	*VNG0404H*	*VNG0404H*
AsnC	*VNG0717H*	*VNG0717H*
AsnC	*VNG0861H*	*VNG0861H*
AsnC	*VNG1002H*	*VNG1002H*
AsnC	*VNG1042H*	*VNG1042H*
AsnC	*VNG1115H*	*VNG1115H*
AsnC	*VNG1229H*	*VNG1229H*
AsnC	*VNG1315H*	*VNG1315H*
AsnC	*VNG1438H*	*VNG1438H*
AsnC	*VNG1484H*	*VNG1484H*
AsnC	*VNG1664H*	*VNG1664H*
AsnC	*VNG1787H*	*VNG1787H*
AsnC	*VNG1865H*	*VNG1865H*
AsnC	*VNG1891H*	*VNG1891H*
AsnC	*VNG1910H*	*VNG1910H*
AsnC	*VNG1920H*	*VNG1920H*

AsnC	*VNG1956H*	*VNG1956H*
AsnC	*VNG2149H*	*VNG2149H*
AsnC	*VNG2497H*	*VNG2497H*
AsnC	*VNG2498H*	*VNG2498H*
AsnC	*VNG2619H*	*VNG2619H*
AsnC	*VNG2656H*	*VNG2656H*
AsnC	*VNG0067H*	*VNG0067H*
AsnC	*VNG1012H*	*VNG1012H*
AsnC	*VNG1261H*	*VNG1261H*
AsnC	*VNG1314H*	*VNG1314H*
AsnC	*VNG1382H*	*VNG1382H*
AsnC	*VNG1487H*	*VNG1487H*
AsnC	*VNG1807H*	*VNG1807H*
AsnC	*VNG2510H*	*VNG2510H*
AsnC	*VNG2581H*	*VNG2581H*
AsnC	*VNG0132C*	*VNG0132C*
AsnC	*VNG1244C*	*VNG1244C*
AsnC	*VNG1325C*	*VNG1325C*
AsnC	*VNG1388H*	*VNG1388H*
AsnC	*VNG1389C*	*VNG1389C*
AsnC	*VNG0094C*	*VNG0094C*
AsnC	*VNG0147C*	*VNG0147C*
AsnC	*VNG0360C*	*VNG0360C*
AsnC	*VNG0537C*	*VNG0537C*
AsnC	*VNG0539C*	*VNG0539C*
AsnC	*VNG0555C*	*VNG0555C*
AsnC	*VNG0602C*	*VNG0602C*
AsnC	*VNG0615C*	*VNG0615C*
AsnC	*VNG0853C*	*VNG0853C*
AsnC	*VNG0983C*	*VNG0983C*
AsnC	*VNG1165G*	*ksgA*
AsnC	*VNG1168C*	*VNG1168C*
AsnC	*VNG1198C*	*VNG1198C*
AsnC	*VNG1228C*	*VNG1228C*
AsnC	*VNG1287C*	*VNG1287C*
AsnC	*VNG1483C*	*VNG1483C*
AsnC	*VNG1681C*	*VNG1681C*
AsnC	*VNG1687C*	*VNG1687C*
AsnC	*VNG2012C*	*VNG2012C*
AsnC	*VNG2180C*	*VNG2180C*
AsnC	*VNG2455C*	*VNG2455C*
AsnC	*VNG2518C*	*VNG2518C*

AsnC	*VNG0013C*	*VNG0013C*
AsnC	*VNG0035C*	*VNG0035C*
AsnC	*VNG0470G*	*trp3*
AsnC	*VNG0598C*	*VNG0598C*
AsnC	*VNG0925C*	*VNG0925C*
AsnC	*VNG2172C*	*VNG2172C*
AsnC	*VNG0006G*	*glmS*
AsnC	*VNG0137G*	*cca*
AsnC	*VNG0163G*	*mutS1*
AsnC	*VNG0164G*	*hef*
AsnC	*VNG0172G*	*mutS2*
AsnC	*VNG0180G*	*hop*
AsnC	*VNG0223G*	*moxR*
AsnC	*VNG0254G*	*tfbG*
AsnC	*VNG0442G*	*rspA*
AsnC	*VNG0444G*	*dapA*
AsnC	*VNG0467G*	*yafB*
AsnC	*VNG0494G*	*grpE*
AsnC	*VNG0504G*	*gbp5*
AsnC	*VNG0610G*	*hhoA*
AsnC	*VNG0614G*	*htr16*
AsnC	*VNG0629G*	*aspB2*
AsnC	*VNG0630G*	*ribE*
AsnC	*VNG0716G*	*afsQ2*
AsnC	*VNG0806G*	*htr4*
AsnC	*VNG0862G*	*hisF*
AsnC	*VNG0864G*	*purL*
AsnC	*VNG0869G*	*tfbD*
AsnC	*VNG0920H*	*VNG0920H*
AsnC	*VNG0921G*	*potA1*
AsnC	*VNG0966G*	*cheR*
AsnC	*VNG1001G*	*guaB*
AsnC	*VNG1079G*	*menB*
AsnC	*VNG1081G*	*menD*
AsnC	*VNG1184G*	*nirJ*
AsnC	*VNG1284G*	*trkH1*
AsnC	*VNG1294G*	*slyD*
AsnC	*VNG1359G*	*rad2*
AsnC	*VNG1369G*	*hemV1*
AsnC	*VNG1465G*	*brp*
AsnC	*VNG1520G*	*mutY*
AsnC	*VNG1592G*	*cysT2*

AsnC	*VNG1607G*	*cheC2*
AsnC	*VNG1754G*	*phr1*
AsnC	*VNG1773G*	*cad*
AsnC	*VNG1815G*	*carA*
AsnC	*VNG1821G*	*adh4*
AsnC	*VNG1862G*	*cef*
AsnC	*VNG1864G*	*hit2*
AsnC	*VNG1929G*	*tmk*
AsnC	*VNG1987G*	*secD*
AsnC	*VNG2051G*	*rpoE''*
AsnC	*VNG2053G*	*rpoE'*
AsnC	*VNG2054H*	*VNG2054H*
AsnC	*VNG2056G*	*eif2g*
AsnC	*VNG2060G*	*phnP*
AsnC	*VNG2093G*	*glnA*
AsnC	*VNG2138G*	*atpB*
AsnC	*VNG2139G*	*atpA*
AsnC	*VNG2140G*	*atpF*
AsnC	*VNG2141G*	*atpC*
AsnC	*VNG2142G*	*atpE*
AsnC	*VNG2284G*	*hisJ*
AsnC	*VNG2462G*	*dpa*
AsnC	*VNG2482G*	*pstB1*
AsnC	*VNG2483G*	*pstA1*
AsnC	*VNG2484G*	*pstC1*
AsnC	*VNG2486G*	*yqgG*
AsnC	*VNG2654G*	*eef2*
AsnC	*VNG2657G*	*rps7p*
AsnC	*VNG0546C*	*VNG0546C*
AsnC	*VNG0548C*	*VNG0548C*
AsnC	*VNG0549G*	*eif2a*
AsnC	*VNG0550G*	*rps27e*
AsnC	*VNG0551G*	*rpl44e*
AsnC	*VNG0626G*	*maoC2*
AsnC	*VNG0841G*	*icfA*
AsnC	*VNG2071G*	*lfl2*
AsnC	*VNG2496G*	*ferB*
AsnC	*VNG0192G*	*ftsZ2*
AsnC	*VNG0194H*	*VNG0194H*
AsnC	*VNG0323H*	*VNG0323H*
AsnC	*VNG1189H*	*VNG1189H*
AsnC	*VNG1376H*	*VNG1376H*

AsnC	*VNG1519H*	*VNG1519H*
AsnC	*VNG1630H*	*VNG1630H*
AsnC	*VNG1832H*	*VNG1832H*
AsnC	*VNG1989H*	*VNG1989H*
AsnC	*VNG1991H*	*VNG1991H*
AsnC	*VNG2177H*	*VNG2177H*
AsnC	*VNG2402H*	*VNG2402H*
AsnC	*VNG2495H*	*VNG2495H*
AsnC	*VNG0054H*	*VNG0054H*
AsnC	*VNG0125H*	*VNG0125H*
AsnC	*VNG0148H*	*VNG0148H*
AsnC	*VNG0198H*	*VNG0198H*
AsnC	*VNG0204H*	*VNG0204H*
AsnC	*VNG0408H*	*VNG0408H*
AsnC	*VNG0420H*	*VNG0420H*
AsnC	*VNG0430H*	*VNG0430H*
AsnC	*VNG0492H*	*VNG0492H*
AsnC	*VNG0612H*	*VNG0612H*
AsnC	*VNG0671H*	*VNG0671H*
AsnC	*VNG0742H*	*VNG0742H*
AsnC	*VNG1144H*	*VNG1144H*
AsnC	*VNG1410H*	*VNG1410H*
AsnC	*VNG1642H*	*VNG1642H*
AsnC	*VNG1777H*	*VNG1777H*
AsnC	*VNG1919H*	*VNG1919H*
AsnC	*VNG1921H*	*VNG1921H*
AsnC	*VNG2014H*	*VNG2014H*
AsnC	*VNG2148H*	*VNG2148H*
AsnC	*VNG2297H*	*VNG2297H*
AsnC	*VNG2403H*	*VNG2403H*
AsnC	*VNG2525H*	*VNG2525H*
AsnC	*VNG2554H*	*VNG2554H*
AsnC	*VNG2562H*	*VNG2562H*
AsnC	*VNG2603H*	*VNG2603H*
AsnC	*VNG2640G*	*gcvT2*
AsnC	*VNG2641H*	*VNG2641H*
AsnC	*VNG5074C*	*VNG5074C*
AsnC	*VNG5118H*	*VNG5118H*
AsnC	*VNG5124H*	*VNG5124H*
AsnC	*VNG5022G*	*gvpJ1*
AsnC	*VNG6071C*	*VNG6071C*
AsnC	*VNG6334H*	*VNG6334H*

AsnC	*VNG6347H*	*VNG6347H*
AsnC	*VNG6378H*	*VNG6378H*
AsnC	*VNG6432H*	*VNG6432H*
AsnC	*VNG6212G*	*iucA*
AsnC	*VNG6213G*	*iucB*
AsnC	*VNG6214G*	*hxyA*
AsnC	*VNG6216G*	*iucC*
AsnC	*VNG6246G*	*gvpO2*
AsnC	*VNG6142C*	*VNG6142C*
AsnC	*VNG6113H*	*VNG6113H*
AsnC	*VNG6115H*	*VNG6115H*
AsnC	*VNG6377H*	*VNG6377H*
AsnC	*VNG6121H*	*VNG6121H*
AsnC	*VNG6144G*	*trsE*
AsnC	*VNG6145H*	*VNG6145H*
AsnC	*VNG6346H*	*VNG6346H*
AsnC	*VNG6404H*	*VNG6404H*
AsnC	*VNG6416H*	*VNG6416H*
AsnC	*VNG6431H*	*VNG6431H*
AsnC	*VNG6022G*	*gvpJ1*
AsnC	*VNG6237G*	*gvpF2*
AsnC	*VNG6233G*	*gvpI2*
AsnC	*VNG6272G*	*orc5*
AsnC	*VNG6294G*	*perA*
VNG1179C	*VNG0171C*	*VNG0171C*
VNG1179C	*VNG0396C*	*VNG0396C*
VNG1179C	*VNG0405C*	*VNG0405C*
VNG1179C	*VNG0421C*	*VNG0421C*
VNG1179C	*VNG0437C*	*VNG0437C*
VNG1179C	*VNG0707C*	*VNG0707C*
VNG1179C	*VNG0875C*	*VNG0875C*
VNG1179C	*VNG1021C*	*VNG1021C*
VNG1179C	*VNG1023C*	*VNG1023C*
VNG1179C	*VNG1024C*	*VNG1024C*
VNG1179C	*VNG1025H*	*VNG1025H*
VNG1179C	*VNG1069C*	*VNG1069C*
VNG1179C	*VNG1237C*	*VNG1237C*
VNG1179C	*VNG1299C*	*VNG1299C*
VNG1179C	*VNG1337C*	*VNG1337C*
VNG1179C	*VNG1375C*	*VNG1375C*
VNG1179C	*VNG1779C*	*VNG1779C*
VNG1179C	*VNG2610C*	*VNG2610C*

VNG1179C	*VNG0713C*	*VNG0713C*
VNG1179C	*VNG0047G*	*graD6*
VNG1179C	*VNG0181G*	*lpl*
VNG1179C	*VNG0398G*	*nthA1*
VNG1179C	*VNG0500G*	*ppd*
VNG1179C	*VNG0627G*	*citE*
VNG1179C	*VNG0667G*	*trp4*
VNG1179C	*VNG0761G*	*dip3*
VNG1179C	*VNG0860G*	*rpoL*
VNG1179C	*VNG0882G*	*pho2*
VNG1179C	*VNG1018G*	*adh3*
VNG1179C	*VNG1020C*	*VNG1020C*
VNG1179C	*VNG1463G*	*blp*
VNG1179C	*VNG1553G*	*cbiF*
VNG1179C	*VNG1554G*	*cbiG*
VNG1179C	*VNG1555G*	*cobH*
VNG1179C	*VNG1557G*	*cbiH*
VNG1179C	*VNG1574G*	*cobI*
VNG1179C	*VNG1576G*	*cbiP*
VNG1179C	*VNG1659G*	*htr1*
VNG1179C	*VNG1660G*	*sop1*
VNG1179C	*VNG1711G*	*rpl32e*
VNG1179C	*VNG1713G*	*rpl19e*
VNG1179C	*VNG1714G*	*rpl18p*
VNG1179C	*VNG1715G*	*rps5p*
VNG1179C	*VNG1716G*	*rpl30p*
VNG1179C	*VNG1718G*	*rpl15p*
VNG1179C	*VNG1719G*	*secY*
VNG1179C	*VNG1785G*	*panF*
VNG1179C	*VNG1914G*	*ppiA*
VNG1179C	*VNG2088G*	*trm1*
VNG1179C	*VNG2150G*	*etfB*
VNG1179C	*VNG2151G*	*etfA*
VNG1179C	*VNG2216G*	*lip*
VNG1179C	*VNG2217G*	*pdhA2*
VNG1179C	*VNG2218G*	*pdhB*
VNG1179C	*VNG2219G*	*dsa*
VNG1179C	*VNG2220G*	*lpdA*
VNG1179C	*VNG2332G*	*cysG*
VNG1179C	*VNG2411G*	*orc7*
VNG1179C	*VNG2420G*	*metA*
VNG1179C	*VNG2421G*	*hal*

VNG1179C	*VNG2620G*	*uvrD*
VNG1179C	*VNG0095G*	*gapB*
VNG1179C	*VNG0438G*	*ferA3*
VNG1179C	*VNG2147G*	*hmp*
VNG1179C	*VNG2320G*	*hdrD*
VNG1179C	*VNG0080H*	*VNG0080H*
VNG1179C	*VNG0184H*	*VNG0184H*
VNG1179C	*VNG0244H*	*VNG0244H*
VNG1179C	*VNG0287H*	*VNG0287H*
VNG1179C	*VNG0352H*	*VNG0352H*
VNG1179C	*VNG0357H*	*VNG0357H*
VNG1179C	*VNG0596H*	*VNG0596H*
VNG1179C	*VNG0861H*	*VNG0861H*
VNG1179C	*VNG0979H*	*VNG0979H*
VNG1179C	*VNG1002H*	*VNG1002H*
VNG1179C	*VNG1042H*	*VNG1042H*
VNG1179C	*VNG1302H*	*VNG1302H*
VNG1179C	*VNG1422H*	*VNG1422H*
VNG1179C	*VNG1466H*	*VNG1466H*
VNG1179C	*VNG1479H*	*VNG1479H*
VNG1179C	*VNG1675H*	*VNG1675H*
VNG1179C	*VNG1783H*	*VNG1783H*
VNG1179C	*VNG1838H*	*VNG1838H*
VNG1179C	*VNG1927H*	*VNG1927H*
VNG1179C	*VNG1993H*	*VNG1993H*
VNG1179C	*VNG2185H*	*VNG2185H*
VNG1179C	*VNG2340H*	*VNG2340H*
VNG1179C	*VNG2585H*	*VNG2585H*
VNG1179C	*VNG1261H*	*VNG1261H*
VNG1179C	*VNG1388H*	*VNG1388H*
VNG1179C	*VNG1389C*	*VNG1389C*
VNG1179C	*VNG0096C*	*VNG0096C*
VNG1179C	*VNG0332C*	*VNG0332C*
VNG1179C	*VNG0394C*	*VNG0394C*
VNG1179C	*VNG0705C*	*VNG0705C*
VNG1179C	*VNG0858C*	*VNG0858C*
VNG1179C	*VNG1251G*	*helA*
VNG1179C	*VNG1252G*	*yhcR*
VNG1179C	*VNG1253C*	*VNG1253C*
VNG1179C	*VNG1287C*	*VNG1287C*
VNG1179C	*VNG1336C*	*VNG1336C*
VNG1179C	*VNG1658C*	*VNG1658C*

VNG1179C	*VNG1903C*	*VNG1903C*
VNG1179C	*VNG2068C*	*VNG2068C*
VNG1179C	*VNG2338G*	*polA2*
VNG1179C	*VNG2339C*	*VNG2339C*
VNG1179C	*VNG2584C*	*VNG2584C*
VNG1179C	*VNG0439C*	*VNG0439C*
VNG1179C	*VNG0546C*	*VNG0546C*
VNG1179C	*VNG1784C*	*VNG1784C*
VNG1179C	*VNG0046G*	*ugd*
VNG1179C	*VNG0180G*	*hop*
VNG1179C	*VNG0494G*	*grpE*
VNG1179C	*VNG0498C*	*VNG0498C*
VNG1179C	*VNG0499G*	*cna*
VNG1179C	*VNG0559G*	*apt*
VNG1179C	*VNG0620G*	*edp*
VNG1179C	*VNG0681G*	*hbd1*
VNG1179C	*VNG0753G*	*ylnA*
VNG1179C	*VNG0862G*	*hisF*
VNG1179C	*VNG0893G*	*udp2*
VNG1179C	*VNG0896G*	*cda*
VNG1179C	*VNG0897G*	*rbsC1*
VNG1179C	*VNG0898G*	*rbsC2*
VNG1179C	*VNG1001G*	*guaB*
VNG1179C	*VNG1103G*	*rpl12p*
VNG1179C	*VNG1104G*	*rpl10p*
VNG1179C	*VNG1105G*	*rpl1p*
VNG1179C	*VNG1108G*	*rpl11p*
VNG1179C	*VNG1162H*	*VNG1162H*
VNG1179C	*VNG1163G*	*hemK*
VNG1179C	*VNG1184G*	*nirJ*
VNG1179C	*VNG1301G*	*cysK*
VNG1179C	*VNG1332G*	*sod2*
VNG1179C	*VNG1462G*	*cdc48a*
VNG1179C	*VNG1478G*	*panB*
VNG1179C	*VNG1592G*	*cysT2*
VNG1179C	*VNG1754G*	*phr1*
VNG1179C	*VNG1764G*	*sop2*
VNG1179C	*VNG1765G*	*htr2*
VNG1179C	*VNG1767G*	*speB*
VNG1179C	*VNG1768G*	*eif5a*
VNG1179C	*VNG1801G*	*hsp1*
VNG1179C	*VNG1866G*	*map*

VNG1179C	*VNG1926G*	*pdhA1*
VNG1179C	*VNG2184G*	*tfbA*
VNG1179C	*VNG2214G*	*dinF*
VNG1179C	*VNG0626G*	*maoC2*
VNG1179C	*VNG1605G*	*gdcH*
VNG1179C	*VNG0978H*	*VNG0978H*
VNG1179C	*VNG1519H*	*VNG1519H*
VNG1179C	*VNG0079H*	*VNG0079H*
VNG1179C	*VNG0204H*	*VNG0204H*
VNG1179C	*VNG0291H*	*VNG0291H*
VNG1179C	*VNG0312H*	*VNG0312H*
VNG1179C	*VNG0408H*	*VNG0408H*
VNG1179C	*VNG0420H*	*VNG0420H*
VNG1179C	*VNG0430H*	*VNG0430H*
VNG1179C	*VNG0492H*	*VNG0492H*
VNG1179C	*VNG0612H*	*VNG0612H*
VNG1179C	*VNG0656H*	*VNG0656H*
VNG1179C	*VNG1017H*	*VNG1017H*
VNG1179C	*VNG1047H*	*VNG1047H*
VNG1179C	*VNG1390H*	*VNG1390H*
VNG1179C	*VNG1394H*	*VNG1394H*
VNG1179C	*VNG1410H*	*VNG1410H*
VNG1179C	*VNG1674H*	*VNG1674H*
VNG1179C	*VNG1777H*	*VNG1777H*
VNG1179C	*VNG1837G*	*ykfB1*
VNG1179C	*VNG1839H*	*VNG1839H*
VNG1179C	*VNG1890H*	*VNG1890H*
VNG1179C	*VNG1902H*	*VNG1902H*
VNG1179C	*VNG2109H*	*VNG2109H*
VNG1179C	*VNG2138G*	*atpB*
VNG1179C	*VNG2139G*	*atpA*
VNG1179C	*VNG2140G*	*atpF*
VNG1179C	*VNG2141G*	*atpC*
VNG1179C	*VNG2142G*	*atpE*
VNG1179C	*VNG2143G*	*atpK*
VNG1179C	*VNG2144G*	*atpI*
VNG1179C	*VNG2146H*	*VNG2146H*
VNG1179C	*VNG2313H*	*VNG2313H*
VNG1179C	*VNG2392H*	*VNG2392H*
VNG1179C	*VNG5141G*	*hepA*
VNG1179C	*VNG5142G*	*tbpC*
VNG1179C	*VNG5177C*	*VNG5177C*

VNG1179C	*VNG6152H*	*VNG6152H*
VNG1179C	*VNG6155H*	*VNG6155H*
VNG1179C	*VNG6153G*	*sojC2*
VNG1179C	*VNG6250G*	*phoT3*
VNG1179C	*VNG6142C*	*VNG6142C*
VNG1179C	*VNG6158H*	*VNG6158H*
VNG1179C	*VNG6157H*	*VNG6157H*
VNG1179C	*VNG6159H*	*VNG6159H*
VNG1179C	*VNG6404H*	*VNG6404H*
VNG1179C	*VNG6416H*	*VNG6416H*
VNG1179C	*VNG6420H*	*VNG6420H*
VNG1179C	*VNG6262G*	*zurM*
VNG1179C	*VNG6264G*	*zurA*
VNG1179C	*VNG6294G*	*perA*
VNG1237C	*VNG0826C*	*VNG0826C*
VNG1237C	*VNG0964C*	*VNG0964C*
VNG1237C	*VNG1238C*	*VNG1238C*
VNG1237C	*VNG1608C*	*VNG1608C*
VNG1237C	*VNG1688C*	*VNG1688C*
VNG1237C	*VNG1689G*	*rpl13p*
VNG1237C	*VNG1690G*	*rpl4e*
VNG1237C	*VNG1691G*	*rpl23p*
VNG1237C	*VNG1692G*	*rpl2p*
VNG1237C	*VNG1693G*	*rps19p*
VNG1237C	*VNG1695G*	*rpl22p*
VNG1237C	*VNG1697G*	*rps3p*
VNG1237C	*VNG1698G*	*rpl29p*
VNG1237C	*VNG1699C*	*VNG1699C*
VNG1237C	*VNG1700G*	*rps17p*
VNG1237C	*VNG1701G*	*rpl14p*
VNG1237C	*VNG1702G*	*rpl24p*
VNG1237C	*VNG1703G*	*rps4e*
VNG1237C	*VNG1705G*	*rpl5p*
VNG1237C	*VNG1706G*	*rps14p*
VNG1237C	*VNG1707G*	*rps8p*
VNG1237C	*VNG1709G*	*rpl6p*
VNG1237C	*VNG1711G*	*rpl32e*
VNG1237C	*VNG1713G*	*rpl19e*
VNG1237C	*VNG1714G*	*rpl18p*
VNG1237C	*VNG1715G*	*rps5p*
VNG1237C	*VNG1716G*	*rpl30p*
VNG1237C	*VNG1718G*	*rpl15p*

VNG1237C	*VNG1719G*	*secY*
VNG1237C	*VNG2296C*	*VNG2296C*
VNG1237C	*VNG1339C*	*VNG1339C*
VNG1237C	*VNG0174G*	*cat1*
VNG1237C	*VNG0245G*	*dtd*
VNG1237C	*VNG0247C*	*VNG0247C*
VNG1237C	*VNG0277G*	*crtI3*
VNG1237C	*VNG0307G*	*trpB*
VNG1237C	*VNG0308G*	*trpA*
VNG1237C	*VNG0309C*	*VNG0309C*
VNG1237C	*VNG0870G*	*gatC*
VNG1237C	*VNG0872G*	*gatA*
VNG1237C	*VNG1150G*	*idsA*
VNG1237C	*VNG1435G*	*asd*
VNG1237C	*VNG1528G*	*nac*
VNG1237C	*VNG1553G*	*cbiF*
VNG1237C	*VNG1554G*	*cbiG*
VNG1237C	*VNG1555G*	*cobH*
VNG1237C	*VNG1557G*	*cbiH*
VNG1237C	*VNG1622G*	*rfcB*
VNG1237C	*VNG1759G*	*htr7*
VNG1237C	*VNG1859G*	*deoC*
VNG1237C	*VNG2397G*	*cysA*
VNG1237C	*VNG1433G*	*rps17e*
VNG1237C	*VNG0049H*	*VNG0049H*
VNG1237C	*VNG0244H*	*VNG0244H*
VNG1237C	*VNG0594H*	*VNG0594H*
VNG1237C	*VNG1034H*	*VNG1034H*
VNG1237C	*VNG1200H*	*VNG1200H*
VNG1237C	*VNG1229H*	*VNG1229H*
VNG1237C	*VNG1380H*	*VNG1380H*
VNG1237C	*VNG1891H*	*VNG1891H*
VNG1237C	*VNG1910H*	*VNG1910H*
VNG1237C	*VNG1956H*	*VNG1956H*
VNG1237C	*VNG2175H*	*VNG2175H*
VNG1237C	*VNG2414H*	*VNG2414H*
VNG1237C	*VNG2415H*	*VNG2415H*
VNG1237C	*VNG1261H*	*VNG1261H*
VNG1237C	*VNG1487H*	*VNG1487H*
VNG1237C	*VNG1672H*	*VNG1672H*
VNG1237C	*VNG0283C*	*VNG0283C*
VNG1237C	*VNG0300C*	*VNG0300C*

VNG1237C	*VNG0563G*	*ndhG2*
VNG1237C	*VNG0565C*	*VNG0565C*
VNG1237C	*VNG0564H*	*VNG0564H*
VNG1237C	*VNG0566C*	*VNG0566C*
VNG1237C	*VNG0570H*	*VNG0570H*
VNG1237C	*VNG0568C*	*VNG0568C*
VNG1237C	*VNG1198C*	*VNG1198C*
VNG1237C	*VNG1228C*	*VNG1228C*
VNG1237C	*VNG1398C*	*VNG1398C*
VNG1237C	*VNG1681C*	*VNG1681C*
VNG1237C	*VNG1687C*	*VNG1687C*
VNG1237C	*VNG1857C*	*VNG1857C*
VNG1237C	*VNG0598C*	*VNG0598C*
VNG1237C	*VNG2138G*	*atpB*
VNG1237C	*VNG2139G*	*atpA*
VNG1237C	*VNG2140G*	*atpF*
VNG1237C	*VNG2141G*	*atpC*
VNG1237C	*VNG2142G*	*atpE*
VNG1237C	*VNG2143G*	*atpK*
VNG1237C	*VNG0137G*	*cca*
VNG1237C	*VNG0172G*	*mutS2*
VNG1237C	*VNG0966G*	*cheR*
VNG1237C	*VNG1030G*	*pgsA*
VNG1237C	*VNG1031C*	*VNG1031C*
VNG1237C	*VNG1033G*	*hisC1*
VNG1237C	*VNG1123G*	*trh7*
VNG1237C	*VNG1607G*	*cheC2*
VNG1237C	*VNG1951G*	*sub*
VNG1237C	*VNG2546G*	*pepB3*
VNG1237C	*VNG0192G*	*ftsZ2*
VNG1237C	*VNG0194H*	*VNG0194H*
VNG1237C	*VNG1376H*	*VNG1376H*
VNG1237C	*VNG1621H*	*VNG1621H*
VNG1237C	*VNG0198H*	*VNG0198H*
VNG1237C	*VNG0492H*	*VNG0492H*
VNG1237C	*VNG0999H*	*VNG0999H*
VNG1237C	*VNG1239H*	*VNG1239H*
VNG1237C	*VNG2174H*	*VNG2174H*
VNG1237C	*VNG2297H*	*VNG2297H*
VNG1237C	*VNG2412H*	*VNG2412H*
VNG1237C	*VNG2413H*	*VNG2413H*
VNG1237C	*VNG5116H*	*VNG5116H*

VNG1237C	*VNG6456H*	*VNG6456H*
VNG1237C	*VNG6113H*	*VNG6113H*
VNG1237C	*VNG6424H*	*VNG6424H*
VNG1237C	*VNG6313G*	*nhaC3*
Trh2	*VNG0419C*	*VNG0419C*
Trh2	*VNG0174G*	*cat1*
Trh2	*VNG1574G*	*cobI*
Trh2	*VNG1576G*	*cbiP*
Trh2	*VNG2363G*	*oppD1*
Trh2	*VNG2365G*	*appF*
Trh2	*VNG2189H*	*VNG2189H*
Trh2	*VNG2035H*	*VNG2035H*
Trh2	*VNG0893G*	*udp2*
Trh2	*VNG0896G*	*cda*
Trh2	*VNG0897G*	*rbsC1*
Trh2	*VNG0898G*	*rbsC2*
Trh2	*VNG0901G*	*rbsA*
Trh2	*VNG0903C*	*VNG0903C*
Trh2	*VNG0172G*	*mutS2*
Trh2	*VNG1951G*	*sub*
Trh2	*VNG2186G*	*hit1*
Trh2	*VNG0697H*	*VNG0697H*
Trh2	*VNG2034H*	*VNG2034H*
Trh2	*VNG6430C*	*VNG6430C*
Trh2	*VNG6437C*	*VNG6437C*
Trh2	*VNG6396H*	*VNG6396H*
Trh2	*VNG6411H*	*VNG6411H*
Trh2	*VNG6432H*	*VNG6432H*
Trh2	*VNG6397H*	*VNG6397H*
Trh2	*VNG6408G*	*phzF*
Trh2	*VNG6401H*	*VNG6401H*
Trh2	*VNG6412H*	*VNG6412H*
Trh2	*VNG6427H*	*VNG6427H*
Trh2	*VNG6395H*	*VNG6395H*
Trh2	*VNG6404H*	*VNG6404H*
Trh2	*VNG6406H*	*VNG6406H*
Trh2	*VNG6407H*	*VNG6407H*
Trh2	*VNG6409H*	*VNG6409H*
Trh2	*VNG6413H*	*VNG6413H*
Trh2	*VNG6416H*	*VNG6416H*
Trh2	*VNG6421H*	*VNG6421H*
Trh2	*VNG6429H*	*VNG6429H*

Trh2	*VNG6431H*	*VNG6431H*
Trh2	*VNG6144G*	*trsE*
Trh3	*VNG1735C*	*VNG1735C*
Trh3	*VNG0181G*	*lpl*
Trh3	*VNG1557G*	*cbiH*
Trh3	*VNG1568G*	*cbiJ*
Trh3	*VNG1700G*	*rps17p*
Trh3	*VNG1701G*	*rpl14p*
Trh3	*VNG1702G*	*rpl24p*
Trh3	*VNG1703G*	*rps4e*
Trh3	*VNG1705G*	*rpl5p*
Trh3	*VNG1706G*	*rps14p*
Trh3	*VNG1707G*	*rps8p*
Trh3	*VNG1709G*	*rpl6p*
Trh3	*VNG1711G*	*rpl32e*
Trh3	*VNG1713G*	*rpl19e*
Trh3	*VNG1714G*	*rpl18p*
Trh3	*VNG1715G*	*rps5p*
Trh3	*VNG1716G*	*rpl30p*
Trh3	*VNG1718G*	*rpl15p*
Trh3	*VNG1719G*	*secY*
Trh3	*VNG1814G*	*carB*
Trh3	*VNG2150G*	*etfB*
Trh3	*VNG2151G*	*etfA*
Trh3	*VNG2420G*	*metA*
Trh3	*VNG2421G*	*hal*
Trh3	*VNG2205H*	*VNG2205H*
Trh3	*VNG1261H*	*VNG1261H*
Trh3	*VNG1907H*	*VNG1907H*
Trh3	*VNG0602C*	*VNG0602C*
Trh3	*VNG0137G*	*cca*
Trh3	*VNG0180G*	*hop*
Trh3	*VNG0966G*	*cheR*
Trh3	*VNG1073G*	*lfl1*
Trh3	*VNG1079G*	*menB*
Trh3	*VNG1197G*	*bcp*
Trh3	*VNG1811G*	*eye*
Trh3	*VNG2648G*	*rps10p*
Trh3	*VNG2649G*	*eef1a*
Trh3	*VNG0488H*	*VNG0488H*
Trh3	*VNG0492H*	*VNG0492H*
Trh3	*VNG2204H*	*VNG2204H*

Trh4	*VNG0268C*	*VNG0268C*
Trh4	*VNG0274C*	*VNG0274C*
Trh4	*VNG0361C*	*VNG0361C*
Trh4	*VNG0363G*	*nfi*
Trh4	*VNG0405C*	*VNG0405C*
Trh4	*VNG0421C*	*VNG0421C*
Trh4	*VNG0525C*	*VNG0525C*
Trh4	*VNG0527C*	*VNG0527C*
Trh4	*VNG1069C*	*VNG1069C*
Trh4	*VNG1296C*	*VNG1296C*
Trh4	*VNG1297C*	*VNG1297C*
Trh4	*VNG1735C*	*VNG1735C*
Trh4	*VNG1779C*	*VNG1779C*
Trh4	*VNG2307C*	*VNG2307C*
Trh4	*VNG2369C*	*VNG2369C*
Trh4	*VNG2466C*	*VNG2466C*
Trh4	*VNG2474C*	*VNG2474C*
Trh4	*VNG2475C*	*VNG2475C*
Trh4	*VNG2610C*	*VNG2610C*
Trh4	*VNG0124C*	*VNG0124C*
Trh4	*VNG0271C*	*VNG0271C*
Trh4	*VNG0713C*	*VNG0713C*
Trh4	*VNG1845C*	*VNG1845C*
Trh4	*VNG2470C*	*VNG2470C*
Trh4	*VNG0166G*	*psmA2*
Trh4	*VNG0174G*	*cat1*
Trh4	*VNG0181G*	*lpl*
Trh4	*VNG0281G*	*soxB*
Trh4	*VNG0307G*	*trpB*
Trh4	*VNG0308G*	*trpA*
Trh4	*VNG0309C*	*VNG0309C*
Trh4	*VNG0371G*	*acd1*
Trh4	*VNG0382G*	*aroE*
Trh4	*VNG0403G*	*proS*
Trh4	*VNG0666G*	*ctaB*
Trh4	*VNG0667G*	*trp4*
Trh4	*VNG0673G*	*mcmA2*
Trh4	*VNG0674C*	*VNG0674C*
Trh4	*VNG0796G*	*cgs*
Trh4	*VNG0872G*	*gatA*
Trh4	*VNG1097G*	*cysS*
Trh4	*VNG1370G*	*hemU*

Trh4	*VNG1371G*	*hemV2*
Trh4	*VNG1432G*	*dhs*
Trh4	*VNG1528G*	*nac*
Trh4	*VNG1550G*	*cbiT*
Trh4	*VNG1551G*	*cbiL*
Trh4	*VNG1553G*	*cbiF*
Trh4	*VNG1554G*	*cbiG*
Trh4	*VNG1555G*	*cobH*
Trh4	*VNG1557G*	*cbiH*
Trh4	*VNG1622G*	*rfcB*
Trh4	*VNG1816G*	*trh3*
Trh4	*VNG1818G*	*idi*
Trh4	*VNG1859G*	*deoC*
Trh4	*VNG1882G*	*nadA*
Trh4	*VNG1883G*	*nadB*
Trh4	*VNG1884G*	*nadC*
Trh4	*VNG2150G*	*etfB*
Trh4	*VNG2151G*	*etfA*
Trh4	*VNG2216G*	*lip*
Trh4	*VNG2217G*	*pdhA2*
Trh4	*VNG2218G*	*pdhB*
Trh4	*VNG2219G*	*dsa*
Trh4	*VNG2220G*	*lpdA*
Trh4	*VNG2290G*	*maoC1*
Trh4	*VNG2291G*	*cat*
Trh4	*VNG2359G*	*appB*
Trh4	*VNG2361G*	*appC*
Trh4	*VNG2363G*	*oppD1*
Trh4	*VNG2365G*	*appF*
Trh4	*VNG2420G*	*metA*
Trh4	*VNG2421G*	*hal*
Trh4	*VNG2604G*	*thi1*
Trh4	*VNG2606G*	*thiD*
Trh4	*VNG1693G*	*rps19p*
Trh4	*VNG1695G*	*rpl22p*
Trh4	*VNG1697G*	*rps3p*
Trh4	*VNG1698G*	*rpl29p*
Trh4	*VNG1699C*	*VNG1699C*
Trh4	*VNG1700G*	*rps17p*
Trh4	*VNG1701G*	*rpl14p*
Trh4	*VNG1702G*	*rpl24p*
Trh4	*VNG1703G*	*rps4e*

Trh4	*VNG1705G*	*rpl5p*
Trh4	*VNG1706G*	*rps14p*
Trh4	*VNG1707G*	*rps8p*
Trh4	*VNG1709G*	*rpl6p*
Trh4	*VNG1711G*	*rpl32e*
Trh4	*VNG1713G*	*rpl19e*
Trh4	*VNG1714G*	*rpl18p*
Trh4	*VNG1715G*	*rps5p*
Trh4	*VNG1716G*	*rpl30p*
Trh4	*VNG1718G*	*rpl15p*
Trh4	*VNG1719G*	*secY*
Trh4	*VNG1406G*	*rhl*
Trh4	*VNG2076G*	*rpl40e*
Trh4	*VNG0055H*	*VNG0055H*
Trh4	*VNG0068H*	*VNG0068H*
Trh4	*VNG0138H*	*VNG0138H*
Trh4	*VNG0184H*	*VNG0184H*
Trh4	*VNG0219H*	*VNG0219H*
Trh4	*VNG0244H*	*VNG0244H*
Trh4	*VNG0296H*	*VNG0296H*
Trh4	*VNG0652H*	*VNG0652H*
Trh4	*VNG0780H*	*VNG0780H*
Trh4	*VNG0861H*	*VNG0861H*
Trh4	*VNG0979H*	*VNG0979H*
Trh4	*VNG1002H*	*VNG1002H*
Trh4	*VNG1025H*	*VNG1025H*
Trh4	*VNG1034H*	*VNG1034H*
Trh4	*VNG1042H*	*VNG1042H*
Trh4	*VNG1302H*	*VNG1302H*
Trh4	*VNG1484H*	*VNG1484H*
Trh4	*VNG1678H*	*VNG1678H*
Trh4	*VNG1940H*	*VNG1940H*
Trh4	*VNG2185H*	*VNG2185H*
Trh4	*VNG2340H*	*VNG2340H*
Trh4	*VNG2451H*	*VNG2451H*
Trh4	*VNG2497H*	*VNG2497H*
Trh4	*VNG2498H*	*VNG2498H*
Trh4	*VNG0067H*	*VNG0067H*
Trh4	*VNG1261H*	*VNG1261H*
Trh4	*VNG1487H*	*VNG1487H*
Trh4	*VNG1558H*	*VNG1558H*
Trh4	*VNG1559H*	*VNG1559H*

Trh4	*VNG1561C*	*VNG1561C*
Trh4	*VNG1562H*	*VNG1562H*
Trh4	*VNG1807H*	*VNG1807H*
Trh4	*VNG2581H*	*VNG2581H*
Trh4	*VNG0463C*	*VNG0463C*
Trh4	*VNG1388H*	*VNG1388H*
Trh4	*VNG1389C*	*VNG1389C*
Trh4	*VNG0147C*	*VNG0147C*
Trh4	*VNG0153C*	*VNG0153C*
Trh4	*VNG0240C*	*VNG0240C*
Trh4	*VNG0360C*	*VNG0360C*
Trh4	*VNG0537C*	*VNG0537C*
Trh4	*VNG0539C*	*VNG0539C*
Trh4	*VNG0602C*	*VNG0602C*
Trh4	*VNG0853C*	*VNG0853C*
Trh4	*VNG1483C*	*VNG1483C*
Trh4	*VNG1548C*	*VNG1548C*
Trh4	*VNG1857C*	*VNG1857C*
Trh4	*VNG2012C*	*VNG2012C*
Trh4	*VNG2338G*	*polA2*
Trh4	*VNG2339C*	*VNG2339C*
Trh4	*VNG0035C*	*VNG0035C*
Trh4	*VNG0006G*	*glmS*
Trh4	*VNG0137G*	*cca*
Trh4	*VNG0164G*	*hef*
Trh4	*VNG0172G*	*mutS2*
Trh4	*VNG0180G*	*hop*
Trh4	*VNG0428G*	*fad2*
Trh4	*VNG0610G*	*hhoA*
Trh4	*VNG0665G*	*coxB1*
Trh4	*VNG0753G*	*ylnA*
Trh4	*VNG0793G*	*htr6*
Trh4	*VNG0806G*	*htr4*
Trh4	*VNG0835G*	*idr2*
Trh4	*VNG0862G*	*hisF*
Trh4	*VNG0873G*	*ykhA*
Trh4	*VNG0920H*	*VNG0920H*
Trh4	*VNG0921G*	*potA1*
Trh4	*VNG0946G*	*minD1*
Trh4	*VNG1154H*	*VNG1154H*
Trh4	*VNG1156G*	*hsp*
Trh4	*VNG1184G*	*nirJ*

Trh4	*VNG1294G*	*slyD*
Trh4	*VNG1395G*	*htr9*
Trh4	*VNG1520G*	*mutY*
Trh4	*VNG1733G*	*htr17*
Trh4	*VNG1760G*	*htr5*
Trh4	*VNG1815G*	*carA*
Trh4	*VNG1853G*	*eif2ba*
Trh4	*VNG1887G*	*gpm*
Trh4	*VNG1987G*	*secD*
Trh4	*VNG2043G*	*ham1*
Trh4	*VNG2138G*	*atpB*
Trh4	*VNG2139G*	*atpA*
Trh4	*VNG2140G*	*atpF*
Trh4	*VNG2141G*	*atpC*
Trh4	*VNG2184G*	*tfbA*
Trh4	*VNG2203G*	*prsA*
Trh4	*VNG2214G*	*dinF*
Trh4	*VNG2377G*	*nosY*
Trh4	*VNG2378G*	*nosF1*
Trh4	*VNG2462G*	*dpa*
Trh4	*VNG2648G*	*rps10p*
Trh4	*VNG2649G*	*eef1a*
Trh4	*VNG0486G*	*hat1*
Trh4	*VNG0626G*	*maoC2*
Trh4	*VNG2060G*	*phnP*
Trh4	*VNG2062G*	*atp*
Trh4	*VNG2496G*	*ferB*
Trh4	*VNG0192G*	*ftsZ2*
Trh4	*VNG0194H*	*VNG0194H*
Trh4	*VNG0978H*	*VNG0978H*
Trh4	*VNG1096H*	*VNG1096H*
Trh4	*VNG1189H*	*VNG1189H*
Trh4	*VNG1376H*	*VNG1376H*
Trh4	*VNG1519H*	*VNG1519H*
Trh4	*VNG1621H*	*VNG1621H*
Trh4	*VNG1832H*	*VNG1832H*
Trh4	*VNG1999H*	*VNG1999H*
Trh4	*VNG2177H*	*VNG2177H*
Trh4	*VNG2495H*	*VNG2495H*
Trh4	*VNG0039H*	*VNG0039H*
Trh4	*VNG0054H*	*VNG0054H*
Trh4	*VNG0297H*	*VNG0297H*

Trh4	*VNG0312H*	*VNG0312H*
Trh4	*VNG0347H*	*VNG0347H*
Trh4	*VNG0370H*	*VNG0370H*
Trh4	*VNG0402H*	*VNG0402H*
Trh4	*VNG0408H*	*VNG0408H*
Trh4	*VNG0420H*	*VNG0420H*
Trh4	*VNG0430H*	*VNG0430H*
Trh4	*VNG0492H*	*VNG0492H*
Trh4	*VNG0671H*	*VNG0671H*
Trh4	*VNG1751H*	*VNG1751H*
Trh4	*VNG1777H*	*VNG1777H*
Trh4	*VNG1965H*	*VNG1965H*
Trh4	*VNG2115H*	*VNG2115H*
Trh4	*VNG2230H*	*VNG2230H*
Trh4	*VNG2392H*	*VNG2392H*
Trh4	*VNG2603H*	*VNG2603H*
Trh4	*VNG5218H*	*VNG5218H*
Trh4	*VNG5022G*	*gvpJ1*
Trh4	*VNG6204H*	*VNG6204H*
Trh4	*VNG6432H*	*VNG6432H*
Trh4	*VNG6209H*	*VNG6209H*
Trh4	*VNG6177G*	*kdpB*
Trh4	*VNG6178G*	*kdpC*
Trh4	*VNG6247G*	*trkA4*
Trh4	*VNG6246G*	*gvpO2*
Trh4	*VNG6303G*	*exsB*
Trh4	*VNG6305C*	*VNG6305C*
Trh4	*VNG6306C*	*VNG6306C*
Trh4	*VNG6143H*	*VNG6143H*
Trh4	*VNG6203H*	*VNG6203H*
Trh4	*VNG6404H*	*VNG6404H*
Trh4	*VNG6406H*	*VNG6406H*
Trh4	*VNG6416H*	*VNG6416H*
Trh4	*VNG6431H*	*VNG6431H*
Trh4	*VNG6022G*	*gvpJ1*
Trh4	*VNG6235G*	*gvpH2*
Trh4	*VNG6144G*	*trsE*
Trh4	*VNG6233G*	*gvpI2*
Trh4	*VNG6262G*	*zurM*
Trh4	*VNG6264G*	*zurA*
Trh4	*VNG6315G*	*arcB*
Trh4	*VNG6316G*	*arcC*

Trh6	*VNG2575G*	*rimI*
Trh6	*VNG0361C*	*VNG0361C*
Trh6	*VNG0363G*	*nfi*
Trh6	*VNG0388C*	*VNG0388C*
Trh6	*VNG0396C*	*VNG0396C*
Trh6	*VNG0405C*	*VNG0405C*
Trh6	*VNG0525C*	*VNG0525C*
Trh6	*VNG0527C*	*VNG0527C*
Trh6	*VNG0875C*	*VNG0875C*
Trh6	*VNG1069C*	*VNG1069C*
Trh6	*VNG1497C*	*VNG1497C*
Trh6	*VNG1735C*	*VNG1735C*
Trh6	*VNG1779C*	*VNG1779C*
Trh6	*VNG1941C*	*VNG1941C*
Trh6	*VNG1982C*	*VNG1982C*
Trh6	*VNG1984G*	*rnh*
Trh6	*VNG2021C*	*VNG2021C*
Trh6	*VNG2307C*	*VNG2307C*
Trh6	*VNG2316C*	*VNG2316C*
Trh6	*VNG2317G*	*cbiO1*
Trh6	*VNG2474C*	*VNG2474C*
Trh6	*VNG2475C*	*VNG2475C*
Trh6	*VNG2610C*	*VNG2610C*
Trh6	*VNG0271C*	*VNG0271C*
Trh6	*VNG0713C*	*VNG0713C*
Trh6	*VNG1874C*	*VNG1874C*
Trh6	*VNG2255C*	*VNG2255C*
Trh6	*VNG2555C*	*VNG2555C*
Trh6	*VNG0166G*	*psmA2*
Trh6	*VNG0174G*	*cat1*
Trh6	*VNG0181G*	*lpl*
Trh6	*VNG0307G*	*trpB*
Trh6	*VNG0308G*	*trpA*
Trh6	*VNG0309C*	*VNG0309C*
Trh6	*VNG0446G*	*gcd*
Trh6	*VNG0448G*	*pyrC*
Trh6	*VNG0666G*	*ctaB*
Trh6	*VNG0667G*	*trp4*
Trh6	*VNG0673G*	*mcmA2*
Trh6	*VNG0674C*	*VNG0674C*
Trh6	*VNG0680G*	*fdfT*
Trh6	*VNG0775G*	*acd2*

Trh6	*VNG0872G*	*gatA*
Trh6	*VNG1172G*	*metB*
Trh6	*VNG1528G*	*nac*
Trh6	*VNG1553G*	*cbiF*
Trh6	*VNG1554G*	*cbiG*
Trh6	*VNG1555G*	*cobH*
Trh6	*VNG1557G*	*cbiH*
Trh6	*VNG1816G*	*trh3*
Trh6	*VNG1818G*	*idi*
Trh6	*VNG1834G*	*hyrA*
Trh6	*VNG1859G*	*deoC*
Trh6	*VNG1914G*	*ppiA*
Trh6	*VNG1932G*	*nolA*
Trh6	*VNG2150G*	*etfB*
Trh6	*VNG2151G*	*etfA*
Trh6	*VNG2216G*	*lip*
Trh6	*VNG2217G*	*pdhA2*
Trh6	*VNG2218G*	*pdhB*
Trh6	*VNG2219G*	*dsa*
Trh6	*VNG2220G*	*lpdA*
Trh6	*VNG2290G*	*maoC1*
Trh6	*VNG2291G*	*cat*
Trh6	*VNG2359G*	*appB*
Trh6	*VNG2361G*	*appC*
Trh6	*VNG2363G*	*oppD1*
Trh6	*VNG2365G*	*appF*
Trh6	*VNG2417G*	*polA1*
Trh6	*VNG2604G*	*thi1*
Trh6	*VNG2606G*	*thiD*
Trh6	*VNG2636G*	*uvrA*
Trh6	*VNG0055H*	*VNG0055H*
Trh6	*VNG0138H*	*VNG0138H*
Trh6	*VNG0184H*	*VNG0184H*
Trh6	*VNG0219H*	*VNG0219H*
Trh6	*VNG0404H*	*VNG0404H*
Trh6	*VNG0717H*	*VNG0717H*
Trh6	*VNG0733H*	*VNG0733H*
Trh6	*VNG0861H*	*VNG0861H*
Trh6	*VNG0883H*	*VNG0883H*
Trh6	*VNG0979H*	*VNG0979H*
Trh6	*VNG1002H*	*VNG1002H*
Trh6	*VNG1042H*	*VNG1042H*

Trh6	*VNG1112H*	*VNG1112H*
Trh6	*VNG1422H*	*VNG1422H*
Trh6	*VNG1891H*	*VNG1891H*
Trh6	*VNG1920H*	*VNG1920H*
Trh6	*VNG2497H*	*VNG2497H*
Trh6	*VNG2498H*	*VNG2498H*
Trh6	*VNG2582H*	*VNG2582H*
Trh6	*VNG1261H*	*VNG1261H*
Trh6	*VNG1382H*	*VNG1382H*
Trh6	*VNG1487H*	*VNG1487H*
Trh6	*VNG1807H*	*VNG1807H*
Trh6	*VNG2581H*	*VNG2581H*
Trh6	*VNG0040C*	*VNG0040C*
Trh6	*VNG0142C*	*VNG0142C*
Trh6	*VNG0463C*	*VNG0463C*
Trh6	*VNG1244C*	*VNG1244C*
Trh6	*VNG1325C*	*VNG1325C*
Trh6	*VNG1388H*	*VNG1388H*
Trh6	*VNG1389C*	*VNG1389C*
Trh6	*VNG0147C*	*VNG0147C*
Trh6	*VNG0153C*	*VNG0153C*
Trh6	*VNG0360C*	*VNG0360C*
Trh6	*VNG0376G*	*ftsZ1*
Trh6	*VNG0378C*	*VNG0378C*
Trh6	*VNG0394C*	*VNG0394C*
Trh6	*VNG0466C*	*VNG0466C*
Trh6	*VNG0537C*	*VNG0537C*
Trh6	*VNG0539C*	*VNG0539C*
Trh6	*VNG0602C*	*VNG0602C*
Trh6	*VNG1249C*	*VNG1249C*
Trh6	*VNG1833C*	*VNG1833C*
Trh6	*VNG1857C*	*VNG1857C*
Trh6	*VNG2116C*	*VNG2116C*
Trh6	*VNG2543C*	*VNG2543C*
Trh6	*VNG0006G*	*glmS*
Trh6	*VNG0098G*	*rimK*
Trh6	*VNG0137G*	*cca*
Trh6	*VNG0163G*	*mutS1*
Trh6	*VNG0164G*	*hef*
Trh6	*VNG0172G*	*mutS2*
Trh6	*VNG0180G*	*hop*
Trh6	*VNG0401G*	*epf2*

Trh6	*VNG0428G*	*fad2*
Trh6	*VNG0494G*	*grpE*
Trh6	*VNG0504G*	*gbp5*
Trh6	*VNG0665G*	*coxB1*
Trh6	*VNG0716G*	*afsQ2*
Trh6	*VNG0720G*	*dip2*
Trh6	*VNG0862G*	*hisF*
Trh6	*VNG0920H*	*VNG0920H*
Trh6	*VNG0921G*	*potA1*
Trh6	*VNG0938G*	*gufA*
Trh6	*VNG0946G*	*minD1*
Trh6	*VNG0966G*	*cheR*
Trh6	*VNG1001G*	*guaB*
Trh6	*VNG1184G*	*nirJ*
Trh6	*VNG1284G*	*trkH1*
Trh6	*VNG1365C*	*VNG1365C*
Trh6	*VNG1366H*	*VNG1366H*
Trh6	*VNG1367G*	*srp19*
Trh6	*VNG1520G*	*mutY*
Trh6	*VNG1733G*	*htr17*
Trh6	*VNG1815G*	*carA*
Trh6	*VNG1853G*	*eif2ba*
Trh6	*VNG1887G*	*gpm*
Trh6	*VNG1929G*	*tmk*
Trh6	*VNG1987G*	*secD*
Trh6	*VNG2003G*	*truA*
Trh6	*VNG2005G*	*hisS*
Trh6	*VNG2138G*	*atpB*
Trh6	*VNG2214G*	*dinF*
Trh6	*VNG2284G*	*hisJ*
Trh6	*VNG2373G*	*tnaA*
Trh6	*VNG2648G*	*rps10p*
Trh6	*VNG2649G*	*eef1a*
Trh6	*VNG2071G*	*lfl2*
Trh6	*VNG0192G*	*ftsZ2*
Trh6	*VNG0194H*	*VNG0194H*
Trh6	*VNG0978H*	*VNG0978H*
Trh6	*VNG1189H*	*VNG1189H*
Trh6	*VNG1519H*	*VNG1519H*
Trh6	*VNG2495H*	*VNG2495H*
Trh6	*VNG0054H*	*VNG0054H*
Trh6	*VNG0125H*	*VNG0125H*

Trh6	*VNG0141H*	*VNG0141H*
Trh6	*VNG0312H*	*VNG0312H*
Trh6	*VNG0408H*	*VNG0408H*
Trh6	*VNG0430H*	*VNG0430H*
Trh6	*VNG0447H*	*VNG0447H*
Trh6	*VNG0472H*	*VNG0472H*
Trh6	*VNG0492H*	*VNG0492H*
Trh6	*VNG0595H*	*VNG0595H*
Trh6	*VNG0617H*	*VNG0617H*
Trh6	*VNG0671H*	*VNG0671H*
Trh6	*VNG0738H*	*VNG0738H*
Trh6	*VNG0782H*	*VNG0782H*
Trh6	*VNG1291H*	*VNG1291H*
Trh6	*VNG1723H*	*VNG1723H*
Trh6	*VNG1777H*	*VNG1777H*
Trh6	*VNG1919H*	*VNG1919H*
Trh6	*VNG1921H*	*VNG1921H*
Trh6	*VNG1983H*	*VNG1983H*
Trh6	*VNG2292H*	*VNG2292H*
Trh6	*VNG2313H*	*VNG2313H*
Trh6	*VNG2554H*	*VNG2554H*
Trh6	*VNG2603H*	*VNG2603H*
Trh6	*VNG2634H*	*VNG2634H*
Trh6	*VNG2640G*	*gcvT2*
Trh6	*VNG2641H*	*VNG2641H*
Trh7	*VNG0421C*	*VNG0421C*
Trh7	*VNG0174G*	*cat1*
Trh7	*VNG0303G*	*lon*
Trh7	*VNG0627G*	*citE*
Trh7	*VNG1557G*	*cbiH*
Trh7	*VNG1816G*	*trh3*
Trh7	*VNG1818G*	*idi*
Trh7	*VNG1859G*	*deoC*
Trh7	*VNG0138H*	*VNG0138H*
Trh7	*VNG0244H*	*VNG0244H*
Trh7	*VNG2626H*	*VNG2626H*
Trh7	*VNG1261H*	*VNG1261H*
Trh7	*VNG1388H*	*VNG1388H*
Trh7	*VNG1389C*	*VNG1389C*
Trh7	*VNG0300C*	*VNG0300C*
Trh7	*VNG0301C*	*VNG0301C*
Trh7	*VNG1857C*	*VNG1857C*

Trh7	*VNG2625C*	*VNG2625C*
Trh7	*VNG0035C*	*VNG0035C*
Trh7	*VNG0172G*	*mutS2*
Trh7	*VNG1733G*	*htr17*
Trh7	*VNG1815G*	*carA*
Trh7	*VNG0626G*	*maoC2*
Trh7	*VNG1376H*	*VNG1376H*
Trh7	*VNG1519H*	*VNG1519H*
Trh7	*VNG2495H*	*VNG2495H*
Trh7	*VNG0312H*	*VNG0312H*
Trh7	*VNG0408H*	*VNG0408H*
Trh7	*VNG0420H*	*VNG0420H*
Trh7	*VNG6152H*	*VNG6152H*
Trh7	*VNG6153G*	*sojC2*
Trh7	*VNG6246G*	*gvpO2*
Trh7	*VNG6157H*	*VNG6157H*
Trh7	*VNG6416H*	*VNG6416H*

Appendix E. Lrp binding sites within each promoter

	Lrp	AsnC	VNG1179C	VNG1237C	Trh2	Trh3	Trh4	Trh6	Trh7	Number_of_binding
Targets										
Canonical_Name	Gene_Name									
VNG1557G	*cbiH*	1	1	1	0	1	1	1	1	7
VNG1261H	*VNG1261H*	1	1	1	0	1	1	1	1	7
VNG0172G	*mutS2*	1	0	1	1	0	1	1	1	6
VNG0492H	*VNG0492H*	1	1	1	0	1	1	1	0	6
VNG1711G	*rpl32e*	1	1	1	0	1	1	0	0	5
VNG1713G	*rpl19e*	1	1	1	0	1	1	0	0	5
VNG1714G	*rpl18p*	1	1	1	0	1	1	0	0	5
VNG1715G	*rps5p*	1	1	1	0	1	1	0	0	5
VNG1716G	*rpl30p*	1	1	1	0	1	1	0	0	5
VNG1718G	*rpl15p*	1	1	1	0	1	1	0	0	5
VNG1719G	*secY*	1	1	1	0	1	1	0	0	5
VNG0181G	*lpl*	1	1	0	0	1	1	1	0	5
VNG1553G	*cbiF*	1	1	1	0	0	1	1	0	5
VNG1554G	*cbiG*	1	1	1	0	0	1	1	0	5
VNG1555G	*cobH*	1	1	1	0	0	1	1	0	5
VNG2150G	*etfB*	1	1	0	0	1	1	1	0	5
VNG2151G	*etfA*	1	1	0	0	1	1	1	0	5
VNG0244H	*VNG0244H*	1	1	1	0	0	1	0	1	5
VNG1388H	*VNG1388H*	1	1	0	0	0	1	1	1	5
VNG1389C	*VNG1389C*	1	1	0	0	0	1	1	1	5
VNG0137G	*cca*	1	0	1	0	1	1	1	0	5
VNG0180G	*hop*	1	1	0	0	1	1	1	0	5
VNG2138G	*atpB*	1	1	1	0	0	1	1	0	5
VNG1519H	*VNG1519H*	1	1	0	0	0	1	1	1	5
VNG0408H	*VNG0408H*	1	1	0	0	0	1	1	1	5
VNG6416H	*VNG6416H*	1	1	0	1	0	1	0	1	5
VNG0174G	*cat1*	0	0	1	1	0	1	1	1	5
VNG0405C	*VNG0405C*	1	1	0	0	0	1	1	0	4
VNG0421C	*VNG0421C*	1	1	0	0	0	1	0	1	4
VNG1069C	*VNG1069C*	1	1	0	0	0	1	1	0	4
VNG1700G	*rps17p*	1	0	1	0	1	1	0	0	4
VNG1701G	*rpl14p*	1	0	1	0	1	1	0	0	4
VNG1702G	*rpl24p*	1	0	1	0	1	1	0	0	4
VNG1703G	*rps4e*	1	0	1	0	1	1	0	0	4
VNG1705G	*rpl5p*	1	0	1	0	1	1	0	0	4
VNG1706G	*rps14p*	1	0	1	0	1	1	0	0	4
VNG1707G	*rps8p*	1	0	1	0	1	1	0	0	4

VNG1709G	*rpl6p*	1	0	1	0	1	1	0	0	4
VNG1735C	*VNG1735C*	1	0	0	0	1	1	1	0	4
VNG1779C	*VNG1779C*	1	1	0	0	0	1	1	0	4
VNG2610C	*VNG2610C*	1	1	0	0	0	1	1	0	4
VNG0713C	*VNG0713C*	1	1	0	0	0	1	1	0	4
VNG0307G	*trpB*	1	0	1	0	0	1	1	0	4
VNG0308G	*trpA*	1	0	1	0	0	1	1	0	4
VNG0309C	*VNG0309C*	1	0	1	0	0	1	1	0	4
VNG0872G	*gatA*	1	0	1	0	0	1	1	0	4
VNG1528G	*nac*	1	0	1	0	0	1	1	0	4
VNG1816G	*trh3*	1	0	0	0	0	1	1	1	4
VNG1818G	*idi*	1	0	0	0	0	1	1	1	4
VNG2220G	*lpdA*	1	1	0	0	0	1	1	0	4
VNG2363G	*oppD1*	1	0	0	1	0	1	1	0	4
VNG2365G	*appF*	1	0	0	1	0	1	1	0	4
VNG0138H	*VNG0138H*	1	0	0	0	0	1	1	1	4
VNG0184H	*VNG0184H*	1	1	0	0	0	1	1	0	4
VNG0861H	*VNG0861H*	1	1	0	0	0	1	1	0	4
VNG1002H	*VNG1002H*	1	1	0	0	0	1	1	0	4
VNG1042H	*VNG1042H*	1	1	0	0	0	1	1	0	4
VNG1487H	*VNG1487H*	1	0	1	0	0	1	1	0	4
VNG0602C	*VNG0602C*	1	0	0	0	1	1	1	0	4
VNG0862G	*hisF*	1	1	0	0	0	1	1	0	4
VNG0966G	*cheR*	1	0	1	0	1	0	1	0	4
VNG1184G	*nirJ*	1	1	0	0	0	1	1	0	4
VNG1815G	*carA*	1	0	0	0	0	1	1	1	4
VNG2139G	*atpA*	1	1	1	0	0	1	0	0	4
VNG2140G	*atpF*	1	1	1	0	0	1	0	0	4
VNG2141G	*atpC*	1	1	1	0	0	1	0	0	4
VNG0626G	*maoC2*	1	1	0	0	0	1	0	1	4
VNG0192G	*ftsZ2*	1	0	1	0	0	1	1	0	4
VNG0194H	*VNG0194H*	1	0	1	0	0	1	1	0	4
VNG1376H	*VNG1376H*	1	0	1	0	0	1	0	1	4
VNG2495H	*VNG2495H*	1	0	0	0	0	1	1	1	4
VNG0420H	*VNG0420H*	1	1	0	0	0	1	0	1	4
VNG0430H	*VNG0430H*	1	1	0	0	0	1	1	0	4
VNG1777H	*VNG1777H*	1	1	0	0	0	1	1	0	4
VNG6404H	*VNG6404H*	1	1	0	1	0	1	0	0	4
VNG0312H	*VNG0312H*	0	1	0	0	0	1	1	1	4
VNG1859G	*deoC*	0	0	1	0	0	1	1	1	4
VNG1857C	*VNG1857C*	0	0	1	0	0	1	1	1	4
VNG0361C	*VNG0361C*	1	0	0	0	0	1	1	0	3
VNG0363G	*nfi*	1	0	0	0	0	1	1	0	3
VNG1693G	*rps19p*	1	0	1	0	0	1	0	0	3
VNG1695G	*rpl22p*	1	0	1	0	0	1	0	0	3

VNG1697G	*rps3p*	1	0	1	0	0	1	0	0	3
VNG1698G	*rpl29p*	1	0	1	0	0	1	0	0	3
VNG1699C	*VNG1699C*	1	0	1	0	0	1	0	0	3
VNG2307C	*VNG2307C*	1	0	0	0	0	1	1	0	3
VNG2474C	*VNG2474C*	1	0	0	0	0	1	1	0	3
VNG2475C	*VNG2475C*	1	0	0	0	0	1	1	0	3
VNG0271C	*VNG0271C*	1	0	0	0	0	1	1	0	3
VNG0166G	*psmA2*	1	0	0	0	0	1	1	0	3
VNG0627G	*citE*	1	1	0	0	0	0	0	1	3
VNG0673G	*mcmA2*	1	0	0	0	0	1	1	0	3
VNG0674C	*VNG0674C*	1	0	0	0	0	1	1	0	3
VNG2290G	*maoC1*	1	0	0	0	0	1	1	0	3
VNG2291G	*cat*	1	0	0	0	0	1	1	0	3
VNG2359G	*appB*	1	0	0	0	0	1	1	0	3
VNG2361G	*appC*	1	0	0	0	0	1	1	0	3
VNG2604G	*thi1*	1	0	0	0	0	1	1	0	3
VNG2606G	*thiD*	1	0	0	0	0	1	1	0	3
VNG0055H	*VNG0055H*	1	0	0	0	0	1	1	0	3
VNG0219H	*VNG0219H*	1	0	0	0	0	1	1	0	3
VNG1891H	*VNG1891H*	1	0	1	0	0	0	1	0	3
VNG2497H	*VNG2497H*	1	0	0	0	0	1	1	0	3
VNG2498H	*VNG2498H*	1	0	0	0	0	1	1	0	3
VNG1807H	*VNG1807H*	1	0	0	0	0	1	1	0	3
VNG2581H	*VNG2581H*	1	0	0	0	0	1	1	0	3
VNG0147C	*VNG0147C*	1	0	0	0	0	1	1	0	3
VNG0360C	*VNG0360C*	1	0	0	0	0	1	1	0	3
VNG0537C	*VNG0537C*	1	0	0	0	0	1	1	0	3
VNG0539C	*VNG0539C*	1	0	0	0	0	1	1	0	3
VNG0035C	*VNG0035C*	1	0	0	0	0	1	0	1	3
VNG0006G	*glmS*	1	0	0	0	0	1	1	0	3
VNG0164G	*hef*	1	0	0	0	0	1	1	0	3
VNG0494G	*grpE*	1	1	0	0	0	0	1	0	3
VNG0920H	*VNG0920H*	1	0	0	0	0	1	1	0	3
VNG0921G	*potA1*	1	0	0	0	0	1	1	0	3
VNG1001G	*guaB*	1	1	0	0	0	0	1	0	3
VNG1520G	*mutY*	1	0	0	0	0	1	1	0	3
VNG1987G	*secD*	1	0	0	0	0	1	1	0	3
VNG2142G	*atpE*	1	1	1	0	0	0	0	0	3
VNG1189H	*VNG1189H*	1	0	0	0	0	1	1	0	3
VNG0054H	*VNG0054H*	1	0	0	0	0	1	1	0	3
VNG0671H	*VNG0671H*	1	0	0	0	0	1	1	0	3
VNG2603H	*VNG2603H*	1	0	0	0	0	1	1	0	3
VNG6432H	*VNG6432H*	1	0	0	1	0	1	0	0	3
VNG6246G	*gvpO2*	1	0	0	0	0	1	0	1	3
VNG6144G	*trsE*	1	0	0	1	0	1	0	0	3

VNG6431H	*VNG6431H*	1	0	0	1	0	1	0	0	3
VNG0667G	*trp4*	0	1	0	0	0	1	1	0	3
VNG2216G	*lip*	0	1	0	0	0	1	1	0	3
VNG2217G	*pdhA2*	0	1	0	0	0	1	1	0	3
VNG2218G	*pdhB*	0	1	0	0	0	1	1	0	3
VNG2219G	*dsa*	0	1	0	0	0	1	1	0	3
VNG2420G	*metA*	0	1	0	0	1	1	0	0	3
VNG2421G	*hal*	0	1	0	0	1	1	0	0	3
VNG0979H	*VNG0979H*	0	1	0	0	0	1	1	0	3
VNG2214G	*dinF*	0	1	0	0	0	1	1	0	3
VNG0978H	*VNG0978H*	0	1	0	0	0	1	1	0	3
VNG2648G	*rps10p*	0	0	0	0	1	1	1	0	3
VNG2649G	*eef1a*	0	0	0	0	1	1	1	0	3
VNG1733G	*htr17*	0	0	0	0	0	1	1	1	3
VNG0826C	*VNG0826C*	1	0	1	0	0	0	0	0	2
VNG1296C	*VNG1296C*	1	0	0	0	0	1	0	0	2
VNG1297C	*VNG1297C*	1	0	0	0	0	1	0	0	2
VNG1608C	*VNG1608C*	1	0	1	0	0	0	0	0	2
VNG1688C	*VNG1688C*	1	0	1	0	0	0	0	0	2
VNG1689G	*rpl13p*	1	0	1	0	0	0	0	0	2
VNG1690G	*rpl4e*	1	0	1	0	0	0	0	0	2
VNG1691G	*rpl23p*	1	0	1	0	0	0	0	0	2
VNG1692G	*rpl2p*	1	0	1	0	0	0	0	0	2
VNG1941C	*VNG1941C*	1	0	0	0	0	0	1	0	2
VNG2296C	*VNG2296C*	1	0	1	0	0	0	0	0	2
VNG2369C	*VNG2369C*	1	0	0	0	0	1	0	0	2
VNG2466C	*VNG2466C*	1	0	0	0	0	1	0	0	2
VNG0124C	*VNG0124C*	1	0	0	0	0	1	0	0	2
VNG1874C	*VNG1874C*	1	0	0	0	0	0	1	0	2
VNG2555C	*VNG2555C*	1	0	0	0	0	0	1	0	2
VNG0277G	*crtI3*	1	0	1	0	0	0	0	0	2
VNG0870G	*gatC*	1	0	1	0	0	0	0	0	2
VNG1150G	*idsA*	1	0	1	0	0	0	0	0	2
VNG1435G	*asd*	1	0	1	0	0	0	0	0	2
VNG1568G	*cbiJ*	1	0	0	0	1	0	0	0	2
VNG1932G	*nolA*	1	0	0	0	0	0	1	0	2
VNG1993H	*VNG1993H*	1	1	0	0	0	0	0	0	2
VNG2397G	*cysA*	1	0	1	0	0	0	0	0	2
VNG1433G	*rps17e*	1	0	1	0	0	0	0	0	2
VNG0296H	*VNG0296H*	1	0	0	0	0	1	0	0	2
VNG0404H	*VNG0404H*	1	0	0	0	0	0	1	0	2
VNG0717H	*VNG0717H*	1	0	0	0	0	0	1	0	2
VNG1229H	*VNG1229H*	1	0	1	0	0	0	0	0	2
VNG1484H	*VNG1484H*	1	0	0	0	0	1	0	0	2
VNG1910H	*VNG1910H*	1	0	1	0	0	0	0	0	2

VNG1920H	*VNG1920H*	1	0	0	0	0	0	1	0	2
VNG1956H	*VNG1956H*	1	0	1	0	0	0	0	0	2
VNG0067H	*VNG0067H*	1	0	0	0	0	1	0	0	2
VNG1382H	*VNG1382H*	1	0	0	0	0	0	1	0	2
VNG1244C	*VNG1244C*	1	0	0	0	0	0	1	0	2
VNG1325C	*VNG1325C*	1	0	0	0	0	0	1	0	2
VNG0853C	*VNG0853C*	1	0	0	0	0	1	0	0	2
VNG1198C	*VNG1198C*	1	0	1	0	0	0	0	0	2
VNG1228C	*VNG1228C*	1	0	1	0	0	0	0	0	2
VNG1287C	*VNG1287C*	1	1	0	0	0	0	0	0	2
VNG1483C	*VNG1483C*	1	0	0	0	0	1	0	0	2
VNG1681C	*VNG1681C*	1	0	1	0	0	0	0	0	2
VNG1687C	*VNG1687C*	1	0	1	0	0	0	0	0	2
VNG2012C	*VNG2012C*	1	0	0	0	0	1	0	0	2
VNG0598C	*VNG0598C*	1	0	1	0	0	0	0	0	2
VNG0163G	*mutS1*	1	0	0	0	0	0	1	0	2
VNG0504G	*gbp5*	1	0	0	0	0	0	1	0	2
VNG0610G	*hhoA*	1	0	0	0	0	1	0	0	2
VNG0716G	*afsQ2*	1	0	0	0	0	0	1	0	2
VNG0806G	*htr4*	1	0	0	0	0	1	0	0	2
VNG1079G	*menB*	1	0	0	0	1	0	0	0	2
VNG1284G	*trkH1*	1	0	0	0	0	0	1	0	2
VNG1294G	*slyD*	1	0	0	0	0	1	0	0	2
VNG1592G	*cysT2*	1	1	0	0	0	0	0	0	2
VNG1607G	*cheC2*	1	0	1	0	0	0	0	0	2
VNG1754G	*phr1*	1	1	0	0	0	0	0	0	2
VNG1929G	*tmk*	1	0	0	0	0	0	1	0	2
VNG2060G	*phnP*	1	0	0	0	0	1	0	0	2
VNG2284G	*hisJ*	1	0	0	0	0	0	1	0	2
VNG2462G	*dpa*	1	0	0	0	0	1	0	0	2
VNG0546C	*VNG0546C*	1	1	0	0	0	0	0	0	2
VNG2071G	*lfl2*	1	0	0	0	0	0	1	0	2
VNG2496G	*ferB*	1	0	0	0	0	1	0	0	2
VNG1832H	*VNG1832H*	1	0	0	0	0	1	0	0	2
VNG2177H	*VNG2177H*	1	0	0	0	0	1	0	0	2
VNG0125H	*VNG0125H*	1	0	0	0	0	0	1	0	2
VNG0198H	*VNG0198H*	1	0	1	0	0	0	0	0	2
VNG0204H	*VNG0204H*	1	1	0	0	0	0	0	0	2
VNG0612H	*VNG0612H*	1	1	0	0	0	0	0	0	2
VNG1410H	*VNG1410H*	1	1	0	0	0	0	0	0	2
VNG1919H	*VNG1919H*	1	0	0	0	0	0	1	0	2
VNG1921H	*VNG1921H*	1	0	0	0	0	0	1	0	2
VNG2297H	*VNG2297H*	1	0	1	0	0	0	0	0	2
VNG2554H	*VNG2554H*	1	0	0	0	0	0	1	0	2
VNG2640G	*gcvT2*	1	0	0	0	0	0	1	0	2

VNG2641H	*VNG2641H*	1	0	0	0	0	0	1	0	2
VNG5022G	*gvpJ1*	1	0	0	0	0	1	0	0	2
VNG6142C	*VNG6142C*	1	1	0	0	0	0	0	0	2
VNG6113H	*VNG6113H*	1	0	1	0	0	0	0	0	2
VNG6022G	*gvpJ1*	1	0	0	0	0	1	0	0	2
VNG6233G	*gvpI2*	1	0	0	0	0	1	0	0	2
VNG6294G	*perA*	1	1	0	0	0	0	0	0	2
VNG0396C	*VNG0396C*	0	1	0	0	0	0	1	0	2
VNG0875C	*VNG0875C*	0	1	0	0	0	0	1	0	2
VNG1025H	*VNG1025H*	0	1	0	0	0	1	0	0	2
VNG1574G	*cobI*	0	1	0	1	0	0	0	0	2
VNG1576G	*cbiP*	0	1	0	1	0	0	0	0	2
VNG1914G	*ppiA*	0	1	0	0	0	0	1	0	2
VNG1302H	*VNG1302H*	0	1	0	0	0	1	0	0	2
VNG1422H	*VNG1422H*	0	1	0	0	0	0	1	0	2
VNG2185H	*VNG2185H*	0	1	0	0	0	1	0	0	2
VNG2340H	*VNG2340H*	0	1	0	0	0	1	0	0	2
VNG0394C	*VNG0394C*	0	1	0	0	0	0	1	0	2
VNG2338G	*polA2*	0	1	0	0	0	1	0	0	2
VNG2339C	*VNG2339C*	0	1	0	0	0	1	0	0	2
VNG0753G	*ylnA*	0	1	0	0	0	1	0	0	2
VNG0893G	*udp2*	0	1	0	1	0	0	0	0	2
VNG0896G	*cda*	0	1	0	1	0	0	0	0	2
VNG0897G	*rbsC1*	0	1	0	1	0	0	0	0	2
VNG0898G	*rbsC2*	0	1	0	1	0	0	0	0	2
VNG2184G	*tfbA*	0	1	0	0	0	1	0	0	2
VNG2143G	*atpK*	0	1	1	0	0	0	0	0	2
VNG2313H	*VNG2313H*	0	1	0	0	0	0	1	0	2
VNG2392H	*VNG2392H*	0	1	0	0	0	1	0	0	2
VNG6152H	*VNG6152H*	0	1	0	0	0	0	0	1	2
VNG6153G	*sojC2*	0	1	0	0	0	0	0	1	2
VNG6157H	*VNG6157H*	0	1	0	0	0	0	0	1	2
VNG6262G	*zurM*	0	1	0	0	0	1	0	0	2
VNG6264G	*zurA*	0	1	0	0	0	1	0	0	2
VNG1622G	*rfcB*	0	0	1	0	0	1	0	0	2
VNG1034H	*VNG1034H*	0	0	1	0	0	1	0	0	2
VNG0300C	*VNG0300C*	0	0	1	0	0	0	0	1	2
VNG1951G	*sub*	0	0	1	1	0	0	0	0	2
VNG1621H	*VNG1621H*	0	0	1	0	0	1	0	0	2
VNG6406H	*VNG6406H*	0	0	0	1	0	1	0	0	2
VNG0525C	*VNG0525C*	0	0	0	0	0	1	1	0	2
VNG0527C	*VNG0527C*	0	0	0	0	0	1	1	0	2
VNG0666G	*ctaB*	0	0	0	0	0	1	1	0	2
VNG0463C	*VNG0463C*	0	0	0	0	0	1	1	0	2
VNG0153C	*VNG0153C*	0	0	0	0	0	1	1	0	2

VNG0428G	*fad2*	0	0	0	0	0	1	1	0	2
VNG0665G	*coxB1*	0	0	0	0	0	1	1	0	2
VNG0946G	*minD1*	0	0	0	0	0	1	1	0	2
VNG1853G	*eif2ba*	0	0	0	0	0	1	1	0	2
VNG1887G	*gpm*	0	0	0	0	0	1	1	0	2
VNG0110C	*VNG0110C*	1	0	0	0	0	0	0	0	1
VNG0255C	*VNG0255C*	1	0	0	0	0	0	0	0	1
VNG0256H	*VNG0256H*	1	0	0	0	0	0	0	0	1
VNG0553C	*VNG0553C*	1	0	0	0	0	0	0	0	1
VNG0631C	*VNG0631C*	1	0	0	0	0	0	0	0	1
VNG0865C	*VNG0865C*	1	0	0	0	0	0	0	0	1
VNG0867G	*asnA*	1	0	0	0	0	0	0	0	1
VNG1323C	*VNG1323C*	1	0	0	0	0	0	0	0	1
VNG2329C	*VNG2329C*	1	0	0	0	0	0	0	0	1
VNG0045C	*VNG0045C*	1	0	0	0	0	0	0	0	1
VNG0505C	*VNG0505C*	1	0	0	0	0	0	0	0	1
VNG1583C	*VNG1583C*	1	0	0	0	0	0	0	0	1
VNG2488C	*VNG2488C*	1	0	0	0	0	0	0	0	1
VNG2490H	*VNG2490H*	1	0	0	0	0	0	0	0	1
VNG0002G	*yvrO*	1	0	0	0	0	0	0	0	1
VNG0003C	*VNG0003C*	1	0	0	0	0	0	0	0	1
VNG0123G	*trp1*	1	0	0	0	0	0	0	0	1
VNG0133G	*rpa*	1	0	0	0	0	0	0	0	1
VNG0134G	*hpyA*	1	0	0	0	0	0	0	0	1
VNG0136G	*aup*	1	0	0	0	0	0	0	0	1
VNG0149G	*zntA*	1	0	0	0	0	0	0	0	1
VNG0226G	*htrA*	1	0	0	0	0	0	0	0	1
VNG0349G	*topA*	1	0	0	0	0	0	0	0	1
VNG0364G	*yusZ3*	1	0	0	0	0	0	0	0	1
VNG0387G	*ilvE1*	1	0	0	0	0	0	0	0	1
VNG0556G	*sgb*	1	0	0	0	0	0	0	0	1
VNG0647G	*nuoM*	1	0	0	0	0	0	0	0	1
VNG0648G	*ndhG3*	1	0	0	0	0	0	0	0	1
VNG0795G	*hcpC*	1	0	0	0	0	0	0	0	1
VNG1143G	*rps2p*	1	0	0	0	0	0	0	0	1
VNG1145G	*mvk*	1	0	0	0	0	0	0	0	1
VNG1148G	*argB*	1	0	0	0	0	0	0	0	1
VNG1160G	*ndk*	1	0	0	0	0	0	0	0	1
VNG1341G	*fabG*	1	0	0	0	0	0	0	0	1
VNG1467G	*bop*	1	0	0	0	0	0	0	0	1
VNG1822G	*moaB*	1	0	0	0	0	0	0	0	1
VNG1823C	*VNG1823C*	1	0	0	0	0	0	0	0	1
VNG1939G	*purC*	1	0	0	0	0	0	0	0	1
VNG1992G	*pgi*	1	0	0	0	0	0	0	0	1
VNG2094G	*trh4*	1	0	0	0	0	0	0	0	1

VNG2294G	*hisA*	1	0	0	0	0	0	0	0	1
VNG2295G	*hisB*	1	0	0	0	0	0	0	0	1
VNG2322G	*hem2*	1	0	0	0	0	0	0	0	1
VNG2326G	*hemL*	1	0	0	0	0	0	0	0	1
VNG2418G	*aspC1*	1	0	0	0	0	0	0	0	1
VNG2526G	*dppF*	1	0	0	0	0	0	0	0	1
VNG2527G	*dppD*	1	0	0	0	0	0	0	0	1
VNG2529G	*dppB2*	1	0	0	0	0	0	0	0	1
VNG2531G	*dppC1*	1	0	0	0	0	0	0	0	1
VNG2617G	*adh2*	1	0	0	0	0	0	0	0	1
VNG0386G	*trpG2*	1	0	0	0	0	0	0	0	1
VNG1159G	*rpl24e*	1	0	0	0	0	0	0	0	1
VNG0022H	*VNG0022H*	1	0	0	0	0	0	0	0	1
VNG0113H	*VNG0113H*	1	0	0	0	0	0	0	0	1
VNG0146H	*VNG0146H*	1	0	0	0	0	0	0	0	1
VNG0217H	*VNG0217H*	1	0	0	0	0	0	0	0	1
VNG0367H	*VNG0367H*	1	0	0	0	0	0	0	0	1
VNG1115H	*VNG1115H*	1	0	0	0	0	0	0	0	1
VNG1315H	*VNG1315H*	1	0	0	0	0	0	0	0	1
VNG1438H	*VNG1438H*	1	0	0	0	0	0	0	0	1
VNG1664H	*VNG1664H*	1	0	0	0	0	0	0	0	1
VNG1787H	*VNG1787H*	1	0	0	0	0	0	0	0	1
VNG1865H	*VNG1865H*	1	0	0	0	0	0	0	0	1
VNG2149H	*VNG2149H*	1	0	0	0	0	0	0	0	1
VNG2619H	*VNG2619H*	1	0	0	0	0	0	0	0	1
VNG2656H	*VNG2656H*	1	0	0	0	0	0	0	0	1
VNG1012H	*VNG1012H*	1	0	0	0	0	0	0	0	1
VNG1314H	*VNG1314H*	1	0	0	0	0	0	0	0	1
VNG2510H	*VNG2510H*	1	0	0	0	0	0	0	0	1
VNG0132C	*VNG0132C*	1	0	0	0	0	0	0	0	1
VNG0094C	*VNG0094C*	1	0	0	0	0	0	0	0	1
VNG0555C	*VNG0555C*	1	0	0	0	0	0	0	0	1
VNG0615C	*VNG0615C*	1	0	0	0	0	0	0	0	1
VNG0983C	*VNG0983C*	1	0	0	0	0	0	0	0	1
VNG1165G	*ksgA*	1	0	0	0	0	0	0	0	1
VNG1168C	*VNG1168C*	1	0	0	0	0	0	0	0	1
VNG2180C	*VNG2180C*	1	0	0	0	0	0	0	0	1
VNG2455C	*VNG2455C*	1	0	0	0	0	0	0	0	1
VNG2518C	*VNG2518C*	1	0	0	0	0	0	0	0	1
VNG0013C	*VNG0013C*	1	0	0	0	0	0	0	0	1
VNG0470G	*trp3*	1	0	0	0	0	0	0	0	1
VNG0925C	*VNG0925C*	1	0	0	0	0	0	0	0	1
VNG2172C	*VNG2172C*	1	0	0	0	0	0	0	0	1
VNG0223G	*moxR*	1	0	0	0	0	0	0	0	1
VNG0254G	*tfbG*	1	0	0	0	0	0	0	0	1

VNG0442G	*rspA*	1	0	0	0	0	0	0	0	1
VNG0444G	*dapA*	1	0	0	0	0	0	0	0	1
VNG0467G	*yafB*	1	0	0	0	0	0	0	0	1
VNG0614G	*htr16*	1	0	0	0	0	0	0	0	1
VNG0629G	*aspB2*	1	0	0	0	0	0	0	0	1
VNG0630G	*ribE*	1	0	0	0	0	0	0	0	1
VNG0864G	*purL*	1	0	0	0	0	0	0	0	1
VNG0869G	*tfbD*	1	0	0	0	0	0	0	0	1
VNG1081G	*menD*	1	0	0	0	0	0	0	0	1
VNG1359G	*rad2*	1	0	0	0	0	0	0	0	1
VNG1369G	*hemV1*	1	0	0	0	0	0	0	0	1
VNG1465G	*brp*	1	0	0	0	0	0	0	0	1
VNG1773G	*cad*	1	0	0	0	0	0	0	0	1
VNG1821G	*adh4*	1	0	0	0	0	0	0	0	1
VNG1862G	*cef*	1	0	0	0	0	0	0	0	1
VNG1864G	*hit2*	1	0	0	0	0	0	0	0	1
VNG2051G	*rpoE''*	1	0	0	0	0	0	0	0	1
VNG2053G	*rpoE'*	1	0	0	0	0	0	0	0	1
VNG2054H	*VNG2054H*	1	0	0	0	0	0	0	0	1
VNG2056G	*eif2g*	1	0	0	0	0	0	0	0	1
VNG2093G	*glnA*	1	0	0	0	0	0	0	0	1
VNG2482G	*pstB1*	1	0	0	0	0	0	0	0	1
VNG2483G	*pstA1*	1	0	0	0	0	0	0	0	1
VNG2484G	*pstC1*	1	0	0	0	0	0	0	0	1
VNG2486G	*yqgG*	1	0	0	0	0	0	0	0	1
VNG2654G	*eef2*	1	0	0	0	0	0	0	0	1
VNG2657G	*rps7p*	1	0	0	0	0	0	0	0	1
VNG0548C	*VNG0548C*	1	0	0	0	0	0	0	0	1
VNG0549G	*eif2a*	1	0	0	0	0	0	0	0	1
VNG0550G	*rps27e*	1	0	0	0	0	0	0	0	1
VNG0551G	*rpl44e*	1	0	0	0	0	0	0	0	1
VNG0841G	*icfA*	1	0	0	0	0	0	0	0	1
VNG0323H	*VNG0323H*	1	0	0	0	0	0	0	0	1
VNG1630H	*VNG1630H*	1	0	0	0	0	0	0	0	1
VNG1989H	*VNG1989H*	1	0	0	0	0	0	0	0	1
VNG1991H	*VNG1991H*	1	0	0	0	0	0	0	0	1
VNG2402H	*VNG2402H*	1	0	0	0	0	0	0	0	1
VNG0148H	*VNG0148H*	1	0	0	0	0	0	0	0	1
VNG0742H	*VNG0742H*	1	0	0	0	0	0	0	0	1
VNG1144H	*VNG1144H*	1	0	0	0	0	0	0	0	1
VNG1642H	*VNG1642H*	1	0	0	0	0	0	0	0	1
VNG2014H	*VNG2014H*	1	0	0	0	0	0	0	0	1
VNG2148H	*VNG2148H*	1	0	0	0	0	0	0	0	1
VNG2403H	*VNG2403H*	1	0	0	0	0	0	0	0	1
VNG2525H	*VNG2525H*	1	0	0	0	0	0	0	0	1

VNG2562H	*VNG2562H*	1	0	0	0	0	0	0	0	1
VNG5074C	*VNG5074C*	1	0	0	0	0	0	0	0	1
VNG5118H	*VNG5118H*	1	0	0	0	0	0	0	0	1
VNG5124H	*VNG5124H*	1	0	0	0	0	0	0	0	1
VNG6071C	*VNG6071C*	1	0	0	0	0	0	0	0	1
VNG6334H	*VNG6334H*	1	0	0	0	0	0	0	0	1
VNG6347H	*VNG6347H*	1	0	0	0	0	0	0	0	1
VNG6378H	*VNG6378H*	1	0	0	0	0	0	0	0	1
VNG6212G	*iucA*	1	0	0	0	0	0	0	0	1
VNG6213G	*iucB*	1	0	0	0	0	0	0	0	1
VNG6214G	*hxyA*	1	0	0	0	0	0	0	0	1
VNG6216G	*iucC*	1	0	0	0	0	0	0	0	1
VNG6115H	*VNG6115H*	1	0	0	0	0	0	0	0	1
VNG6377H	*VNG6377H*	1	0	0	0	0	0	0	0	1
VNG6121H	*VNG6121H*	1	0	0	0	0	0	0	0	1
VNG6145H	*VNG6145H*	1	0	0	0	0	0	0	0	1
VNG6346H	*VNG6346H*	1	0	0	0	0	0	0	0	1
VNG6237G	*gvpF2*	1	0	0	0	0	0	0	0	1
VNG6272G	*orc5*	1	0	0	0	0	0	0	0	1
VNG0171C	*VNG0171C*	0	1	0	0	0	0	0	0	1
VNG0437C	*VNG0437C*	0	1	0	0	0	0	0	0	1
VNG0707C	*VNG0707C*	0	1	0	0	0	0	0	0	1
VNG1021C	*VNG1021C*	0	1	0	0	0	0	0	0	1
VNG1023C	*VNG1023C*	0	1	0	0	0	0	0	0	1
VNG1024C	*VNG1024C*	0	1	0	0	0	0	0	0	1
VNG1237C	*VNG1237C*	0	1	0	0	0	0	0	0	1
VNG1299C	*VNG1299C*	0	1	0	0	0	0	0	0	1
VNG1337C	*VNG1337C*	0	1	0	0	0	0	0	0	1
VNG1375C	*VNG1375C*	0	1	0	0	0	0	0	0	1
VNG0047G	*graD6*	0	1	0	0	0	0	0	0	1
VNG0398G	*nthA1*	0	1	0	0	0	0	0	0	1
VNG0500G	*ppd*	0	1	0	0	0	0	0	0	1
VNG0761G	*dip3*	0	1	0	0	0	0	0	0	1
VNG0860G	*rpoL*	0	1	0	0	0	0	0	0	1
VNG0882G	*pho2*	0	1	0	0	0	0	0	0	1
VNG1018G	*adh3*	0	1	0	0	0	0	0	0	1
VNG1020C	*VNG1020C*	0	1	0	0	0	0	0	0	1
VNG1463G	*blp*	0	1	0	0	0	0	0	0	1
VNG1659G	*htr1*	0	1	0	0	0	0	0	0	1
VNG1660G	*sop1*	0	1	0	0	0	0	0	0	1
VNG1785G	*panF*	0	1	0	0	0	0	0	0	1
VNG2088G	*trm1*	0	1	0	0	0	0	0	0	1
VNG2332G	*cysG*	0	1	0	0	0	0	0	0	1
VNG2411G	*orc7*	0	1	0	0	0	0	0	0	1
VNG2620G	*uvrD*	0	1	0	0	0	0	0	0	1

VNG0095G	*gapB*	0	1	0	0	0	0	0	0	1
VNG0438G	*ferA3*	0	1	0	0	0	0	0	0	1
VNG2147G	*hmp*	0	1	0	0	0	0	0	0	1
VNG2320G	*hdrD*	0	1	0	0	0	0	0	0	1
VNG0080H	*VNG0080H*	0	1	0	0	0	0	0	0	1
VNG0287H	*VNG0287H*	0	1	0	0	0	0	0	0	1
VNG0352H	*VNG0352H*	0	1	0	0	0	0	0	0	1
VNG0357H	*VNG0357H*	0	1	0	0	0	0	0	0	1
VNG0596H	*VNG0596H*	0	1	0	0	0	0	0	0	1
VNG1466H	*VNG1466H*	0	1	0	0	0	0	0	0	1
VNG1479H	*VNG1479H*	0	1	0	0	0	0	0	0	1
VNG1675H	*VNG1675H*	0	1	0	0	0	0	0	0	1
VNG1783H	*VNG1783H*	0	1	0	0	0	0	0	0	1
VNG1838H	*VNG1838H*	0	1	0	0	0	0	0	0	1
VNG1927H	*VNG1927H*	0	1	0	0	0	0	0	0	1
VNG2585H	*VNG2585H*	0	1	0	0	0	0	0	0	1
VNG0096C	*VNG0096C*	0	1	0	0	0	0	0	0	1
VNG0332C	*VNG0332C*	0	1	0	0	0	0	0	0	1
VNG0705C	*VNG0705C*	0	1	0	0	0	0	0	0	1
VNG0858C	*VNG0858C*	0	1	0	0	0	0	0	0	1
VNG1251G	*helA*	0	1	0	0	0	0	0	0	1
VNG1252G	*yhcR*	0	1	0	0	0	0	0	0	1
VNG1253C	*VNG1253C*	0	1	0	0	0	0	0	0	1
VNG1336C	*VNG1336C*	0	1	0	0	0	0	0	0	1
VNG1658C	*VNG1658C*	0	1	0	0	0	0	0	0	1
VNG1903C	*VNG1903C*	0	1	0	0	0	0	0	0	1
VNG2068C	*VNG2068C*	0	1	0	0	0	0	0	0	1
VNG2584C	*VNG2584C*	0	1	0	0	0	0	0	0	1
VNG0439C	*VNG0439C*	0	1	0	0	0	0	0	0	1
VNG1784C	*VNG1784C*	0	1	0	0	0	0	0	0	1
VNG0046G	*ugd*	0	1	0	0	0	0	0	0	1
VNG0498C	*VNG0498C*	0	1	0	0	0	0	0	0	1
VNG0499G	*cna*	0	1	0	0	0	0	0	0	1
VNG0559G	*apt*	0	1	0	0	0	0	0	0	1
VNG0620G	*edp*	0	1	0	0	0	0	0	0	1
VNG0681G	*hbd1*	0	1	0	0	0	0	0	0	1
VNG1103G	*rpl12p*	0	1	0	0	0	0	0	0	1
VNG1104G	*rpl10p*	0	1	0	0	0	0	0	0	1
VNG1105G	*rpl1p*	0	1	0	0	0	0	0	0	1
VNG1108G	*rpl11p*	0	1	0	0	0	0	0	0	1
VNG1162H	*VNG1162H*	0	1	0	0	0	0	0	0	1
VNG1163G	*hemK*	0	1	0	0	0	0	0	0	1
VNG1301G	*cysK*	0	1	0	0	0	0	0	0	1
VNG1332G	*sod2*	0	1	0	0	0	0	0	0	1
VNG1462G	*cdc48a*	0	1	0	0	0	0	0	0	1

VNG1478G	*panB*	0	1	0	0	0	0	0	0	1
VNG1764G	*sop2*	0	1	0	0	0	0	0	0	1
VNG1765G	*htr2*	0	1	0	0	0	0	0	0	1
VNG1767G	*speB*	0	1	0	0	0	0	0	0	1
VNG1768G	*eif5a*	0	1	0	0	0	0	0	0	1
VNG1801G	*hsp1*	0	1	0	0	0	0	0	0	1
VNG1866G	*map*	0	1	0	0	0	0	0	0	1
VNG1926G	*pdhA1*	0	1	0	0	0	0	0	0	1
VNG1605G	*gdcH*	0	1	0	0	0	0	0	0	1
VNG0079H	*VNG0079H*	0	1	0	0	0	0	0	0	1
VNG0291H	*VNG0291H*	0	1	0	0	0	0	0	0	1
VNG0656H	*VNG0656H*	0	1	0	0	0	0	0	0	1
VNG1017H	*VNG1017H*	0	1	0	0	0	0	0	0	1
VNG1047H	*VNG1047H*	0	1	0	0	0	0	0	0	1
VNG1390H	*VNG1390H*	0	1	0	0	0	0	0	0	1
VNG1394H	*VNG1394H*	0	1	0	0	0	0	0	0	1
VNG1674H	*VNG1674H*	0	1	0	0	0	0	0	0	1
VNG1837G	*ykfB1*	0	1	0	0	0	0	0	0	1
VNG1839H	*VNG1839H*	0	1	0	0	0	0	0	0	1
VNG1890H	*VNG1890H*	0	1	0	0	0	0	0	0	1
VNG1902H	*VNG1902H*	0	1	0	0	0	0	0	0	1
VNG2109H	*VNG2109H*	0	1	0	0	0	0	0	0	1
VNG2144G	*atpI*	0	1	0	0	0	0	0	0	1
VNG2146H	*VNG2146H*	0	1	0	0	0	0	0	0	1
VNG5141G	*hepA*	0	1	0	0	0	0	0	0	1
VNG5142G	*tbpC*	0	1	0	0	0	0	0	0	1
VNG5177C	*VNG5177C*	0	1	0	0	0	0	0	0	1
VNG6155H	*VNG6155H*	0	1	0	0	0	0	0	0	1
VNG6250G	*phoT3*	0	1	0	0	0	0	0	0	1
VNG6158H	*VNG6158H*	0	1	0	0	0	0	0	0	1
VNG6159H	*VNG6159H*	0	1	0	0	0	0	0	0	1
VNG6420H	*VNG6420H*	0	1	0	0	0	0	0	0	1
VNG0964C	*VNG0964C*	0	0	1	0	0	0	0	0	1
VNG1238C	*VNG1238C*	0	0	1	0	0	0	0	0	1
VNG1339C	*VNG1339C*	0	0	1	0	0	0	0	0	1
VNG0245G	*dtd*	0	0	1	0	0	0	0	0	1
VNG0247C	*VNG0247C*	0	0	1	0	0	0	0	0	1
VNG1759G	*htr7*	0	0	1	0	0	0	0	0	1
VNG0049H	*VNG0049H*	0	0	1	0	0	0	0	0	1
VNG0594H	*VNG0594H*	0	0	1	0	0	0	0	0	1
VNG1200H	*VNG1200H*	0	0	1	0	0	0	0	0	1
VNG1380H	*VNG1380H*	0	0	1	0	0	0	0	0	1
VNG2175H	*VNG2175H*	0	0	1	0	0	0	0	0	1
VNG2414H	*VNG2414H*	0	0	1	0	0	0	0	0	1
VNG2415H	*VNG2415H*	0	0	1	0	0	0	0	0	1

VNG1672H	*VNG1672H*	0	0	1	0	0	0	0	0	1
VNG0283C	*VNG0283C*	0	0	1	0	0	0	0	0	1
VNG0563G	*ndhG2*	0	0	1	0	0	0	0	0	1
VNG0565C	*VNG0565C*	0	0	1	0	0	0	0	0	1
VNG0564H	*VNG0564H*	0	0	1	0	0	0	0	0	1
VNG0566C	*VNG0566C*	0	0	1	0	0	0	0	0	1
VNG0570H	*VNG0570H*	0	0	1	0	0	0	0	0	1
VNG0568C	*VNG0568C*	0	0	1	0	0	0	0	0	1
VNG1398C	*VNG1398C*	0	0	1	0	0	0	0	0	1
VNG1030G	*pgsA*	0	0	1	0	0	0	0	0	1
VNG1031C	*VNG1031C*	0	0	1	0	0	0	0	0	1
VNG1033G	*hisC1*	0	0	1	0	0	0	0	0	1
VNG1123G	*trh7*	0	0	1	0	0	0	0	0	1
VNG2546G	*pepB3*	0	0	1	0	0	0	0	0	1
VNG0999H	*VNG0999H*	0	0	1	0	0	0	0	0	1
VNG1239H	*VNG1239H*	0	0	1	0	0	0	0	0	1
VNG2174H	*VNG2174H*	0	0	1	0	0	0	0	0	1
VNG2412H	*VNG2412H*	0	0	1	0	0	0	0	0	1
VNG2413H	*VNG2413H*	0	0	1	0	0	0	0	0	1
VNG5116H	*VNG5116H*	0	0	1	0	0	0	0	0	1
VNG6456H	*VNG6456H*	0	0	1	0	0	0	0	0	1
VNG6424H	*VNG6424H*	0	0	1	0	0	0	0	0	1
VNG6313G	*nhaC3*	0	0	1	0	0	0	0	0	1
VNG0419C	*VNG0419C*	0	0	0	1	0	0	0	0	1
VNG2189H	*VNG2189H*	0	0	0	1	0	0	0	0	1
VNG2035H	*VNG2035H*	0	0	0	1	0	0	0	0	1
VNG0901G	*rbsA*	0	0	0	1	0	0	0	0	1
VNG0903C	*VNG0903C*	0	0	0	1	0	0	0	0	1
VNG2186G	*hit1*	0	0	0	1	0	0	0	0	1
VNG0697H	*VNG0697H*	0	0	0	1	0	0	0	0	1
VNG2034H	*VNG2034H*	0	0	0	1	0	0	0	0	1
VNG6430C	*VNG6430C*	0	0	0	1	0	0	0	0	1
VNG6437C	*VNG6437C*	0	0	0	1	0	0	0	0	1
VNG6396H	*VNG6396H*	0	0	0	1	0	0	0	0	1
VNG6411H	*VNG6411H*	0	0	0	1	0	0	0	0	1
VNG6397H	*VNG6397H*	0	0	0	1	0	0	0	0	1
VNG6408G	*phzF*	0	0	0	1	0	0	0	0	1
VNG6401H	*VNG6401H*	0	0	0	1	0	0	0	0	1
VNG6412H	*VNG6412H*	0	0	0	1	0	0	0	0	1
VNG6427H	*VNG6427H*	0	0	0	1	0	0	0	0	1
VNG6395H	*VNG6395H*	0	0	0	1	0	0	0	0	1
VNG6407H	*VNG6407H*	0	0	0	1	0	0	0	0	1
VNG6409H	*VNG6409H*	0	0	0	1	0	0	0	0	1
VNG6413H	*VNG6413H*	0	0	0	1	0	0	0	0	1
VNG6421H	*VNG6421H*	0	0	0	1	0	0	0	0	1

VNG6429H	*VNG6429H*	0	0	0	1	0	0	0	0	1
VNG1814G	*carB*	0	0	0	0	1	0	0	0	1
VNG2205H	*VNG2205H*	0	0	0	0	1	0	0	0	1
VNG1907H	*VNG1907H*	0	0	0	0	1	0	0	0	1
VNG1073G	*lfl1*	0	0	0	0	1	0	0	0	1
VNG1197G	*bcp*	0	0	0	0	1	0	0	0	1
VNG1811G	*eye*	0	0	0	0	1	0	0	0	1
VNG0488H	*VNG0488H*	0	0	0	0	1	0	0	0	1
VNG2204H	*VNG2204H*	0	0	0	0	1	0	0	0	1
VNG0268C	*VNG0268C*	0	0	0	0	0	1	0	0	1
VNG0274C	*VNG0274C*	0	0	0	0	0	1	0	0	1
VNG1845C	*VNG1845C*	0	0	0	0	0	1	0	0	1
VNG2470C	*VNG2470C*	0	0	0	0	0	1	0	0	1
VNG0281G	*soxB*	0	0	0	0	0	1	0	0	1
VNG0371G	*acd1*	0	0	0	0	0	1	0	0	1
VNG0382G	*aroE*	0	0	0	0	0	1	0	0	1
VNG0403G	*proS*	0	0	0	0	0	1	0	0	1
VNG0796G	*cgs*	0	0	0	0	0	1	0	0	1
VNG1097G	*cysS*	0	0	0	0	0	1	0	0	1
VNG1370G	*hemU*	0	0	0	0	0	1	0	0	1
VNG1371G	*hemV2*	0	0	0	0	0	1	0	0	1
VNG1432G	*dhs*	0	0	0	0	0	1	0	0	1
VNG1550G	*cbiT*	0	0	0	0	0	1	0	0	1
VNG1551G	*cbiL*	0	0	0	0	0	1	0	0	1
VNG1882G	*nadA*	0	0	0	0	0	1	0	0	1
VNG1883G	*nadB*	0	0	0	0	0	1	0	0	1
VNG1884G	*nadC*	0	0	0	0	0	1	0	0	1
VNG1406G	*rhl*	0	0	0	0	0	1	0	0	1
VNG2076G	*rpl40e*	0	0	0	0	0	1	0	0	1
VNG0068H	*VNG0068H*	0	0	0	0	0	1	0	0	1
VNG0652H	*VNG0652H*	0	0	0	0	0	1	0	0	1
VNG0780H	*VNG0780H*	0	0	0	0	0	1	0	0	1
VNG1678H	*VNG1678H*	0	0	0	0	0	1	0	0	1
VNG1940H	*VNG1940H*	0	0	0	0	0	1	0	0	1
VNG2451H	*VNG2451H*	0	0	0	0	0	1	0	0	1
VNG1558H	*VNG1558H*	0	0	0	0	0	1	0	0	1
VNG1559H	*VNG1559H*	0	0	0	0	0	1	0	0	1
VNG1561C	*VNG1561C*	0	0	0	0	0	1	0	0	1
VNG1562H	*VNG1562H*	0	0	0	0	0	1	0	0	1
VNG0240C	*VNG0240C*	0	0	0	0	0	1	0	0	1
VNG1548C	*VNG1548C*	0	0	0	0	0	1	0	0	1
VNG0793G	*htr6*	0	0	0	0	0	1	0	0	1
VNG0835G	*idr2*	0	0	0	0	0	1	0	0	1
VNG0873G	*ykhA*	0	0	0	0	0	1	0	0	1
VNG1154H	*VNG1154H*	0	0	0	0	0	1	0	0	1

VNG1156G	*hsp*	0	0	0	0	0	1	0	0	1
VNG1395G	*htr9*	0	0	0	0	0	1	0	0	1
VNG1760G	*htr5*	0	0	0	0	0	1	0	0	1
VNG2043G	*ham1*	0	0	0	0	0	1	0	0	1
VNG2203G	*prsA*	0	0	0	0	0	1	0	0	1
VNG2377G	*nosY*	0	0	0	0	0	1	0	0	1
VNG2378G	*nosF1*	0	0	0	0	0	1	0	0	1
VNG0486G	*hat1*	0	0	0	0	0	1	0	0	1
VNG2062G	*atp*	0	0	0	0	0	1	0	0	1
VNG1096H	*VNG1096H*	0	0	0	0	0	1	0	0	1
VNG1999H	*VNG1999H*	0	0	0	0	0	1	0	0	1
VNG0039H	*VNG0039H*	0	0	0	0	0	1	0	0	1
VNG0297H	*VNG0297H*	0	0	0	0	0	1	0	0	1
VNG0347H	*VNG0347H*	0	0	0	0	0	1	0	0	1
VNG0370H	*VNG0370H*	0	0	0	0	0	1	0	0	1
VNG0402H	*VNG0402H*	0	0	0	0	0	1	0	0	1
VNG1751H	*VNG1751H*	0	0	0	0	0	1	0	0	1
VNG1965H	*VNG1965H*	0	0	0	0	0	1	0	0	1
VNG2115H	*VNG2115H*	0	0	0	0	0	1	0	0	1
VNG2230H	*VNG2230H*	0	0	0	0	0	1	0	0	1
VNG5218H	*VNG5218H*	0	0	0	0	0	1	0	0	1
VNG6204H	*VNG6204H*	0	0	0	0	0	1	0	0	1
VNG6209H	*VNG6209H*	0	0	0	0	0	1	0	0	1
VNG6177G	*kdpB*	0	0	0	0	0	1	0	0	1
VNG6178G	*kdpC*	0	0	0	0	0	1	0	0	1
VNG6247G	*trkA4*	0	0	0	0	0	1	0	0	1
VNG6303G	*exsB*	0	0	0	0	0	1	0	0	1
VNG6305C	*VNG6305C*	0	0	0	0	0	1	0	0	1
VNG6306C	*VNG6306C*	0	0	0	0	0	1	0	0	1
VNG6143H	*VNG6143H*	0	0	0	0	0	1	0	0	1
VNG6203H	*VNG6203H*	0	0	0	0	0	1	0	0	1
VNG6235G	*gvpH2*	0	0	0	0	0	1	0	0	1
VNG6315G	*arcB*	0	0	0	0	0	1	0	0	1
VNG6316G	*arcC*	0	0	0	0	0	1	0	0	1
VNG2575G	*rimI*	0	0	0	0	0	0	1	0	1
VNG0388C	*VNG0388C*	0	0	0	0	0	0	1	0	1
VNG1497C	*VNG1497C*	0	0	0	0	0	0	1	0	1
VNG1982C	*VNG1982C*	0	0	0	0	0	0	1	0	1
VNG1984G	*rnh*	0	0	0	0	0	0	1	0	1
VNG2021C	*VNG2021C*	0	0	0	0	0	0	1	0	1
VNG2316C	*VNG2316C*	0	0	0	0	0	0	1	0	1
VNG2317G	*cbiO1*	0	0	0	0	0	0	1	0	1
VNG2255C	*VNG2255C*	0	0	0	0	0	0	1	0	1
VNG0446G	*gcd*	0	0	0	0	0	0	1	0	1
VNG0448G	*pyrC*	0	0	0	0	0	0	1	0	1

VNG0680G	*fdfT*	0	0	0	0	0	0	1	0	1
VNG0775G	*acd2*	0	0	0	0	0	0	1	0	1
VNG1172G	*metB*	0	0	0	0	0	0	1	0	1
VNG1834G	*hyrA*	0	0	0	0	0	0	1	0	1
VNG2417G	*polA1*	0	0	0	0	0	0	1	0	1
VNG2636G	*uvrA*	0	0	0	0	0	0	1	0	1
VNG0733H	*VNG0733H*	0	0	0	0	0	0	1	0	1
VNG0883H	*VNG0883H*	0	0	0	0	0	0	1	0	1
VNG1112H	*VNG1112H*	0	0	0	0	0	0	1	0	1
VNG2582H	*VNG2582H*	0	0	0	0	0	0	1	0	1
VNG0040C	*VNG0040C*	0	0	0	0	0	0	1	0	1
VNG0142C	*VNG0142C*	0	0	0	0	0	0	1	0	1
VNG0376G	*ftsZ1*	0	0	0	0	0	0	1	0	1
VNG0378C	*VNG0378C*	0	0	0	0	0	0	1	0	1
VNG0466C	*VNG0466C*	0	0	0	0	0	0	1	0	1
VNG1249C	*VNG1249C*	0	0	0	0	0	0	1	0	1
VNG1833C	*VNG1833C*	0	0	0	0	0	0	1	0	1
VNG2116C	*VNG2116C*	0	0	0	0	0	0	1	0	1
VNG2543C	*VNG2543C*	0	0	0	0	0	0	1	0	1
VNG0098G	*rimK*	0	0	0	0	0	0	1	0	1
VNG0401G	*epf2*	0	0	0	0	0	0	1	0	1
VNG0720G	*dip2*	0	0	0	0	0	0	1	0	1
VNG0938G	*gufA*	0	0	0	0	0	0	1	0	1
VNG1365C	*VNG1365C*	0	0	0	0	0	0	1	0	1
VNG1366H	*VNG1366H*	0	0	0	0	0	0	1	0	1
VNG1367G	*srp19*	0	0	0	0	0	0	1	0	1
VNG2003G	*truA*	0	0	0	0	0	0	1	0	1
VNG2005G	*hisS*	0	0	0	0	0	0	1	0	1
VNG2373G	*tnaA*	0	0	0	0	0	0	1	0	1
VNG0141H	*VNG0141H*	0	0	0	0	0	0	1	0	1
VNG0447H	*VNG0447H*	0	0	0	0	0	0	1	0	1
VNG0472H	*VNG0472H*	0	0	0	0	0	0	1	0	1
VNG0595H	*VNG0595H*	0	0	0	0	0	0	1	0	1
VNG0617H	*VNG0617H*	0	0	0	0	0	0	1	0	1
VNG0738H	*VNG0738H*	0	0	0	0	0	0	1	0	1
VNG0782H	*VNG0782H*	0	0	0	0	0	0	1	0	1
VNG1291H	*VNG1291H*	0	0	0	0	0	0	1	0	1
VNG1723H	*VNG1723H*	0	0	0	0	0	0	1	0	1
VNG1983H	*VNG1983H*	0	0	0	0	0	0	1	0	1
VNG2292H	*VNG2292H*	0	0	0	0	0	0	1	0	1
VNG2634H	*VNG2634H*	0	0	0	0	0	0	1	0	1
VNG0303G	*lon*	0	0	0	0	0	0	0	1	1
VNG2626H	*VNG2626H*	0	0	0	0	0	0	0	1	1
VNG0301C	*VNG0301C*	0	0	0	0	0	0	0	1	1
VNG2625C	*VNG2625C*	0	0	0	0	0	0	0	1	1

Target gene names in the first row represent genes whose promoter regions were bound by Lrp. 1 represents the existence of the corresponding Lrp binding; 0 represents the gene was not bound by the corresponding Lrp.

Appendix F. Lrp targets genes with putative feed-forward regulatory structure

Lrp1: Lrp2[a]	Target gene	Lrp1: Lrp2	Target gene
Trh3: AsnC	*rps17p*	Trh4: AsnC	*cca*
Trh3: AsnC	*rpl14p*	Trh4: AsnC	*hef*
Trh3: AsnC	*rpl24p*	Trh4: AsnC	*mutS2*
Trh3: AsnC	*rps4e*	Trh4: AsnC	*hop*
Trh3: AsnC	*rpl5p*	Trh4: AsnC	*hhoA*
Trh3: AsnC	*rps14p*	Trh4: AsnC	*htr4*
Trh3: AsnC	*rps8p*	Trh4: AsnC	*hisF*
Trh3: AsnC	*rpl6p*	Trh4: AsnC	*VNG0920H*
Trh3: AsnC	*rpl32e*	Trh4: AsnC	*potA1*
Trh3: AsnC	*rpl19e*	Trh4: AsnC	*nirJ*
Trh3: AsnC	*rpl18p*	Trh4: AsnC	*slyD*
Trh3: AsnC	*rps5p*	Trh4: AsnC	*mutY*
Trh3: AsnC	*rpl30p*	Trh4: AsnC	*carA*
Trh3: AsnC	*rpl15p*	Trh4: AsnC	*secD*
Trh3: AsnC	*secY*	Trh4: AsnC	*phnP*
Trh3: AsnC	*VNG1735C*	Trh4: AsnC	*atpB*
Trh3: AsnC	*lpl*	Trh4: AsnC	*atpA*
Trh3: AsnC	*cbiH*	Trh4: AsnC	*atpF*
Trh3: AsnC	*cbiJ*	Trh4: AsnC	*atpC*
Trh3: AsnC	*etfB*	Trh4: AsnC	*dpa*
Trh3: AsnC	*etfA*	Trh4: AsnC	*maoC2*
Trh3: AsnC	*VNG1261H*	Trh4: AsnC	*ferB*
Trh3: AsnC	*VNG0602C*	Trh4: AsnC	*ftsZ2*
Trh3: AsnC	*cca*	Trh4: AsnC	*VNG0194H*
Trh3: AsnC	*hop*	Trh4: AsnC	*VNG1189H*
Trh3: AsnC	*cheR*	Trh4: AsnC	*VNG1376H*
Trh3: AsnC	*menB*	Trh4: AsnC	*VNG1519H*
Trh3: AsnC	*VNG0492H*	Trh4: AsnC	*VNG1832H*
Trh4: AsnC	*VNG0361C*	Trh4: AsnC	*VNG2177H*
Trh4: AsnC	*nfi*	Trh4: AsnC	*VNG2495H*
Trh4: AsnC	*VNG0405C*	Trh4: AsnC	*VNG0054H*
Trh4: AsnC	*VNG0421C*	Trh4: AsnC	*VNG0408H*
Trh4: AsnC	*VNG1069C*	Trh4: AsnC	*VNG0420H*
Trh4: AsnC	*VNG1296C*	Trh4: AsnC	*VNG0430H*
Trh4: AsnC	*VNG1297C*	Trh4: AsnC	*VNG0492H*
Trh4: AsnC	*rps19p*	Trh4: AsnC	*VNG0671H*

[a] Lrp1: Lrp2 means Lrp1 binds to the promoter region of Lrp2, and both bind to promoter region of the listed downstream genes

Trh4: AsnC	*rpl22p*	Trh4: AsnC	*VNG1777H*
Trh4: AsnC	*rps3p*	Trh4: AsnC	*VNG2603H*
Trh4: AsnC	*rpl29p*	Trh4: AsnC	*gvpJ1*
Trh4: AsnC	*VNG1699C*	Trh4: AsnC	*VNG6432H*
Trh4: AsnC	*rps17p*	Trh4: AsnC	*gvpO2*
Trh4: AsnC	*rpl14p*	Trh4: AsnC	*trsE*
Trh4: AsnC	*rpl24p*	Trh4: AsnC	*VNG6404H*
Trh4: AsnC	*rps4e*	Trh4: AsnC	*VNG6416H*
Trh4: AsnC	*rpl5p*	Trh4: AsnC	*VNG6431H*
Trh4: AsnC	*rps14p*	Trh4: AsnC	*gvpJ1*
Trh4: AsnC	*rps8p*	Trh4: AsnC	*gvpl2*
Trh4: AsnC	*rpl6p*	VNG1237C:VNG1179C	*cbiF*
Trh4: AsnC	*rpl32e*	VNG1237C:VNG1179C	*cbiG*
Trh4: AsnC	*rpl19e*	VNG1237C:VNG1179C	*cobH*
Trh4: AsnC	*rpl18p*	VNG1237C:VNG1179C	*cbiH*
Trh4: AsnC	*rps5p*	VNG1237C:VNG1179C	*rpl32e*
Trh4: AsnC	*rpl30p*	VNG1237C:VNG1179C	*rpl19e*
Trh4: AsnC	*rpl15p*	VNG1237C:VNG1179C	*rpl18p*
Trh4: AsnC	*secY*	VNG1237C:VNG1179C	*rps5p*
Trh4: AsnC	*VNG1735C*	VNG1237C:VNG1179C	*rpl30p*
Trh4: AsnC	*VNG1779C*	VNG1237C:VNG1179C	*rpl15p*
Trh4: AsnC	*VNG2307C*	VNG1237C:VNG1179C	*secY*
Trh4: AsnC	*VNG2369C*	VNG1237C:VNG1179C	*VNG0244H*
Trh4: AsnC	*VNG2466C*	VNG1237C:VNG1179C	*VNG1261H*
Trh4: AsnC	*VNG2474C*	VNG1237C:VNG1179C	*VNG0492H*
Trh4: AsnC	*VNG2475C*	VNG1237C:VNG1179C	*atpB*
Trh4: AsnC	*VNG2610C*	VNG1237C:VNG1179C	*atpA*
Trh4: AsnC	*VNG0124C*	VNG1237C:VNG1179C	*atpF*
Trh4: AsnC	*VNG0271C*	VNG1237C:VNG1179C	*atpC*
Trh4: AsnC	*VNG0713C*	VNG1237C:VNG1179C	*atpE*
Trh4: AsnC	*psmA2*	VNG1237C:VNG1179C	*atpK*
Trh4: AsnC	*lpl*	Trh7: VNG1237C	*cat1*
Trh4: AsnC	*trpB*	Trh7: VNG1237C	*cbiH*
Trh4: AsnC	*trpA*	Trh7: VNG1237C	*deoC*
Trh4: AsnC	*VNG0309C*	Trh7: VNG1237C	*VNG0244H*
Trh4: AsnC	*mcmA2*	Trh7: VNG1237C	*VNG1261H*
Trh4: AsnC	*VNG0674C*	Trh7: VNG1237C	*VNG0300C*
Trh4: AsnC	*gatA*	Trh7: VNG1237C	*VNG1857C*
Trh4: AsnC	*nac*	Trh7: VNG1237C	*mutS2*
Trh4: AsnC	*cbiF*	Trh7: VNG1237C	*VNG1376H*
Trh4: AsnC	*cbiG*	Trh4: Trh3	*VNG1735C*
Trh4: AsnC	*cobH*	Trh4: Trh3	*lpl*

Trh4: AsnC	*cbiH*	Trh4: Trh3	*cbiH*
Trh4: AsnC	*trh3*	Trh4: Trh3	*rps17p*
Trh4: AsnC	*idi*	Trh4: Trh3	*rpl14p*
Trh4: AsnC	*etfB*	Trh4: Trh3	*rpl24p*
Trh4: AsnC	*etfA*	Trh4: Trh3	*rps4e*
Trh4: AsnC	*lpdA*	Trh4: Trh3	*rpl5p*
Trh4: AsnC	*maoC1*	Trh4: Trh3	*rps14p*
Trh4: AsnC	*cat*	Trh4: Trh3	*rps8p*
Trh4: AsnC	*appB*	Trh4: Trh3	*rpl6p*
Trh4: AsnC	*appC*	Trh4: Trh3	*rpl32e*
Trh4: AsnC	*oppD1*	Trh4: Trh3	*rpl19e*
Trh4: AsnC	*appF*	Trh4: Trh3	*rpl18p*
Trh4: AsnC	*thi1*	Trh4: Trh3	*rps5p*
Trh4: AsnC	*thiD*	Trh4: Trh3	*rpl30p*
Trh4: AsnC	*VNG0055H*	Trh4: Trh3	*rpl15p*
Trh4: AsnC	*VNG0138H*	Trh4: Trh3	*secY*
Trh4: AsnC	*VNG0184H*	Trh4: Trh3	*etfB*
Trh4: AsnC	*VNG0219H*	Trh4: Trh3	*etfA*
Trh4: AsnC	*VNG0244H*	Trh4: Trh3	*metA*
Trh4: AsnC	*VNG0296H*	Trh4: Trh3	*hal*
Trh4: AsnC	*VNG0861H*	Trh4: Trh3	*VNG1261H*
Trh4: AsnC	*VNG1002H*	Trh4: Trh3	*VNG0602C*
Trh4: AsnC	*VNG1042H*	Trh4: Trh3	*cca*
Trh4: AsnC	*VNG1484H*	Trh4: Trh3	*hop*
Trh4: AsnC	*VNG2497H*	Trh4: Trh3	*rps10p*
Trh4: AsnC	*VNG2498H*	Trh4: Trh3	*eef1a*
Trh4: AsnC	*VNG0067H*	Trh4: Trh3	*VNG0492H*
Trh4: AsnC	*VNG1261H*	Trh6: Trh3	*VNG1735C*
Trh4: AsnC	*VNG1487H*	Trh6: Trh3	*lpl*
Trh4: AsnC	*VNG1807H*	Trh6: Trh3	*cbiH*
Trh4: AsnC	*VNG2581H*	Trh6: Trh3	*etfB*
Trh4: AsnC	*VNG1388H*	Trh6: Trh3	*etfA*
Trh4: AsnC	*VNG1389C*	Trh6: Trh3	*VNG1261H*
Trh4: AsnC	*VNG0147C*	Trh6: Trh3	*VNG0602C*
Trh4: AsnC	*VNG0360C*	Trh6: Trh3	*cca*
Trh4: AsnC	*VNG0537C*	Trh6: Trh3	*hop*
Trh4: AsnC	*VNG0539C*	Trh6: Trh3	*cheR*
Trh4: AsnC	*VNG0602C*	Trh6: Trh3	*rps10p*
Trh4: AsnC	*VNG0853C*	Trh6: Trh3	*eef1a*
Trh4: AsnC	*VNG1483C*	Trh6: Trh3	*VNG0492H*
Trh4: AsnC	*VNG2012C*	Trh7: Trh3	*cbiH*
Trh4: AsnC	*VNG0035C*	Trh7: Trh3	*VNG1261H*

Trh4: AsnC	*glmS*		

Appendix G. Growth measurements of the eight Lrp knockout strains

Table F-1 OD measurements of the eight Lrp knockouts in batch culture

Time (hour)		0	10	13.5	18.683	23.85	33.567	37.783	40.633	50.2	67.75	106.25
ΔasnC	replicate_1	0.1	0.1522	0.1725	0.1924	0.2413	0.2886	0.325	0.3473	0.4708	0.6309	0.7426
ΔasnC	replicate_2	0.1	0.1594	0.1831	0.1963	0.2595	0.3206	0.3511	0.3855	0.5017	0.6598	0.8024
ΔVNG1179C	replicate_1	0.1	0.1446	0.1677	0.1894	0.2612	0.3716	0.3426	0.3607	0.3901	0.5399	0.9512
ΔVNG1179C	replicate_2	0.1	0.1406	0.1651	0.181	0.2441	0.3163	0.3148	0.3316	0.3819	0.5103	0.9943
ΔVNG1237C	replicate_1	0.1	0.1394	0.1682	0.1894	0.2528	0.3579	0.4021	0.429	0.5229	0.5344	0.6478
ΔVNG1237C	replicate_2	0.1	0.1232	0.1497	0.169	0.2492	0.3348	0.3733	0.4057	0.4709	0.5231	0.6318
Δtrh2	replicate_1	0.1	0.1128	0.1225	0.1423	0.1879	0.2493	0.2739	0.2925	0.404	0.5314	0.6745
Δtrh2	replicate_2	0.1	0.1258	0.146	0.1577	0.1947	0.2641	0.2937	0.3188	0.4153	0.5538	0.6485
Δtrh3	replicate_1	0.1	0.1356	0.1668	0.1861	0.2436	0.3494	0.3924	0.4158	0.4991	0.5451	0.5925
Δtrh3	replicate_2	0.1	0.1508	0.192	0.1984	0.2803	0.3759	0.4177	0.4425	0.4866	0.5604	0.6048
Δtrh4	replicate_1	0.1	0.1498	0.1726	0.1817	0.2556	0.3024	0.3152	0.3256	0.4642	0.417	0.4814
Δtrh4	replicate_2	0.1	0.1476	0.1811	0.2031	0.2687	0.3616	0.393	0.4105	0.5116	0.5563	0.5781
Δtrh6	replicate_1	0.1	0.1419	0.1624	0.1895	0.2771	0.369	0.4001	0.4064	0.4705	0.5401	0.6275
Δtrh6	replicate_2	0.1	0.1588	0.1842	0.2168	0.2727	0.3843	0.4123	0.4202	0.4587	0.5395	0.634
Δtrh7	replicate_1	0.1	0.1389	0.1693	0.1927	0.2461	0.358	0.4102	0.4458	0.493	0.4817	0.9331
Δtrh7	replicate_2	0.1	0.1626	0.1811	0.2117	0.3077	0.3839	0.444	0.4586	0.5118	0.4956	0.836
Δura3	replicate_1	0.1	0.1533	0.1796	0.2049	0.2709	0.3759	0.4221	0.442	0.5074	0.5478	0.6151
Δura3	replicate_2	0.1	0.1604	0.1932	0.2161	0.2844	0.3754	0.4083	0.4236	0.4902	0.5432	0.5678

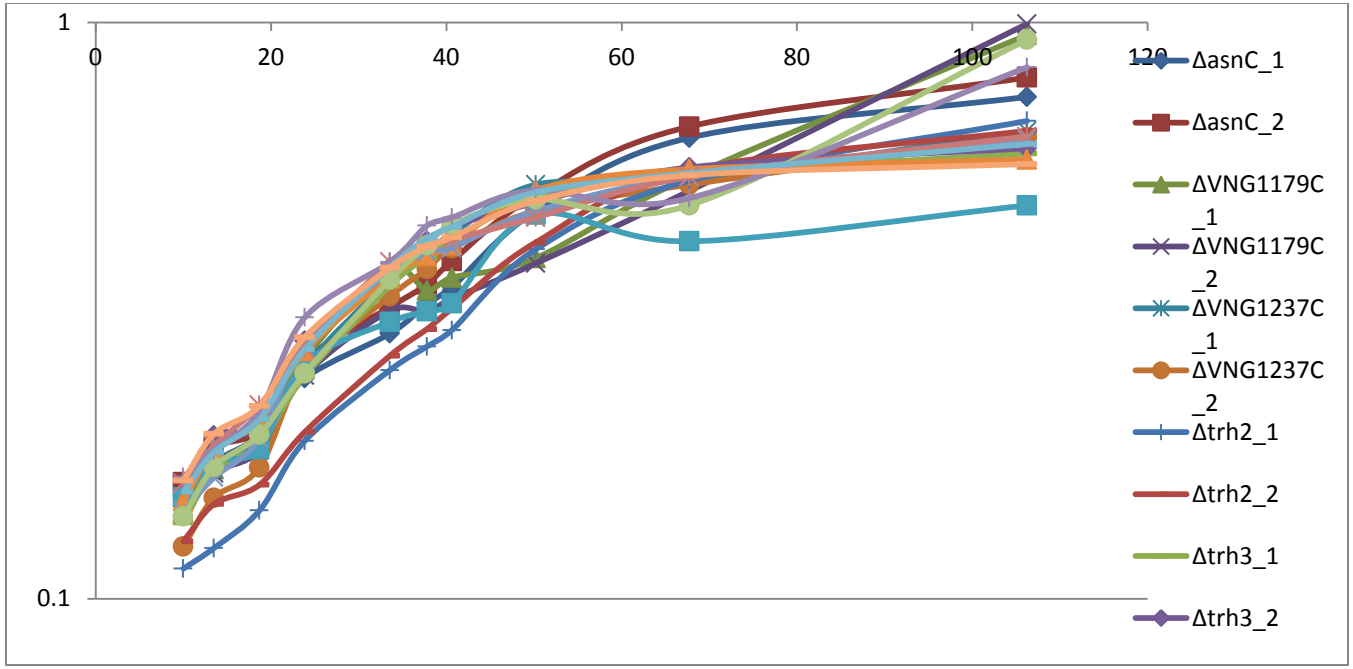

Figure F-1 Plots of growth curve based on Table F-1. Here x-axis represents time in hours and y-axis represents OD measurements in log scale.

Appendix H. p-values and fold changes of genes differentially expressed in *ΔasnC*

canonical_Name	gene_Name	corrected p-val	fold change
VNG0038H	*VNG0038H*	4.29E-03	1.95E+00
VNG0053H	*VNG0053H*	4.19E-02	2.06E+00
VNG0274C	*VNG0274C*	3.25E-02	1.75E+00
VNG0360C	*VNG0360C*	3.85E-02	1.72E+00
VNG0361C	*VNG0361C*	2.97E-02	1.62E+00
VNG0374G	*nusG*	3.33E-02	2.00E+00
VNG0376G	*ftsZ1*	5.65E-03	1.69E+00
VNG0399H	*VNG0399H*	4.52E-02	1.55E+00
VNG0425G	*pimT2*	2.05E-02	1.57E+00
VNG0435H	*VNG0435H*	1.50E-02	1.89E+00
VNG0436G	*nhaC1*	4.52E-02	1.88E+00
VNG0438G	*ferA3*	2.51E-02	1.38E+00
VNG0467G	*yafB*	2.05E-02	3.06E+00
VNG0500G	*ppd*	4.17E-02	1.64E+00
VNG0534C	*VNG0534C*	1.59E-02	1.48E+00
VNG0559G	*apt*	4.19E-02	1.77E+00
VNG0584H	*VNG0584H*	3.40E-02	1.70E+00
VNG0587H	*VNG0587H*	1.54E-02	1.72E+00
VNG0629G	*aspB2*	9.47E-03	1.66E+00
VNG0660H	*VNG0660H*	3.51E-02	1.53E+00
VNG0666G	*ctaB*	3.45E-02	1.62E+00
VNG0680G	*fdfT*	2.51E-02	1.69E+00
VNG0681G	*hbd1*	2.21E-02	1.76E+00
VNG0684G	*fbp*	2.73E-02	1.81E+00
VNG0708H	*VNG0708H*	2.84E-02	1.87E+00
VNG0709C	*VNG0709C*	3.77E-02	1.73E+00
VNG0741H	*VNG0741H*	3.74E-02	2.28E+00
VNG0746C	*VNG0746C*	3.25E-02	2.25E+00
VNG0767H	*VNG0767H*	6.98E-03	1.92E+00
VNG0782H	*VNG0782H*	3.45E-02	2.42E+00
VNG0793G	*htr6*	3.45E-02	1.90E+00
VNG0795G	*hcpC*	2.98E-02	1.59E+00
VNG0804C	*VNG0804C*	2.73E-02	1.50E+00
VNG0810H	*VNG0810H*	3.77E-02	1.74E+00
VNG0821C	*VNG0821C*	4.19E-02	1.48E+00
VNG0834C	*VNG0834C*	3.77E-02	1.44E+00
VNG0847H	*VNG0847H*	4.19E-02	1.44E+00
VNG0849C	*VNG0849C*	6.88E-03	1.66E+00
VNG0853C	*VNG0853C*	3.29E-02	1.91E+00

VNG0860G	*rpoL*	4.29E-03	1.89E+00
VNG0863H	*VNG0863H*	1.71E-02	2.81E+00
VNG0872G	*gatA*	3.45E-02	1.59E+00
VNG0891G	*yjlD*	2.84E-02	1.82E+00
VNG0893G	*udp2*	4.50E-02	1.46E+00
VNG0896G	*cda*	2.43E-02	1.82E+00
VNG0897G	*rbsC1*	3.77E-02	1.82E+00
VNG0898G	*rbsC2*	4.37E-02	1.43E+00
VNG0901G	*rbsA*	4.29E-03	2.20E+00
VNG0905G	*pmu2*	3.25E-02	2.21E+00
VNG0921G	*potA1*	4.19E-02	1.70E+00
VNG0931G	*acaB2*	8.50E-03	1.74E+00
VNG0932C	*VNG0932C*	4.19E-02	1.51E+00
VNG0933G	*yqjM*	4.19E-02	1.75E+00
VNG0940G	*acs3*	1.78E-02	1.88E+00
VNG0941C	*VNG0941C*	2.51E-02	1.66E+00
VNG0942G	*cheW2*	4.29E-03	1.71E+00
VNG0949G	*gspE3*	2.05E-02	1.90E+00
VNG0958G	*htr15*	2.51E-02	1.73E+00
VNG0965C	*VNG0965C*	6.14E-03	1.71E+00
VNG0966G	*cheR*	8.38E-03	1.86E+00
VNG0969H	*VNG0969H*	3.74E-02	2.11E+00
VNG0970G	*cheC1*	4.29E-03	2.08E+00
VNG0971G	*cheA*	8.58E-03	2.18E+00
VNG0974G	*cheY*	3.46E-02	2.04E+00
VNG0976G	*cheW1*	4.29E-03	1.83E+00
VNG0978H	*VNG0978H*	3.74E-02	1.49E+00
VNG0982C	*VNG0982C*	1.50E-02	1.79E+00
VNG0983C	*VNG0983C*	4.26E-02	1.77E+00
VNG0987H	*VNG0987H*	4.50E-02	4.97E+00
VNG0989C	*VNG0989C*	2.21E-02	4.15E+00
VNG1036H	*VNG1036H*	2.51E-02	2.67E+00
VNG1112H	*VNG1112H*	4.26E-02	1.75E+00
VNG1224G	*orc8*	4.32E-02	1.70E+00
VNG1426H	*VNG1426H*	2.51E-02	1.41E+00
VNG1546H	*VNG1546H*	4.44E-02	1.58E+00
VNG1578H	*VNG1578H*	3.77E-02	1.62E+00
VNG1617H	*VNG1617H*	2.51E-02	1.71E+00
VNG1654G	*cdc48e*	2.51E-02	1.45E+00
VNG1679H	*VNG1679H*	3.99E-02	1.69E+00
VNG1879G	*thb*	6.98E-03	1.69E+00
VNG1920H	*VNG1920H*	2.51E-02	1.79E+00

VNG1927H	*VNG1927H*	4.90E-02	2.07E+00
VNG2006C	*VNG2006C*	4.65E-02	1.96E+00
VNG2032G	*fad1*	3.77E-02	2.32E+00
VNG2045G	*gcp*	4.52E-02	1.81E+00
VNG2067H	*VNG2067H*	4.90E-02	1.46E+00
VNG2106G	*sdh*	3.74E-02	1.55E+00
VNG2124C	*VNG2124C*	4.13E-02	1.39E+00
VNG2191H	*VNG2191H*	3.77E-02	1.46E+00
VNG2222G	*pheA*	3.77E-02	1.69E+00
VNG2244H	*VNG2244H*	2.51E-02	1.38E+00
VNG2276G	*pmm*	3.77E-02	2.12E+00
VNG2299H	*VNG2299H*	1.85E-02	1.67E+00
VNG2341H	*VNG2341H*	4.19E-02	1.74E+00
VNG2399H	*VNG2399H*	4.26E-02	1.78E+00
VNG2410G	*gbp3*	4.26E-02	1.41E+00
VNG2422G	*glcD*	3.96E-02	1.52E+00
VNG2451H	*VNG2451H*	4.29E-03	1.75E+00
VNG2452C	*VNG2452C*	2.21E-02	1.77E+00
VNG2495H	*VNG2495H*	4.85E-02	1.43E+00
VNG2563H	*VNG2563H*	3.51E-02	2.32E+00
VNG2646C	*VNG2646C*	2.51E-02	1.40E+00
VNG2673H	*VNG2673H*	3.17E-02	1.47E+00
VNG2675C	*VNG2675C*	1.50E-02	1.63E+00
VNG5019G	*gvpM1*	4.13E-02	3.18E+00
VNG5020G	*gvpL1*	8.50E-03	3.40E+00
VNG5022G	*gvpJ1*	5.65E-03	3.47E+00
VNG5025G	*gvpH1*	4.38E-03	3.81E+00
VNG5027G	*gvpF1*	1.59E-02	4.01E+00
VNG5034G	*gvpO1*	3.77E-02	2.78E+00
VNG5038H	*VNG5038H*	1.50E-02	1.90E+00
VNG5039G	*tbpA*	4.19E-02	2.24E+00
VNG5081H	*VNG5081H*	3.23E-02	1.38E+00
VNG5137H	*VNG5137H*	2.73E-02	2.15E+00
VNG5145H	*VNG5145H*	4.29E-03	2.69E+01
VNG5173H	*VNG5173H*	4.29E-03	5.41E+00
VNG5183G	*arsC*	2.02E-02	6.84E+00
VNG5194C	*VNG5194C*	4.80E-02	1.90E+00
VNG6135C	*VNG6135C*	2.05E-02	1.92E+00
VNG6171H	*VNG6171H*	4.19E-02	2.39E+00
VNG6173C	*VNG6173C*	3.74E-02	2.99E+00
VNG6175G	*trkA2*	4.29E-03	2.84E+00
VNG6179G	*cat3*	1.19E-02	3.15E+00

VNG6181H	*VNG6181H*	3.51E-02	2.34E+00
VNG6182H	*VNG6182H*	2.21E-02	2.55E+00
VNG6194H	*VNG6194H*	2.21E-02	2.82E+00
VNG6199G	*cdc48d*	2.21E-02	5.05E+00
VNG6205C	*VNG6205C*	4.29E-03	2.20E+00
VNG6208C	*VNG6208C*	4.19E-02	2.91E+00
VNG6210G	*gabT*	1.43E-02	3.92E+00
VNG6211G	*bdb*	2.61E-02	5.00E+00
VNG6212G	*iucA*	1.07E-02	4.53E+00
VNG6214G	*hxyA*	3.96E-02	2.64E+00
VNG6216G	*iucC*	5.65E-03	2.77E+00
VNG6218G	*trkA3*	4.29E-03	2.43E+00
VNG6220G	*cat2*	1.59E-02	1.88E+00
VNG6223C	*VNG6223C*	2.21E-02	2.39E+00
VNG6230G	*gvpK2*	3.77E-02	3.92E+00
VNG6232G	*gvpJ2*	2.21E-02	4.22E+00
VNG6233G	*gvpI2*	4.17E-02	3.37E+00
VNG6235G	*gvpH2*	3.51E-02	3.67E+00
VNG6246G	*gvpO2*	8.56E-03	5.58E+00
VNG6247G	*trkA4*	4.29E-03	4.07E+00
VNG6250G	*phoT3*	2.08E-02	1.97E+00
VNG6255C	*VNG6255C*	4.29E-03	3.08E+00
VNG6256G	*lipB*	4.29E-03	2.64E+00
VNG6270G	*gldA*	4.56E-03	3.56E+00
VNG6275H	*VNG6275H*	3.64E-02	2.20E+00
VNG6276H	*VNG6276H*	3.77E-02	1.70E+00
VNG6287H	*VNG6287H*	3.62E-02	2.00E+00
VNG6296C	*VNG6296C*	4.96E-03	2.82E+00
VNG6299G	*hypE*	3.77E-02	3.75E+00
VNG6308G	*gltP*	3.94E-02	2.54E+00
VNG6311G	*pyrI*	3.07E-02	2.88E+00
VNG6318G	*arcR*	2.51E-02	3.33E+00
VNG6321H	*VNG6321H*	2.21E-02	1.95E+00
VNG6326G	*trp6*	2.21E-02	2.71E+00
VNG6329H	*VNG6329H*	3.96E-02	3.52E+00
VNG6332H	*VNG6332H*	2.05E-02	1.83E+00
VNG6334H	*VNG6334H*	3.51E-02	3.75E+00
VNG6335H	*VNG6335H*	8.56E-03	2.07E+00
VNG6339H	*VNG6339H*	4.33E-02	2.66E+00
VNG6347H	*VNG6347H*	3.77E-02	3.66E+00
VNG6348H	*VNG6348H*	1.50E-02	2.95E+00
VNG6351G	*tfbC*	9.47E-03	2.99E+00

VNG6354G	*comA*	4.52E-02	2.79E+00
VNG6355H	*VNG6355H*	3.77E-02	4.30E+00
VNG6357H	*VNG6357H*	1.19E-02	3.48E+00
VNG6361G	*npa*	4.29E-03	2.63E+00
VNG6363G	*orc4*	8.56E-03	2.34E+00
VNG6370H	*VNG6370H*	3.77E-02	3.46E+00
VNG6372H	*VNG6372H*	8.56E-03	3.25E+00
VNG6375H	*VNG6375H*	2.51E-02	2.71E+00
VNG6379C	*VNG6379C*	1.43E-02	1.92E+00
VNG6381H	*VNG6381H*	7.12E-03	1.75E+00
VNG6384H	*VNG6384H*	4.50E-02	2.55E+00

Appendix I. p-values and fold changes of genes differentially expressed in *Δvng1179C*

canonical_Name	gene_Name	corrected p-val	fold
VNG0237H	*VNG0237H*	2.86E-02	1.93E+00
VNG1123G	*trh7*	3.74E-02	1.49E+00
VNG2094G	*trh4*	3.37E-02	2.81E+00
VNG2101H	*VNG2101H*	4.50E-02	1.68E+00
VNG5144H	*VNG5144H*	2.69E-04	3.27E+00
VNG5145H	*VNG5145H*	2.32E-05	1.35E+01
VNG5146H	*VNG5146H*	3.37E-02	1.98E+00
VNG5148H	*VNG5148H*	2.86E-02	2.89E+00
VNG5164C	*VNG5164C*	3.37E-02	2.67E+00
VNG5173H	*VNG5173H*	2.86E-02	7.89E+00
VNG5183G	*arsC*	2.69E-04	2.89E+00
VNG5189H	*VNG5189H*	3.74E-02	1.90E+00
VNG5194C	*VNG5194C*	3.37E-02	1.72E+00
VNG6420H	*VNG6420H*	9.34E-03	4.78E+00

Appendix J. p-values and fold changes of genes differentially expressed in *Δvng1237C*

canonical_Name	gene_Name	corrected p-val	fold
VNG0001H	*VNG0001H*	1.32E-02	1.85E+00
VNG0013C	*VNG0013C*	1.45E-02	1.44E+00
VNG0029H	*VNG0029H*	3.52E-02	4.05E+00
VNG0146H	*VNG0146H*	3.85E-02	4.11E+00
VNG0168H	*VNG0168H*	4.47E-02	2.18E+00
VNG0177G	*rpl15e*	4.56E-02	2.38E+00
VNG0227H	*VNG0227H*	2.47E-02	1.54E+00
VNG0248C	*VNG0248C*	3.82E-02	2.00E+00
VNG0258H	*VNG0258H*	2.12E-02	1.76E+00
VNG0281G	*soxB*	3.94E-02	2.55E+00
VNG0342G	*smc1*	2.99E-02	2.32E+00
VNG0352H	*VNG0352H*	3.08E-02	1.56E+00
VNG0375G	*secE*	4.21E-02	1.71E+00
VNG0376G	*ftsZ1*	2.50E-02	1.97E+00
VNG0383H	*VNG0383H*	2.50E-02	1.58E+00
VNG0399H	*VNG0399H*	3.82E-02	1.61E+00
VNG0410G	*rfbU2*	2.10E-02	2.10E+00
VNG0417H	*VNG0417H*	2.48E-02	1.28E+00
VNG0420H	*VNG0420H*	3.30E-02	1.56E+00
VNG0435H	*VNG0435H*	3.94E-02	1.72E+00
VNG0438G	*ferA3*	2.47E-02	1.67E+00
VNG0439C	*VNG0439C*	9.40E-03	2.36E+00
VNG0461G	*aspS*	3.34E-02	1.46E+00
VNG0507C	*VNG0507C*	1.32E-02	2.28E+00
VNG0508H	*VNG0508H*	1.05E-02	1.57E+00
VNG0509H	*VNG0509H*	6.60E-03	1.53E+00
VNG0516H	*VNG0516H*	1.32E-02	1.74E+00
VNG0518H	*VNG0518H*	1.05E-02	2.55E+00
VNG0534C	*VNG0534C*	3.79E-02	1.37E+00
VNG0535C	*VNG0535C*	2.50E-02	2.32E+00
VNG0536G	*sirR*	3.06E-02	2.09E+00
VNG0546C	*VNG0546C*	2.48E-02	1.71E+00
VNG0563G	*ndhG2*	1.14E-02	1.70E+00
VNG0572G	*dfp*	2.41E-02	1.60E+00
VNG0587H	*VNG0587H*	2.48E-02	1.47E+00
VNG0602C	*VNG0602C*	6.22E-03	2.69E+00
VNG0606G	*yrhA*	2.67E-02	1.42E+00
VNG0617H	*VNG0617H*	1.64E-02	1.71E+00

VNG0620G	*edp*	9.40E-03	2.22E+00
VNG0627G	*citE*	7.64E-03	1.51E+00
VNG0629G	*aspB2*	1.05E-02	1.70E+00
VNG0630G	*ribE*	4.88E-02	2.06E+00
VNG0656H	*VNG0656H*	2.91E-02	1.74E+00
VNG0659H	*VNG0659H*	2.47E-02	5.61E+00
VNG0660H	*VNG0660H*	2.10E-02	1.48E+00
VNG0666G	*ctaB*	4.55E-02	1.48E+00
VNG0675C	*VNG0675C*	1.30E-02	1.59E+00
VNG0677H	*VNG0677H*	1.17E-02	1.61E+00
VNG0679G	*acd4*	2.23E-02	1.54E+00
VNG0680G	*fdfT*	3.30E-02	1.76E+00
VNG0681G	*hbd1*	1.30E-02	1.61E+00
VNG0684G	*fbp*	2.48E-02	1.90E+00
VNG0697H	*VNG0697H*	2.89E-02	1.50E+00
VNG0698H	*VNG0698H*	5.31E-03	1.64E+00
VNG0703H	*VNG0703H*	2.93E-02	1.65E+00
VNG0708H	*VNG0708H*	1.70E-02	1.68E+00
VNG0709C	*VNG0709C*	1.70E-02	2.06E+00
VNG0719G	*araL*	5.61E-03	2.42E+00
VNG0741H	*VNG0741H*	1.84E-02	1.79E+00
VNG0743H	*VNG0743H*	1.30E-02	1.82E+00
VNG0745G	*spoVR*	1.14E-02	2.61E+00
VNG0750C	*VNG0750C*	1.30E-02	1.79E+00
VNG0755C	*VNG0755C*	1.61E-02	1.58E+00
VNG0764C	*VNG0764C*	7.89E-03	1.81E+00
VNG0768H	*VNG0768H*	2.89E-02	1.83E+00
VNG0771G	*aldY2*	4.41E-02	2.28E+00
VNG0782H	*VNG0782H*	2.50E-02	1.94E+00
VNG0790G	*rps15p*	4.41E-02	1.91E+00
VNG0793G	*htr6*	3.25E-03	2.01E+00
VNG0794G	*yufN*	4.27E-03	2.00E+00
VNG0804C	*VNG0804C*	5.61E-03	1.53E+00
VNG0806G	*htr4*	1.52E-02	1.84E+00
VNG0813G	*potD*	4.94E-02	2.18E+00
VNG0823G	*gspE2*	1.05E-02	1.80E+00
VNG0849C	*VNG0849C*	2.91E-02	2.05E+00
VNG0853C	*VNG0853C*	1.61E-02	1.40E+00
VNG0860G	*rpoL*	1.70E-02	1.90E+00
VNG0863H	*VNG0863H*	1.64E-02	2.31E+00
VNG0864G	*purL*	4.56E-02	2.07E+00
VNG0868H	*VNG0868H*	2.95E-02	1.71E+00

VNG0872G	*gatA*	1.75E-02	1.94E+00
VNG0891G	*yjlD*	2.47E-02	1.87E+00
VNG0897G	*rbsC1*	1.05E-02	1.64E+00
VNG0901G	*rbsA*	1.32E-02	2.33E+00
VNG0903C	*VNG0903C*	1.12E-02	2.62E+00
VNG0906H	*VNG0906H*	2.89E-02	1.50E+00
VNG0914H	*VNG0914H*	2.48E-02	1.89E+00
VNG0915G	*hakA*	4.23E-02	2.27E+00
VNG0923G	*sfuB*	1.75E-02	2.06E+00
VNG0930G	*yvbT*	4.26E-02	3.33E+00
VNG0931G	*acaB2*	6.22E-03	1.61E+00
VNG0932C	*VNG0932C*	1.64E-02	1.60E+00
VNG0934H	*VNG0934H*	3.17E-02	1.92E+00
VNG0940G	*acs3*	2.47E-02	1.46E+00
VNG0941C	*VNG0941C*	6.22E-03	1.65E+00
VNG0942G	*cheW2*	5.59E-03	1.73E+00
VNG0946G	*minD1*	1.14E-02	1.64E+00
VNG0949G	*gspE3*	3.56E-03	1.77E+00
VNG0953C	*VNG0953C*	1.89E-02	1.77E+00
VNG0955G	*fapE*	1.36E-03	1.53E+00
VNG0958G	*htr15*	9.40E-03	1.80E+00
VNG0966G	*cheR*	1.36E-03	1.73E+00
VNG0967G	*cheD*	5.59E-03	2.01E+00
VNG0970G	*cheC1*	2.47E-02	1.80E+00
VNG0971G	*cheA*	1.62E-02	1.85E+00
VNG0973G	*cheB*	2.84E-02	2.33E+00
VNG0974G	*cheY*	2.62E-02	1.98E+00
VNG0976G	*cheW1*	4.22E-03	2.14E+00
VNG0982C	*VNG0982C*	5.14E-03	1.62E+00
VNG0987H	*VNG0987H*	2.58E-02	2.20E+00
VNG0993H	*VNG0993H*	3.10E-02	1.96E+00
VNG1001G	*guaB*	2.50E-02	1.60E+00
VNG1006H	*VNG1006H*	2.47E-02	1.45E+00
VNG1042H	*VNG1042H*	4.95E-02	1.85E+00
VNG1100C	*VNG1100C*	2.47E-02	1.41E+00
VNG1123G	*trh7*	2.50E-02	1.73E+00
VNG1168C	*VNG1168C*	3.08E-02	1.56E+00
VNG1196H	*VNG1196H*	4.93E-02	1.57E+00
VNG1212G	*hutH*	4.56E-02	2.30E+00
VNG1216G	*pgk*	6.56E-03	1.44E+00
VNG1241G	*surE*	2.48E-02	1.66E+00
VNG1246H	*VNG1246H*	2.58E-02	1.46E+00

VNG1253C	*VNG1253C*	4.37E-02	1.79E+00
VNG1257H	*VNG1257H*	2.67E-02	1.65E+00
VNG1275G	*hflX2*	4.88E-02	2.05E+00
VNG1320G	*cbp*	1.05E-02	1.99E+00
VNG1323C	*VNG1323C*	4.55E-02	1.58E+00
VNG1343C	*VNG1343C*	2.48E-02	1.99E+00
VNG1350C	*VNG1350C*	3.24E-03	2.27E+00
VNG1407C	*VNG1407C*	4.21E-02	1.37E+00
VNG1412H	*VNG1412H*	7.89E-03	1.77E+00
VNG1420H	*VNG1420H*	3.05E-02	1.36E+00
VNG1426H	*VNG1426H*	3.15E-02	1.51E+00
VNG1447H	*VNG1447H*	2.30E-02	1.65E+00
VNG1534H	*VNG1534H*	1.14E-02	2.19E+00
VNG1543G	*zim*	4.23E-02	2.02E+00
VNG1544G	*clc*	1.06E-02	1.66E+00
VNG1644G	*nrdB2*	3.08E-02	1.44E+00
VNG1646G	*trpG1*	4.88E-02	1.91E+00
VNG1650H	*VNG1650H*	3.53E-02	2.21E+00
VNG1718G	*rpl15p*	3.85E-02	2.62E+00
VNG1774G	*hemA*	4.88E-02	1.92E+00
VNG1776G	*nirH*	3.46E-02	1.58E+00
VNG1814G	*carB*	3.52E-02	3.63E+00
VNG1827H	*VNG1827H*	2.91E-02	1.43E+00
VNG1919H	*VNG1919H*	2.93E-02	1.79E+00
VNG1956H	*VNG1956H*	4.28E-02	2.16E+00
VNG1964H	*VNG1964H*	2.47E-02	1.93E+00
VNG1971G	*gpdB*	3.05E-02	1.56E+00
VNG1976H	*VNG1976H*	3.85E-02	2.22E+00
VNG1997G	*infB*	3.82E-02	1.69E+00
VNG2006C	*VNG2006C*	3.52E-02	2.07E+00
VNG2035H	*VNG2035H*	3.30E-02	1.49E+00
VNG2043G	*ham1*	3.94E-02	1.56E+00
VNG2045G	*gcp*	7.64E-03	2.34E+00
VNG2047G	*rps27e*	2.50E-02	2.04E+00
VNG2048G	*rps24e*	1.14E-02	2.48E+00
VNG2054H	*VNG2054H*	2.55E-02	2.61E+00
VNG2068C	*VNG2068C*	3.30E-02	1.36E+00
VNG2087G	*hisH2*	1.69E-02	2.02E+00
VNG2109H	*VNG2109H*	2.91E-02	1.47E+00
VNG2176H	*VNG2176H*	1.42E-02	1.61E+00
VNG2197H	*VNG2197H*	4.56E-02	2.13E+00
VNG2246H	*VNG2246H*	1.75E-02	2.15E+00

VNG2276G	*pmm*	3.87E-02	1.77E+00
VNG2282C	*VNG2282C*	3.79E-02	1.64E+00
VNG2298H	*VNG2298H*	3.82E-02	1.41E+00
VNG2306H	*VNG2306H*	2.89E-02	1.39E+00
VNG2324H	*VNG2324H*	2.99E-02	1.46E+00
VNG2372G	*rad24c*	3.82E-02	1.32E+00
VNG2377G	*nosY*	2.47E-02	2.09E+00
VNG2378G	*nosF1*	4.04E-02	1.53E+00
VNG2395C	*VNG2395C*	3.85E-02	1.56E+00
VNG2397G	*cysA*	2.13E-02	2.36E+00
VNG2433H	*VNG2433H*	2.47E-02	2.43E+00
VNG2436G	*argH*	2.89E-02	3.39E+00
VNG2437G	*argG*	2.47E-02	3.99E+00
VNG2441G	*rad3b*	3.85E-02	1.52E+00
VNG2466C	*VNG2466C*	4.88E-02	2.20E+00
VNG2480H	*VNG2480H*	3.85E-02	2.79E+00
VNG2521H	*VNG2521H*	4.26E-02	1.31E+00
VNG2541C	*VNG2541C*	2.55E-02	1.74E+00
VNG2593H	*VNG2593H*	4.38E-02	1.51E+00
VNG2627C	*VNG2627C*	2.12E-02	2.28E+00
VNG2662G	*rpoC*	2.91E-02	2.01E+00
VNG2678H	*VNG2678H*	4.23E-02	1.97E+00
VNG5010G	*sojA*	3.70E-02	3.44E+00
VNG5019G	*gvpM1*	1.71E-02	2.70E+00
VNG5020G	*gvpL1*	1.77E-02	3.13E+00
VNG5021G	*gvpK1*	4.27E-03	2.90E+00
VNG5022G	*gvpJ1*	1.61E-02	4.28E+00
VNG5023G	*gvpI1*	1.14E-02	2.94E+00
VNG5025G	*gvpH1*	1.75E-02	3.65E+00
VNG5026G	*gvpG1*	7.89E-03	3.02E+00
VNG5027G	*gvpF1*	1.39E-02	3.60E+00
VNG5034G	*gvpO1*	3.85E-02	2.41E+00
VNG5035G	*sojB*	1.70E-02	2.82E+00
VNG5038H	*VNG5038H*	1.33E-02	2.42E+00
VNG5044H	*VNG5044H*	2.91E-02	2.30E+00
VNG5093C	*VNG5093C*	2.47E-02	2.00E+00
VNG5097H	*VNG5097H*	2.48E-02	2.07E+00
VNG5137H	*VNG5137H*	3.79E-02	2.19E+00
VNG5142G	*tbpC*	2.89E-02	1.56E+00
VNG5144H	*VNG5144H*	4.27E-03	3.17E+00
VNG5145H	*VNG5145H*	1.09E-03	2.25E+01
VNG5146H	*VNG5146H*	1.78E-02	2.11E+00

VNG5148H	*VNG5148H*	1.01E-02	2.50E+00
VNG5154H	*VNG5154H*	2.11E-02	2.21E+00
VNG5156H	*VNG5156H*	3.82E-02	2.25E+00
VNG5167H	*VNG5167H*	2.47E-02	1.92E+00
VNG5173H	*VNG5173H*	2.10E-02	8.89E+00
VNG5178H	*VNG5178H*	5.42E-03	1.35E+00
VNG5180G	*arsA2*	1.15E-02	1.80E+00
VNG5181G	*arsD*	4.25E-03	1.65E+00
VNG5182G	*arsR*	9.33E-03	1.50E+00
VNG5183G	*arsC*	3.25E-03	4.00E+00
VNG5189H	*VNG5189H*	6.22E-03	1.66E+00
VNG5194C	*VNG5194C*	3.90E-02	1.64E+00
VNG5199H	*VNG5199H*	5.61E-03	1.47E+00
VNG6170H	*VNG6170H*	1.78E-02	1.76E+00
VNG6171H	*VNG6171H*	7.64E-03	1.58E+00
VNG6173C	*VNG6173C*	3.24E-03	2.12E+00
VNG6175G	*trkA2*	1.23E-02	2.16E+00
VNG6179G	*cat3*	3.52E-02	2.32E+00
VNG6181H	*VNG6181H*	2.12E-02	2.64E+00
VNG6182H	*VNG6182H*	2.75E-03	2.56E+00
VNG6183C	*VNG6183C*	2.91E-02	1.47E+00
VNG6184G	*cat4*	2.48E-02	1.64E+00
VNG6186H	*VNG6186H*	3.94E-02	2.14E+00
VNG6195H	*VNG6195H*	6.95E-03	2.07E+00
VNG6199G	*cdc48d*	1.30E-02	2.32E+00
VNG6205C	*VNG6205C*	6.15E-03	2.07E+00
VNG6208C	*VNG6208C*	1.75E-02	2.77E+00
VNG6209H	*VNG6209H*	3.11E-02	1.71E+00
VNG6210G	*gabT*	4.27E-03	3.72E+00
VNG6211G	*bdb*	1.30E-02	3.50E+00
VNG6212G	*iucA*	6.66E-03	3.66E+00
VNG6213G	*iucB*	4.41E-02	2.10E+00
VNG6216G	*iucC*	1.70E-02	2.42E+00
VNG6218G	*trkA3*	4.27E-03	2.82E+00
VNG6220G	*cat2*	3.30E-02	1.71E+00
VNG6223C	*VNG6223C*	4.22E-03	2.97E+00
VNG6246G	*gvpO2*	2.48E-02	4.62E+00
VNG6247G	*trkA4*	1.58E-03	2.28E+00
VNG6250G	*phoT3*	2.91E-02	2.07E+00
VNG6251H	*VNG6251H*	1.96E-02	1.75E+00
VNG6255C	*VNG6255C*	3.32E-03	2.45E+00
VNG6256G	*lipB*	1.75E-03	2.72E+00

VNG6260G	*ftsZ5*	3.45E-02	1.70E+00
VNG6269C	*VNG6269C*	4.86E-02	2.46E+00
VNG6270G	*gldA*	2.10E-02	3.86E+00
VNG6276H	*VNG6276H*	4.22E-03	1.73E+00
VNG6279G	*ugpA*	2.42E-02	1.85E+00
VNG6284H	*VNG6284H*	4.19E-02	1.86E+00
VNG6294G	*perA*	2.11E-02	2.66E+00
VNG6296C	*VNG6296C*	5.61E-03	3.52E+00
VNG6303G	*exsB*	9.75E-03	2.11E+00
VNG6306C	*VNG6306C*	2.48E-02	2.37E+00
VNG6312G	*argS*	2.28E-02	2.25E+00
VNG6317G	*arcA*	1.29E-02	1.96E+00
VNG6318G	*arcR*	1.77E-02	1.97E+00
VNG6329H	*VNG6329H*	1.30E-02	2.57E+00
VNG6332H	*VNG6332H*	3.86E-02	2.94E+00
VNG6335H	*VNG6335H*	3.85E-02	2.01E+00
VNG6337G	*sojE*	4.72E-02	2.48E+00
VNG6340H	*VNG6340H*	3.94E-02	1.51E+00
VNG6347H	*VNG6347H*	1.64E-02	2.84E+00
VNG6348H	*VNG6348H*	3.70E-02	1.68E+00
VNG6357H	*VNG6357H*	4.27E-03	2.94E+00
VNG6361G	*npa*	2.47E-02	1.97E+00
VNG6368H	*VNG6368H*	3.80E-02	1.51E+00
VNG6370H	*VNG6370H*	4.27E-03	2.25E+00
VNG6372H	*VNG6372H*	7.64E-03	2.03E+00
VNG6373G	*phrH*	4.55E-02	1.96E+00
VNG6379C	*VNG6379C*	4.66E-02	1.90E+00
VNG6381H	*VNG6381H*	2.62E-02	1.89E+00
VNG6385H	*VNG6385H*	2.66E-02	1.60E+00
VNG6416H	*VNG6416H*	3.17E-02	2.18E+00
VNG6419H	*VNG6419H*	4.21E-02	1.77E+00
VNG6420H	*VNG6420H*	1.94E-02	3.03E+00
VNG6427H	*VNG6427H*	9.40E-03	2.25E+00
VNG6429H	*VNG6429H*	4.21E-02	1.48E+00
VNG6434H	*VNG6434H*	4.26E-02	1.61E+00

Appendix K. p-values and fold changes of genes differentially expressed in *Δtrh2*

canonical_Name	gene_Name	corrected p-val	fold
VNG0153C	*VNG0153C*	2.63E-02	2.40E+00
VNG0311H	*VNG0311H*	3.72E-02	2.12E+00
VNG0374G	*nusG*	1.91E-02	2.02E+00
VNG0376G	*ftsZ1*	1.11E-02	1.63E+00
VNG0399H	*VNG0399H*	1.73E-02	1.44E+00
VNG0424C	*VNG0424C*	1.88E-02	1.52E+00
VNG0425G	*pimT2*	1.18E-02	1.45E+00
VNG0435H	*VNG0435H*	4.48E-02	1.67E+00
VNG0534C	*VNG0534C*	9.14E-03	1.52E+00
VNG0536G	*sirR*	3.25E-02	2.76E+00
VNG0571C	*VNG0571C*	3.46E-02	1.39E+00
VNG0601H	*VNG0601H*	2.03E-02	1.45E+00
VNG0657G	*coxA2*	3.51E-02	1.88E+00
VNG0675C	*VNG0675C*	3.25E-02	1.60E+00
VNG0680G	*fdfT*	4.32E-03	1.79E+00
VNG0681G	*hbd1*	1.18E-02	1.65E+00
VNG0683C	*VNG0683C*	2.63E-02	1.87E+00
VNG0697H	*VNG0697H*	3.25E-02	1.44E+00
VNG0708H	*VNG0708H*	2.99E-02	1.93E+00
VNG0719G	*araL*	1.11E-02	2.24E+00
VNG0741H	*VNG0741H*	1.91E-02	2.16E+00
VNG0764C	*VNG0764C*	5.18E-03	1.49E+00
VNG0780H	*VNG0780H*	3.04E-02	1.49E+00
VNG0795G	*hcpC*	9.14E-03	1.73E+00
VNG0804C	*VNG0804C*	9.14E-03	1.43E+00
VNG0810H	*VNG0810H*	1.18E-02	1.79E+00
VNG0853C	*VNG0853C*	3.35E-02	1.70E+00
VNG0864G	*purL*	4.00E-02	1.92E+00
VNG0865C	*VNG0865C*	3.94E-02	2.55E+00
VNG0867G	*asnA*	3.30E-02	1.83E+00
VNG0872G	*gatA*	2.03E-02	1.52E+00
VNG0898G	*rbsC2*	4.13E-02	1.45E+00
VNG0905G	*pmu2*	2.17E-02	1.96E+00
VNG0911H	*VNG0911H*	2.63E-02	1.60E+00
VNG0921G	*potA1*	3.94E-02	1.63E+00
VNG0931G	*acaB2*	7.17E-03	1.62E+00
VNG0932C	*VNG0932C*	1.03E-02	1.71E+00
VNG0940G	*acs3*	9.54E-03	1.61E+00
VNG0941C	*VNG0941C*	2.17E-02	1.85E+00

VNG0942G	*cheW2*	9.14E-03	1.65E+00
VNG0950G	*fapH*	9.53E-03	1.91E+00
VNG0958G	*htr15*	4.92E-03	1.77E+00
VNG0965C	*VNG0965C*	3.25E-02	1.78E+00
VNG0966G	*cheR*	1.73E-02	1.62E+00
VNG0970G	*cheC1*	3.24E-02	2.22E+00
VNG0971G	*cheA*	2.14E-02	1.90E+00
VNG0976G	*cheW1*	9.14E-03	1.85E+00
VNG0978H	*VNG0978H*	1.88E-02	1.49E+00
VNG0982C	*VNG0982C*	5.53E-03	1.63E+00
VNG0983C	*VNG0983C*	3.72E-02	1.74E+00
VNG1058H	*VNG1058H*	3.70E-02	1.86E+00
VNG1280C	*VNG1280C*	4.06E-02	1.78E+00
VNG1281H	*VNG1281H*	4.32E-03	2.33E+00
VNG1282G	*trkA5*	9.14E-03	3.16E+00
VNG1345H	*VNG1345H*	4.69E-02	1.63E+00
VNG1454C	*VNG1454C*	4.06E-02	1.69E+00
VNG1567G	*cbiC*	3.46E-02	1.90E+00
VNG1613H	*VNG1613H*	3.94E-02	1.45E+00
VNG1680G	*crtB2*	4.88E-02	1.83E+00
VNG1724G	*adk*	1.18E-02	1.58E+00
VNG1766C	*VNG1766C*	3.70E-02	1.33E+00
VNG1814G	*carB*	3.70E-02	3.11E+00
VNG1826H	*VNG1826H*	3.46E-02	1.53E+00
VNG1901C	*VNG1901C*	3.47E-02	1.94E+00
VNG2028H	*VNG2028H*	1.91E-02	2.20E+00
VNG2044H	*VNG2044H*	2.90E-02	1.46E+00
VNG2197H	*VNG2197H*	4.86E-02	2.45E+00
VNG2326G	*hemL*	4.69E-02	1.50E+00
VNG2352G	*glyS*	4.28E-02	1.57E+00
VNG2563H	*VNG2563H*	4.95E-02	2.17E+00
VNG2640G	*gcvT2*	3.25E-02	1.45E+00
VNG2641H	*VNG2641H*	4.28E-02	1.53E+00
VNG5019G	*gvpM1*	1.18E-02	3.03E+00
VNG5022G	*gvpJ1*	4.81E-02	3.42E+00
VNG5025G	*gvpH1*	4.28E-02	3.81E+00
VNG5027G	*gvpF1*	4.28E-02	3.61E+00
VNG5037G	*htlD*	3.94E-02	1.81E+00
VNG5134G	*rad25*	3.90E-02	1.68E+00
VNG5137H	*VNG5137H*	4.70E-02	1.79E+00
VNG5189H	*VNG5189H*	1.91E-02	2.42E+00
VNG5191H	*VNG5191H*	2.78E-02	2.34E+00

VNG5194C	*VNG5194C*	9.80E-04	2.16E+00
VNG6135C	*VNG6135C*	2.17E-02	1.78E+00
VNG6173C	*VNG6173C*	3.25E-02	2.53E+00
VNG6181H	*VNG6181H*	1.18E-02	2.55E+00
VNG6182H	*VNG6182H*	9.14E-03	2.24E+00
VNG6188H	*VNG6188H*	3.70E-02	1.61E+00
VNG6195H	*VNG6195H*	2.24E-02	3.49E+00
VNG6199G	*cdc48d*	4.28E-02	4.52E+00
VNG6201G	*hsp5*	3.30E-02	2.68E+00
VNG6205C	*VNG6205C*	9.14E-03	1.82E+00
VNG6208C	*VNG6208C*	1.18E-02	2.50E+00
VNG6209H	*VNG6209H*	2.63E-02	1.56E+00
VNG6211G	*bdb*	3.66E-02	4.14E+00
VNG6212G	*iucA*	3.22E-02	4.75E+00
VNG6213G	*iucB*	4.24E-02	2.69E+00
VNG6216G	*iucC*	7.92E-03	2.52E+00
VNG6218G	*trkA3*	1.18E-02	2.61E+00
VNG6223C	*VNG6223C*	1.73E-02	3.10E+00
VNG6226H	*VNG6226H*	3.94E-02	1.32E+00
VNG6232G	*gvpJ2*	3.25E-02	4.32E+00
VNG6240G	*gvpD2*	3.94E-02	2.30E+00
VNG6246G	*gvpO2*	2.01E-02	4.45E+00
VNG6247G	*trkA4*	6.34E-03	3.64E+00
VNG6255C	*VNG6255C*	1.45E-03	2.67E+00
VNG6256G	*lipB*	9.14E-03	2.56E+00
VNG6266H	*VNG6266H*	4.00E-02	3.27E+00
VNG6269C	*VNG6269C*	9.14E-03	1.79E+00
VNG6270G	*gldA*	2.92E-02	3.07E+00
VNG6276H	*VNG6276H*	3.04E-02	1.84E+00
VNG6294G	*perA*	4.30E-02	3.20E+00
VNG6296C	*VNG6296C*	4.32E-03	2.82E+00
VNG6299G	*hypE*	2.63E-02	2.91E+00
VNG6302C	*VNG6302C*	4.88E-02	1.94E+00
VNG6308G	*gltP*	2.90E-02	2.35E+00
VNG6316G	*arcC*	3.35E-02	2.45E+00
VNG6318G	*arcR*	9.14E-03	2.42E+00
VNG6321H	*VNG6321H*	4.06E-02	1.79E+00
VNG6329H	*VNG6329H*	3.94E-02	2.08E+00
VNG6420H	*VNG6420H*	9.54E-03	3.73E+00

Appendix L. p-values and fold changes of genes differentially expressed in *Δtrh3*

canonical_Name	gene_Name	corrected p-val	fold
VNG0343H	*VNG0343H*	2.83E-02	1.82E+00
VNG0376G	*ftsZ1*	1.26E-02	1.72E+00
VNG0399H	*VNG0399H*	4.73E-02	1.55E+00
VNG0425G	*pimT2*	2.22E-02	1.51E+00
VNG0583G	*cyb*	2.83E-02	1.56E+00
VNG0617H	*VNG0617H*	4.49E-02	1.76E+00
VNG0629G	*aspB2*	3.39E-02	1.91E+00
VNG0666G	*ctaB*	4.47E-02	1.73E+00
VNG0681G	*hbd1*	1.83E-02	1.60E+00
VNG0703H	*VNG0703H*	2.41E-02	1.66E+00
VNG0764C	*VNG0764C*	2.41E-02	1.55E+00
VNG0793G	*htr6*	1.83E-02	1.74E+00
VNG0804C	*VNG0804C*	2.00E-02	1.55E+00
VNG0849C	*VNG0849C*	2.41E-02	1.67E+00
VNG0921G	*potA1*	4.47E-02	1.59E+00
VNG0931G	*acaB2*	1.83E-02	1.69E+00
VNG0932C	*VNG0932C*	2.44E-02	1.52E+00
VNG0940G	*acs3*	4.75E-02	1.73E+00
VNG0942G	*cheW2*	1.83E-02	1.71E+00
VNG0949G	*gspE3*	4.66E-02	1.52E+00
VNG0955G	*fapE*	4.66E-02	1.66E+00
VNG0958G	*htr15*	4.47E-02	1.73E+00
VNG0963G	*cpcE*	2.38E-02	1.48E+00
VNG0970G	*cheC1*	2.44E-02	1.84E+00
VNG0976G	*cheW1*	4.66E-02	1.76E+00
VNG0978H	*VNG0978H*	4.47E-02	1.61E+00
VNG0982C	*VNG0982C*	2.44E-02	1.68E+00
VNG1642H	*VNG1642H*	4.58E-02	1.51E+00
VNG1654G	*cdc48e*	4.47E-02	1.41E+00
VNG1814G	*carB*	2.83E-02	3.57E+00
VNG1818G	*idi*	1.26E-02	2.63E+00
VNG2059H	*VNG2059H*	4.73E-02	1.76E+00
VNG2599H	*VNG2599H*	1.83E-02	1.50E+00
VNG2673H	*VNG2673H*	2.83E-02	1.38E+00
VNG5037G	*htlD*	2.00E-02	1.65E+00
VNG5038H	*VNG5038H*	2.83E-02	2.10E+00
VNG5139C	*VNG5139C*	4.75E-02	1.93E+00
VNG5144H	*VNG5144H*	3.92E-02	1.98E+00
VNG5148H	*VNG5148H*	4.33E-02	1.85E+00

VNG5173H	*VNG5173H*	1.83E-02	6.73E+00
VNG5183G	*arsC*	3.39E-02	7.26E+00
VNG6135C	*VNG6135C*	1.83E-02	1.68E+00
VNG6159H	*VNG6159H*	4.17E-02	1.87E+00
VNG6181H	*VNG6181H*	1.83E-02	2.39E+00
VNG6182H	*VNG6182H*	1.83E-02	1.81E+00
VNG6205C	*VNG6205C*	3.92E-02	1.80E+00
VNG6218G	*trkA3*	2.85E-02	2.53E+00
VNG6220G	*cat2*	2.41E-02	1.78E+00
VNG6250G	*phoT3*	4.66E-02	1.84E+00
VNG6255C	*VNG6255C*	1.83E-02	2.24E+00
VNG6256G	*lipB*	4.58E-02	2.31E+00
VNG6296C	*VNG6296C*	1.83E-02	2.37E+00
VNG6335H	*VNG6335H*	2.00E-02	2.01E+00
VNG6357H	*VNG6357H*	2.83E-02	2.96E+00
VNG6361G	*npa*	2.83E-02	2.22E+00
VNG6372H	*VNG6372H*	2.83E-02	2.85E+00
VNG6379C	*VNG6379C*	4.66E-02	1.71E+00

Appendix M. p-values and fold changes of genes differentially expressed in *Δtrh4*

canonical_Name	gene_Name	corrected p-val	fold
VNG0289H	*VNG0289H*	2.37E-02	2.13E+00
VNG0322H	*VNG0322H*	3.73E-02	1.42E+00
VNG0361C	*VNG0361C*	2.25E-02	1.73E+00
VNG0376G	*ftsZ1*	2.37E-02	1.58E+00
VNG0404H	*VNG0404H*	3.38E-02	1.57E+00
VNG0420H	*VNG0420H*	1.18E-02	1.67E+00
VNG0424C	*VNG0424C*	4.61E-02	1.44E+00
VNG0436G	*nhaC1*	1.96E-02	1.88E+00
VNG0438G	*ferA3*	3.69E-02	1.52E+00
VNG0471C	*VNG0471C*	1.18E-02	1.53E+00
VNG0473G	*porB*	3.40E-02	2.34E+00
VNG0516H	*VNG0516H*	4.99E-02	1.48E+00
VNG0534C	*VNG0534C*	2.37E-02	1.45E+00
VNG0591C	*VNG0591C*	6.61E-03	1.48E+00
VNG0630G	*ribE*	2.22E-02	1.75E+00
VNG0660H	*VNG0660H*	4.42E-02	1.66E+00
VNG0681G	*hbd1*	1.45E-02	1.55E+00
VNG0702H	*VNG0702H*	2.25E-02	3.33E+00
VNG0738H	*VNG0738H*	4.78E-02	1.44E+00
VNG0757G	*tfeA*	4.42E-02	1.43E+00
VNG0777G	*taqD*	3.73E-02	2.02E+00
VNG0793G	*htr6*	1.58E-02	1.70E+00
VNG0794G	*yufN*	3.38E-02	2.29E+00
VNG0804C	*VNG0804C*	9.41E-03	1.40E+00
VNG0810H	*VNG0810H*	4.00E-02	1.66E+00
VNG0841G	*icfA*	1.79E-02	1.58E+00
VNG0849C	*VNG0849C*	4.42E-02	1.67E+00
VNG0852C	*VNG0852C*	3.73E-02	1.47E+00
VNG0879C	*VNG0879C*	4.00E-02	1.54E+00
VNG0905G	*pmu2*	1.96E-02	2.03E+00
VNG0906H	*VNG0906H*	6.61E-03	1.76E+00
VNG0911H	*VNG0911H*	1.29E-02	1.53E+00
VNG0914H	*VNG0914H*	2.22E-02	1.40E+00
VNG0928G	*mak*	1.39E-02	1.56E+00
VNG0931G	*acaB2*	4.00E-02	1.77E+00
VNG0932C	*VNG0932C*	1.29E-02	1.57E+00
VNG0937G	*gap*	2.15E-02	3.46E+00
VNG0940G	*acs3*	3.13E-02	1.73E+00
VNG0942G	*cheW2*	2.54E-02	1.70E+00

VNG0943C	*VNG0943C*	1.29E-02	1.90E+00
VNG0949G	*gspE3*	2.02E-02	1.69E+00
VNG0950G	*fapH*	1.85E-02	1.85E+00
VNG0953C	*VNG0953C*	3.80E-02	1.59E+00
VNG0955G	*fapE*	4.00E-02	1.66E+00
VNG0958G	*htr15*	6.37E-03	1.78E+00
VNG0966G	*cheR*	2.34E-02	1.73E+00
VNG0969H	*VNG0969H*	3.80E-02	2.09E+00
VNG0970G	*cheC1*	3.67E-02	1.92E+00
VNG0971G	*cheA*	1.29E-02	2.12E+00
VNG0976G	*cheW1*	1.18E-02	1.77E+00
VNG0983C	*VNG0983C*	4.17E-02	2.34E+00
VNG1438H	*VNG1438H*	4.00E-02	1.69E+00
VNG1861C	*VNG1861C*	4.61E-02	1.66E+00
VNG2093G	*glnA*	4.75E-02	2.32E+00
VNG2094G	*trh4*	2.37E-02	1.68E+00
VNG2370C	*VNG2370C*	2.41E-02	1.32E+00
VNG2472G	*nifU*	3.03E-02	1.32E+00
VNG5011H	*VNG5011H*	6.37E-03	1.50E+00
VNG5012H	*VNG5012H*	1.96E-02	2.21E+00
VNG5038H	*VNG5038H*	1.29E-02	2.12E+00
VNG5071C	*VNG5071C*	1.18E-02	2.09E+00
VNG5144H	*VNG5144H*	3.40E-02	1.81E+00
VNG5191H	*VNG5191H*	3.73E-02	2.13E+00
VNG5194C	*VNG5194C*	1.25E-02	1.97E+00
VNG6173C	*VNG6173C*	6.37E-03	2.29E+00
VNG6177G	*kdpB*	4.72E-02	2.86E+00
VNG6181H	*VNG6181H*	2.83E-02	2.07E+00
VNG6182H	*VNG6182H*	2.54E-02	1.91E+00
VNG6195H	*VNG6195H*	1.18E-02	2.37E+00
VNG6199G	*cdc48d*	3.75E-02	4.13E+00
VNG6205C	*VNG6205C*	8.61E-03	2.03E+00
VNG6208C	*VNG6208C*	2.25E-02	2.73E+00
VNG6210G	*gabT*	1.18E-02	3.91E+00
VNG6211G	*bdb*	1.96E-02	4.29E+00
VNG6212G	*iucA*	3.38E-02	4.68E+00
VNG6216G	*iucC*	9.41E-03	2.31E+00
VNG6218G	*trkA3*	1.18E-02	2.45E+00
VNG6220G	*cat2*	3.75E-02	1.76E+00
VNG6223C	*VNG6223C*	1.81E-02	2.80E+00
VNG6247G	*trkA4*	1.18E-02	3.02E+00
VNG6255C	*VNG6255C*	5.55E-07	2.40E+00

VNG6256G	*lipB*	6.37E-03	2.49E+00
VNG6270G	*gldA*	1.29E-02	3.75E+00
VNG6294G	*perA*	1.47E-02	2.83E+00
VNG6296C	*VNG6296C*	4.58E-03	2.38E+00
VNG6308G	*gltP*	2.57E-02	2.61E+00
VNG6312G	*argS*	1.29E-02	1.70E+00
VNG6332H	*VNG6332H*	6.37E-03	1.70E+00
VNG6420H	*VNG6420H*	3.43E-02	3.69E+00

Appendix N. p-values and fold changes of genes differentially expressed in *Δtrh6*

canonical_Name	gene_Name	corrected p-val	fold
VNG1349C	*VNG1349C*	1.09E-02	3.78E+00
VNG1350C	*VNG1350C*	2.42E-02	2.91E+00
VNG1912G	*trpD2*	3.26E-02	1.77E+00
VNG2252G	*hjr*	4.40E-02	1.53E+00
VNG5139C	*VNG5139C*	2.42E-02	2.15E+00
VNG5142G	*tbpC*	1.28E-02	1.74E+00
VNG5144H	*VNG5144H*	6.81E-04	3.21E+00
VNG5145H	*VNG5145H*	4.78E-04	5.00E+01
VNG5146H	*VNG5146H*	3.26E-02	2.11E+00
VNG5148H	*VNG5148H*	2.42E-02	2.97E+00
VNG5164C	*VNG5164C*	3.75E-02	2.62E+00
VNG5167H	*VNG5167H*	3.78E-02	1.81E+00
VNG5173H	*VNG5173H*	2.95E-02	1.02E+01
VNG5176C	*VNG5176C*	6.79E-03	1.65E+00
VNG5178H	*VNG5178H*	7.70E-03	1.60E+00
VNG5183G	*arsC*	3.16E-03	6.08E+00
VNG5189H	*VNG5189H*	2.42E-02	1.82E+00
VNG6210G	*gabT*	3.02E-02	2.98E+00
VNG6420H	*VNG6420H*	3.16E-03	5.74E+00
VNG6429H	*VNG6429H*	2.42E-02	1.71E+00

Appendix O. p-values and fold changes of genes differentially expressed in *Δtrh7*

canonical_Name	gene_Name	corrected p-val	fold
VNG0499G	*cna*	2.68E-02	1.51E+00
VNG1123G	*trh7*	6.93E-03	5.83E+00
VNG1589C	*VNG1589C*	3.99E-03	1.81E+00
VNG5144H	*VNG5144H*	2.93E-02	3.52E+00
VNG5145H	*VNG5145H*	3.90E-03	1.37E+01
VNG5148H	*VNG5148H*	9.74E-03	2.88E+00
VNG5189H	*VNG5189H*	3.90E-03	2.09E+00
VNG5192H	*VNG5192H*	2.29E-02	2.54E+00
VNG6135C	*VNG6135C*	2.68E-02	3.54E+00
VNG6255C	*VNG6255C*	9.74E-03	1.95E+00
VNG6420H	*VNG6420H*	2.93E-02	5.07E+00

Appendix P. Genes with evidence from both ChIP-chip and microarray of deletion strains

Lrp	Direct Targets		
	canonical_Name	gene_Name	Corrected *p*-values
AsnC	*VNG0360C*	*VNG0360C*	3.85E-02
AsnC	*VNG0361C*	*VNG0361C*	2.97E-02
AsnC	*VNG0467G*	*yafB*	2.05E-02
AsnC	*VNG0629G*	*aspB2*	9.47E-03
AsnC	*VNG0795G*	*hcpC*	2.98E-02
AsnC	*VNG0853C*	*VNG0853C*	3.29E-02
AsnC	*VNG0872G*	*gatA*	3.45E-02
AsnC	*VNG0921G*	*potA1*	4.19E-02
AsnC	*VNG0966G*	*cheR*	8.38E-03
AsnC	*VNG0983C*	*VNG0983C*	4.26E-02
AsnC	*VNG1920H*	*VNG1920H*	2.51E-02
AsnC	*VNG2495H*	*VNG2495H*	4.85E-02
AsnC	*VNG5022G*	*gvpJ1*	5.65E-03
AsnC	*VNG6212G*	*iucA*	1.07E-02
AsnC	*VNG6214G*	*hxyA*	3.96E-02
AsnC	*VNG6216G*	*iucC*	5.65E-03
AsnC	*VNG6233G*	*gvpI2*	4.17E-02
AsnC	*VNG6246G*	*gvpO2*	8.56E-03
AsnC	*VNG6334H*	*VNG6334H*	3.51E-02
AsnC	*VNG6347H*	*VNG6347H*	3.77E-02
VNG1179C	*VNG6420H*	*VNG6420H*	9.54E-03
VNG1237C	*VNG0563G*	*ndhG2*	4.63E-02
VNG1237C	*VNG0872G*	*gatA*	1.79E-02
VNG1237C	*VNG0966G*	*cheR*	6.76E-03
VNG1237C	*VNG1123G*	*trh7*	9.11E-01
VNG1237C	*VNG1718G*	*rpl15p*	7.64E-01
VNG1237C	*VNG1956H*	*VNG1956H*	6.88E-01
VNG1237C	*VNG2397G*	*cysA*	8.12E-01
Trh2	*VNG0697H*	*VNG0697H*	2.50E-01
Trh2	*VNG0898G*	*rbsC2*	6.65E-02
Trh3	*VNG0966G*	*cheR*	1.36E-03
Trh3	*VNG1814G*	*carB*	3.52E-02
Trh4	*VNG0361C*	*VNG0361C*	8.82E-01
Trh4	*VNG0420H*	*VNG0420H*	5.10E-01
Trh4	*VNG0793G*	*htr6*	2.83E-01
Trh4	*VNG0920H*	*VNG0920H*	3.53E-01
Trh4	*VNG6177G*	*kdpB*	8.41E-01
Trh4	*VNG6247G*	*trkA4*	7.71E-01

Appendix Q. Detailed list of 66 condition sets and corresponding experiments

Name of condition sets	Name of experiments[a]	Description
circadian	light2__1440m_vs_light1_3960m	light:dark changes on a 12:12 hour cyclic schedule
circadian	light2__1620m_vs_light1_3960m	light:dark changes on a 12:12 hour cyclic schedule
circadian	light2__1800m_vs_light1_3960m	light:dark changes on a 12:12 hour cyclic schedule
circadian	light2__1980m_vs_light1_3960m	light:dark changes on a 12:12 hour cyclic schedule
circadian	light2__2160m_vs_light1_3960m	light:dark changes on a 12:12 hour cyclic schedule
circadian	light2__2340m_vs_light1_3960m	light:dark changes on a 12:12 hour cyclic schedule
circadian	light2__2520m_vs_light1_3960m	light:dark changes on a 12:12 hour cyclic schedule
circadian	light2__2700m_vs_light1_3960m	light:dark changes on a 12:12 hour cyclic schedule
circadian	light2__2880m_vs_light1_3960m	light:dark changes on a 12:12 hour cyclic schedule
circadian	light2__3060m_vs_light1_3960m	light:dark changes on a 12:12 hour cyclic schedule
circadian	light2__3240m_vs_light1_3960m	light:dark changes on a 12:12 hour cyclic schedule
circadian	light2__3420m_vs_light1_3960m	light:dark changes on a 12:12 hour cyclic schedule
circadian	light2__3600m_vs_light1_3960m	light:dark changes on a 12:12 hour cyclic schedule
circadian	light2__3780m_vs_light1_3960m	light:dark changes on a 12:12 hour cyclic schedule
circadian	light2__3960m_vs_light1_3960m	light:dark changes on a 12:12 hour cyclic schedule
circadian	light2__4140m_vs_light1_3960m	light:dark changes on a 12:12 hour cyclic schedule
circadian	light2__4320m_vs_light1_3960m	light:dark changes on a 12:12 hour cyclic schedule
circadian	light2__4500m_vs_light1_3960m	light:dark changes on a 12:12 hour cyclic schedule
circadian	light2__4680m_vs_light1_3960m	light:dark changes on a 12:12 hour cyclic schedule
circadian	light2__4860m_vs_light1_3960m	light:dark changes on a 12:12 hour cyclic schedule
circadian	light2__5040m_vs_light1_3960m	light:dark changes on a 12:12 hour cyclic schedule
circadian	light2__5220m_vs_light1_3960m	light:dark changes on a 12:12 hour cyclic schedule

[a] See **Appendix R** for more detailed description of each experiment.

circadian	light2__5400m_vs_light1_3960m	light:dark changes on a 12:12 hour cyclic schedule
circadian	light2__5580m_vs_light1_3960m	light:dark changes on a 12:12 hour cyclic schedule
circadian	light2__5760m_vs_light1_3960m	light:dark changes on a 12:12 hour cyclic schedule
circadian	dark2__0000m_vs_NRC-1c	light:dark changes on a 12:12 hour cyclic schedule
circadian	dark2__0060m_vs_NRC-1c	light:dark changes on a 12:12 hour cyclic schedule
circadian	dark2__0300m_vs_NRC-1c	light:dark changes on a 12:12 hour cyclic schedule
circadian	dark2__0540m_vs_NRC-1c	light:dark changes on a 12:12 hour cyclic schedule
circadian	dark2__0780m_vs_NRC-1c	light:dark changes on a 12:12 hour cyclic schedule
circadian	dark2__1020m_vs_NRC-1c	light:dark changes on a 12:12 hour cyclic schedule
circadian	dark2__1260m_vs_NRC-1c	light:dark changes on a 12:12 hour cyclic schedule
circadian	dark2__1500m_vs_NRC-1c	light:dark changes on a 12:12 hour cyclic schedule
circadian	dark2__1740m_vs_NRC-1c	light:dark changes on a 12:12 hour cyclic schedule
circadian	dark2__1980m_vs_NRC-1c	light:dark changes on a 12:12 hour cyclic schedule
circadian	dark2__2220m_vs_NRC-1c	light:dark changes on a 12:12 hour cyclic schedule
circadian	dark2__2460m_vs_NRC-1c	light:dark changes on a 12:12 hour cyclic schedule
circadian	dark2__2700m_vs_NRC-1c	light:dark changes on a 12:12 hour cyclic schedule
circadian	dark2__2940m_vs_NRC-1c	light:dark changes on a 12:12 hour cyclic schedule
circadian	dark2__3180m_vs_NRC-1c	light:dark changes on a 12:12 hour cyclic schedule
circadian	dark2__3420m_vs_NRC-1c	light:dark changes on a 12:12 hour cyclic schedule
circadian	dark2__3660m_vs_NRC-1c	light:dark changes on a 12:12 hour cyclic schedule
circadian	dark2__3900m_vs_NRC-1c	light:dark changes on a 12:12 hour cyclic schedule
circadian	dark1__0000m_vs_NRC-1c	light:dark changes on a 12:12 hour cyclic schedule
circadian	dark1__0240m_vs_NRC-1c	light:dark changes on a 12:12 hour cyclic schedule
circadian	dark1__0480m_vs_NRC-1c	light:dark changes on a 12:12 hour cyclic schedule
circadian	dark1__0720m_vs_NRC-1c	light:dark changes on a 12:12 hour cyclic schedule

circadian	dark1__0960m_vs_NRC-1c	light:dark changes on a 12:12 hour cyclic schedule
circadian	dark1__1200m_vs_NRC-1c	light:dark changes on a 12:12 hour cyclic schedule
circadian	dark1__1440m_vs_NRC-1c	light:dark changes on a 12:12 hour cyclic schedule
circadian	dark1__1680m_vs_NRC-1c	light:dark changes on a 12:12 hour cyclic schedule
circadian	dark1__1920m_vs_NRC-1c	light:dark changes on a 12:12 hour cyclic schedule
circadian	dark1__2160m_vs_NRC-1c	light:dark changes on a 12:12 hour cyclic schedule
circadian	dark1__2400m_vs_NRC-1c	light:dark changes on a 12:12 hour cyclic schedule
circadian	dark1__2640m_vs_NRC-1c	light:dark changes on a 12:12 hour cyclic schedule
circadian	dark1__2880m_vs_NRC-1c	light:dark changes on a 12:12 hour cyclic schedule
circadian	dark1__3120m_vs_NRC-1c	light:dark changes on a 12:12 hour cyclic schedule
circadian	dark1__3360m_vs_NRC-1c	light:dark changes on a 12:12 hour cyclic schedule
circadian	dark1__3600m_vs_NRC-1c	light:dark changes on a 12:12 hour cyclic schedule
circadian	dark1__3870m_vs_NRC-1c	light:dark changes on a 12:12 hour cyclic schedule
circadian	dark1__4110m_vs_NRC-1c	light:dark changes on a 12:12 hour cyclic schedule
circadian	circadian_Dphr1_drk_cycling__1440min_vs_NRC-1d.sig	light:dark changes on a 12:12 hour cyclic schedule
circadian	circadian_Dphr1_drk_cycling__1665min_vs_NRC-1d.sig	light:dark changes on a 12:12 hour cyclic schedule
circadian	circadian_Dphr1_drk_cycling__1800min_vs_NRC-1d.sig	light:dark changes on a 12:12 hour cyclic schedule
circadian	circadian_Dphr1_drk_cycling__1980min_vs_NRC-1d.sig	light:dark changes on a 12:12 hour cyclic schedule
circadian	circadian_Dphr1_drk_cycling__2175min_vs_NRC-1d.sig	light:dark changes on a 12:12 hour cyclic schedule
circadian	circadian_Dphr1_drk_cycling__2340min_vs_NRC-1d.sig	light:dark changes on a 12:12 hour cyclic schedule
circadian	circadian_Dphr1_drk_cycling__2595min_vs_NRC-1d.sig	light:dark changes on a 12:12 hour cyclic schedule
circadian	circadian_Dphr1_drk_cycling__2705min_vs_NRC-1d.sig	light:dark changes on a 12:12 hour cyclic schedule
circadian	circadian_Dphr1_drk_cycling__2880min_vs_NRC-1d.sig	light:dark changes on a 12:12 hour cyclic schedule
circadian	circadian_drk8_cycling_0000min_vs_NRC-1e.sig	light:dark changes on a 12:12 hour cyclic schedule
circadian	circadian_drk8_cycling_0180min_vs_NRC-1e.sig	light:dark changes on a 12:12 hour cyclic schedule

circadian	circadian_drk8_cycling_0360min_vs_NRC-1e.sig	light:dark changes on a 12:12 hour cyclic schedule
circadian	circadian_drk8_cycling_0540min_vs_NRC-1e.sig	light:dark changes on a 12:12 hour cyclic schedule
circadian	circadian_drk8_cycling_0720min_vs_NRC-1e.sig	light:dark changes on a 12:12 hour cyclic schedule
circadian	circadian_drk8_cycling_0900min_vs_NRC-1e.sig	light:dark changes on a 12:12 hour cyclic schedule
circadian	circadian_drk8_cycling_1080min_vs_NRC-1e.sig	light:dark changes on a 12:12 hour cyclic schedule
circadian	circadian_drk8_cycling_1260min_vs_NRC-1e.sig	light:dark changes on a 12:12 hour cyclic schedule
circadian	circadian_drk8_cycling_1440min_vs_NRC-1e.sig	light:dark changes on a 12:12 hour cyclic schedule
circadian	circadian_drk8_cycling_1620min_vs_NRC-1e.sig	light:dark changes on a 12:12 hour cyclic schedule
circadian	circadian_drk8_cycling_1800min_vs_NRC-1e.sig	light:dark changes on a 12:12 hour cyclic schedule
circadian	circadian_drk8_cycling_1980min_vs_NRC-1e.sig	light:dark changes on a 12:12 hour cyclic schedule
circadian	circadian_drk8_cycling_2160min_vs_NRC-1e.sig	light:dark changes on a 12:12 hour cyclic schedule
circadian	circadian_drk8_cycling_2340min_vs_NRC-1e.sig	light:dark changes on a 12:12 hour cyclic schedule
circadian	circadian_drk8_cycling_2520min_vs_NRC-1e.sig	light:dark changes on a 12:12 hour cyclic schedule
circadian	circadian_drk8_cycling_2700min_vs_NRC-1e.sig	light:dark changes on a 12:12 hour cyclic schedule
circadian	circadian_drk8_cycling_2880min_vs_NRC-1e.sig	light:dark changes on a 12:12 hour cyclic schedule
circadian	circadian_drk8_cycling_3060min_vs_NRC-1e.sig	light:dark changes on a 12:12 hour cyclic schedule
circadian	circadian_drk8_cycling_3240min_vs_NRC-1e.sig	light:dark changes on a 12:12 hour cyclic schedule
circadian	circadian_drk7_cycling_0000min_vs_NRC-1d.sig	light:dark changes on a 12:12 hour cyclic schedule
circadian	circadian_drk7_cycling_0180min_vs_NRC-1d.sig	light:dark changes on a 12:12 hour cyclic schedule
circadian	circadian_drk7_cycling_0360min_vs_NRC-1d.sig	light:dark changes on a 12:12 hour cyclic schedule
circadian	circadian_drk7_cycling_0540min_vs_NRC-1d.sig	light:dark changes on a 12:12 hour cyclic schedule
circadian	circadian_drk7_cycling_0720min_vs_NRC-1d.sig	light:dark changes on a 12:12 hour cyclic schedule
circadian	circadian_drk7_cycling_0900min_vs_NRC-1d.sig	light:dark changes on a 12:12 hour cyclic schedule
circadian	circadian_drk7_cycling_1080min_vs_NRC-1d.sig	light:dark changes on a 12:12 hour cyclic schedule
circadian	circadian_drk7_cycling_1260min_vs_NRC-1d.sig	light:dark changes on a 12:12 hour cyclic schedule

circadian	circadian_drk7_cycling_1440min_vs_NRC-1d.sig	light:dark changes on a 12:12 hour cyclic schedule
circadian	circadian_drk7_cycling_1620min_vs_NRC-1d.sig	light:dark changes on a 12:12 hour cyclic schedule
circadian	circadian_drk7_cycling_1800min_vs_NRC-1d.sig	light:dark changes on a 12:12 hour cyclic schedule
circadian	circadian_drk7_cycling_1980min_vs_NRC-1d.sig	light:dark changes on a 12:12 hour cyclic schedule
circadian	circadian_drk7_cycling_2160min_vs_NRC-1d.sig	light:dark changes on a 12:12 hour cyclic schedule
circadian	circadian_drk7_cycling_2340min_vs_NRC-1d.sig	light:dark changes on a 12:12 hour cyclic schedule
circadian	circadian_drk7_cycling_2520min_vs_NRC-1d.sig	light:dark changes on a 12:12 hour cyclic schedule
circadian	circadian_drk7_cycling_2700min_vs_NRC-1d.sig	light:dark changes on a 12:12 hour cyclic schedule
circadian	circadian_drk7_cycling_2880min_vs_NRC-1d.sig	light:dark changes on a 12:12 hour cyclic schedule
circadian	circadian_drk7_cycling_3060min_vs_NRC-1d.sig	light:dark changes on a 12:12 hour cyclic schedule
circadian	circadian_drk7_cycling_3240min_vs_NRC-1d.sig	light:dark changes on a 12:12 hour cyclic schedule
circadian	circadian_drk6_cycling_0000min_vs_NRC-1e.sig	light:dark changes on a 12:12 hour cyclic schedule
circadian	circadian_drk6_cycling_0180min_vs_NRC-1e.sig	light:dark changes on a 12:12 hour cyclic schedule
circadian	circadian_drk6_cycling_0360min_vs_NRC-1e.sig	light:dark changes on a 12:12 hour cyclic schedule
circadian	circadian_drk6_cycling_0540min_vs_NRC-1e.sig	light:dark changes on a 12:12 hour cyclic schedule
circadian	circadian_drk6_cycling_0720min_vs_NRC-1e.sig	light:dark changes on a 12:12 hour cyclic schedule
circadian	circadian_drk6_cycling_0912min_vs_NRC-1e.sig	light:dark changes on a 12:12 hour cyclic schedule
circadian	circadian_drk6_cycling_1080min_vs_NRC-1e.sig	light:dark changes on a 12:12 hour cyclic schedule
circadian	circadian_drk6_cycling_1260min_vs_NRC-1e.sig	light:dark changes on a 12:12 hour cyclic schedule
circadian	circadian_drk6_cycling_1440min_vs_NRC-1e.sig	light:dark changes on a 12:12 hour cyclic schedule
circadian	circadian__dark5_cycling_30C_1440min_vs_NRC-1d.sig	light:dark changes on a 12:12 hour cyclic schedule
circadian	circadian__dark5_cycling_30C_1630min_vs_NRC-1d.sig	light:dark changes on a 12:12 hour cyclic schedule
circadian	circadian__dark5_cycling_30C_1815min_vs_NRC-1d.sig	light:dark changes on a 12:12 hour cyclic schedule
circadian	circadian__dark5_cycling_30C_1980min_vs_NRC-1d.sig	light:dark changes on a 12:12 hour cyclic schedule
circadian	circadian__dark5_cycling_30C_2160min_vs_NRC-1d.sig	light:dark changes on a 12:12 hour cyclic schedule

circadian	circadian__dark5_cycling_30C_2355min_vs_NRC-1d.sig	light:dark changes on a 12:12 hour cyclic schedule
circadian	circadian__dark5_cycling_30C_2590min_vs_NRC-1d.sig	light:dark changes on a 12:12 hour cyclic schedule
circadian	circadian__dark5_cycling_30C_2700min_vs_NRC-1d.sig	light:dark changes on a 12:12 hour cyclic schedule
circadian	circadian__dark5_cycling_30C_2880min_vs_NRC-1d.sig	light:dark changes on a 12:12 hour cyclic schedule
circadian	circadian_20051021_cycling_dark_42oC_1440min_vs_NRC-1d.sig	light:dark changes on a 12:12 hour cyclic schedule
circadian	circadian_20051021_cycling_dark_42oC_1615min_vs_NRC-1d.sig	light:dark changes on a 12:12 hour cyclic schedule
circadian	circadian_20051021_cycling_dark_42oC_1800min_vs_NRC-1d.sig	light:dark changes on a 12:12 hour cyclic schedule
circadian	circadian_20051021_cycling_dark_42oC_1985min_vs_NRC-1d.sig	light:dark changes on a 12:12 hour cyclic schedule
circadian	circadian_20051021_cycling_dark_42oC_2160min_vs_NRC-1d.sig	light:dark changes on a 12:12 hour cyclic schedule
circadian	circadian_20051021_cycling_dark_42oC_2340min_vs_NRC-1d.sig	light:dark changes on a 12:12 hour cyclic schedule
circadian	circadian_20051021_cycling_dark_42oC_2515min_vs_NRC-1d.sig	light:dark changes on a 12:12 hour cyclic schedule
circadian	circadian_20051021_cycling_dark_42oC_2705min_vs_NRC-1d.sig	light:dark changes on a 12:12 hour cyclic schedule
circadian	circadian_20051021_cycling_dark_42oC_2880min_vs_NRC-1d.sig	light:dark changes on a 12:12 hour cyclic schedule
circadian	circadian_dark3_cycling_1380min_vs_NRC-1d.sig	light:dark changes on a 12:12 hour cyclic schedule
circadian	circadian_dark3_cycling_1440min_vs_NRC-1d.sig	light:dark changes on a 12:12 hour cyclic schedule
circadian	circadian_dark3_cycling_1500min_vs_NRC-1d.sig	light:dark changes on a 12:12 hour cyclic schedule
circadian	circadian_dark3_cycling_1620min_vs_NRC-1d.sig	light:dark changes on a 12:12 hour cyclic schedule
circadian	circadian_dark3_cycling_1800min_vs_NRC-1d.sig	light:dark changes on a 12:12 hour cyclic schedule
circadian	circadian_dark3_cycling_1980min_vs_NRC-1d.sig	light:dark changes on a 12:12 hour cyclic schedule
circadian	circadian_dark3_cycling_2160min_vs_NRC-1d.sig	light:dark changes on a 12:12 hour cyclic schedule
circadian	circadian_dark3_cycling_2220min_vs_NRC-1d.sig	light:dark changes on a 12:12 hour cyclic schedule
circadian	circadian_dark3_cycling_2340min_vs_NRC-1d.sig	light:dark changes on a 12:12 hour cyclic schedule
circadian	circadian_dark3_cycling_2520min_vs_NRC-1d.sig	light:dark changes on a 12:12 hour cyclic schedule
circadian	circadian_dark3_cycling_2700min_vs_NRC-1d.sig	light:dark changes on a 12:12 hour cyclic schedule
circadian	circadian_dark3_cycling_2880min_vs_NRC-1d.sig	light:dark changes on a 12:12 hour cyclic schedule

circadian	circadian_dark3_ctrl_1380min_vs_NRC-1d.sig	light:dark changes on a 12:12 hour cyclic schedule
circadian	circadian_dark3_ctrl_1440min_vs_NRC-1d.sig	light:dark changes on a 12:12 hour cyclic schedule
circadian	circadian_dark3_ctrl_1500min_vs_NRC-1d.sig	light:dark changes on a 12:12 hour cyclic schedule
circadian	circadian_dark3_ctrl_1620min_vs_NRC-1d.sig	light:dark changes on a 12:12 hour cyclic schedule
circadian	circadian_dark3_ctrl_1800min_vs_NRC-1d.sig	light:dark changes on a 12:12 hour cyclic schedule
circadian	circadian_dark3_ctrl_1980min_vs_NRC-1d.sig	light:dark changes on a 12:12 hour cyclic schedule
circadian	circadian_dark3_ctrl_2160min_vs_NRC-1d.sig	light:dark changes on a 12:12 hour cyclic schedule
circadian	circadian_dark3_ctrl_2220min_vs_NRC-1d.sig	light:dark changes on a 12:12 hour cyclic schedule
circadian	circadian_dark3_ctrl_2340min_vs_NRC-1d.sig	light:dark changes on a 12:12 hour cyclic schedule
circadian	circadian_dark3_ctrl_2520min_vs_NRC-1d.sig	light:dark changes on a 12:12 hour cyclic schedule
circadian	circadian_dark3_ctrl_2700min_vs_NRC-1d.sig	light:dark changes on a 12:12 hour cyclic schedule
circadian	circadian_dark3_ctrl_2880min_vs_NRC-1d.sig	light:dark changes on a 12:12 hour cyclic schedule
circadian	circadian_drk8_control_0000min_vs_NRC-1e.sig	light:dark changes on a 12:12 hour cyclic schedule
circadian	circadian_drk8_control_0180min_vs_NRC-1e.sig	light:dark changes on a 12:12 hour cyclic schedule
circadian	circadian_drk8_control_0360min_vs_NRC-1e.sig	light:dark changes on a 12:12 hour cyclic schedule
circadian	circadian_drk8_control_0540min_vs_NRC-1e.sig	light:dark changes on a 12:12 hour cyclic schedule
circadian	circadian_drk8_control_0720min_vs_NRC-1e.sig	light:dark changes on a 12:12 hour cyclic schedule
circadian	circadian_drk8_control_0900min_vs_NRC-1e.sig	light:dark changes on a 12:12 hour cyclic schedule
circadian	circadian_drk8_control_1080min_vs_NRC-1e.sig	light:dark changes on a 12:12 hour cyclic schedule
circadian	circadian_drk8_control_1260min_vs_NRC-1e.sig	light:dark changes on a 12:12 hour cyclic schedule
circadian	circadian_drk8_control_1440min_vs_NRC-1e.sig	light:dark changes on a 12:12 hour cyclic schedule
circadian	circadian_drk8_control_1620min_vs_NRC-1e.sig	light:dark changes on a 12:12 hour cyclic schedule
circadian	circadian_drk8_control_1800min_vs_NRC-1e.sig	light:dark changes on a 12:12 hour cyclic schedule
circadian	circadian_drk8_control_1980min_vs_NRC-1e.sig	light:dark changes on a 12:12 hour cyclic schedule
circadian	circadian_drk8_control_2160min_vs_NRC-1e.sig	light:dark changes on a 12:12 hour cyclic schedule

circadian	circadian_drk8_control_2340min_vs_NRC-1e.sig	light:dark changes on a 12:12 hour cyclic schedule
circadian	circadian_drk8_control_2520min_vs_NRC-1e.sig	light:dark changes on a 12:12 hour cyclic schedule
circadian	circadian_drk8_control_2700min_vs_NRC-1e.sig	light:dark changes on a 12:12 hour cyclic schedule
circadian	circadian_drk8_control_2880min_vs_NRC-1e.sig	light:dark changes on a 12:12 hour cyclic schedule
circadian	circadian_drk8_control_3060min_vs_NRC-1e.sig	light:dark changes on a 12:12 hour cyclic schedule
circadian	circadian_drk8_control_3240min_vs_NRC-1e.sig	light:dark changes on a 12:12 hour cyclic schedule
circadian	Circadian_Dark9_Cycling_0000min_vs_NRC-1g.sig	light:dark changes on a 12:12 hour cyclic schedule
circadian	Circadian_Dark9_Cycling_0180min_vs_NRC-1g.sig	light:dark changes on a 12:12 hour cyclic schedule
circadian	Circadian_Dark9_Cycling_0360min_vs_NRC-1g.sig	light:dark changes on a 12:12 hour cyclic schedule
circadian	Circadian_Dark9_Cycling_0535min_vs_NRC-1g.sig	light:dark changes on a 12:12 hour cyclic schedule
circadian	Circadian_Dark9_Cycling_0720min_vs_NRC-1g.sig	light:dark changes on a 12:12 hour cyclic schedule
circadian	Circadian_Dark9_Cycling_0900min_vs_NRC-1g.sig	light:dark changes on a 12:12 hour cyclic schedule
circadian	Circadian_Dark9_Cycling_1080min_vs_NRC-1g.sig	light:dark changes on a 12:12 hour cyclic schedule
circadian	Circadian_Dark9_Cycling_1265min_vs_NRC-1g.sig	light:dark changes on a 12:12 hour cyclic schedule
circadian	Circadian_Dark9_Cycling_1440min_vs_NRC-1g.sig	light:dark changes on a 12:12 hour cyclic schedule
circadian	Circadian_Dark9_Cycling_1620min_vs_NRC-1g.sig	light:dark changes on a 12:12 hour cyclic schedule
circadian	Circadian_Dark9_Cycling_1800min_vs_NRC-1g.sig	light:dark changes on a 12:12 hour cyclic schedule
circadian	Circadian_Dark9_Cycling_1980min_vs_NRC-1g.sig	light:dark changes on a 12:12 hour cyclic schedule
circadian	Circadian_Dark9_Cycling_2160min_vs_NRC-1g.sig	light:dark changes on a 12:12 hour cyclic schedule
circadian	Circadian_Dark9_Cycling_2340min_vs_NRC-1g.sig	light:dark changes on a 12:12 hour cyclic schedule
circadian	Circadian_Dark9_Cycling_2520min_vs_NRC-1g.sig	light:dark changes on a 12:12 hour cyclic schedule
circadian	Circadian_Dark9_Cycling_2700min_vs_NRC-1g.sig	light:dark changes on a 12:12 hour cyclic schedule
circadian	Circadian_Dark9_Cycling_2880min_vs_NRC-1g.sig	light:dark changes on a 12:12 hour cyclic schedule
circadian	Circadian_Dark9_Cycling_3060min_vs_NRC-1g.sig	light:dark changes on a 12:12 hour cyclic schedule
circadian	Circadian_Dark9_Cycling_3240min_vs_NRC-1g.sig	light:dark changes on a 12:12 hour cyclic schedule

circadian	Circadian_Dark9_Cycling_3420min_vs_NRC-1g.sig	light:dark changes on a 12:12 hour cyclic schedule
circadian	Circadian_Dark9_Cycling_3600min_vs_NRC-1g.sig	light:dark changes on a 12:12 hour cyclic schedule
circadian	Circadian_Dark9_Cycling_3780min_vs_NRC-1g.sig	light:dark changes on a 12:12 hour cyclic schedule
circadian	Circadian_Dark9_Cycling_3960min_vs_NRC-1g.sig	light:dark changes on a 12:12 hour cyclic schedule
circadian	Circadian_Dark9_Cycling_4140min_vs_NRC-1g.sig	light:dark changes on a 12:12 hour cyclic schedule
circadian	Circadian_Dark9_Cycling_4320min_vs_NRC-1g.sig	light:dark changes on a 12:12 hour cyclic schedule
circadian	Circadian_Dark9_Cycling_4500min_vs_NRC-1g.sig	light:dark changes on a 12:12 hour cyclic schedule
circadian	Circadian_Dark9_Control_0000min_vs_NRC-1g.sig	light:dark changes on a 12:12 hour cyclic schedule
circadian	Circadian_Dark9_Control_0180min_vs_NRC-1g.sig	light:dark changes on a 12:12 hour cyclic schedule
circadian	Circadian_Dark9_Control_0360min_vs_NRC-1g.sig	light:dark changes on a 12:12 hour cyclic schedule
circadian	Circadian_Dark9_Control_0535min_vs_NRC-1g.sig	light:dark changes on a 12:12 hour cyclic schedule
circadian	Circadian_Dark9_Control_0720min_vs_NRC-1g.sig	light:dark changes on a 12:12 hour cyclic schedule
circadian	Circadian_Dark9_Control_1080min_vs_NRC-1g.sig	light:dark changes on a 12:12 hour cyclic schedule
circadian	Circadian_Dark9_Control_1265min_vs_NRC-1g.sig	light:dark changes on a 12:12 hour cyclic schedule
circadian	Circadian_Dark9_Control_1440min_vs_NRC-1g.sig	light:dark changes on a 12:12 hour cyclic schedule
circadian	Circadian_Dark9_Control_1620min_vs_NRC-1g.sig	light:dark changes on a 12:12 hour cyclic schedule
circadian	Circadian_Dark9_Control_1800min_vs_NRC-1g.sig	light:dark changes on a 12:12 hour cyclic schedule
circadian	Circadian_Dark9_Control_1980min_vs_NRC-1g.sig	light:dark changes on a 12:12 hour cyclic schedule
circadian	Circadian_Dark9_Control_2160min_vs_NRC-1g.sig	light:dark changes on a 12:12 hour cyclic schedule
circadian	Circadian_Dark9_Control_2340min_vs_NRC-1g.sig	light:dark changes on a 12:12 hour cyclic schedule
circadian	Circadian_Dark9_Control_2520min_vs_NRC-1g.sig	light:dark changes on a 12:12 hour cyclic schedule
circadian	Circadian_Dark9_Control_2700min_vs_NRC-1g.sig	light:dark changes on a 12:12 hour cyclic schedule
circadian	Circadian_Dark9_Control_2880min_vs_NRC-1g.sig	light:dark changes on a 12:12 hour cyclic schedule
circadian	Circadian_Dark9_Control_3060min_vs_NRC-1g.sig	light:dark changes on a 12:12 hour cyclic schedule
circadian	Circadian_Dark9_Control_3240min_vs_NRC-1g.sig	light:dark changes on a 12:12 hour cyclic schedule

circadian	Circadian_Dark9_Control_3420min_vs_NRC-1g.sig	light:dark changes on a 12:12 hour cyclic schedule
circadian	Circadian_Dark9_Control_3600min_vs_NRC-1g.sig	light:dark changes on a 12:12 hour cyclic schedule
circadian	Circadian_Dark9_Control_3780min_vs_NRC-1g.sig	light:dark changes on a 12:12 hour cyclic schedule
circadian	Circadian_Dark9_Control_3960min_vs_NRC-1g.sig	light:dark changes on a 12:12 hour cyclic schedule
circadian	Circadian_Dark9_Control_4140min_vs_NRC-1g.sig	light:dark changes on a 12:12 hour cyclic schedule
circadian	Circadian_Dark9_Control_4320min_vs_NRC-1g.sig	light:dark changes on a 12:12 hour cyclic schedule
circadian	Circadian_Dark9_Control_4500min_vs_NRC-1g.sig	light:dark changes on a 12:12 hour cyclic schedule
circadian	Circadian_Dark10_Cycling_-2873min_vs_NRC-1h1.sig	light:dark changes on a 12:12 hour cyclic schedule
circadian	Circadian_Dark10_Cycling_-2670min_vs_NRC-1h1.sig	light:dark changes on a 12:12 hour cyclic schedule
circadian	Circadian_Dark10_Cycling_-2490min_vs_NRC-1h1.sig	light:dark changes on a 12:12 hour cyclic schedule
circadian	Circadian_Dark10_Cycling_-2315min_vs_NRC-1h1.sig	light:dark changes on a 12:12 hour cyclic schedule
circadian	Circadian_Dark10_Cycling_-2120min_vs_NRC-1h1.sig	light:dark changes on a 12:12 hour cyclic schedule
circadian	Circadian_Dark10_Cycling_-1960min_vs_NRC-1h1.sig	light:dark changes on a 12:12 hour cyclic schedule
circadian	Circadian_Dark10_Cycling_-1785min_vs_NRC-1h1.sig	light:dark changes on a 12:12 hour cyclic schedule
circadian	Circadian_Dark10_Cycling_-1595min_vs_NRC-1h1.sig	light:dark changes on a 12:12 hour cyclic schedule
circadian	Circadian_Dark10_Cycling_-1410min_vs_NRC-1h1.sig	light:dark changes on a 12:12 hour cyclic schedule
circadian	Circadian_Dark10_Cycling_-1245min_vs_NRC-1h1.sig	light:dark changes on a 12:12 hour cyclic schedule
circadian	Circadian_Dark10_Cycling_-1060min_vs_NRC-1h1.sig	light:dark changes on a 12:12 hour cyclic schedule
circadian	Circadian_Dark10_Cycling_-0880min_vs_NRC-1h1.sig	light:dark changes on a 12:12 hour cyclic schedule
circadian	Circadian_Dark10_Cycling_-0690min_vs_NRC-1h1.sig	light:dark changes on a 12:12 hour cyclic schedule
circadian	Circadian_Dark10_Cycling_-0525min_vs_NRC-1h1.sig	light:dark changes on a 12:12 hour cyclic schedule
circadian	Circadian_Dark10_Cycling_-0360min_vs_NRC-1h1.sig	light:dark changes on a 12:12 hour cyclic schedule
circadian	Circadian_Dark10_Cycling_-0165min_vs_NRC-1h1.sig	light:dark changes on a 12:12 hour cyclic schedule
circadian	Circadian_Dark10_Cycling_0000min_vs_NRC-1h1.sig	light:dark changes on a 12:12 hour cyclic schedule
circadian	Circadian_Dark10_Cycling_0195min_vs_NRC-1h1.sig	light:dark changes on a 12:12 hour cyclic schedule

circadian	Circadian_Dark10_Cycling_0370min_vs_NRC-1h1.sig	light:dark changes on a 12:12 hour cyclic schedule
circadian	Circadian_Dark10_Cycling_0560min_vs_NRC-1h1.sig	light:dark changes on a 12:12 hour cyclic schedule
circadian	Circadian_Dark10_Cycling_0750min_vs_NRC-1h1.sig	light:dark changes on a 12:12 hour cyclic schedule
circadian	Circadian_Dark10_Cycling_0915min_vs_NRC-1h1.sig	light:dark changes on a 12:12 hour cyclic schedule
circadian	Circadian_Dark10_Cycling_1100min_vs_NRC-1h1.sig	light:dark changes on a 12:12 hour cyclic schedule
circadian	Circadian_Dark10_Cycling_1270min_vs_NRC-1h1.sig	light:dark changes on a 12:12 hour cyclic schedule
circadian	Circadian_Dark10_Cycling_1450min_vs_NRC-1h1.sig	light:dark changes on a 12:12 hour cyclic schedule
circadian	Circadian_Dark10_Cycling_1635min_vs_NRC-1h1.sig	light:dark changes on a 12:12 hour cyclic schedule
circadian	Circadian_Dark10_Cycling_1810min_vs_NRC-1h1.sig	light:dark changes on a 12:12 hour cyclic schedule
circadian	Circadian_Dark10_Cycling_1980min_vs_NRC-1h1.sig	light:dark changes on a 12:12 hour cyclic schedule
circadian	Circadian_Dark10_Cycling_2200min_vs_NRC-1h1.sig	light:dark changes on a 12:12 hour cyclic schedule
circadian	Circadian_Dark10_Cycling_2345min_vs_NRC-1h1.sig	light:dark changes on a 12:12 hour cyclic schedule
circadian	Circadian_Dark10_Cycling_2535min_vs_NRC-1h1.sig	light:dark changes on a 12:12 hour cyclic schedule
circadian	Circadian_Dark10_Cycling_2711min_vs_NRC-1h1.sig	light:dark changes on a 12:12 hour cyclic schedule
circadian	Circadian_Dark10_Cycling_2895min_vs_NRC-1h1.sig	light:dark changes on a 12:12 hour cyclic schedule
circadian	Circadian_Dark10_Cycling_3070min_vs_NRC-1h1.sig	light:dark changes on a 12:12 hour cyclic schedule
circadian	Circadian_Dark10_Cycling_3252min_vs_NRC-1h1.sig	light:dark changes on a 12:12 hour cyclic schedule
circadian	Circadian_Dark10_Cycling_3430min_vs_NRC-1h1.sig	light:dark changes on a 12:12 hour cyclic schedule
circadian	Circadian_Dark10_Cycling_3630min_vs_NRC-1h1.sig	light:dark changes on a 12:12 hour cyclic schedule
circadian	Circadian_Dark10_Cycling_3790min_vs_NRC-1h1.sig	light:dark changes on a 12:12 hour cyclic schedule
circadian	Circadian_Dark10_Cycling_3980min_vs_NRC-1h1.sig	light:dark changes on a 12:12 hour cyclic schedule
circadian	Circadian_Dark10_Cycling_4150min_vs_NRC-1h1.sig	light:dark changes on a 12:12 hour cyclic schedule
circadian	Circadian_Dark10_Cycling_4330min_vs_NRC-1h1.sig	light:dark changes on a 12:12 hour cyclic schedule
circadian	zn__0005um_vs_NRC-1	light:dark changes on a 12:12 hour cyclic schedule
circadian	zn__0010um_vs_NRC-1	light:dark changes on a 12:12 hour cyclic schedule

circadian	zn__0020um_vs_NRC-1	light:dark changes on a 12:12 hour cyclic schedule
circadian	cu__0700um_vs_NRC-1	light:dark changes on a 12:12 hour cyclic schedule
circadian	cu__0850um_vs_NRC-1	light:dark changes on a 12:12 hour cyclic schedule
circadian	cu__1000um_vs_NRC-1	light:dark changes on a 12:12 hour cyclic schedule
circadian	Cu_NRC1_set1_-030min_vs_NRC-1h1.sig	light:dark changes on a 12:12 hour cyclic schedule
circadian	Cu_NRC1_set1_000min_vs_NRC-1h1.sig	light:dark changes on a 12:12 hour cyclic schedule
circadian	Cu_NRC1_set1_005min_vs_NRC-1h1.sig	light:dark changes on a 12:12 hour cyclic schedule
circadian	Cu_NRC1_set1_010min_vs_NRC-1h1.sig	light:dark changes on a 12:12 hour cyclic schedule
circadian	Cu_NRC1_set1_020min_vs_NRC-1h1.sig	light:dark changes on a 12:12 hour cyclic schedule
circadian	Cu_NRC1_set1_040min_vs_NRC-1h1.sig	light:dark changes on a 12:12 hour cyclic schedule
circadian	Cu_NRC1_set1_080min_vs_NRC-1h1.sig	light:dark changes on a 12:12 hour cyclic schedule
circadian	Cu_NRC1_set1_160min_vs_NRC-1h1.sig	light:dark changes on a 12:12 hour cyclic schedule
circadian	Cu_ura3_KO_set1_-030min_vs_NRC-1h1.sig	light:dark changes on a 12:12 hour cyclic schedule
circadian	Cu_ura3_KO_set1_000min_vs_NRC-1h1.sig	light:dark changes on a 12:12 hour cyclic schedule
circadian	Cu_ura3_KO_set1_005min_vs_NRC-1h1.sig	light:dark changes on a 12:12 hour cyclic schedule
circadian	Cu_ura3_KO_set1_010min_vs_NRC-1h1.sig	light:dark changes on a 12:12 hour cyclic schedule
circadian	Cu_ura3_KO_set1_020min_vs_NRC-1h1.sig	light:dark changes on a 12:12 hour cyclic schedule
circadian	Cu_ura3_KO_set1_040min_vs_NRC-1h1.sig	light:dark changes on a 12:12 hour cyclic schedule
circadian	Cu_ura3_KO_set1_080min_vs_NRC-1h1.sig	light:dark changes on a 12:12 hour cyclic schedule
circadian	Cu_ura3_KO_set1_160min_vs_NRC-1h1.sig	light:dark changes on a 12:12 hour cyclic schedule
circadian	feso4__-0001m_vs_NRC-1	light:dark changes on a 12:12 hour cyclic schedule
circadian	feso4__0000m_vs_NRC-1	light:dark changes on a 12:12 hour cyclic schedule
circadian	feso4__0005m_vs_NRC-1b	light:dark changes on a 12:12 hour cyclic schedule
circadian	feso4__0010m_vs_NRC-1b	light:dark changes on a 12:12 hour cyclic schedule
circadian	feso4__0015m_vs_NRC-1b	light:dark changes on a 12:12 hour cyclic schedule

circadian	feso4__0020m_vs_NRC-1	light:dark changes on a 12:12 hour cyclic schedule
circadian	feso4__0025m_vs_NRC-1b	light:dark changes on a 12:12 hour cyclic schedule
circadian	feso4__0040m_vs_NRC-1	light:dark changes on a 12:12 hour cyclic schedule
circadian	feso4__0080m_vs_NRC-1	light:dark changes on a 12:12 hour cyclic schedule
circadian	feso4__0160m_vs_NRC-1	light:dark changes on a 12:12 hour cyclic schedule
circadian	feso4__0320m_vs_NRC-1	light:dark changes on a 12:12 hour cyclic schedule
circadian	zim__HO_D_vs_NRC-1	light:dark changes on a 12:12 hour cyclic schedule
circadian	zim__HO_L_vs_NRC-1	light:dark changes on a 12:12 hour cyclic schedule
circadian	zim__LO_D_vs_NRC-1	light:dark changes on a 12:12 hour cyclic schedule
circadian	zim__LO_L_vs_NRC-1	light:dark changes on a 12:12 hour cyclic schedule
circadian	VNG2334C__HO_D_vs_NRC-1	light:dark changes on a 12:12 hour cyclic schedule
circadian	VNG2334C__HO_L_vs_NRC-1	light:dark changes on a 12:12 hour cyclic schedule
circadian	VNG2334C__LO_D_vs_NRC-1	light:dark changes on a 12:12 hour cyclic schedule
circadian	VNG2334C__LO_L_vs_NRC-1	light:dark changes on a 12:12 hour cyclic schedule
circadian	VNG1296C__HO_D_vs_NRC-1	light:dark changes on a 12:12 hour cyclic schedule
circadian	VNG1296C__HO_L_vs_NRC-1	light:dark changes on a 12:12 hour cyclic schedule
circadian	VNG1296C__LO_D_vs_NRC-1	light:dark changes on a 12:12 hour cyclic schedule
circadian	VNG1296C__LO_L_vs_NRC-1	light:dark changes on a 12:12 hour cyclic schedule
circadian	VNG0750C__HO_D_vs_NRC-1	light:dark changes on a 12:12 hour cyclic schedule
circadian	VNG0750C__HO_L_vs_NRC-1	light:dark changes on a 12:12 hour cyclic schedule
circadian	VNG0750C__LO_D_vs_NRC-1	light:dark changes on a 12:12 hour cyclic schedule
circadian	VNG0750C__LO_L_vs_NRC-1	light:dark changes on a 12:12 hour cyclic schedule
circadian	VNG0019H__HO_D_vs_NRC-1c	light:dark changes on a 12:12 hour cyclic schedule
circadian	VNG0019H__HO_L_vs_NRC-1c	light:dark changes on a 12:12 hour cyclic schedule
circadian	VNG0019H__LO_D_vs_NRC-1c	light:dark changes on a 12:12 hour cyclic schedule

circadian	VNG0019H__LO_L_vs_NRC-1c	light:dark changes on a 12:12 hour cyclic schedule
circadian	uv__000jm2_CL_060m	light:dark changes on a 12:12 hour cyclic schedule
circadian	ura3__HO_D_vs_NRC-1	light:dark changes on a 12:12 hour cyclic schedule
circadian	ura3__HO_L_vs_NRC-1	light:dark changes on a 12:12 hour cyclic schedule
circadian	ura3__LO_D_vs_NRC-1	light:dark changes on a 12:12 hour cyclic schedule
circadian	ura3__LO_L_vs_NRC-1	light:dark changes on a 12:12 hour cyclic schedule
circadian	NRC-1__HO_D_vs_NRC-1	light:dark changes on a 12:12 hour cyclic schedule
circadian	NRC-1__HO_L_vs_NRC-1	light:dark changes on a 12:12 hour cyclic schedule
circadian	NRC-1__LO_D_vs_NRC-1	light:dark changes on a 12:12 hour cyclic schedule
circadian	NRC-1__LO_L_vs_NRC-1	light:dark changes on a 12:12 hour cyclic schedule
circadian	circadian__dark_cycling_125w/m2_42C_1440min_vs_NRC-1d.sig	light:dark changes on a 12:12 hour cyclic schedule
circadian	circadian__dark_cycling_125w/m2_42C_1615min_vs_NRC-1d.sig	light:dark changes on a 12:12 hour cyclic schedule
circadian	circadian__dark_cycling_125w/m2_42C_1800min_vs_NRC-1d.sig	light:dark changes on a 12:12 hour cyclic schedule
circadian	circadian__dark_cycling_125w/m2_42C_1985min_vs_NRC-1d.sig	light:dark changes on a 12:12 hour cyclic schedule
circadian	circadian__dark_cycling_125w/m2_42C_2160min_vs_NRC-1d.sig	light:dark changes on a 12:12 hour cyclic schedule
circadian	circadian__dark_cycling_125w/m2_42C_2340min_vs_NRC-1d.sig	light:dark changes on a 12:12 hour cyclic schedule
circadian	circadian__dark_cycling_125w/m2_42C_2515min_vs_NRC-1d.sig	light:dark changes on a 12:12 hour cyclic schedule
circadian	circadian__dark_cycling_125w/m2_42C_2705min_vs_NRC-1d.sig	light:dark changes on a 12:12 hour cyclic schedule
circadian	circadian__dark_cycling_125w/m2_42C_2880min_vs_NRC-1d.sig	light:dark changes on a 12:12 hour cyclic schedule
circadian	Dun_F2_000minb_vs_NRC-1g.sig	light:dark changes on a 12:12 hour cyclic schedule
circadian	Dun_F2_005minb_vs_NRC-1g.sig	light:dark changes on a 12:12 hour cyclic schedule
circadian	Dun_F2_010minb_vs_NRC-1g.sig	light:dark changes on a 12:12 hour cyclic schedule
circadian	Dun_F2_020minb_vs_NRC-1g.sig	light:dark changes on a 12:12 hour cyclic schedule
circadian	Dun_F2_040minb_vs_NRC-1g.sig	light:dark changes on a 12:12 hour cyclic schedule
circadian	Dun_F2_080minb_vs_NRC-1g.sig	light:dark changes on a 12:12 hour cyclic schedule

circadian	Dun_F2_160minb_vs_NRC-1g.sig	light:dark changes on a 12:12 hour cyclic schedule
circadian	Dun_F2_320minb_vs_NRC-1g.sig	light:dark changes on a 12:12 hour cyclic schedule
circadian	NRC1_03720_0.234_rep2_vs_NRC-1g.sig	light:dark changes on a 12:12 hour cyclic schedule
circadian	NRC1_03960_0.409_rep2_vs_NRC-1g.sig	light:dark changes on a 12:12 hour cyclic schedule
circadian	NRC1_04320_0.578_rep2_vs_NRC-1g.sig	light:dark changes on a 12:12 hour cyclic schedule
circadian	NRC1_04476_0.715_rep2_vs_NRC-1g.sig	light:dark changes on a 12:12 hour cyclic schedule
circadian	NRC1_05400_0.786_rep2_vs_NRC-1g.sig	light:dark changes on a 12:12 hour cyclic schedule
circadian	NRC1_05778_0.722_rep2_vs_NRC-1g.sig	light:dark changes on a 12:12 hour cyclic schedule
circadian	NRC1_07020_1.318_rep2_vs_NRC-1g.sig	light:dark changes on a 12:12 hour cyclic schedule
circadian	NRC1_07740_2.681_rep2_vs_NRC-1g.sig	light:dark changes on a 12:12 hour cyclic schedule
circadian	NRC1_08460_3.840_rep2_vs_NRC-1g.sig	light:dark changes on a 12:12 hour cyclic schedule
circadian	NRC1_09540_4.690_rep2_vs_NRC-1g.sig	light:dark changes on a 12:12 hour cyclic schedule
circadian	NRC1_10260_4.540_rep2_vs_NRC-1g.sig	light:dark changes on a 12:12 hour cyclic schedule
circadian	NRC1_10980_4.935_rep2_vs_NRC-1g.sig	light:dark changes on a 12:12 hour cyclic schedule
circadian	NRC1_11700_5.730_rep2_vs_NRC-1g.sig	light:dark changes on a 12:12 hour cyclic schedule
circadian	NRC1_03720_0.259_rep1_vs_NRC-1g.sig	light:dark changes on a 12:12 hour cyclic schedule
circadian	NRC1_03960_0.364_rep1_vs_NRC-1g.sig	light:dark changes on a 12:12 hour cyclic schedule
circadian	NRC1_04320_0.590_rep1_vs_NRC-1g.sig	light:dark changes on a 12:12 hour cyclic schedule
circadian	NRC1_04476_0.762_rep1_vs_NRC-1g.sig	light:dark changes on a 12:12 hour cyclic schedule
circadian	NRC1_05400_0.803_rep1_vs_NRC-1g.sig	light:dark changes on a 12:12 hour cyclic schedule
circadian	NRC1_05778_0.710_rep1vs_NRC-1g.sig	light:dark changes on a 12:12 hour cyclic schedule
circadian	NRC1_07020_1.329_rep1_vs_NRC-1g.sig	light:dark changes on a 12:12 hour cyclic schedule
circadian	NRC1_07740_2.580_rep1_vs_NRC-1g.sig	light:dark changes on a 12:12 hour cyclic schedule
circadian	NRC1_08460_3.510_rep1_vs_NRC-1g.sig	light:dark changes on a 12:12 hour cyclic schedule
circadian	NRC1_09540_4.860_rep1_vs_NRC-1g.sig	light:dark changes on a 12:12 hour cyclic schedule

circadian	NRC1_10260_4.860_rep1_vs_NRC-1g.sig	light:dark changes on a 12:12 hour cyclic schedule
circadian	NRC1_10980_5.130_rep1_vs_NRC-1g.sig	light:dark changes on a 12:12 hour cyclic schedule
circadian	NRC1_11700_5.640_rep1_vs_NRC-1g.sig	light:dark changes on a 12:12 hour cyclic schedule
circadian	uv__200jm2_D_030m	light:dark changes on a 12:12 hour cyclic schedule
circadian	uv__200jm2_D_060m	light:dark changes on a 12:12 hour cyclic schedule
circadian	uv__200jm2_L_030m	light:dark changes on a 12:12 hour cyclic schedule
circadian	uv__200jm2_L_060m	light:dark changes on a 12:12 hour cyclic schedule
circadian	o2_set1_-001m_L2H_005_vs_NRC-1c	light:dark changes on a 12:12 hour cyclic schedule
circadian	o2_set1_0001m_L2H_500_vs_NRC-1c	light:dark changes on a 12:12 hour cyclic schedule
circadian	o2_set1_0005m_H_922_vs_NRC-1c	light:dark changes on a 12:12 hour cyclic schedule
circadian	o2_set1_0010m_H_947_vs_NRC-1c	light:dark changes on a 12:12 hour cyclic schedule
circadian	o2_set1_0020m_H_937_vs_NRC-1c	light:dark changes on a 12:12 hour cyclic schedule
circadian	o2_set1_0030m_H_931_vs_NRC-1c	light:dark changes on a 12:12 hour cyclic schedule
circadian	o2_set1_0045m_H_939_vs_NRC-1c	light:dark changes on a 12:12 hour cyclic schedule
circadian	o2_set1_0090m_H_941_vs_NRC-1c	light:dark changes on a 12:12 hour cyclic schedule
circadian	o2_set1_0180m_H_930_vs_NRC-1c	light:dark changes on a 12:12 hour cyclic schedule
circadian	o2_set1_0360m_H_903_vs_NRC-1c	light:dark changes on a 12:12 hour cyclic schedule
circadian	o2_set1_0362m_H2L_860_vs_NRC-1c	light:dark changes on a 12:12 hour cyclic schedule
circadian	o2_set1_0367m_H2L_215_vs_NRC-1c	light:dark changes on a 12:12 hour cyclic schedule
circadian	o2_set1_0372m_H2L_079_vs_NRC-1c	light:dark changes on a 12:12 hour cyclic schedule
circadian	o2_set1_0382m_H2L_048_vs_NRC-1c	light:dark changes on a 12:12 hour cyclic schedule
circadian	o2_set1_0387m_L_041_vs_NRC-1c	light:dark changes on a 12:12 hour cyclic schedule
circadian	o2_set1_0392m_L_037_vs_NRC-1c	light:dark changes on a 12:12 hour cyclic schedule
circadian	o2_set1_0397m_L_035_vs_NRC-1c	light:dark changes on a 12:12 hour cyclic schedule
circadian	o2_set1_0407m_L_030_vs_NRC-1c	light:dark changes on a 12:12 hour cyclic schedule

circadian	o2_set1_0417m_L_027_vs_NRC-1c	light:dark changes on a 12:12 hour cyclic schedule
circadian	o2_set1_0432m_L_024_vs_NRC-1c	light:dark changes on a 12:12 hour cyclic schedule
circadian	o2_set1_0477m_L_017_vs_NRC-1c	light:dark changes on a 12:12 hour cyclic schedule
circadian	o2_set1_0567m_L_011_vs_NRC-1c	light:dark changes on a 12:12 hour cyclic schedule
circadian	o2_set1_0747m_L_008_vs_NRC-1c	light:dark changes on a 12:12 hour cyclic schedule
circadian	o2_set1_0750m_L2H_540_vs_NRC-1c	light:dark changes on a 12:12 hour cyclic schedule
circadian	o2_set1_0755m_L2H_825_vs_NRC-1c	light:dark changes on a 12:12 hour cyclic schedule
circadian	o2_set1_0760m_L2H_847_vs_NRC-1c	light:dark changes on a 12:12 hour cyclic schedule
circadian	o2_set1_0770m_L2H_852_vs_NRC-1c	light:dark changes on a 12:12 hour cyclic schedule
circadian	o2_set1_0780m_L2H_847_vs_NRC-1c	light:dark changes on a 12:12 hour cyclic schedule
circadian	20061006_Cmyc_rep2_0.179_vs_NRC-1e.sig	light:dark changes on a 12:12 hour cyclic schedule
circadian	20061006_Cmyc_rep2_0.399_vs_NRC-1e.sig	light:dark changes on a 12:12 hour cyclic schedule
circadian	20061006_Cmyc_rep2_0.833_vs_NRC-1e.sig	light:dark changes on a 12:12 hour cyclic schedule
circadian	20061006_Cmyc_rep1_0.175_vs_NRC-1e.sig	light:dark changes on a 12:12 hour cyclic schedule
circadian	20061006_Cmyc_rep1_0.417_vs_NRC-1e.sig	light:dark changes on a 12:12 hour cyclic schedule
circadian	20061006_Cmyc_rep1_0.835_vs_NRC-1e.sig	light:dark changes on a 12:12 hour cyclic schedule
circadian	20060818_KO_ura3_rep2_0.189_vs_NRC-1e.sig	light:dark changes on a 12:12 hour cyclic schedule
circadian	20060818_KO_ura3_rep2_0.376_vs_NRC-1e.sig	light:dark changes on a 12:12 hour cyclic schedule
circadian	20060818_KO_ura3_rep2_0.828_vs_NRC-1e.sig	light:dark changes on a 12:12 hour cyclic schedule
circadian	20060818_KO_ura3_rep1_0.178_vs_NRC-1e.sig	light:dark changes on a 12:12 hour cyclic schedule
circadian	20060818_KO_ura3_rep1_0.405_vs_NRC-1e.sig	light:dark changes on a 12:12 hour cyclic schedule
circadian	20060818_KO_ura3_rep1_0.842_vs_NRC-1e.sig	light:dark changes on a 12:12 hour cyclic schedule
circadian	20060717_Cmyc_rep2_0.223_vs_NRC-1e.sig	light:dark changes on a 12:12 hour cyclic schedule
circadian	20060717_Cmyc_rep2_0.407_vs_NRC-1e.sig	light:dark changes on a 12:12 hour cyclic schedule
circadian	20060717_Cmyc_rep2_0.883_vs_NRC-1e.sig	light:dark changes on a 12:12 hour cyclic schedule

circadian	20060717_Cmyc_rep1_0.221_vs_NRC-1e.sig	light:dark changes on a 12:12 hour cyclic schedule
circadian	20060717_Cmyc_rep1_0.402_vs_NRC-1e.sig	light:dark changes on a 12:12 hour cyclic schedule
circadian	20060717_Cmyc_rep1_0.827_vs_NRC-1e.sig	light:dark changes on a 12:12 hour cyclic schedule
circadian	20060308_KO_ura3_0.189_vs_NRC-1e.sig	light:dark changes on a 12:12 hour cyclic schedule
circadian	20060308_KO_ura3_0.448_vs_NRC-1e.sig	light:dark changes on a 12:12 hour cyclic schedule
circadian	20060308_KO_ura3_0.853_vs_NRC-1e.sig	light:dark changes on a 12:12 hour cyclic schedule
circadian	20050620_NRC1_rep2_0.183_vs_NRC-1d.sig	light:dark changes on a 12:12 hour cyclic schedule
circadian	20050620_NRC1_rep2_0.505_vs_NRC-1d.sig	light:dark changes on a 12:12 hour cyclic schedule
circadian	20050620_NRC1_rep2_1.030_vs_NRC-1d.sig	light:dark changes on a 12:12 hour cyclic schedule
circadian	20050620_NRC1_rep1_0.173_vs_NRC-1d.sig	light:dark changes on a 12:12 hour cyclic schedule
circadian	20050620_NRC1_rep1_0.484_vs_NRC-1d.sig	light:dark changes on a 12:12 hour cyclic schedule
circadian	20050620_NRC1_rep1_1.276_vs_NRC-1d.sig	light:dark changes on a 12:12 hour cyclic schedule
circadian	20050620_Cmyc_rep2_0.177_vs_NRC-1d.sig	light:dark changes on a 12:12 hour cyclic schedule
circadian	20050620_Cmyc_rep2_0.457_vs_NRC-1d.sig	light:dark changes on a 12:12 hour cyclic schedule
circadian	20050620_Cmyc_rep2_1.072_vs_NRC-1d.sig	light:dark changes on a 12:12 hour cyclic schedule
circadian	20050620_Cmyc_rep1_0.207_vs_NRC-1d.sig	light:dark changes on a 12:12 hour cyclic schedule
circadian	20050620_Cmyc_rep1_0.474_vs_NRC-1d.sig	light:dark changes on a 12:12 hour cyclic schedule
circadian	20050620_Cmyc_rep1_1.052_vs_NRC-1d.sig	light:dark changes on a 12:12 hour cyclic schedule
circadian	sDura3_pCu_d0.100mM_t+015m_vs_NRC-1h1.sig	light:dark changes on a 12:12 hour cyclic schedule
circadian	sDura3_pCu_d0.100mM_t+030m_vs_NRC-1h1.sig	light:dark changes on a 12:12 hour cyclic schedule
circadian	sDura3_pCu_d0.100mM_t+060m_vs_NRC-1h1.sig	light:dark changes on a 12:12 hour cyclic schedule
circadian	sDura3_pCu_d0.100mM_t+180m_vs_NRC-1h1.sig	light:dark changes on a 12:12 hour cyclic schedule
circadian	sDura3_pCu_d0.100mM_t-015m_vs_NRC-1h1.sig	light:dark changes on a 12:12 hour cyclic schedule
circadian	sDura3_pCu_d0.700mM_t+015m_vs_NRC-1h1.sig	light:dark changes on a 12:12 hour cyclic schedule
circadian	sDura3_pCu_d0.700mM_t+030m_vs_NRC-1h1.sig	light:dark changes on a 12:12 hour cyclic schedule

circadian	sDura3_pCu_d0.700mM_t+060m_vs_NRC-1h1.sig	light:dark changes on a 12:12 hour cyclic schedule
circadian	sDura3_pCu_d0.700mM_t+180m_vs_NRC-1h1.sig	light:dark changes on a 12:12 hour cyclic schedule
circadian	sDura3_pCu_d0.700mM_t-015m_vs_NRC-1h1.sig	light:dark changes on a 12:12 hour cyclic schedule
circadian	sDura3_pCu_d1.000mM_t+015m_vs_NRC-1h1.sig	light:dark changes on a 12:12 hour cyclic schedule
circadian	sDura3_pCu_d1.000mM_t+030m_vs_NRC-1h1.sig	light:dark changes on a 12:12 hour cyclic schedule
circadian	sDura3_pCu_d1.000mM_t+060m_vs_NRC-1h1.sig	light:dark changes on a 12:12 hour cyclic schedule
circadian	sDura3_pCu_d1.000mM_t+180m_vs_NRC-1h1.sig	light:dark changes on a 12:12 hour cyclic schedule
circadian	sDura3_pCu_d1.000mM_t-015m_vs_NRC-1h1.sig	light:dark changes on a 12:12 hour cyclic schedule
circadian	sDura3_pNULL_d0.000mM_t+015m_vs_NRC-1h1.sig	light:dark changes on a 12:12 hour cyclic schedule
circadian	sDura3_pNULL_d0.000mM_t+030m_vs_NRC-1h1.sig	light:dark changes on a 12:12 hour cyclic schedule
circadian	sDura3_pNULL_d0.000mM_t+060m_vs_NRC-1h1.sig	light:dark changes on a 12:12 hour cyclic schedule
circadian	sDura3_pNULL_d0.000mM_t+180m_vs_NRC-1h1.sig	light:dark changes on a 12:12 hour cyclic schedule
circadian	sDura3_pNULL_d0.000mM_t-015m_vs_NRC-1h1.sig	light:dark changes on a 12:12 hour cyclic schedule
circadian	sDura3_pZn_d0.005mM_t+015m_vs_NRC-1h1.sig	light:dark changes on a 12:12 hour cyclic schedule
circadian	sDura3_pZn_d0.005mM_t+030m_vs_NRC-1h1.sig	light:dark changes on a 12:12 hour cyclic schedule
circadian	sDura3_pZn_d0.005mM_t+060m_vs_NRC-1h1.sig	light:dark changes on a 12:12 hour cyclic schedule
circadian	sDura3_pZn_d0.005mM_t+180m_vs_NRC-1h1.sig	light:dark changes on a 12:12 hour cyclic schedule
circadian	sDura3_pZn_d0.005mM_t-015m_vs_NRC-1h1.sig	light:dark changes on a 12:12 hour cyclic schedule
circadian	sDura3_pZn_d0.020mM_t+015m_vs_NRC-1h1.sig	light:dark changes on a 12:12 hour cyclic schedule
circadian	sDura3_pZn_d0.020mM_t+030m_vs_NRC-1h1.sig	light:dark changes on a 12:12 hour cyclic schedule
circadian	sDura3_pZn_d0.020mM_t+060m_vs_NRC-1h1.sig	light:dark changes on a 12:12 hour cyclic schedule
circadian	sDura3_pZn_d0.020mM_t+180m_vs_NRC-1h1.sig	light:dark changes on a 12:12 hour cyclic schedule
circadian	sDura3_pZn_d0.020mM_t-015m_vs_NRC-1h1.sig	light:dark changes on a 12:12 hour cyclic schedule
circadian	sDura3_pZn_d0.050mM_t+015m_vs_NRC-1h1.sig	light:dark changes on a 12:12 hour cyclic schedule
circadian	sDura3_pZn_d0.050mM_t+030m_vs_NRC-1h1.sig	light:dark changes on a 12:12 hour cyclic schedule

circadian	sDura3_pZn_d0.050mM_t+060m_vs_NRC-1h1.sig	light:dark changes on a 12:12 hour cyclic schedule
circadian	sDura3_pZn_d0.050mM_t+180m_vs_NRC-1h1.sig	light:dark changes on a 12:12 hour cyclic schedule
circadian	sDura3_pZn_d0.050mM_t-015m_vs_NRC-1h1.sig	light:dark changes on a 12:12 hour cyclic schedule
cobalt	Co_0.2_vs_NRC-1d.sig	2e-3<=mol/L=<5.0e-3.
cobalt	Co_0.3_vs_NRC-1d.sig	2e-3<=mol/L=<5.0e-3.
cobalt	Co_0.5_vs_NRC-1d.sig	2e-3<=mol/L=<5.0e-3.
cobalt	Co_0.0_vs_NRC-1d.sig	2e-3<=mol/L=<5.0e-3.
cobalt	co__0000um_vs_NRC-1c	2e-3<=mol/L=<5.0e-3.
cobalt	co__0200um_vs_NRC-1c	2e-3<=mol/L=<5.0e-3.
cobalt	co__0300um_vs_NRC-1c	2e-3<=mol/L=<5.0e-3.
cobalt	co__0500um_vs_NRC-1c	2e-3<=mol/L=<5.0e-3.
copper	cu__0700um_vs_NRC-1	1e-4<=mol/L=<1.0e-3.
copper	cu__0850um_vs_NRC-1	1e-4<=mol/L=<1.0e-3.
copper	cu__1000um_vs_NRC-1	1e-4<=mol/L=<1.0e-3.
copper	Cu_-5_vs_NRC-1.sig	1e-4<=mol/L=<1.0e-3.
copper	Cu_000_vs_NRC-1.sig	1e-4<=mol/L=<1.0e-3.
copper	Cu_005_vs_NRC-1.sig	1e-4<=mol/L=<1.0e-3.
copper	Cu_010_vs_NRC-1.sig	1e-4<=mol/L=<1.0e-3.
copper	Cu_020_vs_NRC-1.sig	1e-4<=mol/L=<1.0e-3.
copper	Cu_040_vs_NRC-1.sig	1e-4<=mol/L=<1.0e-3.
copper	Cu_080_vs_NRC-1.sig	1e-4<=mol/L=<1.0e-3.
copper	Cu_160_vs_NRC-1.sig	1e-4<=mol/L=<1.0e-3.
copper	Cu_-1_vs_NRC-1e.sig	1e-4<=mol/L=<1.0e-3.
copper	Cu_000_vs_NRC-1e.sig	1e-4<=mol/L=<1.0e-3.
copper	Cu_005_vs_NRC-1e.sig	1e-4<=mol/L=<1.0e-3.
copper	Cu_010_vs_NRC-1e.sig	1e-4<=mol/L=<1.0e-3.
copper	Cu_020_vs_NRC-1e.sig	1e-4<=mol/L=<1.0e-3.
copper	Cu_040_vs_NRC-1e.sig	1e-4<=mol/L=<1.0e-3.
copper	Cu_080_vs_NRC-1e.sig	1e-4<=mol/L=<1.0e-3.
copper	Cu_160_vs_NRC-1e.sig	1e-4<=mol/L=<1.0e-3.
copper	Cu_320_vs_NRC-1e.sig	1e-4<=mol/L=<1.0e-3.
copper	Cu_NRC1_set1_-030min_vs_NRC-1h1.sig	1e-4<=mol/L=<1.0e-3.
copper	Cu_NRC1_set1_000min_vs_NRC-1h1.sig	1e-4<=mol/L=<1.0e-3.
copper	Cu_NRC1_set1_005min_vs_NRC-1h1.sig	1e-4<=mol/L=<1.0e-3.
copper	Cu_NRC1_set1_010min_vs_NRC-1h1.sig	1e-4<=mol/L=<1.0e-3.
copper	Cu_NRC1_set1_020min_vs_NRC-1h1.sig	1e-4<=mol/L=<1.0e-3.
copper	Cu_NRC1_set1_040min_vs_NRC-1h1.sig	1e-4<=mol/L=<1.0e-3.
copper	Cu_NRC1_set1_080min_vs_NRC-1h1.sig	1e-4<=mol/L=<1.0e-3.
copper	Cu_NRC1_set1_160min_vs_NRC-1h1.sig	1e-4<=mol/L=<1.0e-3.
copper	Cu_ura3_KO_set1_-030min_vs_NRC-	1e-4<=mol/L=<1.0e-3.

	1h1.sig	
copper	Cu_ura3_KO_set1_000min_vs_NRC-1h1.sig	1e-4<=mol/L=<1.0e-3.
copper	Cu_ura3_KO_set1_005min_vs_NRC-1h1.sig	1e-4<=mol/L=<1.0e-3.
copper	Cu_ura3_KO_set1_010min_vs_NRC-1h1.sig	1e-4<=mol/L=<1.0e-3.
copper	Cu_ura3_KO_set1_020min_vs_NRC-1h1.sig	1e-4<=mol/L=<1.0e-3.
copper	Cu_ura3_KO_set1_040min_vs_NRC-1h1.sig	1e-4<=mol/L=<1.0e-3.
copper	Cu_ura3_KO_set1_080min_vs_NRC-1h1.sig	1e-4<=mol/L=<1.0e-3.
copper	Cu_ura3_KO_set1_160min_vs_NRC-1h1.sig	1e-4<=mol/L=<1.0e-3.
copper	Cu_ura3_KO_set2_-030min_vs_NRC-1h1.sig	1e-4<=mol/L=<1.0e-3.
copper	Cu_ura3_KO_set2_000min_vs_NRC-1h1.sig	1e-4<=mol/L=<1.0e-3.
copper	Cu_ura3_KO_set2_005min_vs_NRC-1h1.sig	1e-4<=mol/L=<1.0e-3.
copper	Cu_ura3_KO_set2_010min_vs_NRC-1h1.sig	1e-4<=mol/L=<1.0e-3.
copper	Cu_ura3_KO_set2_020min_vs_NRC-1h1.sig	1e-4<=mol/L=<1.0e-3.
copper	Cu_ura3_KO_set2_040min_vs_NRC-1h1.sig	1e-4<=mol/L=<1.0e-3.
copper	Cu_ura3_KO_set2_080min_vs_NRC-1h1.sig	1e-4<=mol/L=<1.0e-3.
copper	Cu_ura3_KO_set2_160min_vs_NRC-1h1.sig	1e-4<=mol/L=<1.0e-3.
copper	Cu_NRC1_set2_-030min_vs_NRC-1h1.sig	1e-4<=mol/L=<1.0e-3.
copper	Cu_NRC1_set2_000min_vs_NRC-1h1.sig	1e-4<=mol/L=<1.0e-3.
copper	Cu_NRC1_set2_005min_vs_NRC-1h1.sig	1e-4<=mol/L=<1.0e-3.
copper	Cu_NRC1_set2_010min_vs_NRC-1h1.sig	1e-4<=mol/L=<1.0e-3.
copper	Cu_NRC1_set2_020min_vs_NRC-1h1.sig	1e-4<=mol/L=<1.0e-3.
copper	Cu_NRC1_set2_040min_vs_NRC-1h1.sig	1e-4<=mol/L=<1.0e-3.
copper	Cu_NRC1_set2_080min_vs_NRC-1h1.sig	1e-4<=mol/L=<1.0e-3.
copper	Cu_NRC1_set2_160min_vs_NRC-1h1.sig	1e-4<=mol/L=<1.0e-3.
copper	ura3_0a_vs_NRC-1d.sig	1e-4<=mol/L=<1.0e-3.
copper	ura3_0b_vs_NRC-1d.sig	1e-4<=mol/L=<1.0e-3.
copper	ura3_Cu_0700um_a_vs_NRC-1d.sig	1e-4<=mol/L=<1.0e-3.
copper	ura3_Cu_0700um_b_vs_NRC-1d.sig	1e-4<=mol/L=<1.0e-3.
copper	ura3_Cu_0850um_a_vs_NRC-1d.sig	1e-4<=mol/L=<1.0e-3.
copper	ura3_Cu_0850um_b_vs_NRC-1d.sig	1e-4<=mol/L=<1.0e-3.
copper	ura3_Cu_1000um_a_vs_NRC-1d.sig	1e-4<=mol/L=<1.0e-3.
copper	ura3_Cu_1000um_b_vs_NRC-1d.sig	1e-4<=mol/L=<1.0e-3.

copper	sDura3_pCu_d0.100mM_t+015m_vs_NRC-1h1.sig	1e-4<=mol/L=<1.0e-3.
copper	sDura3_pCu_d0.100mM_t+030m_vs_NRC-1h1.sig	1e-4<=mol/L=<1.0e-3.
copper	sDura3_pCu_d0.100mM_t+060m_vs_NRC-1h1.sig	1e-4<=mol/L=<1.0e-3.
copper	sDura3_pCu_d0.100mM_t+180m_vs_NRC-1h1.sig	1e-4<=mol/L=<1.0e-3.
copper	sDura3_pCu_d0.100mM_t-015m_vs_NRC-1h1.sig	1e-4<=mol/L=<1.0e-3.
copper	sDura3_pCu_d0.700mM_t+015m_vs_NRC-1h1.sig	1e-4<=mol/L=<1.0e-3.
copper	sDura3_pCu_d0.700mM_t+030m_vs_NRC-1h1.sig	1e-4<=mol/L=<1.0e-3.
copper	sDura3_pCu_d0.700mM_t+060m_vs_NRC-1h1.sig	1e-4<=mol/L=<1.0e-3.
copper	sDura3_pCu_d0.700mM_t+180m_vs_NRC-1h1.sig	1e-4<=mol/L=<1.0e-3.
copper	sDura3_pCu_d0.700mM_t-015m_vs_NRC-1h1.sig	1e-4<=mol/L=<1.0e-3.
copper	sDura3_pCu_d1.000mM_t+015m_vs_NRC-1h1.sig	1e-4<=mol/L=<1.0e-3.
copper	sDura3_pCu_d1.000mM_t+030m_vs_NRC-1h1.sig	1e-4<=mol/L=<1.0e-3.
copper	sDura3_pCu_d1.000mM_t+060m_vs_NRC-1h1.sig	1e-4<=mol/L=<1.0e-3.
copper	sDura3_pCu_d1.000mM_t+180m_vs_NRC-1h1.sig	1e-4<=mol/L=<1.0e-3.
copper	sDura3_pCu_d1.000mM_t-015m_vs_NRC-1h1.sig	1e-4<=mol/L=<1.0e-3.
dark	dark2__0000m_vs_NRC-1c	= 0umol/m2/s.
dark	dark2__0060m_vs_NRC-1c	= 0umol/m2/s.
dark	dark2__0300m_vs_NRC-1c	= 0umol/m2/s.
dark	dark2__0540m_vs_NRC-1c	= 0umol/m2/s.
dark	dark2__0780m_vs_NRC-1c	= 0umol/m2/s.
dark	dark2__1020m_vs_NRC-1c	= 0umol/m2/s.
dark	dark2__1260m_vs_NRC-1c	= 0umol/m2/s.
dark	dark2__1500m_vs_NRC-1c	= 0umol/m2/s.
dark	dark2__1740m_vs_NRC-1c	= 0umol/m2/s.
dark	dark2__1980m_vs_NRC-1c	= 0umol/m2/s.
dark	dark2__2220m_vs_NRC-1c	= 0umol/m2/s.
dark	dark2__2460m_vs_NRC-1c	= 0umol/m2/s.
dark	dark2__2700m_vs_NRC-1c	= 0umol/m2/s.
dark	dark2__2940m_vs_NRC-1c	= 0umol/m2/s.
dark	dark2__3180m_vs_NRC-1c	= 0umol/m2/s.
dark	dark2__3420m_vs_NRC-1c	= 0umol/m2/s.
dark	dark2__3660m_vs_NRC-1c	= 0umol/m2/s.

dark	dark2__3900m_vs_NRC-1c	= 0umol/m2/s.
dark	dark1__0000m_vs_NRC-1c	= 0umol/m2/s.
dark	dark1__0240m_vs_NRC-1c	= 0umol/m2/s.
dark	dark1__0480m_vs_NRC-1c	= 0umol/m2/s.
dark	dark1__0720m_vs_NRC-1c	= 0umol/m2/s.
dark	dark1__0960m_vs_NRC-1c	= 0umol/m2/s.
dark	dark1__1200m_vs_NRC-1c	= 0umol/m2/s.
dark	dark1__1440m_vs_NRC-1c	= 0umol/m2/s.
dark	dark1__1680m_vs_NRC-1c	= 0umol/m2/s.
dark	dark1__1920m_vs_NRC-1c	= 0umol/m2/s.
dark	dark1__2160m_vs_NRC-1c	= 0umol/m2/s.
dark	dark1__2400m_vs_NRC-1c	= 0umol/m2/s.
dark	dark1__2640m_vs_NRC-1c	= 0umol/m2/s.
dark	dark1__2880m_vs_NRC-1c	= 0umol/m2/s.
dark	dark1__3120m_vs_NRC-1c	= 0umol/m2/s.
dark	dark1__3360m_vs_NRC-1c	= 0umol/m2/s.
dark	dark1__3600m_vs_NRC-1c	= 0umol/m2/s.
dark	dark1__3870m_vs_NRC-1c	= 0umol/m2/s.
dark	dark1__4110m_vs_NRC-1c	= 0umol/m2/s.
dark	circadian_Dphr1_drk_cycling__1440min_vs_NRC-1d.sig	= 0umol/m2/s.
dark	circadian_Dphr1_drk_cycling__1665min_vs_NRC-1d.sig	= 0umol/m2/s.
dark	circadian_Dphr1_drk_cycling__1800min_vs_NRC-1d.sig	= 0umol/m2/s.
dark	circadian_Dphr1_drk_cycling__1980min_vs_NRC-1d.sig	= 0umol/m2/s.
dark	circadian_Dphr1_drk_cycling__2175min_vs_NRC-1d.sig	= 0umol/m2/s.
dark	circadian_Dphr1_drk_cycling__2340min_vs_NRC-1d.sig	= 0umol/m2/s.
dark	circadian_Dphr1_drk_cycling__2595min_vs_NRC-1d.sig	= 0umol/m2/s.
dark	circadian_Dphr1_drk_cycling__2705min_vs_NRC-1d.sig	= 0umol/m2/s.
dark	circadian_Dphr1_drk_cycling__2880min_vs_NRC-1d.sig	= 0umol/m2/s.
dark	circadian_drk8_cycling_0000min_vs_NRC-1e.sig	= 0umol/m2/s.
dark	circadian_drk8_cycling_0180min_vs_NRC-1e.sig	= 0umol/m2/s.
dark	circadian_drk8_cycling_0360min_vs_NRC-1e.sig	= 0umol/m2/s.
dark	circadian_drk8_cycling_0540min_vs_NRC-1e.sig	= 0umol/m2/s.
dark	circadian_drk8_cycling_0720min_vs_NRC-1e.sig	= 0umol/m2/s.

dark	circadian_drk8_cycling_0900min_vs_NRC-1e.sig	= 0umol/m2/s.
dark	circadian_drk8_cycling_1080min_vs_NRC-1e.sig	= 0umol/m2/s.
dark	circadian_drk8_cycling_1260min_vs_NRC-1e.sig	= 0umol/m2/s.
dark	circadian_drk8_cycling_1440min_vs_NRC-1e.sig	= 0umol/m2/s.
dark	circadian_drk8_cycling_1620min_vs_NRC-1e.sig	= 0umol/m2/s.
dark	circadian_drk8_cycling_1800min_vs_NRC-1e.sig	= 0umol/m2/s.
dark	circadian_drk8_cycling_1980min_vs_NRC-1e.sig	= 0umol/m2/s.
dark	circadian_drk8_cycling_2160min_vs_NRC-1e.sig	= 0umol/m2/s.
dark	circadian_drk8_cycling_2340min_vs_NRC-1e.sig	= 0umol/m2/s.
dark	circadian_drk8_cycling_2520min_vs_NRC-1e.sig	= 0umol/m2/s.
dark	circadian_drk8_cycling_2700min_vs_NRC-1e.sig	= 0umol/m2/s.
dark	circadian_drk8_cycling_2880min_vs_NRC-1e.sig	= 0umol/m2/s.
dark	circadian_drk8_cycling_3060min_vs_NRC-1e.sig	= 0umol/m2/s.
dark	circadian_drk8_cycling_3240min_vs_NRC-1e.sig	= 0umol/m2/s.
dark	circadian_drk7_cycling_0000min_vs_NRC-1d.sig	= 0umol/m2/s.
dark	circadian_drk7_cycling_0180min_vs_NRC-1d.sig	= 0umol/m2/s.
dark	circadian_drk7_cycling_0360min_vs_NRC-1d.sig	= 0umol/m2/s.
dark	circadian_drk7_cycling_0540min_vs_NRC-1d.sig	= 0umol/m2/s.
dark	circadian_drk7_cycling_0720min_vs_NRC-1d.sig	= 0umol/m2/s.
dark	circadian_drk7_cycling_0900min_vs_NRC-1d.sig	= 0umol/m2/s.
dark	circadian_drk7_cycling_1080min_vs_NRC-1d.sig	= 0umol/m2/s.
dark	circadian_drk7_cycling_1260min_vs_NRC-1d.sig	= 0umol/m2/s.
dark	circadian_drk7_cycling_1440min_vs_NRC-1d.sig	= 0umol/m2/s.
dark	circadian_drk7_cycling_1620min_vs_NRC-1d.sig	= 0umol/m2/s.
dark	circadian_drk7_cycling_1800min_vs_NRC-1d.sig	= 0umol/m2/s.

dark	circadian_drk7_cycling_1980min_vs_NRC-1d.sig	= 0umol/m2/s.
dark	circadian_drk7_cycling_2160min_vs_NRC-1d.sig	= 0umol/m2/s.
dark	circadian_drk7_cycling_2340min_vs_NRC-1d.sig	= 0umol/m2/s.
dark	circadian_drk7_cycling_2520min_vs_NRC-1d.sig	= 0umol/m2/s.
dark	circadian_drk7_cycling_2700min_vs_NRC-1d.sig	= 0umol/m2/s.
dark	circadian_drk7_cycling_2880min_vs_NRC-1d.sig	= 0umol/m2/s.
dark	circadian_drk7_cycling_3060min_vs_NRC-1d.sig	= 0umol/m2/s.
dark	circadian_drk7_cycling_3240min_vs_NRC-1d.sig	= 0umol/m2/s.
dark	circadian_drk6_cycling_0000min_vs_NRC-1e.sig	= 0umol/m2/s.
dark	circadian_drk6_cycling_0180min_vs_NRC-1e.sig	= 0umol/m2/s.
dark	circadian_drk6_cycling_0360min_vs_NRC-1e.sig	= 0umol/m2/s.
dark	circadian_drk6_cycling_0540min_vs_NRC-1e.sig	= 0umol/m2/s.
dark	circadian_drk6_cycling_0720min_vs_NRC-1e.sig	= 0umol/m2/s.
dark	circadian_drk6_cycling_0912min_vs_NRC-1e.sig	= 0umol/m2/s.
dark	circadian_drk6_cycling_1080min_vs_NRC-1e.sig	= 0umol/m2/s.
dark	circadian_drk6_cycling_1260min_vs_NRC-1e.sig	= 0umol/m2/s.
dark	circadian_drk6_cycling_1440min_vs_NRC-1e.sig	= 0umol/m2/s.
dark	circadian__dark5_cycling_30C_1440min_vs_NRC-1d.sig	= 0umol/m2/s.
dark	circadian__dark5_cycling_30C_1630min_vs_NRC-1d.sig	= 0umol/m2/s.
dark	circadian__dark5_cycling_30C_1815min_vs_NRC-1d.sig	= 0umol/m2/s.
dark	circadian__dark5_cycling_30C_1980min_vs_NRC-1d.sig	= 0umol/m2/s.
dark	circadian__dark5_cycling_30C_2160min_vs_NRC-1d.sig	= 0umol/m2/s.
dark	circadian__dark5_cycling_30C_2355min_vs_NRC-1d.sig	= 0umol/m2/s.
dark	circadian__dark5_cycling_30C_2590min_vs_NRC-1d.sig	= 0umol/m2/s.
dark	circadian__dark5_cycling_30C_2700min_vs_NRC-1d.sig	= 0umol/m2/s.

dark	circadian__dark5_cycling_30C_2880min_vs_NRC-1d.sig	= 0umol/m2/s.
dark	circadian_20051021_cycling_dark_42oC_1440min_vs_NRC-1d.sig	= 0umol/m2/s.
dark	circadian_20051021_cycling_dark_42oC_1615min_vs_NRC-1d.sig	= 0umol/m2/s.
dark	circadian_20051021_cycling_dark_42oC_1800min_vs_NRC-1d.sig	= 0umol/m2/s.
dark	circadian_20051021_cycling_dark_42oC_1985min_vs_NRC-1d.sig	= 0umol/m2/s.
dark	circadian_20051021_cycling_dark_42oC_2160min_vs_NRC-1d.sig	= 0umol/m2/s.
dark	circadian_20051021_cycling_dark_42oC_2340min_vs_NRC-1d.sig	= 0umol/m2/s.
dark	circadian_20051021_cycling_dark_42oC_2515min_vs_NRC-1d.sig	= 0umol/m2/s.
dark	circadian_20051021_cycling_dark_42oC_2705min_vs_NRC-1d.sig	= 0umol/m2/s.
dark	circadian_20051021_cycling_dark_42oC_2880min_vs_NRC-1d.sig	= 0umol/m2/s.
dark	circadian_dark3_cycling_1380min_vs_NRC-1d.sig	= 0umol/m2/s.
dark	circadian_dark3_cycling_1440min_vs_NRC-1d.sig	= 0umol/m2/s.
dark	circadian_dark3_cycling_1500min_vs_NRC-1d.sig	= 0umol/m2/s.
dark	circadian_dark3_cycling_1620min_vs_NRC-1d.sig	= 0umol/m2/s.
dark	circadian_dark3_cycling_1800min_vs_NRC-1d.sig	= 0umol/m2/s.
dark	circadian_dark3_cycling_1980min_vs_NRC-1d.sig	= 0umol/m2/s.
dark	circadian_dark3_cycling_2160min_vs_NRC-1d.sig	= 0umol/m2/s.
dark	circadian_dark3_cycling_2220min_vs_NRC-1d.sig	= 0umol/m2/s.
dark	circadian_dark3_cycling_2340min_vs_NRC-1d.sig	= 0umol/m2/s.
dark	circadian_dark3_cycling_2520min_vs_NRC-1d.sig	= 0umol/m2/s.
dark	circadian_dark3_cycling_2700min_vs_NRC-1d.sig	= 0umol/m2/s.
dark	circadian_dark3_cycling_2880min_vs_NRC-1d.sig	= 0umol/m2/s.
dark	circadian_dark3_ctrl_1380min_vs_NRC-1d.sig	= 0umol/m2/s.
dark	circadian_dark3_ctrl_1440min_vs_NRC-1d.sig	= 0umol/m2/s.
dark	circadian_dark3_ctrl_1500min_vs_NRC-1d.sig	= 0umol/m2/s.

dark	circadian_dark3_ctrl_1620min_vs_NRC-1d.sig	= 0umol/m2/s.
dark	circadian_dark3_ctrl_1800min_vs_NRC-1d.sig	= 0umol/m2/s.
dark	circadian_dark3_ctrl_1980min_vs_NRC-1d.sig	= 0umol/m2/s.
dark	circadian_dark3_ctrl_2160min_vs_NRC-1d.sig	= 0umol/m2/s.
dark	circadian_dark3_ctrl_2220min_vs_NRC-1d.sig	= 0umol/m2/s.
dark	circadian_dark3_ctrl_2340min_vs_NRC-1d.sig	= 0umol/m2/s.
dark	circadian_dark3_ctrl_2520min_vs_NRC-1d.sig	= 0umol/m2/s.
dark	circadian_dark3_ctrl_2700min_vs_NRC-1d.sig	= 0umol/m2/s.
dark	circadian_dark3_ctrl_2880min_vs_NRC-1d.sig	= 0umol/m2/s.
dark	circadian_drk8_control_0000min_vs_NRC-1e.sig	= 0umol/m2/s.
dark	circadian_drk8_control_0180min_vs_NRC-1e.sig	= 0umol/m2/s.
dark	circadian_drk8_control_0360min_vs_NRC-1e.sig	= 0umol/m2/s.
dark	circadian_drk8_control_0540min_vs_NRC-1e.sig	= 0umol/m2/s.
dark	circadian_drk8_control_0720min_vs_NRC-1e.sig	= 0umol/m2/s.
dark	circadian_drk8_control_0900min_vs_NRC-1e.sig	= 0umol/m2/s.
dark	circadian_drk8_control_1080min_vs_NRC-1e.sig	= 0umol/m2/s.
dark	circadian_drk8_control_1260min_vs_NRC-1e.sig	= 0umol/m2/s.
dark	circadian_drk8_control_1440min_vs_NRC-1e.sig	= 0umol/m2/s.
dark	circadian_drk8_control_1620min_vs_NRC-1e.sig	= 0umol/m2/s.
dark	circadian_drk8_control_1800min_vs_NRC-1e.sig	= 0umol/m2/s.
dark	circadian_drk8_control_1980min_vs_NRC-1e.sig	= 0umol/m2/s.
dark	circadian_drk8_control_2160min_vs_NRC-1e.sig	= 0umol/m2/s.
dark	circadian_drk8_control_2340min_vs_NRC-1e.sig	= 0umol/m2/s.
dark	circadian_drk8_control_2520min_vs_NRC-1e.sig	= 0umol/m2/s.
dark	circadian_drk8_control_2700min_vs_NRC-1e.sig	= 0umol/m2/s.

dark	circadian_drk8_control_2880min_vs_NRC-1e.sig	= 0umol/m2/s.
dark	circadian_drk8_control_3060min_vs_NRC-1e.sig	= 0umol/m2/s.
dark	circadian_drk8_control_3240min_vs_NRC-1e.sig	= 0umol/m2/s.
dark	Circadian_Dark9_Cycling_0000min_vs_NRC-1g.sig	= 0umol/m2/s.
dark	Circadian_Dark9_Cycling_0180min_vs_NRC-1g.sig	= 0umol/m2/s.
dark	Circadian_Dark9_Cycling_0360min_vs_NRC-1g.sig	= 0umol/m2/s.
dark	Circadian_Dark9_Cycling_0535min_vs_NRC-1g.sig	= 0umol/m2/s.
dark	Circadian_Dark9_Cycling_0720min_vs_NRC-1g.sig	= 0umol/m2/s.
dark	Circadian_Dark9_Cycling_0900min_vs_NRC-1g.sig	= 0umol/m2/s.
dark	Circadian_Dark9_Cycling_1080min_vs_NRC-1g.sig	= 0umol/m2/s.
dark	Circadian_Dark9_Cycling_1265min_vs_NRC-1g.sig	= 0umol/m2/s.
dark	Circadian_Dark9_Cycling_1440min_vs_NRC-1g.sig	= 0umol/m2/s.
dark	Circadian_Dark9_Cycling_1620min_vs_NRC-1g.sig	= 0umol/m2/s.
dark	Circadian_Dark9_Cycling_1800min_vs_NRC-1g.sig	= 0umol/m2/s.
dark	Circadian_Dark9_Cycling_1980min_vs_NRC-1g.sig	= 0umol/m2/s.
dark	Circadian_Dark9_Cycling_2160min_vs_NRC-1g.sig	= 0umol/m2/s.
dark	Circadian_Dark9_Cycling_2340min_vs_NRC-1g.sig	= 0umol/m2/s.
dark	Circadian_Dark9_Cycling_2520min_vs_NRC-1g.sig	= 0umol/m2/s.
dark	Circadian_Dark9_Cycling_2700min_vs_NRC-1g.sig	= 0umol/m2/s.
dark	Circadian_Dark9_Cycling_2880min_vs_NRC-1g.sig	= 0umol/m2/s.
dark	Circadian_Dark9_Cycling_3060min_vs_NRC-1g.sig	= 0umol/m2/s.
dark	Circadian_Dark9_Cycling_3240min_vs_NRC-1g.sig	= 0umol/m2/s.
dark	Circadian_Dark9_Cycling_3420min_vs_NRC-1g.sig	= 0umol/m2/s.
dark	Circadian_Dark9_Cycling_3600min_vs_NRC-1g.sig	= 0umol/m2/s.
dark	Circadian_Dark9_Cycling_3780min_vs_NRC-1g.sig	= 0umol/m2/s.

dark	Circadian_Dark9_Cycling_3960min_vs_NRC-1g.sig	= 0umol/m2/s.
dark	Circadian_Dark9_Cycling_4140min_vs_NRC-1g.sig	= 0umol/m2/s.
dark	Circadian_Dark9_Cycling_4320min_vs_NRC-1g.sig	= 0umol/m2/s.
dark	Circadian_Dark9_Cycling_4500min_vs_NRC-1g.sig	= 0umol/m2/s.
dark	Circadian_Dark9_Control_0000min_vs_NRC-1g.sig	= 0umol/m2/s.
dark	Circadian_Dark9_Control_0180min_vs_NRC-1g.sig	= 0umol/m2/s.
dark	Circadian_Dark9_Control_0360min_vs_NRC-1g.sig	= 0umol/m2/s.
dark	Circadian_Dark9_Control_0535min_vs_NRC-1g.sig	= 0umol/m2/s.
dark	Circadian_Dark9_Control_0720min_vs_NRC-1g.sig	= 0umol/m2/s.
dark	Circadian_Dark9_Control_1080min_vs_NRC-1g.sig	= 0umol/m2/s.
dark	Circadian_Dark9_Control_1265min_vs_NRC-1g.sig	= 0umol/m2/s.
dark	Circadian_Dark9_Control_1440min_vs_NRC-1g.sig	= 0umol/m2/s.
dark	Circadian_Dark9_Control_1620min_vs_NRC-1g.sig	= 0umol/m2/s.
dark	Circadian_Dark9_Control_1800min_vs_NRC-1g.sig	= 0umol/m2/s.
dark	Circadian_Dark9_Control_1980min_vs_NRC-1g.sig	= 0umol/m2/s.
dark	Circadian_Dark9_Control_2160min_vs_NRC-1g.sig	= 0umol/m2/s.
dark	Circadian_Dark9_Control_2340min_vs_NRC-1g.sig	= 0umol/m2/s.
dark	Circadian_Dark9_Control_2520min_vs_NRC-1g.sig	= 0umol/m2/s.
dark	Circadian_Dark9_Control_2700min_vs_NRC-1g.sig	= 0umol/m2/s.
dark	Circadian_Dark9_Control_2880min_vs_NRC-1g.sig	= 0umol/m2/s.
dark	Circadian_Dark9_Control_3060min_vs_NRC-1g.sig	= 0umol/m2/s.
dark	Circadian_Dark9_Control_3240min_vs_NRC-1g.sig	= 0umol/m2/s.
dark	Circadian_Dark9_Control_3420min_vs_NRC-1g.sig	= 0umol/m2/s.
dark	Circadian_Dark9_Control_3600min_vs_NRC-1g.sig	= 0umol/m2/s.
dark	Circadian_Dark9_Control_3780min_vs_NRC-1g.sig	= 0umol/m2/s.

dark	Circadian_Dark9_Control_3960min_vs_NRC-1g.sig	= 0umol/m2/s.
dark	Circadian_Dark9_Control_4140min_vs_NRC-1g.sig	= 0umol/m2/s.
dark	Circadian_Dark9_Control_4320min_vs_NRC-1g.sig	= 0umol/m2/s.
dark	Circadian_Dark9_Control_4500min_vs_NRC-1g.sig	= 0umol/m2/s.
dark	Circadian_Dark10_Cycling_-2873min_vs_NRC-1h1.sig	= 0umol/m2/s.
dark	Circadian_Dark10_Cycling_-2670min_vs_NRC-1h1.sig	= 0umol/m2/s.
dark	Circadian_Dark10_Cycling_-2490min_vs_NRC-1h1.sig	= 0umol/m2/s.
dark	Circadian_Dark10_Cycling_-2315min_vs_NRC-1h1.sig	= 0umol/m2/s.
dark	Circadian_Dark10_Cycling_-1410min_vs_NRC-1h1.sig	= 0umol/m2/s.
dark	Circadian_Dark10_Cycling_-1245min_vs_NRC-1h1.sig	= 0umol/m2/s.
dark	Circadian_Dark10_Cycling_-1060min_vs_NRC-1h1.sig	= 0umol/m2/s.
dark	Circadian_Dark10_Cycling_-0880min_vs_NRC-1h1.sig	= 0umol/m2/s.
dark	Circadian_Dark10_Cycling_0000min_vs_NRC-1h1.sig	= 0umol/m2/s.
dark	Circadian_Dark10_Cycling_0195min_vs_NRC-1h1.sig	= 0umol/m2/s.
dark	Circadian_Dark10_Cycling_0370min_vs_NRC-1h1.sig	= 0umol/m2/s.
dark	Circadian_Dark10_Cycling_0560min_vs_NRC-1h1.sig	= 0umol/m2/s.
dark	Circadian_Dark10_Cycling_0750min_vs_NRC-1h1.sig	= 0umol/m2/s.
dark	Circadian_Dark10_Cycling_0915min_vs_NRC-1h1.sig	= 0umol/m2/s.
dark	Circadian_Dark10_Cycling_1100min_vs_NRC-1h1.sig	= 0umol/m2/s.
dark	Circadian_Dark10_Cycling_1270min_vs_NRC-1h1.sig	= 0umol/m2/s.
dark	Circadian_Dark10_Cycling_1450min_vs_NRC-1h1.sig	= 0umol/m2/s.
dark	Circadian_Dark10_Cycling_1635min_vs_NRC-1h1.sig	= 0umol/m2/s.
dark	Circadian_Dark10_Cycling_1810min_vs_NRC-1h1.sig	= 0umol/m2/s.
dark	Circadian_Dark10_Cycling_1980min_vs_NRC-1h1.sig	= 0umol/m2/s.
dark	Circadian_Dark10_Cycling_2200min_vs_NRC-1h1.sig	= 0umol/m2/s.

dark	Circadian_Dark10_Cycling_2345min_vs_NRC-1h1.sig	= 0umol/m2/s.
dark	Circadian_Dark10_Cycling_2535min_vs_NRC-1h1.sig	= 0umol/m2/s.
dark	Circadian_Dark10_Cycling_2711min_vs_NRC-1h1.sig	= 0umol/m2/s.
dark	Circadian_Dark10_Cycling_2895min_vs_NRC-1h1.sig	= 0umol/m2/s.
dark	Circadian_Dark10_Cycling_3070min_vs_NRC-1h1.sig	= 0umol/m2/s.
dark	Circadian_Dark10_Cycling_3252min_vs_NRC-1h1.sig	= 0umol/m2/s.
dark	Circadian_Dark10_Cycling_3430min_vs_NRC-1h1.sig	= 0umol/m2/s.
dark	Circadian_Dark10_Cycling_3630min_vs_NRC-1h1.sig	= 0umol/m2/s.
dark	Circadian_Dark10_Cycling_3790min_vs_NRC-1h1.sig	= 0umol/m2/s.
dark	Circadian_Dark10_Cycling_3980min_vs_NRC-1h1.sig	= 0umol/m2/s.
dark	Circadian_Dark10_Cycling_4150min_vs_NRC-1h1.sig	= 0umol/m2/s.
dark	Circadian_Dark10_Cycling_4330min_vs_NRC-1h1.sig	= 0umol/m2/s.
dark	zim__HO_D_vs_NRC-1	= 0umol/m2/s.
dark	zim__LO_D_vs_NRC-1	= 0umol/m2/s.
dark	VNG2334C__HO_D_vs_NRC-1	= 0umol/m2/s.
dark	VNG2334C__LO_D_vs_NRC-1	= 0umol/m2/s.
dark	VNG1296C__HO_D_vs_NRC-1	= 0umol/m2/s.
dark	VNG1296C__LO_D_vs_NRC-1	= 0umol/m2/s.
dark	VNG0750C__HO_D_vs_NRC-1	= 0umol/m2/s.
dark	VNG0750C__LO_D_vs_NRC-1	= 0umol/m2/s.
dark	VNG0019H__HO_D_vs_NRC-1c	= 0umol/m2/s.
dark	VNG0019H__LO_D_vs_NRC-1c	= 0umol/m2/s.
dark	uv__000jm2_CL_060m	= 0umol/m2/s.
dark	ura3__HO_D_vs_NRC-1	= 0umol/m2/s.
dark	ura3__LO_D_vs_NRC-1	= 0umol/m2/s.
dark	NRC-1__HO_D_vs_NRC-1	= 0umol/m2/s.
dark	NRC-1__LO_D_vs_NRC-1	= 0umol/m2/s.
dark	circadian__dark_cycling_125w/m2_42C_2160min_vs_NRC-1d.sig	= 0umol/m2/s.
dark	circadian__dark_cycling_125w/m2_42C_2340min_vs_NRC-1d.sig	= 0umol/m2/s.
dark	circadian__dark_cycling_125w/m2_42C_2515min_vs_NRC-1d.sig	= 0umol/m2/s.
dark	circadian__dark_cycling_125w/m2_42C_2705min_vs_NRC-1d.sig	= 0umol/m2/s.

dark	uv__200jm2_D_030m	= 0umol/m2/s.
dark	uv__200jm2_D_060m	= 0umol/m2/s.
early-exponential phase	light2__1440m_vs_light1_3960m	0.2 >= OD < 0.4.
early-exponential phase	light2__1620m_vs_light1_3960m	0.2 >= OD < 0.4.
early-exponential phase	light2__1800m_vs_light1_3960m	0.2 >= OD < 0.4.
early-exponential phase	light2__1980m_vs_light1_3960m	0.2 >= OD < 0.4.
early-exponential phase	light2__2160m_vs_light1_3960m	0.2 >= OD < 0.4.
early-exponential phase	light2__2340m_vs_light1_3960m	0.2 >= OD < 0.4.
early-exponential phase	light2__2520m_vs_light1_3960m	0.2 >= OD < 0.4.
early-exponential phase	light2__2700m_vs_light1_3960m	0.2 >= OD < 0.4.
early-exponential phase	light2__2880m_vs_light1_3960m	0.2 >= OD < 0.4.
early-exponential phase	light2__3060m_vs_light1_3960m	0.2 >= OD < 0.4.
early-exponential phase	light2__3240m_vs_light1_3960m	0.2 >= OD < 0.4.
early-exponential phase	circadian_drk8_cycling_0000min_vs_NRC-1e.sig	0.2 >= OD < 0.4.
early-exponential phase	circadian_dark3_cycling_1380min_vs_NRC-1d.sig	0.2 >= OD < 0.4.
early-exponential phase	circadian_dark3_cycling_1440min_vs_NRC-1d.sig	0.2 >= OD < 0.4.
early-exponential phase	circadian_dark3_cycling_1500min_vs_NRC-1d.sig	0.2 >= OD < 0.4.
early-exponential phase	circadian_dark3_ctrl_1380min_vs_NRC-1d.sig	0.2 >= OD < 0.4.
early-exponential phase	circadian_dark3_ctrl_1440min_vs_NRC-1d.sig	0.2 >= OD < 0.4.
early-exponential phase	circadian_dark3_ctrl_1500min_vs_NRC-1d.sig	0.2 >= OD < 0.4.
early-exponential phase	circadian_drk8_control_0000min_vs_NRC-1e.sig	0.2 >= OD < 0.4.
early-exponential phase	Circadian_Dark9_Cycling_0000min_vs_NRC-1g.sig	0.2 >= OD < 0.4.
early-exponential phase	Circadian_Dark9_Cycling_0180min_vs_NRC-1g.sig	0.2 >= OD < 0.4.
early-exponential phase	Circadian_Dark9_Cycling_0360min_vs_NRC-1g.sig	0.2 >= OD < 0.4.
early-exponential phase	Circadian_Dark9_Cycling_0535min_vs_NRC-1g.sig	0.2 >= OD < 0.4.
early-exponential phase	Circadian_Dark9_Cycling_0720min_vs_NRC-1g.sig	0.2 >= OD < 0.4.

early-exponential phase	Circadian_Dark9_Cycling_0900min_vs_NRC-1g.sig	0.2 >= OD < 0.4.
early-exponential phase	Circadian_Dark9_Cycling_1080min_vs_NRC-1g.sig	0.2 >= OD < 0.4.
early-exponential phase	Circadian_Dark9_Cycling_1440min_vs_NRC-1g.sig	0.2 >= OD < 0.4.
early-exponential phase	Circadian_Dark9_Cycling_1620min_vs_NRC-1g.sig	0.2 >= OD < 0.4.
early-exponential phase	Circadian_Dark9_Cycling_1800min_vs_NRC-1g.sig	0.2 >= OD < 0.4.
early-exponential phase	Circadian_Dark9_Cycling_1980min_vs_NRC-1g.sig	0.2 >= OD < 0.4.
early-exponential phase	Circadian_Dark9_Cycling_2160min_vs_NRC-1g.sig	0.2 >= OD < 0.4.
early-exponential phase	Circadian_Dark9_Cycling_2340min_vs_NRC-1g.sig	0.2 >= OD < 0.4.
early-exponential phase	Circadian_Dark9_Cycling_2520min_vs_NRC-1g.sig	0.2 >= OD < 0.4.
early-exponential phase	Circadian_Dark9_Cycling_2700min_vs_NRC-1g.sig	0.2 >= OD < 0.4.
early-exponential phase	Circadian_Dark9_Cycling_2880min_vs_NRC-1g.sig	0.2 >= OD < 0.4.
early-exponential phase	Circadian_Dark9_Cycling_3060min_vs_NRC-1g.sig	0.2 >= OD < 0.4.
early-exponential phase	Circadian_Dark9_Cycling_3240min_vs_NRC-1g.sig	0.2 >= OD < 0.4.
early-exponential phase	Circadian_Dark9_Cycling_3420min_vs_NRC-1g.sig	0.2 >= OD < 0.4.
early-exponential phase	Circadian_Dark9_Cycling_3600min_vs_NRC-1g.sig	0.2 >= OD < 0.4.
early-exponential phase	Circadian_Dark9_Cycling_3780min_vs_NRC-1g.sig	0.2 >= OD < 0.4.
early-exponential phase	Circadian_Dark9_Cycling_3960min_vs_NRC-1g.sig	0.2 >= OD < 0.4.
early-exponential phase	Circadian_Dark9_Cycling_4140min_vs_NRC-1g.sig	0.2 >= OD < 0.4.
early-exponential phase	Circadian_Dark9_Cycling_4320min_vs_NRC-1g.sig	0.2 >= OD < 0.4.
early-exponential phase	Circadian_Dark9_Cycling_4500min_vs_NRC-1g.sig	0.2 >= OD < 0.4.
early-exponential phase	Circadian_Dark9_Control_0000min_vs_NRC-1g.sig	0.2 >= OD < 0.4.
early-exponential phase	Circadian_Dark9_Control_0180min_vs_NRC-1g.sig	0.2 >= OD < 0.4.
early-exponential phase	Circadian_Dark9_Control_0360min_vs_NRC-1g.sig	0.2 >= OD < 0.4.
early-exponential phase	Circadian_Dark9_Control_0535min_vs_NRC-1g.sig	0.2 >= OD < 0.4.
early-exponential phase	Circadian_Dark9_Control_0720min_vs_NRC-1g.sig	0.2 >= OD < 0.4.

early-exponential phase	Circadian_Dark9_Control_1080min_vs_NRC-1g.sig	0.2 >= OD < 0.4.
early-exponential phase	Circadian_Dark9_Control_1265min_vs_NRC-1g.sig	0.2 >= OD < 0.4.
early-exponential phase	Circadian_Dark9_Control_1440min_vs_NRC-1g.sig	0.2 >= OD < 0.4.
early-exponential phase	Circadian_Dark9_Control_1620min_vs_NRC-1g.sig	0.2 >= OD < 0.4.
early-exponential phase	Circadian_Dark9_Control_1800min_vs_NRC-1g.sig	0.2 >= OD < 0.4.
early-exponential phase	Circadian_Dark9_Control_1980min_vs_NRC-1g.sig	0.2 >= OD < 0.4.
early-exponential phase	Circadian_Dark9_Control_2160min_vs_NRC-1g.sig	0.2 >= OD < 0.4.
early-exponential phase	Circadian_Dark9_Control_2340min_vs_NRC-1g.sig	0.2 >= OD < 0.4.
early-exponential phase	Circadian_Dark9_Control_2520min_vs_NRC-1g.sig	0.2 >= OD < 0.4.
early-exponential phase	Circadian_Dark9_Control_2700min_vs_NRC-1g.sig	0.2 >= OD < 0.4.
early-exponential phase	Circadian_Dark9_Control_2880min_vs_NRC-1g.sig	0.2 >= OD < 0.4.
early-exponential phase	Circadian_Dark9_Control_3060min_vs_NRC-1g.sig	0.2 >= OD < 0.4.
early-exponential phase	Circadian_Dark9_Control_3240min_vs_NRC-1g.sig	0.2 >= OD < 0.4.
early-exponential phase	Circadian_Dark9_Control_3420min_vs_NRC-1g.sig	0.2 >= OD < 0.4.
early-exponential phase	Circadian_Dark9_Control_3600min_vs_NRC-1g.sig	0.2 >= OD < 0.4.
early-exponential phase	Circadian_Dark9_Control_3780min_vs_NRC-1g.sig	0.2 >= OD < 0.4.
early-exponential phase	Circadian_Dark9_Control_3960min_vs_NRC-1g.sig	0.2 >= OD < 0.4.
early-exponential phase	Circadian_Dark9_Control_4140min_vs_NRC-1g.sig	0.2 >= OD < 0.4.
early-exponential phase	Circadian_Dark9_Control_4320min_vs_NRC-1g.sig	0.2 >= OD < 0.4.
early-exponential phase	Circadian_Dark9_Control_4500min_vs_NRC-1g.sig	0.2 >= OD < 0.4.
early-exponential phase	Cu_ura3_KO_set2_160min_vs_NRC-1h1.sig	0.2 >= OD < 0.4.
early-exponential phase	VNG1296C__HO_D_vs_NRC-1	0.2 >= OD < 0.4.
early-exponential phase	VNG1296C__HO_L_vs_NRC-1	0.2 >= OD < 0.4.
early-exponential phase	VNG1296C__LO_D_vs_NRC-1	0.2 >= OD < 0.4.
early-exponential phase	VNG1296C__LO_L_vs_NRC-1	0.2 >= OD < 0.4.

early-exponential phase	EMS_Treated__000uM-000	0.2 >= OD < 0.4.
early-exponential phase	EMS_Treated__000uM-010	0.2 >= OD < 0.4.
early-exponential phase	EMS_Treated__000uM-020	0.2 >= OD < 0.4.
early-exponential phase	EMS_Treated__000uM-030	0.2 >= OD < 0.4.
early-exponential phase	EMS_Treated__000uM-040	0.2 >= OD < 0.4.
early-exponential phase	EMS_Treated__000uM-050	0.2 >= OD < 0.4.
early-exponential phase	EMS_Treated__000uM-060	0.2 >= OD < 0.4.
early-exponential phase	EMS_Treated__000uM-120	0.2 >= OD < 0.4.
early-exponential phase	circadian__dark_cycling_125w/m2_42C_1440min_vs_NRC-1d.sig	0.2 >= OD < 0.4.
early-exponential phase	NRC1_H2O_0540_0.220_rep2_vs_NRC-1g.sig	0.2 >= OD < 0.4.
early-exponential phase	NRC1_H2O_0540_0.225_rep1_vs_NRC-1g.sig	0.2 >= OD < 0.4.
early-exponential phase	NRC1_Uracil_0540_0.205_rep2_vs_NRC-1g.sig	0.2 >= OD < 0.4.
early-exponential phase	NRC1_Uracil_0540_0.200_rep1_vs_NRC-1g.sig	0.2 >= OD < 0.4.
early-exponential phase	Dura3_Uracil_0690_0.200_rep2_vs_NRC-1g.sig	0.2 >= OD < 0.4.
early-exponential phase	NRC1_03720_0.234_rep2_vs_NRC-1g.sig	0.2 >= OD < 0.4.
early-exponential phase	NRC1_03720_0.259_rep1_vs_NRC-1g.sig	0.2 >= OD < 0.4.
early-exponential phase	NRC1_03960_0.364_rep1_vs_NRC-1g.sig	0.2 >= OD < 0.4.
early-exponential phase	MDM200gSalt_0.388_vs_NRC-1e.sig	0.2 >= OD < 0.4.
early-exponential phase	KO_ura3.2_0.3207_vs_NRC-1_h1.sig	0.2 >= OD < 0.4.
early-exponential phase	ura3_growth_t1_exp2_0.3OD_vs_NRC1f.sig	0.2 >= OD < 0.4.
early-exponential phase	ura3_growth_t1_exp3_0.3OD_vs_NRC1f.sig	0.2 >= OD < 0.4.
early-exponential phase	ura3_+glu_a_OD0.6repl_vs_NRC1e.sig	0.2 >= OD < 0.4.
early-exponential phase	ura3_+glu_b_OD0.6repl_vs_NRC1g.sig	0.2 >= OD < 0.4.
early-exponential phase	ura3_-glu_a_OD0.2_vs_NRC1e.sig	0.2 >= OD < 0.4.
early-exponential phase	ura3_-glu_b_OD0.2_vs_NRC1g.sig	0.2 >= OD < 0.4.

early-exponential phase	EMS_Treated__100000uM-000	0.2 >= OD < 0.4.
early-exponential phase	EMS_Treated__100000uM-010	0.2 >= OD < 0.4.
early-exponential phase	EMS_Treated__100000uM-020	0.2 >= OD < 0.4.
early-exponential phase	EMS_Treated__100000uM-040	0.2 >= OD < 0.4.
early-exponential phase	EMS_Treated__100000uM-050	0.2 >= OD < 0.4.
early-exponential phase	EMS_Treated__100000uM-060	0.2 >= OD < 0.4.
early-exponential phase	EMS_Treated__100000uM-120	0.2 >= OD < 0.4.
early-exponential phase	MDM250gSalt_0.204_vs_NRC-1e.sig	0.2 >= OD < 0.4.
early-exponential phase	MDM250gSalt_0.396_vs_NRC-1e.sig	0.2 >= OD < 0.4.
early-exponential phase	H2O2_Recov._set_2_25mM_000min_vs_NRC-1f.sig	0.2 >= OD < 0.4.
early-exponential phase	H2O2_Recov._set_2_25mM_010min_vs_NRC-1f.sig	0.2 >= OD < 0.4.
early-exponential phase	H2O2_Recov._set_2_25mM_020min_vs_NRC-1f.sig	0.2 >= OD < 0.4.
early-exponential phase	H2O2_Recov._set_2_25mM_030min_vs_NRC-1f.sig	0.2 >= OD < 0.4.
early-exponential phase	H2O2_Recov._set_2_25mM_040min_vs_NRC-1f.sig	0.2 >= OD < 0.4.
early-exponential phase	H2O2_Recov._set_2_25mM_050min_vs_NRC-1f.sig	0.2 >= OD < 0.4.
early-exponential phase	H2O2_Recov._set_2_25mM_060min_vs_NRC-1f.sig	0.2 >= OD < 0.4.
early-exponential phase	H2O2_Recov._set_2_25mM_120min_vs_NRC-1f.sig	0.2 >= OD < 0.4.
early-exponential phase	H2O2_Recov._set_2_25mM_240min_vs_NRC-1f.sig	0.2 >= OD < 0.4.
early-exponential phase	KO_ura3.3_0.274_vs_NRC-1_h1.sig	0.2 >= OD < 0.4.
early-exponential phase	KO_ura3.4_0.2812_vs_NRC-1_h1.sig	0.2 >= OD < 0.4.
early-exponential phase	o2_set3_-0005_min_LO2_vs_NRC1f.sig	0.2 >= OD < 0.4.
early-exponential phase	o2_set3_0000_min_L2HO2_vs_NRC1f.sig	0.2 >= OD < 0.4.
early-exponential phase	o2_set3_0005_min_HO2_vs_NRC1f.sig	0.2 >= OD < 0.4.
early-exponential phase	o2_set3_0360_min_HO2_vs_NRC1f.sig	0.2 >= OD < 0.4.
early-exponential phase	20061006_Cmyc_rep2_0.399_vs_NRC-1e.sig	0.2 >= OD < 0.4.

early-exponential phase	20060818_KO_ura3_rep2_0.376_vs_NRC-1e.sig	0.2 >= OD < 0.4.
early-exponential phase	20060717_Cmyc_rep2_0.223_vs_NRC-1e.sig	0.2 >= OD < 0.4.
early-exponential phase	20060717_Cmyc_rep1_0.221_vs_NRC-1e.sig	0.2 >= OD < 0.4.
early-exponential phase	20050620_Cmyc_rep1_0.207_vs_NRC-1d.sig	0.2 >= OD < 0.4.
early-exponential phase	H2O2_Recov._set_1_0mM_000min_vs_NRC-1d.sig	0.2 >= OD < 0.4.
early-exponential phase	H2O2_Recov._set_1_0mM_010min_vs_NRC-1d.sig	0.2 >= OD < 0.4.
early-exponential phase	H2O2_Recov._set_1_0mM_020min_vs_NRC-1d.sig	0.2 >= OD < 0.4.
early-exponential phase	H2O2_Recov._set_1_0mM_030min_vs_NRC-1d.sig	0.2 >= OD < 0.4.
early-exponential phase	H2O2_Recov._set_1_0mM_040min_vs_NRC-1d.sig	0.2 >= OD < 0.4.
early-exponential phase	H2O2_Recov._set_1_0mM_050min_vs_NRC-1d.sig	0.2 >= OD < 0.4.
early-exponential phase	H2O2_Recov._set_1_0mM_060min_vs_NRC-1d.sig	0.2 >= OD < 0.4.
early-exponential phase	H2O2_Recov._set_1_0mM_120min_vs_NRC-1d.sig	0.2 >= OD < 0.4.
early-exponential phase	NRC-1.2_0.3063_vs_NRC-1_h1.sig	0.2 >= OD < 0.4.
early-exponential phase	NRC-1.2_0.3895_vs_NRC-1_h1.sig	0.2 >= OD < 0.4.
early-exponential phase	KO_ura3.1_0.3501_vs_NRC-1_h1.sig	0.2 >= OD < 0.4.
early-exponential phase	NRC-1_0.3279_vs_NRC-1_h1.sig	0.2 >= OD < 0.4.
early-exponential phase	NRC-1_0.3882_vs_NRC-1_h1.sig	0.2 >= OD < 0.4.
early-exponential phase	H2O2_Recov._set_1_50mM_000min_vs_NRC-1d.sig	0.2 >= OD < 0.4.
early-exponential phase	H2O2_Recov._set_1_50mM_010min_vs_NRC-1d.sig	0.2 >= OD < 0.4.
early-exponential phase	H2O2_Recov._set_1_50mM_020min_vs_NRC-1d.sig	0.2 >= OD < 0.4.
early-exponential phase	H2O2_Recov._set_1_50mM_030min_vs_NRC-1d.sig	0.2 >= OD < 0.4.
early-exponential phase	H2O2_Recov._set_1_50mM_040min_vs_NRC-1d.sig	0.2 >= OD < 0.4.
early-exponential phase	H2O2_Recov._set_1_50mM_050min_vs_NRC-1d.sig	0.2 >= OD < 0.4.
early-exponential phase	H2O2_Recov._set_1_50mM_060min_vs_NRC-1d.sig	0.2 >= OD < 0.4.
early-exponential phase	H2O2_Recov._set_1_50mM_120min_vs_NRC-1d.sig	0.2 >= OD < 0.4.

edta	ura3_0min_-EDTA_CM_vs_NRC1-h1.sig	1e-3 mol/L.
edta	ura3_20min_-EDTA_CM_vs_NRC1-h1.sig	1e-3 mol/L.
edta	ura3_40min_-EDTA_CM_vs_NRC1-h1.sig	1e-3 mol/L.
edta	ura3_60min_-EDTA_CM_vs_NRC1-h1.sig	1e-3 mol/L.
edta	ura3_0min_1mM_EDTA_vs_NRC1-h1.sig	1e-3 mol/L.
edta	ura3_20min_1mM_EDTA_vs_NRC1-h1.sig	1e-3 mol/L.
edta	ura3_40min_1mM_EDTA_vs_NRC1-h1.sig	1e-3 mol/L.
edta	ura3_60min_1mM_EDTA_vs_NRC1-h1.sig	1e-3 mol/L.
ems	EMS_Treated__100000uM-000	0.1 mol/L.
ems	EMS_Treated__100000uM-010	0.1 mol/L.
ems	EMS_Treated__100000uM-020	0.1 mol/L.
ems	EMS_Treated__100000uM-030	0.1 mol/L.
ems	EMS_Treated__100000uM-040	0.1 mol/L.
ems	EMS_Treated__100000uM-050	0.1 mol/L.
ems	EMS_Treated__100000uM-060	0.1 mol/L.
ems	EMS_Treated__100000uM-120	0.1 mol/L.
expects dark	circadian_Dphr1_drk_cycling__2175min_vs_NRC-1d.sig	= 50umol/m2/s.
expects dark	circadian_Dphr1_drk_cycling__2340min_vs_NRC-1d.sig	= 50umol/m2/s.
expects dark	circadian_Dphr1_drk_cycling__2595min_vs_NRC-1d.sig	= 50umol/m2/s.
expects dark	circadian_Dphr1_drk_cycling__2705min_vs_NRC-1d.sig	= 50umol/m2/s.
expects dark	circadian_drk8_cycling_0720min_vs_NRC-1e.sig	= 50umol/m2/s.
expects dark	circadian_drk8_cycling_0900min_vs_NRC-1e.sig	= 50umol/m2/s.
expects dark	circadian_drk8_cycling_1080min_vs_NRC-1e.sig	= 50umol/m2/s.
expects dark	circadian_drk8_cycling_1260min_vs_NRC-1e.sig	= 50umol/m2/s.
expects dark	circadian_drk8_cycling_2160min_vs_NRC-1e.sig	= 50umol/m2/s.
expects dark	circadian_drk8_cycling_2340min_vs_NRC-1e.sig	= 50umol/m2/s.
expects dark	circadian_drk8_cycling_2520min_vs_NRC-1e.sig	= 50umol/m2/s.
expects dark	circadian_drk8_cycling_2700min_vs_NRC-1e.sig	= 50umol/m2/s.
expects dark	circadian_drk7_cycling_0720min_vs_NRC-1d.sig	= 50umol/m2/s.
expects dark	circadian_drk7_cycling_0900min_vs_NRC-1d.sig	= 50umol/m2/s.
expects dark	circadian_drk7_cycling_1080min_vs_NRC-1d.sig	= 50umol/m2/s.

expects dark	circadian_drk7_cycling_1260min_vs_NRC-1d.sig	= 50umol/m2/s.
expects dark	circadian_drk7_cycling_2160min_vs_NRC-1d.sig	= 50umol/m2/s.
expects dark	circadian_drk7_cycling_2340min_vs_NRC-1d.sig	= 50umol/m2/s.
expects dark	circadian_drk7_cycling_2520min_vs_NRC-1d.sig	= 50umol/m2/s.
expects dark	circadian_drk7_cycling_2700min_vs_NRC-1d.sig	= 50umol/m2/s.
expects dark	circadian_drk6_cycling_0720min_vs_NRC-1e.sig	= 50umol/m2/s.
expects dark	circadian_drk6_cycling_0912min_vs_NRC-1e.sig	= 50umol/m2/s.
expects dark	circadian_drk6_cycling_1080min_vs_NRC-1e.sig	= 50umol/m2/s.
expects dark	circadian_drk6_cycling_1260min_vs_NRC-1e.sig	= 50umol/m2/s.
expects dark	circadian__dark5_cycling_30C_2160min_vs_NRC-1d.sig	= 50umol/m2/s.
expects dark	circadian__dark5_cycling_30C_2355min_vs_NRC-1d.sig	= 50umol/m2/s.
expects dark	circadian__dark5_cycling_30C_2590min_vs_NRC-1d.sig	= 50umol/m2/s.
expects dark	circadian__dark5_cycling_30C_2700min_vs_NRC-1d.sig	= 50umol/m2/s.
expects dark	circadian_20051021_cycling_dark_42oC_2160min_vs_NRC-1d.sig	= 50umol/m2/s.
expects dark	circadian_20051021_cycling_dark_42oC_2340min_vs_NRC-1d.sig	= 50umol/m2/s.
expects dark	circadian_20051021_cycling_dark_42oC_2515min_vs_NRC-1d.sig	= 50umol/m2/s.
expects dark	circadian_20051021_cycling_dark_42oC_2705min_vs_NRC-1d.sig	= 50umol/m2/s.
expects dark	circadian_dark3_cycling_1380min_vs_NRC-1d.sig	= 50umol/m2/s.
expects dark	circadian_dark3_cycling_2160min_vs_NRC-1d.sig	= 50umol/m2/s.
expects dark	circadian_dark3_cycling_2220min_vs_NRC-1d.sig	= 50umol/m2/s.
expects dark	circadian_dark3_cycling_2340min_vs_NRC-1d.sig	= 50umol/m2/s.
expects dark	circadian_dark3_cycling_2520min_vs_NRC-1d.sig	= 50umol/m2/s.
expects dark	circadian_dark3_cycling_2700min_vs_NRC-1d.sig	= 50umol/m2/s.
expects dark	circadian_dark3_ctrl_1380min_vs_NRC-1d.sig	= 50umol/m2/s.
expects dark	circadian_dark3_ctrl_1440min_vs_NRC-1d.sig	= 50umol/m2/s.

expects dark	circadian_dark3_ctrl_1500min_vs_NRC-1d.sig	= 50umol/m2/s.
expects dark	circadian_dark3_ctrl_1620min_vs_NRC-1d.sig	= 50umol/m2/s.
expects dark	circadian_dark3_ctrl_1800min_vs_NRC-1d.sig	= 50umol/m2/s.
expects dark	circadian_dark3_ctrl_1980min_vs_NRC-1d.sig	= 50umol/m2/s.
expects dark	circadian_dark3_ctrl_2160min_vs_NRC-1d.sig	= 50umol/m2/s.
expects dark	circadian_dark3_ctrl_2220min_vs_NRC-1d.sig	= 50umol/m2/s.
expects dark	circadian_dark3_ctrl_2340min_vs_NRC-1d.sig	= 50umol/m2/s.
expects dark	circadian_dark3_ctrl_2520min_vs_NRC-1d.sig	= 50umol/m2/s.
expects dark	circadian_dark3_ctrl_2700min_vs_NRC-1d.sig	= 50umol/m2/s.
expects dark	circadian_dark3_ctrl_2880min_vs_NRC-1d.sig	= 50umol/m2/s.
expects dark	circadian_drk8_control_0000min_vs_NRC-1e.sig	= 50umol/m2/s.
expects dark	circadian_drk8_control_0180min_vs_NRC-1e.sig	= 50umol/m2/s.
expects dark	circadian_drk8_control_0360min_vs_NRC-1e.sig	= 50umol/m2/s.
expects dark	circadian_drk8_control_0540min_vs_NRC-1e.sig	= 50umol/m2/s.
expects dark	circadian_drk8_control_0720min_vs_NRC-1e.sig	= 50umol/m2/s.
expects dark	circadian_drk8_control_0900min_vs_NRC-1e.sig	= 50umol/m2/s.
expects dark	circadian_drk8_control_1080min_vs_NRC-1e.sig	= 50umol/m2/s.
expects dark	circadian_drk8_control_1260min_vs_NRC-1e.sig	= 50umol/m2/s.
expects dark	circadian_drk8_control_1440min_vs_NRC-1e.sig	= 50umol/m2/s.
expects dark	circadian_drk8_control_1620min_vs_NRC-1e.sig	= 50umol/m2/s.
expects dark	circadian_drk8_control_1800min_vs_NRC-1e.sig	= 50umol/m2/s.
expects dark	circadian_drk8_control_1980min_vs_NRC-1e.sig	= 50umol/m2/s.
expects dark	circadian_drk8_control_2160min_vs_NRC-1e.sig	= 50umol/m2/s.
expects dark	circadian_drk8_control_2340min_vs_NRC-1e.sig	= 50umol/m2/s.
expects dark	circadian_drk8_control_2520min_vs_NRC-1e.sig	= 50umol/m2/s.

expects dark	circadian_drk8_control_2700min_vs_NRC-1e.sig	= 50umol/m2/s.
expects dark	circadian_drk8_control_2880min_vs_NRC-1e.sig	= 50umol/m2/s.
expects dark	circadian_drk8_control_3060min_vs_NRC-1e.sig	= 50umol/m2/s.
expects dark	circadian_drk8_control_3240min_vs_NRC-1e.sig	= 50umol/m2/s.
expects dark	Circadian_Dark9_Cycling_0720min_vs_NRC-1g.sig	= 50umol/m2/s.
expects dark	Circadian_Dark9_Cycling_0900min_vs_NRC-1g.sig	= 50umol/m2/s.
expects dark	Circadian_Dark9_Cycling_1080min_vs_NRC-1g.sig	= 50umol/m2/s.
expects dark	Circadian_Dark9_Cycling_1265min_vs_NRC-1g.sig	= 50umol/m2/s.
expects dark	Circadian_Dark9_Cycling_2160min_vs_NRC-1g.sig	= 50umol/m2/s.
expects dark	Circadian_Dark9_Cycling_2340min_vs_NRC-1g.sig	= 50umol/m2/s.
expects dark	Circadian_Dark9_Cycling_2520min_vs_NRC-1g.sig	= 50umol/m2/s.
expects dark	Circadian_Dark9_Cycling_2700min_vs_NRC-1g.sig	= 50umol/m2/s.
expects dark	Circadian_Dark9_Cycling_3600min_vs_NRC-1g.sig	= 50umol/m2/s.
expects dark	Circadian_Dark9_Cycling_3780min_vs_NRC-1g.sig	= 50umol/m2/s.
expects dark	Circadian_Dark9_Cycling_3960min_vs_NRC-1g.sig	= 50umol/m2/s.
expects dark	Circadian_Dark9_Cycling_4140min_vs_NRC-1g.sig	= 50umol/m2/s.
expects dark	Circadian_Dark9_Control_0000min_vs_NRC-1g.sig	= 50umol/m2/s.
expects dark	Circadian_Dark9_Control_0180min_vs_NRC-1g.sig	= 50umol/m2/s.
expects dark	Circadian_Dark9_Control_0360min_vs_NRC-1g.sig	= 50umol/m2/s.
expects dark	Circadian_Dark9_Control_0535min_vs_NRC-1g.sig	= 50umol/m2/s.
expects dark	Circadian_Dark9_Control_0720min_vs_NRC-1g.sig	= 50umol/m2/s.
expects dark	Circadian_Dark9_Control_1080min_vs_NRC-1g.sig	= 50umol/m2/s.
expects dark	Circadian_Dark9_Control_1265min_vs_NRC-1g.sig	= 50umol/m2/s.
expects dark	Circadian_Dark9_Control_1440min_vs_NRC-1g.sig	= 50umol/m2/s.
expects dark	Circadian_Dark9_Control_1620min_vs_NRC-1g.sig	= 50umol/m2/s.

expects dark	Circadian_Dark9_Control_1800min_vs_NRC-1g.sig	= 50umol/m2/s.
expects dark	Circadian_Dark9_Control_1980min_vs_NRC-1g.sig	= 50umol/m2/s.
expects dark	Circadian_Dark9_Control_2160min_vs_NRC-1g.sig	= 50umol/m2/s.
expects dark	Circadian_Dark9_Control_2340min_vs_NRC-1g.sig	= 50umol/m2/s.
expects dark	Circadian_Dark9_Control_2520min_vs_NRC-1g.sig	= 50umol/m2/s.
expects dark	Circadian_Dark9_Control_2700min_vs_NRC-1g.sig	= 50umol/m2/s.
expects dark	Circadian_Dark9_Control_2880min_vs_NRC-1g.sig	= 50umol/m2/s.
expects dark	Circadian_Dark9_Control_3060min_vs_NRC-1g.sig	= 50umol/m2/s.
expects dark	Circadian_Dark9_Control_3240min_vs_NRC-1g.sig	= 50umol/m2/s.
expects dark	Circadian_Dark9_Control_3420min_vs_NRC-1g.sig	= 50umol/m2/s.
expects dark	Circadian_Dark9_Control_3600min_vs_NRC-1g.sig	= 50umol/m2/s.
expects dark	Circadian_Dark9_Control_3780min_vs_NRC-1g.sig	= 50umol/m2/s.
expects dark	Circadian_Dark9_Control_3960min_vs_NRC-1g.sig	= 50umol/m2/s.
expects dark	Circadian_Dark9_Control_4140min_vs_NRC-1g.sig	= 50umol/m2/s.
expects dark	Circadian_Dark9_Control_4320min_vs_NRC-1g.sig	= 50umol/m2/s.
expects dark	Circadian_Dark9_Control_4500min_vs_NRC-1g.sig	= 50umol/m2/s.
expects dark	Circadian_Dark10_Cycling_-2873min_vs_NRC-1h1.sig	= 50umol/m2/s.
expects dark	Circadian_Dark10_Cycling_-2670min_vs_NRC-1h1.sig	= 50umol/m2/s.
expects dark	Circadian_Dark10_Cycling_-2490min_vs_NRC-1h1.sig	= 50umol/m2/s.
expects dark	Circadian_Dark10_Cycling_-2315min_vs_NRC-1h1.sig	= 50umol/m2/s.
expects dark	Circadian_Dark10_Cycling_-1410min_vs_NRC-1h1.sig	= 50umol/m2/s.
expects dark	Circadian_Dark10_Cycling_-1245min_vs_NRC-1h1.sig	= 50umol/m2/s.
expects dark	Circadian_Dark10_Cycling_-1060min_vs_NRC-1h1.sig	= 50umol/m2/s.
expects dark	Circadian_Dark10_Cycling_-0880min_vs_NRC-1h1.sig	= 50umol/m2/s.
expects dark	Circadian_Dark10_Cycling_0000min_vs_NRC-1h1.sig	= 50umol/m2/s.

expects dark	Circadian_Dark10_Cycling_0195min_vs_NRC-1h1.sig	= 50umol/m2/s.
expects dark	Circadian_Dark10_Cycling_0370min_vs_NRC-1h1.sig	= 50umol/m2/s.
expects dark	Circadian_Dark10_Cycling_0560min_vs_NRC-1h1.sig	= 50umol/m2/s.
expects dark	Circadian_Dark10_Cycling_1450min_vs_NRC-1h1.sig	= 50umol/m2/s.
expects dark	Circadian_Dark10_Cycling_1635min_vs_NRC-1h1.sig	= 50umol/m2/s.
expects dark	Circadian_Dark10_Cycling_1810min_vs_NRC-1h1.sig	= 50umol/m2/s.
expects dark	Circadian_Dark10_Cycling_1980min_vs_NRC-1h1.sig	= 50umol/m2/s.
expects dark	Circadian_Dark10_Cycling_2895min_vs_NRC-1h1.sig	= 50umol/m2/s.
expects dark	Circadian_Dark10_Cycling_3070min_vs_NRC-1h1.sig	= 50umol/m2/s.
expects dark	Circadian_Dark10_Cycling_3252min_vs_NRC-1h1.sig	= 50umol/m2/s.
expects dark	Circadian_Dark10_Cycling_3430min_vs_NRC-1h1.sig	= 50umol/m2/s.
expects dark	Circadian_Dark10_Cycling_4330min_vs_NRC-1h1.sig	= 50umol/m2/s.
expects high light	circadian_Dphr1_drk_cycling__1440min_vs_NRC-1d.sig	> 100 mol/m2/s.
expects high light	circadian_Dphr1_drk_cycling__1665min_vs_NRC-1d.sig	> 100 mol/m2/s.
expects high light	circadian_Dphr1_drk_cycling__1800min_vs_NRC-1d.sig	> 100 mol/m2/s.
expects high light	circadian_Dphr1_drk_cycling__1980min_vs_NRC-1d.sig	> 100 mol/m2/s.
expects high light	circadian_Dphr1_drk_cycling__2880min_vs_NRC-1d.sig	> 100 mol/m2/s.
expects high light	circadian_drk8_cycling_0000min_vs_NRC-1e.sig	> 100 mol/m2/s.
expects high light	circadian_drk8_cycling_0180min_vs_NRC-1e.sig	> 100 mol/m2/s.
expects high light	circadian_drk8_cycling_0360min_vs_NRC-1e.sig	> 100 mol/m2/s.
expects high light	circadian_drk8_cycling_0540min_vs_NRC-1e.sig	> 100 mol/m2/s.
expects high light	circadian_drk8_cycling_1440min_vs_NRC-1e.sig	> 100 mol/m2/s.
expects high light	circadian_drk8_cycling_1620min_vs_NRC-1e.sig	> 100 mol/m2/s.
expects high light	circadian_drk8_cycling_1800min_vs_NRC-1e.sig	> 100 mol/m2/s.
expects high light	circadian_drk8_cycling_1980min_vs_NRC-1e.sig	> 100 mol/m2/s.

expects high light	circadian_drk8_cycling_2880min_vs_NRC-1e.sig	> 100 mol/m2/s.
expects high light	circadian_drk8_cycling_3060min_vs_NRC-1e.sig	> 100 mol/m2/s.
expects high light	circadian_drk8_cycling_3240min_vs_NRC-1e.sig	> 100 mol/m2/s.
expects high light	circadian_drk6_cycling_0000min_vs_NRC-1e.sig	> 100 mol/m2/s.
expects high light	circadian_drk6_cycling_0180min_vs_NRC-1e.sig	> 100 mol/m2/s.
expects high light	circadian_drk6_cycling_0360min_vs_NRC-1e.sig	> 100 mol/m2/s.
expects high light	circadian_drk6_cycling_0540min_vs_NRC-1e.sig	> 100 mol/m2/s.
expects high light	circadian_drk6_cycling_1440min_vs_NRC-1e.sig	> 100 mol/m2/s.
expects high light	circadian__dark5_cycling_30C_1440min_vs_NRC-1d.sig	> 100 mol/m2/s.
expects high light	circadian__dark5_cycling_30C_1630min_vs_NRC-1d.sig	> 100 mol/m2/s.
expects high light	circadian__dark5_cycling_30C_1815min_vs_NRC-1d.sig	> 100 mol/m2/s.
expects high light	circadian__dark5_cycling_30C_1980min_vs_NRC-1d.sig	> 100 mol/m2/s.
expects high light	circadian__dark5_cycling_30C_2880min_vs_NRC-1d.sig	> 100 mol/m2/s.
expects high light	circadian_20051021_cycling_dark_42oC_1440min_vs_NRC-1d.sig	> 100 mol/m2/s.
expects high light	circadian_20051021_cycling_dark_42oC_1615min_vs_NRC-1d.sig	> 100 mol/m2/s.
expects high light	circadian_20051021_cycling_dark_42oC_1800min_vs_NRC-1d.sig	> 100 mol/m2/s.
expects high light	circadian_20051021_cycling_dark_42oC_1985min_vs_NRC-1d.sig	> 100 mol/m2/s.
expects high light	circadian_20051021_cycling_dark_42oC_2880min_vs_NRC-1d.sig	> 100 mol/m2/s.
expects high light	circadian_dark3_cycling_1440min_vs_NRC-1d.sig	> 100 mol/m2/s.
expects high light	circadian_dark3_cycling_1500min_vs_NRC-1d.sig	> 100 mol/m2/s.
expects high light	circadian_dark3_cycling_1620min_vs_NRC-1d.sig	> 100 mol/m2/s.
expects high light	circadian_dark3_cycling_1800min_vs_NRC-1d.sig	> 100 mol/m2/s.
expects high light	circadian_dark3_cycling_1980min_vs_NRC-1d.sig	> 100 mol/m2/s.
expects high light	circadian_dark3_cycling_2880min_vs_NRC-1d.sig	> 100 mol/m2/s.
expects high light	Circadian_Dark9_Cycling_0000min_vs_NRC-1g.sig	> 100 mol/m2/s.

expects high light	Circadian_Dark9_Cycling_0180min_vs_NRC-1g.sig	> 100 mol/m2/s.
expects high light	Circadian_Dark9_Cycling_0360min_vs_NRC-1g.sig	> 100 mol/m2/s.
expects high light	Circadian_Dark9_Cycling_0535min_vs_NRC-1g.sig	> 100 mol/m2/s.
expects high light	Circadian_Dark9_Cycling_1440min_vs_NRC-1g.sig	> 100 mol/m2/s.
expects high light	Circadian_Dark9_Cycling_1620min_vs_NRC-1g.sig	> 100 mol/m2/s.
expects high light	Circadian_Dark9_Cycling_1800min_vs_NRC-1g.sig	> 100 mol/m2/s.
expects high light	Circadian_Dark9_Cycling_1980min_vs_NRC-1g.sig	> 100 mol/m2/s.
expects high light	Circadian_Dark9_Cycling_2880min_vs_NRC-1g.sig	> 100 mol/m2/s.
expects high light	Circadian_Dark9_Cycling_3060min_vs_NRC-1g.sig	> 100 mol/m2/s.
expects high light	Circadian_Dark9_Cycling_3240min_vs_NRC-1g.sig	> 100 mol/m2/s.
expects high light	Circadian_Dark9_Cycling_3420min_vs_NRC-1g.sig	> 100 mol/m2/s.
expects high light	Circadian_Dark9_Cycling_4320min_vs_NRC-1g.sig	> 100 mol/m2/s.
expects high light	Circadian_Dark9_Cycling_4500min_vs_NRC-1g.sig	> 100 mol/m2/s.
expects high light	Circadian_Dark10_Cycling_-2120min_vs_NRC-1h1.sig	> 100 mol/m2/s.
expects high light	Circadian_Dark10_Cycling_-1960min_vs_NRC-1h1.sig	> 100 mol/m2/s.
expects high light	Circadian_Dark10_Cycling_-1785min_vs_NRC-1h1.sig	> 100 mol/m2/s.
expects high light	Circadian_Dark10_Cycling_-1595min_vs_NRC-1h1.sig	> 100 mol/m2/s.
expects high light	Circadian_Dark10_Cycling_-0690min_vs_NRC-1h1.sig	> 100 mol/m2/s.
expects high light	Circadian_Dark10_Cycling_-0525min_vs_NRC-1h1.sig	> 100 mol/m2/s.
expects high light	Circadian_Dark10_Cycling_-0360min_vs_NRC-1h1.sig	> 100 mol/m2/s.
expects high light	Circadian_Dark10_Cycling_-0165min_vs_NRC-1h1.sig	> 100 mol/m2/s.
expects high light	Circadian_Dark10_Cycling_0750min_vs_NRC-1h1.sig	> 100 mol/m2/s.
expects high light	Circadian_Dark10_Cycling_0915min_vs_NRC-1h1.sig	> 100 mol/m2/s.
expects high light	Circadian_Dark10_Cycling_1100min_vs_NRC-1h1.sig	> 100 mol/m2/s.
expects high light	Circadian_Dark10_Cycling_1270min_vs_NRC-1h1.sig	> 100 mol/m2/s.

expects high light	Circadian_Dark10_Cycling_2200min_vs_NRC-1h1.sig	> 100 mol/m2/s.
expects high light	Circadian_Dark10_Cycling_2345min_vs_NRC-1h1.sig	> 100 mol/m2/s.
expects high light	Circadian_Dark10_Cycling_2535min_vs_NRC-1h1.sig	> 100 mol/m2/s.
expects high light	Circadian_Dark10_Cycling_2711min_vs_NRC-1h1.sig	> 100 mol/m2/s.
expects high light	Circadian_Dark10_Cycling_3630min_vs_NRC-1h1.sig	> 100 mol/m2/s.
expects high light	Circadian_Dark10_Cycling_3790min_vs_NRC-1h1.sig	> 100 mol/m2/s.
expects high light	Circadian_Dark10_Cycling_3980min_vs_NRC-1h1.sig	> 100 mol/m2/s.
expects high light	Circadian_Dark10_Cycling_4150min_vs_NRC-1h1.sig	> 100 mol/m2/s.
expects low light	circadian_drk7_cycling_0000min_vs_NRC-1d.sig	0 < mol/m2/s < 100.
expects low light	circadian_drk7_cycling_0180min_vs_NRC-1d.sig	0 < mol/m2/s < 100.
expects low light	circadian_drk7_cycling_0360min_vs_NRC-1d.sig	0 < mol/m2/s < 100.
expects low light	circadian_drk7_cycling_0540min_vs_NRC-1d.sig	0 < mol/m2/s < 100.
expects low light	circadian_drk7_cycling_1440min_vs_NRC-1d.sig	0 < mol/m2/s < 100.
expects low light	circadian_drk7_cycling_1620min_vs_NRC-1d.sig	0 < mol/m2/s < 100.
expects low light	circadian_drk7_cycling_1800min_vs_NRC-1d.sig	0 < mol/m2/s < 100.
expects low light	circadian_drk7_cycling_1980min_vs_NRC-1d.sig	0 < mol/m2/s < 100.
expects low light	circadian_drk7_cycling_2880min_vs_NRC-1d.sig	0 < mol/m2/s < 100.
expects low light	circadian_drk7_cycling_3060min_vs_NRC-1d.sig	0 < mol/m2/s < 100.
expects low light	circadian_drk7_cycling_3240min_vs_NRC-1d.sig	0 < mol/m2/s < 100.
exponential phase	light2__1440m_vs_light1_3960m	0.2 > OD < 0.8.
exponential phase	light2__1620m_vs_light1_3960m	0.2 > OD < 0.8.
exponential phase	light2__1800m_vs_light1_3960m	0.2 > OD < 0.8.
exponential phase	light2__1980m_vs_light1_3960m	0.2 > OD < 0.8.
exponential phase	light2__2160m_vs_light1_3960m	0.2 > OD < 0.8.
exponential phase	light2__2340m_vs_light1_3960m	0.2 > OD < 0.8.
exponential phase	light2__2520m_vs_light1_3960m	0.2 > OD < 0.8.
exponential phase	light2__2700m_vs_light1_3960m	0.2 > OD < 0.8.
exponential phase	light2__2880m_vs_light1_3960m	0.2 > OD < 0.8.
exponential phase	light2__3060m_vs_light1_3960m	0.2 > OD < 0.8.

exponential phase	light2__3240m_vs_light1_3960m	0.2 > OD < 0.8.
exponential phase	dark1__1200m_vs_NRC-1c	0.2 > OD < 0.8.
exponential phase	dark1__1440m_vs_NRC-1c	0.2 > OD < 0.8.
exponential phase	dark1__1680m_vs_NRC-1c	0.2 > OD < 0.8.
exponential phase	dark1__3120m_vs_NRC-1c	0.2 > OD < 0.8.
exponential phase	dark1__3360m_vs_NRC-1c	0.2 > OD < 0.8.
exponential phase	circadian_Dphr1_drk_cycling__1440min_vs_NRC-1d.sig	0.2 > OD < 0.8.
exponential phase	circadian_Dphr1_drk_cycling__1665min_vs_NRC-1d.sig	0.2 > OD < 0.8.
exponential phase	circadian_Dphr1_drk_cycling__1800min_vs_NRC-1d.sig	0.2 > OD < 0.8.
exponential phase	circadian_drk8_cycling_0000min_vs_NRC-1e.sig	0.2 > OD < 0.8.
exponential phase	circadian_drk8_cycling_0540min_vs_NRC-1e.sig	0.2 > OD < 0.8.
exponential phase	circadian_drk8_cycling_0720min_vs_NRC-1e.sig	0.2 > OD < 0.8.
exponential phase	circadian_drk8_cycling_0900min_vs_NRC-1e.sig	0.2 > OD < 0.8.
exponential phase	circadian_drk8_cycling_1080min_vs_NRC-1e.sig	0.2 > OD < 0.8.
exponential phase	circadian_drk8_cycling_1260min_vs_NRC-1e.sig	0.2 > OD < 0.8.
exponential phase	circadian_drk8_cycling_1440min_vs_NRC-1e.sig	0.2 > OD < 0.8.
exponential phase	circadian_drk8_cycling_1620min_vs_NRC-1e.sig	0.2 > OD < 0.8.
exponential phase	circadian_drk8_cycling_1800min_vs_NRC-1e.sig	0.2 > OD < 0.8.
exponential phase	circadian_drk8_cycling_1980min_vs_NRC-1e.sig	0.2 > OD < 0.8.
exponential phase	circadian_drk8_cycling_2160min_vs_NRC-1e.sig	0.2 > OD < 0.8.
exponential phase	circadian_drk8_cycling_2340min_vs_NRC-1e.sig	0.2 > OD < 0.8.
exponential phase	circadian_drk8_cycling_2520min_vs_NRC-1e.sig	0.2 > OD < 0.8.
exponential phase	circadian_drk8_cycling_2700min_vs_NRC-1e.sig	0.2 > OD < 0.8.
exponential phase	circadian_drk8_cycling_2880min_vs_NRC-1e.sig	0.2 > OD < 0.8.
exponential phase	circadian_drk8_cycling_3060min_vs_NRC-1e.sig	0.2 > OD < 0.8.
exponential phase	circadian_drk8_cycling_3240min_vs_NRC-1e.sig	0.2 > OD < 0.8.
exponential phase	circadian_drk7_cycling_0000min_vs_NRC-1d.sig	0.2 > OD < 0.8.

exponential phase	circadian_drk7_cycling_0180min_vs_NRC-1d.sig	0.2 > OD < 0.8.
exponential phase	circadian_drk7_cycling_0540min_vs_NRC-1d.sig	0.2 > OD < 0.8.
exponential phase	circadian_drk7_cycling_0720min_vs_NRC-1d.sig	0.2 > OD < 0.8.
exponential phase	circadian_drk7_cycling_0900min_vs_NRC-1d.sig	0.2 > OD < 0.8.
exponential phase	circadian_drk7_cycling_3060min_vs_NRC-1d.sig	0.2 > OD < 0.8.
exponential phase	circadian_drk6_cycling_0000min_vs_NRC-1e.sig	0.2 > OD < 0.8.
exponential phase	circadian_drk6_cycling_0180min_vs_NRC-1e.sig	0.2 > OD < 0.8.
exponential phase	circadian_drk6_cycling_0360min_vs_NRC-1e.sig	0.2 > OD < 0.8.
exponential phase	circadian_drk6_cycling_0540min_vs_NRC-1e.sig	0.2 > OD < 0.8.
exponential phase	circadian_drk6_cycling_0720min_vs_NRC-1e.sig	0.2 > OD < 0.8.
exponential phase	circadian_drk6_cycling_0912min_vs_NRC-1e.sig	0.2 > OD < 0.8.
exponential phase	circadian_drk6_cycling_1080min_vs_NRC-1e.sig	0.2 > OD < 0.8.
exponential phase	circadian_drk6_cycling_1260min_vs_NRC-1e.sig	0.2 > OD < 0.8.
exponential phase	circadian_drk6_cycling_1440min_vs_NRC-1e.sig	0.2 > OD < 0.8.
exponential phase	circadian__dark5_cycling_30C_1440min_vs_NRC-1d.sig	0.2 > OD < 0.8.
exponential phase	circadian__dark5_cycling_30C_1630min_vs_NRC-1d.sig	0.2 > OD < 0.8.
exponential phase	circadian__dark5_cycling_30C_1815min_vs_NRC-1d.sig	0.2 > OD < 0.8.
exponential phase	circadian_dark3_cycling_1380min_vs_NRC-1d.sig	0.2 > OD < 0.8.
exponential phase	circadian_dark3_cycling_1440min_vs_NRC-1d.sig	0.2 > OD < 0.8.
exponential phase	circadian_dark3_cycling_1500min_vs_NRC-1d.sig	0.2 > OD < 0.8.
exponential phase	circadian_dark3_cycling_1620min_vs_NRC-1d.sig	0.2 > OD < 0.8.
exponential phase	circadian_dark3_cycling_1800min_vs_NRC-1d.sig	0.2 > OD < 0.8.
exponential phase	circadian_dark3_cycling_1980min_vs_NRC-1d.sig	0.2 > OD < 0.8.
exponential phase	circadian_dark3_cycling_2160min_vs_NRC-1d.sig	0.2 > OD < 0.8.
exponential phase	circadian_dark3_cycling_2220min_vs_NRC-1d.sig	0.2 > OD < 0.8.

exponential phase	circadian_dark3_cycling_2340min_vs_NRC-1d.sig	0.2 > OD < 0.8.
exponential phase	circadian_dark3_cycling_2520min_vs_NRC-1d.sig	0.2 > OD < 0.8.
exponential phase	circadian_dark3_ctrl_1380min_vs_NRC-1d.sig	0.2 > OD < 0.8.
exponential phase	circadian_dark3_ctrl_1440min_vs_NRC-1d.sig	0.2 > OD < 0.8.
exponential phase	circadian_dark3_ctrl_1500min_vs_NRC-1d.sig	0.2 > OD < 0.8.
exponential phase	circadian_dark3_ctrl_1620min_vs_NRC-1d.sig	0.2 > OD < 0.8.
exponential phase	circadian_dark3_ctrl_1800min_vs_NRC-1d.sig	0.2 > OD < 0.8.
exponential phase	circadian_dark3_ctrl_1980min_vs_NRC-1d.sig	0.2 > OD < 0.8.
exponential phase	circadian_dark3_ctrl_2160min_vs_NRC-1d.sig	0.2 > OD < 0.8.
exponential phase	circadian_dark3_ctrl_2220min_vs_NRC-1d.sig	0.2 > OD < 0.8.
exponential phase	circadian_drk8_control_0000min_vs_NRC-1e.sig	0.2 > OD < 0.8.
exponential phase	circadian_drk8_control_0180min_vs_NRC-1e.sig	0.2 > OD < 0.8.
exponential phase	circadian_drk8_control_0360min_vs_NRC-1e.sig	0.2 > OD < 0.8.
exponential phase	circadian_drk8_control_0540min_vs_NRC-1e.sig	0.2 > OD < 0.8.
exponential phase	circadian_drk8_control_0720min_vs_NRC-1e.sig	0.2 > OD < 0.8.
exponential phase	circadian_drk8_control_0900min_vs_NRC-1e.sig	0.2 > OD < 0.8.
exponential phase	circadian_drk8_control_1080min_vs_NRC-1e.sig	0.2 > OD < 0.8.
exponential phase	circadian_drk8_control_1260min_vs_NRC-1e.sig	0.2 > OD < 0.8.
exponential phase	circadian_drk8_control_1440min_vs_NRC-1e.sig	0.2 > OD < 0.8.
exponential phase	circadian_drk8_control_1620min_vs_NRC-1e.sig	0.2 > OD < 0.8.
exponential phase	circadian_drk8_control_1800min_vs_NRC-1e.sig	0.2 > OD < 0.8.
exponential phase	circadian_drk8_control_1980min_vs_NRC-1e.sig	0.2 > OD < 0.8.
exponential phase	circadian_drk8_control_2160min_vs_NRC-1e.sig	0.2 > OD < 0.8.
exponential phase	circadian_drk8_control_2340min_vs_NRC-1e.sig	0.2 > OD < 0.8.
exponential phase	circadian_drk8_control_2520min_vs_NRC-1e.sig	0.2 > OD < 0.8.

exponential phase	circadian_drk8_control_2700min_vs_NRC-1e.sig	0.2 > OD < 0.8.
exponential phase	circadian_drk8_control_3060min_vs_NRC-1e.sig	0.2 > OD < 0.8.
exponential phase	circadian_drk8_control_3240min_vs_NRC-1e.sig	0.2 > OD < 0.8.
exponential phase	Circadian_Dark9_Cycling_0000min_vs_NRC-1g.sig	0.2 > OD < 0.8.
exponential phase	Circadian_Dark9_Cycling_0180min_vs_NRC-1g.sig	0.2 > OD < 0.8.
exponential phase	Circadian_Dark9_Cycling_0360min_vs_NRC-1g.sig	0.2 > OD < 0.8.
exponential phase	Circadian_Dark9_Cycling_0535min_vs_NRC-1g.sig	0.2 > OD < 0.8.
exponential phase	Circadian_Dark9_Cycling_0720min_vs_NRC-1g.sig	0.2 > OD < 0.8.
exponential phase	Circadian_Dark9_Cycling_0900min_vs_NRC-1g.sig	0.2 > OD < 0.8.
exponential phase	Circadian_Dark9_Cycling_1080min_vs_NRC-1g.sig	0.2 > OD < 0.8.
exponential phase	Circadian_Dark9_Cycling_1265min_vs_NRC-1g.sig	0.2 > OD < 0.8.
exponential phase	Circadian_Dark9_Cycling_1440min_vs_NRC-1g.sig	0.2 > OD < 0.8.
exponential phase	Circadian_Dark9_Cycling_1620min_vs_NRC-1g.sig	0.2 > OD < 0.8.
exponential phase	Circadian_Dark9_Cycling_1800min_vs_NRC-1g.sig	0.2 > OD < 0.8.
exponential phase	Circadian_Dark9_Cycling_1980min_vs_NRC-1g.sig	0.2 > OD < 0.8.
exponential phase	Circadian_Dark9_Cycling_2160min_vs_NRC-1g.sig	0.2 > OD < 0.8.
exponential phase	Circadian_Dark9_Cycling_2340min_vs_NRC-1g.sig	0.2 > OD < 0.8.
exponential phase	Circadian_Dark9_Cycling_2520min_vs_NRC-1g.sig	0.2 > OD < 0.8.
exponential phase	Circadian_Dark9_Cycling_2700min_vs_NRC-1g.sig	0.2 > OD < 0.8.
exponential phase	Circadian_Dark9_Cycling_2880min_vs_NRC-1g.sig	0.2 > OD < 0.8.
exponential phase	Circadian_Dark9_Cycling_3060min_vs_NRC-1g.sig	0.2 > OD < 0.8.
exponential phase	Circadian_Dark9_Cycling_3240min_vs_NRC-1g.sig	0.2 > OD < 0.8.
exponential phase	Circadian_Dark9_Cycling_3420min_vs_NRC-1g.sig	0.2 > OD < 0.8.
exponential phase	Circadian_Dark9_Cycling_3600min_vs_NRC-1g.sig	0.2 > OD < 0.8.
exponential phase	Circadian_Dark9_Cycling_3780min_vs_NRC-1g.sig	0.2 > OD < 0.8.

exponential phase	Circadian_Dark9_Cycling_3960min_vs_NRC-1g.sig	0.2 > OD < 0.8.
exponential phase	Circadian_Dark9_Cycling_4140min_vs_NRC-1g.sig	0.2 > OD < 0.8.
exponential phase	Circadian_Dark9_Cycling_4320min_vs_NRC-1g.sig	0.2 > OD < 0.8.
exponential phase	Circadian_Dark9_Cycling_4500min_vs_NRC-1g.sig	0.2 > OD < 0.8.
exponential phase	Circadian_Dark9_Control_0000min_vs_NRC-1g.sig	0.2 > OD < 0.8.
exponential phase	Circadian_Dark9_Control_0180min_vs_NRC-1g.sig	0.2 > OD < 0.8.
exponential phase	Circadian_Dark9_Control_0360min_vs_NRC-1g.sig	0.2 > OD < 0.8.
exponential phase	Circadian_Dark9_Control_0535min_vs_NRC-1g.sig	0.2 > OD < 0.8.
exponential phase	Circadian_Dark9_Control_0720min_vs_NRC-1g.sig	0.2 > OD < 0.8.
exponential phase	Circadian_Dark9_Control_1080min_vs_NRC-1g.sig	0.2 > OD < 0.8.
exponential phase	Circadian_Dark9_Control_1265min_vs_NRC-1g.sig	0.2 > OD < 0.8.
exponential phase	Circadian_Dark9_Control_1440min_vs_NRC-1g.sig	0.2 > OD < 0.8.
exponential phase	Circadian_Dark9_Control_1620min_vs_NRC-1g.sig	0.2 > OD < 0.8.
exponential phase	Circadian_Dark9_Control_1800min_vs_NRC-1g.sig	0.2 > OD < 0.8.
exponential phase	Circadian_Dark9_Control_1980min_vs_NRC-1g.sig	0.2 > OD < 0.8.
exponential phase	Circadian_Dark9_Control_2160min_vs_NRC-1g.sig	0.2 > OD < 0.8.
exponential phase	Circadian_Dark9_Control_2340min_vs_NRC-1g.sig	0.2 > OD < 0.8.
exponential phase	Circadian_Dark9_Control_2520min_vs_NRC-1g.sig	0.2 > OD < 0.8.
exponential phase	Circadian_Dark9_Control_2700min_vs_NRC-1g.sig	0.2 > OD < 0.8.
exponential phase	Circadian_Dark9_Control_2880min_vs_NRC-1g.sig	0.2 > OD < 0.8.
exponential phase	Circadian_Dark9_Control_3060min_vs_NRC-1g.sig	0.2 > OD < 0.8.
exponential phase	Circadian_Dark9_Control_3240min_vs_NRC-1g.sig	0.2 > OD < 0.8.
exponential phase	Circadian_Dark9_Control_3420min_vs_NRC-1g.sig	0.2 > OD < 0.8.
exponential phase	Circadian_Dark9_Control_3600min_vs_NRC-1g.sig	0.2 > OD < 0.8.
exponential phase	Circadian_Dark9_Control_3780min_vs_NRC-1g.sig	0.2 > OD < 0.8.

exponential phase	Circadian_Dark9_Control_3960min_vs_NRC-1g.sig	0.2 > OD < 0.8.
exponential phase	Circadian_Dark9_Control_4140min_vs_NRC-1g.sig	0.2 > OD < 0.8.
exponential phase	Circadian_Dark9_Control_4320min_vs_NRC-1g.sig	0.2 > OD < 0.8.
exponential phase	Circadian_Dark9_Control_4500min_vs_NRC-1g.sig	0.2 > OD < 0.8.
exponential phase	Circadian_Dark10_Cycling_-2873min_vs_NRC-1h1.sig	0.2 > OD < 0.8.
exponential phase	Circadian_Dark10_Cycling_-2670min_vs_NRC-1h1.sig	0.2 > OD < 0.8.
exponential phase	Circadian_Dark10_Cycling_-2315min_vs_NRC-1h1.sig	0.2 > OD < 0.8.
exponential phase	Circadian_Dark10_Cycling_-2120min_vs_NRC-1h1.sig	0.2 > OD < 0.8.
exponential phase	Circadian_Dark10_Cycling_-1960min_vs_NRC-1h1.sig	0.2 > OD < 0.8.
exponential phase	Circadian_Dark10_Cycling_-1785min_vs_NRC-1h1.sig	0.2 > OD < 0.8.
exponential phase	Circadian_Dark10_Cycling_-1595min_vs_NRC-1h1.sig	0.2 > OD < 0.8.
exponential phase	Circadian_Dark10_Cycling_-1060min_vs_NRC-1h1.sig	0.2 > OD < 0.8.
exponential phase	Circadian_Dark10_Cycling_-0360min_vs_NRC-1h1.sig	0.2 > OD < 0.8.
exponential phase	Circadian_Dark10_Cycling_0195min_vs_NRC-1h1.sig	0.2 > OD < 0.8.
exponential phase	Circadian_Dark10_Cycling_0560min_vs_NRC-1h1.sig	0.2 > OD < 0.8.
exponential phase	Cu_-5_vs_NRC-1.sig	0.2 > OD < 0.8.
exponential phase	Cu_000_vs_NRC-1.sig	0.2 > OD < 0.8.
exponential phase	Cu_005_vs_NRC-1.sig	0.2 > OD < 0.8.
exponential phase	Cu_010_vs_NRC-1.sig	0.2 > OD < 0.8.
exponential phase	Cu_020_vs_NRC-1.sig	0.2 > OD < 0.8.
exponential phase	Cu_160_vs_NRC-1.sig	0.2 > OD < 0.8.
exponential phase	Cu_-1_vs_NRC-1e.sig	0.2 > OD < 0.8.
exponential phase	Cu_000_vs_NRC-1e.sig	0.2 > OD < 0.8.
exponential phase	Cu_005_vs_NRC-1e.sig	0.2 > OD < 0.8.
exponential phase	Cu_010_vs_NRC-1e.sig	0.2 > OD < 0.8.
exponential phase	Cu_020_vs_NRC-1e.sig	0.2 > OD < 0.8.
exponential phase	Cu_160_vs_NRC-1e.sig	0.2 > OD < 0.8.
exponential phase	Cu_NRC1_set1_160min_vs_NRC-1h1.sig	0.2 > OD < 0.8.
exponential phase	Cu_ura3_KO_set1_-030min_vs_NRC-1h1.sig	0.2 > OD < 0.8.
exponential phase	Cu_ura3_KO_set1_000min_vs_NRC-1h1.sig	0.2 > OD < 0.8.
exponential phase	Cu_ura3_KO_set1_005min_vs_NRC-	0.2 > OD < 0.8.

	1h1.sig	
exponential phase	Cu_ura3_KO_set1_010min_vs_NRC-1h1.sig	0.2 > OD < 0.8.
exponential phase	Cu_ura3_KO_set1_020min_vs_NRC-1h1.sig	0.2 > OD < 0.8.
exponential phase	Cu_ura3_KO_set1_040min_vs_NRC-1h1.sig	0.2 > OD < 0.8.
exponential phase	Cu_ura3_KO_set1_080min_vs_NRC-1h1.sig	0.2 > OD < 0.8.
exponential phase	Cu_ura3_KO_set1_160min_vs_NRC-1h1.sig	0.2 > OD < 0.8.
exponential phase	Cu_ura3_KO_set2_-030min_vs_NRC-1h1.sig	0.2 > OD < 0.8.
exponential phase	Cu_ura3_KO_set2_000min_vs_NRC-1h1.sig	0.2 > OD < 0.8.
exponential phase	Cu_ura3_KO_set2_005min_vs_NRC-1h1.sig	0.2 > OD < 0.8.
exponential phase	Cu_ura3_KO_set2_010min_vs_NRC-1h1.sig	0.2 > OD < 0.8.
exponential phase	Cu_ura3_KO_set2_020min_vs_NRC-1h1.sig	0.2 > OD < 0.8.
exponential phase	Cu_ura3_KO_set2_040min_vs_NRC-1h1.sig	0.2 > OD < 0.8.
exponential phase	Cu_ura3_KO_set2_080min_vs_NRC-1h1.sig	0.2 > OD < 0.8.
exponential phase	Cu_ura3_KO_set2_160min_vs_NRC-1h1.sig	0.2 > OD < 0.8.
exponential phase	Cu_NRC1_set2_-030min_vs_NRC-1h1.sig	0.2 > OD < 0.8.
exponential phase	Cu_NRC1_set2_000min_vs_NRC-1h1.sig	0.2 > OD < 0.8.
exponential phase	Cu_NRC1_set2_005min_vs_NRC-1h1.sig	0.2 > OD < 0.8.
exponential phase	Cu_NRC1_set2_010min_vs_NRC-1h1.sig	0.2 > OD < 0.8.
exponential phase	Cu_NRC1_set2_020min_vs_NRC-1h1.sig	0.2 > OD < 0.8.
exponential phase	Cu_NRC1_set2_040min_vs_NRC-1h1.sig	0.2 > OD < 0.8.
exponential phase	Cu_NRC1_set2_080min_vs_NRC-1h1.sig	0.2 > OD < 0.8.
exponential phase	Cu_NRC1_set2_160min_vs_NRC-1h1.sig	0.2 > OD < 0.8.
exponential phase	ura3_40min_+Fe_vs_NRC1-h1.sig	0.2 > OD < 0.8.
exponential phase	zim__HO_D_vs_NRC-1	0.2 > OD < 0.8.
exponential phase	zim__HO_L_vs_NRC-1	0.2 > OD < 0.8.
exponential phase	zim__LO_D_vs_NRC-1	0.2 > OD < 0.8.
exponential phase	zim__LO_L_vs_NRC-1	0.2 > OD < 0.8.
exponential phase	VNG2334C__HO_D_vs_NRC-1	0.2 > OD < 0.8.
exponential phase	VNG2334C__HO_L_vs_NRC-1	0.2 > OD < 0.8.
exponential phase	VNG2334C__LO_D_vs_NRC-1	0.2 > OD < 0.8.
exponential phase	VNG2334C__LO_L_vs_NRC-1	0.2 > OD < 0.8.
exponential phase	VNG1296C__HO_D_vs_NRC-1	0.2 > OD < 0.8.
exponential phase	VNG1296C__HO_L_vs_NRC-1	0.2 > OD < 0.8.

exponential phase	VNG1296C__LO_D_vs_NRC-1	0.2 > OD < 0.8.
exponential phase	VNG1296C__LO_L_vs_NRC-1	0.2 > OD < 0.8.
exponential phase	EMS_Treated__000uM-000	0.2 > OD < 0.8.
exponential phase	EMS_Treated__000uM-010	0.2 > OD < 0.8.
exponential phase	EMS_Treated__000uM-020	0.2 > OD < 0.8.
exponential phase	EMS_Treated__000uM-030	0.2 > OD < 0.8.
exponential phase	EMS_Treated__000uM-040	0.2 > OD < 0.8.
exponential phase	EMS_Treated__000uM-050	0.2 > OD < 0.8.
exponential phase	EMS_Treated__000uM-060	0.2 > OD < 0.8.
exponential phase	EMS_Treated__000uM-120	0.2 > OD < 0.8.
exponential phase	circadian__dark_cycling_125w/m2_42C_1440min_vs_NRC-1d.sig	0.2 > OD < 0.8.
exponential phase	circadian__dark_cycling_125w/m2_42C_1615min_vs_NRC-1d.sig	0.2 > OD < 0.8.
exponential phase	circadian__dark_cycling_125w/m2_42C_1800min_vs_NRC-1d.sig	0.2 > OD < 0.8.
exponential phase	circadian__dark_cycling_125w/m2_42C_1985min_vs_NRC-1d.sig	0.2 > OD < 0.8.
exponential phase	circadian__dark_cycling_125w/m2_42C_2160min_vs_NRC-1d.sig	0.2 > OD < 0.8.
exponential phase	circadian__dark_cycling_125w/m2_42C_2340min_vs_NRC-1d.sig	0.2 > OD < 0.8.
exponential phase	circadian__dark_cycling_125w/m2_42C_2515min_vs_NRC-1d.sig	0.2 > OD < 0.8.
exponential phase	NRC1_H2O_0540_0.220_rep2_vs_NRC-1g.sig	0.2 > OD < 0.8.
exponential phase	NRC1_H2O_0890_0.468_rep2_vs_NRC-1g.sig	0.2 > OD < 0.8.
exponential phase	NRC1_H2O_0540_0.225_rep1_vs_NRC-1g.sig	0.2 > OD < 0.8.
exponential phase	NRC1_H2O_0890_0.496_rep1_vs_NRC-1g.sig	0.2 > OD < 0.8.
exponential phase	NRC1_Uracil_0540_0.205_rep2_vs_NRC-1g.sig	0.2 > OD < 0.8.
exponential phase	NRC1_Uracil_0890_0.420_rep2_vs_NRC-1g.sig	0.2 > OD < 0.8.
exponential phase	NRC1_Uracil_0540_0.200_rep1_vs_NRC-1g.sig	0.2 > OD < 0.8.
exponential phase	NRC1_Uracil_0890_0.440_rep1_vs_NRC-1g.sig	0.2 > OD < 0.8.
exponential phase	Dura3_Uracil_0690_0.200_rep2_vs_NRC-1g.sig	0.2 > OD < 0.8.
exponential phase	Dura3_Uracil_1200_0.467_rep2_vs_NRC-1g.sig	0.2 > OD < 0.8.
exponential phase	Dura3_Uracil_1200_0.465_rep1_vs_NRC-1g.sig	0.2 > OD < 0.8.
exponential phase	NRC1_03720_0.234_rep2_vs_NRC-1g.sig	0.2 > OD < 0.8.
exponential phase	NRC1_03960_0.409_rep2_vs_NRC-1g.sig	0.2 > OD < 0.8.

exponential phase	NRC1_04320_0.578_rep2_vs_NRC-1g.sig	0.2 > OD < 0.8.
exponential phase	NRC1_03720_0.259_rep1_vs_NRC-1g.sig	0.2 > OD < 0.8.
exponential phase	NRC1_03960_0.364_rep1_vs_NRC-1g.sig	0.2 > OD < 0.8.
exponential phase	NRC1_04320_0.590_rep1_vs_NRC-1g.sig	0.2 > OD < 0.8.
exponential phase	H2O2_Recov._set_3_0mM_000min_vs_NRC-1f.sig	0.2 > OD < 0.8.
exponential phase	H2O2_Recov._set_3_0mM_010min_vs_NRC-1f.sig	0.2 > OD < 0.8.
exponential phase	H2O2_Recov._set_3_0mM_020min_vs_NRC-1f.sig	0.2 > OD < 0.8.
exponential phase	H2O2_Recov._set_3_0mM_030min_vs_NRC-1f.sig	0.2 > OD < 0.8.
exponential phase	H2O2_Recov._set_3_0mM_040min_vs_NRC-1f.sig	0.2 > OD < 0.8.
exponential phase	H2O2_Recov._set_3_0mM_050min_vs_NRC-1f.sig	0.2 > OD < 0.8.
exponential phase	H2O2_Recov._set_3_0mM_060min_vs_NRC-1f.sig	0.2 > OD < 0.8.
exponential phase	H2O2_Recov._set_3_0mM_120min_vs_NRC-1f.sig	0.2 > OD < 0.8.
exponential phase	H2O2_Const._set_2_0mM_000min_vs_NRC-1f.sig	0.2 > OD < 0.8.
exponential phase	H2O2_Const._set_2_0mM_030min_vs_NRC-1f.sig	0.2 > OD < 0.8.
exponential phase	H2O2_Const._set_2_0mM_060min_vs_NRC-1f.sig	0.2 > OD < 0.8.
exponential phase	H2O2_Const._set_2_0mM_120min_vs_NRC-1f.sig	0.2 > OD < 0.8.
exponential phase	PQ_Recov._set_2_0mM_000min_vs_NRC-1f.sig	0.2 > OD < 0.8.
exponential phase	PQ_Recov._set_2_0mM_010min_vs_NRC-1f.sig	0.2 > OD < 0.8.
exponential phase	PQ_Recov._set_2_0mM_020min_vs_NRC-1f.sig	0.2 > OD < 0.8.
exponential phase	PQ_Recov._set_2_0mM_030min_vs_NRC-1f.sig	0.2 > OD < 0.8.
exponential phase	PQ_Recov._set_2_0mM_040min_vs_NRC-1f.sig	0.2 > OD < 0.8.
exponential phase	PQ_Recov._set_2_0mM_050min_vs_NRC-1f.sig	0.2 > OD < 0.8.
exponential phase	PQ_Recov._set_2_0mM_060min_vs_NRC-1f.sig	0.2 > OD < 0.8.
exponential phase	PQ_Recov._set_2_0mM_120min_vs_NRC-1f.sig	0.2 > OD < 0.8.
exponential phase	PQ_Const._set_2_0mM_000min_vs_NRC-1f.sig	0.2 > OD < 0.8.
exponential phase	PQ_Const._set_2_0mM_030min_vs_NRC-1f.sig	0.2 > OD < 0.8.
exponential phase	PQ_Const._set_2_0mM_060min_vs_NRC-1f.sig	0.2 > OD < 0.8.

exponential phase	H2O2_Recov._set_2_0mM_000min_vs_NRC-1f.sig	0.2 > OD < 0.8.
exponential phase	H2O2_Recov._set_2_0mM_010min_vs_NRC-1f.sig	0.2 > OD < 0.8.
exponential phase	H2O2_Recov._set_2_0mM_020min_vs_NRC-1f.sig	0.2 > OD < 0.8.
exponential phase	H2O2_Recov._set_2_0mM_030min_vs_NRC-1f.sig	0.2 > OD < 0.8.
exponential phase	H2O2_Recov._set_2_0mM_040min_vs_NRC-1f.sig	0.2 > OD < 0.8.
exponential phase	H2O2_Recov._set_2_0mM_050min_vs_NRC-1f.sig	0.2 > OD < 0.8.
exponential phase	H2O2_Recov._set_2_0mM_060min_vs_NRC-1f.sig	0.2 > OD < 0.8.
exponential phase	H2O2_Recov._set_2_0mM_120min_vs_NRC-1f.sig	0.2 > OD < 0.8.
exponential phase	H2O2_Const._set_1_0mM_000min_vs_NRC-1f.sig	0.2 > OD < 0.8.
exponential phase	H2O2_Const._set_1_0mM_030min_vs_NRC-1f.sig	0.2 > OD < 0.8.
exponential phase	H2O2_Const._set_1_0mM_060min_vs_NRC-1f.sig	0.2 > OD < 0.8.
exponential phase	H2O2_Const._set_1_0mM_120min_vs_NRC-1f.sig	0.2 > OD < 0.8.
exponential phase	PQ_Recov._set_1_0mM_000min_vs_NRC-1f.sig	0.2 > OD < 0.8.
exponential phase	PQ_Recov._set_1_0mM_010min_vs_NRC-1f.sig	0.2 > OD < 0.8.
exponential phase	PQ_Recov._set_1_0mM_020min_vs_NRC-1f.sig	0.2 > OD < 0.8.
exponential phase	PQ_Recov._set_1_0mM_030min_vs_NRC-1f.sig	0.2 > OD < 0.8.
exponential phase	PQ_Recov._set_1_0mM_040min_vs_NRC-1f.sig	0.2 > OD < 0.8.
exponential phase	PQ_Recov._set_1_0mM_050min_vs_NRC-1f.sig	0.2 > OD < 0.8.
exponential phase	PQ_Recov._set_1_0mM_060min_vs_NRC-1f.sig	0.2 > OD < 0.8.
exponential phase	PQ_Const._set_1_0mM_000min_vs_NRC-1f.sig	0.2 > OD < 0.8.
exponential phase	PQ_Const._set_1_0mM_030min_vs_NRC-1f.sig	0.2 > OD < 0.8.
exponential phase	PQ_Const._set_1_0mM_060min_vs_NRC-1f.sig	0.2 > OD < 0.8.
exponential phase	MDM200gSalt_0.388_vs_NRC-1e.sig	0.2 > OD < 0.8.
exponential phase	MDM200gSalt_0.466_vs_NRC-1e.sig	0.2 > OD < 0.8.
exponential phase	MDM200gSalt_0.534_vs_NRC-1e.sig	0.2 > OD < 0.8.
exponential phase	20060818_NRC1_rep2_0.424_vs_NRC-1e.sig	0.2 > OD < 0.8.
exponential phase	20060818_NRC1_rep1_0.430_vs_NRC-	0.2 > OD < 0.8.

	1e.sig	
exponential phase	KO_ura3.2_0.3207_vs_NRC-1_h1.sig	0.2 > OD < 0.8.
exponential phase	KO_ura3.2_0.4308_vs_NRC-1_h1.sig	0.2 > OD < 0.8.
exponential phase	KO_ura3.2_0.5084_vs_NRC-1_h1.sig	0.2 > OD < 0.8.
exponential phase	ura3_growth_t2exp1_0.5OD_vs_NRC1e.sig	0.2 > OD < 0.8.
exponential phase	ura3_growth_t1_exp2_0.3OD_vs_NRC1f.sig	0.2 > OD < 0.8.
exponential phase	ura3_growth_t2_exp2_0.5OD_vs_NRC1f.sig	0.2 > OD < 0.8.
exponential phase	ura3_+glu_a_OD1.2_vs_NRC1e.sig	0.2 > OD < 0.8.
exponential phase	ura3_growth_t1_exp3_0.3OD_vs_NRC1f.sig	0.2 > OD < 0.8.
exponential phase	ura3_growth_t2_exp3_0.5OD_vs_NRC1f.sig	0.2 > OD < 0.8.
exponential phase	ura3_+glu_a_OD0.6repl_vs_NRC1e.sig	0.2 > OD < 0.8.
exponential phase	ura3_+glu_a_OD1.2repl_vs_NRC1e.sig	0.2 > OD < 0.8.
exponential phase	ura3_+glu_b_OD0.6repl_vs_NRC1g.sig	0.2 > OD < 0.8.
exponential phase	ura3_+glu_b_OD1.2repl_vs_NRC1g.sig	0.2 > OD < 0.8.
exponential phase	ura3_-glu_a_OD0.2_vs_NRC1e.sig	0.2 > OD < 0.8.
exponential phase	ura3_-glu_b_OD0.2_vs_NRC1g.sig	0.2 > OD < 0.8.
exponential phase	EMS_Treated__100000uM-000	0.2 > OD < 0.8.
exponential phase	EMS_Treated__100000uM-010	0.2 > OD < 0.8.
exponential phase	EMS_Treated__100000uM-020	0.2 > OD < 0.8.
exponential phase	EMS_Treated__100000uM-040	0.2 > OD < 0.8.
exponential phase	EMS_Treated__100000uM-050	0.2 > OD < 0.8.
exponential phase	EMS_Treated__100000uM-060	0.2 > OD < 0.8.
exponential phase	EMS_Treated__100000uM-120	0.2 > OD < 0.8.
exponential phase	MDM250gSalt_0.204_vs_NRC-1e.sig	0.2 > OD < 0.8.
exponential phase	MDM250gSalt_0.396_vs_NRC-1e.sig	0.2 > OD < 0.8.
exponential phase	MDM250gSalt_0.481_vs_NRC-1e.sig	0.2 > OD < 0.8.
exponential phase	MDM250gSalt_0.49_vs_NRC-1e.sig	0.2 > OD < 0.8.
exponential phase	H2O2_Recov._set_3_25mM_000min_vs_NRC-1f.sig	0.2 > OD < 0.8.
exponential phase	H2O2_Recov._set_3_25mM_010min_vs_NRC-1f.sig	0.2 > OD < 0.8.
exponential phase	H2O2_Recov._set_3_25mM_020min_vs_NRC-1f.sig	0.2 > OD < 0.8.
exponential phase	H2O2_Recov._set_3_25mM_030min_vs_NRC-1f.sig	0.2 > OD < 0.8.
exponential phase	H2O2_Recov._set_3_25mM_040min_vs_NRC-1f.sig	0.2 > OD < 0.8.
exponential phase	H2O2_Recov._set_3_25mM_050min_vs_NRC-1f.sig	0.2 > OD < 0.8.
exponential phase	H2O2_Recov._set_3_25mM_060min_vs_NRC-1f.sig	0.2 > OD < 0.8.

exponential phase	H2O2_Recov._set_3_25mM_120min_vs_NRC-1f.sig	0.2 > OD < 0.8.
exponential phase	H2O2_Recov._set_3_25mM_240min_vs_NRC-1f.sig	0.2 > OD < 0.8.
exponential phase	H2O2_Const._set_2_25mM_000min_vs_NRC-1f.sig	0.2 > OD < 0.8.
exponential phase	H2O2_Const._set_2_25mM_030min_vs_NRC-1f.sig	0.2 > OD < 0.8.
exponential phase	H2O2_Const._set_2_25mM_060min_vs_NRC-1f.sig	0.2 > OD < 0.8.
exponential phase	H2O2_Const._set_2_25mM_120min_vs_NRC-1f.sig	0.2 > OD < 0.8.
exponential phase	PQ_Recov._set_2_4mM_000min_vs_NRC-1f.sig	0.2 > OD < 0.8.
exponential phase	PQ_Recov._set_2_4mM_010min_vs_NRC-1f.sig	0.2 > OD < 0.8.
exponential phase	PQ_Recov._set_2_4mM_020min_vs_NRC-1f.sig	0.2 > OD < 0.8.
exponential phase	PQ_Recov._set_2_4mM_030min_vs_NRC-1f.sig	0.2 > OD < 0.8.
exponential phase	PQ_Recov._set_2_4mM_040min_vs_NRC-1f.sig	0.2 > OD < 0.8.
exponential phase	PQ_Recov._set_2_4mM_050min_vs_NRC-1f.sig	0.2 > OD < 0.8.
exponential phase	PQ_Recov._set_2_4mM_060min_vs_NRC-1f.sig	0.2 > OD < 0.8.
exponential phase	PQ_Recov._set_2_4mM_120min_vs_NRC-1f.sig	0.2 > OD < 0.8.
exponential phase	PQ_Recov._set_2_4mM_240min_vs_NRC-1f.sig	0.2 > OD < 0.8.
exponential phase	PQ_Const._set_2_4mM_000min_vs_NRC-1f.sig	0.2 > OD < 0.8.
exponential phase	PQ_Const._set_2_4mM_030min_vs_NRC-1f.sig	0.2 > OD < 0.8.
exponential phase	PQ_Const._set_2_4mM_060min_vs_NRC-1f.sig	0.2 > OD < 0.8.
exponential phase	PQ_Const._set_2_4mM_120min_vs_NRC-1f.sig	0.2 > OD < 0.8.
exponential phase	PQ_Const._set_2_4mM_240min_vs_NRC-1f.sig	0.2 > OD < 0.8.
exponential phase	H2O2_Recov._set_2_25mM_000min_vs_NRC-1f.sig	0.2 > OD < 0.8.
exponential phase	H2O2_Recov._set_2_25mM_010min_vs_NRC-1f.sig	0.2 > OD < 0.8.
exponential phase	H2O2_Recov._set_2_25mM_020min_vs_NRC-1f.sig	0.2 > OD < 0.8.
exponential phase	H2O2_Recov._set_2_25mM_030min_vs_NRC-1f.sig	0.2 > OD < 0.8.
exponential phase	H2O2_Recov._set_2_25mM_040min_vs_NRC-1f.sig	0.2 > OD < 0.8.

exponential phase	H2O2_Recov._set_2_25mM_050min_vs_NRC-1f.sig	0.2 > OD < 0.8.
exponential phase	H2O2_Recov._set_2_25mM_060min_vs_NRC-1f.sig	0.2 > OD < 0.8.
exponential phase	H2O2_Recov._set_2_25mM_120min_vs_NRC-1f.sig	0.2 > OD < 0.8.
exponential phase	H2O2_Recov._set_2_25mM_240min_vs_NRC-1f.sig	0.2 > OD < 0.8.
exponential phase	H2O2_Const._set_1_25mM_000min_vs_NRC-1f.sig	0.2 > OD < 0.8.
exponential phase	H2O2_Const._set_1_25mM_030min_vs_NRC-1f.sig	0.2 > OD < 0.8.
exponential phase	H2O2_Const._set_1_25mM_060min_vs_NRC-1f.sig	0.2 > OD < 0.8.
exponential phase	H2O2_Const._set_1_25mM_120min_vs_NRC-1f.sig	0.2 > OD < 0.8.
exponential phase	PQ_Recov._set_1_4mM_000min_vs_NRC-1f.sig	0.2 > OD < 0.8.
exponential phase	PQ_Recov._set_1_4mM_010min_vs_NRC-1f.sig	0.2 > OD < 0.8.
exponential phase	PQ_Recov._set_1_4mM_020min_vs_NRC-1f.sig	0.2 > OD < 0.8.
exponential phase	PQ_Recov._set_1_4mM_030min_vs_NRC-1f.sig	0.2 > OD < 0.8.
exponential phase	PQ_Recov._set_1_4mM_040min_vs_NRC-1f.sig	0.2 > OD < 0.8.
exponential phase	PQ_Recov._set_1_4mM_050min_vs_NRC-1f.sig	0.2 > OD < 0.8.
exponential phase	PQ_Recov._set_1_4mM_060min_vs_NRC-1f.sig	0.2 > OD < 0.8.
exponential phase	PQ_Recov._set_1_4mM_120min_vs_NRC-1f.sig	0.2 > OD < 0.8.
exponential phase	PQ_Recov._set_1_4mM_240min_vs_NRC-1f.sig	0.2 > OD < 0.8.
exponential phase	PQ_Const._set_1_4mM_000min_vs_NRC-1f.sig	0.2 > OD < 0.8.
exponential phase	PQ_Const._set_1_4mM_030min_vs_NRC-1f.sig	0.2 > OD < 0.8.
exponential phase	PQ_Const._set_1_4mM_060min_vs_NRC-1f.sig	0.2 > OD < 0.8.
exponential phase	PQ_Const._set_1_4mM_120min_vs_NRC-1f.sig	0.2 > OD < 0.8.
exponential phase	PQ_Const._set_1_4mM_240min_vs_NRC-1f.sig	0.2 > OD < 0.8.
exponential phase	KO_ura3.3_0.274_vs_NRC-1_h1.sig	0.2 > OD < 0.8.
exponential phase	KO_ura3.3_0.4452_vs_NRC-1_h1.sig	0.2 > OD < 0.8.
exponential phase	KO_ura3.4_0.2812_vs_NRC-1_h1.sig	0.2 > OD < 0.8.
exponential phase	KO_ura3.4_0.4645_vs_NRC-1_h1.sig	0.2 > OD < 0.8.
exponential phase	o2_set1_-001m_L2H_005_vs_NRC-1c	0.2 > OD < 0.8.
exponential phase	o2_set1_0001m_L2H_500_vs_NRC-1c	0.2 > OD < 0.8.

exponential phase	o2_set1_0005m_H_922_vs_NRC-1c	0.2 > OD < 0.8.
exponential phase	o2_set1_0010m_H_947_vs_NRC-1c	0.2 > OD < 0.8.
exponential phase	o2_set1_0020m_H_937_vs_NRC-1c	0.2 > OD < 0.8.
exponential phase	o2_set1_0030m_H_931_vs_NRC-1c	0.2 > OD < 0.8.
exponential phase	o2_set1_0045m_H_939_vs_NRC-1c	0.2 > OD < 0.8.
exponential phase	o2_set1_0090m_H_941_vs_NRC-1c	0.2 > OD < 0.8.
exponential phase	o2_set1_0180m_H_930_vs_NRC-1c	0.2 > OD < 0.8.
exponential phase	o2_set2_L_020_vs_NRC-1d.sig	0.2 > OD < 0.8.
exponential phase	o2_set2_L_030_vs_NRC-1d.sig	0.2 > OD < 0.8.
exponential phase	o2_set2_L_045_vs_NRC-1d.sig	0.2 > OD < 0.8.
exponential phase	o2_set2_L_090_vs_NRC-1d.sig	0.2 > OD < 0.8.
exponential phase	o2_set2_L_135_vs_NRC-1d.sig	0.2 > OD < 0.8.
exponential phase	o2_set2_L_180_vs_NRC-1d.sig	0.2 > OD < 0.8.
exponential phase	o2_set2_L_270_vs_NRC-1d.sig	0.2 > OD < 0.8.
exponential phase	o2_set2_L_360_vs_NRC-1d.sig	0.2 > OD < 0.8.
exponential phase	o2_set3_-0005_min_LO2_vs_NRC1f.sig	0.2 > OD < 0.8.
exponential phase	o2_set3_0000_min_L2HO2_vs_NRC1f.sig	0.2 > OD < 0.8.
exponential phase	o2_set3_0005_min_HO2_vs_NRC1f.sig	0.2 > OD < 0.8.
exponential phase	o2_set3_0010_min_HO2_vs_NRC1f.sig	0.2 > OD < 0.8.
exponential phase	o2_set3_0020_min_HO2_vs_NRC1f.sig	0.2 > OD < 0.8.
exponential phase	o2_set3_0030_min_HO2_vs_NRC1f.sig	0.2 > OD < 0.8.
exponential phase	o2_set3_0045_min_HO2_vs_NRC1f.sig	0.2 > OD < 0.8.
exponential phase	o2_set3_0060_min_HO2_vs_NRC1f.sig	0.2 > OD < 0.8.
exponential phase	o2_set3_0090_min_HO2_vs_NRC1f.sig	0.2 > OD < 0.8.
exponential phase	o2_set3_0120_min_HO2_vs_NRC1f.sig	0.2 > OD < 0.8.
exponential phase	o2_set3_0180_min_HO2_vs_NRC1f.sig	0.2 > OD < 0.8.
exponential phase	o2_set3_0240_min_HO2_vs_NRC1f.sig	0.2 > OD < 0.8.
exponential phase	o2_set3_0300_min_HO2_vs_NRC1f.sig	0.2 > OD < 0.8.
exponential phase	o2_set3_0360_min_HO2_vs_NRC1f.sig	0.2 > OD < 0.8.
exponential phase	o2_set3_0420_min_HO2_vs_NRC1f.sig	0.2 > OD < 0.8.
exponential phase	o2_set3_0540_min_HO2_vs_NRC1f.sig	0.2 > OD < 0.8.
exponential phase	o2_set3_0600_min_HO2_vs_NRC1f.sig	0.2 > OD < 0.8.
exponential phase	o2_set3_0660_min_HO2_vs_NRC1f.sig	0.2 > OD < 0.8.
exponential phase	PQ_Const._set_1_0.25mM_320m_vs_NRC-1f.sig	0.2 > OD < 0.8.
exponential phase	20061006_Cmyc_rep2_0.399_vs_NRC-1e.sig	0.2 > OD < 0.8.
exponential phase	20061006_Cmyc_rep1_0.417_vs_NRC-1e.sig	0.2 > OD < 0.8.
exponential phase	20060818_KO_ura3_rep2_0.376_vs_NRC-1e.sig	0.2 > OD < 0.8.
exponential phase	20060818_KO_ura3_rep1_0.405_vs_NRC-1e.sig	0.2 > OD < 0.8.
exponential phase	20060717_Cmyc_rep2_0.223_vs_NRC-	0.2 > OD < 0.8.

	1e.sig	
exponential phase	20060717_Cmyc_rep2_0.407_vs_NRC-1e.sig	0.2 > OD < 0.8.
exponential phase	20060717_Cmyc_rep1_0.221_vs_NRC-1e.sig	0.2 > OD < 0.8.
exponential phase	20060717_Cmyc_rep1_0.402_vs_NRC-1e.sig	0.2 > OD < 0.8.
exponential phase	20060308_KO_ura3_0.448_vs_NRC-1e.sig	0.2 > OD < 0.8.
exponential phase	20050620_NRC1_rep2_0.505_vs_NRC-1d.sig	0.2 > OD < 0.8.
exponential phase	20050620_NRC1_rep1_0.484_vs_NRC-1d.sig	0.2 > OD < 0.8.
exponential phase	20050620_Cmyc_rep2_0.457_vs_NRC-1d.sig	0.2 > OD < 0.8.
exponential phase	20050620_Cmyc_rep1_0.207_vs_NRC-1d.sig	0.2 > OD < 0.8.
exponential phase	20050620_Cmyc_rep1_0.474_vs_NRC-1d.sig	0.2 > OD < 0.8.
exponential phase	NRC-1e_vs_NRC-1h1.sig	0.2 > OD < 0.8.
exponential phase	H2O2_Recov._set_1_0mM_000min_vs_NRC-1d.sig	0.2 > OD < 0.8.
exponential phase	H2O2_Recov._set_1_0mM_010min_vs_NRC-1d.sig	0.2 > OD < 0.8.
exponential phase	H2O2_Recov._set_1_0mM_020min_vs_NRC-1d.sig	0.2 > OD < 0.8.
exponential phase	H2O2_Recov._set_1_0mM_030min_vs_NRC-1d.sig	0.2 > OD < 0.8.
exponential phase	H2O2_Recov._set_1_0mM_040min_vs_NRC-1d.sig	0.2 > OD < 0.8.
exponential phase	H2O2_Recov._set_1_0mM_050min_vs_NRC-1d.sig	0.2 > OD < 0.8.
exponential phase	H2O2_Recov._set_1_0mM_060min_vs_NRC-1d.sig	0.2 > OD < 0.8.
exponential phase	H2O2_Recov._set_1_0mM_120min_vs_NRC-1d.sig	0.2 > OD < 0.8.
exponential phase	NRC-1.2_0.3063_vs_NRC-1_h1.sig	0.2 > OD < 0.8.
exponential phase	NRC-1.2_0.3895_vs_NRC-1_h1.sig	0.2 > OD < 0.8.
exponential phase	KO_ura3.1_0.3501_vs_NRC-1_h1.sig	0.2 > OD < 0.8.
exponential phase	KO_ura3.1_0.4424_vs_NRC-1_h1.sig	0.2 > OD < 0.8.
exponential phase	KO_ura3.1_0.525_vs_NRC-1_h1.sig	0.2 > OD < 0.8.
exponential phase	NRC-1_0.3279_vs_NRC-1_h1.sig	0.2 > OD < 0.8.
exponential phase	NRC-1_0.3882_vs_NRC-1_h1.sig	0.2 > OD < 0.8.
exponential phase	H2O2_Recov._set_1_50mM_000min_vs_NRC-1d.sig	0.2 > OD < 0.8.
exponential phase	H2O2_Recov._set_1_50mM_010min_vs_NRC-1d.sig	0.2 > OD < 0.8.
exponential phase	H2O2_Recov._set_1_50mM_020min_vs_NRC-1d.sig	0.2 > OD < 0.8.

exponential phase	H2O2_Recov._set_1_50mM_030min_vs_NRC-1d.sig	0.2 > OD < 0.8.
exponential phase	H2O2_Recov._set_1_50mM_040min_vs_NRC-1d.sig	0.2 > OD < 0.8.
exponential phase	H2O2_Recov._set_1_50mM_050min_vs_NRC-1d.sig	0.2 > OD < 0.8.
exponential phase	H2O2_Recov._set_1_50mM_060min_vs_NRC-1d.sig	0.2 > OD < 0.8.
exponential phase	H2O2_Recov._set_1_50mM_120min_vs_NRC-1d.sig	0.2 > OD < 0.8.
gamma	gamma4__2500gy-000min	2500 gy.
gamma	gamma4__2500gy-010min	2500 gy.
gamma	gamma4__2500gy-020min	2500 gy.
gamma	gamma4__2500gy-030min	2500 gy.
gamma	gamma4__2500gy-040min	2500 gy.
gamma	gamma4__2500gy-050min	2500 gy.
gamma	gamma4__2500gy-060min	2500 gy.
gamma	gamma4__2500gy-120min	2500 gy.
gamma	gamma4__2500gy-240min	2500 gy.
gamma	gamma__2500gy-0000m	2500 gy.
gamma	gamma__2500gy-0010m	2500 gy.
gamma	gamma__2500gy-0020m	2500 gy.
gamma	gamma__2500gy-0030m	2500 gy.
gamma	gamma__2500gy-0040m	2500 gy.
gamma	gamma__2500gy-0060m	2500 gy.
gamma	gamma__2500gy-0120m	2500 gy.
gamma	gamma__2500gy-0240m	2500 gy.
gamma	gamma__2500gy-0480m	2500 gy.
gamma	gamma__2500gy-0960m	2500 gy.
gamma	gamma3__2500gy-0000m	2500 gy.
gamma	gamma3__2500gy-0010m	2500 gy.
gamma	gamma3__2500gy-0020m	2500 gy.
gamma	gamma3__2500gy-0030m	2500 gy.
gamma	gamma3__2500gy-0040m	2500 gy.
gamma	gamma3__2500gy-0050m	2500 gy.
gamma	gamma3__2500gy-0060m	2500 gy.
gamma	gamma3__2500gy-0120m	2500 gy.
gamma	gamma3__2500gy-0240m	2500 gy.
gamma	gamma2__2500gy-0000m	2500 gy.
gamma	gamma2__2500gy-0010m	2500 gy.
gamma	gamma2__2500gy-0020m	2500 gy.
gamma	gamma2__2500gy-0030m	2500 gy.
gamma	gamma2__2500gy-0040m	2500 gy.
gamma	gamma2__2500gy-0050m	2500 gy.

gamma	gamma2__2500gy-0060m	2500 gy.
gamma	gamma2__2500gy-0120m	2500 gy.
gamma	gamma2__2500gy-0240m	2500 gy.
glucose perturbation	ura3_+glu_a_OD0.6_vs_NRC1e.sig	7% wv.
glucose perturbation	ura3_+glu_a_OD1.2_vs_NRC1e.sig	7% wv.
glucose perturbation	ura3_+glu_a_OD0.2_vs_NRC1e.sig	7% wv.
glucose perturbation	ura3_+glu_a_OD0.6repl_vs_NRC1e.sig	7% wv.
glucose perturbation	ura3_+glu_a_OD1.2repl_vs_NRC1e.sig	7% wv.
glucose perturbation	ura3_+glu_b_OD0.2_vs_NRC1g.sig	7% wv.
glucose perturbation	ura3_+glu_b_OD0.6repl_vs_NRC1g.sig	7% wv.
glucose perturbation	ura3_+glu_b_OD1.2repl_vs_NRC1g.sig	7% wv.
h202 recovery	H2O2_Recov._set_3_25mM_000min_vs_NRC-1f.sig	cells received perturbation then washed off. Samples were collected when cells were in revocovery
h202 recovery	H2O2_Recov._set_3_25mM_010min_vs_NRC-1f.sig	cells received perturbation then washed off. Samples were collected when cells were in revocovery
h202 recovery	H2O2_Recov._set_3_25mM_020min_vs_NRC-1f.sig	cells received perturbation then washed off. Samples were collected when cells were in revocovery
h202 recovery	H2O2_Recov._set_3_25mM_030min_vs_NRC-1f.sig	cells received perturbation then washed off. Samples were collected when cells were in revocovery
h202 recovery	H2O2_Recov._set_3_25mM_040min_vs_NRC-1f.sig	cells received perturbation then washed off. Samples were collected when cells were in revocovery
h202 recovery	H2O2_Recov._set_3_25mM_050min_vs_NRC-1f.sig	cells received perturbation then washed off. Samples were collected when cells were in revocovery
h202 recovery	H2O2_Recov._set_3_25mM_060min_vs_NRC-1f.sig	cells received perturbation then washed off. Samples were collected when cells were in revocovery
h202 recovery	H2O2_Recov._set_3_25mM_120min_vs_NRC-1f.sig	cells received perturbation then washed off. Samples were collected when cells were in revocovery
h202 recovery	H2O2_Recov._set_3_25mM_240min_vs_NRC-1f.sig	cells received perturbation then washed off. Samples were collected when cells were in revocovery
h202 recovery	H2O2_Recov._set_2_25mM_000min_vs_NRC-1f.sig	cells received perturbation then washed off. Samples were collected when cells were in revocovery

h202 recovery	H2O2_Recov._set_2_25mM_010min_vs_NRC-1f.sig	cells received perturbation then washed off. Samples were collected when cells were in revocovery
h202 recovery	H2O2_Recov._set_2_25mM_020min_vs_NRC-1f.sig	cells received perturbation then washed off. Samples were collected when cells were in revocovery
h202 recovery	H2O2_Recov._set_2_25mM_030min_vs_NRC-1f.sig	cells received perturbation then washed off. Samples were collected when cells were in revocovery
h202 recovery	H2O2_Recov._set_2_25mM_040min_vs_NRC-1f.sig	cells received perturbation then washed off. Samples were collected when cells were in revocovery
h202 recovery	H2O2_Recov._set_2_25mM_050min_vs_NRC-1f.sig	cells received perturbation then washed off. Samples were collected when cells were in revocovery
h202 recovery	H2O2_Recov._set_2_25mM_060min_vs_NRC-1f.sig	cells received perturbation then washed off. Samples were collected when cells were in revocovery
h202 recovery	H2O2_Recov._set_2_25mM_120min_vs_NRC-1f.sig	cells received perturbation then washed off. Samples were collected when cells were in revocovery
h202 recovery	H2O2_Recov._set_2_25mM_240min_vs_NRC-1f.sig	cells received perturbation then washed off. Samples were collected when cells were in revocovery
h202 recovery	H2O2_Recov._set_1_50mM_000min_vs_NRC-1d.sig	cells received perturbation then washed off. Samples were collected when cells were in revocovery
h202 recovery	H2O2_Recov._set_1_50mM_010min_vs_NRC-1d.sig	cells received perturbation then washed off. Samples were collected when cells were in revocovery
h202 recovery	H2O2_Recov._set_1_50mM_020min_vs_NRC-1d.sig	cells received perturbation then washed off. Samples were collected when cells were in revocovery
h202 recovery	H2O2_Recov._set_1_50mM_030min_vs_NRC-1d.sig	cells received perturbation then washed off. Samples were collected when cells were in revocovery
h202 recovery	H2O2_Recov._set_1_50mM_040min_vs_NRC-1d.sig	cells received perturbation then washed off. Samples were collected when cells were in revocovery
h202 recovery	H2O2_Recov._set_1_50mM_050min_vs_NRC-1d.sig	cells received perturbation then washed off. Samples were collected when cells were in revocovery
h202 recovery	H2O2_Recov._set_1_50mM_060min_vs_NRC-1d.sig	cells received perturbation then washed off. Samples were collected when cells were in revocovery
h202 recovery	H2O2_Recov._set_1_50mM_120min_vs_NRC-1d.sig	cells received perturbation then washed off. Samples were collected when cells were in revocovery
h202	H2O2_Const._set_3_25mM_-001min_vs_NRC-1h1.sig	2.5e-2<=mol/L=<5.0e-2.

h202	H2O2_Const._set_3_25mM_005min_vs_NRC-1h1.sig	2.5e-2<=mol/L=<5.0e-2.
h202	H2O2_Const._set_3_25mM_010min_vs_NRC-1h1.sig	2.5e-2<=mol/L=<5.0e-2.
h202	H2O2_Const._set_3_25mM_020min_vs_NRC-1h1.sig	2.5e-2<=mol/L=<5.0e-2.
h202	H2O2_Const._set_3_25mM_040min_vs_NRC-1h1.sig	2.5e-2<=mol/L=<5.0e-2.
h202	H2O2_Const._set_3_25mM_080min_vs_NRC-1h1.sig	2.5e-2<=mol/L=<5.0e-2.
h202	H2O2_Const._set_3_25mM_160min_vs_NRC-1h1.sig	2.5e-2<=mol/L=<5.0e-2.
h202	H2O2_Const._set_4_25mM_-001min_vs_NRC-1h1.sig	2.5e-2<=mol/L=<5.0e-2.
h202	H2O2_Const._set_4_25mM_005min_vs_NRC-1h1.sig	2.5e-2<=mol/L=<5.0e-2.
h202	H2O2_Const._set_4_25mM_010min_vs_NRC-1h1.sig	2.5e-2<=mol/L=<5.0e-2.
h202	H2O2_Const._set_4_25mM_020min_vs_NRC-1h1.sig	2.5e-2<=mol/L=<5.0e-2.
h202	H2O2_Const._set_4_25mM_040min_vs_NRC-1h1.sig	2.5e-2<=mol/L=<5.0e-2.
h202	H2O2_Const._set_4_25mM_080min_vs_NRC-1h1.sig	2.5e-2<=mol/L=<5.0e-2.
h202	H2O2_Const._set_4_25mM_160min_vs_NRC-1h1.sig	2.5e-2<=mol/L=<5.0e-2.
h202	H2O2_Recov._set_3_25mM_000min_vs_NRC-1f.sig	2.5e-2<=mol/L=<5.0e-2.
h202	H2O2_Recov._set_3_25mM_010min_vs_NRC-1f.sig	2.5e-2<=mol/L=<5.0e-2.
h202	H2O2_Recov._set_3_25mM_020min_vs_NRC-1f.sig	2.5e-2<=mol/L=<5.0e-2.
h202	H2O2_Recov._set_3_25mM_030min_vs_NRC-1f.sig	2.5e-2<=mol/L=<5.0e-2.
h202	H2O2_Recov._set_3_25mM_040min_vs_NRC-1f.sig	2.5e-2<=mol/L=<5.0e-2.
h202	H2O2_Recov._set_3_25mM_050min_vs_NRC-1f.sig	2.5e-2<=mol/L=<5.0e-2.
h202	H2O2_Recov._set_3_25mM_060min_vs_NRC-1f.sig	2.5e-2<=mol/L=<5.0e-2.
h202	H2O2_Recov._set_3_25mM_120min_vs_NRC-1f.sig	2.5e-2<=mol/L=<5.0e-2.
h202	H2O2_Recov._set_3_25mM_240min_vs_NRC-1f.sig	2.5e-2<=mol/L=<5.0e-2.
h202	H2O2_Const._set_2_25mM_000min_vs_NRC-1f.sig	2.5e-2<=mol/L=<5.0e-2.
h202	H2O2_Const._set_2_25mM_030min_vs_NRC-1f.sig	2.5e-2<=mol/L=<5.0e-2.
h202	H2O2_Const._set_2_25mM_060min_vs_NRC-1f.sig	2.5e-2<=mol/L=<5.0e-2.

h202	H2O2_Const._set_2_25mM_120min_vs_NRC-1f.sig	2.5e-2<=mol/L=<5.0e-2.
h202	H2O2_Const._set_2_25mM_240min_vs_NRC-1f.sig	2.5e-2<=mol/L=<5.0e-2.
h202	H2O2_Recov._set_2_25mM_000min_vs_NRC-1f.sig	2.5e-2<=mol/L=<5.0e-2.
h202	H2O2_Recov._set_2_25mM_010min_vs_NRC-1f.sig	2.5e-2<=mol/L=<5.0e-2.
h202	H2O2_Recov._set_2_25mM_020min_vs_NRC-1f.sig	2.5e-2<=mol/L=<5.0e-2.
h202	H2O2_Recov._set_2_25mM_030min_vs_NRC-1f.sig	2.5e-2<=mol/L=<5.0e-2.
h202	H2O2_Recov._set_2_25mM_040min_vs_NRC-1f.sig	2.5e-2<=mol/L=<5.0e-2.
h202	H2O2_Recov._set_2_25mM_050min_vs_NRC-1f.sig	2.5e-2<=mol/L=<5.0e-2.
h202	H2O2_Recov._set_2_25mM_060min_vs_NRC-1f.sig	2.5e-2<=mol/L=<5.0e-2.
h202	H2O2_Recov._set_2_25mM_120min_vs_NRC-1f.sig	2.5e-2<=mol/L=<5.0e-2.
h202	H2O2_Recov._set_2_25mM_240min_vs_NRC-1f.sig	2.5e-2<=mol/L=<5.0e-2.
h202	H2O2_Const._set_1_25mM_000min_vs_NRC-1f.sig	2.5e-2<=mol/L=<5.0e-2.
h202	H2O2_Const._set_1_25mM_030min_vs_NRC-1f.sig	2.5e-2<=mol/L=<5.0e-2.
h202	H2O2_Const._set_1_25mM_060min_vs_NRC-1f.sig	2.5e-2<=mol/L=<5.0e-2.
h202	H2O2_Const._set_1_25mM_120min_vs_NRC-1f.sig	2.5e-2<=mol/L=<5.0e-2.
h202	H2O2_Const._set_1_25mM_240min_vs_NRC-1f.sig	2.5e-2<=mol/L=<5.0e-2.
h202	H2O2_Recov._set_1_50mM_000min_vs_NRC-1d.sig	2.5e-2<=mol/L=<5.0e-2.
h202	H2O2_Recov._set_1_50mM_010min_vs_NRC-1d.sig	2.5e-2<=mol/L=<5.0e-2.
h202	H2O2_Recov._set_1_50mM_020min_vs_NRC-1d.sig	2.5e-2<=mol/L=<5.0e-2.
h202	H2O2_Recov._set_1_50mM_030min_vs_NRC-1d.sig	2.5e-2<=mol/L=<5.0e-2.
h202	H2O2_Recov._set_1_50mM_040min_vs_NRC-1d.sig	2.5e-2<=mol/L=<5.0e-2.
h202	H2O2_Recov._set_1_50mM_050min_vs_NRC-1d.sig	2.5e-2<=mol/L=<5.0e-2.
h202	H2O2_Recov._set_1_50mM_060min_vs_NRC-1d.sig	2.5e-2<=mol/L=<5.0e-2.
h202	H2O2_Recov._set_1_50mM_120min_vs_NRC-1d.sig	2.5e-2<=mol/L=<5.0e-2.
high atp level	o2_set3_0360_min_HO2_vs_NRC1f.sig	atp (mol/L) > 1.5.
high atp level	o2_set3_0540_min_HO2_vs_NRC1f.sig	atp (mol/L) > 1.5.

high atp level	o2_set3_0600_min_HO2_vs_NRC1f.sig	atp (mol/L) > 1.5.
high atp level	o2_set3_0660_min_HO2_vs_NRC1f.sig	atp (mol/L) > 1.5.
high copper	cu__0850um_vs_NRC-1	mol/L>0.8e-3.
high copper	cu__1000um_vs_NRC-1	mol/L>0.8e-3.
high copper	Cu_-5_vs_NRC-1.sig	mol/L>0.8e-3.
high copper	Cu_000_vs_NRC-1.sig	mol/L>0.8e-3.
high copper	Cu_005_vs_NRC-1.sig	mol/L>0.8e-3.
high copper	Cu_010_vs_NRC-1.sig	mol/L>0.8e-3.
high copper	Cu_020_vs_NRC-1.sig	mol/L>0.8e-3.
high copper	Cu_040_vs_NRC-1.sig	mol/L>0.8e-3.
high copper	Cu_080_vs_NRC-1.sig	mol/L>0.8e-3.
high copper	Cu_160_vs_NRC-1.sig	mol/L>0.8e-3.
high copper	Cu_-1_vs_NRC-1e.sig	mol/L>0.8e-3.
high copper	Cu_000_vs_NRC-1e.sig	mol/L>0.8e-3.
high copper	Cu_005_vs_NRC-1e.sig	mol/L>0.8e-3.
high copper	Cu_010_vs_NRC-1e.sig	mol/L>0.8e-3.
high copper	Cu_020_vs_NRC-1e.sig	mol/L>0.8e-3.
high copper	Cu_040_vs_NRC-1e.sig	mol/L>0.8e-3.
high copper	Cu_080_vs_NRC-1e.sig	mol/L>0.8e-3.
high copper	Cu_160_vs_NRC-1e.sig	mol/L>0.8e-3.
high copper	Cu_320_vs_NRC-1e.sig	mol/L>0.8e-3.
high copper	Cu_NRC1_set1_-030min_vs_NRC-1h1.sig	mol/L>0.8e-3.
high copper	Cu_NRC1_set1_000min_vs_NRC-1h1.sig	mol/L>0.8e-3.
high copper	Cu_NRC1_set1_005min_vs_NRC-1h1.sig	mol/L>0.8e-3.
high copper	Cu_NRC1_set1_010min_vs_NRC-1h1.sig	mol/L>0.8e-3.
high copper	Cu_NRC1_set1_020min_vs_NRC-1h1.sig	mol/L>0.8e-3.
high copper	Cu_NRC1_set1_040min_vs_NRC-1h1.sig	mol/L>0.8e-3.
high copper	Cu_NRC1_set1_080min_vs_NRC-1h1.sig	mol/L>0.8e-3.
high copper	Cu_NRC1_set1_160min_vs_NRC-1h1.sig	mol/L>0.8e-3.
high copper	Cu_ura3_KO_set1_-030min_vs_NRC-1h1.sig	mol/L>0.8e-3.
high copper	Cu_ura3_KO_set1_000min_vs_NRC-1h1.sig	mol/L>0.8e-3.
high copper	Cu_ura3_KO_set1_005min_vs_NRC-1h1.sig	mol/L>0.8e-3.
high copper	Cu_ura3_KO_set1_010min_vs_NRC-1h1.sig	mol/L>0.8e-3.
high copper	Cu_ura3_KO_set1_020min_vs_NRC-1h1.sig	mol/L>0.8e-3.
high copper	Cu_ura3_KO_set1_040min_vs_NRC-1h1.sig	mol/L>0.8e-3.
high copper	Cu_ura3_KO_set1_080min_vs_NRC-1h1.sig	mol/L>0.8e-3.
high copper	Cu_ura3_KO_set1_160min_vs_NRC-1h1.sig	mol/L>0.8e-3.

high copper	Cu_ura3_KO_set2_-030min_vs_NRC-1h1.sig	mol/L>0.8e-3.
high copper	Cu_ura3_KO_set2_000min_vs_NRC-1h1.sig	mol/L>0.8e-3.
high copper	Cu_ura3_KO_set2_005min_vs_NRC-1h1.sig	mol/L>0.8e-3.
high copper	Cu_ura3_KO_set2_010min_vs_NRC-1h1.sig	mol/L>0.8e-3.
high copper	Cu_ura3_KO_set2_020min_vs_NRC-1h1.sig	mol/L>0.8e-3.
high copper	Cu_ura3_KO_set2_040min_vs_NRC-1h1.sig	mol/L>0.8e-3.
high copper	Cu_ura3_KO_set2_080min_vs_NRC-1h1.sig	mol/L>0.8e-3.
high copper	Cu_ura3_KO_set2_160min_vs_NRC-1h1.sig	mol/L>0.8e-3.
high copper	Cu_NRC1_set2_-030min_vs_NRC-1h1.sig	mol/L>0.8e-3.
high copper	Cu_NRC1_set2_000min_vs_NRC-1h1.sig	mol/L>0.8e-3.
high copper	Cu_NRC1_set2_005min_vs_NRC-1h1.sig	mol/L>0.8e-3.
high copper	Cu_NRC1_set2_010min_vs_NRC-1h1.sig	mol/L>0.8e-3.
high copper	Cu_NRC1_set2_020min_vs_NRC-1h1.sig	mol/L>0.8e-3.
high copper	Cu_NRC1_set2_040min_vs_NRC-1h1.sig	mol/L>0.8e-3.
high copper	Cu_NRC1_set2_080min_vs_NRC-1h1.sig	mol/L>0.8e-3.
high copper	Cu_NRC1_set2_160min_vs_NRC-1h1.sig	mol/L>0.8e-3.
high copper	ura3_Cu_0850um_a_vs_NRC-1d.sig	mol/L>0.8e-3.
high copper	ura3_Cu_0850um_b_vs_NRC-1d.sig	mol/L>0.8e-3.
high copper	ura3_Cu_1000um_a_vs_NRC-1d.sig	mol/L>0.8e-3.
high copper	ura3_Cu_1000um_b_vs_NRC-1d.sig	mol/L>0.8e-3.
high copper	sDura3_pCu_d1.000mM_t+015m_vs_NRC-1h1.sig	mol/L>0.8e-3.
high copper	sDura3_pCu_d1.000mM_t+030m_vs_NRC-1h1.sig	mol/L>0.8e-3.
high copper	sDura3_pCu_d1.000mM_t+060m_vs_NRC-1h1.sig	mol/L>0.8e-3.
high copper	sDura3_pCu_d1.000mM_t+180m_vs_NRC-1h1.sig	mol/L>0.8e-3.
high copper	sDura3_pCu_d1.000mM_t-015m_vs_NRC-1h1.sig	mol/L>0.8e-3.
high h202 recovery	H2O2_Recov._set_1_50mM_000min_vs_NRC-1d.sig	5e-2 mol/L.
high h202 recovery	H2O2_Recov._set_1_50mM_010min_vs_NRC-1d.sig	5e-2 mol/L.
high h202 recovery	H2O2_Recov._set_1_50mM_020min_vs_NRC-1d.sig	5e-2 mol/L.
high h202 recovery	H2O2_Recov._set_1_50mM_030min_vs_NRC-1d.sig	5e-2 mol/L.
high h202 recovery	H2O2_Recov._set_1_50mM_040min_vs_NRC-1d.sig	5e-2 mol/L.

high h202 recovery	H2O2_Recov._set_1_50mM_050min_vs_NRC-1d.sig	5e-2 mol/L.
high h202 recovery	H2O2_Recov._set_1_50mM_060min_vs_NRC-1d.sig	5e-2 mol/L.
high h202 recovery	H2O2_Recov._set_1_50mM_120min_vs_NRC-1d.sig	5e-2 mol/L.
high iron	fe__4000um_vs_NRC-1	>=4e-3 mol/L.
high iron	fe__6000um_vs_NRC-1	>=4e-3 mol/L.
high iron	fe__7000um_vs_NRC-1	>=4e-3 mol/L.
high iron	feso4__-0001m_vs_NRC-1	>=4e-3 mol/L.
high iron	feso4__0000m_vs_NRC-1	>=4e-3 mol/L.
high iron	feso4__0005m_vs_NRC-1b	>=4e-3 mol/L.
high iron	feso4__0010m_vs_NRC-1b	>=4e-3 mol/L.
high iron	feso4__0015m_vs_NRC-1b	>=4e-3 mol/L.
high iron	feso4__0020m_vs_NRC-1	>=4e-3 mol/L.
high iron	feso4__0025m_vs_NRC-1b	>=4e-3 mol/L.
high iron	feso4__0040m_vs_NRC-1	>=4e-3 mol/L.
high iron	feso4__0080m_vs_NRC-1	>=4e-3 mol/L.
high iron	feso4__0160m_vs_NRC-1	>=4e-3 mol/L.
high iron	feso4__0320m_vs_NRC-1	>=4e-3 mol/L.
high light	light2__1440m_vs_light1_3960m	> 100 mol/m2/s.
high light	light2__1620m_vs_light1_3960m	> 100 mol/m2/s.
high light	light2__1800m_vs_light1_3960m	> 100 mol/m2/s.
high light	light2__1980m_vs_light1_3960m	> 100 mol/m2/s.
high light	light2__2160m_vs_light1_3960m	> 100 mol/m2/s.
high light	light2__2340m_vs_light1_3960m	> 100 mol/m2/s.
high light	light2__2520m_vs_light1_3960m	> 100 mol/m2/s.
high light	light2__2700m_vs_light1_3960m	> 100 mol/m2/s.
high light	light2__2880m_vs_light1_3960m	> 100 mol/m2/s.
high light	light2__3060m_vs_light1_3960m	> 100 mol/m2/s.
high light	light2__3240m_vs_light1_3960m	> 100 mol/m2/s.
high light	light2__3420m_vs_light1_3960m	> 100 mol/m2/s.
high light	light2__3600m_vs_light1_3960m	> 100 mol/m2/s.
high light	light2__3780m_vs_light1_3960m	> 100 mol/m2/s.
high light	light2__3960m_vs_light1_3960m	> 100 mol/m2/s.
high light	light2__4140m_vs_light1_3960m	> 100 mol/m2/s.
high light	light2__4320m_vs_light1_3960m	> 100 mol/m2/s.
high light	light2__4500m_vs_light1_3960m	> 100 mol/m2/s.
high light	light2__4680m_vs_light1_3960m	> 100 mol/m2/s.
high light	light2__4860m_vs_light1_3960m	> 100 mol/m2/s.
high light	light2__5040m_vs_light1_3960m	> 100 mol/m2/s.
high light	light2__5220m_vs_light1_3960m	> 100 mol/m2/s.
high light	light2__5400m_vs_light1_3960m	> 100 mol/m2/s.

high light	light2__5580m_vs_light1_3960m	> 100 mol/m2/s.
high light	light2__5760m_vs_light1_3960m	> 100 mol/m2/s.
high light	Circadian_Dark10_Cycling_-2120min_vs_NRC-1h1.sig	> 100 mol/m2/s.
high light	Circadian_Dark10_Cycling_-1960min_vs_NRC-1h1.sig	> 100 mol/m2/s.
high light	Circadian_Dark10_Cycling_-1785min_vs_NRC-1h1.sig	> 100 mol/m2/s.
high light	Circadian_Dark10_Cycling_-1595min_vs_NRC-1h1.sig	> 100 mol/m2/s.
high light	Circadian_Dark10_Cycling_-0690min_vs_NRC-1h1.sig	> 100 mol/m2/s.
high light	Circadian_Dark10_Cycling_-0525min_vs_NRC-1h1.sig	> 100 mol/m2/s.
high light	Circadian_Dark10_Cycling_-0360min_vs_NRC-1h1.sig	> 100 mol/m2/s.
high light	Circadian_Dark10_Cycling_-0165min_vs_NRC-1h1.sig	> 100 mol/m2/s.
high light	circadian__dark_cycling_125w/m2_42C_1440min_vs_NRC-1d.sig	> 100 mol/m2/s.
high light	circadian__dark_cycling_125w/m2_42C_1615min_vs_NRC-1d.sig	> 100 mol/m2/s.
high light	circadian__dark_cycling_125w/m2_42C_1800min_vs_NRC-1d.sig	> 100 mol/m2/s.
high light	circadian__dark_cycling_125w/m2_42C_1985min_vs_NRC-1d.sig	> 100 mol/m2/s.
high light	circadian__dark_cycling_125w/m2_42C_2880min_vs_NRC-1d.sig	> 100 mol/m2/s.
high light	Dun_F2_000minb_vs_NRC-1g.sig	> 100 mol/m2/s.
high light	Dun_F2_005minb_vs_NRC-1g.sig	> 100 mol/m2/s.
high light	Dun_F2_010minb_vs_NRC-1g.sig	> 100 mol/m2/s.
high light	Dun_F2_020minb_vs_NRC-1g.sig	> 100 mol/m2/s.
high light	Dun_F2_040minb_vs_NRC-1g.sig	> 100 mol/m2/s.
high light	Dun_F2_080minb_vs_NRC-1g.sig	> 100 mol/m2/s.
high light	Dun_F2_160minb_vs_NRC-1g.sig	> 100 mol/m2/s.
high light	Dun_F2_320minb_vs_NRC-1g.sig	> 100 mol/m2/s.
high light	NRC1_03720_0.234_rep2_vs_NRC-1g.sig	> 100 mol/m2/s.
high light	NRC1_03960_0.409_rep2_vs_NRC-1g.sig	> 100 mol/m2/s.
high light	NRC1_04320_0.578_rep2_vs_NRC-1g.sig	> 100 mol/m2/s.
high light	NRC1_04476_0.715_rep2_vs_NRC-1g.sig	> 100 mol/m2/s.
high light	NRC1_05400_0.786_rep2_vs_NRC-1g.sig	> 100 mol/m2/s.
high light	NRC1_05778_0.722_rep2_vs_NRC-1g.sig	> 100 mol/m2/s.
high light	NRC1_07020_1.318_rep2_vs_NRC-1g.sig	> 100 mol/m2/s.
high light	NRC1_07740_2.681_rep2_vs_NRC-1g.sig	> 100 mol/m2/s.
high light	NRC1_08460_3.840_rep2_vs_NRC-1g.sig	> 100 mol/m2/s.
high light	NRC1_09540_4.690_rep2_vs_NRC-1g.sig	> 100 mol/m2/s.

high light	NRC1_10260_4.540_rep2_vs_NRC-1g.sig	> 100 mol/m2/s.
high light	NRC1_10980_4.935_rep2_vs_NRC-1g.sig	> 100 mol/m2/s.
high light	NRC1_11700_5.730_rep2_vs_NRC-1g.sig	> 100 mol/m2/s.
high light	NRC1_03720_0.259_rep1_vs_NRC-1g.sig	> 100 mol/m2/s.
high light	NRC1_03960_0.364_rep1_vs_NRC-1g.sig	> 100 mol/m2/s.
high light	NRC1_04320_0.590_rep1_vs_NRC-1g.sig	> 100 mol/m2/s.
high light	NRC1_04476_0.762_rep1_vs_NRC-1g.sig	> 100 mol/m2/s.
high light	NRC1_05400_0.803_rep1_vs_NRC-1g.sig	> 100 mol/m2/s.
high light	NRC1_05778_0.710_rep1vs_NRC-1g.sig	> 100 mol/m2/s.
high light	NRC1_07020_1.329_rep1_vs_NRC-1g.sig	> 100 mol/m2/s.
high light	NRC1_07740_2.580_rep1_vs_NRC-1g.sig	> 100 mol/m2/s.
high light	NRC1_08460_3.510_rep1_vs_NRC-1g.sig	> 100 mol/m2/s.
high light	NRC1_09540_4.860_rep1_vs_NRC-1g.sig	> 100 mol/m2/s.
high light	NRC1_10260_4.860_rep1_vs_NRC-1g.sig	> 100 mol/m2/s.
high light	NRC1_10980_5.130_rep1_vs_NRC-1g.sig	> 100 mol/m2/s.
high light	NRC1_11700_5.640_rep1_vs_NRC-1g.sig	> 100 mol/m2/s.
high manganese	sirR_Mn_1500um_a_vs_NRC-1d.sig	1.5e-3 mol/L.
high manganese	sirR_Mn_1500um_b_vs_NRC-1d.sig	1.5e-3 mol/L.
high manganese	ura3_Mn_1500um_a_vs_NRC-1d.sig	1.5e-3 mol/L.
high manganese	ura3_Mn_1500um_b_vs_NRC-1d.sig	1.5e-3 mol/L.
high manganese	mn__1500um_vs_NRC-1	1.5e-3 mol/L.
high oxygen	o2_set1_-001m_L2H_005_vs_NRC-1c	>75 pct
high oxygen	o2_set1_0001m_L2H_500_vs_NRC-1c	>75 pct
high oxygen	o2_set1_0005m_H_922_vs_NRC-1c	>75 pct
high oxygen	o2_set1_0010m_H_947_vs_NRC-1c	>75 pct
high oxygen	o2_set1_0020m_H_937_vs_NRC-1c	>75 pct
high oxygen	o2_set1_0030m_H_931_vs_NRC-1c	>75 pct
high oxygen	o2_set1_0045m_H_939_vs_NRC-1c	>75 pct
high oxygen	o2_set1_0090m_H_941_vs_NRC-1c	>75 pct
high oxygen	o2_set1_0180m_H_930_vs_NRC-1c	>75 pct
high oxygen	o2_set1_0360m_H_903_vs_NRC-1c	>75 pct
high oxygen	o2_set1_0362m_H2L_860_vs_NRC-1c	>75 pct
high oxygen	o2_set1_0755m_L2H_825_vs_NRC-1c	>75 pct
high oxygen	o2_set1_0760m_L2H_847_vs_NRC-1c	>75 pct
high oxygen	o2_set1_0770m_L2H_852_vs_NRC-1c	>75 pct
high oxygen	o2_set1_0780m_L2H_847_vs_NRC-1c	>75 pct
high oxygen	o2_set2_H_L_000_vs_NRC-1d.sig	>75 pct
high oxygen	o2_set3_-0005_min_LO2_vs_NRC1f.sig	>75 pct
high oxygen	o2_set3_0000_min_L2HO2_vs_NRC1f.sig	>75 pct
high oxygen	o2_set3_0005_min_HO2_vs_NRC1f.sig	>75 pct
high oxygen	o2_set3_0010_min_HO2_vs_NRC1f.sig	>75 pct
high oxygen	o2_set3_0020_min_HO2_vs_NRC1f.sig	>75 pct

high oxygen	o2_set3_0030_min_HO2_vs_NRC1f.sig	>75 pct
high oxygen	o2_set3_0045_min_HO2_vs_NRC1f.sig	>75 pct
high oxygen	o2_set3_0060_min_HO2_vs_NRC1f.sig	>75 pct
high oxygen	o2_set3_0090_min_HO2_vs_NRC1f.sig	>75 pct
high oxygen	o2_set3_0120_min_HO2_vs_NRC1f.sig	>75 pct
high oxygen	o2_set3_0180_min_HO2_vs_NRC1f.sig	>75 pct
high oxygen	o2_set3_0240_min_HO2_vs_NRC1f.sig	>75 pct
high oxygen	o2_set3_0300_min_HO2_vs_NRC1f.sig	>75 pct
high oxygen	o2_set3_0360_min_HO2_vs_NRC1f.sig	>75 pct
high oxygen	o2_set3_0420_min_HO2_vs_NRC1f.sig	>75 pct
high oxygen	o2_set3_0540_min_HO2_vs_NRC1f.sig	>75 pct
high oxygen	o2_set3_0600_min_HO2_vs_NRC1f.sig	>75 pct
high oxygen	o2_set3_0660_min_HO2_vs_NRC1f.sig	>75 pct
high oxygen shift	o2_set1_-001m_L2H_005_vs_NRC-1c	high oxygen (chemostat) 90.3%-94.7%
high oxygen shift	o2_set1_0001m_L2H_500_vs_NRC-1c	high oxygen (chemostat) 90.3%-94.7%
high oxygen shift	o2_set1_0005m_H_922_vs_NRC-1c	high oxygen (chemostat) 90.3%-94.7%
high oxygen shift	o2_set1_0010m_H_947_vs_NRC-1c	high oxygen (chemostat) 90.3%-94.7%
high oxygen shift	o2_set1_0020m_H_937_vs_NRC-1c	high oxygen (chemostat) 90.3%-94.7%
high oxygen shift	o2_set1_0030m_H_931_vs_NRC-1c	high oxygen (chemostat) 90.3%-94.7%
high oxygen shift	o2_set1_0045m_H_939_vs_NRC-1c	high oxygen (chemostat) 90.3%-94.7%
high oxygen shift	o2_set1_0090m_H_941_vs_NRC-1c	high oxygen (chemostat) 90.3%-94.7%
high oxygen shift	o2_set1_0180m_H_930_vs_NRC-1c	high oxygen (chemostat) 90.3%-94.7%
high oxygen shift	o2_set1_0360m_H_903_vs_NRC-1c	high oxygen (chemostat) 90.3%-94.7%
high paraquat constant	PQ_Const._set_3_4mM_-001min_vs_NRC-1h1.sig	constant perturbation
high paraquat constant	PQ_Const._set_3_4mM_005min_vs_NRC-1h1.sig	constant perturbation
high paraquat constant	PQ_Const._set_3_4mM_010min_vs_NRC-1h1.sig	constant perturbation
high paraquat constant	PQ_Const._set_3_4mM_020min_vs_NRC-1h1.sig	constant perturbation
high paraquat constant	PQ_Const._set_3_4mM_040min_vs_NRC-1h1.sig	constant perturbation
high paraquat constant	PQ_Const._set_3_4mM_080min_vs_NRC-1h1.sig	constant perturbation
high paraquat constant	PQ_Const._set_3_4mM_160min_vs_NRC-1h1.sig	constant perturbation
high paraquat constant	PQ_Const._set_4_4mM_-001min_vs_NRC-1h1.sig	constant perturbation
high paraquat constant	PQ_Const._set_4_4mM_005min_vs_NRC-1h1.sig	constant perturbation
high paraquat constant	PQ_Const._set_4_4mM_010min_vs_NRC-1h1.sig	constant perturbation
high paraquat constant	PQ_Const._set_4_4mM_020min_vs_NRC-1h1.sig	constant perturbation

high paraquat constant	PQ_Const._set_4_4mM_040min_vs_NRC-1h1.sig	constant perturbation
high paraquat constant	PQ_Const._set_4_4mM_080min_vs_NRC-1h1.sig	constant perturbation
high paraquat constant	PQ_Const._set_4_4mM_160min_vs_NRC-1h1.sig	constant perturbation
high paraquat constant	PQ_Const._set_2_4mM_000min_vs_NRC-1f.sig	constant perturbation
high paraquat constant	PQ_Const._set_2_4mM_030min_vs_NRC-1f.sig	constant perturbation
high paraquat constant	PQ_Const._set_2_4mM_060min_vs_NRC-1f.sig	constant perturbation
high paraquat constant	PQ_Const._set_2_4mM_120min_vs_NRC-1f.sig	constant perturbation
high paraquat constant	PQ_Const._set_2_4mM_240min_vs_NRC-1f.sig	constant perturbation
high paraquat constant	PQ_Const._set_1_4mM_000min_vs_NRC-1f.sig	constant perturbation
high paraquat constant	PQ_Const._set_1_4mM_030min_vs_NRC-1f.sig	constant perturbation
high paraquat constant	PQ_Const._set_1_4mM_060min_vs_NRC-1f.sig	constant perturbation
high paraquat constant	PQ_Const._set_1_4mM_120min_vs_NRC-1f.sig	constant perturbation
high paraquat constant	PQ_Const._set_1_4mM_240min_vs_NRC-1f.sig	constant perturbation
high paraquat recovery	PQ_Recov._set_2_4mM_000min_vs_NRC-1f.sig	cells received perturbation then washed off. Samples were collected when cells were in revocovery
high paraquat recovery	PQ_Recov._set_2_4mM_010min_vs_NRC-1f.sig	cells received perturbation then washed off. Samples were collected when cells were in revocovery
high paraquat recovery	PQ_Recov._set_2_4mM_020min_vs_NRC-1f.sig	cells received perturbation then washed off. Samples were collected when cells were in revocovery
high paraquat recovery	PQ_Recov._set_2_4mM_030min_vs_NRC-1f.sig	cells received perturbation then washed off. Samples were collected when cells were in revocovery
high paraquat recovery	PQ_Recov._set_2_4mM_040min_vs_NRC-1f.sig	cells received perturbation then washed off. Samples were collected when cells were in revocovery
high paraquat recovery	PQ_Recov._set_2_4mM_050min_vs_NRC-1f.sig	cells received perturbation then washed off. Samples were collected when cells were in revocovery
high paraquat recovery	PQ_Recov._set_2_4mM_060min_vs_NRC-1f.sig	cells received perturbation then washed off. Samples were collected when cells were in revocovery
high paraquat recovery	PQ_Recov._set_2_4mM_120min_vs_NRC-1f.sig	cells received perturbation then washed off. Samples were collected when cells were in revocovery

high paraquat recovery	PQ_Recov._set_2_4mM_240min_vs_NRC-1f.sig	cells received perturbation then washed off. Samples were collected when cells were in revocovery
high paraquat recovery	PQ_Recov._set_1_4mM_000min_vs_NRC-1f.sig	cells received perturbation then washed off. Samples were collected when cells were in revocovery
high paraquat recovery	PQ_Recov._set_1_4mM_010min_vs_NRC-1f.sig	cells received perturbation then washed off. Samples were collected when cells were in revocovery
high paraquat recovery	PQ_Recov._set_1_4mM_020min_vs_NRC-1f.sig	cells received perturbation then washed off. Samples were collected when cells were in revocovery
high paraquat recovery	PQ_Recov._set_1_4mM_030min_vs_NRC-1f.sig	cells received perturbation then washed off. Samples were collected when cells were in revocovery
high paraquat recovery	PQ_Recov._set_1_4mM_040min_vs_NRC-1f.sig	cells received perturbation then washed off. Samples were collected when cells were in revocovery
high paraquat recovery	PQ_Recov._set_1_4mM_050min_vs_NRC-1f.sig	cells received perturbation then washed off. Samples were collected when cells were in revocovery
high paraquat recovery	PQ_Recov._set_1_4mM_060min_vs_NRC-1f.sig	cells received perturbation then washed off. Samples were collected when cells were in revocovery
high paraquat recovery	PQ_Recov._set_1_4mM_120min_vs_NRC-1f.sig	cells received perturbation then washed off. Samples were collected when cells were in revocovery
high paraquat recovery	PQ_Recov._set_1_4mM_240min_vs_NRC-1f.sig	cells received perturbation then washed off. Samples were collected when cells were in revocovery
high paraquat	PQ_Const._set_3_4mM_-001min_vs_NRC-1h1.sig	4e-3 mol/L.
high paraquat	PQ_Const._set_3_4mM_005min_vs_NRC-1h1.sig	4e-3 mol/L.
high paraquat	PQ_Const._set_3_4mM_010min_vs_NRC-1h1.sig	4e-3 mol/L.
high paraquat	PQ_Const._set_3_4mM_020min_vs_NRC-1h1.sig	4e-3 mol/L.
high paraquat	PQ_Const._set_3_4mM_040min_vs_NRC-1h1.sig	4e-3 mol/L.
high paraquat	PQ_Const._set_3_4mM_080min_vs_NRC-1h1.sig	4e-3 mol/L.
high paraquat	PQ_Const._set_3_4mM_160min_vs_NRC-1h1.sig	4e-3 mol/L.
high paraquat	PQ_Const._set_4_4mM_-001min_vs_NRC-1h1.sig	4e-3 mol/L.
high paraquat	PQ_Const._set_4_4mM_005min_vs_NRC-1h1.sig	4e-3 mol/L.
high paraquat	PQ_Const._set_4_4mM_010min_vs_NRC-1h1.sig	4e-3 mol/L.
high paraquat	PQ_Const._set_4_4mM_020min_vs_NRC-	4e-3 mol/L.

	1h1.sig	
high paraquat	PQ_Const._set_4_4mM_040min_vs_NRC-1h1.sig	4e-3 mol/L.
high paraquat	PQ_Const._set_4_4mM_080min_vs_NRC-1h1.sig	4e-3 mol/L.
high paraquat	PQ_Const._set_4_4mM_160min_vs_NRC-1h1.sig	4e-3 mol/L.
high paraquat	PQ_Recov._set_2_4mM_000min_vs_NRC-1f.sig	4e-3 mol/L.
high paraquat	PQ_Recov._set_2_4mM_010min_vs_NRC-1f.sig	4e-3 mol/L.
high paraquat	PQ_Recov._set_2_4mM_020min_vs_NRC-1f.sig	4e-3 mol/L.
high paraquat	PQ_Recov._set_2_4mM_030min_vs_NRC-1f.sig	4e-3 mol/L.
high paraquat	PQ_Recov._set_2_4mM_040min_vs_NRC-1f.sig	4e-3 mol/L.
high paraquat	PQ_Recov._set_2_4mM_050min_vs_NRC-1f.sig	4e-3 mol/L.
high paraquat	PQ_Recov._set_2_4mM_060min_vs_NRC-1f.sig	4e-3 mol/L.
high paraquat	PQ_Recov._set_2_4mM_120min_vs_NRC-1f.sig	4e-3 mol/L.
high paraquat	PQ_Recov._set_2_4mM_240min_vs_NRC-1f.sig	4e-3 mol/L.
high paraquat	PQ_Const._set_2_4mM_000min_vs_NRC-1f.sig	4e-3 mol/L.
high paraquat	PQ_Const._set_2_4mM_030min_vs_NRC-1f.sig	4e-3 mol/L.
high paraquat	PQ_Const._set_2_4mM_060min_vs_NRC-1f.sig	4e-3 mol/L.
high paraquat	PQ_Const._set_2_4mM_120min_vs_NRC-1f.sig	4e-3 mol/L.
high paraquat	PQ_Const._set_2_4mM_240min_vs_NRC-1f.sig	4e-3 mol/L.
high paraquat	PQ_Recov._set_1_4mM_000min_vs_NRC-1f.sig	4e-3 mol/L.
high paraquat	PQ_Recov._set_1_4mM_010min_vs_NRC-1f.sig	4e-3 mol/L.
high paraquat	PQ_Recov._set_1_4mM_020min_vs_NRC-1f.sig	4e-3 mol/L.
high paraquat	PQ_Recov._set_1_4mM_030min_vs_NRC-1f.sig	4e-3 mol/L.
high paraquat	PQ_Recov._set_1_4mM_040min_vs_NRC-1f.sig	4e-3 mol/L.
high paraquat	PQ_Recov._set_1_4mM_050min_vs_NRC-1f.sig	4e-3 mol/L.
high paraquat	PQ_Recov._set_1_4mM_060min_vs_NRC-1f.sig	4e-3 mol/L.
high paraquat	PQ_Recov._set_1_4mM_120min_vs_NRC-1f.sig	4e-3 mol/L.

high paraquat	PQ_Recov._set_1_4mM_240min_vs_NRC-1f.sig	4e-3 mol/L.
high paraquat	PQ_Const._set_1_4mM_000min_vs_NRC-1f.sig	4e-3 mol/L.
high paraquat	PQ_Const._set_1_4mM_030min_vs_NRC-1f.sig	4e-3 mol/L.
high paraquat	PQ_Const._set_1_4mM_060min_vs_NRC-1f.sig	4e-3 mol/L.
high paraquat	PQ_Const._set_1_4mM_120min_vs_NRC-1f.sig	4e-3 mol/L.
high paraquat	PQ_Const._set_1_4mM_240min_vs_NRC-1f.sig	4e-3 mol/L.
high temperature	circadian_20051021_cycling_dark_42oC_1440min_vs_NRC-1d.sig	> 40 C
high temperature	circadian_20051021_cycling_dark_42oC_1615min_vs_NRC-1d.sig	> 40 C
high temperature	circadian_20051021_cycling_dark_42oC_1800min_vs_NRC-1d.sig	> 40 C
high temperature	circadian_20051021_cycling_dark_42oC_1985min_vs_NRC-1d.sig	> 40 C
high temperature	circadian_20051021_cycling_dark_42oC_2160min_vs_NRC-1d.sig	> 40 C
high temperature	circadian_20051021_cycling_dark_42oC_2340min_vs_NRC-1d.sig	> 40 C
high temperature	circadian_20051021_cycling_dark_42oC_2515min_vs_NRC-1d.sig	> 40 C
high temperature	circadian_20051021_cycling_dark_42oC_2705min_vs_NRC-1d.sig	> 40 C
high temperature	circadian_20051021_cycling_dark_42oC_2880min_vs_NRC-1d.sig	> 40 C
high temperature	uv__000jm2_CL_060m	> 40 C
high temperature	gamma4__0000gy-000min	> 40 C
high temperature	gamma4__0000gy-010min	> 40 C
high temperature	gamma4__0000gy-020min	> 40 C
high temperature	gamma4__0000gy-030min	> 40 C
high temperature	gamma4__0000gy-040min	> 40 C
high temperature	gamma4__0000gy-050min	> 40 C
high temperature	gamma4__0000gy-060min	> 40 C
high temperature	gamma4__0000gy-120min	> 40 C
high temperature	gamma4__0000gy-240min	> 40 C
high temperature	gamma__0000gy-0000m	> 40 C
high temperature	gamma__0000gy-0010m	> 40 C
high temperature	gamma__0000gy-0030m	> 40 C
high temperature	gamma__0000gy-0060m	> 40 C
high temperature	gamma__0000gy-0240m	> 40 C
high temperature	gamma__0000gy-0960m	> 40 C

high temperature	circadian__dark_cycling_125w/m2_42C_1440min_vs_NRC-1d.sig	> 40 C
high temperature	circadian__dark_cycling_125w/m2_42C_1615min_vs_NRC-1d.sig	> 40 C
high temperature	circadian__dark_cycling_125w/m2_42C_1800min_vs_NRC-1d.sig	> 40 C
high temperature	circadian__dark_cycling_125w/m2_42C_1985min_vs_NRC-1d.sig	> 40 C
high temperature	circadian__dark_cycling_125w/m2_42C_2160min_vs_NRC-1d.sig	> 40 C
high temperature	circadian__dark_cycling_125w/m2_42C_2340min_vs_NRC-1d.sig	> 40 C
high temperature	circadian__dark_cycling_125w/m2_42C_2515min_vs_NRC-1d.sig	> 40 C
high temperature	circadian__dark_cycling_125w/m2_42C_2705min_vs_NRC-1d.sig	> 40 C
high temperature	circadian__dark_cycling_125w/m2_42C_2880min_vs_NRC-1d.sig	> 40 C
high temperature	H2O2_Recov._set_3_0mM_000min_vs_NRC-1f.sig	> 40 C
high temperature	H2O2_Recov._set_3_0mM_010min_vs_NRC-1f.sig	> 40 C
high temperature	H2O2_Recov._set_3_0mM_020min_vs_NRC-1f.sig	> 40 C
high temperature	H2O2_Recov._set_3_0mM_030min_vs_NRC-1f.sig	> 40 C
high temperature	H2O2_Recov._set_3_0mM_040min_vs_NRC-1f.sig	> 40 C
high temperature	H2O2_Recov._set_3_0mM_050min_vs_NRC-1f.sig	> 40 C
high temperature	H2O2_Recov._set_3_0mM_060min_vs_NRC-1f.sig	> 40 C
high temperature	H2O2_Recov._set_3_0mM_120min_vs_NRC-1f.sig	> 40 C
high temperature	H2O2_Recov._set_3_0mM_240min_vs_NRC-1f.sig	> 40 C
high temperature	H2O2_Const._set_2_0mM_000min_vs_NRC-1f.sig	> 40 C
high temperature	H2O2_Const._set_2_0mM_030min_vs_NRC-1f.sig	> 40 C
high temperature	H2O2_Const._set_2_0mM_060min_vs_NRC-1f.sig	> 40 C
high temperature	H2O2_Const._set_2_0mM_120min_vs_NRC-1f.sig	> 40 C
high temperature	H2O2_Const._set_2_0mM_240min_vs_NRC-1f.sig	> 40 C
high temperature	PQ_Recov._set_2_0mM_000min_vs_NRC-1f.sig	> 40 C
high temperature	PQ_Recov._set_2_0mM_010min_vs_NRC-1f.sig	> 40 C

high temperature	PQ_Recov._set_2_0mM_020min_vs_NRC-1f.sig	> 40 C
high temperature	PQ_Recov._set_2_0mM_030min_vs_NRC-1f.sig	> 40 C
high temperature	PQ_Recov._set_2_0mM_040min_vs_NRC-1f.sig	> 40 C
high temperature	PQ_Recov._set_2_0mM_050min_vs_NRC-1f.sig	> 40 C
high temperature	PQ_Recov._set_2_0mM_060min_vs_NRC-1f.sig	> 40 C
high temperature	PQ_Recov._set_2_0mM_120min_vs_NRC-1f.sig	> 40 C
high temperature	PQ_Recov._set_2_0mM_240min_vs_NRC-1f.sig	> 40 C
high temperature	PQ_Const._set_2_0mM_000min_vs_NRC-1f.sig	> 40 C
high temperature	PQ_Const._set_2_0mM_030min_vs_NRC-1f.sig	> 40 C
high temperature	PQ_Const._set_2_0mM_060min_vs_NRC-1f.sig	> 40 C
high temperature	PQ_Const._set_2_0mM_120min_vs_NRC-1f.sig	> 40 C
high temperature	PQ_Const._set_2_0mM_240min_vs_NRC-1f.sig	> 40 C
high temperature	H2O2_Recov._set_2_0mM_000min_vs_NRC-1f.sig	> 40 C
high temperature	H2O2_Recov._set_2_0mM_010min_vs_NRC-1f.sig	> 40 C
high temperature	H2O2_Recov._set_2_0mM_020min_vs_NRC-1f.sig	> 40 C
high temperature	H2O2_Recov._set_2_0mM_030min_vs_NRC-1f.sig	> 40 C
high temperature	H2O2_Recov._set_2_0mM_040min_vs_NRC-1f.sig	> 40 C
high temperature	H2O2_Recov._set_2_0mM_050min_vs_NRC-1f.sig	> 40 C
high temperature	H2O2_Recov._set_2_0mM_060min_vs_NRC-1f.sig	> 40 C
high temperature	H2O2_Recov._set_2_0mM_120min_vs_NRC-1f.sig	> 40 C
high temperature	H2O2_Recov._set_2_0mM_240min_vs_NRC-1f.sig	> 40 C
high temperature	H2O2_Const._set_1_0mM_000min_vs_NRC-1f.sig	> 40 C
high temperature	H2O2_Const._set_1_0mM_030min_vs_NRC-1f.sig	> 40 C
high temperature	H2O2_Const._set_1_0mM_060min_vs_NRC-1f.sig	> 40 C
high temperature	H2O2_Const._set_1_0mM_120min_vs_NRC-1f.sig	> 40 C

high temperature	H2O2_Const._set_1_0mM_240min_vs_NRC-1f.sig	> 40 C
high temperature	PQ_Recov._set_1_0mM_000min_vs_NRC-1f.sig	> 40 C
high temperature	PQ_Recov._set_1_0mM_010min_vs_NRC-1f.sig	> 40 C
high temperature	PQ_Recov._set_1_0mM_020min_vs_NRC-1f.sig	> 40 C
high temperature	PQ_Recov._set_1_0mM_030min_vs_NRC-1f.sig	> 40 C
high temperature	PQ_Recov._set_1_0mM_040min_vs_NRC-1f.sig	> 40 C
high temperature	PQ_Recov._set_1_0mM_050min_vs_NRC-1f.sig	> 40 C
high temperature	PQ_Recov._set_1_0mM_060min_vs_NRC-1f.sig	> 40 C
high temperature	PQ_Recov._set_1_0mM_120min_vs_NRC-1f.sig	> 40 C
high temperature	PQ_Recov._set_1_0mM_240min_vs_NRC-1f.sig	> 40 C
high temperature	PQ_Const._set_1_0mM_000min_vs_NRC-1f.sig	> 40 C
high temperature	PQ_Const._set_1_0mM_030min_vs_NRC-1f.sig	> 40 C
high temperature	PQ_Const._set_1_0mM_060min_vs_NRC-1f.sig	> 40 C
high temperature	PQ_Const._set_1_0mM_120min_vs_NRC-1f.sig	> 40 C
high temperature	PQ_Const._set_1_0mM_240min_vs_NRC-1f.sig	> 40 C
high temperature	EMS_Treated__100000uM-000	> 40 C
high temperature	EMS_Treated__100000uM-010	> 40 C
high temperature	EMS_Treated__100000uM-020	> 40 C
high temperature	EMS_Treated__100000uM-030	> 40 C
high temperature	EMS_Treated__100000uM-040	> 40 C
high temperature	EMS_Treated__100000uM-050	> 40 C
high temperature	EMS_Treated__100000uM-060	> 40 C
high temperature	EMS_Treated__100000uM-120	> 40 C
high temperature	gamma4__2500gy-000min	> 40 C
high temperature	gamma4__2500gy-010min	> 40 C
high temperature	gamma4__2500gy-020min	> 40 C
high temperature	gamma4__2500gy-030min	> 40 C
high temperature	gamma4__2500gy-040min	> 40 C
high temperature	gamma4__2500gy-050min	> 40 C
high temperature	gamma4__2500gy-060min	> 40 C
high temperature	gamma4__2500gy-120min	> 40 C
high temperature	gamma4__2500gy-240min	> 40 C

high temperature	gamma__2500gy-0000m	> 40 C
high temperature	gamma__2500gy-0010m	> 40 C
high temperature	gamma__2500gy-0020m	> 40 C
high temperature	gamma__2500gy-0030m	> 40 C
high temperature	gamma__2500gy-0040m	> 40 C
high temperature	gamma__2500gy-0060m	> 40 C
high temperature	gamma__2500gy-0120m	> 40 C
high temperature	gamma__2500gy-0240m	> 40 C
high temperature	gamma__2500gy-0480m	> 40 C
high temperature	gamma__2500gy-0960m	> 40 C
high temperature	H2O2_Recov._set_3_25mM_000min_vs_NRC-1f.sig	> 40 C
high temperature	H2O2_Recov._set_3_25mM_010min_vs_NRC-1f.sig	> 40 C
high temperature	H2O2_Recov._set_3_25mM_020min_vs_NRC-1f.sig	> 40 C
high temperature	H2O2_Recov._set_3_25mM_030min_vs_NRC-1f.sig	> 40 C
high temperature	H2O2_Recov._set_3_25mM_040min_vs_NRC-1f.sig	> 40 C
high temperature	H2O2_Recov._set_3_25mM_050min_vs_NRC-1f.sig	> 40 C
high temperature	H2O2_Recov._set_3_25mM_060min_vs_NRC-1f.sig	> 40 C
high temperature	H2O2_Recov._set_3_25mM_120min_vs_NRC-1f.sig	> 40 C
high temperature	H2O2_Recov._set_3_25mM_240min_vs_NRC-1f.sig	> 40 C
high temperature	H2O2_Const._set_2_25mM_000min_vs_NRC-1f.sig	> 40 C
high temperature	H2O2_Const._set_2_25mM_030min_vs_NRC-1f.sig	> 40 C
high temperature	H2O2_Const._set_2_25mM_060min_vs_NRC-1f.sig	> 40 C
high temperature	H2O2_Const._set_2_25mM_120min_vs_NRC-1f.sig	> 40 C
high temperature	H2O2_Const._set_2_25mM_240min_vs_NRC-1f.sig	> 40 C
high temperature	PQ_Recov._set_2_4mM_000min_vs_NRC-1f.sig	> 40 C
high temperature	PQ_Recov._set_2_4mM_010min_vs_NRC-1f.sig	> 40 C
high temperature	PQ_Recov._set_2_4mM_020min_vs_NRC-1f.sig	> 40 C
high temperature	PQ_Recov._set_2_4mM_030min_vs_NRC-1f.sig	> 40 C
high temperature	PQ_Recov._set_2_4mM_040min_vs_NRC-1f.sig	> 40 C

high temperature	PQ_Recov._set_2_4mM_050min_vs_NRC-1f.sig	> 40 C
high temperature	PQ_Recov._set_2_4mM_060min_vs_NRC-1f.sig	> 40 C
high temperature	PQ_Recov._set_2_4mM_120min_vs_NRC-1f.sig	> 40 C
high temperature	PQ_Recov._set_2_4mM_240min_vs_NRC-1f.sig	> 40 C
high temperature	PQ_Const._set_2_4mM_000min_vs_NRC-1f.sig	> 40 C
high temperature	PQ_Const._set_2_4mM_030min_vs_NRC-1f.sig	> 40 C
high temperature	PQ_Const._set_2_4mM_060min_vs_NRC-1f.sig	> 40 C
high temperature	PQ_Const._set_2_4mM_120min_vs_NRC-1f.sig	> 40 C
high temperature	PQ_Const._set_2_4mM_240min_vs_NRC-1f.sig	> 40 C
high temperature	H2O2_Recov._set_2_25mM_000min_vs_NRC-1f.sig	> 40 C
high temperature	H2O2_Recov._set_2_25mM_010min_vs_NRC-1f.sig	> 40 C
high temperature	H2O2_Recov._set_2_25mM_020min_vs_NRC-1f.sig	> 40 C
high temperature	H2O2_Recov._set_2_25mM_030min_vs_NRC-1f.sig	> 40 C
high temperature	H2O2_Recov._set_2_25mM_040min_vs_NRC-1f.sig	> 40 C
high temperature	H2O2_Recov._set_2_25mM_050min_vs_NRC-1f.sig	> 40 C
high temperature	H2O2_Recov._set_2_25mM_060min_vs_NRC-1f.sig	> 40 C
high temperature	H2O2_Recov._set_2_25mM_120min_vs_NRC-1f.sig	> 40 C
high temperature	H2O2_Recov._set_2_25mM_240min_vs_NRC-1f.sig	> 40 C
high temperature	H2O2_Const._set_1_25mM_000min_vs_NRC-1f.sig	> 40 C
high temperature	H2O2_Const._set_1_25mM_030min_vs_NRC-1f.sig	> 40 C
high temperature	H2O2_Const._set_1_25mM_060min_vs_NRC-1f.sig	> 40 C
high temperature	H2O2_Const._set_1_25mM_120min_vs_NRC-1f.sig	> 40 C
high temperature	H2O2_Const._set_1_25mM_240min_vs_NRC-1f.sig	> 40 C
high temperature	PQ_Recov._set_1_4mM_000min_vs_NRC-1f.sig	> 40 C
high temperature	PQ_Recov._set_1_4mM_010min_vs_NRC-1f.sig	> 40 C
high temperature	PQ_Recov._set_1_4mM_020min_vs_NRC-	> 40 C

	1f.sig	
high temperature	PQ_Recov._set_1_4mM_030min_vs_NRC-1f.sig	> 40 C
high temperature	PQ_Recov._set_1_4mM_040min_vs_NRC-1f.sig	> 40 C
high temperature	PQ_Recov._set_1_4mM_050min_vs_NRC-1f.sig	> 40 C
high temperature	PQ_Recov._set_1_4mM_060min_vs_NRC-1f.sig	> 40 C
high temperature	PQ_Recov._set_1_4mM_120min_vs_NRC-1f.sig	> 40 C
high temperature	PQ_Recov._set_1_4mM_240min_vs_NRC-1f.sig	> 40 C
high temperature	PQ_Const._set_1_4mM_000min_vs_NRC-1f.sig	> 40 C
high temperature	PQ_Const._set_1_4mM_030min_vs_NRC-1f.sig	> 40 C
high temperature	PQ_Const._set_1_4mM_060min_vs_NRC-1f.sig	> 40 C
high temperature	PQ_Const._set_1_4mM_120min_vs_NRC-1f.sig	> 40 C
high temperature	PQ_Const._set_1_4mM_240min_vs_NRC-1f.sig	> 40 C
high temperature	uv__200jm2_D_030m	> 40 C
high temperature	uv__200jm2_D_060m	> 40 C
high temperature	uv__200jm2_L_030m	> 40 C
high temperature	uv__200jm2_L_060m	> 40 C
high temperature	gamma3__0000gy-0000m	> 40 C
high temperature	gamma3__0000gy-0010m	> 40 C
high temperature	gamma3__0000gy-0020m	> 40 C
high temperature	gamma3__0000gy-0030m	> 40 C
high temperature	gamma3__0000gy-0040m	> 40 C
high temperature	gamma3__0000gy-0050m	> 40 C
high temperature	gamma3__0000gy-0060m	> 40 C
high temperature	gamma3__0000gy-0120m	> 40 C
high temperature	gamma3__0000gy-0240m	> 40 C
high temperature	gamma2__0000gy-0000m	> 40 C
high temperature	gamma2__0000gy-0010m	> 40 C
high temperature	gamma2__0000gy-0020m	> 40 C
high temperature	gamma2__0000gy-0030m	> 40 C
high temperature	gamma2__0000gy-0040m	> 40 C
high temperature	gamma2__0000gy-0050m	> 40 C
high temperature	gamma2__0000gy-0060m	> 40 C
high temperature	gamma2__0000gy-0120m	> 40 C
high temperature	gamma2__0000gy-0240m	> 40 C
high temperature	PQ_Const._set_1_0.25mM_-	> 40 C

	001m_vs_NRC-1f.sig	
high temperature	PQ_Const._set_1_0.25mM_000m_vs_NRC-1f.sig	> 40 C
high temperature	PQ_Const._set_1_0.25mM_005m_vs_NRC-1f.sig	> 40 C
high temperature	PQ_Const._set_1_0.25mM_010m_vs_NRC-1f.sig	> 40 C
high temperature	PQ_Const._set_1_0.25mM_020m_vs_NRC-1f.sig	> 40 C
high temperature	PQ_Const._set_1_0.25mM_040m_vs_NRC-1f.sig	> 40 C
high temperature	PQ_Const._set_1_0.25mM_080m_vs_NRC-1f.sig	> 40 C
high temperature	PQ_Const._set_1_0.25mM_160m_vs_NRC-1f.sig	> 40 C
high temperature	PQ_Const._set_1_0.25mM_320m_vs_NRC-1f.sig	> 40 C
high temperature	H2O2_Recov._set_1_0mM_000min_vs_NRC-1d.sig	> 40 C
high temperature	H2O2_Recov._set_1_0mM_010min_vs_NRC-1d.sig	> 40 C
high temperature	H2O2_Recov._set_1_0mM_020min_vs_NRC-1d.sig	> 40 C
high temperature	H2O2_Recov._set_1_0mM_030min_vs_NRC-1d.sig	> 40 C
high temperature	H2O2_Recov._set_1_0mM_040min_vs_NRC-1d.sig	> 40 C
high temperature	H2O2_Recov._set_1_0mM_050min_vs_NRC-1d.sig	> 40 C
high temperature	H2O2_Recov._set_1_0mM_060min_vs_NRC-1d.sig	> 40 C
high temperature	H2O2_Recov._set_1_0mM_120min_vs_NRC-1d.sig	> 40 C
high temperature	H2O2_Recov._set_1_50mM_000min_vs_NRC-1d.sig	> 40 C
high temperature	H2O2_Recov._set_1_50mM_010min_vs_NRC-1d.sig	> 40 C
high temperature	H2O2_Recov._set_1_50mM_020min_vs_NRC-1d.sig	> 40 C
high temperature	H2O2_Recov._set_1_50mM_030min_vs_NRC-1d.sig	> 40 C
high temperature	H2O2_Recov._set_1_50mM_040min_vs_NRC-1d.sig	> 40 C
high temperature	H2O2_Recov._set_1_50mM_050min_vs_NRC-1d.sig	> 40 C
high temperature	H2O2_Recov._set_1_50mM_060min_vs_NRC-1d.sig	> 40 C
high temperature	H2O2_Recov._set_1_50mM_120min_vs_NRC-1d.sig	> 40 C
high temperature	gamma3__2500gy-0000m	> 40 C

high temperature	gamma3__2500gy-0010m	> 40 C
high temperature	gamma3__2500gy-0020m	> 40 C
high temperature	gamma3__2500gy-0030m	> 40 C
high temperature	gamma3__2500gy-0040m	> 40 C
high temperature	gamma3__2500gy-0050m	> 40 C
high temperature	gamma3__2500gy-0060m	> 40 C
high temperature	gamma3__2500gy-0120m	> 40 C
high temperature	gamma3__2500gy-0240m	> 40 C
high temperature	gamma2__2500gy-0000m	> 40 C
high temperature	gamma2__2500gy-0010m	> 40 C
high temperature	gamma2__2500gy-0020m	> 40 C
high temperature	gamma2__2500gy-0030m	> 40 C
high temperature	gamma2__2500gy-0040m	> 40 C
high temperature	gamma2__2500gy-0050m	> 40 C
high temperature	gamma2__2500gy-0060m	> 40 C
high temperature	gamma2__2500gy-0120m	> 40 C
high temperature	gamma2__2500gy-0240m	> 40 C
high zinc	sDura3_pZn_d0.050mM_t+015m_vs_NRC-1h1.sig	> 2 mol/L.
high zinc	sDura3_pZn_d0.050mM_t+030m_vs_NRC-1h1.sig	> 2 mol/L.
high zinc	sDura3_pZn_d0.050mM_t+060m_vs_NRC-1h1.sig	> 2 mol/L.
high zinc	sDura3_pZn_d0.050mM_t+180m_vs_NRC-1h1.sig	> 2 mol/L.
high zinc	sDura3_pZn_d0.050mM_t-015m_vs_NRC-1h1.sig	> 2 mol/L.
high2low	o2_set1_0362m_H2L_860_vs_NRC-1c	oxygen shift from high to low(86%->4.8%)
high2low	o2_set1_0367m_H2L_215_vs_NRC-1c	oxygen shift from high to low(86%->4.8%)
high2low	o2_set1_0372m_H2L_079_vs_NRC-1c	oxygen shift from high to low(86%->4.8%)
high2low	o2_set1_0382m_H2L_048_vs_NRC-1c	oxygen shift from high to low(86%->4.8%)
iron	fe__2000um_vs_NRC-1	1e-5<=mol/L=<7.0e-3.
iron	fe__4000um_vs_NRC-1	1e-5<=mol/L=<7.0e-3.
iron	fe__6000um_vs_NRC-1	1e-5<=mol/L=<7.0e-3.
iron	fe__7000um_vs_NRC-1	1e-5<=mol/L=<7.0e-3.
iron	feso4__-0001m_vs_NRC-1	1e-5<=mol/L=<7.0e-3.
iron	feso4__0000m_vs_NRC-1	1e-5<=mol/L=<7.0e-3.
iron	feso4__0005m_vs_NRC-1b	1e-5<=mol/L=<7.0e-3.
iron	feso4__0010m_vs_NRC-1b	1e-5<=mol/L=<7.0e-3.
iron	feso4__0015m_vs_NRC-1b	1e-5<=mol/L=<7.0e-3.
iron	feso4__0020m_vs_NRC-1	1e-5<=mol/L=<7.0e-3.
iron	feso4__0025m_vs_NRC-1b	1e-5<=mol/L=<7.0e-3.
iron	feso4__0040m_vs_NRC-1	1e-5<=mol/L=<7.0e-3.
iron	feso4__0080m_vs_NRC-1	1e-5<=mol/L=<7.0e-3.

iron	feso4__0160m_vs_NRC-1	1e-5<=mol/L=<7.0e-3.
iron	feso4__0320m_vs_NRC-1	1e-5<=mol/L=<7.0e-3.
iron	ura3_40min_+Fe_vs_NRC1-h1.sig	1e-5<=mol/L=<7.0e-3.
irradiation	gamma4__2500gy-000min	including gamma(2500 gy) and uv (200 J/m2)
irradiation	gamma4__2500gy-010min	including gamma(2500 gy) and uv (200 J/m2)
irradiation	gamma4__2500gy-020min	including gamma(2500 gy) and uv (200 J/m2)
irradiation	gamma4__2500gy-030min	including gamma(2500 gy) and uv (200 J/m2)
irradiation	gamma4__2500gy-040min	including gamma(2500 gy) and uv (200 J/m2)
irradiation	gamma4__2500gy-050min	including gamma(2500 gy) and uv (200 J/m2)
irradiation	gamma4__2500gy-060min	including gamma(2500 gy) and uv (200 J/m2)
irradiation	gamma4__2500gy-120min	including gamma(2500 gy) and uv (200 J/m2)
irradiation	gamma4__2500gy-240min	including gamma(2500 gy) and uv (200 J/m2)
irradiation	gamma__2500gy-0000m	including gamma(2500 gy) and uv (200 J/m2)
irradiation	gamma__2500gy-0010m	including gamma(2500 gy) and uv (200 J/m2)
irradiation	gamma__2500gy-0020m	including gamma(2500 gy) and uv (200 J/m2)
irradiation	gamma__2500gy-0030m	including gamma(2500 gy) and uv (200 J/m2)
irradiation	gamma__2500gy-0040m	including gamma(2500 gy) and uv (200 J/m2)
irradiation	gamma__2500gy-0060m	including gamma(2500 gy) and uv (200 J/m2)
irradiation	gamma__2500gy-0120m	including gamma(2500 gy) and uv (200 J/m2)
irradiation	gamma__2500gy-0240m	including gamma(2500 gy) and uv (200 J/m2)
irradiation	gamma__2500gy-0480m	including gamma(2500 gy) and uv (200 J/m2)
irradiation	gamma__2500gy-0960m	including gamma(2500 gy) and uv (200 J/m2)
irradiation	uv__200jm2_D_030m	including gamma(2500 gy) and uv (200 J/m2)
irradiation	uv__200jm2_D_060m	including gamma(2500 gy) and uv (200 J/m2)
irradiation	uv__200jm2_L_030m	including gamma(2500 gy) and uv (200 J/m2)
irradiation	uv__200jm2_L_060m	including gamma(2500 gy) and uv (200 J/m2)
irradiation	gamma3__2500gy-0000m	including gamma(2500 gy) and uv (200

		J/m2)
irradiation	gamma3__2500gy-0010m	including gamma(2500 gy) and uv (200 J/m2)
irradiation	gamma3__2500gy-0020m	including gamma(2500 gy) and uv (200 J/m2)
irradiation	gamma3__2500gy-0030m	including gamma(2500 gy) and uv (200 J/m2)
irradiation	gamma3__2500gy-0040m	including gamma(2500 gy) and uv (200 J/m2)
irradiation	gamma3__2500gy-0050m	including gamma(2500 gy) and uv (200 J/m2)
irradiation	gamma3__2500gy-0060m	including gamma(2500 gy) and uv (200 J/m2)
irradiation	gamma3__2500gy-0120m	including gamma(2500 gy) and uv (200 J/m2)
irradiation	gamma3__2500gy-0240m	including gamma(2500 gy) and uv (200 J/m2)
irradiation	gamma2__2500gy-0000m	including gamma(2500 gy) and uv (200 J/m2)
irradiation	gamma2__2500gy-0010m	including gamma(2500 gy) and uv (200 J/m2)
irradiation	gamma2__2500gy-0020m	including gamma(2500 gy) and uv (200 J/m2)
irradiation	gamma2__2500gy-0030m	including gamma(2500 gy) and uv (200 J/m2)
irradiation	gamma2__2500gy-0040m	including gamma(2500 gy) and uv (200 J/m2)
irradiation	gamma2__2500gy-0050m	including gamma(2500 gy) and uv (200 J/m2)
irradiation	gamma2__2500gy-0060m	including gamma(2500 gy) and uv (200 J/m2)
irradiation	gamma2__2500gy-0120m	including gamma(2500 gy) and uv (200 J/m2)
irradiation	gamma2__2500gy-0240m	including gamma(2500 gy) and uv (200 J/m2)
lag phase	Dura3_Uracil_0690_0.197_rep1_vs_NRC-1g.sig	OD < 0.2.
lag phase	MDM200gSalt_0.199_vs_NRC-1e.sig	OD < 0.2.
lag phase	20060818_NRC1_rep2_0.194_vs_NRC-1e.sig	OD < 0.2.
lag phase	20060818_NRC1_rep1_0.195_vs_NRC-1e.sig	OD < 0.2.
lag phase	KO_ura3.2_0.1716_vs_NRC-1_h1.sig	OD < 0.2.
lag phase	ura3_+glu_a_OD0.2_vs_NRC1e.sig	OD < 0.2.
lag phase	ura3_+glu_b_OD0.2_vs_NRC1g.sig	OD < 0.2.
lag phase	EMS_Treated__100000uM-030	OD < 0.2.
lag phase	KO_ura3.3_0.1673_vs_NRC-1_h1.sig	OD < 0.2.
lag phase	KO_ura3.4_0.1642_vs_NRC-1_h1.sig	OD < 0.2.
lag phase	20061006_Cmyc_rep2_0.179_vs_NRC-	OD < 0.2.

	1e.sig	
lag phase	20061006_Cmyc_rep1_0.175_vs_NRC-1e.sig	OD < 0.2.
lag phase	20060818_KO_ura3_rep2_0.189_vs_NRC-1e.sig	OD < 0.2.
lag phase	20060818_KO_ura3_rep1_0.178_vs_NRC-1e.sig	OD < 0.2.
lag phase	20060308_KO_ura3_0.189_vs_NRC-1e.sig	OD < 0.2.
lag phase	20050620_NRC1_rep2_0.183_vs_NRC-1d.sig	OD < 0.2.
lag phase	20050620_NRC1_rep1_0.173_vs_NRC-1d.sig	OD < 0.2.
lag phase	20050620_Cmyc_rep2_0.177_vs_NRC-1d.sig	OD < 0.2.
lag phase	NRC-1.2_0.1684_vs_NRC-1_h1.sig	OD < 0.2.
lag phase	KO_ura3.1_0.1857_vs_NRC-1_h1.sig	OD < 0.2.
lag phase	NRC-1_0.1779_vs_NRC-1_h1.sig	OD < 0.2.
low atp level	o2_set3_-0005_min_LO2_vs_NRC1f.sig	atp (mol/L) < 1.0.
low atp level	o2_set3_0000_min_L2HO2_vs_NRC1f.sig	atp (mol/L) < 1.0.
low atp level	o2_set3_0005_min_HO2_vs_NRC1f.sig	atp (mol/L) < 1.0.
low atp level	o2_set3_0010_min_HO2_vs_NRC1f.sig	atp (mol/L) < 1.0.
low atp level	o2_set3_0020_min_HO2_vs_NRC1f.sig	atp (mol/L) < 1.0.
low atp level	o2_set3_0030_min_HO2_vs_NRC1f.sig	atp (mol/L) < 1.0.
low atp level	o2_set3_0045_min_HO2_vs_NRC1f.sig	atp (mol/L) < 1.0.
low atp level	o2_set3_0090_min_HO2_vs_NRC1f.sig	atp (mol/L) < 1.0.
low copper	Cu_vng700_KO_set1_-030min_vs_NRC-1h1.sig	mol/L<1e-4.
low copper	Cu_vng700_KO_set1_000min_vs_NRC-1h1.sig	mol/L<1e-4.
low copper	Cu_vng700_KO_set1_005min_vs_NRC-1h1.sig	mol/L<1e-4.
low copper	Cu_vng700_KO_set1_010min_vs_NRC-1h1.sig	mol/L<1e-4.
low copper	Cu_vng700_KO_set1_020min_vs_NRC-1h1.sig	mol/L<1e-4.
low copper	Cu_vng700_KO_set1_040min_vs_NRC-1h1.sig	mol/L<1e-4.
low copper	Cu_vng700_KO_set1_080min_vs_NRC-1h1.sig	mol/L<1e-4.
low copper	Cu_vng700_KO_set1_160min_vs_NRC-1h1.sig	mol/L<1e-4.
low copper	Cu_vng700_KO_set2_-030min_vs_NRC-1h1.sig	mol/L<1e-4.
low copper	Cu_vng700_KO_set2_000min_vs_NRC-1h1.sig	mol/L<1e-4.
low copper	Cu_vng700_KO_set2_005min_vs_NRC-1h1.sig	mol/L<1e-4.
low copper	Cu_vng700_KO_set2_010min_vs_NRC-	mol/L<1e-4.

	1h1.sig	
low copper	Cu_vng700_KO_set2_020min_vs_NRC-1h1.sig	mol/L<1e-4.
low copper	Cu_vng700_KO_set2_040min_vs_NRC-1h1.sig	mol/L<1e-4.
low copper	Cu_vng700_KO_set2_080min_vs_NRC-1h1.sig	mol/L<1e-4.
low copper	Cu_vng700_KO_set2_160min_vs_NRC-1h1.sig	mol/L<1e-4.
h202 constant	H2O2_Const._set_3_25mM_-001min_vs_NRC-1h1.sig	2.5e-2 mol/L.
h202 constant	H2O2_Const._set_3_25mM_005min_vs_NRC-1h1.sig	2.5e-2 mol/L.
h202 constant	H2O2_Const._set_3_25mM_010min_vs_NRC-1h1.sig	2.5e-2 mol/L.
h202 constant	H2O2_Const._set_3_25mM_020min_vs_NRC-1h1.sig	2.5e-2 mol/L.
h202 constant	H2O2_Const._set_3_25mM_040min_vs_NRC-1h1.sig	2.5e-2 mol/L.
h202 constant	H2O2_Const._set_3_25mM_080min_vs_NRC-1h1.sig	2.5e-2 mol/L.
h202 constant	H2O2_Const._set_3_25mM_160min_vs_NRC-1h1.sig	2.5e-2 mol/L.
h202 constant	H2O2_Const._set_4_25mM_-001min_vs_NRC-1h1.sig	2.5e-2 mol/L.
h202 constant	H2O2_Const._set_4_25mM_005min_vs_NRC-1h1.sig	2.5e-2 mol/L.
h202 constant	H2O2_Const._set_4_25mM_010min_vs_NRC-1h1.sig	2.5e-2 mol/L.
h202 constant	H2O2_Const._set_4_25mM_020min_vs_NRC-1h1.sig	2.5e-2 mol/L.
h202 constant	H2O2_Const._set_4_25mM_040min_vs_NRC-1h1.sig	2.5e-2 mol/L.
h202 constant	H2O2_Const._set_4_25mM_080min_vs_NRC-1h1.sig	2.5e-2 mol/L.
h202 constant	H2O2_Const._set_4_25mM_160min_vs_NRC-1h1.sig	2.5e-2 mol/L.
h202 constant	H2O2_Const._set_2_25mM_000min_vs_NRC-1f.sig	2.5e-2 mol/L.
h202 constant	H2O2_Const._set_2_25mM_030min_vs_NRC-1f.sig	2.5e-2 mol/L.
h202 constant	H2O2_Const._set_2_25mM_060min_vs_NRC-1f.sig	2.5e-2 mol/L.
h202 constant	H2O2_Const._set_2_25mM_120min_vs_NRC-1f.sig	2.5e-2 mol/L.
h202 constant	H2O2_Const._set_2_25mM_240min_vs_NRC-1f.sig	2.5e-2 mol/L.
h202 constant	H2O2_Const._set_1_25mM_000min_vs_NRC-1f.sig	2.5e-2 mol/L.

h202 constant	H2O2_Const._set_1_25mM_030min_vs_NRC-1f.sig	2.5e-2 mol/L.
h202 constant	H2O2_Const._set_1_25mM_060min_vs_NRC-1f.sig	2.5e-2 mol/L.
h202 constant	H2O2_Const._set_1_25mM_120min_vs_NRC-1f.sig	2.5e-2 mol/L.
h202 constant	H2O2_Const._set_1_25mM_240min_vs_NRC-1f.sig	2.5e-2 mol/L.
low h202 recovery	H2O2_Recov._set_3_25mM_000min_vs_NRC-1f.sig	2.5e-2 mol/L.
low h202 recovery	H2O2_Recov._set_3_25mM_010min_vs_NRC-1f.sig	2.5e-2 mol/L.
low h202 recovery	H2O2_Recov._set_3_25mM_020min_vs_NRC-1f.sig	2.5e-2 mol/L.
low h202 recovery	H2O2_Recov._set_3_25mM_030min_vs_NRC-1f.sig	2.5e-2 mol/L.
low h202 recovery	H2O2_Recov._set_3_25mM_040min_vs_NRC-1f.sig	2.5e-2 mol/L.
low h202 recovery	H2O2_Recov._set_3_25mM_050min_vs_NRC-1f.sig	2.5e-2 mol/L.
low h202 recovery	H2O2_Recov._set_3_25mM_060min_vs_NRC-1f.sig	2.5e-2 mol/L.
low h202 recovery	H2O2_Recov._set_3_25mM_120min_vs_NRC-1f.sig	2.5e-2 mol/L.
low h202 recovery	H2O2_Recov._set_3_25mM_240min_vs_NRC-1f.sig	2.5e-2 mol/L.
low h202 recovery	H2O2_Recov._set_2_25mM_000min_vs_NRC-1f.sig	2.5e-2 mol/L.
low h202 recovery	H2O2_Recov._set_2_25mM_010min_vs_NRC-1f.sig	2.5e-2 mol/L.
low h202 recovery	H2O2_Recov._set_2_25mM_020min_vs_NRC-1f.sig	2.5e-2 mol/L.
low h202 recovery	H2O2_Recov._set_2_25mM_030min_vs_NRC-1f.sig	2.5e-2 mol/L.
low h202 recovery	H2O2_Recov._set_2_25mM_040min_vs_NRC-1f.sig	2.5e-2 mol/L.
low h202 recovery	H2O2_Recov._set_2_25mM_050min_vs_NRC-1f.sig	2.5e-2 mol/L.
low h202 recovery	H2O2_Recov._set_2_25mM_060min_vs_NRC-1f.sig	2.5e-2 mol/L.
low h202 recovery	H2O2_Recov._set_2_25mM_120min_vs_NRC-1f.sig	2.5e-2 mol/L.
low h202 recovery	H2O2_Recov._set_2_25mM_240min_vs_NRC-1f.sig	2.5e-2 mol/L.
low h202	H2O2_Const._set_3_25mM_-001min_vs_NRC-1h1.sig	2.5e-2 mol/L.
low h202	H2O2_Const._set_3_25mM_005min_vs_NRC-1h1.sig	2.5e-2 mol/L.
low h202	H2O2_Const._set_3_25mM_010min_vs_NRC-1h1.sig	2.5e-2 mol/L.

low h202	H2O2_Const._set_3_25mM_020min_vs_NRC-1h1.sig	2.5e-2 mol/L.
low h202	H2O2_Const._set_3_25mM_040min_vs_NRC-1h1.sig	2.5e-2 mol/L.
low h202	H2O2_Const._set_3_25mM_080min_vs_NRC-1h1.sig	2.5e-2 mol/L.
low h202	H2O2_Const._set_3_25mM_160min_vs_NRC-1h1.sig	2.5e-2 mol/L.
low h202	H2O2_Const._set_4_25mM_-001min_vs_NRC-1h1.sig	2.5e-2 mol/L.
low h202	H2O2_Const._set_4_25mM_005min_vs_NRC-1h1.sig	2.5e-2 mol/L.
low h202	H2O2_Const._set_4_25mM_010min_vs_NRC-1h1.sig	2.5e-2 mol/L.
low h202	H2O2_Const._set_4_25mM_020min_vs_NRC-1h1.sig	2.5e-2 mol/L.
low h202	H2O2_Const._set_4_25mM_040min_vs_NRC-1h1.sig	2.5e-2 mol/L.
low h202	H2O2_Const._set_4_25mM_080min_vs_NRC-1h1.sig	2.5e-2 mol/L.
low h202	H2O2_Const._set_4_25mM_160min_vs_NRC-1h1.sig	2.5e-2 mol/L.
low h202	H2O2_Recov._set_3_25mM_000min_vs_NRC-1f.sig	2.5e-2 mol/L.
low h202	H2O2_Recov._set_3_25mM_010min_vs_NRC-1f.sig	2.5e-2 mol/L.
low h202	H2O2_Recov._set_3_25mM_020min_vs_NRC-1f.sig	2.5e-2 mol/L.
low h202	H2O2_Recov._set_3_25mM_030min_vs_NRC-1f.sig	2.5e-2 mol/L.
low h202	H2O2_Recov._set_3_25mM_040min_vs_NRC-1f.sig	2.5e-2 mol/L.
low h202	H2O2_Recov._set_3_25mM_050min_vs_NRC-1f.sig	2.5e-2 mol/L.
low h202	H2O2_Recov._set_3_25mM_060min_vs_NRC-1f.sig	2.5e-2 mol/L.
low h202	H2O2_Recov._set_3_25mM_120min_vs_NRC-1f.sig	2.5e-2 mol/L.
low h202	H2O2_Recov._set_3_25mM_240min_vs_NRC-1f.sig	2.5e-2 mol/L.
low h202	H2O2_Const._set_2_25mM_000min_vs_NRC-1f.sig	2.5e-2 mol/L.
low h202	H2O2_Const._set_2_25mM_030min_vs_NRC-1f.sig	2.5e-2 mol/L.
low h202	H2O2_Const._set_2_25mM_060min_vs_NRC-1f.sig	2.5e-2 mol/L.
low h202	H2O2_Const._set_2_25mM_120min_vs_NRC-1f.sig	2.5e-2 mol/L.
low h202	H2O2_Const._set_2_25mM_240min_vs_NRC-1f.sig	2.5e-2 mol/L.

low h202	H2O2_Recov._set_2_25mM_000min_vs_NRC-1f.sig	2.5e-2 mol/L.
low h202	H2O2_Recov._set_2_25mM_010min_vs_NRC-1f.sig	2.5e-2 mol/L.
low h202	H2O2_Recov._set_2_25mM_020min_vs_NRC-1f.sig	2.5e-2 mol/L.
low h202	H2O2_Recov._set_2_25mM_030min_vs_NRC-1f.sig	2.5e-2 mol/L.
low h202	H2O2_Recov._set_2_25mM_040min_vs_NRC-1f.sig	2.5e-2 mol/L.
low h202	H2O2_Recov._set_2_25mM_050min_vs_NRC-1f.sig	2.5e-2 mol/L.
low h202	H2O2_Recov._set_2_25mM_060min_vs_NRC-1f.sig	2.5e-2 mol/L.
low h202	H2O2_Recov._set_2_25mM_120min_vs_NRC-1f.sig	2.5e-2 mol/L.
low h202	H2O2_Recov._set_2_25mM_240min_vs_NRC-1f.sig	2.5e-2 mol/L.
low h202	H2O2_Const._set_1_25mM_000min_vs_NRC-1f.sig	2.5e-2 mol/L.
low h202	H2O2_Const._set_1_25mM_030min_vs_NRC-1f.sig	2.5e-2 mol/L.
low h202	H2O2_Const._set_1_25mM_060min_vs_NRC-1f.sig	2.5e-2 mol/L.
low h202	H2O2_Const._set_1_25mM_120min_vs_NRC-1f.sig	2.5e-2 mol/L.
low h202	H2O2_Const._set_1_25mM_240min_vs_NRC-1f.sig	2.5e-2 mol/L.
low iron	fe__2000um_vs_NRC-1	<4e-3 mol/L.
low iron	idr1_40min_+Fe_vs_NRC1-h1.sig	<4e-3 mol/L.
low iron	idr1_60min_+Fe_vs_NRC1-h1.sig	<4e-3 mol/L.
low iron	idr2_20min_+Fe_vs_NRC1-h1.sig	<4e-3 mol/L.
low iron	idr2_40min_+Fe_vs_NRC1-h1.sig	<4e-3 mol/L.
low iron	idr2_60min_+Fe_vs_NRC1-h1.sig	<4e-3 mol/L.
low iron	idr2_60min_-Fe_vs_NRC1-h1.sig	<4e-3 mol/L.
low iron	sirR_20min_+Fe_vs_NRC1_h1.sig	<4e-3 mol/L.
low iron	sirR_40min_+Fe_vs_NRC1_h1.sig	<4e-3 mol/L.
low iron	sirR_60min_+Fe_vs_NRC1_h1.sig	<4e-3 mol/L.
low iron	ura3_40min_+Fe_vs_NRC1-h1.sig	<4e-3 mol/L.
low light	zn__0005um_vs_NRC-1	0 < mol/m2/s < 100.
low light	zn__0010um_vs_NRC-1	0 < mol/m2/s < 100.
low light	zn__0020um_vs_NRC-1	0 < mol/m2/s < 100.
low light	cu__0700um_vs_NRC-1	0 < mol/m2/s < 100.
low light	cu__0850um_vs_NRC-1	0 < mol/m2/s < 100.
low light	cu__1000um_vs_NRC-1	0 < mol/m2/s < 100.
low light	Cu_NRC1_set1_-030min_vs_NRC-1h1.sig	0 < mol/m2/s < 100.
low light	Cu_NRC1_set1_000min_vs_NRC-1h1.sig	0 < mol/m2/s < 100.

low light	Cu_NRC1_set1_005min_vs_NRC-1h1.sig	0 < mol/m2/s < 100.
low light	Cu_NRC1_set1_010min_vs_NRC-1h1.sig	0 < mol/m2/s < 100.
low light	Cu_NRC1_set1_020min_vs_NRC-1h1.sig	0 < mol/m2/s < 100.
low light	Cu_NRC1_set1_040min_vs_NRC-1h1.sig	0 < mol/m2/s < 100.
low light	Cu_NRC1_set1_080min_vs_NRC-1h1.sig	0 < mol/m2/s < 100.
low light	Cu_NRC1_set1_160min_vs_NRC-1h1.sig	0 < mol/m2/s < 100.
low light	Cu_ura3_KO_set1_-030min_vs_NRC-1h1.sig	0 < mol/m2/s < 100.
low light	Cu_ura3_KO_set1_000min_vs_NRC-1h1.sig	0 < mol/m2/s < 100.
low light	Cu_ura3_KO_set1_005min_vs_NRC-1h1.sig	0 < mol/m2/s < 100.
low light	Cu_ura3_KO_set1_010min_vs_NRC-1h1.sig	0 < mol/m2/s < 100.
low light	Cu_ura3_KO_set1_020min_vs_NRC-1h1.sig	0 < mol/m2/s < 100.
low light	Cu_ura3_KO_set1_040min_vs_NRC-1h1.sig	0 < mol/m2/s < 100.
low light	Cu_ura3_KO_set1_080min_vs_NRC-1h1.sig	0 < mol/m2/s < 100.
low light	Cu_ura3_KO_set1_160min_vs_NRC-1h1.sig	0 < mol/m2/s < 100.
low light	feso4__-0001m_vs_NRC-1	0 < mol/m2/s < 100.
low light	feso4__0000m_vs_NRC-1	0 < mol/m2/s < 100.
low light	feso4__0005m_vs_NRC-1b	0 < mol/m2/s < 100.
low light	feso4__0010m_vs_NRC-1b	0 < mol/m2/s < 100.
low light	feso4__0015m_vs_NRC-1b	0 < mol/m2/s < 100.
low light	feso4__0020m_vs_NRC-1	0 < mol/m2/s < 100.
low light	feso4__0025m_vs_NRC-1b	0 < mol/m2/s < 100.
low light	feso4__0040m_vs_NRC-1	0 < mol/m2/s < 100.
low light	feso4__0080m_vs_NRC-1	0 < mol/m2/s < 100.
low light	feso4__0160m_vs_NRC-1	0 < mol/m2/s < 100.
low light	feso4__0320m_vs_NRC-1	0 < mol/m2/s < 100.
low light	zim__HO_L_vs_NRC-1	0 < mol/m2/s < 100.
low light	zim__LO_L_vs_NRC-1	0 < mol/m2/s < 100.
low light	VNG2334C__HO_L_vs_NRC-1	0 < mol/m2/s < 100.
low light	VNG2334C__LO_L_vs_NRC-1	0 < mol/m2/s < 100.
low light	VNG1296C__HO_L_vs_NRC-1	0 < mol/m2/s < 100.
low light	VNG1296C__LO_L_vs_NRC-1	0 < mol/m2/s < 100.
low light	VNG0750C__HO_L_vs_NRC-1	0 < mol/m2/s < 100.
low light	VNG0750C__LO_L_vs_NRC-1	0 < mol/m2/s < 100.
low light	VNG0019H__HO_L_vs_NRC-1c	0 < mol/m2/s < 100.
low light	VNG0019H__LO_L_vs_NRC-1c	0 < mol/m2/s < 100.
low light	ura3__HO_L_vs_NRC-1	0 < mol/m2/s < 100.
low light	ura3__LO_L_vs_NRC-1	0 < mol/m2/s < 100.

low light	NRC-1__HO_L_vs_NRC-1	0 < mol/m2/s < 100.
low light	NRC-1__LO_L_vs_NRC-1	0 < mol/m2/s < 100.
low light	uv__200jm2_L_030m	0 < mol/m2/s < 100.
low light	uv__200jm2_L_060m	0 < mol/m2/s < 100.
low light	o2_set1_-001m_L2H_005_vs_NRC-1c	0 < mol/m2/s < 100.
low light	o2_set1_0001m_L2H_500_vs_NRC-1c	0 < mol/m2/s < 100.
low light	o2_set1_0005m_H_922_vs_NRC-1c	0 < mol/m2/s < 100.
low light	o2_set1_0010m_H_947_vs_NRC-1c	0 < mol/m2/s < 100.
low light	o2_set1_0020m_H_937_vs_NRC-1c	0 < mol/m2/s < 100.
low light	o2_set1_0030m_H_931_vs_NRC-1c	0 < mol/m2/s < 100.
low light	o2_set1_0045m_H_939_vs_NRC-1c	0 < mol/m2/s < 100.
low light	o2_set1_0090m_H_941_vs_NRC-1c	0 < mol/m2/s < 100.
low light	o2_set1_0180m_H_930_vs_NRC-1c	0 < mol/m2/s < 100.
low light	o2_set1_0360m_H_903_vs_NRC-1c	0 < mol/m2/s < 100.
low light	o2_set1_0362m_H2L_860_vs_NRC-1c	0 < mol/m2/s < 100.
low light	o2_set1_0367m_H2L_215_vs_NRC-1c	0 < mol/m2/s < 100.
low light	o2_set1_0372m_H2L_079_vs_NRC-1c	0 < mol/m2/s < 100.
low light	o2_set1_0382m_H2L_048_vs_NRC-1c	0 < mol/m2/s < 100.
low light	o2_set1_0387m_L_041_vs_NRC-1c	0 < mol/m2/s < 100.
low light	o2_set1_0392m_L_037_vs_NRC-1c	0 < mol/m2/s < 100.
low light	o2_set1_0397m_L_035_vs_NRC-1c	0 < mol/m2/s < 100.
low light	o2_set1_0407m_L_030_vs_NRC-1c	0 < mol/m2/s < 100.
low light	o2_set1_0417m_L_027_vs_NRC-1c	0 < mol/m2/s < 100.
low light	o2_set1_0432m_L_024_vs_NRC-1c	0 < mol/m2/s < 100.
low light	o2_set1_0477m_L_017_vs_NRC-1c	0 < mol/m2/s < 100.
low light	o2_set1_0567m_L_011_vs_NRC-1c	0 < mol/m2/s < 100.
low light	o2_set1_0747m_L_008_vs_NRC-1c	0 < mol/m2/s < 100.
low light	o2_set1_0750m_L2H_540_vs_NRC-1c	0 < mol/m2/s < 100.
low light	o2_set1_0755m_L2H_825_vs_NRC-1c	0 < mol/m2/s < 100.
low light	o2_set1_0760m_L2H_847_vs_NRC-1c	0 < mol/m2/s < 100.
low light	o2_set1_0770m_L2H_852_vs_NRC-1c	0 < mol/m2/s < 100.
low light	o2_set1_0780m_L2H_847_vs_NRC-1c	0 < mol/m2/s < 100.
low light	20061006_Cmyc_rep2_0.179_vs_NRC-1e.sig	0 < mol/m2/s < 100.
low light	20061006_Cmyc_rep2_0.399_vs_NRC-1e.sig	0 < mol/m2/s < 100.
low light	20061006_Cmyc_rep2_0.833_vs_NRC-1e.sig	0 < mol/m2/s < 100.
low light	20061006_Cmyc_rep1_0.175_vs_NRC-1e.sig	0 < mol/m2/s < 100.
low light	20061006_Cmyc_rep1_0.417_vs_NRC-1e.sig	0 < mol/m2/s < 100.
low light	20061006_Cmyc_rep1_0.835_vs_NRC-1e.sig	0 < mol/m2/s < 100.

low light	20060818_KO_ura3_rep2_0.189_vs_NRC-1e.sig	0 < mol/m2/s < 100.
low light	20060818_KO_ura3_rep2_0.376_vs_NRC-1e.sig	0 < mol/m2/s < 100.
low light	20060818_KO_ura3_rep2_0.828_vs_NRC-1e.sig	0 < mol/m2/s < 100.
low light	20060818_KO_ura3_rep1_0.178_vs_NRC-1e.sig	0 < mol/m2/s < 100.
low light	20060818_KO_ura3_rep1_0.405_vs_NRC-1e.sig	0 < mol/m2/s < 100.
low light	20060818_KO_ura3_rep1_0.842_vs_NRC-1e.sig	0 < mol/m2/s < 100.
low light	20060717_Cmyc_rep2_0.223_vs_NRC-1e.sig	0 < mol/m2/s < 100.
low light	20060717_Cmyc_rep2_0.407_vs_NRC-1e.sig	0 < mol/m2/s < 100.
low light	20060717_Cmyc_rep2_0.883_vs_NRC-1e.sig	0 < mol/m2/s < 100.
low light	20060717_Cmyc_rep1_0.221_vs_NRC-1e.sig	0 < mol/m2/s < 100.
low light	20060717_Cmyc_rep1_0.402_vs_NRC-1e.sig	0 < mol/m2/s < 100.
low light	20060717_Cmyc_rep1_0.827_vs_NRC-1e.sig	0 < mol/m2/s < 100.
low light	20060308_KO_ura3_0.189_vs_NRC-1e.sig	0 < mol/m2/s < 100.
low light	20060308_KO_ura3_0.448_vs_NRC-1e.sig	0 < mol/m2/s < 100.
low light	20060308_KO_ura3_0.853_vs_NRC-1e.sig	0 < mol/m2/s < 100.
low light	20050620_NRC1_rep2_0.183_vs_NRC-1d.sig	0 < mol/m2/s < 100.
low light	20050620_NRC1_rep2_0.505_vs_NRC-1d.sig	0 < mol/m2/s < 100.
low light	20050620_NRC1_rep2_1.030_vs_NRC-1d.sig	0 < mol/m2/s < 100.
low light	20050620_NRC1_rep1_0.173_vs_NRC-1d.sig	0 < mol/m2/s < 100.
low light	20050620_NRC1_rep1_0.484_vs_NRC-1d.sig	0 < mol/m2/s < 100.
low light	20050620_NRC1_rep1_1.276_vs_NRC-1d.sig	0 < mol/m2/s < 100.
low light	20050620_Cmyc_rep2_0.177_vs_NRC-1d.sig	0 < mol/m2/s < 100.
low light	20050620_Cmyc_rep2_0.457_vs_NRC-1d.sig	0 < mol/m2/s < 100.
low light	20050620_Cmyc_rep2_1.072_vs_NRC-1d.sig	0 < mol/m2/s < 100.
low light	20050620_Cmyc_rep1_0.207_vs_NRC-1d.sig	0 < mol/m2/s < 100.
low light	20050620_Cmyc_rep1_0.474_vs_NRC-1d.sig	0 < mol/m2/s < 100.
low light	20050620_Cmyc_rep1_1.052_vs_NRC-	0 < mol/m2/s < 100.

	1d.sig	
low light	sDura3_pCu_d0.100mM_t+015m_vs_NRC-1h1.sig	0 < mol/m2/s < 100.
low light	sDura3_pCu_d0.100mM_t+030m_vs_NRC-1h1.sig	0 < mol/m2/s < 100.
low light	sDura3_pCu_d0.100mM_t+060m_vs_NRC-1h1.sig	0 < mol/m2/s < 100.
low light	sDura3_pCu_d0.100mM_t+180m_vs_NRC-1h1.sig	0 < mol/m2/s < 100.
low light	sDura3_pCu_d0.100mM_t-015m_vs_NRC-1h1.sig	0 < mol/m2/s < 100.
low light	sDura3_pCu_d0.700mM_t+015m_vs_NRC-1h1.sig	0 < mol/m2/s < 100.
low light	sDura3_pCu_d0.700mM_t+030m_vs_NRC-1h1.sig	0 < mol/m2/s < 100.
low light	sDura3_pCu_d0.700mM_t+060m_vs_NRC-1h1.sig	0 < mol/m2/s < 100.
low light	sDura3_pCu_d0.700mM_t+180m_vs_NRC-1h1.sig	0 < mol/m2/s < 100.
low light	sDura3_pCu_d0.700mM_t-015m_vs_NRC-1h1.sig	0 < mol/m2/s < 100.
low light	sDura3_pCu_d1.000mM_t+015m_vs_NRC-1h1.sig	0 < mol/m2/s < 100.
low light	sDura3_pCu_d1.000mM_t+030m_vs_NRC-1h1.sig	0 < mol/m2/s < 100.
low light	sDura3_pCu_d1.000mM_t+060m_vs_NRC-1h1.sig	0 < mol/m2/s < 100.
low light	sDura3_pCu_d1.000mM_t+180m_vs_NRC-1h1.sig	0 < mol/m2/s < 100.
low light	sDura3_pCu_d1.000mM_t-015m_vs_NRC-1h1.sig	0 < mol/m2/s < 100.
low light	sDura3_pNULL_d0.000mM_t+015m_vs_NRC-1h1.sig	0 < mol/m2/s < 100.
low light	sDura3_pNULL_d0.000mM_t+030m_vs_NRC-1h1.sig	0 < mol/m2/s < 100.
low light	sDura3_pNULL_d0.000mM_t+060m_vs_NRC-1h1.sig	0 < mol/m2/s < 100.
low light	sDura3_pNULL_d0.000mM_t+180m_vs_NRC-1h1.sig	0 < mol/m2/s < 100.
low light	sDura3_pNULL_d0.000mM_t-015m_vs_NRC-1h1.sig	0 < mol/m2/s < 100.
low light	sDura3_pZn_d0.005mM_t+015m_vs_NRC-1h1.sig	0 < mol/m2/s < 100.
low light	sDura3_pZn_d0.005mM_t+030m_vs_NRC-1h1.sig	0 < mol/m2/s < 100.
low light	sDura3_pZn_d0.005mM_t+060m_vs_NRC-1h1.sig	0 < mol/m2/s < 100.
low light	sDura3_pZn_d0.005mM_t+180m_vs_NRC-1h1.sig	0 < mol/m2/s < 100.

low light	sDura3_pZn_d0.005mM_t-015m_vs_NRC-1h1.sig	0 < mol/m2/s < 100.
low light	sDura3_pZn_d0.020mM_t+015m_vs_NRC-1h1.sig	0 < mol/m2/s < 100.
low light	sDura3_pZn_d0.020mM_t+030m_vs_NRC-1h1.sig	0 < mol/m2/s < 100.
low light	sDura3_pZn_d0.020mM_t+060m_vs_NRC-1h1.sig	0 < mol/m2/s < 100.
low light	sDura3_pZn_d0.020mM_t+180m_vs_NRC-1h1.sig	0 < mol/m2/s < 100.
low light	sDura3_pZn_d0.020mM_t-015m_vs_NRC-1h1.sig	0 < mol/m2/s < 100.
low light	sDura3_pZn_d0.050mM_t+015m_vs_NRC-1h1.sig	0 < mol/m2/s < 100.
low light	sDura3_pZn_d0.050mM_t+030m_vs_NRC-1h1.sig	0 < mol/m2/s < 100.
low light	sDura3_pZn_d0.050mM_t+060m_vs_NRC-1h1.sig	0 < mol/m2/s < 100.
low light	sDura3_pZn_d0.050mM_t+180m_vs_NRC-1h1.sig	0 < mol/m2/s < 100.
low light	sDura3_pZn_d0.050mM_t-015m_vs_NRC-1h1.sig	0 < mol/m2/s < 100.
low manganese	sirR_Mn_0800um_a_vs_NRC-1d.sig	8.0e-4 mol/L.
low manganese	sirR_Mn_0800um_b_vs_NRC-1d.sig	8.0e-4 mol/L.
low manganese	ura3_Mn_0800um_a_vs_NRC-1d.sig	8.0e-4 mol/L.
low manganese	ura3_Mn_0800um_b_vs_NRC-1d.sig	8.0e-4 mol/L.
low manganese	mn__0800um_vs_NRC-1	8.0e-4 mol/L.
low oxygen	o2_set1_-001m_L2H_005_vs_NRC-1c	< 25 pct.
low oxygen	o2_set1_0367m_H2L_215_vs_NRC-1c	< 25 pct.
low oxygen	o2_set1_0372m_H2L_079_vs_NRC-1c	< 25 pct.
low oxygen	o2_set1_0382m_H2L_048_vs_NRC-1c	< 25 pct.
low oxygen	o2_set1_0387m_L_041_vs_NRC-1c	< 25 pct.
low oxygen	o2_set1_0392m_L_037_vs_NRC-1c	< 25 pct.
low oxygen	o2_set1_0397m_L_035_vs_NRC-1c	< 25 pct.
low oxygen	o2_set1_0407m_L_030_vs_NRC-1c	< 25 pct.
low oxygen	o2_set1_0417m_L_027_vs_NRC-1c	< 25 pct.
low oxygen	o2_set1_0432m_L_024_vs_NRC-1c	< 25 pct.
low oxygen	o2_set1_0477m_L_017_vs_NRC-1c	< 25 pct.
low oxygen	o2_set1_0567m_L_011_vs_NRC-1c	< 25 pct.
low oxygen	o2_set1_0747m_L_008_vs_NRC-1c	< 25 pct.
low oxygen	o2_set2_H_L_010_vs_NRC-1d.sig	< 25 pct.
low oxygen	o2_set2_H_L_020_vs_NRC-1d.sig	< 25 pct.
low oxygen	o2_set2_L_000_vs_NRC-1d.sig	< 25 pct.
low oxygen	o2_set2_L_005_vs_NRC-1d.sig	< 25 pct.
low oxygen	o2_set2_L_010_vs_NRC-1d.sig	< 25 pct.
low oxygen	o2_set2_L_020_vs_NRC-1d.sig	< 25 pct.

low oxygen	o2_set2_L_030_vs_NRC-1d.sig	< 25 pct.
low oxygen	o2_set2_L_045_vs_NRC-1d.sig	< 25 pct.
low oxygen	o2_set2_L_090_vs_NRC-1d.sig	< 25 pct.
low oxygen	o2_set2_L_135_vs_NRC-1d.sig	< 25 pct.
low oxygen	o2_set2_L_180_vs_NRC-1d.sig	< 25 pct.
low oxygen	o2_set2_L_270_vs_NRC-1d.sig	< 25 pct.
low oxygen	o2_set2_L_360_vs_NRC-1d.sig	< 25 pct.
low oxygen	o2_set3_-0005_min_LO2_vs_NRC1f.sig	< 25 pct.
low oxygen	o2_set3_0000_min_L2HO2_vs_NRC1f.sig	< 25 pct.
low oxygen shift	o2_set1_0387m_L_041_vs_NRC-1c	low oxygen(chemostat) 1.1%-4.1%
low oxygen shift	o2_set1_0392m_L_037_vs_NRC-1c	low oxygen(chemostat) 1.1%-4.1%
low oxygen shift	o2_set1_0397m_L_035_vs_NRC-1c	low oxygen(chemostat) 1.1%-4.1%
low oxygen shift	o2_set1_0407m_L_030_vs_NRC-1c	low oxygen(chemostat) 1.1%-4.1%
low oxygen shift	o2_set1_0417m_L_027_vs_NRC-1c	low oxygen(chemostat) 1.1%-4.1%
low oxygen shift	o2_set1_0432m_L_024_vs_NRC-1c	low oxygen(chemostat) 1.1%-4.1%
low oxygen shift	o2_set1_0477m_L_017_vs_NRC-1c	low oxygen(chemostat) 1.1%-4.1%
low oxygen shift	o2_set1_0567m_L_011_vs_NRC-1c	low oxygen(chemostat) 1.1%-4.1%
low oxygen shift	o2_set1_0747m_L_008_vs_NRC-1c	low oxygen(chemostat) 1.1%-4.1%
low paraquat constant	PQ_Const._set_1_0.25mM_000m_vs_NRC-1f.sig	2.5e-4 mol/L.
low paraquat constant	PQ_Const._set_1_0.25mM_005m_vs_NRC-1f.sig	2.5e-4 mol/L.
low paraquat constant	PQ_Const._set_1_0.25mM_010m_vs_NRC-1f.sig	2.5e-4 mol/L.
low paraquat constant	PQ_Const._set_1_0.25mM_020m_vs_NRC-1f.sig	2.5e-4 mol/L.
low paraquat constant	PQ_Const._set_1_0.25mM_040m_vs_NRC-1f.sig	2.5e-4 mol/L.
low paraquat constant	PQ_Const._set_1_0.25mM_080m_vs_NRC-1f.sig	2.5e-4 mol/L.
low paraquat constant	PQ_Const._set_1_0.25mM_160m_vs_NRC-1f.sig	2.5e-4 mol/L.
low paraquat constant	PQ_Const._set_1_0.25mM_320m_vs_NRC-1f.sig	2.5e-4 mol/L.
low salt	Dun_F2_000minb_vs_NRC-1g.sig	200 g/L NaCl.
low salt	Dun_F2_005minb_vs_NRC-1g.sig	200 g/L NaCl.
low salt	Dun_F2_010minb_vs_NRC-1g.sig	200 g/L NaCl.
low salt	Dun_F2_020minb_vs_NRC-1g.sig	200 g/L NaCl.
low salt	Dun_F2_040minb_vs_NRC-1g.sig	200 g/L NaCl.
low salt	Dun_F2_080minb_vs_NRC-1g.sig	200 g/L NaCl.
low salt	Dun_F2_160minb_vs_NRC-1g.sig	200 g/L NaCl.
low salt	Dun_F2_320minb_vs_NRC-1g.sig	200 g/L NaCl.
low salt	MDM200gSalt_0.199_vs_NRC-1e.sig	200 g/L NaCl.
low salt	MDM200gSalt_0.388_vs_NRC-1e.sig	200 g/L NaCl.
low salt	MDM200gSalt_0.466_vs_NRC-1e.sig	200 g/L NaCl.

low salt	MDM200gSalt_0.534_vs_NRC-1e.sig	200 g/L NaCl.
low salt	Dun_Supernat._000minb_vs_NRC-1g.sig	200 g/L NaCl.
low salt	Dun_Supernat._005minb_vs_NRC-1g.sig	200 g/L NaCl.
low salt	Dun_Supernat._010minb_vs_NRC-1g.sig	200 g/L NaCl.
low salt	Dun_Supernat._020minb_vs_NRC-1g.sig	200 g/L NaCl.
low salt	Dun_Supernat._040minb_vs_NRC-1g.sig	200 g/L NaCl.
low salt	Dun_Supernat._080minb_vs_NRC-1g.sig	200 g/L NaCl.
low salt	Dun_Supernat._160minb_vs_NRC-1g.sig	200 g/L NaCl.
low salt	Dun_Supernat._320minb_vs_NRC-1g.sig	200 g/L NaCl.
low temperature	circadian__dark5_cycling_30C_1440min_vs_NRC-1d.sig	<= 30C.
low temperature	circadian__dark5_cycling_30C_1630min_vs_NRC-1d.sig	<= 30C.
low temperature	circadian__dark5_cycling_30C_1815min_vs_NRC-1d.sig	<= 30C.
low temperature	circadian__dark5_cycling_30C_1980min_vs_NRC-1d.sig	<= 30C.
low temperature	circadian__dark5_cycling_30C_2160min_vs_NRC-1d.sig	<= 30C.
low temperature	circadian__dark5_cycling_30C_2355min_vs_NRC-1d.sig	<= 30C.
low temperature	circadian__dark5_cycling_30C_2590min_vs_NRC-1d.sig	<= 30C.
low temperature	circadian__dark5_cycling_30C_2700min_vs_NRC-1d.sig	<= 30C.
low temperature	circadian__dark5_cycling_30C_2880min_vs_NRC-1d.sig	<= 30C.
low temperature	Dun_F2_000minb_vs_NRC-1g.sig	<= 30C.
low temperature	Dun_F2_005minb_vs_NRC-1g.sig	<= 30C.
low temperature	Dun_F2_010minb_vs_NRC-1g.sig	<= 30C.
low temperature	Dun_F2_020minb_vs_NRC-1g.sig	<= 30C.
low temperature	Dun_F2_040minb_vs_NRC-1g.sig	<= 30C.
low temperature	Dun_F2_080minb_vs_NRC-1g.sig	<= 30C.
low temperature	Dun_F2_160minb_vs_NRC-1g.sig	<= 30C.
low temperature	Dun_F2_320minb_vs_NRC-1g.sig	<= 30C.
low temperature	Dun_Supernat._000minb_vs_NRC-1g.sig	<= 30C.
low zinc	Zn_0.000_vs_NRC-1d.sig	<=.1e-5 mol/L zinc.
low zinc	Zn_0.005_vs_NRC-1d.sig	<=.1e-5 mol/L zinc.
low zinc	Zn_0.010_vs_NRC-1d.sig	<=.1e-5 mol/L zinc.
low zinc	zn__0005um_vs_NRC-1	<=.1e-5 mol/L zinc.
low zinc	zn__0010um_vs_NRC-1	<=.1e-5 mol/L zinc.
low zinc	sDura3_pZn_d0.005mM_t+015m_vs_NRC-1h1.sig	<=.1e-5 mol/L zinc.
low zinc	sDura3_pZn_d0.005mM_t+030m_vs_NRC-1h1.sig	<=.1e-5 mol/L zinc.

low zinc	sDura3_pZn_d0.005mM_t+060m_vs_NRC-1h1.sig	<=.1e-5 mol/L zinc.
low zinc	sDura3_pZn_d0.005mM_t+180m_vs_NRC-1h1.sig	<=.1e-5 mol/L zinc.
low zinc	sDura3_pZn_d0.005mM_t-015m_vs_NRC-1h1.sig	<=.1e-5 mol/L zinc.
low2high	o2_set1_-001m_L2H_005_vs_NRC-1c	oxygen shift from low to high(0.5%->84.7%)
low2high	o2_set1_0001m_L2H_500_vs_NRC-1c	oxygen shift from low to high(0.5%->84.7%)
low2high	o2_set1_0750m_L2H_540_vs_NRC-1c	oxygen shift from low to high(0.5%->84.7%)
low2high	o2_set1_0755m_L2H_825_vs_NRC-1c	oxygen shift from low to high(0.5%->84.7%)
low2high	o2_set1_0760m_L2H_847_vs_NRC-1c	oxygen shift from low to high(0.5%->84.7%)
low2high	o2_set1_0770m_L2H_852_vs_NRC-1c	oxygen shift from low to high(0.5%->84.7%)
low2high	o2_set1_0780m_L2H_847_vs_NRC-1c	oxygen shift from low to high(0.5%->84.7%)
manganese	sirR_Mn_0800um_a_vs_NRC-1d.sig	8e-4 mol/L
manganese	sirR_Mn_0800um_b_vs_NRC-1d.sig	8e-4 mol/L
manganese	sirR_Mn_1500um_a_vs_NRC-1d.sig	8e-4 mol/L
manganese	sirR_Mn_1500um_b_vs_NRC-1d.sig	8e-4 mol/L
manganese	sirR_Mn_1000um_a_vs_NRC-1d.sig	8e-4 mol/L
manganese	sirR_Mn_1000um_b_vs_NRC-1d.sig	8e-4 mol/L
manganese	ura3_Mn_0800um_a_vs_NRC-1d.sig	8e-4 mol/L
manganese	ura3_Mn_0800um_b_vs_NRC-1d.sig	8e-4 mol/L
manganese	ura3_Mn_1500um_a_vs_NRC-1d.sig	8e-4 mol/L
manganese	ura3_Mn_1500um_b_vs_NRC-1d.sig	8e-4 mol/L
manganese	ura3_Mn_1000um_a_vs_NRC-1d.sig	8e-4 mol/L
manganese	ura3_Mn_1000um_b_vs_NRC-1d.sig	8e-4 mol/L
manganese	mn__0800um_vs_NRC-1	8e-4 mol/L
manganese	mn__1000um_vs_NRC-1	8e-4 mol/L
manganese	mn__1500um_vs_NRC-1	8e-4 mol/L
medium atp level	o2_set3_0060_min_HO2_vs_NRC1f.sig	1.0 > atp (mol/L) < 1.5.
medium atp level	o2_set3_0120_min_HO2_vs_NRC1f.sig	1.0 > atp (mol/L) < 1.5.
medium atp level	o2_set3_0180_min_HO2_vs_NRC1f.sig	1.0 > atp (mol/L) < 1.5.
medium atp level	o2_set3_0240_min_HO2_vs_NRC1f.sig	1.0 > atp (mol/L) < 1.5.
medium atp level	o2_set3_0300_min_HO2_vs_NRC1f.sig	1.0 > atp (mol/L) < 1.5.
medium atp level	o2_set3_0420_min_HO2_vs_NRC1f.sig	1.0 > atp (mol/L) < 1.5.
medium copper	cu__0700um_vs_NRC-1	1e-4>mol/L<0.8e-3.
medium copper	ura3_Cu_0700um_a_vs_NRC-1d.sig	1e-4>mol/L<0.8e-3.
medium copper	ura3_Cu_0700um_b_vs_NRC-1d.sig	1e-4>mol/L<0.8e-3.
medium copper	sDura3_pCu_d0.100mM_t+015m_vs_NRC-1h1.sig	1e-4>mol/L<0.8e-3.
medium copper	sDura3_pCu_d0.100mM_t+030m_vs_NRC-1h1.sig	1e-4>mol/L<0.8e-3.
medium copper	sDura3_pCu_d0.100mM_t+060m_vs_NRC-1h1.sig	1e-4>mol/L<0.8e-3.

medium copper	sDura3_pCu_d0.100mM_t+180m_vs_NRC-1h1.sig	1e-4>mol/L<0.8e-3.
medium copper	sDura3_pCu_d0.700mM_t+015m_vs_NRC-1h1.sig	1e-4>mol/L<0.8e-3.
medium copper	sDura3_pCu_d0.700mM_t+030m_vs_NRC-1h1.sig	1e-4>mol/L<0.8e-3.
medium copper	sDura3_pCu_d0.700mM_t+060m_vs_NRC-1h1.sig	1e-4>mol/L<0.8e-3.
medium copper	sDura3_pCu_d0.700mM_t+180m_vs_NRC-1h1.sig	1e-4>mol/L<0.8e-3.
medium manganese	sirR_Mn_1000um_a_vs_NRC-1d.sig	1.0e-3 mol/L.
medium manganese	sirR_Mn_1000um_b_vs_NRC-1d.sig	1.0e-3 mol/L.
medium manganese	ura3_Mn_1000um_a_vs_NRC-1d.sig	1.0e-3 mol/L.
medium manganese	ura3_Mn_1000um_b_vs_NRC-1d.sig	1.0e-3 mol/L.
medium manganese	mn__1000um_vs_NRC-1	1.0e-3 mol/L.
medium zinc	Zn_0.015_vs_NRC-1d.sig	1.5e-5<mol/L<-2e-5.
medium zinc	zn__0020um_vs_NRC-1	1.5e-5<mol/L<-2e-5.
medium zinc	ZnSO4_ts_set-1_-005min_vs_NRC-1h1.sig	1.5e-5<mol/L<-2e-5.
medium zinc	ZnSO4_ts_set-1_000min_vs_NRC-1h1.sig	1.5e-5<mol/L<-2e-5.
medium zinc	ZnSO4_ts_set-1_005min_vs_NRC-1h1.sig	1.5e-5<mol/L<-2e-5.
medium zinc	ZnSO4_ts_set-1_010min_vs_NRC-1h1.sig	1.5e-5<mol/L<-2e-5.
medium zinc	ZnSO4_ts_set-1_020min_vs_NRC-1h1.sig	1.5e-5<mol/L<-2e-5.
medium zinc	ZnSO4_ts_set-1_040min_vs_NRC-1h1.sig	1.5e-5<mol/L<-2e-5.
medium zinc	ZnSO4_ts_set-1_080min_vs_NRC-1h1.sig	1.5e-5<mol/L<-2e-5.
medium zinc	ZnSO4_ts_set-1_160min_vs_NRC-1h1.sig	1.5e-5<mol/L<-2e-5.
medium zinc	ZnSO4_set2_-005min_vs_NRC-1h1.sig	1.5e-5<mol/L<-2e-5.
medium zinc	ZnSO4_set2_000min_vs_NRC-1h1.sig	1.5e-5<mol/L<-2e-5.
medium zinc	ZnSO4_set2_005min_vs_NRC-1h1.sig	1.5e-5<mol/L<-2e-5.
medium zinc	ZnSO4_set2_010min_vs_NRC-1h1.sig	1.5e-5<mol/L<-2e-5.
medium zinc	ZnSO4_set2_015min_vs_NRC-1h1.sig	1.5e-5<mol/L<-2e-5.
medium zinc	ZnSO4_set2_020min_vs_NRC-1h1.sig	1.5e-5<mol/L<-2e-5.
medium zinc	ZnSO4_set2_025min_vs_NRC-1h1.sig	1.5e-5<mol/L<-2e-5.
medium zinc	ZnSO4_set2_030min_vs_NRC-1h1.sig	1.5e-5<mol/L<-2e-5.
medium zinc	ZnSO4_set2_040min_vs_NRC-1h1.sig	1.5e-5<mol/L<-2e-5.
medium zinc	ZnSO4_set2_060min_vs_NRC-1h1.sig	1.5e-5<mol/L<-2e-5.
medium zinc	ZnSO4_set2_080min_vs_NRC-1h1.sig	1.5e-5<mol/L<-2e-5.
medium zinc	ZnSO4_set2_120min_vs_NRC-1h1.sig	1.5e-5<mol/L<-2e-5.
medium zinc	ZnSO4_set2_160min_vs_NRC-1h1.sig	1.5e-5<mol/L<-2e-5.
medium zinc	ZnSO4_set2_320min_vs_NRC-1h1.sig	1.5e-5<mol/L<-2e-5.
medium zinc	sDura3_pZn_d0.005mM_t-015m_vs_NRC-1h1.sig	1.5e-5<mol/L<-2e-5.

medium zinc	sDura3_pZn_d0.020mM_t+015m_vs_NRC-1h1.sig	1.5e-5<mol/L<-2e-5.
medium zinc	sDura3_pZn_d0.020mM_t+030m_vs_NRC-1h1.sig	1.5e-5<mol/L<-2e-5.
medium zinc	sDura3_pZn_d0.020mM_t+060m_vs_NRC-1h1.sig	1.5e-5<mol/L<-2e-5.
medium zinc	sDura3_pZn_d0.020mM_t+180m_vs_NRC-1h1.sig	1.5e-5<mol/L<-2e-5.
medium-high oxygen	uv__200jm2_D_030m	50 < pct < 75.
medium-high oxygen	uv__200jm2_D_060m	50 < pct < 75.
medium-high oxygen	uv__200jm2_L_030m	50 < pct < 75.
medium-high oxygen	uv__200jm2_L_060m	50 < pct < 75.
medium-high oxygen	o2_set1_0001m_L2H_500_vs_NRC-1c	50 < pct < 75.
medium-high oxygen	o2_set1_0750m_L2H_540_vs_NRC-1c	50 < pct < 75.
medium-high oxygen	20061006_Cmyc_rep2_0.179_vs_NRC-1e.sig	50 < pct < 75.
medium-high oxygen	20061006_Cmyc_rep2_0.399_vs_NRC-1e.sig	50 < pct < 75.
medium-high oxygen	20061006_Cmyc_rep2_0.833_vs_NRC-1e.sig	50 < pct < 75.
medium-high oxygen	20061006_Cmyc_rep1_0.175_vs_NRC-1e.sig	50 < pct < 75.
medium-high oxygen	20061006_Cmyc_rep1_0.417_vs_NRC-1e.sig	50 < pct < 75.
medium-high oxygen	20061006_Cmyc_rep1_0.835_vs_NRC-1e.sig	50 < pct < 75.
medium-high oxygen	20060818_KO_ura3_rep2_0.189_vs_NRC-1e.sig	50 < pct < 75.
medium-high oxygen	20060818_KO_ura3_rep2_0.376_vs_NRC-1e.sig	50 < pct < 75.
medium-high oxygen	20060818_KO_ura3_rep2_0.828_vs_NRC-1e.sig	50 < pct < 75.
medium-high oxygen	20060818_KO_ura3_rep1_0.178_vs_NRC-1e.sig	50 < pct < 75.
medium-high oxygen	20060818_KO_ura3_rep1_0.405_vs_NRC-1e.sig	50 < pct < 75.
medium-high oxygen	20060818_KO_ura3_rep1_0.842_vs_NRC-1e.sig	50 < pct < 75.
medium-high oxygen	20060717_Cmyc_rep2_0.223_vs_NRC-1e.sig	50 < pct < 75.
medium-high oxygen	20060717_Cmyc_rep2_0.407_vs_NRC-1e.sig	50 < pct < 75.
medium-high oxygen	20060717_Cmyc_rep2_0.883_vs_NRC-1e.sig	50 < pct < 75.

medium-high oxygen	20060717_Cmyc_rep1_0.221_vs_NRC-1e.sig	50 < pct < 75.
medium-high oxygen	20060717_Cmyc_rep1_0.402_vs_NRC-1e.sig	50 < pct < 75.
medium-high oxygen	20060717_Cmyc_rep1_0.827_vs_NRC-1e.sig	50 < pct < 75.
medium-high oxygen	20050620_NRC1_rep2_0.183_vs_NRC-1d.sig	50 < pct < 75.
medium-high oxygen	20050620_NRC1_rep2_0.505_vs_NRC-1d.sig	50 < pct < 75.
medium-high oxygen	20050620_NRC1_rep2_1.030_vs_NRC-1d.sig	50 < pct < 75.
medium-high oxygen	20050620_NRC1_rep1_0.173_vs_NRC-1d.sig	50 < pct < 75.
medium-high oxygen	20050620_NRC1_rep1_0.484_vs_NRC-1d.sig	50 < pct < 75.
medium-high oxygen	20050620_NRC1_rep1_1.276_vs_NRC-1d.sig	50 < pct < 75.
medium-high oxygen	20050620_Cmyc_rep2_0.177_vs_NRC-1d.sig	50 < pct < 75.
medium-high oxygen	20050620_Cmyc_rep2_0.457_vs_NRC-1d.sig	50 < pct < 75.
medium-high oxygen	20050620_Cmyc_rep2_1.072_vs_NRC-1d.sig	50 < pct < 75.
medium-high oxygen	20050620_Cmyc_rep1_0.207_vs_NRC-1d.sig	50 < pct < 75.
medium-high oxygen	20050620_Cmyc_rep1_0.474_vs_NRC-1d.sig	50 < pct < 75.
medium-high oxygen	20050620_Cmyc_rep1_1.052_vs_NRC-1d.sig	50 < pct < 75.
medium-low oxygen	o2_set2_H_L_005_vs_NRC-1d.sig	25 < pct < 50.
medium-low oxygen	PQ_Const._set_1_0.25mM_-001m_vs_NRC-1f.sig	25 < pct < 50.
medium-low oxygen	PQ_Const._set_1_0.25mM_000m_vs_NRC-1f.sig	25 < pct < 50.
medium-low oxygen	PQ_Const._set_1_0.25mM_005m_vs_NRC-1f.sig	25 < pct < 50.
medium-low oxygen	PQ_Const._set_1_0.25mM_010m_vs_NRC-1f.sig	25 < pct < 50.
medium-low oxygen	PQ_Const._set_1_0.25mM_020m_vs_NRC-1f.sig	25 < pct < 50.
medium-low oxygen	PQ_Const._set_1_0.25mM_040m_vs_NRC-1f.sig	25 < pct < 50.
medium-low oxygen	PQ_Const._set_1_0.25mM_080m_vs_NRC-1f.sig	25 < pct < 50.
medium-low oxygen	PQ_Const._set_1_0.25mM_160m_vs_NRC-1f.sig	25 < pct < 50.
medium-low oxygen	PQ_Const._set_1_0.25mM_320m_vs_NRC-1f.sig	25 < pct < 50.

metal chelation	Dip_0.025_vs_NRC-1d.sig	dip (2.5e-5<=mol/L<=2.5e-4)or edta(1e-3 mol/L)
metal chelation	Dip_0.100_vs_NRC-1d.sig	dip (2.5e-5<=mol/L<=2.5e-4)or edta(1e-3 mol/L)
metal chelation	Dip_0.250_vs_NRC-1d.sig	dip (2.5e-5<=mol/L<=2.5e-4)or edta(1e-3 mol/L)
metal chelation	Dip_0.000_vs_NRC-1d.sig	dip (2.5e-5<=mol/L<=2.5e-4)or edta(1e-3 mol/L)
metal chelation	ura3_0min_-EDTA_CM_vs_NRC1-h1.sig	dip (2.5e-5<=mol/L<=2.5e-4)or edta(1e-3 mol/L)
metal chelation	ura3_20min_-EDTA_CM_vs_NRC1-h1.sig	dip (2.5e-5<=mol/L<=2.5e-4)or edta(1e-3 mol/L)
metal chelation	ura3_40min_-EDTA_CM_vs_NRC1-h1.sig	dip (2.5e-5<=mol/L<=2.5e-4)or edta(1e-3 mol/L)
metal chelation	ura3_60min_-EDTA_CM_vs_NRC1-h1.sig	dip (2.5e-5<=mol/L<=2.5e-4)or edta(1e-3 mol/L)
metal chelation	ura3_0min_1mM_EDTA_vs_NRC1-h1.sig	dip (2.5e-5<=mol/L<=2.5e-4)or edta(1e-3 mol/L)
metal chelation	ura3_20min_1mM_EDTA_vs_NRC1-h1.sig	dip (2.5e-5<=mol/L<=2.5e-4)or edta(1e-3 mol/L)
metal chelation	ura3_40min_1mM_EDTA_vs_NRC1-h1.sig	dip (2.5e-5<=mol/L<=2.5e-4)or edta(1e-3 mol/L)
metal chelation	ura3_60min_1mM_EDTA_vs_NRC1-h1.sig	dip (2.5e-5<=mol/L<=2.5e-4)or edta(1e-3 mol/L)
mid-exponential phase	dark1__1200m_vs_NRC-1c	0.4 >= OD < 0.6.
mid-exponential phase	dark1__1440m_vs_NRC-1c	0.4 >= OD < 0.6.
mid-exponential phase	dark1__1680m_vs_NRC-1c	0.4 >= OD < 0.6.
mid-exponential phase	dark1__3120m_vs_NRC-1c	0.4 >= OD < 0.6.
mid-exponential phase	dark1__3360m_vs_NRC-1c	0.4 >= OD < 0.6.
mid-exponential phase	circadian_Dphr1_drk_cycling__1440min_vs_NRC-1d.sig	0.4 >= OD < 0.6.
mid-exponential phase	circadian_Dphr1_drk_cycling__1665min_vs_NRC-1d.sig	0.4 >= OD < 0.6.
mid-exponential phase	circadian_Dphr1_drk_cycling__1800min_vs_NRC-1d.sig	0.4 >= OD < 0.6.
mid-exponential phase	circadian_drk8_cycling_0540min_vs_NRC-1e.sig	0.4 >= OD < 0.6.
mid-exponential phase	circadian_drk8_cycling_0720min_vs_NRC-1e.sig	0.4 >= OD < 0.6.
mid-exponential phase	circadian_drk8_cycling_0900min_vs_NRC-1e.sig	0.4 >= OD < 0.6.
mid-exponential phase	circadian_drk8_cycling_1080min_vs_NRC-1e.sig	0.4 >= OD < 0.6.
mid-exponential phase	circadian_drk8_cycling_1260min_vs_NRC-1e.sig	0.4 >= OD < 0.6.

mid-exponential phase	circadian_drk8_cycling_1440min_vs_NRC-1e.sig	0.4 >= OD < 0.6.
mid-exponential phase	circadian_drk8_cycling_1620min_vs_NRC-1e.sig	0.4 >= OD < 0.6.
mid-exponential phase	circadian_drk8_cycling_1800min_vs_NRC-1e.sig	0.4 >= OD < 0.6.
mid-exponential phase	circadian_drk8_cycling_1980min_vs_NRC-1e.sig	0.4 >= OD < 0.6.
mid-exponential phase	circadian_drk8_cycling_2160min_vs_NRC-1e.sig	0.4 >= OD < 0.6.
mid-exponential phase	circadian_drk8_cycling_2340min_vs_NRC-1e.sig	0.4 >= OD < 0.6.
mid-exponential phase	circadian_drk8_cycling_2520min_vs_NRC-1e.sig	0.4 >= OD < 0.6.
mid-exponential phase	circadian_drk8_cycling_2700min_vs_NRC-1e.sig	0.4 >= OD < 0.6.
mid-exponential phase	circadian_drk8_cycling_2880min_vs_NRC-1e.sig	0.4 >= OD < 0.6.
mid-exponential phase	circadian_drk8_cycling_3060min_vs_NRC-1e.sig	0.4 >= OD < 0.6.
mid-exponential phase	circadian_drk8_cycling_3240min_vs_NRC-1e.sig	0.4 >= OD < 0.6.
mid-exponential phase	circadian_drk7_cycling_0000min_vs_NRC-1d.sig	0.4 >= OD < 0.6.
mid-exponential phase	circadian_drk7_cycling_0180min_vs_NRC-1d.sig	0.4 >= OD < 0.6.
mid-exponential phase	circadian_drk7_cycling_0540min_vs_NRC-1d.sig	0.4 >= OD < 0.6.
mid-exponential phase	circadian_drk7_cycling_0720min_vs_NRC-1d.sig	0.4 >= OD < 0.6.
mid-exponential phase	circadian_drk7_cycling_0900min_vs_NRC-1d.sig	0.4 >= OD < 0.6.
mid-exponential phase	circadian_drk7_cycling_3060min_vs_NRC-1d.sig	0.4 >= OD < 0.6.
mid-exponential phase	circadian_drk6_cycling_0000min_vs_NRC-1e.sig	0.4 >= OD < 0.6.
mid-exponential phase	circadian_drk6_cycling_0180min_vs_NRC-1e.sig	0.4 >= OD < 0.6.
mid-exponential phase	circadian_drk6_cycling_0360min_vs_NRC-1e.sig	0.4 >= OD < 0.6.
mid-exponential phase	circadian_drk6_cycling_0540min_vs_NRC-1e.sig	0.4 >= OD < 0.6.
mid-exponential phase	circadian_drk6_cycling_0720min_vs_NRC-1e.sig	0.4 >= OD < 0.6.
mid-exponential phase	circadian_drk6_cycling_0912min_vs_NRC-1e.sig	0.4 >= OD < 0.6.
mid-exponential phase	circadian_drk6_cycling_1080min_vs_NRC-1e.sig	0.4 >= OD < 0.6.
mid-exponential phase	circadian_drk6_cycling_1260min_vs_NRC-1e.sig	0.4 >= OD < 0.6.

mid-exponential phase	circadian_drk6_cycling_1440min_vs_NRC-1e.sig	0.4 >= OD < 0.6.
mid-exponential phase	circadian__dark5_cycling_30C_1440min_vs_NRC-1d.sig	0.4 >= OD < 0.6.
mid-exponential phase	circadian__dark5_cycling_30C_1630min_vs_NRC-1d.sig	0.4 >= OD < 0.6.
mid-exponential phase	circadian__dark5_cycling_30C_1815min_vs_NRC-1d.sig	0.4 >= OD < 0.6.
mid-exponential phase	circadian_dark3_cycling_1620min_vs_NRC-1d.sig	0.4 >= OD < 0.6.
mid-exponential phase	circadian_dark3_cycling_1800min_vs_NRC-1d.sig	0.4 >= OD < 0.6.
mid-exponential phase	circadian_dark3_cycling_1980min_vs_NRC-1d.sig	0.4 >= OD < 0.6.
mid-exponential phase	circadian_dark3_cycling_2160min_vs_NRC-1d.sig	0.4 >= OD < 0.6.
mid-exponential phase	circadian_dark3_cycling_2220min_vs_NRC-1d.sig	0.4 >= OD < 0.6.
mid-exponential phase	circadian_dark3_cycling_2340min_vs_NRC-1d.sig	0.4 >= OD < 0.6.
mid-exponential phase	circadian_dark3_cycling_2520min_vs_NRC-1d.sig	0.4 >= OD < 0.6.
mid-exponential phase	circadian_dark3_ctrl_1620min_vs_NRC-1d.sig	0.4 >= OD < 0.6.
mid-exponential phase	circadian_dark3_ctrl_1800min_vs_NRC-1d.sig	0.4 >= OD < 0.6.
mid-exponential phase	circadian_dark3_ctrl_1980min_vs_NRC-1d.sig	0.4 >= OD < 0.6.
mid-exponential phase	circadian_dark3_ctrl_2160min_vs_NRC-1d.sig	0.4 >= OD < 0.6.
mid-exponential phase	circadian_dark3_ctrl_2220min_vs_NRC-1d.sig	0.4 >= OD < 0.6.
mid-exponential phase	circadian_drk8_control_0180min_vs_NRC-1e.sig	0.4 >= OD < 0.6.
mid-exponential phase	circadian_drk8_control_0360min_vs_NRC-1e.sig	0.4 >= OD < 0.6.
mid-exponential phase	circadian_drk8_control_0540min_vs_NRC-1e.sig	0.4 >= OD < 0.6.
mid-exponential phase	circadian_drk8_control_0720min_vs_NRC-1e.sig	0.4 >= OD < 0.6.
mid-exponential phase	circadian_drk8_control_0900min_vs_NRC-1e.sig	0.4 >= OD < 0.6.
mid-exponential phase	circadian_drk8_control_1080min_vs_NRC-1e.sig	0.4 >= OD < 0.6.
mid-exponential phase	circadian_drk8_control_1260min_vs_NRC-1e.sig	0.4 >= OD < 0.6.
mid-exponential phase	circadian_drk8_control_1440min_vs_NRC-1e.sig	0.4 >= OD < 0.6.
mid-exponential phase	circadian_drk8_control_1620min_vs_NRC-1e.sig	0.4 >= OD < 0.6.

mid-exponential phase	circadian_drk8_control_1800min_vs_NRC-1e.sig	0.4 >= OD < 0.6.
mid-exponential phase	circadian_drk8_control_1980min_vs_NRC-1e.sig	0.4 >= OD < 0.6.
mid-exponential phase	circadian_drk8_control_2160min_vs_NRC-1e.sig	0.4 >= OD < 0.6.
mid-exponential phase	circadian_drk8_control_2340min_vs_NRC-1e.sig	0.4 >= OD < 0.6.
mid-exponential phase	circadian_drk8_control_2520min_vs_NRC-1e.sig	0.4 >= OD < 0.6.
mid-exponential phase	circadian_drk8_control_2700min_vs_NRC-1e.sig	0.4 >= OD < 0.6.
mid-exponential phase	circadian_drk8_control_3060min_vs_NRC-1e.sig	0.4 >= OD < 0.6.
mid-exponential phase	circadian_drk8_control_3240min_vs_NRC-1e.sig	0.4 >= OD < 0.6.
mid-exponential phase	Circadian_Dark9_Cycling_1265min_vs_NRC-1g.sig	0.4 >= OD < 0.6.
mid-exponential phase	Circadian_Dark10_Cycling_-2873min_vs_NRC-1h1.sig	0.4 >= OD < 0.6.
mid-exponential phase	Circadian_Dark10_Cycling_-2670min_vs_NRC-1h1.sig	0.4 >= OD < 0.6.
mid-exponential phase	Circadian_Dark10_Cycling_-2315min_vs_NRC-1h1.sig	0.4 >= OD < 0.6.
mid-exponential phase	Circadian_Dark10_Cycling_-2120min_vs_NRC-1h1.sig	0.4 >= OD < 0.6.
mid-exponential phase	Circadian_Dark10_Cycling_-1960min_vs_NRC-1h1.sig	0.4 >= OD < 0.6.
mid-exponential phase	Circadian_Dark10_Cycling_-1785min_vs_NRC-1h1.sig	0.4 >= OD < 0.6.
mid-exponential phase	Circadian_Dark10_Cycling_-1595min_vs_NRC-1h1.sig	0.4 >= OD < 0.6.
mid-exponential phase	Circadian_Dark10_Cycling_-1060min_vs_NRC-1h1.sig	0.4 >= OD < 0.6.
mid-exponential phase	Circadian_Dark10_Cycling_-0360min_vs_NRC-1h1.sig	0.4 >= OD < 0.6.
mid-exponential phase	Circadian_Dark10_Cycling_0195min_vs_NRC-1h1.sig	0.4 >= OD < 0.6.
mid-exponential phase	Circadian_Dark10_Cycling_0560min_vs_NRC-1h1.sig	0.4 >= OD < 0.6.
mid-exponential phase	Cu_-5_vs_NRC-1.sig	0.4 >= OD < 0.6.
mid-exponential phase	Cu_000_vs_NRC-1.sig	0.4 >= OD < 0.6.
mid-exponential phase	Cu_005_vs_NRC-1.sig	0.4 >= OD < 0.6.
mid-exponential phase	Cu_010_vs_NRC-1.sig	0.4 >= OD < 0.6.
mid-exponential phase	Cu_020_vs_NRC-1.sig	0.4 >= OD < 0.6.

mid-exponential phase	Cu_160_vs_NRC-1.sig	0.4 >= OD < 0.6.
mid-exponential phase	Cu_-1_vs_NRC-1e.sig	0.4 >= OD < 0.6.
mid-exponential phase	Cu_000_vs_NRC-1e.sig	0.4 >= OD < 0.6.
mid-exponential phase	Cu_005_vs_NRC-1e.sig	0.4 >= OD < 0.6.
mid-exponential phase	Cu_010_vs_NRC-1e.sig	0.4 >= OD < 0.6.
mid-exponential phase	Cu_020_vs_NRC-1e.sig	0.4 >= OD < 0.6.
mid-exponential phase	Cu_160_vs_NRC-1e.sig	0.4 >= OD < 0.6.
mid-exponential phase	Cu_NRC1_set1_160min_vs_NRC-1h1.sig	0.4 >= OD < 0.6.
mid-exponential phase	Cu_ura3_KO_set1_-030min_vs_NRC-1h1.sig	0.4 >= OD < 0.6.
mid-exponential phase	Cu_ura3_KO_set1_000min_vs_NRC-1h1.sig	0.4 >= OD < 0.6.
mid-exponential phase	Cu_ura3_KO_set1_005min_vs_NRC-1h1.sig	0.4 >= OD < 0.6.
mid-exponential phase	Cu_ura3_KO_set1_010min_vs_NRC-1h1.sig	0.4 >= OD < 0.6.
mid-exponential phase	Cu_ura3_KO_set1_020min_vs_NRC-1h1.sig	0.4 >= OD < 0.6.
mid-exponential phase	Cu_ura3_KO_set1_040min_vs_NRC-1h1.sig	0.4 >= OD < 0.6.
mid-exponential phase	Cu_ura3_KO_set1_080min_vs_NRC-1h1.sig	0.4 >= OD < 0.6.
mid-exponential phase	Cu_ura3_KO_set1_160min_vs_NRC-1h1.sig	0.4 >= OD < 0.6.
mid-exponential phase	Cu_ura3_KO_set2_-030min_vs_NRC-1h1.sig	0.4 >= OD < 0.6.
mid-exponential phase	Cu_ura3_KO_set2_000min_vs_NRC-1h1.sig	0.4 >= OD < 0.6.
mid-exponential phase	Cu_ura3_KO_set2_005min_vs_NRC-1h1.sig	0.4 >= OD < 0.6.
mid-exponential phase	Cu_ura3_KO_set2_010min_vs_NRC-1h1.sig	0.4 >= OD < 0.6.
mid-exponential phase	Cu_ura3_KO_set2_020min_vs_NRC-1h1.sig	0.4 >= OD < 0.6.
mid-exponential phase	Cu_ura3_KO_set2_040min_vs_NRC-1h1.sig	0.4 >= OD < 0.6.
mid-exponential phase	Cu_ura3_KO_set2_080min_vs_NRC-1h1.sig	0.4 >= OD < 0.6.
mid-exponential phase	Cu_NRC1_set2_-030min_vs_NRC-1h1.sig	0.4 >= OD < 0.6.
mid-exponential phase	Cu_NRC1_set2_000min_vs_NRC-1h1.sig	0.4 >= OD < 0.6.

mid-exponential phase	Cu_NRC1_set2_005min_vs_NRC-1h1.sig	0.4 >= OD < 0.6.
mid-exponential phase	Cu_NRC1_set2_010min_vs_NRC-1h1.sig	0.4 >= OD < 0.6.
mid-exponential phase	Cu_NRC1_set2_020min_vs_NRC-1h1.sig	0.4 >= OD < 0.6.
mid-exponential phase	Cu_NRC1_set2_040min_vs_NRC-1h1.sig	0.4 >= OD < 0.6.
mid-exponential phase	Cu_NRC1_set2_080min_vs_NRC-1h1.sig	0.4 >= OD < 0.6.
mid-exponential phase	Cu_NRC1_set2_160min_vs_NRC-1h1.sig	0.4 >= OD < 0.6.
mid-exponential phase	ura3_40min_+Fe_vs_NRC1-h1.sig	0.4 >= OD < 0.6.
mid-exponential phase	zim__HO_D_vs_NRC-1	0.4 >= OD < 0.6.
mid-exponential phase	zim__HO_L_vs_NRC-1	0.4 >= OD < 0.6.
mid-exponential phase	zim__LO_D_vs_NRC-1	0.4 >= OD < 0.6.
mid-exponential phase	zim__LO_L_vs_NRC-1	0.4 >= OD < 0.6.
mid-exponential phase	VNG2334C__HO_D_vs_NRC-1	0.4 >= OD < 0.6.
mid-exponential phase	VNG2334C__HO_L_vs_NRC-1	0.4 >= OD < 0.6.
mid-exponential phase	VNG2334C__LO_D_vs_NRC-1	0.4 >= OD < 0.6.
mid-exponential phase	VNG2334C__LO_L_vs_NRC-1	0.4 >= OD < 0.6.
mid-exponential phase	circadian__dark_cycling_125w/m2_42C_1615min_vs_NRC-1d.sig	0.4 >= OD < 0.6.
mid-exponential phase	circadian__dark_cycling_125w/m2_42C_1800min_vs_NRC-1d.sig	0.4 >= OD < 0.6.
mid-exponential phase	circadian__dark_cycling_125w/m2_42C_1985min_vs_NRC-1d.sig	0.4 >= OD < 0.6.
mid-exponential phase	circadian__dark_cycling_125w/m2_42C_2160min_vs_NRC-1d.sig	0.4 >= OD < 0.6.
mid-exponential phase	circadian__dark_cycling_125w/m2_42C_2340min_vs_NRC-1d.sig	0.4 >= OD < 0.6.
mid-exponential phase	circadian__dark_cycling_125w/m2_42C_2515min_vs_NRC-1d.sig	0.4 >= OD < 0.6.
mid-exponential phase	NRC1_H2O_0890_0.468_rep2_vs_NRC-1g.sig	0.4 >= OD < 0.6.
mid-exponential phase	NRC1_H2O_0890_0.496_rep1_vs_NRC-1g.sig	0.4 >= OD < 0.6.
mid-exponential phase	NRC1_Uracil_0890_0.420_rep2_vs_NRC-1g.sig	0.4 >= OD < 0.6.
mid-exponential phase	NRC1_Uracil_0890_0.440_rep1_vs_NRC-1g.sig	0.4 >= OD < 0.6.

mid-exponential phase	Dura3_Uracil_1200_0.467_rep2_vs_NRC-1g.sig	0.4 >= OD < 0.6.
mid-exponential phase	Dura3_Uracil_1200_0.465_rep1_vs_NRC-1g.sig	0.4 >= OD < 0.6.
mid-exponential phase	NRC1_03960_0.409_rep2_vs_NRC-1g.sig	0.4 >= OD < 0.6.
mid-exponential phase	NRC1_04320_0.578_rep2_vs_NRC-1g.sig	0.4 >= OD < 0.6.
mid-exponential phase	NRC1_04320_0.590_rep1_vs_NRC-1g.sig	0.4 >= OD < 0.6.
mid-exponential phase	H2O2_Recov._set_3_0mM_000min_vs_NRC-1f.sig	0.4 >= OD < 0.6.
mid-exponential phase	H2O2_Recov._set_3_0mM_010min_vs_NRC-1f.sig	0.4 >= OD < 0.6.
mid-exponential phase	H2O2_Recov._set_3_0mM_020min_vs_NRC-1f.sig	0.4 >= OD < 0.6.
mid-exponential phase	H2O2_Recov._set_3_0mM_030min_vs_NRC-1f.sig	0.4 >= OD < 0.6.
mid-exponential phase	H2O2_Recov._set_3_0mM_040min_vs_NRC-1f.sig	0.4 >= OD < 0.6.
mid-exponential phase	H2O2_Recov._set_3_0mM_050min_vs_NRC-1f.sig	0.4 >= OD < 0.6.
mid-exponential phase	H2O2_Recov._set_3_0mM_060min_vs_NRC-1f.sig	0.4 >= OD < 0.6.
mid-exponential phase	H2O2_Recov._set_3_0mM_120min_vs_NRC-1f.sig	0.4 >= OD < 0.6.
mid-exponential phase	H2O2_Const._set_2_0mM_000min_vs_NRC-1f.sig	0.4 >= OD < 0.6.
mid-exponential phase	H2O2_Const._set_2_0mM_030min_vs_NRC-1f.sig	0.4 >= OD < 0.6.
mid-exponential phase	H2O2_Const._set_2_0mM_060min_vs_NRC-1f.sig	0.4 >= OD < 0.6.
mid-exponential phase	H2O2_Const._set_2_0mM_120min_vs_NRC-1f.sig	0.4 >= OD < 0.6.
mid-exponential phase	PQ_Recov._set_2_0mM_000min_vs_NRC-1f.sig	0.4 >= OD < 0.6.
mid-exponential phase	PQ_Recov._set_2_0mM_010min_vs_NRC-1f.sig	0.4 >= OD < 0.6.
mid-exponential phase	PQ_Recov._set_2_0mM_020min_vs_NRC-1f.sig	0.4 >= OD < 0.6.
mid-exponential phase	PQ_Recov._set_2_0mM_030min_vs_NRC-1f.sig	0.4 >= OD < 0.6.
mid-exponential phase	PQ_Recov._set_2_0mM_040min_vs_NRC-1f.sig	0.4 >= OD < 0.6.
mid-exponential phase	PQ_Recov._set_2_0mM_050min_vs_NRC-1f.sig	0.4 >= OD < 0.6.
mid-exponential phase	PQ_Recov._set_2_0mM_060min_vs_NRC-1f.sig	0.4 >= OD < 0.6.
mid-exponential phase	PQ_Recov._set_2_0mM_120min_vs_NRC-1f.sig	0.4 >= OD < 0.6.

mid-exponential phase	PQ_Const._set_2_0mM_000min_vs_NRC-1f.sig	0.4 >= OD < 0.6.
mid-exponential phase	PQ_Const._set_2_0mM_030min_vs_NRC-1f.sig	0.4 >= OD < 0.6.
mid-exponential phase	PQ_Const._set_2_0mM_060min_vs_NRC-1f.sig	0.4 >= OD < 0.6.
mid-exponential phase	H2O2_Recov._set_2_0mM_000min_vs_NRC-1f.sig	0.4 >= OD < 0.6.
mid-exponential phase	H2O2_Recov._set_2_0mM_010min_vs_NRC-1f.sig	0.4 >= OD < 0.6.
mid-exponential phase	H2O2_Recov._set_2_0mM_020min_vs_NRC-1f.sig	0.4 >= OD < 0.6.
mid-exponential phase	H2O2_Recov._set_2_0mM_030min_vs_NRC-1f.sig	0.4 >= OD < 0.6.
mid-exponential phase	H2O2_Recov._set_2_0mM_040min_vs_NRC-1f.sig	0.4 >= OD < 0.6.
mid-exponential phase	H2O2_Recov._set_2_0mM_050min_vs_NRC-1f.sig	0.4 >= OD < 0.6.
mid-exponential phase	H2O2_Recov._set_2_0mM_060min_vs_NRC-1f.sig	0.4 >= OD < 0.6.
mid-exponential phase	H2O2_Recov._set_2_0mM_120min_vs_NRC-1f.sig	0.4 >= OD < 0.6.
mid-exponential phase	H2O2_Const._set_1_0mM_000min_vs_NRC-1f.sig	0.4 >= OD < 0.6.
mid-exponential phase	H2O2_Const._set_1_0mM_030min_vs_NRC-1f.sig	0.4 >= OD < 0.6.
mid-exponential phase	H2O2_Const._set_1_0mM_060min_vs_NRC-1f.sig	0.4 >= OD < 0.6.
mid-exponential phase	H2O2_Const._set_1_0mM_120min_vs_NRC-1f.sig	0.4 >= OD < 0.6.
mid-exponential phase	PQ_Recov._set_1_0mM_000min_vs_NRC-1f.sig	0.4 >= OD < 0.6.
mid-exponential phase	PQ_Recov._set_1_0mM_010min_vs_NRC-1f.sig	0.4 >= OD < 0.6.
mid-exponential phase	PQ_Recov._set_1_0mM_020min_vs_NRC-1f.sig	0.4 >= OD < 0.6.
mid-exponential phase	PQ_Recov._set_1_0mM_030min_vs_NRC-1f.sig	0.4 >= OD < 0.6.
mid-exponential phase	PQ_Recov._set_1_0mM_040min_vs_NRC-1f.sig	0.4 >= OD < 0.6.
mid-exponential phase	PQ_Recov._set_1_0mM_050min_vs_NRC-1f.sig	0.4 >= OD < 0.6.
mid-exponential phase	PQ_Recov._set_1_0mM_060min_vs_NRC-1f.sig	0.4 >= OD < 0.6.
mid-exponential phase	PQ_Const._set_1_0mM_000min_vs_NRC-1f.sig	0.4 >= OD < 0.6.
mid-exponential phase	PQ_Const._set_1_0mM_030min_vs_NRC-1f.sig	0.4 >= OD < 0.6.
mid-exponential phase	PQ_Const._set_1_0mM_060min_vs_NRC-1f.sig	0.4 >= OD < 0.6.

mid-exponential phase	MDM200gSalt_0.466_vs_NRC-1e.sig	0.4 >= OD < 0.6.
mid-exponential phase	MDM200gSalt_0.534_vs_NRC-1e.sig	0.4 >= OD < 0.6.
mid-exponential phase	20060818_NRC1_rep2_0.424_vs_NRC-1e.sig	0.4 >= OD < 0.6.
mid-exponential phase	20060818_NRC1_rep1_0.430_vs_NRC-1e.sig	0.4 >= OD < 0.6.
mid-exponential phase	KO_ura3.2_0.4308_vs_NRC-1_h1.sig	0.4 >= OD < 0.6.
mid-exponential phase	KO_ura3.2_0.5084_vs_NRC-1_h1.sig	0.4 >= OD < 0.6.
mid-exponential phase	ura3_growth_t2exp1_0.5OD_vs_NRC1e.sig	0.4 >= OD < 0.6.
mid-exponential phase	ura3_growth_t2_exp2_0.5OD_vs_NRC1f.sig	0.4 >= OD < 0.6.
mid-exponential phase	ura3_+glu_a_OD1.2_vs_NRC1e.sig	0.4 >= OD < 0.6.
mid-exponential phase	ura3_growth_t2_exp3_0.5OD_vs_NRC1f.sig	0.4 >= OD < 0.6.
mid-exponential phase	ura3_+glu_a_OD1.2repl_vs_NRC1e.sig	0.4 >= OD < 0.6.
mid-exponential phase	ura3_+glu_b_OD1.2repl_vs_NRC1g.sig	0.4 >= OD < 0.6.
mid-exponential phase	MDM250gSalt_0.481_vs_NRC-1e.sig	0.4 >= OD < 0.6.
mid-exponential phase	MDM250gSalt_0.49_vs_NRC-1e.sig	0.4 >= OD < 0.6.
mid-exponential phase	H2O2_Recov._set_3_25mM_000min_vs_NRC-1f.sig	0.4 >= OD < 0.6.
mid-exponential phase	H2O2_Recov._set_3_25mM_010min_vs_NRC-1f.sig	0.4 >= OD < 0.6.
mid-exponential phase	H2O2_Recov._set_3_25mM_020min_vs_NRC-1f.sig	0.4 >= OD < 0.6.
mid-exponential phase	H2O2_Recov._set_3_25mM_030min_vs_NRC-1f.sig	0.4 >= OD < 0.6.
mid-exponential phase	H2O2_Recov._set_3_25mM_040min_vs_NRC-1f.sig	0.4 >= OD < 0.6.
mid-exponential phase	H2O2_Recov._set_3_25mM_050min_vs_NRC-1f.sig	0.4 >= OD < 0.6.
mid-exponential phase	H2O2_Recov._set_3_25mM_060min_vs_NRC-1f.sig	0.4 >= OD < 0.6.
mid-exponential phase	H2O2_Recov._set_3_25mM_120min_vs_NRC-1f.sig	0.4 >= OD < 0.6.
mid-exponential phase	H2O2_Recov._set_3_25mM_240min_vs_NRC-1f.sig	0.4 >= OD < 0.6.
mid-exponential phase	H2O2_Const._set_2_25mM_000min_vs_NRC-1f.sig	0.4 >= OD < 0.6.
mid-exponential phase	H2O2_Const._set_2_25mM_030min_vs_NRC-1f.sig	0.4 >= OD < 0.6.

mid-exponential phase	H2O2_Const._set_2_25mM_060min_vs_NRC-1f.sig	0.4 >= OD < 0.6.
mid-exponential phase	H2O2_Const._set_2_25mM_120min_vs_NRC-1f.sig	0.4 >= OD < 0.6.
mid-exponential phase	PQ_Recov._set_2_4mM_000min_vs_NRC-1f.sig	0.4 >= OD < 0.6.
mid-exponential phase	PQ_Recov._set_2_4mM_010min_vs_NRC-1f.sig	0.4 >= OD < 0.6.
mid-exponential phase	PQ_Recov._set_2_4mM_020min_vs_NRC-1f.sig	0.4 >= OD < 0.6.
mid-exponential phase	PQ_Recov._set_2_4mM_030min_vs_NRC-1f.sig	0.4 >= OD < 0.6.
mid-exponential phase	PQ_Recov._set_2_4mM_040min_vs_NRC-1f.sig	0.4 >= OD < 0.6.
mid-exponential phase	PQ_Recov._set_2_4mM_050min_vs_NRC-1f.sig	0.4 >= OD < 0.6.
mid-exponential phase	PQ_Recov._set_2_4mM_060min_vs_NRC-1f.sig	0.4 >= OD < 0.6.
mid-exponential phase	PQ_Recov._set_2_4mM_120min_vs_NRC-1f.sig	0.4 >= OD < 0.6.
mid-exponential phase	PQ_Recov._set_2_4mM_240min_vs_NRC-1f.sig	0.4 >= OD < 0.6.
mid-exponential phase	PQ_Const._set_2_4mM_000min_vs_NRC-1f.sig	0.4 >= OD < 0.6.
mid-exponential phase	PQ_Const._set_2_4mM_030min_vs_NRC-1f.sig	0.4 >= OD < 0.6.
mid-exponential phase	PQ_Const._set_2_4mM_060min_vs_NRC-1f.sig	0.4 >= OD < 0.6.
mid-exponential phase	PQ_Const._set_2_4mM_120min_vs_NRC-1f.sig	0.4 >= OD < 0.6.
mid-exponential phase	PQ_Const._set_2_4mM_240min_vs_NRC-1f.sig	0.4 >= OD < 0.6.
mid-exponential phase	H2O2_Const._set_1_25mM_000min_vs_NRC-1f.sig	0.4 >= OD < 0.6.
mid-exponential phase	H2O2_Const._set_1_25mM_030min_vs_NRC-1f.sig	0.4 >= OD < 0.6.
mid-exponential phase	H2O2_Const._set_1_25mM_060min_vs_NRC-1f.sig	0.4 >= OD < 0.6.
mid-exponential phase	H2O2_Const._set_1_25mM_120min_vs_NRC-1f.sig	0.4 >= OD < 0.6.
mid-exponential phase	PQ_Recov._set_1_4mM_000min_vs_NRC-1f.sig	0.4 >= OD < 0.6.
mid-exponential phase	PQ_Recov._set_1_4mM_010min_vs_NRC-1f.sig	0.4 >= OD < 0.6.
mid-exponential phase	PQ_Recov._set_1_4mM_020min_vs_NRC-1f.sig	0.4 >= OD < 0.6.
mid-exponential phase	PQ_Recov._set_1_4mM_030min_vs_NRC-1f.sig	0.4 >= OD < 0.6.
mid-exponential phase	PQ_Recov._set_1_4mM_040min_vs_NRC-1f.sig	0.4 >= OD < 0.6.

mid-exponential phase	PQ_Recov._set_1_4mM_050min_vs_NRC-1f.sig	0.4 >= OD < 0.6.
mid-exponential phase	PQ_Recov._set_1_4mM_060min_vs_NRC-1f.sig	0.4 >= OD < 0.6.
mid-exponential phase	PQ_Recov._set_1_4mM_120min_vs_NRC-1f.sig	0.4 >= OD < 0.6.
mid-exponential phase	PQ_Recov._set_1_4mM_240min_vs_NRC-1f.sig	0.4 >= OD < 0.6.
mid-exponential phase	PQ_Const._set_1_4mM_000min_vs_NRC-1f.sig	0.4 >= OD < 0.6.
mid-exponential phase	PQ_Const._set_1_4mM_030min_vs_NRC-1f.sig	0.4 >= OD < 0.6.
mid-exponential phase	PQ_Const._set_1_4mM_060min_vs_NRC-1f.sig	0.4 >= OD < 0.6.
mid-exponential phase	PQ_Const._set_1_4mM_120min_vs_NRC-1f.sig	0.4 >= OD < 0.6.
mid-exponential phase	PQ_Const._set_1_4mM_240min_vs_NRC-1f.sig	0.4 >= OD < 0.6.
mid-exponential phase	KO_ura3.3_0.4452_vs_NRC-1_h1.sig	0.4 >= OD < 0.6.
mid-exponential phase	KO_ura3.4_0.4645_vs_NRC-1_h1.sig	0.4 >= OD < 0.6.
mid-exponential phase	o2_set1_-001m_L2H_005_vs_NRC-1c	0.4 >= OD < 0.6.
mid-exponential phase	o2_set1_0001m_L2H_500_vs_NRC-1c	0.4 >= OD < 0.6.
mid-exponential phase	o2_set1_0005m_H_922_vs_NRC-1c	0.4 >= OD < 0.6.
mid-exponential phase	o2_set1_0010m_H_947_vs_NRC-1c	0.4 >= OD < 0.6.
mid-exponential phase	o2_set1_0020m_H_937_vs_NRC-1c	0.4 >= OD < 0.6.
mid-exponential phase	o2_set1_0030m_H_931_vs_NRC-1c	0.4 >= OD < 0.6.
mid-exponential phase	o2_set1_0045m_H_939_vs_NRC-1c	0.4 >= OD < 0.6.
mid-exponential phase	o2_set1_0090m_H_941_vs_NRC-1c	0.4 >= OD < 0.6.
mid-exponential phase	o2_set1_0180m_H_930_vs_NRC-1c	0.4 >= OD < 0.6.
mid-exponential phase	o2_set2_L_020_vs_NRC-1d.sig	0.4 >= OD < 0.6.
mid-exponential phase	o2_set2_L_030_vs_NRC-1d.sig	0.4 >= OD < 0.6.
mid-exponential phase	o2_set2_L_045_vs_NRC-1d.sig	0.4 >= OD < 0.6.
mid-exponential phase	o2_set2_L_090_vs_NRC-1d.sig	0.4 >= OD < 0.6.
mid-exponential phase	o2_set2_L_135_vs_NRC-1d.sig	0.4 >= OD < 0.6.

mid-exponential phase	o2_set2_L_180_vs_NRC-1d.sig	0.4 >= OD < 0.6.
mid-exponential phase	o2_set2_L_270_vs_NRC-1d.sig	0.4 >= OD < 0.6.
mid-exponential phase	o2_set2_L_360_vs_NRC-1d.sig	0.4 >= OD < 0.6.
mid-exponential phase	o2_set3_0010_min_HO2_vs_NRC1f.sig	0.4 >= OD < 0.6.
mid-exponential phase	o2_set3_0020_min_HO2_vs_NRC1f.sig	0.4 >= OD < 0.6.
mid-exponential phase	o2_set3_0030_min_HO2_vs_NRC1f.sig	0.4 >= OD < 0.6.
mid-exponential phase	o2_set3_0045_min_HO2_vs_NRC1f.sig	0.4 >= OD < 0.6.
mid-exponential phase	o2_set3_0060_min_HO2_vs_NRC1f.sig	0.4 >= OD < 0.6.
mid-exponential phase	o2_set3_0090_min_HO2_vs_NRC1f.sig	0.4 >= OD < 0.6.
mid-exponential phase	o2_set3_0120_min_HO2_vs_NRC1f.sig	0.4 >= OD < 0.6.
mid-exponential phase	o2_set3_0180_min_HO2_vs_NRC1f.sig	0.4 >= OD < 0.6.
mid-exponential phase	o2_set3_0240_min_HO2_vs_NRC1f.sig	0.4 >= OD < 0.6.
mid-exponential phase	o2_set3_0300_min_HO2_vs_NRC1f.sig	0.4 >= OD < 0.6.
mid-exponential phase	o2_set3_0420_min_HO2_vs_NRC1f.sig	0.4 >= OD < 0.6.
mid-exponential phase	o2_set3_0540_min_HO2_vs_NRC1f.sig	0.4 >= OD < 0.6.
mid-exponential phase	o2_set3_0600_min_HO2_vs_NRC1f.sig	0.4 >= OD < 0.6.
mid-exponential phase	o2_set3_0660_min_HO2_vs_NRC1f.sig	0.4 >= OD < 0.6.
mid-exponential phase	PQ_Const._set_1_0.25mM_320m_vs_NRC-1f.sig	0.4 >= OD < 0.6.
mid-exponential phase	20061006_Cmyc_rep1_0.417_vs_NRC-1e.sig	0.4 >= OD < 0.6.
mid-exponential phase	20060818_KO_ura3_rep1_0.405_vs_NRC-1e.sig	0.4 >= OD < 0.6.
mid-exponential phase	20060717_Cmyc_rep2_0.407_vs_NRC-1e.sig	0.4 >= OD < 0.6.
mid-exponential phase	20060717_Cmyc_rep1_0.402_vs_NRC-1e.sig	0.4 >= OD < 0.6.
mid-exponential phase	20060308_KO_ura3_0.448_vs_NRC-1e.sig	0.4 >= OD < 0.6.
mid-exponential phase	20050620_NRC1_rep2_0.505_vs_NRC-1d.sig	0.4 >= OD < 0.6.
mid-exponential phase	20050620_NRC1_rep1_0.484_vs_NRC-1d.sig	0.4 >= OD < 0.6.

mid-exponential phase	20050620_Cmyc_rep2_0.457_vs_NRC-1d.sig	0.4 >= OD < 0.6.
mid-exponential phase	20050620_Cmyc_rep1_0.474_vs_NRC-1d.sig	0.4 >= OD < 0.6.
mid-exponential phase	NRC-1e_vs_NRC-1h1.sig	0.4 >= OD < 0.6.
mid-exponential phase	KO_ura3.1_0.4424_vs_NRC-1_h1.sig	0.4 >= OD < 0.6.
mid-exponential phase	KO_ura3.1_0.525_vs_NRC-1_h1.sig	0.4 >= OD < 0.6.
nickel	Ni_0.5_vs_NRC-1d.sig	5e-4<=mol/L<=1.5e-3.
nickel	Ni_0.75_vs_NRC-1d.sig	5e-4<=mol/L<=1.5e-3.
nickel	Ni_1.5_vs_NRC-1d.sig	5e-4<=mol/L<=1.5e-3.
nickel	Ni_0.0_vs_NRC-1d.sig	5e-4<=mol/L<=1.5e-3.
nickel	ni__0000um_vs_NRC-1c	5e-4<=mol/L<=1.5e-3.
nickel	ni__0500um_vs_NRC-1c	5e-4<=mol/L<=1.5e-3.
nickel	ni__0750um_vs_NRC-1c	5e-4<=mol/L<=1.5e-3.
nickel	ni__1500um_vs_NRC-1c	5e-4<=mol/L<=1.5e-3.
oxygen shift	o2_set1_-001m_L2H_005_vs_NRC-1c	high oxygen shift, low oxygen shift, high oxygen shift to low oxygen, or low oxygen shift to high oxygen
oxygen shift	o2_set1_0001m_L2H_500_vs_NRC-1c	high oxygen shift, low oxygen shift, high oxygen shift to low oxygen, or low oxygen shift to high oxygen
oxygen shift	o2_set1_0005m_H_922_vs_NRC-1c	high oxygen shift, low oxygen shift, high oxygen shift to low oxygen, or low oxygen shift to high oxygen
oxygen shift	o2_set1_0010m_H_947_vs_NRC-1c	high oxygen shift, low oxygen shift, high oxygen shift to low oxygen, or low oxygen shift to high oxygen
oxygen shift	o2_set1_0020m_H_937_vs_NRC-1c	high oxygen shift, low oxygen shift, high oxygen shift to low oxygen, or low oxygen shift to high oxygen
oxygen shift	o2_set1_0030m_H_931_vs_NRC-1c	high oxygen shift, low oxygen shift, high oxygen shift to low oxygen, or low oxygen shift to high oxygen
oxygen shift	o2_set1_0045m_H_939_vs_NRC-1c	high oxygen shift, low oxygen shift, high oxygen shift to low oxygen, or low oxygen shift to high oxygen
oxygen shift	o2_set1_0090m_H_941_vs_NRC-1c	high oxygen shift, low oxygen shift, high oxygen shift to low oxygen, or low oxygen shift to high oxygen
oxygen shift	o2_set1_0180m_H_930_vs_NRC-1c	high oxygen shift, low oxygen shift, high oxygen shift to low oxygen, or low oxygen shift to high oxygen
oxygen shift	o2_set1_0360m_H_903_vs_NRC-1c	high oxygen shift, low oxygen shift, high oxygen shift to low oxygen, or low oxygen shift to high oxygen

oxygen shift	o2_set1_0362m_H2L_860_vs_NRC-1c	high oxygen shift, low oxygen shift, high oxygen shift to low oxygen, or low oxygen shift to high oxygen
oxygen shift	o2_set1_0367m_H2L_215_vs_NRC-1c	high oxygen shift, low oxygen shift, high oxygen shift to low oxygen, or low oxygen shift to high oxygen
oxygen shift	o2_set1_0372m_H2L_079_vs_NRC-1c	high oxygen shift, low oxygen shift, high oxygen shift to low oxygen, or low oxygen shift to high oxygen
oxygen shift	o2_set1_0382m_H2L_048_vs_NRC-1c	high oxygen shift, low oxygen shift, high oxygen shift to low oxygen, or low oxygen shift to high oxygen
oxygen shift	o2_set1_0387m_L_041_vs_NRC-1c	high oxygen shift, low oxygen shift, high oxygen shift to low oxygen, or low oxygen shift to high oxygen
oxygen shift	o2_set1_0392m_L_037_vs_NRC-1c	high oxygen shift, low oxygen shift, high oxygen shift to low oxygen, or low oxygen shift to high oxygen
oxygen shift	o2_set1_0397m_L_035_vs_NRC-1c	high oxygen shift, low oxygen shift, high oxygen shift to low oxygen, or low oxygen shift to high oxygen
oxygen shift	o2_set1_0407m_L_030_vs_NRC-1c	high oxygen shift, low oxygen shift, high oxygen shift to low oxygen, or low oxygen shift to high oxygen
oxygen shift	o2_set1_0417m_L_027_vs_NRC-1c	high oxygen shift, low oxygen shift, high oxygen shift to low oxygen, or low oxygen shift to high oxygen
oxygen shift	o2_set1_0432m_L_024_vs_NRC-1c	high oxygen shift, low oxygen shift, high oxygen shift to low oxygen, or low oxygen shift to high oxygen
oxygen shift	o2_set1_0477m_L_017_vs_NRC-1c	high oxygen shift, low oxygen shift, high oxygen shift to low oxygen, or low oxygen shift to high oxygen
oxygen shift	o2_set1_0567m_L_011_vs_NRC-1c	high oxygen shift, low oxygen shift, high oxygen shift to low oxygen, or low oxygen shift to high oxygen
oxygen shift	o2_set1_0747m_L_008_vs_NRC-1c	high oxygen shift, low oxygen shift, high oxygen shift to low oxygen, or low oxygen shift to high oxygen
oxygen shift	o2_set1_0750m_L2H_540_vs_NRC-1c	high oxygen shift, low oxygen shift, high oxygen shift to low oxygen, or low oxygen shift to high oxygen
oxygen shift	o2_set1_0755m_L2H_825_vs_NRC-1c	high oxygen shift, low oxygen shift, high oxygen shift to low oxygen, or low oxygen shift to high oxygen
oxygen shift	o2_set1_0760m_L2H_847_vs_NRC-1c	high oxygen shift, low oxygen shift, high oxygen shift to low oxygen, or low oxygen shift to high oxygen
oxygen shift	o2_set1_0770m_L2H_852_vs_NRC-1c	high oxygen shift, low oxygen shift, high oxygen shift to low oxygen, or low oxygen shift to high oxygen

oxygen shift	o2_set1_0780m_L2H_847_vs_NRC-1c	high oxygen shift, low oxygen shift, high oxygen shift to low oxygen, or low oxygen shift to high oxygen
paraquat constant	PQ_Const._set_3_4mM_005min_vs_NRC-1h1.sig	constant perturbation
paraquat constant	PQ_Const._set_3_4mM_010min_vs_NRC-1h1.sig	constant perturbation
paraquat constant	PQ_Const._set_3_4mM_020min_vs_NRC-1h1.sig	constant perturbation
paraquat constant	PQ_Const._set_3_4mM_040min_vs_NRC-1h1.sig	constant perturbation
paraquat constant	PQ_Const._set_3_4mM_080min_vs_NRC-1h1.sig	constant perturbation
paraquat constant	PQ_Const._set_3_4mM_160min_vs_NRC-1h1.sig	constant perturbation
paraquat constant	PQ_Const._set_4_4mM_-001min_vs_NRC-1h1.sig	constant perturbation
paraquat constant	PQ_Const._set_4_4mM_005min_vs_NRC-1h1.sig	constant perturbation
paraquat constant	PQ_Const._set_4_4mM_010min_vs_NRC-1h1.sig	constant perturbation
paraquat constant	PQ_Const._set_4_4mM_020min_vs_NRC-1h1.sig	constant perturbation
paraquat constant	PQ_Const._set_4_4mM_040min_vs_NRC-1h1.sig	constant perturbation
paraquat constant	PQ_Const._set_4_4mM_080min_vs_NRC-1h1.sig	constant perturbation
paraquat constant	PQ_Const._set_4_4mM_160min_vs_NRC-1h1.sig	constant perturbation
paraquat constant	PQ_Const._set_2_4mM_000min_vs_NRC-1f.sig	constant perturbation
paraquat constant	PQ_Const._set_2_4mM_030min_vs_NRC-1f.sig	constant perturbation
paraquat constant	PQ_Const._set_2_4mM_060min_vs_NRC-1f.sig	constant perturbation
paraquat constant	PQ_Const._set_2_4mM_120min_vs_NRC-1f.sig	constant perturbation
paraquat constant	PQ_Const._set_2_4mM_240min_vs_NRC-1f.sig	constant perturbation
paraquat constant	PQ_Const._set_1_4mM_000min_vs_NRC-1f.sig	constant perturbation
paraquat constant	PQ_Const._set_1_4mM_030min_vs_NRC-1f.sig	constant perturbation
paraquat constant	PQ_Const._set_1_4mM_060min_vs_NRC-1f.sig	constant perturbation
paraquat constant	PQ_Const._set_1_4mM_120min_vs_NRC-1f.sig	constant perturbation
paraquat constant	PQ_Const._set_1_4mM_240min_vs_NRC-1f.sig	constant perturbation
paraquat constant	PQ_Const._set_1_0.25mM_-001m_vs_NRC-1f.sig	constant perturbation

paraquat constant	PQ_Const._set_1_0.25mM_000m_vs_NRC-1f.sig	constant perturbation
paraquat constant	PQ_Const._set_1_0.25mM_005m_vs_NRC-1f.sig	constant perturbation
paraquat constant	PQ_Const._set_1_0.25mM_010m_vs_NRC-1f.sig	constant perturbation
paraquat constant	PQ_Const._set_1_0.25mM_020m_vs_NRC-1f.sig	constant perturbation
paraquat constant	PQ_Const._set_1_0.25mM_040m_vs_NRC-1f.sig	constant perturbation
paraquat constant	PQ_Const._set_1_0.25mM_080m_vs_NRC-1f.sig	constant perturbation
paraquat constant	PQ_Const._set_1_0.25mM_160m_vs_NRC-1f.sig	constant perturbation
paraquat constant	PQ_Const._set_1_0.25mM_320m_vs_NRC-1f.sig	constant perturbation
paraquat	PQ_Const._set_3_4mM_005min_vs_NRC-1h1.sig	2.5e-5<=mol/L<=4e-3.
paraquat	PQ_Const._set_3_4mM_010min_vs_NRC-1h1.sig	2.5e-5<=mol/L<=4e-3.
paraquat	PQ_Const._set_3_4mM_020min_vs_NRC-1h1.sig	2.5e-5<=mol/L<=4e-3.
paraquat	PQ_Const._set_3_4mM_040min_vs_NRC-1h1.sig	2.5e-5<=mol/L<=4e-3.
paraquat	PQ_Const._set_3_4mM_080min_vs_NRC-1h1.sig	2.5e-5<=mol/L<=4e-3.
paraquat	PQ_Const._set_3_4mM_160min_vs_NRC-1h1.sig	2.5e-5<=mol/L<=4e-3.
paraquat	PQ_Const._set_4_4mM_-001min_vs_NRC-1h1.sig	2.5e-5<=mol/L<=4e-3.
paraquat	PQ_Const._set_4_4mM_005min_vs_NRC-1h1.sig	2.5e-5<=mol/L<=4e-3.
paraquat	PQ_Const._set_4_4mM_010min_vs_NRC-1h1.sig	2.5e-5<=mol/L<=4e-3.
paraquat	PQ_Const._set_4_4mM_020min_vs_NRC-1h1.sig	2.5e-5<=mol/L<=4e-3.
paraquat	PQ_Const._set_4_4mM_040min_vs_NRC-1h1.sig	2.5e-5<=mol/L<=4e-3.
paraquat	PQ_Const._set_4_4mM_080min_vs_NRC-1h1.sig	2.5e-5<=mol/L<=4e-3.
paraquat	PQ_Const._set_4_4mM_160min_vs_NRC-1h1.sig	2.5e-5<=mol/L<=4e-3.
paraquat	PQ_Recov._set_2_4mM_000min_vs_NRC-1f.sig	2.5e-5<=mol/L<=4e-3.
paraquat	PQ_Recov._set_2_4mM_010min_vs_NRC-1f.sig	2.5e-5<=mol/L<=4e-3.
paraquat	PQ_Recov._set_2_4mM_020min_vs_NRC-1f.sig	2.5e-5<=mol/L<=4e-3.
paraquat	PQ_Recov._set_2_4mM_030min_vs_NRC-1f.sig	2.5e-5<=mol/L<=4e-3.
paraquat	PQ_Recov._set_2_4mM_040min_vs_NRC-	2.5e-5<=mol/L<=4e-3.

	1f.sig	
paraquat	PQ_Recov._set_2_4mM_050min_vs_NRC-1f.sig	2.5e-5<=mol/L<=4e-3.
paraquat	PQ_Recov._set_2_4mM_060min_vs_NRC-1f.sig	2.5e-5<=mol/L<=4e-3.
paraquat	PQ_Recov._set_2_4mM_120min_vs_NRC-1f.sig	2.5e-5<=mol/L<=4e-3.
paraquat	PQ_Recov._set_2_4mM_240min_vs_NRC-1f.sig	2.5e-5<=mol/L<=4e-3.
paraquat	PQ_Const._set_2_4mM_000min_vs_NRC-1f.sig	2.5e-5<=mol/L<=4e-3.
paraquat	PQ_Const._set_2_4mM_030min_vs_NRC-1f.sig	2.5e-5<=mol/L<=4e-3.
paraquat	PQ_Const._set_2_4mM_060min_vs_NRC-1f.sig	2.5e-5<=mol/L<=4e-3.
paraquat	PQ_Const._set_2_4mM_120min_vs_NRC-1f.sig	2.5e-5<=mol/L<=4e-3.
paraquat	PQ_Const._set_2_4mM_240min_vs_NRC-1f.sig	2.5e-5<=mol/L<=4e-3.
paraquat	PQ_Recov._set_1_4mM_000min_vs_NRC-1f.sig	2.5e-5<=mol/L<=4e-3.
paraquat	PQ_Recov._set_1_4mM_010min_vs_NRC-1f.sig	2.5e-5<=mol/L<=4e-3.
paraquat	PQ_Recov._set_1_4mM_020min_vs_NRC-1f.sig	2.5e-5<=mol/L<=4e-3.
paraquat	PQ_Recov._set_1_4mM_030min_vs_NRC-1f.sig	2.5e-5<=mol/L<=4e-3.
paraquat	PQ_Recov._set_1_4mM_040min_vs_NRC-1f.sig	2.5e-5<=mol/L<=4e-3.
paraquat	PQ_Recov._set_1_4mM_050min_vs_NRC-1f.sig	2.5e-5<=mol/L<=4e-3.
paraquat	PQ_Recov._set_1_4mM_060min_vs_NRC-1f.sig	2.5e-5<=mol/L<=4e-3.
paraquat	PQ_Recov._set_1_4mM_120min_vs_NRC-1f.sig	2.5e-5<=mol/L<=4e-3.
paraquat	PQ_Recov._set_1_4mM_240min_vs_NRC-1f.sig	2.5e-5<=mol/L<=4e-3.
paraquat	PQ_Const._set_1_4mM_000min_vs_NRC-1f.sig	2.5e-5<=mol/L<=4e-3.
paraquat	PQ_Const._set_1_4mM_030min_vs_NRC-1f.sig	2.5e-5<=mol/L<=4e-3.
paraquat	PQ_Const._set_1_4mM_060min_vs_NRC-1f.sig	2.5e-5<=mol/L<=4e-3.
paraquat	PQ_Const._set_1_4mM_120min_vs_NRC-1f.sig	2.5e-5<=mol/L<=4e-3.
paraquat	PQ_Const._set_1_4mM_240min_vs_NRC-1f.sig	2.5e-5<=mol/L<=4e-3.
paraquat	PQ_Const._set_1_0.25mM_-001m_vs_NRC-1f.sig	2.5e-5<=mol/L<=4e-3.
paraquat	PQ_Const._set_1_0.25mM_000m_vs_NRC-1f.sig	2.5e-5<=mol/L<=4e-3.

paraquat	PQ_Const._set_1_0.25mM_005m_vs_NRC-1f.sig	2.5e-5<=mol/L<=4e-3.
paraquat	PQ_Const._set_1_0.25mM_010m_vs_NRC-1f.sig	2.5e-5<=mol/L<=4e-3.
paraquat	PQ_Const._set_1_0.25mM_020m_vs_NRC-1f.sig	2.5e-5<=mol/L<=4e-3.
paraquat	PQ_Const._set_1_0.25mM_040m_vs_NRC-1f.sig	2.5e-5<=mol/L<=4e-3.
paraquat	PQ_Const._set_1_0.25mM_080m_vs_NRC-1f.sig	2.5e-5<=mol/L<=4e-3.
paraquat	PQ_Const._set_1_0.25mM_160m_vs_NRC-1f.sig	2.5e-5<=mol/L<=4e-3.
paraquat	PQ_Const._set_1_0.25mM_320m_vs_NRC-1f.sig	2.5e-5<=mol/L<=4e-3.
ros constant	H2O2_Const._set_3_25mM_-001min_vs_NRC-1h1.sig	constant perturbation
ros constant	H2O2_Const._set_3_25mM_005min_vs_NRC-1h1.sig	constant perturbation
ros constant	H2O2_Const._set_3_25mM_010min_vs_NRC-1h1.sig	constant perturbation
ros constant	H2O2_Const._set_3_25mM_020min_vs_NRC-1h1.sig	constant perturbation
ros constant	H2O2_Const._set_3_25mM_040min_vs_NRC-1h1.sig	constant perturbation
ros constant	H2O2_Const._set_3_25mM_080min_vs_NRC-1h1.sig	constant perturbation
ros constant	H2O2_Const._set_3_25mM_160min_vs_NRC-1h1.sig	constant perturbation
ros constant	H2O2_Const._set_4_25mM_-001min_vs_NRC-1h1.sig	constant perturbation
ros constant	H2O2_Const._set_4_25mM_005min_vs_NRC-1h1.sig	constant perturbation
ros constant	H2O2_Const._set_4_25mM_010min_vs_NRC-1h1.sig	constant perturbation
ros constant	H2O2_Const._set_4_25mM_020min_vs_NRC-1h1.sig	constant perturbation
ros constant	H2O2_Const._set_4_25mM_040min_vs_NRC-1h1.sig	constant perturbation
ros constant	H2O2_Const._set_4_25mM_080min_vs_NRC-1h1.sig	constant perturbation
ros constant	H2O2_Const._set_4_25mM_160min_vs_NRC-1h1.sig	constant perturbation
ros constant	PQ_Const._set_3_4mM_-001min_vs_NRC-1h1.sig	constant perturbation
ros constant	PQ_Const._set_3_4mM_005min_vs_NRC-1h1.sig	constant perturbation
ros constant	PQ_Const._set_3_4mM_010min_vs_NRC-1h1.sig	constant perturbation
ros constant	PQ_Const._set_3_4mM_020min_vs_NRC-1h1.sig	constant perturbation
ros constant	PQ_Const._set_3_4mM_040min_vs_NRC-	constant perturbation

	1h1.sig	
ros constant	PQ_Const._set_3_4mM_080min_vs_NRC-1h1.sig	constant perturbation
ros constant	PQ_Const._set_3_4mM_160min_vs_NRC-1h1.sig	constant perturbation
ros constant	PQ_Const._set_4_4mM_-001min_vs_NRC-1h1.sig	constant perturbation
ros constant	PQ_Const._set_4_4mM_005min_vs_NRC-1h1.sig	constant perturbation
ros constant	PQ_Const._set_4_4mM_010min_vs_NRC-1h1.sig	constant perturbation
ros constant	PQ_Const._set_4_4mM_020min_vs_NRC-1h1.sig	constant perturbation
ros constant	PQ_Const._set_4_4mM_040min_vs_NRC-1h1.sig	constant perturbation
ros constant	PQ_Const._set_4_4mM_080min_vs_NRC-1h1.sig	constant perturbation
ros constant	PQ_Const._set_4_4mM_160min_vs_NRC-1h1.sig	constant perturbation
ros constant	H2O2_Const._set_2_25mM_000min_vs_NRC-1f.sig	constant perturbation
ros constant	H2O2_Const._set_2_25mM_030min_vs_NRC-1f.sig	constant perturbation
ros constant	H2O2_Const._set_2_25mM_060min_vs_NRC-1f.sig	constant perturbation
ros constant	H2O2_Const._set_2_25mM_120min_vs_NRC-1f.sig	constant perturbation
ros constant	H2O2_Const._set_2_25mM_240min_vs_NRC-1f.sig	constant perturbation
ros constant	PQ_Const._set_2_4mM_000min_vs_NRC-1f.sig	constant perturbation
ros constant	PQ_Const._set_2_4mM_030min_vs_NRC-1f.sig	constant perturbation
ros constant	PQ_Const._set_2_4mM_060min_vs_NRC-1f.sig	constant perturbation
ros constant	PQ_Const._set_2_4mM_120min_vs_NRC-1f.sig	constant perturbation
ros constant	PQ_Const._set_2_4mM_240min_vs_NRC-1f.sig	constant perturbation
ros constant	H2O2_Const._set_1_25mM_000min_vs_NRC-1f.sig	constant perturbation
ros constant	H2O2_Const._set_1_25mM_030min_vs_NRC-1f.sig	constant perturbation
ros constant	H2O2_Const._set_1_25mM_060min_vs_NRC-1f.sig	constant perturbation
ros constant	H2O2_Const._set_1_25mM_120min_vs_NRC-1f.sig	constant perturbation
ros constant	H2O2_Const._set_1_25mM_240min_vs_NRC-1f.sig	constant perturbation
ros constant	PQ_Const._set_1_4mM_000min_vs_NRC-1f.sig	constant perturbation

ros constant	PQ_Const._set_1_4mM_030min_vs_NRC-1f.sig	constant perturbation
ros constant	PQ_Const._set_1_4mM_060min_vs_NRC-1f.sig	constant perturbation
ros constant	PQ_Const._set_1_4mM_120min_vs_NRC-1f.sig	constant perturbation
ros constant	PQ_Const._set_1_4mM_240min_vs_NRC-1f.sig	constant perturbation
ros constant	PQ_Const._set_1_0.25mM_-001m_vs_NRC-1f.sig	constant perturbation
ros constant	PQ_Const._set_1_0.25mM_000m_vs_NRC-1f.sig	constant perturbation
ros constant	PQ_Const._set_1_0.25mM_005m_vs_NRC-1f.sig	constant perturbation
ros constant	PQ_Const._set_1_0.25mM_010m_vs_NRC-1f.sig	constant perturbation
ros constant	PQ_Const._set_1_0.25mM_020m_vs_NRC-1f.sig	constant perturbation
ros constant	PQ_Const._set_1_0.25mM_040m_vs_NRC-1f.sig	constant perturbation
ros constant	PQ_Const._set_1_0.25mM_080m_vs_NRC-1f.sig	constant perturbation
ros constant	PQ_Const._set_1_0.25mM_160m_vs_NRC-1f.sig	constant perturbation
ros constant	PQ_Const._set_1_0.25mM_320m_vs_NRC-1f.sig	constant perturbation
ros recovery	H2O2_Recov._set_3_25mM_000min_vs_NRC-1f.sig	cells received perturbation then washed off. Samples were collected when cells were in revocovery
ros recovery	H2O2_Recov._set_3_25mM_010min_vs_NRC-1f.sig	cells received perturbation then washed off. Samples were collected when cells were in revocovery
ros recovery	H2O2_Recov._set_3_25mM_020min_vs_NRC-1f.sig	cells received perturbation then washed off. Samples were collected when cells were in revocovery
ros recovery	H2O2_Recov._set_3_25mM_030min_vs_NRC-1f.sig	cells received perturbation then washed off. Samples were collected when cells were in revocovery
ros recovery	H2O2_Recov._set_3_25mM_040min_vs_NRC-1f.sig	cells received perturbation then washed off. Samples were collected when cells were in revocovery
ros recovery	H2O2_Recov._set_3_25mM_050min_vs_NRC-1f.sig	cells received perturbation then washed off. Samples were collected when cells were in revocovery
ros recovery	H2O2_Recov._set_3_25mM_060min_vs_NRC-1f.sig	cells received perturbation then washed off. Samples were collected when cells were in revocovery
ros recovery	H2O2_Recov._set_3_25mM_120min_vs_NRC-1f.sig	cells received perturbation then washed off. Samples were collected when cells were in revocovery

ros recovery	H2O2_Recov._set_3_25mM_240min_vs_NRC-1f.sig	cells received perturbation then washed off. Samples were collected when cells were in revocovery
ros recovery	PQ_Recov._set_2_4mM_000min_vs_NRC-1f.sig	cells received perturbation then washed off. Samples were collected when cells were in revocovery
ros recovery	PQ_Recov._set_2_4mM_010min_vs_NRC-1f.sig	cells received perturbation then washed off. Samples were collected when cells were in revocovery
ros recovery	PQ_Recov._set_2_4mM_020min_vs_NRC-1f.sig	cells received perturbation then washed off. Samples were collected when cells were in revocovery
ros recovery	PQ_Recov._set_2_4mM_030min_vs_NRC-1f.sig	cells received perturbation then washed off. Samples were collected when cells were in revocovery
ros recovery	PQ_Recov._set_2_4mM_040min_vs_NRC-1f.sig	cells received perturbation then washed off. Samples were collected when cells were in revocovery
ros recovery	PQ_Recov._set_2_4mM_050min_vs_NRC-1f.sig	cells received perturbation then washed off. Samples were collected when cells were in revocovery
ros recovery	PQ_Recov._set_2_4mM_060min_vs_NRC-1f.sig	cells received perturbation then washed off. Samples were collected when cells were in revocovery
ros recovery	PQ_Recov._set_2_4mM_120min_vs_NRC-1f.sig	cells received perturbation then washed off. Samples were collected when cells were in revocovery
ros recovery	PQ_Recov._set_2_4mM_240min_vs_NRC-1f.sig	cells received perturbation then washed off. Samples were collected when cells were in revocovery
ros recovery	H2O2_Recov._set_2_25mM_000min_vs_NRC-1f.sig	cells received perturbation then washed off. Samples were collected when cells were in revocovery
ros recovery	H2O2_Recov._set_2_25mM_010min_vs_NRC-1f.sig	cells received perturbation then washed off. Samples were collected when cells were in revocovery
ros recovery	H2O2_Recov._set_2_25mM_020min_vs_NRC-1f.sig	cells received perturbation then washed off. Samples were collected when cells were in revocovery
ros recovery	H2O2_Recov._set_2_25mM_030min_vs_NRC-1f.sig	cells received perturbation then washed off. Samples were collected when cells were in revocovery
ros recovery	H2O2_Recov._set_2_25mM_040min_vs_NRC-1f.sig	cells received perturbation then washed off. Samples were collected when cells were in revocovery
ros recovery	H2O2_Recov._set_2_25mM_050min_vs_NRC-1f.sig	cells received perturbation then washed off. Samples were collected when cells were in revocovery
ros recovery	H2O2_Recov._set_2_25mM_060min_vs_NRC-1f.sig	cells received perturbation then washed off. Samples were collected when cells were in revocovery

ros recovery	H2O2_Recov._set_2_25mM_120min_vs_NRC-1f.sig	cells received perturbation then washed off. Samples were collected when cells were in revocovery
ros recovery	H2O2_Recov._set_2_25mM_240min_vs_NRC-1f.sig	cells received perturbation then washed off. Samples were collected when cells were in revocovery
ros recovery	PQ_Recov._set_1_4mM_000min_vs_NRC-1f.sig	cells received perturbation then washed off. Samples were collected when cells were in revocovery
ros recovery	PQ_Recov._set_1_4mM_010min_vs_NRC-1f.sig	cells received perturbation then washed off. Samples were collected when cells were in revocovery
ros recovery	PQ_Recov._set_1_4mM_020min_vs_NRC-1f.sig	cells received perturbation then washed off. Samples were collected when cells were in revocovery
ros recovery	PQ_Recov._set_1_4mM_030min_vs_NRC-1f.sig	cells received perturbation then washed off. Samples were collected when cells were in revocovery
ros recovery	PQ_Recov._set_1_4mM_040min_vs_NRC-1f.sig	cells received perturbation then washed off. Samples were collected when cells were in revocovery
ros recovery	PQ_Recov._set_1_4mM_050min_vs_NRC-1f.sig	cells received perturbation then washed off. Samples were collected when cells were in revocovery
ros recovery	PQ_Recov._set_1_4mM_060min_vs_NRC-1f.sig	cells received perturbation then washed off. Samples were collected when cells were in revocovery
ros recovery	PQ_Recov._set_1_4mM_120min_vs_NRC-1f.sig	cells received perturbation then washed off. Samples were collected when cells were in revocovery
ros recovery	PQ_Recov._set_1_4mM_240min_vs_NRC-1f.sig	cells received perturbation then washed off. Samples were collected when cells were in revocovery
ros recovery	H2O2_Recov._set_1_50mM_000min_vs_NRC-1d.sig	cells received perturbation then washed off. Samples were collected when cells were in revocovery
ros recovery	H2O2_Recov._set_1_50mM_010min_vs_NRC-1d.sig	cells received perturbation then washed off. Samples were collected when cells were in revocovery
ros recovery	H2O2_Recov._set_1_50mM_020min_vs_NRC-1d.sig	cells received perturbation then washed off. Samples were collected when cells were in revocovery
ros recovery	H2O2_Recov._set_1_50mM_030min_vs_NRC-1d.sig	cells received perturbation then washed off. Samples were collected when cells were in revocovery
ros recovery	H2O2_Recov._set_1_50mM_040min_vs_NRC-1d.sig	cells received perturbation then washed off. Samples were collected when cells were in revocovery
ros recovery	H2O2_Recov._set_1_50mM_050min_vs_NRC-1d.sig	cells received perturbation then washed off. Samples were collected when cells were in revocovery

ros recovery	H2O2_Recov._set_1_50mM_060min_vs_NRC-1d.sig	cells received perturbation then washed off. Samples were collected when cells were in revocovery
ros recovery	H2O2_Recov._set_1_50mM_120min_vs_NRC-1d.sig	cells received perturbation then washed off. Samples were collected when cells were in revocovery
ros	H2O2_Const._set_3_25mM_-001min_vs_NRC-1h1.sig	h2o2 and paraquat
ros	H2O2_Const._set_3_25mM_005min_vs_NRC-1h1.sig	h2o2 and paraquat
ros	H2O2_Const._set_3_25mM_010min_vs_NRC-1h1.sig	h2o2 and paraquat
ros	H2O2_Const._set_3_25mM_020min_vs_NRC-1h1.sig	h2o2 and paraquat
ros	H2O2_Const._set_3_25mM_040min_vs_NRC-1h1.sig	h2o2 and paraquat
ros	H2O2_Const._set_3_25mM_080min_vs_NRC-1h1.sig	h2o2 and paraquat
ros	H2O2_Const._set_3_25mM_160min_vs_NRC-1h1.sig	h2o2 and paraquat
ros	H2O2_Const._set_4_25mM_-001min_vs_NRC-1h1.sig	h2o2 and paraquat
ros	H2O2_Const._set_4_25mM_005min_vs_NRC-1h1.sig	h2o2 and paraquat
ros	H2O2_Const._set_4_25mM_010min_vs_NRC-1h1.sig	h2o2 and paraquat
ros	H2O2_Const._set_4_25mM_020min_vs_NRC-1h1.sig	h2o2 and paraquat
ros	H2O2_Const._set_4_25mM_040min_vs_NRC-1h1.sig	h2o2 and paraquat
ros	H2O2_Const._set_4_25mM_080min_vs_NRC-1h1.sig	h2o2 and paraquat
ros	H2O2_Const._set_4_25mM_160min_vs_NRC-1h1.sig	h2o2 and paraquat
ros	PQ_Const._set_3_4mM_-001min_vs_NRC-1h1.sig	h2o2 and paraquat
ros	PQ_Const._set_3_4mM_005min_vs_NRC-1h1.sig	h2o2 and paraquat
ros	PQ_Const._set_3_4mM_010min_vs_NRC-1h1.sig	h2o2 and paraquat
ros	PQ_Const._set_3_4mM_020min_vs_NRC-1h1.sig	h2o2 and paraquat
ros	PQ_Const._set_3_4mM_040min_vs_NRC-1h1.sig	h2o2 and paraquat
ros	PQ_Const._set_3_4mM_080min_vs_NRC-1h1.sig	h2o2 and paraquat
ros	PQ_Const._set_3_4mM_160min_vs_NRC-1h1.sig	h2o2 and paraquat
ros	PQ_Const._set_4_4mM_-001min_vs_NRC-1h1.sig	h2o2 and paraquat
ros	PQ_Const._set_4_4mM_005min_vs_NRC-	h2o2 and paraquat

	1h1.sig	
ros	PQ_Const._set_4_4mM_010min_vs_NRC-1h1.sig	h2o2 and paraquat
ros	PQ_Const._set_4_4mM_020min_vs_NRC-1h1.sig	h2o2 and paraquat
ros	PQ_Const._set_4_4mM_040min_vs_NRC-1h1.sig	h2o2 and paraquat
ros	PQ_Const._set_4_4mM_080min_vs_NRC-1h1.sig	h2o2 and paraquat
ros	PQ_Const._set_4_4mM_160min_vs_NRC-1h1.sig	h2o2 and paraquat
ros	H2O2_Recov._set_3_25mM_000min_vs_NRC-1f.sig	h2o2 and paraquat
ros	H2O2_Recov._set_3_25mM_010min_vs_NRC-1f.sig	h2o2 and paraquat
ros	H2O2_Recov._set_3_25mM_020min_vs_NRC-1f.sig	h2o2 and paraquat
ros	H2O2_Recov._set_3_25mM_030min_vs_NRC-1f.sig	h2o2 and paraquat
ros	H2O2_Recov._set_3_25mM_040min_vs_NRC-1f.sig	h2o2 and paraquat
ros	H2O2_Recov._set_3_25mM_050min_vs_NRC-1f.sig	h2o2 and paraquat
ros	H2O2_Recov._set_3_25mM_060min_vs_NRC-1f.sig	h2o2 and paraquat
ros	H2O2_Recov._set_3_25mM_120min_vs_NRC-1f.sig	h2o2 and paraquat
ros	H2O2_Recov._set_3_25mM_240min_vs_NRC-1f.sig	h2o2 and paraquat
ros	H2O2_Const._set_2_25mM_000min_vs_NRC-1f.sig	h2o2 and paraquat
ros	H2O2_Const._set_2_25mM_030min_vs_NRC-1f.sig	h2o2 and paraquat
ros	H2O2_Const._set_2_25mM_060min_vs_NRC-1f.sig	h2o2 and paraquat
ros	H2O2_Const._set_2_25mM_120min_vs_NRC-1f.sig	h2o2 and paraquat
ros	H2O2_Const._set_2_25mM_240min_vs_NRC-1f.sig	h2o2 and paraquat
ros	PQ_Recov._set_2_4mM_000min_vs_NRC-1f.sig	h2o2 and paraquat
ros	PQ_Recov._set_2_4mM_010min_vs_NRC-1f.sig	h2o2 and paraquat
ros	PQ_Recov._set_2_4mM_020min_vs_NRC-1f.sig	h2o2 and paraquat
ros	PQ_Recov._set_2_4mM_030min_vs_NRC-1f.sig	h2o2 and paraquat
ros	PQ_Recov._set_2_4mM_040min_vs_NRC-1f.sig	h2o2 and paraquat
ros	PQ_Recov._set_2_4mM_050min_vs_NRC-1f.sig	h2o2 and paraquat

ros	PQ_Recov._set_2_4mM_060min_vs_NRC-1f.sig	h2o2 and paraquat
ros	PQ_Recov._set_2_4mM_120min_vs_NRC-1f.sig	h2o2 and paraquat
ros	PQ_Recov._set_2_4mM_240min_vs_NRC-1f.sig	h2o2 and paraquat
ros	PQ_Const._set_2_4mM_000min_vs_NRC-1f.sig	h2o2 and paraquat
ros	PQ_Const._set_2_4mM_030min_vs_NRC-1f.sig	h2o2 and paraquat
ros	PQ_Const._set_2_4mM_060min_vs_NRC-1f.sig	h2o2 and paraquat
ros	PQ_Const._set_2_4mM_120min_vs_NRC-1f.sig	h2o2 and paraquat
ros	PQ_Const._set_2_4mM_240min_vs_NRC-1f.sig	h2o2 and paraquat
ros	H2O2_Recov._set_2_25mM_000min_vs_NRC-1f.sig	h2o2 and paraquat
ros	H2O2_Recov._set_2_25mM_010min_vs_NRC-1f.sig	h2o2 and paraquat
ros	H2O2_Recov._set_2_25mM_020min_vs_NRC-1f.sig	h2o2 and paraquat
ros	H2O2_Recov._set_2_25mM_030min_vs_NRC-1f.sig	h2o2 and paraquat
ros	H2O2_Recov._set_2_25mM_040min_vs_NRC-1f.sig	h2o2 and paraquat
ros	H2O2_Recov._set_2_25mM_050min_vs_NRC-1f.sig	h2o2 and paraquat
ros	H2O2_Recov._set_2_25mM_060min_vs_NRC-1f.sig	h2o2 and paraquat
ros	H2O2_Recov._set_2_25mM_120min_vs_NRC-1f.sig	h2o2 and paraquat
ros	H2O2_Recov._set_2_25mM_240min_vs_NRC-1f.sig	h2o2 and paraquat
ros	H2O2_Const._set_1_25mM_000min_vs_NRC-1f.sig	h2o2 and paraquat
ros	H2O2_Const._set_1_25mM_030min_vs_NRC-1f.sig	h2o2 and paraquat
ros	H2O2_Const._set_1_25mM_060min_vs_NRC-1f.sig	h2o2 and paraquat
ros	H2O2_Const._set_1_25mM_120min_vs_NRC-1f.sig	h2o2 and paraquat
ros	H2O2_Const._set_1_25mM_240min_vs_NRC-1f.sig	h2o2 and paraquat
ros	PQ_Recov._set_1_4mM_000min_vs_NRC-1f.sig	h2o2 and paraquat
ros	PQ_Recov._set_1_4mM_010min_vs_NRC-1f.sig	h2o2 and paraquat
ros	PQ_Recov._set_1_4mM_020min_vs_NRC-1f.sig	h2o2 and paraquat
ros	PQ_Recov._set_1_4mM_030min_vs_NRC-	h2o2 and paraquat

	1f.sig	
ros	PQ_Recov._set_1_4mM_040min_vs_NRC-1f.sig	h2o2 and paraquat
ros	PQ_Recov._set_1_4mM_050min_vs_NRC-1f.sig	h2o2 and paraquat
ros	PQ_Recov._set_1_4mM_060min_vs_NRC-1f.sig	h2o2 and paraquat
ros	PQ_Recov._set_1_4mM_120min_vs_NRC-1f.sig	h2o2 and paraquat
ros	PQ_Recov._set_1_4mM_240min_vs_NRC-1f.sig	h2o2 and paraquat
ros	PQ_Const._set_1_4mM_000min_vs_NRC-1f.sig	h2o2 and paraquat
ros	PQ_Const._set_1_4mM_030min_vs_NRC-1f.sig	h2o2 and paraquat
ros	PQ_Const._set_1_4mM_060min_vs_NRC-1f.sig	h2o2 and paraquat
ros	PQ_Const._set_1_4mM_120min_vs_NRC-1f.sig	h2o2 and paraquat
ros	PQ_Const._set_1_4mM_240min_vs_NRC-1f.sig	h2o2 and paraquat
ros	PQ_Const._set_1_0.25mM_-001m_vs_NRC-1f.sig	h2o2 and paraquat
ros	PQ_Const._set_1_0.25mM_000m_vs_NRC-1f.sig	h2o2 and paraquat
ros	PQ_Const._set_1_0.25mM_005m_vs_NRC-1f.sig	h2o2 and paraquat
ros	PQ_Const._set_1_0.25mM_010m_vs_NRC-1f.sig	h2o2 and paraquat
ros	PQ_Const._set_1_0.25mM_020m_vs_NRC-1f.sig	h2o2 and paraquat
ros	PQ_Const._set_1_0.25mM_040m_vs_NRC-1f.sig	h2o2 and paraquat
ros	PQ_Const._set_1_0.25mM_080m_vs_NRC-1f.sig	h2o2 and paraquat
ros	PQ_Const._set_1_0.25mM_160m_vs_NRC-1f.sig	h2o2 and paraquat
ros	PQ_Const._set_1_0.25mM_320m_vs_NRC-1f.sig	h2o2 and paraquat
ros	H2O2_Recov._set_1_50mM_000min_vs_NRC-1d.sig	h2o2 and paraquat
ros	H2O2_Recov._set_1_50mM_010min_vs_NRC-1d.sig	h2o2 and paraquat
ros	H2O2_Recov._set_1_50mM_020min_vs_NRC-1d.sig	h2o2 and paraquat
ros	H2O2_Recov._set_1_50mM_030min_vs_NRC-1d.sig	h2o2 and paraquat
ros	H2O2_Recov._set_1_50mM_040min_vs_NRC-1d.sig	h2o2 and paraquat
ros	H2O2_Recov._set_1_50mM_050min_vs_NRC-1d.sig	h2o2 and paraquat

ros	H2O2_Recov._set_1_50mM_060min_vs_NRC-1d.sig	h2o2 and paraquat
ros	H2O2_Recov._set_1_50mM_120min_vs_NRC-1d.sig	h2o2 and paraquat
saturation phase	dark1__0000m_vs_NRC-1c	optical density > 0.8.
saturation phase	dark1__0240m_vs_NRC-1c	optical density > 0.8.
saturation phase	dark1__0480m_vs_NRC-1c	optical density > 0.8.
saturation phase	dark1__0720m_vs_NRC-1c	optical density > 0.8.
saturation phase	dark1__0960m_vs_NRC-1c	optical density > 0.8.
saturation phase	dark1__1920m_vs_NRC-1c	optical density > 0.8.
saturation phase	dark1__2160m_vs_NRC-1c	optical density > 0.8.
saturation phase	dark1__2400m_vs_NRC-1c	optical density > 0.8.
saturation phase	dark1__2640m_vs_NRC-1c	optical density > 0.8.
saturation phase	dark1__2880m_vs_NRC-1c	optical density > 0.8.
saturation phase	dark1__3600m_vs_NRC-1c	optical density > 0.8.
saturation phase	dark1__3870m_vs_NRC-1c	optical density > 0.8.
saturation phase	dark1__4110m_vs_NRC-1c	optical density > 0.8.
saturation phase	circadian_Dphr1_drk_cycling__1980min_vs_NRC-1d.sig	optical density > 0.8.
saturation phase	circadian_Dphr1_drk_cycling__2175min_vs_NRC-1d.sig	optical density > 0.8.
saturation phase	circadian_Dphr1_drk_cycling__2340min_vs_NRC-1d.sig	optical density > 0.8.
saturation phase	circadian_Dphr1_drk_cycling__2595min_vs_NRC-1d.sig	optical density > 0.8.
saturation phase	circadian_Dphr1_drk_cycling__2705min_vs_NRC-1d.sig	optical density > 0.8.
saturation phase	circadian_Dphr1_drk_cycling__2880min_vs_NRC-1d.sig	optical density > 0.8.
saturation phase	circadian_drk8_cycling_0180min_vs_NRC-1e.sig	optical density > 0.8.
saturation phase	circadian_drk8_cycling_0360min_vs_NRC-1e.sig	optical density > 0.8.
saturation phase	circadian_drk7_cycling_0360min_vs_NRC-1d.sig	optical density > 0.8.
saturation phase	circadian_drk7_cycling_1080min_vs_NRC-1d.sig	optical density > 0.8.
saturation phase	circadian_drk7_cycling_1260min_vs_NRC-1d.sig	optical density > 0.8.
saturation phase	circadian_drk7_cycling_1440min_vs_NRC-1d.sig	optical density > 0.8.
saturation phase	circadian_drk7_cycling_1620min_vs_NRC-1d.sig	optical density > 0.8.
saturation phase	circadian_drk7_cycling_1800min_vs_NRC-1d.sig	optical density > 0.8.
saturation phase	circadian_drk7_cycling_1980min_vs_NRC-1d.sig	optical density > 0.8.

saturation phase	circadian_drk7_cycling_2160min_vs_NRC-1d.sig	optical density > 0.8.
saturation phase	circadian_drk7_cycling_2340min_vs_NRC-1d.sig	optical density > 0.8.
saturation phase	circadian_drk7_cycling_2520min_vs_NRC-1d.sig	optical density > 0.8.
saturation phase	circadian_drk7_cycling_2700min_vs_NRC-1d.sig	optical density > 0.8.
saturation phase	circadian_drk7_cycling_2880min_vs_NRC-1d.sig	optical density > 0.8.
saturation phase	circadian_drk7_cycling_3240min_vs_NRC-1d.sig	optical density > 0.8.
saturation phase	circadian__dark5_cycling_30C_1980min_vs_NRC-1d.sig	optical density > 0.8.
saturation phase	circadian__dark5_cycling_30C_2160min_vs_NRC-1d.sig	optical density > 0.8.
saturation phase	circadian__dark5_cycling_30C_2355min_vs_NRC-1d.sig	optical density > 0.8.
saturation phase	circadian__dark5_cycling_30C_2590min_vs_NRC-1d.sig	optical density > 0.8.
saturation phase	circadian__dark5_cycling_30C_2700min_vs_NRC-1d.sig	optical density > 0.8.
saturation phase	circadian__dark5_cycling_30C_2880min_vs_NRC-1d.sig	optical density > 0.8.
saturation phase	circadian_20051021_cycling_dark_42oC_1440min_vs_NRC-1d.sig	optical density > 0.8.
saturation phase	circadian_20051021_cycling_dark_42oC_1615min_vs_NRC-1d.sig	optical density > 0.8.
saturation phase	circadian_20051021_cycling_dark_42oC_1800min_vs_NRC-1d.sig	optical density > 0.8.
saturation phase	circadian_20051021_cycling_dark_42oC_1985min_vs_NRC-1d.sig	optical density > 0.8.
saturation phase	circadian_20051021_cycling_dark_42oC_2160min_vs_NRC-1d.sig	optical density > 0.8.
saturation phase	circadian_20051021_cycling_dark_42oC_2340min_vs_NRC-1d.sig	optical density > 0.8.
saturation phase	circadian_20051021_cycling_dark_42oC_2515min_vs_NRC-1d.sig	optical density > 0.8.
saturation phase	circadian_20051021_cycling_dark_42oC_2705min_vs_NRC-1d.sig	optical density > 0.8.
saturation phase	circadian_20051021_cycling_dark_42oC_2880min_vs_NRC-1d.sig	optical density > 0.8.
saturation phase	circadian_dark3_cycling_2700min_vs_NRC-1d.sig	optical density > 0.8.
saturation phase	circadian_dark3_cycling_2880min_vs_NRC-1d.sig	optical density > 0.8.
saturation phase	circadian_dark3_ctrl_2340min_vs_NRC-1d.sig	optical density > 0.8.
saturation phase	circadian_dark3_ctrl_2520min_vs_NRC-1d.sig	optical density > 0.8.

saturation phase	circadian_dark3_ctrl_2700min_vs_NRC-1d.sig	optical density > 0.8.
saturation phase	circadian_dark3_ctrl_2880min_vs_NRC-1d.sig	optical density > 0.8.
saturation phase	circadian_drk8_control_2880min_vs_NRC-1e.sig	optical density > 0.8.
saturation phase	Circadian_Dark10_Cycling_-2490min_vs_NRC-1h1.sig	optical density > 0.8.
saturation phase	Circadian_Dark10_Cycling_-1410min_vs_NRC-1h1.sig	optical density > 0.8.
saturation phase	Circadian_Dark10_Cycling_-1245min_vs_NRC-1h1.sig	optical density > 0.8.
saturation phase	Circadian_Dark10_Cycling_-0880min_vs_NRC-1h1.sig	optical density > 0.8.
saturation phase	Circadian_Dark10_Cycling_-0690min_vs_NRC-1h1.sig	optical density > 0.8.
saturation phase	Circadian_Dark10_Cycling_-0525min_vs_NRC-1h1.sig	optical density > 0.8.
saturation phase	Circadian_Dark10_Cycling_-0165min_vs_NRC-1h1.sig	optical density > 0.8.
saturation phase	Circadian_Dark10_Cycling_0000min_vs_NRC-1h1.sig	optical density > 0.8.
saturation phase	Circadian_Dark10_Cycling_0370min_vs_NRC-1h1.sig	optical density > 0.8.
saturation phase	Circadian_Dark10_Cycling_0750min_vs_NRC-1h1.sig	optical density > 0.8.
saturation phase	Circadian_Dark10_Cycling_0915min_vs_NRC-1h1.sig	optical density > 0.8.
saturation phase	Circadian_Dark10_Cycling_1100min_vs_NRC-1h1.sig	optical density > 0.8.
saturation phase	Circadian_Dark10_Cycling_1270min_vs_NRC-1h1.sig	optical density > 0.8.
saturation phase	Circadian_Dark10_Cycling_1450min_vs_NRC-1h1.sig	optical density > 0.8.
saturation phase	Circadian_Dark10_Cycling_1635min_vs_NRC-1h1.sig	optical density > 0.8.
saturation phase	Circadian_Dark10_Cycling_1810min_vs_NRC-1h1.sig	optical density > 0.8.
saturation phase	Circadian_Dark10_Cycling_1980min_vs_NRC-1h1.sig	optical density > 0.8.
saturation phase	Circadian_Dark10_Cycling_2200min_vs_NRC-1h1.sig	optical density > 0.8.
saturation phase	Circadian_Dark10_Cycling_2345min_vs_NRC-1h1.sig	optical density > 0.8.
saturation phase	Circadian_Dark10_Cycling_2535min_vs_NRC-1h1.sig	optical density > 0.8.
saturation phase	Circadian_Dark10_Cycling_2711min_vs_NRC-1h1.sig	optical density > 0.8.
saturation phase	Circadian_Dark10_Cycling_2895min_vs_NRC-1h1.sig	optical density > 0.8.

saturation phase	Circadian_Dark10_Cycling_3070min_vs_NRC-1h1.sig	optical density > 0.8.
saturation phase	Circadian_Dark10_Cycling_3252min_vs_NRC-1h1.sig	optical density > 0.8.
saturation phase	Circadian_Dark10_Cycling_3430min_vs_NRC-1h1.sig	optical density > 0.8.
saturation phase	Circadian_Dark10_Cycling_3630min_vs_NRC-1h1.sig	optical density > 0.8.
saturation phase	Circadian_Dark10_Cycling_3790min_vs_NRC-1h1.sig	optical density > 0.8.
saturation phase	Circadian_Dark10_Cycling_3980min_vs_NRC-1h1.sig	optical density > 0.8.
saturation phase	Circadian_Dark10_Cycling_4150min_vs_NRC-1h1.sig	optical density > 0.8.
saturation phase	Circadian_Dark10_Cycling_4330min_vs_NRC-1h1.sig	optical density > 0.8.
saturation phase	Cu_040_vs_NRC-1.sig	optical density > 0.8.
saturation phase	Cu_080_vs_NRC-1.sig	optical density > 0.8.
saturation phase	Cu_040_vs_NRC-1e.sig	optical density > 0.8.
saturation phase	Cu_080_vs_NRC-1e.sig	optical density > 0.8.
saturation phase	Cu_320_vs_NRC-1e.sig	optical density > 0.8.
saturation phase	ZnSO4_ts_set-1_-005min_vs_NRC-1h1.sig	optical density > 0.8.
saturation phase	ZnSO4_ts_set-1_000min_vs_NRC-1h1.sig	optical density > 0.8.
saturation phase	ZnSO4_ts_set-1_005min_vs_NRC-1h1.sig	optical density > 0.8.
saturation phase	ZnSO4_ts_set-1_010min_vs_NRC-1h1.sig	optical density > 0.8.
saturation phase	ZnSO4_ts_set-1_020min_vs_NRC-1h1.sig	optical density > 0.8.
saturation phase	ZnSO4_ts_set-1_040min_vs_NRC-1h1.sig	optical density > 0.8.
saturation phase	ZnSO4_ts_set-1_080min_vs_NRC-1h1.sig	optical density > 0.8.
saturation phase	ZnSO4_ts_set-1_160min_vs_NRC-1h1.sig	optical density > 0.8.
saturation phase	ZnSO4_set2_-005min_vs_NRC-1h1.sig	optical density > 0.8.
saturation phase	ZnSO4_set2_000min_vs_NRC-1h1.sig	optical density > 0.8.
saturation phase	ZnSO4_set2_005min_vs_NRC-1h1.sig	optical density > 0.8.
saturation phase	ZnSO4_set2_010min_vs_NRC-1h1.sig	optical density > 0.8.
saturation phase	ZnSO4_set2_015min_vs_NRC-1h1.sig	optical density > 0.8.
saturation phase	ZnSO4_set2_020min_vs_NRC-1h1.sig	optical density > 0.8.
saturation phase	ZnSO4_set2_025min_vs_NRC-1h1.sig	optical density > 0.8.
saturation phase	ZnSO4_set2_030min_vs_NRC-1h1.sig	optical density > 0.8.
saturation phase	ZnSO4_set2_040min_vs_NRC-1h1.sig	optical density > 0.8.
saturation phase	ZnSO4_set2_060min_vs_NRC-1h1.sig	optical density > 0.8.
saturation phase	ZnSO4_set2_080min_vs_NRC-1h1.sig	optical density > 0.8.
saturation phase	ZnSO4_set2_120min_vs_NRC-1h1.sig	optical density > 0.8.
saturation phase	ZnSO4_set2_160min_vs_NRC-1h1.sig	optical density > 0.8.
saturation phase	ZnSO4_set2_320min_vs_NRC-1h1.sig	optical density > 0.8.
saturation phase	Cu_NRC1_set1_-030min_vs_NRC-1h1.sig	optical density > 0.8.
saturation phase	Cu_NRC1_set1_000min_vs_NRC-1h1.sig	optical density > 0.8.

saturation phase	Cu_NRC1_set1_005min_vs_NRC-1h1.sig	optical density > 0.8.
saturation phase	Cu_NRC1_set1_010min_vs_NRC-1h1.sig	optical density > 0.8.
saturation phase	Cu_NRC1_set1_020min_vs_NRC-1h1.sig	optical density > 0.8.
saturation phase	Cu_NRC1_set1_040min_vs_NRC-1h1.sig	optical density > 0.8.
saturation phase	Cu_NRC1_set1_080min_vs_NRC-1h1.sig	optical density > 0.8.
saturation phase	VNG0750C__HO_D_vs_NRC-1	optical density > 0.8.
saturation phase	VNG0750C__HO_L_vs_NRC-1	optical density > 0.8.
saturation phase	VNG0750C__LO_D_vs_NRC-1	optical density > 0.8.
saturation phase	VNG0750C__LO_L_vs_NRC-1	optical density > 0.8.
saturation phase	VNG0019H__HO_D_vs_NRC-1c	optical density > 0.8.
saturation phase	VNG0019H__HO_L_vs_NRC-1c	optical density > 0.8.
saturation phase	VNG0019H__LO_D_vs_NRC-1c	optical density > 0.8.
saturation phase	VNG0019H__LO_L_vs_NRC-1c	optical density > 0.8.
saturation phase	ura3__HO_D_vs_NRC-1	optical density > 0.8.
saturation phase	ura3__HO_L_vs_NRC-1	optical density > 0.8.
saturation phase	ura3__LO_D_vs_NRC-1	optical density > 0.8.
saturation phase	ura3__LO_L_vs_NRC-1	optical density > 0.8.
saturation phase	NRC1e_vs_NRC1f.sig	optical density > 0.8.
saturation phase	NRC-1__HO_D_vs_NRC-1	optical density > 0.8.
saturation phase	NRC-1__HO_L_vs_NRC-1	optical density > 0.8.
saturation phase	NRC-1__LO_D_vs_NRC-1	optical density > 0.8.
saturation phase	NRC-1__LO_L_vs_NRC-1	optical density > 0.8.
saturation phase	circadian__dark_cycling_125w/m2_42C_2705min_vs_NRC-1d.sig	optical density > 0.8.
saturation phase	circadian__dark_cycling_125w/m2_42C_2880min_vs_NRC-1d.sig	optical density > 0.8.
saturation phase	NRC-1b_vs_NRC-1a.sig	optical density > 0.8.
saturation phase	NRC-1_vs_NRC-1c.sig	optical density > 0.8.
saturation phase	NRC-1c_vs_NRC-1d.sig	optical density > 0.8.
saturation phase	NRC1_H2O_1260_0.830_rep2_vs_NRC-1g.sig	optical density > 0.8.
saturation phase	NRC1_H2O_1860_0.733_rep2_vs_NRC-1g.sig	optical density > 0.8.
saturation phase	NRC1_H2O_2280_0.764_rep2_vs_NRC-1g.sig	optical density > 0.8.
saturation phase	NRC1_H2O_2760_0.913_rep2_vs_NRC-1g.sig	optical density > 0.8.
saturation phase	NRC1_H2O_3120_1.086_rep2_vs_NRC-1g.sig	optical density > 0.8.
saturation phase	NRC1_H2O_1260_0.807_rep1_vs_NRC-1g.sig	optical density > 0.8.
saturation phase	NRC1_H2O_1860_0.758_rep1_vs_NRC-1g.sig	optical density > 0.8.
saturation phase	NRC1_H2O_2280_0.781_rep1_vs_NRC-1g.sig	optical density > 0.8.

saturation phase	NRC1_H2O_2760_0.913_rep1_vs_NRC-1g.sig	optical density > 0.8.
saturation phase	NRC1_H2O_3120_1.023_rep1_vs_NRC-1g.sig	optical density > 0.8.
saturation phase	NRC1_Uracil_1260_0.812_rep2_vs_NRC-1g.sig	optical density > 0.8.
saturation phase	NRC1_Uracil_1860_0.912_rep2_vs_NRC-1g.sig	optical density > 0.8.
saturation phase	NRC1_Uracil_2280_0.881_rep2_vs_NRC-1g.sig	optical density > 0.8.
saturation phase	NRC1_Uracil_2760_1.133_rep2_vs_NRC-1g.sig	optical density > 0.8.
saturation phase	NRC1_Uracil_3120_1.296_rep2_vs_NRC-1g.sig	optical density > 0.8.
saturation phase	NRC1_Uracil_1260_0.785_rep1_vs_NRC-1g.sig	optical density > 0.8.
saturation phase	NRC1_Uracil_1860_0.882_rep1_vs_NRC-1g.sig	optical density > 0.8.
saturation phase	NRC1_Uracil_2280_0.876_rep1_vs_NRC-1g.sig	optical density > 0.8.
saturation phase	NRC1_Uracil_2760_1.039_rep1_vs_NRC-1g.sig	optical density > 0.8.
saturation phase	NRC1_Uracil_3120_1.341_rep1_vs_NRC-1g.sig	optical density > 0.8.
saturation phase	Dura3_Uracil_1860_0.756_rep2_vs_NRC-1g.sig	optical density > 0.8.
saturation phase	Dura3_Uracil_2280_0.830_rep2_vs_NRC-1g.sig	optical density > 0.8.
saturation phase	Dura3_Uracil_2760_0.970_rep2_vs_NRC-1g.sig	optical density > 0.8.
saturation phase	Dura3_Uracil_3120_1.147_rep2_vs_NRC-1g.sig	optical density > 0.8.
saturation phase	Dura3_Uracil_1860_0.755_rep1_vs_NRC-1g.sig	optical density > 0.8.
saturation phase	Dura3_Uracil_2280_0.832_rep1_vs_NRC-1g.sig	optical density > 0.8.
saturation phase	Dura3_Uracil_2760_0.975_rep1_vs_NRC-1g.sig	optical density > 0.8.
saturation phase	Dura3_Uracil_3120_1.136_rep1_vs_NRC-1g.sig	optical density > 0.8.
saturation phase	NRC-1f_vs_NRC-1g.sig	optical density > 0.8.
saturation phase	NRC1_04476_0.715_rep2_vs_NRC-1g.sig	optical density > 0.8.
saturation phase	NRC1_05400_0.786_rep2_vs_NRC-1g.sig	optical density > 0.8.
saturation phase	NRC1_05778_0.722_rep2_vs_NRC-1g.sig	optical density > 0.8.
saturation phase	NRC1_07020_1.318_rep2_vs_NRC-1g.sig	optical density > 0.8.
saturation phase	NRC1_07740_2.681_rep2_vs_NRC-1g.sig	optical density > 0.8.
saturation phase	NRC1_08460_3.840_rep2_vs_NRC-1g.sig	optical density > 0.8.
saturation phase	NRC1_09540_4.690_rep2_vs_NRC-1g.sig	optical density > 0.8.
saturation phase	NRC1_10260_4.540_rep2_vs_NRC-1g.sig	optical density > 0.8.

saturation phase	NRC1_10980_4.935_rep2_vs_NRC-1g.sig	optical density > 0.8.
saturation phase	NRC1_11700_5.730_rep2_vs_NRC-1g.sig	optical density > 0.8.
saturation phase	NRC1_04476_0.762_rep1_vs_NRC-1g.sig	optical density > 0.8.
saturation phase	NRC1_05400_0.803_rep1_vs_NRC-1g.sig	optical density > 0.8.
saturation phase	NRC1_05778_0.710_rep1vs_NRC-1g.sig	optical density > 0.8.
saturation phase	NRC1_07020_1.329_rep1_vs_NRC-1g.sig	optical density > 0.8.
saturation phase	NRC1_07740_2.580_rep1_vs_NRC-1g.sig	optical density > 0.8.
saturation phase	NRC1_08460_3.510_rep1_vs_NRC-1g.sig	optical density > 0.8.
saturation phase	NRC1_09540_4.860_rep1_vs_NRC-1g.sig	optical density > 0.8.
saturation phase	NRC1_10260_4.860_rep1_vs_NRC-1g.sig	optical density > 0.8.
saturation phase	NRC1_10980_5.130_rep1_vs_NRC-1g.sig	optical density > 0.8.
saturation phase	NRC1_11700_5.640_rep1_vs_NRC-1g.sig	optical density > 0.8.
saturation phase	H2O2_Recov._set_3_0mM_240min_vs_NRC-1f.sig	optical density > 0.8.
saturation phase	H2O2_Const._set_2_0mM_240min_vs_NRC-1f.sig	optical density > 0.8.
saturation phase	PQ_Recov._set_2_0mM_240min_vs_NRC-1f.sig	optical density > 0.8.
saturation phase	PQ_Const._set_2_0mM_120min_vs_NRC-1f.sig	optical density > 0.8.
saturation phase	PQ_Const._set_2_0mM_240min_vs_NRC-1f.sig	optical density > 0.8.
saturation phase	H2O2_Recov._set_2_0mM_240min_vs_NRC-1f.sig	optical density > 0.8.
saturation phase	H2O2_Const._set_1_0mM_240min_vs_NRC-1f.sig	optical density > 0.8.
saturation phase	PQ_Recov._set_1_0mM_120min_vs_NRC-1f.sig	optical density > 0.8.
saturation phase	PQ_Recov._set_1_0mM_240min_vs_NRC-1f.sig	optical density > 0.8.
saturation phase	PQ_Const._set_1_0mM_120min_vs_NRC-1f.sig	optical density > 0.8.
saturation phase	PQ_Const._set_1_0mM_240min_vs_NRC-1f.sig	optical density > 0.8.
saturation phase	20060818_NRC1_rep2_0.821_vs_NRC-1e.sig	optical density > 0.8.
saturation phase	20060818_NRC1_rep1_0.816_vs_NRC-1e.sig	optical density > 0.8.
saturation phase	ura3_growth_t3exp1_0.8OD_vs_NRC1e.sig	optical density > 0.8.
saturation phase	ura3_growth_t3_exp2_0.8OD_vs_NRC1f.sig	optical density > 0.8.
saturation phase	ura3_+glu_a_OD0.6_vs_NRC1e.sig	optical density > 0.8.
saturation phase	ura3_-glu_a_OD0.6_vs_NRC1e.sig	optical density > 0.8.
saturation phase	ura3_-glu_a_OD1.2_vs_NRC1e.sig	optical density > 0.8.
saturation phase	ura3_growth_t4_exp2_1.2OD_vs_NRC1f.sig	optical density > 0.8.

saturation phase	ura3_growth_t3_exp3_0.8OD_vs_NRC1f.sig	optical density > 0.8.
saturation phase	ura3_growth_t4_exp3_1.2OD_vs_NRC1f.sig	optical density > 0.8.
saturation phase	ura3_-glu_a_OD0.6repl_vs_NRC1e.sig	optical density > 0.8.
saturation phase	ura3_-glu_a_OD1.2repl_vs_NRC1e.sig	optical density > 0.8.
saturation phase	ura3_-glu_b_OD0.6repl_vs_NRC1g.sig	optical density > 0.8.
saturation phase	ura3_-glu_b_OD1.2repl_vs_NRC1g.sig	optical density > 0.8.
saturation phase	H2O2_Const._set_2_25mM_240min_vs_NRC-1f.sig	optical density > 0.8.
saturation phase	H2O2_Const._set_1_25mM_240min_vs_NRC-1f.sig	optical density > 0.8.
saturation phase	ura3_0min_-EDTA_CM_vs_NRC1-h1.sig	optical density > 0.8.
saturation phase	ura3_20min_-EDTA_CM_vs_NRC1-h1.sig	optical density > 0.8.
saturation phase	ura3_40min_-EDTA_CM_vs_NRC1-h1.sig	optical density > 0.8.
saturation phase	ura3_60min_-EDTA_CM_vs_NRC1-h1.sig	optical density > 0.8.
saturation phase	ura3_0min_1mM_EDTA_vs_NRC1-h1.sig	optical density > 0.8.
saturation phase	ura3_20min_1mM_EDTA_vs_NRC1-h1.sig	optical density > 0.8.
saturation phase	ura3_40min_1mM_EDTA_vs_NRC1-h1.sig	optical density > 0.8.
saturation phase	ura3_60min_1mM_EDTA_vs_NRC1-h1.sig	optical density > 0.8.
saturation phase	KO_ura3.3_0.8976_vs_NRC-1_h1.sig	optical density > 0.8.
saturation phase	KO_ura3.4_0.9128_vs_NRC-1_h1.sig	optical density > 0.8.
saturation phase	o2_set1_0360m_H_903_vs_NRC-1c	optical density > 0.8.
saturation phase	o2_set1_0362m_H2L_860_vs_NRC-1c	optical density > 0.8.
saturation phase	o2_set1_0367m_H2L_215_vs_NRC-1c	optical density > 0.8.
saturation phase	o2_set1_0372m_H2L_079_vs_NRC-1c	optical density > 0.8.
saturation phase	o2_set1_0382m_H2L_048_vs_NRC-1c	optical density > 0.8.
saturation phase	o2_set1_0387m_L_041_vs_NRC-1c	optical density > 0.8.
saturation phase	o2_set1_0392m_L_037_vs_NRC-1c	optical density > 0.8.
saturation phase	o2_set1_0397m_L_035_vs_NRC-1c	optical density > 0.8.
saturation phase	o2_set1_0407m_L_030_vs_NRC-1c	optical density > 0.8.
saturation phase	o2_set1_0417m_L_027_vs_NRC-1c	optical density > 0.8.
saturation phase	o2_set1_0432m_L_024_vs_NRC-1c	optical density > 0.8.
saturation phase	o2_set1_0477m_L_017_vs_NRC-1c	optical density > 0.8.
saturation phase	o2_set1_0567m_L_011_vs_NRC-1c	optical density > 0.8.
saturation phase	o2_set1_0747m_L_008_vs_NRC-1c	optical density > 0.8.
saturation phase	o2_set1_0750m_L2H_540_vs_NRC-1c	optical density > 0.8.
saturation phase	o2_set1_0755m_L2H_825_vs_NRC-1c	optical density > 0.8.
saturation phase	o2_set1_0760m_L2H_847_vs_NRC-1c	optical density > 0.8.
saturation phase	o2_set1_0770m_L2H_852_vs_NRC-1c	optical density > 0.8.
saturation phase	o2_set1_0780m_L2H_847_vs_NRC-1c	optical density > 0.8.
saturation phase	o2_set2_H_L_000_vs_NRC-1d.sig	optical density > 0.8.
saturation phase	o2_set2_H_L_005_vs_NRC-1d.sig	optical density > 0.8.

saturation phase	o2_set2_H_L_010_vs_NRC-1d.sig	optical density > 0.8.
saturation phase	o2_set2_H_L_020_vs_NRC-1d.sig	optical density > 0.8.
saturation phase	o2_set2_L_000_vs_NRC-1d.sig	optical density > 0.8.
saturation phase	o2_set2_L_005_vs_NRC-1d.sig	optical density > 0.8.
saturation phase	o2_set2_L_010_vs_NRC-1d.sig	optical density > 0.8.
saturation phase	PQ_Const._set_1_0.25mM_-001m_vs_NRC-1f.sig	optical density > 0.8.
saturation phase	PQ_Const._set_1_0.25mM_000m_vs_NRC-1f.sig	optical density > 0.8.
saturation phase	PQ_Const._set_1_0.25mM_005m_vs_NRC-1f.sig	optical density > 0.8.
saturation phase	PQ_Const._set_1_0.25mM_010m_vs_NRC-1f.sig	optical density > 0.8.
saturation phase	PQ_Const._set_1_0.25mM_020m_vs_NRC-1f.sig	optical density > 0.8.
saturation phase	PQ_Const._set_1_0.25mM_040m_vs_NRC-1f.sig	optical density > 0.8.
saturation phase	PQ_Const._set_1_0.25mM_080m_vs_NRC-1f.sig	optical density > 0.8.
saturation phase	PQ_Const._set_1_0.25mM_160m_vs_NRC-1f.sig	optical density > 0.8.
saturation phase	20061006_Cmyc_rep2_0.833_vs_NRC-1e.sig	optical density > 0.8.
saturation phase	20061006_Cmyc_rep1_0.835_vs_NRC-1e.sig	optical density > 0.8.
saturation phase	20060818_KO_ura3_rep2_0.828_vs_NRC-1e.sig	optical density > 0.8.
saturation phase	20060818_KO_ura3_rep1_0.842_vs_NRC-1e.sig	optical density > 0.8.
saturation phase	20060717_Cmyc_rep2_0.883_vs_NRC-1e.sig	optical density > 0.8.
saturation phase	20060717_Cmyc_rep1_0.827_vs_NRC-1e.sig	optical density > 0.8.
saturation phase	NRC-1d_vs_NRC-1e.sig	optical density > 0.8.
saturation phase	20060308_KO_ura3_0.853_vs_NRC-1e.sig	optical density > 0.8.
saturation phase	20050620_NRC1_rep2_1.030_vs_NRC-1d.sig	optical density > 0.8.
saturation phase	20050620_NRC1_rep1_1.276_vs_NRC-1d.sig	optical density > 0.8.
saturation phase	20050620_Cmyc_rep2_1.072_vs_NRC-1d.sig	optical density > 0.8.
saturation phase	20050620_Cmyc_rep1_1.052_vs_NRC-1d.sig	optical density > 0.8.
saturation phase	NRC-1.2_1.1065_vs_NRC-1_h1.sig	optical density > 0.8.
saturation phase	NRC-1_1.0338_vs_NRC-1_h1.sig	optical density > 0.8.
uv	uv__000jm2_CL_060m	200 J/m2.
uv	uv__200jm2_D_030m	200 J/m2.
uv	uv__200jm2_D_060m	200 J/m2.

uv	uv__200jm2_L_030m	200 J/m2.
uv	uv__200jm2_L_060m	200 J/m2.
zinc	Zn_0.000_vs_NRC-1d.sig	5e-6<=mol/L<=5e-5.
zinc	Zn_0.005_vs_NRC-1d.sig	5e-6<=mol/L<=5e-5.
zinc	Zn_0.010_vs_NRC-1d.sig	5e-6<=mol/L<=5e-5.
zinc	Zn_0.015_vs_NRC-1d.sig	5e-6<=mol/L<=5e-5.
zinc	zn__0005um_vs_NRC-1	5e-6<=mol/L<=5e-5.
zinc	zn__0010um_vs_NRC-1	5e-6<=mol/L<=5e-5.
zinc	zn__0020um_vs_NRC-1	5e-6<=mol/L<=5e-5.
zinc	ZnSO4_ts_set-1_-005min_vs_NRC-1h1.sig	5e-6<=mol/L<=5e-5.
zinc	ZnSO4_ts_set-1_000min_vs_NRC-1h1.sig	5e-6<=mol/L<=5e-5.
zinc	ZnSO4_ts_set-1_005min_vs_NRC-1h1.sig	5e-6<=mol/L<=5e-5.
zinc	ZnSO4_ts_set-1_010min_vs_NRC-1h1.sig	5e-6<=mol/L<=5e-5.
zinc	ZnSO4_ts_set-1_020min_vs_NRC-1h1.sig	5e-6<=mol/L<=5e-5.
zinc	ZnSO4_ts_set-1_040min_vs_NRC-1h1.sig	5e-6<=mol/L<=5e-5.
zinc	ZnSO4_ts_set-1_080min_vs_NRC-1h1.sig	5e-6<=mol/L<=5e-5.
zinc	ZnSO4_ts_set-1_160min_vs_NRC-1h1.sig	5e-6<=mol/L<=5e-5.
zinc	ZnSO4_set2_-005min_vs_NRC-1h1.sig	5e-6<=mol/L<=5e-5.
zinc	ZnSO4_set2_000min_vs_NRC-1h1.sig	5e-6<=mol/L<=5e-5.
zinc	ZnSO4_set2_005min_vs_NRC-1h1.sig	5e-6<=mol/L<=5e-5.
zinc	ZnSO4_set2_010min_vs_NRC-1h1.sig	5e-6<=mol/L<=5e-5.
zinc	ZnSO4_set2_015min_vs_NRC-1h1.sig	5e-6<=mol/L<=5e-5.
zinc	ZnSO4_set2_020min_vs_NRC-1h1.sig	5e-6<=mol/L<=5e-5.
zinc	ZnSO4_set2_025min_vs_NRC-1h1.sig	5e-6<=mol/L<=5e-5.
zinc	ZnSO4_set2_030min_vs_NRC-1h1.sig	5e-6<=mol/L<=5e-5.
zinc	ZnSO4_set2_040min_vs_NRC-1h1.sig	5e-6<=mol/L<=5e-5.
zinc	ZnSO4_set2_060min_vs_NRC-1h1.sig	5e-6<=mol/L<=5e-5.
zinc	ZnSO4_set2_080min_vs_NRC-1h1.sig	5e-6<=mol/L<=5e-5.
zinc	ZnSO4_set2_120min_vs_NRC-1h1.sig	5e-6<=mol/L<=5e-5.
zinc	ZnSO4_set2_160min_vs_NRC-1h1.sig	5e-6<=mol/L<=5e-5.
zinc	ZnSO4_set2_320min_vs_NRC-1h1.sig	5e-6<=mol/L<=5e-5.
zinc	sDura3_pZn_d0.005mM_t+015m_vs_NRC-1h1.sig	5e-6<=mol/L<=5e-5.
zinc	sDura3_pZn_d0.005mM_t+030m_vs_NRC-1h1.sig	5e-6<=mol/L<=5e-5.
zinc	sDura3_pZn_d0.005mM_t+060m_vs_NRC-1h1.sig	5e-6<=mol/L<=5e-5.
zinc	sDura3_pZn_d0.005mM_t+180m_vs_NRC-1h1.sig	5e-6<=mol/L<=5e-5.
zinc	sDura3_pZn_d0.005mM_t-015m_vs_NRC-1h1.sig	5e-6<=mol/L<=5e-5.
zinc	sDura3_pZn_d0.020mM_t+015m_vs_NRC-1h1.sig	5e-6<=mol/L<=5e-5.

zinc	sDura3_pZn_d0.020mM_t+030m_vs_NRC-1h1.sig	5e-6<=mol/L<=5e-5.
zinc	sDura3_pZn_d0.020mM_t+060m_vs_NRC-1h1.sig	5e-6<=mol/L<=5e-5.
zinc	sDura3_pZn_d0.020mM_t+180m_vs_NRC-1h1.sig	5e-6<=mol/L<=5e-5.
zinc	sDura3_pZn_d0.020mM_t-015m_vs_NRC-1h1.sig	5e-6<=mol/L<=5e-5.
zinc	sDura3_pZn_d0.050mM_t+015m_vs_NRC-1h1.sig	5e-6<=mol/L<=5e-5.
zinc	sDura3_pZn_d0.050mM_t+030m_vs_NRC-1h1.sig	5e-6<=mol/L<=5e-5.
zinc	sDura3_pZn_d0.050mM_t+060m_vs_NRC-1h1.sig	5e-6<=mol/L<=5e-5.
zinc	sDura3_pZn_d0.050mM_t+180m_vs_NRC-1h1.sig	5e-6<=mol/L<=5e-5.
zinc	sDura3_pZn_d0.050mM_t-015m_vs_NRC-1h1.sig	5e-6<=mol/L<=5e-5.

Appendix R. Experimental details of each experiment

# units	mol /L	mol /L	mol /L	mol /L	mol /L	mol /L	gy	pct w/v	mol /L	umol/ m2/ s	umol/ m2/ s	mol /L	mol /L	600 nm	NA	pct	mol /L	rpm	NA	min	J/m 2	mol /L	NA	deg C
condition	ATP	CoSO 4.7 H2 O	CuSO 4.5 H2 O	EDTA	EMS	FeSO4. 7H2 O	gamma	glucose	H2 O2	illumination	irradiation history	MnSO 4.H 2O	NiSO4. H2 O	Optical density	overexpressed gene	oxygen	paraquat	shaking_agitation (rpm)	tag	Time	uv	ZnSO4. 7H2 O	growth media	temperature
light2__1440m_vs_light1_3960m	NA	NA	NA	NA	NA	NA	NA	NA	NA	150	NA	NA	NA	0.26	NA	NA	NA	125	NA	1440	NA	NA	CM	37
light2__1620m_vs_light1_3960m	NA	NA	NA	NA	NA	NA	NA	NA	NA	150	NA	NA	NA	0.26	NA	NA	NA	125	NA	1620	NA	NA	CM	37
light2__1800m_vs_light1_3960m	NA	NA	NA	NA	NA	NA	NA	NA	NA	150	NA	NA	NA	0.26	NA	NA	NA	125	NA	1800	NA	NA	CM	37
light2__1980m_vs_light1_3960m	NA	NA	NA	NA	NA	NA	NA	NA	NA	150	NA	NA	NA	0.26	NA	NA	NA	125	NA	1980	NA	NA	CM	37
light2__2160m_vs_light1_3960m	NA	NA	NA	NA	NA	NA	NA	NA	NA	150	NA	NA	NA	0.26	NA	NA	NA	125	NA	2160	NA	NA	CM	37
light2__2340m_vs_light1_3960m	NA	NA	NA	NA	NA	NA	NA	NA	NA	150	NA	NA	NA	0.26	NA	NA	NA	125	NA	2340	NA	NA	CM	37
light2__2520m_vs_light1_3960m	NA	NA	NA	NA	NA	NA	NA	NA	NA	150	NA	NA	NA	0.26	NA	NA	NA	125	NA	2520	NA	NA	CM	37
light2__2700m_vs_light1_3960m	NA	NA	NA	NA	NA	NA	NA	NA	NA	150	NA	NA	NA	0.26	NA	NA	NA	125	NA	2700	NA	NA	CM	37
light2__2880m_vs_light1_3960m	NA	NA	NA	NA	NA	NA	NA	NA	NA	150	NA	NA	NA	0.26	NA	NA	NA	125	NA	2880	NA	NA	CM	37
light2__3060m_vs_light1_3960m	NA	NA	NA	NA	NA	NA	NA	NA	NA	150	NA	NA	NA	0.26	NA	NA	NA	125	NA	3060	NA	NA	CM	37
light2__3240m_vs_light1_3960m	NA	NA	NA	NA	NA	NA	NA	NA	NA	150	NA	NA	NA	0.26	NA	NA	NA	125	NA	3240	NA	NA	CM	37
light2__3420m_vs_light1_3960m	NA	NA	NA	NA	NA	NA	NA	NA	NA	150	NA	NA	NA	NA	NA	NA	NA	125	NA	3420	NA	NA	CM	37
light2__3600m_vs_light1_3960m	NA	NA	NA	NA	NA	NA	NA	NA	NA	150	NA	NA	NA	NA	NA	NA	NA	125	NA	3600	NA	NA	CM	37
light2__3780m_vs_light1_3960m	NA	NA	NA	NA	NA	NA	NA	NA	NA	150	NA	NA	NA	NA	NA	NA	NA	125	NA	3780	NA	NA	CM	37

light2__3960m_vs_light1_3960m	NA	NA	NA	NA	NA	NA	NA	NA	NA	150	NA	NA	NA	NA	NA	NA	NA	125	NA	3960	NA	NA	CM	37
light2__4140m_vs_light1_3960m	NA	NA	NA	NA	NA	NA	NA	NA	NA	150	NA	NA	NA	NA	NA	NA	NA	125	NA	4140	NA	NA	CM	37
light2__4320m_vs_light1_3960m	NA	NA	NA	NA	NA	NA	NA	NA	NA	150	NA	NA	NA	NA	NA	NA	NA	125	NA	4320	NA	NA	CM	37
light2__4500m_vs_light1_3960m	NA	NA	NA	NA	NA	NA	NA	NA	NA	150	NA	NA	NA	NA	NA	NA	NA	125	NA	4500	NA	NA	CM	37
light2__4680m_vs_light1_3960m	NA	NA	NA	NA	NA	NA	NA	NA	NA	150	NA	NA	NA	NA	NA	NA	NA	125	NA	4680	NA	NA	CM	37
light2__4860m_vs_light1_3960m	NA	NA	NA	NA	NA	NA	NA	NA	NA	150	NA	NA	NA	NA	NA	NA	NA	125	NA	4860	NA	NA	CM	37
light2__5040m_vs_light1_3960m	NA	NA	NA	NA	NA	NA	NA	NA	NA	150	NA	NA	NA	NA	NA	NA	NA	125	NA	5040	NA	NA	CM	37
light2__5220m_vs_light1_3960m	NA	NA	NA	NA	NA	NA	NA	NA	NA	150	NA	NA	NA	NA	NA	NA	NA	125	NA	5220	NA	NA	CM	37
light2__5400m_vs_light1_3960m	NA	NA	NA	NA	NA	NA	NA	NA	NA	150	NA	NA	NA	NA	NA	NA	NA	125	NA	5400	NA	NA	CM	37
light2__5580m_vs_light1_3960m	NA	NA	NA	NA	NA	NA	NA	NA	NA	150	NA	NA	NA	NA	NA	NA	NA	125	NA	5580	NA	NA	CM	37
light2__5760m_vs_light1_3960m	NA	NA	NA	NA	NA	NA	NA	NA	NA	150	NA	NA	NA	NA	NA	NA	NA	125	NA	5760	NA	NA	CM	37
dark2__0000m_vs_NRC-1c	NA	NA	NA	NA	NA	NA	NA	NA	NA	0	NA	NA	NA	NA	NA	NA	NA	125	NA	0	NA	NA	CM	37
dark2__0060m_vs_NRC-1c	NA	NA	NA	NA	NA	NA	NA	NA	NA	0	NA	NA	NA	NA	NA	NA	NA	125	NA	60	NA	NA	CM	37
dark2__0300m_vs_NRC-1c	NA	NA	NA	NA	NA	NA	NA	NA	NA	0	NA	NA	NA	NA	NA	NA	NA	125	NA	300	NA	NA	CM	37
dark2__0540m_vs_NRC-1c	NA	NA	NA	NA	NA	NA	NA	NA	NA	0	NA	NA	NA	NA	NA	NA	NA	125	NA	540	NA	NA	CM	37
dark2__0780m_vs_NRC-1c	NA	NA	NA	NA	NA	NA	NA	NA	NA	0	NA	NA	NA	NA	NA	NA	NA	125	NA	780	NA	NA	CM	37
dark2__1020m_vs_NRC-1c	NA	NA	NA	NA	NA	NA	NA	NA	NA	0	NA	NA	NA	NA	NA	NA	NA	125	NA	1020	NA	NA	CM	37
dark2__1260m_vs_NRC-1c	NA	NA	NA	NA	NA	NA	NA	NA	NA	0	NA	NA	NA	NA	NA	NA	NA	125	NA	1260	NA	NA	CM	37
dark2__1500m_vs_NRC-1c	NA	NA	NA	NA	NA	NA	NA	NA	NA	0	NA	NA	NA	NA	NA	NA	NA	125	NA	1500	NA	NA	CM	37
dark2__1740m_vs_NRC-1c	NA	NA	NA	NA	NA	NA	NA	NA	NA	0	NA	NA	NA	NA	NA	NA	NA	125	NA	1740	NA	NA	CM	37
dark2__1980m_vs_NRC-1c	NA	NA	NA	NA	NA	NA	NA	NA	NA	0	NA	NA	NA	NA	NA	NA	NA	125	NA	1980	NA	NA	CM	37
dark2__2220m_vs_NRC-1c	NA	NA	NA	NA	NA	NA	NA	NA	NA	0	NA	NA	NA	NA	NA	NA	NA	125	NA	2220	NA	NA	CM	37

dark2__2460m_vs_NRC-1c	NA	NA	NA	NA	NA	NA	NA	NA	NA	0	NA	NA	NA	NA	NA	NA	NA	125	NA	2460	NA	NA	CM	37
dark2__2700m_vs_NRC-1c	NA	NA	NA	NA	NA	NA	NA	NA	NA	0	NA	NA	NA	NA	NA	NA	NA	125	NA	2700	NA	NA	CM	37
dark2__2940m_vs_NRC-1c	NA	NA	NA	NA	NA	NA	NA	NA	NA	0	NA	NA	NA	NA	NA	NA	NA	125	NA	2940	NA	NA	CM	37
dark2__3180m_vs_NRC-1c	NA	NA	NA	NA	NA	NA	NA	NA	NA	0	NA	NA	NA	NA	NA	NA	NA	125	NA	3180	NA	NA	CM	37
dark2__3420m_vs_NRC-1c	NA	NA	NA	NA	NA	NA	NA	NA	NA	0	NA	NA	NA	NA	NA	NA	NA	125	NA	3420	NA	NA	CM	37
dark2__3660m_vs_NRC-1c	NA	NA	NA	NA	NA	NA	NA	NA	NA	0	NA	NA	NA	NA	NA	NA	NA	125	NA	3660	NA	NA	CM	37
dark2__3900m_vs_NRC-1c	NA	NA	NA	NA	NA	NA	NA	NA	NA	0	NA	NA	NA	NA	NA	NA	NA	125	NA	3900	NA	NA	CM	37
dark1__0000m_vs_NRC-1c	NA	NA	NA	NA	NA	NA	NA	NA	NA	0	NA	NA	NA	0.63	NA	NA	NA	125	NA	0	NA	NA	CM	37
dark1__0240m_vs_NRC-1c	NA	NA	NA	NA	NA	NA	NA	NA	NA	0	NA	NA	NA	0.66	NA	NA	NA	125	NA	240	NA	NA	CM	37
dark1__0480m_vs_NRC-1c	NA	NA	NA	NA	NA	NA	NA	NA	NA	0	NA	NA	NA	0.69	NA	NA	NA	125	NA	480	NA	NA	CM	37
dark1__0720m_vs_NRC-1c	NA	NA	NA	NA	NA	NA	NA	NA	NA	0	NA	NA	NA	0.64	NA	NA	NA	125	NA	720	NA	NA	CM	37
dark1__0960m_vs_NRC-1c	NA	NA	NA	NA	NA	NA	NA	NA	NA	0	NA	NA	NA	0.61	NA	NA	NA	125	NA	960	NA	NA	CM	37
dark1__1200m_vs_NRC-1c	NA	NA	NA	NA	NA	NA	NA	NA	NA	0	NA	NA	NA	0.58	NA	NA	NA	125	NA	1200	NA	NA	CM	37
dark1__1440m_vs_NRC-1c	NA	NA	NA	NA	NA	NA	NA	NA	NA	0	NA	NA	NA	0.57	NA	NA	NA	125	NA	1440	NA	NA	CM	37
dark1__1680m_vs_NRC-1c	NA	NA	NA	NA	NA	NA	NA	NA	NA	0	NA	NA	NA	0.54	NA	NA	NA	125	NA	1680	NA	NA	CM	37
dark1__1920m_vs_NRC-1c	NA	NA	NA	NA	NA	NA	NA	NA	NA	0	NA	NA	NA	0.61	NA	NA	NA	125	NA	1920	NA	NA	CM	37
dark1__2160m_vs_NRC-1c	NA	NA	NA	NA	NA	NA	NA	NA	NA	0	NA	NA	NA	0.63	NA	NA	NA	125	NA	2160	NA	NA	CM	37
dark1__2400m_vs_NRC-1c	NA	NA	NA	NA	NA	NA	NA	NA	NA	0	NA	NA	NA	0.61	NA	NA	NA	125	NA	2400	NA	NA	CM	37
dark1__2640m_vs_NRC-1c	NA	NA	NA	NA	NA	NA	NA	NA	NA	0	NA	NA	NA	0.61	NA	NA	NA	125	NA	2640	NA	NA	CM	37
dark1__2880m_vs_NRC-1c	NA	NA	NA	NA	NA	NA	NA	NA	NA	0	NA	NA	NA	0.65	NA	NA	NA	125	NA	2880	NA	NA	CM	37
dark1__3120m_vs_NRC-1c	NA	NA	NA	NA	NA	NA	NA	NA	NA	0	NA	NA	NA	0.59	NA	NA	NA	125	NA	3120	NA	NA	CM	37
dark1__3360m_vs_NRC-1c	NA	NA	NA	NA	NA	NA	NA	NA	NA	0	NA	NA	NA	0.55	NA	NA	NA	125	NA	3360	NA	NA	CM	37
dark1__3600m_vs_NRC-1c	NA	NA	NA	NA	NA	NA	NA	NA	NA	0	NA	NA	NA	0.61	NA	NA	NA	125	NA	3600	NA	NA	CM	37
dark1__3870m_vs_NRC-1c	NA	NA	NA	NA	NA	NA	NA	NA	NA	0	NA	NA	NA	0.65	NA	NA	NA	125	NA	3870	NA	NA	CM	37

dark1__4110m_vs_NRC-1c	NA	NA	NA	NA	NA	NA	NA	NA	NA	0	NA	NA	NA	0.66	NA	NA	NA	125	NA	4110	NA	NA	CM	37
circadian_Dphr1_drk_cycling__1440min_vs_NRC-1d.sig	NA	NA	NA	NA	NA	NA	NA	NA	NA	0	150	NA	NA	0.41	NA	NA	NA	125	NA	1440	NA	NA	CM	37
circadian_Dphr1_drk_cycling__1665min_vs_NRC-1d.sig	NA	NA	NA	NA	NA	NA	NA	NA	NA	0	150	NA	NA	0.52	NA	NA	NA	125	NA	1665	NA	NA	CM	37
circadian_Dphr1_drk_cycling__1800min_vs_NRC-1d.sig	NA	NA	NA	NA	NA	NA	NA	NA	NA	0	150	NA	NA	0.57	NA	NA	NA	125	NA	1800	NA	NA	CM	37
circadian_Dphr1_drk_cycling__1980min_vs_NRC-1d.sig	NA	NA	NA	NA	NA	NA	NA	NA	NA	0	150	NA	NA	0.72	NA	NA	NA	125	NA	1980	NA	NA	CM	37
circadian_Dphr1_drk_cycling__2175min_vs_NRC-1d.sig	NA	NA	NA	NA	NA	NA	NA	NA	NA	0	0	NA	NA	0.87	NA	NA	NA	125	NA	2175	NA	NA	CM	37
circadian_Dphr1_drk_cycling__2340min_vs_NRC-1d.sig	NA	NA	NA	NA	NA	NA	NA	NA	NA	0	0	NA	NA	1.01	NA	NA	NA	125	NA	2340	NA	NA	CM	37
circadian_Dphr1_drk_cycling__2595min_vs_NRC-1d.sig	NA	NA	NA	NA	NA	NA	NA	NA	NA	0	0	NA	NA	1.31	NA	NA	NA	125	NA	2595	NA	NA	CM	37
circadian_Dphr1_drk_cycling__2705min_vs_NRC-1d.sig	NA	NA	NA	NA	NA	NA	NA	NA	NA	0	0	NA	NA	1.31	NA	NA	NA	125	NA	2705	NA	NA	CM	37
circadian_Dphr1_drk_cycling__2880min_vs_NRC-1d.sig	NA	NA	NA	NA	NA	NA	NA	NA	NA	0	150	NA	NA	1.43	NA	NA	NA	125	NA	2880	NA	NA	CM	37
circadian_drk8_cycling_0000min_vs_NRC-1e.sig	NA	NA	NA	NA	NA	NA	NA	NA	NA	0	150	NA	NA	0.33	NA	NA	NA	125	NA	0	NA	NA	CM	37
circadian_drk8_cycling_0180min_vs_NRC-1e.sig	NA	NA	NA	NA	NA	NA	NA	NA	NA	0	150	NA	NA	0.66	NA	NA	NA	125	NA	180	NA	NA	CM	37
circadian_drk8_cycling_0360min_vs_NRC-1e.sig	NA	NA	NA	NA	NA	NA	NA	NA	NA	0	150	NA	NA	0.62	NA	NA	NA	125	NA	360	NA	NA	CM	37
circadian_drk8_cycling_0540min_vs_NRC-1e.sig	NA	NA	NA	NA	NA	NA	NA	NA	NA	0	150	NA	NA	0.56	NA	NA	NA	125	NA	540	NA	NA	CM	37
circadian_drk8_cycling_0720min_vs_NRC-1e.sig	NA	NA	NA	NA	NA	NA	NA	NA	NA	0	0	NA	NA	0.44	NA	NA	NA	125	NA	720	NA	NA	CM	37
circadian_drk8_cycling_0900min_vs_NRC-1e.sig	NA	NA	NA	NA	NA	NA	NA	NA	NA	0	0	NA	NA	0.5	NA	NA	NA	125	NA	900	NA	NA	CM	37
circadian_drk8_cycling_1080min_vs_	NA	NA	NA	NA	NA	NA	NA	NA	NA	0	0	NA	NA	0.48	NA	NA	NA	125	NA	1080	NA	NA	CM	37

NRC-1e.sig																								
circadian_drk8_cycling_1260min_vs_NRC-1e.sig	NA	NA	NA	NA	NA	NA	NA	NA	NA	0	0	NA	NA	0.51	NA	NA	NA	125	NA	1260	NA	NA	CM	37
circadian_drk8_cycling_1440min_vs_NRC-1e.sig	NA	NA	NA	NA	NA	NA	NA	NA	NA	0	150	NA	NA	0.5	NA	NA	NA	125	NA	1440	NA	NA	CM	37
circadian_drk8_cycling_1620min_vs_NRC-1e.sig	NA	NA	NA	NA	NA	NA	NA	NA	NA	0	150	NA	NA	0.44	NA	NA	NA	125	NA	1620	NA	NA	CM	37
circadian_drk8_cycling_1800min_vs_NRC-1e.sig	NA	NA	NA	NA	NA	NA	NA	NA	NA	0	150	NA	NA	0.48	NA	NA	NA	125	NA	1800	NA	NA	CM	37
circadian_drk8_cycling_1980min_vs_NRC-1e.sig	NA	NA	NA	NA	NA	NA	NA	NA	NA	0	150	NA	NA	0.46	NA	NA	NA	125	NA	1980	NA	NA	CM	37
circadian_drk8_cycling_2160min_vs_NRC-1e.sig	NA	NA	NA	NA	NA	NA	NA	NA	NA	0	0	NA	NA	0.48	NA	NA	NA	125	NA	2160	NA	NA	CM	37
circadian_drk8_cycling_2340min_vs_NRC-1e.sig	NA	NA	NA	NA	NA	NA	NA	NA	NA	0	0	NA	NA	0.5	NA	NA	NA	125	NA	2340	NA	NA	CM	37
circadian_drk8_cycling_2520min_vs_NRC-1e.sig	NA	NA	NA	NA	NA	NA	NA	NA	NA	0	0	NA	NA	0.56	NA	NA	NA	125	NA	2520	NA	NA	CM	37
circadian_drk8_cycling_2700min_vs_NRC-1e.sig	NA	NA	NA	NA	NA	NA	NA	NA	NA	0	0	NA	NA	0.52	NA	NA	NA	125	NA	2700	NA	NA	CM	37
circadian_drk8_cycling_2880min_vs_NRC-1e.sig	NA	NA	NA	NA	NA	NA	NA	NA	NA	0	150	NA	NA	0.55	NA	NA	NA	125	NA	2880	NA	NA	CM	37
circadian_drk8_cycling_3060min_vs_NRC-1e.sig	NA	NA	NA	NA	NA	NA	NA	NA	NA	0	150	NA	NA	0.57	NA	NA	NA	125	NA	3060	NA	NA	CM	37
circadian_drk8_cycling_3240min_vs_NRC-1e.sig	NA	NA	NA	NA	NA	NA	NA	NA	NA	0	150	NA	NA	0.56	NA	NA	NA	125	NA	3240	NA	NA	CM	37
circadian_drk7_cycling_0000min_vs_NRC-1d.sig	NA	NA	NA	NA	NA	NA	NA	NA	NA	0	21.3	NA	NA	0.55	NA	NA	NA	125	NA	0	NA	NA	CM	37
circadian_drk7_cycling_0180min_vs_NRC-1d.sig	NA	NA	NA	NA	NA	NA	NA	NA	NA	0	21.3	NA	NA	0.57	NA	NA	NA	125	NA	180	NA	NA	CM	37
circadian_drk7_cycling_0360min_vs_NRC-1d.sig	NA	NA	NA	NA	NA	NA	NA	NA	NA	0	21.3	NA	NA	0.64	NA	NA	NA	125	NA	360	NA	NA	CM	37

circadian_drk7_cycling_0540min_vs_NRC-1d.sig	NA	NA	NA	NA	NA	NA	NA	NA	NA	0	21.3	NA	NA	0.58	NA	NA	NA	125	NA	540	NA	NA	CM	37
circadian_drk7_cycling_0720min_vs_NRC-1d.sig	NA	NA	NA	NA	NA	NA	NA	NA	NA	0	0	NA	NA	0.59	NA	NA	NA	125	NA	720	NA	NA	CM	37
circadian_drk7_cycling_0900min_vs_NRC-1d.sig	NA	NA	NA	NA	NA	NA	NA	NA	NA	0	0	NA	NA	0.6	NA	NA	NA	125	NA	900	NA	NA	CM	37
circadian_drk7_cycling_1080min_vs_NRC-1d.sig	NA	NA	NA	NA	NA	NA	NA	NA	NA	0	0	NA	NA	0.6	NA	NA	NA	125	NA	1080	NA	NA	CM	37
circadian_drk7_cycling_1260min_vs_NRC-1d.sig	NA	NA	NA	NA	NA	NA	NA	NA	NA	0	0	NA	NA	0.7	NA	NA	NA	125	NA	1260	NA	NA	CM	37
circadian_drk7_cycling_1440min_vs_NRC-1d.sig	NA	NA	NA	NA	NA	NA	NA	NA	NA	0	21.3	NA	NA	0.77	NA	NA	NA	125	NA	1440	NA	NA	CM	37
circadian_drk7_cycling_1620min_vs_NRC-1d.sig	NA	NA	NA	NA	NA	NA	NA	NA	NA	0	21.3	NA	NA	0.62	NA	NA	NA	125	NA	1620	NA	NA	CM	37
circadian_drk7_cycling_1800min_vs_NRC-1d.sig	NA	NA	NA	NA	NA	NA	NA	NA	NA	0	21.3	NA	NA	0.63	NA	NA	NA	125	NA	1800	NA	NA	CM	37
circadian_drk7_cycling_1980min_vs_NRC-1d.sig	NA	NA	NA	NA	NA	NA	NA	NA	NA	0	21.3	NA	NA	0.63	NA	NA	NA	125	NA	1980	NA	NA	CM	37
circadian_drk7_cycling_2160min_vs_NRC-1d.sig	NA	NA	NA	NA	NA	NA	NA	NA	NA	0	0	NA	NA	0.67	NA	NA	NA	125	NA	2160	NA	NA	CM	37
circadian_drk7_cycling_2340min_vs_NRC-1d.sig	NA	NA	NA	NA	NA	NA	NA	NA	NA	0	0	NA	NA	0.66	NA	NA	NA	125	NA	2340	NA	NA	CM	37
circadian_drk7_cycling_2520min_vs_NRC-1d.sig	NA	NA	NA	NA	NA	NA	NA	NA	NA	0	0	NA	NA	0.65	NA	NA	NA	125	NA	2520	NA	NA	CM	37
circadian_drk7_cycling_2700min_vs_NRC-1d.sig	NA	NA	NA	NA	NA	NA	NA	NA	NA	0	0	NA	NA	0.63	NA	NA	NA	125	NA	2700	NA	NA	CM	37
circadian_drk7_cycling_2880min_vs_NRC-1d.sig	NA	NA	NA	NA	NA	NA	NA	NA	NA	0	21.3	NA	NA	0.7	NA	NA	NA	125	NA	2880	NA	NA	CM	37
circadian_drk7_cycling_3060min_vs_NRC-1d.sig	NA	NA	NA	NA	NA	NA	NA	NA	NA	0	21.3	NA	NA	0.44	NA	NA	NA	125	NA	3060	NA	NA	CM	37
circadian_drk7_cycling_3240min_vs_NRC-1d.sig	NA	NA	NA	NA	NA	NA	NA	NA	NA	0	21.3	NA	NA	0.68	NA	NA	NA	125	NA	3240	NA	NA	CM	37

circadian_drk6_cycling_0000min_vs_NRC-1e.sig	NA	NA	NA	NA	NA	NA	NA	NA	NA	0	250	NA	NA	0.51	NA	NA	NA	20	NA	0	NA	NA	CM	37
circadian_drk6_cycling_0180min_vs_NRC-1e.sig	NA	NA	NA	NA	NA	NA	NA	NA	NA	0	250	NA	NA	0.51	NA	NA	NA	20	NA	180	NA	NA	CM	37
circadian_drk6_cycling_0360min_vs_NRC-1e.sig	NA	NA	NA	NA	NA	NA	NA	NA	NA	0	250	NA	NA	0.51	NA	NA	NA	20	NA	360	NA	NA	CM	37
circadian_drk6_cycling_0540min_vs_NRC-1e.sig	NA	NA	NA	NA	NA	NA	NA	NA	NA	0	250	NA	NA	0.51	NA	NA	NA	20	NA	540	NA	NA	CM	37
circadian_drk6_cycling_0720min_vs_NRC-1e.sig	NA	NA	NA	NA	NA	NA	NA	NA	NA	0	0	NA	NA	0.51	NA	NA	NA	20	NA	720	NA	NA	CM	37
circadian_drk6_cycling_0912min_vs_NRC-1e.sig	NA	NA	NA	NA	NA	NA	NA	NA	NA	0	0	NA	NA	0.51	NA	NA	NA	20	NA	912	NA	NA	CM	37
circadian_drk6_cycling_1080min_vs_NRC-1e.sig	NA	NA	NA	NA	NA	NA	NA	NA	NA	0	0	NA	NA	0.51	NA	NA	NA	20	NA	1080	NA	NA	CM	37
circadian_drk6_cycling_1260min_vs_NRC-1e.sig	NA	NA	NA	NA	NA	NA	NA	NA	NA	0	0	NA	NA	0.51	NA	NA	NA	20	NA	1260	NA	NA	CM	37
circadian_drk6_cycling_1440min_vs_NRC-1e.sig	NA	NA	NA	NA	NA	NA	NA	NA	NA	0	250	NA	NA	0.51	NA	NA	NA	20	NA	1440	NA	NA	CM	37
circadian__dark5_cycling_30C_1440min_vs_NRC-1d.sig	NA	NA	NA	NA	NA	NA	NA	NA	NA	0	150	NA	NA	0.45	NA	NA	NA	125	NA	1440	NA	NA	CM	30
circadian__dark5_cycling_30C_1630min_vs_NRC-1d.sig	NA	NA	NA	NA	NA	NA	NA	NA	NA	0	150	NA	NA	0.49	NA	NA	NA	125	NA	1630	NA	NA	CM	30
circadian__dark5_cycling_30C_1815min_vs_NRC-1d.sig	NA	NA	NA	NA	NA	NA	NA	NA	NA	0	150	NA	NA	0.54	NA	NA	NA	125	NA	1815	NA	NA	CM	30
circadian__dark5_cycling_30C_1980min_vs_NRC-1d.sig	NA	NA	NA	NA	NA	NA	NA	NA	NA	0	150	NA	NA	0.6	NA	NA	NA	125	NA	1980	NA	NA	CM	30
circadian__dark5_cycling_30C_2160min_vs_NRC-1d.sig	NA	NA	NA	NA	NA	NA	NA	NA	NA	0	0	NA	NA	0.63	NA	NA	NA	125	NA	2160	NA	NA	CM	30
circadian__dark5_cycling_30C_2355	NA	NA	NA	NA	NA	NA	NA	NA	NA	0	0	NA	NA	0.61	NA	NA	NA	125	NA	2355	NA	NA	CM	30

min_vs_NRC-1d.sig																								
circadian__dark5_cycling_30C_2590min_vs_NRC-1d.sig	NA	NA	NA	NA	NA	NA	NA	NA	NA	0	0	NA	NA	0.79	NA	NA	NA	125	NA	2590	NA	NA	CM	30
circadian__dark5_cycling_30C_2700min_vs_NRC-1d.sig	NA	NA	NA	NA	NA	NA	NA	NA	NA	0	0	NA	NA	0.8	NA	NA	NA	125	NA	2705	NA	NA	CM	30
circadian__dark5_cycling_30C_2880min_vs_NRC-1d.sig	NA	NA	NA	NA	NA	NA	NA	NA	NA	0	150	NA	NA	0.86	NA	NA	NA	125	NA	2880	NA	NA	CM	30
circadian_20051021_cycling_dark_42oC_1440min_vs_NRC-1d.sig	NA	NA	NA	NA	NA	NA	NA	NA	NA	0	150	NA	NA	0.89	NA	NA	NA	125	NA	1440	NA	NA	CM	42
circadian_20051021_cycling_dark_42oC_1615min_vs_NRC-1d.sig	NA	NA	NA	NA	NA	NA	NA	NA	NA	0	150	NA	NA	1.07	NA	NA	NA	125	NA	1615	NA	NA	CM	42
circadian_20051021_cycling_dark_42oC_1800min_vs_NRC-1d.sig	NA	NA	NA	NA	NA	NA	NA	NA	NA	0	150	NA	NA	1.17	NA	NA	NA	125	NA	1800	NA	NA	CM	42
circadian_20051021_cycling_dark_42oC_1985min_vs_NRC-1d.sig	NA	NA	NA	NA	NA	NA	NA	NA	NA	0	150	NA	NA	1.13	NA	NA	NA	125	NA	1985	NA	NA	CM	42
circadian_20051021_cycling_dark_42oC_2160min_vs_NRC-1d.sig	NA	NA	NA	NA	NA	NA	NA	NA	NA	0	0	NA	NA	1.25	NA	NA	NA	125	NA	2160	NA	NA	CM	42
circadian_20051021_cycling_dark_42oC_2340min_vs_NRC-1d.sig	NA	NA	NA	NA	NA	NA	NA	NA	NA	0	0	NA	NA	1.33	NA	NA	NA	125	NA	2340	NA	NA	CM	42
circadian_20051021_cycling_dark_42oC_2515min_vs_NRC-1d.sig	NA	NA	NA	NA	NA	NA	NA	NA	NA	0	0	NA	NA	1.52	NA	NA	NA	125	NA	2515	NA	NA	CM	42
circadian_20051021_cycling_dark_42oC_2705min_vs_NRC-1d.sig	NA	NA	NA	NA	NA	NA	NA	NA	NA	0	0	NA	NA	1.67	NA	NA	NA	125	NA	2705	NA	NA	CM	42

circadian_20051021_cycling_dark_42oC_2880min_vs_NRC-1d.sig	NA	NA	NA	NA	NA	NA	NA	NA	NA	0	150	NA	NA	1.8	NA	NA	NA	125	NA	2880	NA	NA	CM	42
circadian_dark3_cycling_1380min_vs_NRC-1d.sig	NA	NA	NA	NA	NA	NA	NA	NA	NA	0	0	NA	NA	0.36	NA	NA	NA	125	NA	1380	NA	NA	CM	37
circadian_dark3_cycling_1440min_vs_NRC-1d.sig	NA	NA	NA	NA	NA	NA	NA	NA	NA	0	150	NA	NA	0.37	NA	NA	NA	125	NA	1440	NA	NA	CM	37
circadian_dark3_cycling_1500min_vs_NRC-1d.sig	NA	NA	NA	NA	NA	NA	NA	NA	NA	0	150	NA	NA	0.32	NA	NA	NA	125	NA	1500	NA	NA	CM	37
circadian_dark3_cycling_1620min_vs_NRC-1d.sig	NA	NA	NA	NA	NA	NA	NA	NA	NA	0	150	NA	NA	0.41	NA	NA	NA	125	NA	1620	NA	NA	CM	37
circadian_dark3_cycling_1800min_vs_NRC-1d.sig	NA	NA	NA	NA	NA	NA	NA	NA	NA	0	150	NA	NA	0.47	NA	NA	NA	125	NA	1800	NA	NA	CM	37
circadian_dark3_cycling_1980min_vs_NRC-1d.sig	NA	NA	NA	NA	NA	NA	NA	NA	NA	0	150	NA	NA	0.42	NA	NA	NA	125	NA	1980	NA	NA	CM	37
circadian_dark3_cycling_2160min_vs_NRC-1d.sig	NA	NA	NA	NA	NA	NA	NA	NA	NA	0	0	NA	NA	0.5	NA	NA	NA	125	NA	2160	NA	NA	CM	37
circadian_dark3_cycling_2220min_vs_NRC-1d.sig	NA	NA	NA	NA	NA	NA	NA	NA	NA	0	0	NA	NA	0.52	NA	NA	NA	125	NA	2220	NA	NA	CM	37
circadian_dark3_cycling_2340min_vs_NRC-1d.sig	NA	NA	NA	NA	NA	NA	NA	NA	NA	0	0	NA	NA	0.56	NA	NA	NA	125	NA	2340	NA	NA	CM	37
circadian_dark3_cycling_2520min_vs_NRC-1d.sig	NA	NA	NA	NA	NA	NA	NA	NA	NA	0	0	NA	NA	0.57	NA	NA	NA	125	NA	2520	NA	NA	CM	37
circadian_dark3_cycling_2700min_vs_NRC-1d.sig	NA	NA	NA	NA	NA	NA	NA	NA	NA	0	0	NA	NA	0.75	NA	NA	NA	125	NA	2700	NA	NA	CM	37
circadian_dark3_cycling_2880min_vs_NRC-1d.sig	NA	NA	NA	NA	NA	NA	NA	NA	NA	0	150	NA	NA	0.86	NA	NA	NA	125	NA	2880	NA	NA	CM	37
circadian_dark3_ctrl_1380min_vs_NRC-1d.sig	NA	NA	NA	NA	NA	NA	NA	NA	NA	0	0	NA	NA	0.37	NA	NA	NA	125	NA	1380	NA	NA	CM	37
circadian_dark3_ctrl_1440min_vs_NRC-1d.sig	NA	NA	NA	NA	NA	NA	NA	NA	NA	0	0	NA	NA	0.39	NA	NA	NA	125	NA	1440	NA	NA	CM	37
circadian_dark3_ctrl_1500min_vs_NRC-1d.sig	NA	NA	NA	NA	NA	NA	NA	NA	NA	0	0	NA	NA	0.38	NA	NA	NA	125	NA	1500	NA	NA	CM	37

circadian_dark3_ctrl_1620min_vs_NRC-1d.sig	NA	NA	NA	NA	NA	NA	NA	NA	NA	0	0	NA	NA	0.42	NA	NA	NA	125	NA	1620	NA	NA	CM	37
circadian_dark3_ctrl_1800min_vs_NRC-1d.sig	NA	NA	NA	NA	NA	NA	NA	NA	NA	0	0	NA	NA	0.52	NA	NA	NA	125	NA	1800	NA	NA	CM	37
circadian_dark3_ctrl_1980min_vs_NRC-1d.sig	NA	NA	NA	NA	NA	NA	NA	NA	NA	0	0	NA	NA	0.41	NA	NA	NA	125	NA	1980	NA	NA	CM	37
circadian_dark3_ctrl_2160min_vs_NRC-1d.sig	NA	NA	NA	NA	NA	NA	NA	NA	NA	0	0	NA	NA	0.52	NA	NA	NA	125	NA	2160	NA	NA	CM	37
circadian_dark3_ctrl_2220min_vs_NRC-1d.sig	NA	NA	NA	NA	NA	NA	NA	NA	NA	0	0	NA	NA	0.56	NA	NA	NA	125	NA	2220	NA	NA	CM	37
circadian_dark3_ctrl_2340min_vs_NRC-1d.sig	NA	NA	NA	NA	NA	NA	NA	NA	NA	0	0	NA	NA	0.62	NA	NA	NA	125	NA	2340	NA	NA	CM	37
circadian_dark3_ctrl_2520min_vs_NRC-1d.sig	NA	NA	NA	NA	NA	NA	NA	NA	NA	0	0	NA	NA	0.66	NA	NA	NA	125	NA	2520	NA	NA	CM	37
circadian_dark3_ctrl_2700min_vs_NRC-1d.sig	NA	NA	NA	NA	NA	NA	NA	NA	NA	0	0	NA	NA	0.81	NA	NA	NA	125	NA	2700	NA	NA	CM	37
circadian_dark3_ctrl_2880min_vs_NRC-1d.sig	NA	NA	NA	NA	NA	NA	NA	NA	NA	0	0	NA	NA	0.97	NA	NA	NA	125	NA	2880	NA	NA	CM	37
circadian_drk8_control_0000min_vs_NRC-1e.sig	NA	NA	NA	NA	NA	NA	NA	NA	NA	0	0	NA	NA	0.287	NA	NA	NA	125	NA	0	NA	NA	CM	37
circadian_drk8_control_0180min_vs_NRC-1e.sig	NA	NA	NA	NA	NA	NA	NA	NA	NA	0	0	NA	NA	0.512	NA	NA	NA	125	NA	180	NA	NA	CM	37
circadian_drk8_control_0360min_vs_NRC-1e.sig	NA	NA	NA	NA	NA	NA	NA	NA	NA	0	0	NA	NA	0.593	NA	NA	NA	125	NA	360	NA	NA	CM	37
circadian_drk8_control_0540min_vs_NRC-1e.sig	NA	NA	NA	NA	NA	NA	NA	NA	NA	0	0	NA	NA	0.495	NA	NA	NA	125	NA	540	NA	NA	CM	37
circadian_drk8_control_0720min_vs_NRC-1e.sig	NA	NA	NA	NA	NA	NA	NA	NA	NA	0	0	NA	NA	0.527	NA	NA	NA	125	NA	720	NA	NA	CM	37
circadian_drk8_control_0900min_vs_NRC-1e.sig	NA	NA	NA	NA	NA	NA	NA	NA	NA	0	0	NA	NA	0.471	NA	NA	NA	125	NA	900	NA	NA	CM	37
circadian_drk8_control_1080min_vs_NRC-1e.sig	NA	NA	NA	NA	NA	NA	NA	NA	NA	0	0	NA	NA	0.468	NA	NA	NA	125	NA	1080	NA	NA	CM	37

circadian_drk8_control_1260min_vs_NRC-1e.sig	NA	NA	NA	NA	NA	NA	NA	NA	NA	0	0	NA	NA	0.509	NA	NA	NA	125	NA	1260	NA	NA	CM	37
circadian_drk8_control_1440min_vs_NRC-1e.sig	NA	NA	NA	NA	NA	NA	NA	NA	NA	0	0	NA	NA	0.521	NA	NA	NA	125	NA	1440	NA	NA	CM	37
circadian_drk8_control_1620min_vs_NRC-1e.sig	NA	NA	NA	NA	NA	NA	NA	NA	NA	0	0	NA	NA	0.500	NA	NA	NA	125	NA	1620	NA	NA	CM	37
circadian_drk8_control_1800min_vs_NRC-1e.sig	NA	NA	NA	NA	NA	NA	NA	NA	NA	0	0	NA	NA	0.451	NA	NA	NA	125	NA	1800	NA	NA	CM	37
circadian_drk8_control_1980min_vs_NRC-1e.sig	NA	NA	NA	NA	NA	NA	NA	NA	NA	0	0	NA	NA	0.467	NA	NA	NA	125	NA	1980	NA	NA	CM	37
circadian_drk8_control_2160min_vs_NRC-1e.sig	NA	NA	NA	NA	NA	NA	NA	NA	NA	0	0	NA	NA	0.451	NA	NA	NA	125	NA	2160	NA	NA	CM	37
circadian_drk8_control_2340min_vs_NRC-1e.sig	NA	NA	NA	NA	NA	NA	NA	NA	NA	0	0	NA	NA	0.492	NA	NA	NA	125	NA	2340	NA	NA	CM	37
circadian_drk8_control_2520min_vs_NRC-1e.sig	NA	NA	NA	NA	NA	NA	NA	NA	NA	0	0	NA	NA	0.497	NA	NA	NA	125	NA	2520	NA	NA	CM	37
circadian_drk8_control_2700min_vs_NRC-1e.sig	NA	NA	NA	NA	NA	NA	NA	NA	NA	0	0	NA	NA	0.539	NA	NA	NA	125	NA	2700	NA	NA	CM	37
circadian_drk8_control_2880min_vs_NRC-1e.sig	NA	NA	NA	NA	NA	NA	NA	NA	NA	0	0	NA	NA	0.659	NA	NA	NA	125	NA	2880	NA	NA	CM	37
circadian_drk8_control_3060min_vs_NRC-1e.sig	NA	NA	NA	NA	NA	NA	NA	NA	NA	0	0	NA	NA	0.484	NA	NA	NA	125	NA	3060	NA	NA	CM	37
circadian_drk8_control_3240min_vs_NRC-1e.sig	NA	NA	NA	NA	NA	NA	NA	NA	NA	0	0	NA	NA	0.543	NA	NA	NA	125	NA	3240	NA	NA	CM	37
Circadian_Dark9_Cycling_0000min_vs_NRC-1g.sig	NA	NA	NA	NA	NA	NA	NA	NA	NA	0	150	NA	NA	0.25	NA	NA	NA	125	NA	0	NA	NA	CM	37
Circadian_Dark9_Cycling_0180min_vs_NRC-1g.sig	NA	NA	NA	NA	NA	NA	NA	NA	NA	0	150	NA	NA	0.35	NA	NA	NA	125	NA	180	NA	NA	CM	37
Circadian_Dark9_Cycling_0360min_vs_NRC-1g.sig	NA	NA	NA	NA	NA	NA	NA	NA	NA	0	150	NA	NA	0.3	NA	NA	NA	125	NA	360	NA	NA	CM	37
Circadian_Dark9_Cycling_0535min_vs_NRC-1g.sig	NA	NA	NA	NA	NA	NA	NA	NA	NA	0	150	NA	NA	0.32	NA	NA	NA	125	NA	535	NA	NA	CM	37

Circadian_Dark9_Cycling_0720min_vs_NRC-1g.sig	NA	NA	NA	NA	NA	NA	NA	NA	NA	0	0	NA	NA	0.36	NA	NA	NA	125	NA	720	NA	NA	CM	37
Circadian_Dark9_Cycling_0900min_vs_NRC-1g.sig	NA	NA	NA	NA	NA	NA	NA	NA	NA	0	0	NA	NA	0.35	NA	NA	NA	125	NA	900	NA	NA	CM	37
Circadian_Dark9_Cycling_1080min_vs_NRC-1g.sig	NA	NA	NA	NA	NA	NA	NA	NA	NA	0	0	NA	NA	0.35	NA	NA	NA	125	NA	1080	NA	NA	CM	37
Circadian_Dark9_Cycling_1265min_vs_NRC-1g.sig	NA	NA	NA	NA	NA	NA	NA	NA	NA	0	0	NA	NA	0.41	NA	NA	NA	125	NA	1265	NA	NA	CM	37
Circadian_Dark9_Cycling_1440min_vs_NRC-1g.sig	NA	NA	NA	NA	NA	NA	NA	NA	NA	0	150	NA	NA	0.33	NA	NA	NA	125	NA	1440	NA	NA	CM	37
Circadian_Dark9_Cycling_1620min_vs_NRC-1g.sig	NA	NA	NA	NA	NA	NA	NA	NA	NA	0	150	NA	NA	0.31	NA	NA	NA	125	NA	1620	NA	NA	CM	37
Circadian_Dark9_Cycling_1800min_vs_NRC-1g.sig	NA	NA	NA	NA	NA	NA	NA	NA	NA	0	150	NA	NA	0.38	NA	NA	NA	125	NA	1800	NA	NA	CM	37
Circadian_Dark9_Cycling_1980min_vs_NRC-1g.sig	NA	NA	NA	NA	NA	NA	NA	NA	NA	0	150	NA	NA	0.23	NA	NA	NA	125	NA	1980	NA	NA	CM	37
Circadian_Dark9_Cycling_2160min_vs_NRC-1g.sig	NA	NA	NA	NA	NA	NA	NA	NA	NA	0	0	NA	NA	0.31	NA	NA	NA	125	NA	2160	NA	NA	CM	37
Circadian_Dark9_Cycling_2340min_vs_NRC-1g.sig	NA	NA	NA	NA	NA	NA	NA	NA	NA	0	0	NA	NA	0.31	NA	NA	NA	125	NA	2340	NA	NA	CM	37
Circadian_Dark9_Cycling_2520min_vs_NRC-1g.sig	NA	NA	NA	NA	NA	NA	NA	NA	NA	0	0	NA	NA	0.27	NA	NA	NA	125	NA	2520	NA	NA	CM	37
Circadian_Dark9_Cycling_2700min_vs_NRC-1g.sig	NA	NA	NA	NA	NA	NA	NA	NA	NA	0	0	NA	NA	0.37	NA	NA	NA	125	NA	2700	NA	NA	CM	37
Circadian_Dark9_Cycling_2880min_vs_NRC-1g.sig	NA	NA	NA	NA	NA	NA	NA	NA	NA	0	150	NA	NA	0.33	NA	NA	NA	125	NA	2880	NA	NA	CM	37
Circadian_Dark9_Cycling_3060min_vs_NRC-1g.sig	NA	NA	NA	NA	NA	NA	NA	NA	NA	0	150	NA	NA	0.35	NA	NA	NA	125	NA	3060	NA	NA	CM	37
Circadian_Dark9_Cycling_3240min_vs_NRC-1g.sig	NA	NA	NA	NA	NA	NA	NA	NA	NA	0	150	NA	NA	0.29	NA	NA	NA	125	NA	3240	NA	NA	CM	37
Circadian_Dark9_Cycling_3420min_vs_NRC-1g.sig	NA	NA	NA	NA	NA	NA	NA	NA	NA	0	150	NA	NA	0.29	NA	NA	NA	125	NA	3420	NA	NA	CM	37

Circadian_Dark9_Cycling_3600min_vs_NRC-1g.sig	NA	NA	NA	NA	NA	NA	NA	NA	NA	0	0	NA	NA	0.28	NA	NA	NA	125	NA	3600	NA	NA	CM	37
Circadian_Dark9_Cycling_3780min_vs_NRC-1g.sig	NA	NA	NA	NA	NA	NA	NA	NA	NA	0	0	NA	NA	0.3	NA	NA	NA	125	NA	3780	NA	NA	CM	37
Circadian_Dark9_Cycling_3960min_vs_NRC-1g.sig	NA	NA	NA	NA	NA	NA	NA	NA	NA	0	0	NA	NA	0.28	NA	NA	NA	125	NA	3960	NA	NA	CM	37
Circadian_Dark9_Cycling_4140min_vs_NRC-1g.sig	NA	NA	NA	NA	NA	NA	NA	NA	NA	0	0	NA	NA	0.31	NA	NA	NA	125	NA	4140	NA	NA	CM	37
Circadian_Dark9_Cycling_4320min_vs_NRC-1g.sig	NA	NA	NA	NA	NA	NA	NA	NA	NA	0	150	NA	NA	0.29	NA	NA	NA	125	NA	4320	NA	NA	CM	37
Circadian_Dark9_Cycling_4500min_vs_NRC-1g.sig	NA	NA	NA	NA	NA	NA	NA	NA	NA	0	150	NA	NA	0.32	NA	NA	NA	125	NA	4500	NA	NA	CM	37
Circadian_Dark9_Control_0000min_vs_NRC-1g.sig	NA	NA	NA	NA	NA	NA	NA	NA	NA	0	0	NA	NA	0.23	NA	NA	NA	125	NA	0	NA	NA	CM	37
Circadian_Dark9_Control_0180min_vs_NRC-1g.sig	NA	NA	NA	NA	NA	NA	NA	NA	NA	0	0	NA	NA	0.36	NA	NA	NA	125	NA	180	NA	NA	CM	37
Circadian_Dark9_Control_0360min_vs_NRC-1g.sig	NA	NA	NA	NA	NA	NA	NA	NA	NA	0	0	NA	NA	0.31	NA	NA	NA	125	NA	360	NA	NA	CM	37
Circadian_Dark9_Control_0535min_vs_NRC-1g.sig	NA	NA	NA	NA	NA	NA	NA	NA	NA	0	0	NA	NA	0.33	NA	NA	NA	125	NA	535	NA	NA	CM	37
Circadian_Dark9_Control_0720min_vs_NRC-1g.sig	NA	NA	NA	NA	NA	NA	NA	NA	NA	0	0	NA	NA	0.32	NA	NA	NA	125	NA	720	NA	NA	CM	37
Circadian_Dark9_Control_1080min_vs_NRC-1g.sig	NA	NA	NA	NA	NA	NA	NA	NA	NA	0	0	NA	NA	0.34	NA	NA	NA	125	NA	1080	NA	NA	CM	37
Circadian_Dark9_Control_1265min_vs_NRC-1g.sig	NA	NA	NA	NA	NA	NA	NA	NA	NA	0	0	NA	NA	0.33	NA	NA	NA	125	NA	1265	NA	NA	CM	37
Circadian_Dark9_Control_1440min_vs_NRC-1g.sig	NA	NA	NA	NA	NA	NA	NA	NA	NA	0	0	NA	NA	0.33	NA	NA	NA	125	NA	1440	NA	NA	CM	37
Circadian_Dark9_Control_1620min_vs_NRC-1g.sig	NA	NA	NA	NA	NA	NA	NA	NA	NA	0	0	NA	NA	0.27	NA	NA	NA	125	NA	1620	NA	NA	CM	37
Circadian_Dark9_Control_1800min_vs_NRC-1g.sig	NA	NA	NA	NA	NA	NA	NA	NA	NA	0	0	NA	NA	0.29	NA	NA	NA	125	NA	1800	NA	NA	CM	37

Circadian_Dark9_Control_1980min_vs_NRC-1g.sig	NA	NA	NA	NA	NA	NA	NA	NA	NA	0	0	NA	NA	0.31	NA	NA	NA	125	NA	1980	NA	NA	CM	37
Circadian_Dark9_Control_2160min_vs_NRC-1g.sig	NA	NA	NA	NA	NA	NA	NA	NA	NA	0	0	NA	NA	0.31	NA	NA	NA	125	NA	2160	NA	NA	CM	37
Circadian_Dark9_Control_2340min_vs_NRC-1g.sig	NA	NA	NA	NA	NA	NA	NA	NA	NA	0	0	NA	NA	0.29	NA	NA	NA	125	NA	2340	NA	NA	CM	37
Circadian_Dark9_Control_2520min_vs_NRC-1g.sig	NA	NA	NA	NA	NA	NA	NA	NA	NA	0	0	NA	NA	0.3	NA	NA	NA	125	NA	2520	NA	NA	CM	37
Circadian_Dark9_Control_2700min_vs_NRC-1g.sig	NA	NA	NA	NA	NA	NA	NA	NA	NA	0	0	NA	NA	0.37	NA	NA	NA	125	NA	2700	NA	NA	CM	37
Circadian_Dark9_Control_2880min_vs_NRC-1g.sig	NA	NA	NA	NA	NA	NA	NA	NA	NA	0	0	NA	NA	0.32	NA	NA	NA	125	NA	2880	NA	NA	CM	37
Circadian_Dark9_Control_3060min_vs_NRC-1g.sig	NA	NA	NA	NA	NA	NA	NA	NA	NA	0	0	NA	NA	0.29	NA	NA	NA	125	NA	3060	NA	NA	CM	37
Circadian_Dark9_Control_3240min_vs_NRC-1g.sig	NA	NA	NA	NA	NA	NA	NA	NA	NA	0	0	NA	NA	0.31	NA	NA	NA	125	NA	3240	NA	NA	CM	37
Circadian_Dark9_Control_3420min_vs_NRC-1g.sig	NA	NA	NA	NA	NA	NA	NA	NA	NA	0	0	NA	NA	0.29	NA	NA	NA	125	NA	3420	NA	NA	CM	37
Circadian_Dark9_Control_3600min_vs_NRC-1g.sig	NA	NA	NA	NA	NA	NA	NA	NA	NA	0	0	NA	NA	0.28	NA	NA	NA	125	NA	3600	NA	NA	CM	37
Circadian_Dark9_Control_3780min_vs_NRC-1g.sig	NA	NA	NA	NA	NA	NA	NA	NA	NA	0	0	NA	NA	0.27	NA	NA	NA	125	NA	3780	NA	NA	CM	37
Circadian_Dark9_Control_3960min_vs_NRC-1g.sig	NA	NA	NA	NA	NA	NA	NA	NA	NA	0	0	NA	NA	0.25	NA	NA	NA	125	NA	3960	NA	NA	CM	37
Circadian_Dark9_Control_4140min_vs_NRC-1g.sig	NA	NA	NA	NA	NA	NA	NA	NA	NA	0	0	NA	NA	0.29	NA	NA	NA	125	NA	4140	NA	NA	CM	37
Circadian_Dark9_Control_4320min_vs_NRC-1g.sig	NA	NA	NA	NA	NA	NA	NA	NA	NA	0	0	NA	NA	0.26	NA	NA	NA	125	NA	4320	NA	NA	CM	37
Circadian_Dark9_Control_4500min_vs_NRC-1g.sig	NA	NA	NA	NA	NA	NA	NA	NA	NA	0	0	NA	NA	0.29	NA	NA	NA	125	NA	4500	NA	NA	CM	37
Circadian_Dark10_Cycling_-2873min_vs_NRC-1h1.sig	NA	NA	NA	NA	NA	NA	NA	NA	NA	0	0	NA	NA	0.58	NA	NA	NA	125	NA	-2873	NA	NA	CM	37

Circadian_Dark10_Cycling_-2670min_vs_NRC-1h1.sig	NA	NA	NA	NA	NA	NA	NA	NA	NA	0	0	NA	NA	0.59	NA	NA	NA	125	NA	-2670	NA	NA	CM	37
Circadian_Dark10_Cycling_-2490min_vs_NRC-1h1.sig	NA	NA	NA	NA	NA	NA	NA	NA	NA	0	0	NA	NA	0.62	NA	NA	NA	125	NA	-2490	NA	NA	CM	37
Circadian_Dark10_Cycling_-2315min_vs_NRC-1h1.sig	NA	NA	NA	NA	NA	NA	NA	NA	NA	0	0	NA	NA	0.57	NA	NA	NA	125	NA	-2315	NA	NA	CM	37
Circadian_Dark10_Cycling_-2120min_vs_NRC-1h1.sig	NA	NA	NA	NA	NA	NA	NA	NA	NA	150	150	NA	NA	0.53	NA	NA	NA	125	NA	-2120	NA	NA	CM	37
Circadian_Dark10_Cycling_-1960min_vs_NRC-1h1.sig	NA	NA	NA	NA	NA	NA	NA	NA	NA	150	150	NA	NA	0.55	NA	NA	NA	125	NA	-1960	NA	NA	CM	37
Circadian_Dark10_Cycling_-1785min_vs_NRC-1h1.sig	NA	NA	NA	NA	NA	NA	NA	NA	NA	150	150	NA	NA	0.54	NA	NA	NA	125	NA	-1785	NA	NA	CM	37
Circadian_Dark10_Cycling_-1595min_vs_NRC-1h1.sig	NA	NA	NA	NA	NA	NA	NA	NA	NA	150	150	NA	NA	0.6	NA	NA	NA	125	NA	-1595	NA	NA	CM	37
Circadian_Dark10_Cycling_-1410min_vs_NRC-1h1.sig	NA	NA	NA	NA	NA	NA	NA	NA	NA	0	0	NA	NA	0.61	NA	NA	NA	125	NA	-1410	NA	NA	CM	37
Circadian_Dark10_Cycling_-1245min_vs_NRC-1h1.sig	NA	NA	NA	NA	NA	NA	NA	NA	NA	0	0	NA	NA	0.64	NA	NA	NA	125	NA	-1245	NA	NA	CM	37
Circadian_Dark10_Cycling_-1060min_vs_NRC-1h1.sig	NA	NA	NA	NA	NA	NA	NA	NA	NA	0	0	NA	NA	0.58	NA	NA	NA	125	NA	-1060	NA	NA	CM	37
Circadian_Dark10_Cycling_-0880min_vs_NRC-1h1.sig	NA	NA	NA	NA	NA	NA	NA	NA	NA	0	0	NA	NA	0.8	NA	NA	NA	125	NA	-880	NA	NA	CM	37
Circadian_Dark10_Cycling_-0690min_vs_NRC-1h1.sig	NA	NA	NA	NA	NA	NA	NA	NA	NA	150	150	NA	NA	0.65	NA	NA	NA	125	NA	-690	NA	NA	CM	37

Circadian_Dark10_Cycling_-0525min_vs_NRC-1h1.sig	NA	NA	NA	NA	NA	NA	NA	NA	NA	150	150	NA	NA	0.67	NA	NA	NA	125	NA	-525	NA	NA	CM	37
Circadian_Dark10_Cycling_-0360min_vs_NRC-1h1.sig	NA	NA	NA	NA	NA	NA	NA	NA	NA	150	150	NA	NA	0.58	NA	NA	NA	125	NA	-360	NA	NA	CM	37
Circadian_Dark10_Cycling_-0165min_vs_NRC-1h1.sig	NA	NA	NA	NA	NA	NA	NA	NA	NA	150	150	NA	NA	0.76	NA	NA	NA	125	NA	-165	NA	NA	CM	37
Circadian_Dark10_Cycling_0000min_vs_NRC-1h1.sig	NA	NA	NA	NA	NA	NA	NA	NA	NA	0	0	NA	NA	0.65	NA	NA	NA	125	NA	0	NA	NA	CM	37
Circadian_Dark10_Cycling_0195min_vs_NRC-1h1.sig	NA	NA	NA	NA	NA	NA	NA	NA	NA	0	0	NA	NA	0.58	NA	NA	NA	125	NA	195	NA	NA	CM	37
Circadian_Dark10_Cycling_0370min_vs_NRC-1h1.sig	NA	NA	NA	NA	NA	NA	NA	NA	NA	0	0	NA	NA	0.63	NA	NA	NA	125	NA	370	NA	NA	CM	37
Circadian_Dark10_Cycling_0560min_vs_NRC-1h1.sig	NA	NA	NA	NA	NA	NA	NA	NA	NA	0	0	NA	NA	0.55	NA	NA	NA	125	NA	560	NA	NA	CM	37
Circadian_Dark10_Cycling_0750min_vs_NRC-1h1.sig	NA	NA	NA	NA	NA	NA	NA	NA	NA	0	150	NA	NA	0.67	NA	NA	NA	125	NA	750	NA	NA	CM	37
Circadian_Dark10_Cycling_0915min_vs_NRC-1h1.sig	NA	NA	NA	NA	NA	NA	NA	NA	NA	0	150	NA	NA	0.63	NA	NA	NA	125	NA	915	NA	NA	CM	37
Circadian_Dark10_Cycling_1100min_vs_NRC-1h1.sig	NA	NA	NA	NA	NA	NA	NA	NA	NA	0	150	NA	NA	0.68	NA	NA	NA	125	NA	1100	NA	NA	CM	37
Circadian_Dark10_Cycling_1270min_vs_NRC-1h1.sig	NA	NA	NA	NA	NA	NA	NA	NA	NA	0	150	NA	NA	0.65	NA	NA	NA	125	NA	1270	NA	NA	CM	37
Circadian_Dark10_Cycling_1450min_vs_NRC-1h1.sig	NA	NA	NA	NA	NA	NA	NA	NA	NA	0	0	NA	NA	0.66	NA	NA	NA	125	NA	1450	NA	NA	CM	37
Circadian_Dark10_Cycling_1635min_vs_NRC-1h1.sig	NA	NA	NA	NA	NA	NA	NA	NA	NA	0	0	NA	NA	0.66	NA	NA	NA	125	NA	1635	NA	NA	CM	37
Circadian_Dark10_Cycling_1810min_vs_NRC-1h1.sig	NA	NA	NA	NA	NA	NA	NA	NA	NA	0	0	NA	NA	0.66	NA	NA	NA	125	NA	1810	NA	NA	CM	37
Circadian_Dark10_Cycling_1980min_vs_NRC-1h1.sig	NA	NA	NA	NA	NA	NA	NA	NA	NA	0	0	NA	NA	0.64	NA	NA	NA	125	NA	1980	NA	NA	CM	37

Circadian_Dark10_Cycling_2200min_vs_NRC-1h1.sig	NA	NA	NA	NA	NA	NA	NA	NA	NA	0	150	NA	NA	0.64	NA	NA	NA	125	NA	2200	NA	NA	CM	37
Circadian_Dark10_Cycling_2345min_vs_NRC-1h1.sig	NA	NA	NA	NA	NA	NA	NA	NA	NA	0	150	NA	NA	0.7	NA	NA	NA	125	NA	2345	NA	NA	CM	37
Circadian_Dark10_Cycling_2535min_vs_NRC-1h1.sig	NA	NA	NA	NA	NA	NA	NA	NA	NA	0	150	NA	NA	0.65	NA	NA	NA	125	NA	2535	NA	NA	CM	37
Circadian_Dark10_Cycling_2711min_vs_NRC-1h1.sig	NA	NA	NA	NA	NA	NA	NA	NA	NA	0	150	NA	NA	0.68	NA	NA	NA	125	NA	2711	NA	NA	CM	37
Circadian_Dark10_Cycling_2895min_vs_NRC-1h1.sig	NA	NA	NA	NA	NA	NA	NA	NA	NA	0	0	NA	NA	0.65	NA	NA	NA	125	NA	2895	NA	NA	CM	37
Circadian_Dark10_Cycling_3070min_vs_NRC-1h1.sig	NA	NA	NA	NA	NA	NA	NA	NA	NA	0	0	NA	NA	0.61	NA	NA	NA	125	NA	3070	NA	NA	CM	37
Circadian_Dark10_Cycling_3252min_vs_NRC-1h1.sig	NA	NA	NA	NA	NA	NA	NA	NA	NA	0	0	NA	NA	0.64	NA	NA	NA	125	NA	3252	NA	NA	CM	37
Circadian_Dark10_Cycling_3430min_vs_NRC-1h1.sig	NA	NA	NA	NA	NA	NA	NA	NA	NA	0	0	NA	NA	0.68	NA	NA	NA	125	NA	3430	NA	NA	CM	37
Circadian_Dark10_Cycling_3630min_vs_NRC-1h1.sig	NA	NA	NA	NA	NA	NA	NA	NA	NA	0	150	NA	NA	0.67	NA	NA	NA	125	NA	3630	NA	NA	CM	37
Circadian_Dark10_Cycling_3790min_vs_NRC-1h1.sig	NA	NA	NA	NA	NA	NA	NA	NA	NA	0	150	NA	NA	0.65	NA	NA	NA	125	NA	3790	NA	NA	CM	37
Circadian_Dark10_Cycling_3980min_vs_NRC-1h1.sig	NA	NA	NA	NA	NA	NA	NA	NA	NA	0	150	NA	NA	0.68	NA	NA	NA	125	NA	3980	NA	NA	CM	37
Circadian_Dark10_Cycling_4150min_vs_NRC-1h1.sig	NA	NA	NA	NA	NA	NA	NA	NA	NA	0	150	NA	NA	0.64	NA	NA	NA	125	NA	4150	NA	NA	CM	37
Circadian_Dark10_Cycling_4330min_vs_NRC-1h1.sig	NA	NA	NA	NA	NA	NA	NA	NA	NA	0	0	NA	NA	0.66	NA	NA	NA	125	NA	4330	NA	NA	CM	37
Zn_0.000_vs_NRC-1d.sig	NA	NA	NA	NA	NA	NA	NA	NA	NA	NA	NA	NA	NA	NA	NA	NA	NA	225	NA	NA	NA	0	CM	37
Zn_0.005_vs_NRC-1d.sig	NA	NA	NA	NA	NA	NA	NA	NA	NA	NA	NA	NA	NA	NA	NA	NA	NA	225	NA	NA	NA	0	CM	37
Zn_0.010_vs_NRC-1d.sig	NA	NA	NA	NA	NA	NA	NA	NA	NA	NA	NA	NA	NA	NA	NA	NA	NA	225	NA	NA	NA	0	CM	37
Zn_0.015_vs_NRC-1d.sig	NA	NA	NA	NA	NA	NA	NA	NA	NA	NA	NA	NA	NA	NA	NA	NA	NA	225	NA	NA	NA	0	CM	37
zn__0005um_vs_NRC-1	NA	NA	NA	NA	NA	NA	NA	NA	NA	35	NA	NA	NA	NA	NA	NA	NA	225	NA	NA	NA	0	CM	37

zn__0010um_vs_NRC-1	NA	NA	NA	NA	NA	NA	NA	NA	NA	35	NA	NA	NA	NA	NA	NA	NA	225	NA	NA	NA	0	CM	37
zn__0020um_vs_NRC-1	NA	NA	NA	NA	NA	NA	NA	NA	NA	35	NA	NA	NA	NA	NA	NA	NA	225	NA	NA	NA	0	CM	37
cu__0700um_vs_NRC-1	NA	NA	0	NA	NA	NA	NA	NA	NA	35	NA	NA	NA	NA	NA	NA	NA	225	NA	NA	NA	NA	CM	37
cu__0850um_vs_NRC-1	NA	NA	0	NA	NA	NA	NA	NA	NA	35	NA	NA	NA	NA	NA	NA	NA	225	NA	NA	NA	NA	CM	37
cu__1000um_vs_NRC-1	NA	NA	0	NA	NA	NA	NA	NA	NA	35	NA	NA	NA	NA	NA	NA	NA	225	NA	NA	NA	NA	CM	37
Cu_-5_vs_NRC-1.sig	NA	NA	0	NA	NA	NA	NA	NA	NA	NA	NA	NA	NA	0.59	NA	NA	NA	NA	NA	-5	NA	NA	CM	37
Cu_000_vs_NRC-1.sig	NA	NA	0	NA	NA	NA	NA	NA	NA	NA	NA	NA	NA	0.56	NA	NA	NA	NA	NA	0	NA	NA	CM	37
Cu_005_vs_NRC-1.sig	NA	NA	0	NA	NA	NA	NA	NA	NA	NA	NA	NA	NA	0.58	NA	NA	NA	NA	NA	5	NA	NA	CM	37
Cu_010_vs_NRC-1.sig	NA	NA	0	NA	NA	NA	NA	NA	NA	NA	NA	NA	NA	0.57	NA	NA	NA	NA	NA	10	NA	NA	CM	37
Cu_020_vs_NRC-1.sig	NA	NA	0	NA	NA	NA	NA	NA	NA	NA	NA	NA	NA	0.56	NA	NA	NA	NA	NA	20	NA	NA	CM	37
Cu_040_vs_NRC-1.sig	NA	NA	0	NA	NA	NA	NA	NA	NA	NA	NA	NA	NA	0.61	NA	NA	NA	NA	NA	40	NA	NA	CM	37
Cu_080_vs_NRC-1.sig	NA	NA	0	NA	NA	NA	NA	NA	NA	NA	NA	NA	NA	0.65	NA	NA	NA	NA	NA	80	NA	NA	CM	37
Cu_160_vs_NRC-1.sig	NA	NA	0	NA	NA	NA	NA	NA	NA	NA	NA	NA	NA	0.55	NA	NA	NA	NA	NA	160	NA	NA	CM	37
Cu_-1_vs_NRC-1e.sig	NA	NA	0	NA	NA	NA	NA	NA	NA	NA	NA	NA	NA	0.59	NA	NA	NA	NA	NA	-1	NA	NA	CM	37
Cu_000_vs_NRC-1e.sig	NA	NA	0	NA	NA	NA	NA	NA	NA	NA	NA	NA	NA	0.56	NA	NA	NA	NA	NA	0	NA	NA	CM	37
Cu_005_vs_NRC-1e.sig	NA	NA	0	NA	NA	NA	NA	NA	NA	NA	NA	NA	NA	0.58	NA	NA	NA	NA	NA	5	NA	NA	CM	37
Cu_010_vs_NRC-1e.sig	NA	NA	0	NA	NA	NA	NA	NA	NA	NA	NA	NA	NA	0.57	NA	NA	NA	NA	NA	10	NA	NA	CM	37
Cu_020_vs_NRC-1e.sig	NA	NA	0	NA	NA	NA	NA	NA	NA	NA	NA	NA	NA	0.56	NA	NA	NA	NA	NA	20	NA	NA	CM	37
Cu_040_vs_NRC-1e.sig	NA	NA	0	NA	NA	NA	NA	NA	NA	NA	NA	NA	NA	0.61	NA	NA	NA	NA	NA	40	NA	NA	CM	37
Cu_080_vs_NRC-1e.sig	NA	NA	0	NA	NA	NA	NA	NA	NA	NA	NA	NA	NA	0.65	NA	NA	NA	NA	NA	80	NA	NA	CM	37
Cu_160_vs_NRC-1e.sig	NA	NA	0	NA	NA	NA	NA	NA	NA	NA	NA	NA	NA	0.55	NA	NA	NA	NA	NA	160	NA	NA	CM	37
Cu_320_vs_NRC-1e.sig	NA	NA	0	NA	NA	NA	NA	NA	NA	NA	NA	NA	NA	0.61	NA	NA	NA	NA	NA	320	NA	NA	CM	37
ZnSO4_ts_set-1_-005min_vs_NRC-1h1.sig	NA	NA	NA	NA	NA	NA	NA	NA	NA	NA	NA	NA	NA	0.65	NA	NA	NA	NA	NA	-5	NA	0	CM	37

ZnSO4_ts_set-1_000min_vs_NRC-1h1.sig	NA	NA	NA	NA	NA	NA	NA	NA	NA	NA	NA	NA	NA	0.65	NA	NA	NA	NA	NA	0	NA	0	CM	37
ZnSO4_ts_set-1_005min_vs_NRC-1h1.sig	NA	NA	NA	NA	NA	NA	NA	NA	NA	NA	NA	NA	NA	0.64	NA	NA	NA	NA	NA	5	NA	0	CM	37
ZnSO4_ts_set-1_010min_vs_NRC-1h1.sig	NA	NA	NA	NA	NA	NA	NA	NA	NA	NA	NA	NA	NA	0.63	NA	NA	NA	NA	NA	10	NA	0	CM	37
ZnSO4_ts_set-1_020min_vs_NRC-1h1.sig	NA	NA	NA	NA	NA	NA	NA	NA	NA	NA	NA	NA	NA	0.62	NA	NA	NA	NA	NA	20	NA	0	CM	37
ZnSO4_ts_set-1_040min_vs_NRC-1h1.sig	NA	NA	NA	NA	NA	NA	NA	NA	NA	NA	NA	NA	NA	0.64	NA	NA	NA	NA	NA	40	NA	0	CM	37
ZnSO4_ts_set-1_080min_vs_NRC-1h1.sig	NA	NA	NA	NA	NA	NA	NA	NA	NA	NA	NA	NA	NA	0.68	NA	NA	NA	NA	NA	80	NA	0	CM	37
ZnSO4_ts_set-1_160min_vs_NRC-1h1.sig	NA	NA	NA	NA	NA	NA	NA	NA	NA	NA	NA	NA	NA	0.66	NA	NA	NA	NA	NA	160	NA	0	CM	37
ZnSO4_set2_-005min_vs_NRC-1h1.sig	NA	NA	NA	NA	NA	NA	NA	NA	NA	NA	NA	NA	NA	0.67	NA	NA	NA	NA	NA	-5	NA	0	CM	37
ZnSO4_set2_000min_vs_NRC-1h1.sig	NA	NA	NA	NA	NA	NA	NA	NA	NA	NA	NA	NA	NA	0.67	NA	NA	NA	NA	NA	0	NA	0	CM	37
ZnSO4_set2_005min_vs_NRC-1h1.sig	NA	NA	NA	NA	NA	NA	NA	NA	NA	NA	NA	NA	NA	0.67	NA	NA	NA	NA	NA	5	NA	0	CM	37
ZnSO4_set2_010min_vs_NRC-1h1.sig	NA	NA	NA	NA	NA	NA	NA	NA	NA	NA	NA	NA	NA	0.7	NA	NA	NA	NA	NA	10	NA	0	CM	37
ZnSO4_set2_015min_vs_NRC-1h1.sig	NA	NA	NA	NA	NA	NA	NA	NA	NA	NA	NA	NA	NA	0.64	NA	NA	NA	NA	NA	15	NA	0	CM	37
ZnSO4_set2_020min_vs_NRC-1h1.sig	NA	NA	NA	NA	NA	NA	NA	NA	NA	NA	NA	NA	NA	0.66	NA	NA	NA	NA	NA	20	NA	0	CM	37
ZnSO4_set2_025min_vs_NRC-1h1.sig	NA	NA	NA	NA	NA	NA	NA	NA	NA	NA	NA	NA	NA	0.71	NA	NA	NA	NA	NA	25	NA	0	CM	37
ZnSO4_set2_030min_vs_NRC-1h1.sig	NA	NA	NA	NA	NA	NA	NA	NA	NA	NA	NA	NA	NA	0.67	NA	NA	NA	NA	NA	30	NA	0	CM	37
ZnSO4_set2_040min_vs_NRC-1h1.sig	NA	NA	NA	NA	NA	NA	NA	NA	NA	NA	NA	NA	NA	0.65	NA	NA	NA	NA	NA	40	NA	0	CM	37
ZnSO4_set2_060min_vs_NRC-1h1.sig	NA	NA	NA	NA	NA	NA	NA	NA	NA	NA	NA	NA	NA	0.63	NA	NA	NA	NA	NA	60	NA	0	CM	37
ZnSO4_set2_080min_vs_NRC-1h1.sig	NA	NA	NA	NA	NA	NA	NA	NA	NA	NA	NA	NA	NA	0.63	NA	NA	NA	NA	NA	80	NA	0	CM	37

ZnSO4_set2_120min_vs_NRC-1h1.sig	NA	NA	NA	NA	NA	NA	NA	NA	NA	NA	NA	NA	NA	0.61	NA	NA	NA	NA	NA	120	NA	0	CM	37
ZnSO4_set2_160min_vs_NRC-1h1.sig	NA	NA	NA	NA	NA	NA	NA	NA	NA	NA	NA	NA	NA	0.63	NA	NA	NA	NA	NA	160	NA	0	CM	37
ZnSO4_set2_320min_vs_NRC-1h1.sig	NA	NA	NA	NA	NA	NA	NA	NA	NA	NA	NA	NA	NA	0.69	NA	NA	NA	NA	NA	320	NA	0	CM	37
Cu_NRC1_set1_-030min_vs_NRC-1h1.sig	NA	NA	0	NA	NA	NA	NA	NA	NA	7	NA	NA	NA	0.61	NA	NA	NA	225	NA	-30	NA	NA	CM	37
Cu_NRC1_set1_000min_vs_NRC-1h1.sig	NA	NA	0	NA	NA	NA	NA	NA	NA	7	NA	NA	NA	0.61	NA	NA	NA	225	NA	0	NA	NA	CM	37
Cu_NRC1_set1_005min_vs_NRC-1h1.sig	NA	NA	0	NA	NA	NA	NA	NA	NA	7	NA	NA	NA	0.61	NA	NA	NA	225	NA	5	NA	NA	CM	37
Cu_NRC1_set1_010min_vs_NRC-1h1.sig	NA	NA	0	NA	NA	NA	NA	NA	NA	7	NA	NA	NA	0.61	NA	NA	NA	225	NA	10	NA	NA	CM	37
Cu_NRC1_set1_020min_vs_NRC-1h1.sig	NA	NA	0	NA	NA	NA	NA	NA	NA	7	NA	NA	NA	0.61	NA	NA	NA	225	NA	20	NA	NA	CM	37
Cu_NRC1_set1_040min_vs_NRC-1h1.sig	NA	NA	0	NA	NA	NA	NA	NA	NA	7	NA	NA	NA	0.61	NA	NA	NA	225	NA	40	NA	NA	CM	37
Cu_NRC1_set1_080min_vs_NRC-1h1.sig	NA	NA	0	NA	NA	NA	NA	NA	NA	7	NA	NA	NA	0.61	NA	NA	NA	225	NA	80	NA	NA	CM	37
Cu_NRC1_set1_160min_vs_NRC-1h1.sig	NA	NA	0	NA	NA	NA	NA	NA	NA	7	NA	NA	NA	0.6	NA	NA	NA	225	NA	160	NA	NA	CM	37
Cu_ura3_KO_set1_-030min_vs_NRC-1h1.sig	NA	NA	0	NA	NA	NA	NA	NA	NA	7	NA	NA	NA	0.57	NA	NA	NA	225	NA	-30	NA	NA	CM	37
Cu_ura3_KO_set1_000min_vs_NRC-1h1.sig	NA	NA	0	NA	NA	NA	NA	NA	NA	7	NA	NA	NA	0.57	NA	NA	NA	225	NA	0	NA	NA	CM	37
Cu_ura3_KO_set1_005min_vs_NRC-1h1.sig	NA	NA	0	NA	NA	NA	NA	NA	NA	7	NA	NA	NA	0.57	NA	NA	NA	225	NA	5	NA	NA	CM	37
Cu_ura3_KO_set1_010min_vs_NRC-1h1.sig	NA	NA	0	NA	NA	NA	NA	NA	NA	7	NA	NA	NA	0.57	NA	NA	NA	225	NA	10	NA	NA	CM	37
Cu_ura3_KO_set1_020min_vs_NRC-1h1.sig	NA	NA	0	NA	NA	NA	NA	NA	NA	7	NA	NA	NA	0.57	NA	NA	NA	225	NA	20	NA	NA	CM	37
Cu_ura3_KO_set1_040min_vs_NRC-1h1.sig	NA	NA	0	NA	NA	NA	NA	NA	NA	7	NA	NA	NA	0.57	NA	NA	NA	225	NA	40	NA	NA	CM	37

Cu_ura3_KO_set1_080min_vs_NRC-1h1.sig	NA	NA	0	NA	NA	NA	NA	NA	NA	7	NA	NA	NA	0.57	NA	NA	NA	225	NA	80	NA	NA	CM	37
Cu_ura3_KO_set1_160min_vs_NRC-1h1.sig	NA	NA	0	NA	NA	NA	NA	NA	NA	7	NA	NA	NA	0.46	NA	NA	NA	225	NA	160	NA	NA	CM	37
Cu_vng1179_KO_set1_-030min_vs_NRC-1h1.sig	NA	NA	0	NA	NA	NA	NA	NA	NA	NA	NA	NA	NA	0.38	NA	NA	NA	225	NA	-30	NA	NA	CM	37
Cu_vng1179_KO_set1_000min_vs_NRC-1h1.sig	NA	NA	0	NA	NA	NA	NA	NA	NA	NA	NA	NA	NA	0.38	NA	NA	NA	225	NA	0	NA	NA	CM	37
Cu_vng1179_KO_set1_005min_vs_NRC-1h1.sig	NA	NA	0	NA	NA	NA	NA	NA	NA	NA	NA	NA	NA	0.38	NA	NA	NA	225	NA	5	NA	NA	CM	37
Cu_vng1179_KO_set1_010min_vs_NRC-1h1.sig	NA	NA	0	NA	NA	NA	NA	NA	NA	NA	NA	NA	NA	0.38	NA	NA	NA	225	NA	10	NA	NA	CM	37
Cu_vng1179_KO_set1_020min_vs_NRC-1h1.sig	NA	NA	0	NA	NA	NA	NA	NA	NA	NA	NA	NA	NA	0.38	NA	NA	NA	225	NA	20	NA	NA	CM	37
Cu_vng1179_KO_set1_040min_vs_NRC-1h1.sig	NA	NA	0	NA	NA	NA	NA	NA	NA	NA	NA	NA	NA	0.38	NA	NA	NA	225	NA	40	NA	NA	CM	37
Cu_vng1179_KO_set1_080min_vs_NRC-1h1.sig	NA	NA	0	NA	NA	NA	NA	NA	NA	NA	NA	NA	NA	0.38	NA	NA	NA	225	NA	80	NA	NA	CM	37
Cu_vng1179_KO_set1_160min_vs_NRC-1h1.sig	NA	NA	0	NA	NA	NA	NA	NA	NA	NA	NA	NA	NA	0.38	NA	NA	NA	225	NA	160	NA	NA	CM	37
Cu_vng700_KO_set1_-030min_vs_NRC-1h1.sig	NA	NA	0	NA	NA	NA	NA	NA	NA	NA	NA	NA	NA	NA	NA	NA	NA	225	NA	-30	NA	NA	CM	37
Cu_vng700_KO_set1_000min_vs_NRC-1h1.sig	NA	NA	0	NA	NA	NA	NA	NA	NA	NA	NA	NA	NA	NA	NA	NA	NA	225	NA	0	NA	NA	CM	37
Cu_vng700_KO_set1_005min_vs_NRC-1h1.sig	NA	NA	0	NA	NA	NA	NA	NA	NA	NA	NA	NA	NA	NA	NA	NA	NA	225	NA	5	NA	NA	CM	37
Cu_vng700_KO_set1_010min_vs_NRC-1h1.sig	NA	NA	0	NA	NA	NA	NA	NA	NA	NA	NA	NA	NA	NA	NA	NA	NA	225	NA	10	NA	NA	CM	37
Cu_vng700_KO_set1_020min_vs_NRC-1h1.sig	NA	NA	0	NA	NA	NA	NA	NA	NA	NA	NA	NA	NA	NA	NA	NA	NA	225	NA	20	NA	NA	CM	37
Cu_vng700_KO_set1_040min_vs_NR	NA	NA	0	NA	NA	NA	NA	NA	NA	NA	NA	NA	NA	NA	NA	NA	NA	225	NA	40	NA	NA	CM	37

C-1h1.sig																								
Cu_vng700_KO_set1_080min_vs_NRC-1h1.sig	NA	NA	0	NA	NA	NA	NA	NA	NA	NA	NA	NA	NA	NA	NA	NA	NA	225	NA	80	NA	NA	CM	37
Cu_vng700_KO_set1_160min_vs_NRC-1h1.sig	NA	NA	0	NA	NA	NA	NA	NA	NA	NA	NA	NA	NA	NA	NA	NA	NA	225	NA	160	NA	NA	CM	37
Cu_vng149_KO_set1_-030min_vs_NRC-1h1.sig	NA	NA	0	NA	NA	NA	NA	NA	NA	NA	NA	NA	NA	NA	NA	NA	NA	225	NA	-30	NA	NA	CM	37
Cu_vng149_KO_set1_000min_vs_NRC-1h1.sig	NA	NA	0	NA	NA	NA	NA	NA	NA	NA	NA	NA	NA	NA	NA	NA	NA	225	NA	0	NA	NA	CM	37
Cu_vng149_KO_set1_005min_vs_NRC-1h1.sig	NA	NA	0	NA	NA	NA	NA	NA	NA	NA	NA	NA	NA	NA	NA	NA	NA	225	NA	5	NA	NA	CM	37
Cu_vng149_KO_set1_010min_vs_NRC-1h1.sig	NA	NA	0	NA	NA	NA	NA	NA	NA	NA	NA	NA	NA	NA	NA	NA	NA	225	NA	10	NA	NA	CM	37
Cu_vng149_KO_set1_020min_vs_NRC-1h1.sig	NA	NA	0	NA	NA	NA	NA	NA	NA	NA	NA	NA	NA	NA	NA	NA	NA	225	NA	20	NA	NA	CM	37
Cu_vng149_KO_set1_040min_vs_NRC-1h1.sig	NA	NA	0	NA	NA	NA	NA	NA	NA	NA	NA	NA	NA	NA	NA	NA	NA	225	NA	40	NA	NA	CM	37
Cu_vng149_KO_set1_080min_vs_NRC-1h1.sig	NA	NA	0	NA	NA	NA	NA	NA	NA	NA	NA	NA	NA	NA	NA	NA	NA	225	NA	80	NA	NA	CM	37
Cu_vng149_KO_set1_160min_vs_NRC-1h1.sig	NA	NA	0	NA	NA	NA	NA	NA	NA	NA	NA	NA	NA	NA	NA	NA	NA	225	NA	160	NA	NA	CM	37
Cu_ura3_KO_set2_-030min_vs_NRC-1h1.sig	NA	NA	0	NA	NA	NA	NA	NA	NA	NA	NA	NA	NA	0.46	NA	NA	NA	225	NA	-30	NA	NA	CM	37
Cu_ura3_KO_set2_000min_vs_NRC-1h1.sig	NA	NA	0	NA	NA	NA	NA	NA	NA	NA	NA	NA	NA	0.46	NA	NA	NA	225	NA	0	NA	NA	CM	37
Cu_ura3_KO_set2_005min_vs_NRC-1h1.sig	NA	NA	0	NA	NA	NA	NA	NA	NA	NA	NA	NA	NA	0.46	NA	NA	NA	225	NA	5	NA	NA	CM	37
Cu_ura3_KO_set2_010min_vs_NRC-1h1.sig	NA	NA	0	NA	NA	NA	NA	NA	NA	NA	NA	NA	NA	0.46	NA	NA	NA	225	NA	10	NA	NA	CM	37
Cu_ura3_KO_set2_020min_vs_NRC-1h1.sig	NA	NA	0	NA	NA	NA	NA	NA	NA	NA	NA	NA	NA	0.46	NA	NA	NA	225	NA	20	NA	NA	CM	37

Cu_ura3_KO_set2_040min_vs_NRC-1h1.sig	NA	NA	0	NA	NA	NA	NA	NA	NA	NA	NA	NA	NA	0.46	NA	NA	NA	225	NA	40	NA	NA	CM	37
Cu_ura3_KO_set2_080min_vs_NRC-1h1.sig	NA	NA	0	NA	NA	NA	NA	NA	NA	NA	NA	NA	NA	0.46	NA	NA	NA	225	NA	80	NA	NA	CM	37
Cu_ura3_KO_set2_160min_vs_NRC-1h1.sig	NA	NA	0	NA	NA	NA	NA	NA	NA	NA	NA	NA	NA	0.38	NA	NA	NA	225	NA	160	NA	NA	CM	37
Cu_vng700_KO_set2_-030min_vs_NRC-1h1.sig	NA	NA	0	NA	NA	NA	NA	NA	NA	NA	NA	NA	NA	NA	NA	NA	NA	225	NA	-30	NA	NA	CM	37
Cu_vng700_KO_set2_000min_vs_NRC-1h1.sig	NA	NA	0	NA	NA	NA	NA	NA	NA	NA	NA	NA	NA	NA	NA	NA	NA	225	NA	0	NA	NA	CM	37
Cu_vng700_KO_set2_005min_vs_NRC-1h1.sig	NA	NA	0	NA	NA	NA	NA	NA	NA	NA	NA	NA	NA	NA	NA	NA	NA	225	NA	5	NA	NA	CM	37
Cu_vng700_KO_set2_010min_vs_NRC-1h1.sig	NA	NA	0	NA	NA	NA	NA	NA	NA	NA	NA	NA	NA	NA	NA	NA	NA	225	NA	10	NA	NA	CM	37
Cu_vng700_KO_set2_020min_vs_NRC-1h1.sig	NA	NA	0	NA	NA	NA	NA	NA	NA	NA	NA	NA	NA	NA	NA	NA	NA	225	NA	20	NA	NA	CM	37
Cu_vng700_KO_set2_040min_vs_NRC-1h1.sig	NA	NA	0	NA	NA	NA	NA	NA	NA	NA	NA	NA	NA	NA	NA	NA	NA	225	NA	40	NA	NA	CM	37
Cu_vng700_KO_set2_080min_vs_NRC-1h1.sig	NA	NA	0	NA	NA	NA	NA	NA	NA	NA	NA	NA	NA	NA	NA	NA	NA	225	NA	80	NA	NA	CM	37
Cu_vng700_KO_set2_160min_vs_NRC-1h1.sig	NA	NA	0	NA	NA	NA	NA	NA	NA	NA	NA	NA	NA	NA	NA	NA	NA	225	NA	160	NA	NA	CM	37
Cu_vng149_KO_set2_-030min_vs_NRC-1h1.sig	NA	NA	0	NA	NA	NA	NA	NA	NA	NA	NA	NA	NA	NA	NA	NA	NA	225	NA	-30	NA	NA	CM	37
Cu_vng149_KO_set2_000min_vs_NRC-1h1.sig	NA	NA	0	NA	NA	NA	NA	NA	NA	NA	NA	NA	NA	NA	NA	NA	NA	225	NA	0	NA	NA	CM	37
Cu_vng149_KO_set2_005min_vs_NRC-1h1.sig	NA	NA	0	NA	NA	NA	NA	NA	NA	NA	NA	NA	NA	NA	NA	NA	NA	225	NA	5	NA	NA	CM	37
Cu_vng149_KO_set2_010min_vs_NRC-1h1.sig	NA	NA	0	NA	NA	NA	NA	NA	NA	NA	NA	NA	NA	NA	NA	NA	NA	225	NA	10	NA	NA	CM	37
Cu_vng149_KO_set2_020min_vs_NR	NA	NA	0	NA	NA	NA	NA	NA	NA	NA	NA	NA	NA	NA	NA	NA	NA	225	NA	20	NA	NA	CM	37

C-1h1.sig																								
Cu_vng149_KO_set2_040min_vs_NRC-1h1.sig	NA	NA	0	NA	NA	NA	NA	NA	NA	NA	NA	NA	NA	NA	NA	NA	NA	225	NA	40	NA	NA	CM	37
Cu_vng149_KO_set2_080min_vs_NRC-1h1.sig	NA	NA	0	NA	NA	NA	NA	NA	NA	NA	NA	NA	NA	NA	NA	NA	NA	225	NA	80	NA	NA	CM	37
Cu_vng149_KO_set2_160min_vs_NRC-1h1.sig	NA	NA	0	NA	NA	NA	NA	NA	NA	NA	NA	NA	NA	NA	NA	NA	NA	225	NA	160	NA	NA	CM	37
Cu_vng1179_set2_-030min_vs_NRC-1h1.sig	NA	NA	0	NA	NA	NA	NA	NA	NA	NA	NA	NA	NA	0.38	NA	NA	NA	225	NA	-30	NA	NA	CM	37
Cu_vng1179_set2_000min_vs_NRC-1h1.sig	NA	NA	0	NA	NA	NA	NA	NA	NA	NA	NA	NA	NA	0.38	NA	NA	NA	225	NA	0	NA	NA	CM	37
Cu_vng1179_set2_005min_vs_NRC-1h1.sig	NA	NA	0	NA	NA	NA	NA	NA	NA	NA	NA	NA	NA	0.38	NA	NA	NA	225	NA	5	NA	NA	CM	37
Cu_vng1179_set2_010min_vs_NRC-1h1.sig	NA	NA	0	NA	NA	NA	NA	NA	NA	NA	NA	NA	NA	0.38	NA	NA	NA	225	NA	10	NA	NA	CM	37
Cu_vng1179_set2_020min_vs_NRC-1h1.sig	NA	NA	0	NA	NA	NA	NA	NA	NA	NA	NA	NA	NA	0.38	NA	NA	NA	225	NA	20	NA	NA	CM	37
Cu_vng1179_set2_040min_vs_NRC-1h1.sig	NA	NA	0	NA	NA	NA	NA	NA	NA	NA	NA	NA	NA	0.38	NA	NA	NA	225	NA	40	NA	NA	CM	37
Cu_vng1179_set2_080min_vs_NRC-1h1.sig	NA	NA	0	NA	NA	NA	NA	NA	NA	NA	NA	NA	NA	0.38	NA	NA	NA	225	NA	80	NA	NA	CM	37
Cu_vng1179_set2_160min_vs_NRC-1h1.sig	NA	NA	0	NA	NA	NA	NA	NA	NA	NA	NA	NA	NA	0.4	NA	NA	NA	225	NA	160	NA	NA	CM	37
Cu_NRC1_set2_-030min_vs_NRC-1h1.sig	NA	NA	0	NA	NA	NA	NA	NA	NA	NA	NA	NA	NA	0.6	NA	NA	NA	225	NA	-30	NA	NA	CM	37
Cu_NRC1_set2_000min_vs_NRC-1h1.sig	NA	NA	0	NA	NA	NA	NA	NA	NA	NA	NA	NA	NA	0.6	NA	NA	NA	225	NA	0	NA	NA	CM	37
Cu_NRC1_set2_005min_vs_NRC-1h1.sig	NA	NA	0	NA	NA	NA	NA	NA	NA	NA	NA	NA	NA	0.6	NA	NA	NA	225	NA	5	NA	NA	CM	37
Cu_NRC1_set2_010min_vs_NRC-1h1.sig	NA	NA	0	NA	NA	NA	NA	NA	NA	NA	NA	NA	NA	0.6	NA	NA	NA	225	NA	10	NA	NA	CM	37

Cu_NRC1_set2_020min_vs_NRC-1h1.sig	NA	NA	0	NA	NA	NA	NA	NA	NA	NA	NA	NA	NA	0.6	NA	NA	NA	225	NA	20	NA	NA	CM	37
Cu_NRC1_set2_040min_vs_NRC-1h1.sig	NA	NA	0	NA	NA	NA	NA	NA	NA	NA	NA	NA	NA	0.6	NA	NA	NA	225	NA	40	NA	NA	CM	37
Cu_NRC1_set2_080min_vs_NRC-1h1.sig	NA	NA	0	NA	NA	NA	NA	NA	NA	NA	NA	NA	NA	0.6	NA	NA	NA	225	NA	80	NA	NA	CM	37
Cu_NRC1_set2_160min_vs_NRC-1h1.sig	NA	NA	0	NA	NA	NA	NA	NA	NA	NA	NA	NA	NA	0.57	NA	NA	NA	225	NA	160	NA	NA	CM	37
Ni_0.5_vs_NRC-1d.sig	NA	NA	NA	NA	NA	NA	NA	NA	NA	NA	NA	NA	0	NA	NA	NA	NA	225	NA	NA	NA	NA	CM	37
Ni_0.75_vs_NRC-1d.sig	NA	NA	NA	NA	NA	NA	NA	NA	NA	NA	NA	NA	0	NA	NA	NA	NA	225	NA	NA	NA	NA	CM	37
Ni_1.5_vs_NRC-1d.sig	NA	NA	NA	NA	NA	NA	NA	NA	NA	NA	NA	NA	0	NA	NA	NA	NA	225	NA	NA	NA	NA	CM	37
Ni_0.0_vs_NRC-1d.sig	NA	NA	NA	NA	NA	NA	NA	NA	NA	NA	NA	NA	0	NA	NA	NA	NA	225	NA	NA	NA	NA	CM	37
ni__0000um_vs_NRC-1c	NA	NA	NA	NA	NA	NA	NA	NA	NA	NA	NA	NA	0	NA	NA	NA	NA	225	NA	NA	NA	NA	CM	37
ni__0500um_vs_NRC-1c	NA	NA	NA	NA	NA	NA	NA	NA	NA	NA	NA	NA	0	NA	NA	NA	NA	225	NA	NA	NA	NA	CM	37
ni__0750um_vs_NRC-1c	NA	NA	NA	NA	NA	NA	NA	NA	NA	NA	NA	NA	0	NA	NA	NA	NA	225	NA	NA	NA	NA	CM	37
ni__1500um_vs_NRC-1c	NA	NA	NA	NA	NA	NA	NA	NA	NA	NA	NA	NA	0	NA	NA	NA	NA	225	NA	NA	NA	NA	CM	37
sirR_0a_vs_NRC-1d.sig	NA	NA	NA	NA	NA	NA	NA	NA	NA	NA	NA	NA	NA	NA	NA	NA	NA	225	NA	NA	NA	NA	CM	37
sirR_0b_vs_NRC-1d.sig	NA	NA	NA	NA	NA	NA	NA	NA	NA	NA	NA	NA	NA	NA	NA	NA	NA	225	NA	NA	NA	NA	CM	37
sirR_Mn_0800um_a_vs_NRC-1d.sig	NA	NA	NA	NA	NA	NA	NA	NA	NA	NA	NA	0	NA	NA	NA	NA	NA	225	NA	NA	NA	NA	CM	37
sirR_Mn_0800um_b_vs_NRC-1d.sig	NA	NA	NA	NA	NA	NA	NA	NA	NA	NA	NA	0	NA	NA	NA	NA	NA	225	NA	NA	NA	NA	CM	37
sirR_Mn_1500um_a_vs_NRC-1d.sig	NA	NA	NA	NA	NA	NA	NA	NA	NA	NA	NA	0	NA	NA	NA	NA	NA	225	NA	NA	NA	NA	CM	37
sirR_Mn_1500um_b_vs_NRC-1d.sig	NA	NA	NA	NA	NA	NA	NA	NA	NA	NA	NA	0	NA	NA	NA	NA	NA	225	NA	NA	NA	NA	CM	37
sirR_Mn_1000um_a_vs_NRC-1d.sig	NA	NA	NA	NA	NA	NA	NA	NA	NA	NA	NA	0	NA	NA	NA	NA	NA	225	NA	NA	NA	NA	CM	37
sirR_Mn_1000um_b_vs_NRC-1d.sig	NA	NA	NA	NA	NA	NA	NA	NA	NA	NA	NA	0	NA	NA	NA	NA	NA	225	NA	NA	NA	NA	CM	37
ura3_0a_vs_NRC-1d.sig	NA	NA	NA	NA	NA	NA	NA	NA	NA	NA	NA	NA	NA	NA	NA	NA	NA	225	NA	NA	NA	NA	CM	37

ura3_0b_vs_NRC-1d.sig	NA	NA	NA	NA	NA	NA	NA	NA	NA	NA	NA	NA	NA	NA	NA	NA	NA	225	NA	NA	NA	NA	CM	37
ura3_Cu_0700um_a_vs_NRC-1d.sig	NA	NA	0	NA	NA	NA	NA	NA	NA	NA	NA	NA	NA	NA	NA	NA	NA	225	NA	NA	NA	NA	CM	37
ura3_Cu_0700um_b_vs_NRC-1d.sig	NA	NA	0	NA	NA	NA	NA	NA	NA	NA	NA	NA	NA	NA	NA	NA	NA	225	NA	NA	NA	NA	CM	37
ura3_Cu_0850um_a_vs_NRC-1d.sig	NA	NA	0	NA	NA	NA	NA	NA	NA	NA	NA	NA	NA	NA	NA	NA	NA	225	NA	NA	NA	NA	CM	37
ura3_Cu_0850um_b_vs_NRC-1d.sig	NA	NA	0	NA	NA	NA	NA	NA	NA	NA	NA	NA	NA	NA	NA	NA	NA	225	NA	NA	NA	NA	CM	37
ura3_Cu_1000um_a_vs_NRC-1d.sig	NA	NA	0	NA	NA	NA	NA	NA	NA	NA	NA	NA	NA	NA	NA	NA	NA	225	NA	NA	NA	NA	CM	37
ura3_Cu_1000um_b_vs_NRC-1d.sig	NA	NA	0	NA	NA	NA	NA	NA	NA	NA	NA	NA	NA	NA	NA	NA	NA	225	NA	NA	NA	NA	CM	37
ura3_Mn_0800um_a_vs_NRC-1d.sig	NA	NA	NA	NA	NA	NA	NA	NA	NA	NA	NA	0	NA	NA	NA	NA	NA	225	NA	NA	NA	NA	CM	37
ura3_Mn_0800um_b_vs_NRC-1d.sig	NA	NA	NA	NA	NA	NA	NA	NA	NA	NA	NA	0	NA	NA	NA	NA	NA	225	NA	NA	NA	NA	CM	37
ura3_Mn_1500um_a_vs_NRC-1d.sig	NA	NA	NA	NA	NA	NA	NA	NA	NA	NA	NA	0	NA	NA	NA	NA	NA	225	NA	NA	NA	NA	CM	37
ura3_Mn_1500um_b_vs_NRC-1d.sig	NA	NA	NA	NA	NA	NA	NA	NA	NA	NA	NA	0	NA	NA	NA	NA	NA	225	NA	NA	NA	NA	CM	37
ura3_Mn_1000um_a_vs_NRC-1d.sig	NA	NA	NA	NA	NA	NA	NA	NA	NA	NA	NA	0	NA	NA	NA	NA	NA	225	NA	NA	NA	NA	CM	37
ura3_Mn_1000um_b_vs_NRC-1d.sig	NA	NA	NA	NA	NA	NA	NA	NA	NA	NA	NA	0	NA	NA	NA	NA	NA	225	NA	NA	NA	NA	CM	37
vng1179_0a_vs_NRC-1d.sig	NA	NA	NA	NA	NA	NA	NA	NA	NA	NA	NA	NA	NA	NA	NA	NA	NA	225	NA	NA	NA	NA	CM	37
vng1179_0b_vs_NRC-1d.sig	NA	NA	NA	NA	NA	NA	NA	NA	NA	NA	NA	NA	NA	NA	NA	NA	NA	225	NA	NA	NA	NA	CM	37
vng1179_Cu_0700um_a_vs_NRC-1d.sig	NA	NA	0	NA	NA	NA	NA	NA	NA	NA	NA	NA	NA	NA	NA	NA	NA	225	NA	NA	NA	NA	CM	37
vng1179_Cu_0700um_b_vs_NRC-1d.sig	NA	NA	0	NA	NA	NA	NA	NA	NA	NA	NA	NA	NA	NA	NA	NA	NA	225	NA	NA	NA	NA	CM	37
vng1179_Cu_0850um_a_vs_NRC-1d.sig	NA	NA	0	NA	NA	NA	NA	NA	NA	NA	NA	NA	NA	NA	NA	NA	NA	225	NA	NA	NA	NA	CM	37
vng1179_Cu_0850um_b_vs_NRC-1d.sig	NA	NA	0	NA	NA	NA	NA	NA	NA	NA	NA	NA	NA	NA	NA	NA	NA	225	NA	NA	NA	NA	CM	37
vng1179_Cu_1000um_a_vs_NRC-	NA	NA	0	NA	NA	NA	NA	NA	NA	NA	NA	NA	NA	NA	NA	NA	NA	225	NA	NA	NA	NA	CM	37

1d.sig																								
vng1179_Cu_1000um_b_vs_NRC-1d.sig	NA	NA	0	NA	NA	NA	NA	NA	NA	NA	NA	NA	NA	NA	NA	NA	NA	225	NA	NA	NA	NA	CM	37
mn__0800um_vs_NRC-1	NA	NA	NA	NA	NA	NA	NA	NA	NA	NA	NA	0	NA	NA	NA	NA	NA	NA	NA	NA	NA	NA	CM	37
mn__1000um_vs_NRC-1	NA	NA	NA	NA	NA	NA	NA	NA	NA	NA	NA	0	NA	NA	NA	NA	NA	NA	NA	NA	NA	NA	CM	37
mn__1500um_vs_NRC-1	NA	NA	NA	NA	NA	NA	NA	NA	NA	NA	NA	0	NA	NA	NA	NA	NA	NA	NA	NA	NA	NA	CM	37
fe__2000um_vs_NRC-1	NA	NA	NA	NA	NA	0	NA	NA	NA	NA	NA	NA	NA	NA	NA	NA	NA	NA	NA	NA	NA	NA	CM	37
fe__4000um_vs_NRC-1	NA	NA	NA	NA	NA	0	NA	NA	NA	NA	NA	NA	NA	NA	NA	NA	NA	NA	NA	NA	NA	NA	CM	37
fe__6000um_vs_NRC-1	NA	NA	NA	NA	NA	0.01	NA	NA	NA	NA	NA	NA	NA	NA	NA	NA	NA	NA	NA	NA	NA	NA	CM	37
fe__7000um_vs_NRC-1	NA	NA	NA	NA	NA	0.01	NA	NA	NA	NA	NA	NA	NA	NA	NA	NA	NA	NA	NA	NA	NA	NA	CM	37
feso4__-0001m_vs_NRC-1	NA	NA	NA	NA	NA	0	NA	NA	NA	35	NA	NA	NA	NA	NA	NA	NA	NA	NA	-1	NA	NA	CM	37
feso4__0000m_vs_NRC-1	NA	NA	NA	NA	NA	0	NA	NA	NA	35	NA	NA	NA	NA	NA	NA	NA	NA	NA	0	NA	NA	CM	37
feso4__0005m_vs_NRC-1b	NA	NA	NA	NA	NA	0.01	NA	NA	NA	35	NA	NA	NA	NA	NA	NA	NA	NA	NA	5	NA	NA	CM	37
feso4__0010m_vs_NRC-1b	NA	NA	NA	NA	NA	0.01	NA	NA	NA	35	NA	NA	NA	NA	NA	NA	NA	NA	NA	10	NA	NA	CM	37
feso4__0015m_vs_NRC-1b	NA	NA	NA	NA	NA	0.01	NA	NA	NA	35	NA	NA	NA	NA	NA	NA	NA	NA	NA	15	NA	NA	CM	37
feso4__0020m_vs_NRC-1	NA	NA	NA	NA	NA	0.01	NA	NA	NA	35	NA	NA	NA	NA	NA	NA	NA	NA	NA	20	NA	NA	CM	37
feso4__0025m_vs_NRC-1b	NA	NA	NA	NA	NA	0.01	NA	NA	NA	35	NA	NA	NA	NA	NA	NA	NA	NA	NA	25	NA	NA	CM	37
feso4__0040m_vs_NRC-1	NA	NA	NA	NA	NA	0.01	NA	NA	NA	35	NA	NA	NA	NA	NA	NA	NA	NA	NA	40	NA	NA	CM	37
feso4__0080m_vs_NRC-1	NA	NA	NA	NA	NA	0.01	NA	NA	NA	35	NA	NA	NA	NA	NA	NA	NA	NA	NA	80	NA	NA	CM	37
feso4__0160m_vs_NRC-1	NA	NA	NA	NA	NA	0.01	NA	NA	NA	35	NA	NA	NA	NA	NA	NA	NA	NA	NA	160	NA	NA	CM	37
feso4__0320m_vs_NRC-1	NA	NA	NA	NA	NA	0.01	NA	NA	NA	35	NA	NA	NA	NA	NA	NA	NA	NA	NA	320	NA	NA	CM	37
Dip_0.025_vs_NRC-1d.sig	NA	NA	NA	NA	NA	NA	NA	NA	NA	NA	NA	NA	NA	NA	NA	NA	NA	NA	NA	NA	NA	NA	CM	37
Dip_0.100_vs_NRC-1d.sig	NA	NA	NA	NA	NA	NA	NA	NA	NA	NA	NA	NA	NA	NA	NA	NA	NA	NA	NA	NA	NA	NA	CM	37
Dip_0.250_vs_NRC-1d.sig	NA	NA	NA	NA	NA	NA	NA	NA	NA	NA	NA	NA	NA	NA	NA	NA	NA	NA	NA	NA	NA	NA	CM	37
Dip_0.000_vs_NRC	NA	NA	NA	NA	NA	NA	NA	NA	NA	NA	NA	NA	NA	NA	NA	NA	NA	NA	NA	NA	NA	NA	CM	37

-1d.sig																									
Co_0.2_vs_NRC-1d.sig	NA	0	NA	NA	NA	NA	NA	NA	NA	NA	NA	NA	NA	NA	NA	NA	NA	NA	NA	NA	NA	NA	CM	37
Co_0.3_vs_NRC-1d.sig	NA	0	NA	NA	NA	NA	NA	NA	NA	NA	NA	NA	NA	NA	NA	NA	NA	NA	NA	NA	NA	NA	CM	37
Co_0.5_vs_NRC-1d.sig	NA	0	NA	NA	NA	NA	NA	NA	NA	NA	NA	NA	NA	NA	NA	NA	NA	NA	NA	NA	NA	NA	CM	37
Co_0.0_vs_NRC-1d.sig	NA	0	NA	NA	NA	NA	NA	NA	NA	NA	NA	NA	NA	NA	NA	NA	NA	NA	NA	NA	NA	NA	CM	37
co__0000um_vs_NRC-1c	NA	0	NA	NA	NA	NA	NA	NA	NA	NA	NA	NA	NA	NA	NA	NA	NA	NA	NA	NA	NA	NA	CM	37
co__0200um_vs_NRC-1c	NA	0	NA	NA	NA	NA	NA	NA	NA	NA	NA	NA	NA	NA	NA	NA	NA	NA	NA	NA	NA	NA	CM	37
co__0300um_vs_NRC-1c	NA	0	NA	NA	NA	NA	NA	NA	NA	NA	NA	NA	NA	NA	NA	NA	NA	NA	NA	NA	NA	NA	CM	37
co__0500um_vs_NRC-1c	NA	0	NA	NA	NA	NA	NA	NA	NA	NA	NA	NA	NA	NA	NA	NA	NA	NA	NA	NA	NA	NA	CM	37
idr1_40min_+Fe_vs_NRC1-h1.sig	NA	NA	NA	NA	NA	0	NA	NA	NA	NA	NA	NA	NA	0.56	NA	NA	NA	225	NA	40	NA	NA	CM	37
idr1_40min_-Fe_vs_NRC1-h1.sig	NA	NA	NA	NA	NA	0	NA	NA	NA	NA	NA	NA	NA	0.56	NA	NA	NA	225	NA	40	NA	NA	CM	37
idr1_60_min_-Fe_vs_NRC1-h1.sig	NA	NA	NA	NA	NA	0	NA	NA	NA	NA	NA	NA	NA	0.79	NA	NA	NA	225	NA	60	NA	NA	CM	37
idr1_60min_+Fe_vs_NRC1-h1.sig	NA	NA	NA	NA	NA	0	NA	NA	NA	NA	NA	NA	NA	0.79	NA	NA	NA	225	NA	60	NA	NA	CM	37
idr2_0min_vs_NRC1-h1.sig	NA	NA	NA	NA	NA	0	NA	NA	NA	NA	NA	NA	NA	0.31	NA	NA	NA	225	NA	0	NA	NA	CM	37
idr2_20min_+Fe_vs_NRC1-h1.sig	NA	NA	NA	NA	NA	0	NA	NA	NA	NA	NA	NA	NA	0.32	NA	NA	NA	225	NA	20	NA	NA	CM	37
idr2_20min_-Fe_vs_NRC1-h1.sig	NA	NA	NA	NA	NA	0	NA	NA	NA	NA	NA	NA	NA	0.31	NA	NA	NA	225	NA	20	NA	NA	CM	37
idr2_40min_+Fe_vs_NRC1-h1.sig	NA	NA	NA	NA	NA	0	NA	NA	NA	NA	NA	NA	NA	0.32	NA	NA	NA	225	NA	40	NA	NA	CM	37
idr2_40min_-Fe_vs_NRC1-h1.sig	NA	NA	NA	NA	NA	0	NA	NA	NA	NA	NA	NA	NA	0.31	NA	NA	NA	225	NA	40	NA	NA	CM	37
idr2_60min_+Fe_vs_NRC1-h1.sig	NA	NA	NA	NA	NA	0	NA	NA	NA	NA	NA	NA	NA	0.32	NA	NA	NA	225	NA	60	NA	NA	CM	37
idr2_60min_-Fe_vs_NRC1-h1.sig	NA	NA	NA	NA	NA	0	NA	NA	NA	NA	NA	NA	NA	0.31	NA	NA	NA	225	NA	60	NA	NA	CM	37
sirR_0min_vs_NRC1_h1.sig	NA	NA	NA	NA	NA	0	NA	NA	NA	NA	NA	NA	NA	0.5	NA	NA	NA	225	NA	0	NA	NA	CM	37

sirR_20min_+Fe_vs_NRC1_h1.sig	NA	NA	NA	NA	NA	0	NA	NA	NA	NA	NA	NA	NA	0.46	NA	NA	NA	225	NA	20	NA	NA	CM	37
sirR_20min_-Fe_vs_NRC1_h1.sig	NA	NA	NA	NA	NA	0	NA	NA	NA	NA	NA	NA	NA	0.5	NA	NA	NA	225	NA	20	NA	NA	CM	37
sirR_40min_+Fe_vs_NRC1_h1.sig	NA	NA	NA	NA	NA	0	NA	NA	NA	NA	NA	NA	NA	0.46	NA	NA	NA	225	NA	40	NA	NA	CM	37
sirR_40min_-Fe_vs_NRC1_h1.sig	NA	NA	NA	NA	NA	0	NA	NA	NA	NA	NA	NA	NA	0.5	NA	NA	NA	225	NA	40	NA	NA	CM	37
sirR_60min_+Fe_vs_NRC1_h1.sig	NA	NA	NA	NA	NA	0	NA	NA	NA	NA	NA	NA	NA	0.46	NA	NA	NA	225	NA	60	NA	NA	CM	37
sirR_60min_-Fe_vs_NRC1_h1.sig	NA	NA	NA	NA	NA	0	NA	NA	NA	NA	NA	NA	NA	0.5	NA	NA	NA	225	NA	60	NA	NA	CM	37
ura3_40min_+Fe_vs_NRC1-h1.sig	NA	NA	NA	NA	NA	0	NA	NA	NA	NA	NA	NA	NA	0.4	NA	NA	NA	225	NA	40	NA	NA	CM	37
zim__HO_D_vs_NRC-1	NA	NA	NA	NA	NA	NA	NA	NA	NA	0	NA	NA	NA	0.53	NA	NA	NA	220	NA	NA	NA	NA	CM	37
zim__HO_L_vs_NRC-1	NA	NA	NA	NA	NA	NA	NA	NA	NA	35	NA	NA	NA	0.57	NA	NA	NA	220	NA	NA	NA	NA	CM	37
zim__LO_D_vs_NRC-1	NA	NA	NA	NA	NA	NA	NA	NA	NA	0	NA	NA	NA	0.49	NA	NA	NA	100	NA	NA	NA	NA	CM	37
zim__LO_L_vs_NRC-1	NA	NA	NA	NA	NA	NA	NA	NA	NA	35	NA	NA	NA	0.49	NA	NA	NA	100	NA	NA	NA	NA	CM	37
VNG2334C__HO_D_vs_NRC-1	NA	NA	NA	NA	NA	NA	NA	NA	NA	0	NA	NA	NA	0.47	NA	NA	NA	220	NA	NA	NA	NA	CM	37
VNG2334C__HO_L_vs_NRC-1	NA	NA	NA	NA	NA	NA	NA	NA	NA	35	NA	NA	NA	0.48	NA	NA	NA	220	NA	NA	NA	NA	CM	37
VNG2334C__LO_D_vs_NRC-1	NA	NA	NA	NA	NA	NA	NA	NA	NA	0	NA	NA	NA	0.43	NA	NA	NA	100	NA	NA	NA	NA	CM	37
VNG2334C__LO_L_vs_NRC-1	NA	NA	NA	NA	NA	NA	NA	NA	NA	35	NA	NA	NA	0.5	NA	NA	NA	100	NA	NA	NA	NA	CM	37
VNG1296C__HO_D_vs_NRC-1	NA	NA	NA	NA	NA	NA	NA	NA	NA	0	NA	NA	NA	0.37	NA	NA	NA	220	NA	NA	NA	NA	CM	37
VNG1296C__HO_L_vs_NRC-1	NA	NA	NA	NA	NA	NA	NA	NA	NA	35	NA	NA	NA	0.36	NA	NA	NA	220	NA	NA	NA	NA	CM	37
VNG1296C__LO_D_vs_NRC-1	NA	NA	NA	NA	NA	NA	NA	NA	NA	0	NA	NA	NA	0.31	NA	NA	NA	100	NA	NA	NA	NA	CM	37
VNG1296C__LO_L_vs_NRC-1	NA	NA	NA	NA	NA	NA	NA	NA	NA	35	NA	NA	NA	0.33	NA	NA	NA	100	NA	NA	NA	NA	CM	37
VNG0750C__HO_D_vs_NRC-1	NA	NA	NA	NA	NA	NA	NA	NA	NA	0	NA	NA	NA	0.77	NA	NA	NA	220	NA	NA	NA	NA	CM	37
VNG0750C__HO_L_vs_NRC-1	NA	NA	NA	NA	NA	NA	NA	NA	NA	35	NA	NA	NA	0.68	NA	NA	NA	220	NA	NA	NA	NA	CM	37
VNG0750C__LO_D_vs_NRC-1	NA	NA	NA	NA	NA	NA	NA	NA	NA	0	NA	NA	NA	0.71	NA	NA	NA	100	NA	NA	NA	NA	CM	37

VNG0750C__LO_L_vs_NRC-1	NA	NA	NA	NA	NA	NA	NA	NA	NA	35	NA	NA	NA	0.77	NA	NA	NA	100	NA	NA	NA	NA	CM	37
VNG0019H__HO_D_vs_NRC-1c	NA	NA	NA	NA	NA	NA	NA	NA	NA	0	NA	NA	NA	0.77	NA	NA	NA	220	NA	NA	NA	NA	CM	37
VNG0019H__HO_L_vs_NRC-1c	NA	NA	NA	NA	NA	NA	NA	NA	NA	35	NA	NA	NA	0.81	NA	NA	NA	220	NA	NA	NA	NA	CM	37
VNG0019H__LO_D_vs_NRC-1c	NA	NA	NA	NA	NA	NA	NA	NA	NA	0	NA	NA	NA	0.77	NA	NA	NA	100	NA	NA	NA	NA	CM	37
VNG0019H__LO_L_vs_NRC-1c	NA	NA	NA	NA	NA	NA	NA	NA	NA	35	NA	NA	NA	0.69	NA	NA	NA	100	NA	NA	NA	NA	CM	37
uv__000jm2_CL_060m	NA	NA	NA	NA	NA	NA	NA	NA	NA	0	NA	NA	NA	NA	NA	High	NA	NA	NA	60	0	NA	CM	42
ura3__HO_D_vs_NRC-1	NA	NA	NA	NA	NA	NA	NA	NA	NA	0	NA	NA	NA	0.83	NA	NA	NA	220	NA	NA	NA	NA	CM	37
ura3__HO_L_vs_NRC-1	NA	NA	NA	NA	NA	NA	NA	NA	NA	35	NA	NA	NA	0.83	NA	NA	NA	220	NA	NA	NA	NA	CM	37
ura3__LO_D_vs_NRC-1	NA	NA	NA	NA	NA	NA	NA	NA	NA	0	NA	NA	NA	0.75	NA	NA	NA	100	NA	NA	NA	NA	CM	37
ura3__LO_L_vs_NRC-1	NA	NA	NA	NA	NA	NA	NA	NA	NA	35	NA	NA	NA	0.79	NA	NA	NA	100	NA	NA	NA	NA	CM	37
tfbG_CHIS_over	NA	NA	NA	NA	NA	NA	NA	NA	NA	NA	NA	NA	NA	NA	tfbG	NA	NA	225	Chis	NA	NA	NA	CM	37
tfb_D_vs_NRC-1c	NA	NA	NA	NA	NA	NA	NA	NA	NA	NA	NA	NA	NA	0.61	NA	NA	NA	225	NA	NA	NA	NA	CM	37
tfb_C_vs_NRC-1c	NA	NA	NA	NA	NA	NA	NA	NA	NA	NA	NA	NA	NA	0.69	NA	NA	NA	225	NA	NA	NA	NA	CM	37
tfb_B_vs_NRC-1c	NA	NA	NA	NA	NA	NA	NA	NA	NA	NA	NA	NA	NA	0.71	NA	NA	NA	225	NA	NA	NA	NA	CM	37
tfb_A_vs_NRC-1c	NA	NA	NA	NA	NA	NA	NA	NA	NA	NA	NA	NA	NA	0.63	NA	NA	NA	225	NA	NA	NA	NA	CM	37
tbp_D_vs_NRC-1c	NA	NA	NA	NA	NA	NA	NA	NA	NA	NA	NA	NA	NA	0.71	NA	NA	NA	225	NA	NA	NA	NA	CM	37
tbp_C_vs_NRC-1c	NA	NA	NA	NA	NA	NA	NA	NA	NA	NA	NA	NA	NA	0.72	NA	NA	NA	225	NA	NA	NA	NA	CM	37
tbp_A_vs_NRC-1c	NA	NA	NA	NA	NA	NA	NA	NA	NA	NA	NA	NA	NA	0.59	NA	NA	NA	225	NA	NA	NA	NA	CM	37
sop2_II__HO_D_vs_NRC-1c	NA	NA	NA	NA	NA	NA	NA	NA	NA	0	NA	NA	NA	0.81	NA	NA	NA	220	NA	NA	NA	NA	CM	37
sop2_II__HO_L_vs_NRC-1c	NA	NA	NA	NA	NA	NA	NA	NA	NA	35	NA	NA	NA	0.76	NA	NA	NA	220	NA	NA	NA	NA	CM	37
sop2_II__LO_D_vs_NRC-1c	NA	NA	NA	NA	NA	NA	NA	NA	NA	0	NA	NA	NA	0.7	NA	NA	NA	100	NA	NA	NA	NA	CM	37
sop2_II__LO_L_vs_NRC-1c	NA	NA	NA	NA	NA	NA	NA	NA	NA	35	NA	NA	NA	0.76	NA	NA	NA	100	NA	NA	NA	NA	CM	37
sop2_I__HO_D_vs_NRC-1	NA	NA	NA	NA	NA	NA	NA	NA	NA	0	NA	NA	NA	0.74	NA	NA	NA	220	NA	NA	NA	NA	CM	37
sop2_I__HO_L_vs_NRC-1	NA	NA	NA	NA	NA	NA	NA	NA	NA	35	NA	NA	NA	0.71	NA	NA	NA	220	NA	NA	NA	NA	CM	37

sop2_l__LO_D_vs_NRC-1	NA	NA	NA	NA	NA	NA	NA	NA	NA	0	NA	NA	NA	0.73	NA	NA	NA	100	NA	NA	NA	NA	CM	37
sop2_l__LO_L_vs_NRC-1	NA	NA	NA	NA	NA	NA	NA	NA	NA	35	NA	NA	NA	0.72	NA	NA	NA	100	NA	NA	NA	NA	CM	37
phr2__HO_D_vs_NRC-1	NA	NA	NA	NA	NA	NA	NA	NA	NA	0	NA	NA	NA	0.87	NA	NA	NA	220	NA	NA	NA	NA	CM	37
phr2__HO_L_vs_NRC-1	NA	NA	NA	NA	NA	NA	NA	NA	NA	35	NA	NA	NA	0.82	NA	NA	NA	220	NA	NA	NA	NA	CM	37
phr2__LO_D_vs_NRC-1	NA	NA	NA	NA	NA	NA	NA	NA	NA	0	NA	NA	NA	0.72	NA	NA	NA	100	NA	NA	NA	NA	CM	37
phr2__LO_L_vs_NRC-1	NA	NA	NA	NA	NA	NA	NA	NA	NA	35	NA	NA	NA	0.78	NA	NA	NA	100	NA	NA	NA	NA	CM	37
phr1_and_2__HO_D_vs_NRC-1	NA	NA	NA	NA	NA	NA	NA	NA	NA	0	NA	NA	NA	0.83	NA	NA	NA	220	NA	NA	NA	NA	CM	37
phr1_and_2__HO_L_vs_NRC-1	NA	NA	NA	NA	NA	NA	NA	NA	NA	35	NA	NA	NA	0.78	NA	NA	NA	220	NA	NA	NA	NA	CM	37
phr1_and_2__LO_D_vs_NRC-1	NA	NA	NA	NA	NA	NA	NA	NA	NA	0	NA	NA	NA	0.75	NA	NA	NA	100	NA	NA	NA	NA	CM	37
phr1_and_2__LO_L_vs_NRC-1	NA	NA	NA	NA	NA	NA	NA	NA	NA	35	NA	NA	NA	0.8	NA	NA	NA	100	NA	NA	NA	NA	CM	37
phr1__HO_D_vs_NRC-1	NA	NA	NA	NA	NA	NA	NA	NA	NA	0	NA	NA	NA	0.78	NA	NA	NA	220	NA	NA	NA	NA	CM	37
phr1__HO_L_vs_NRC-1	NA	NA	NA	NA	NA	NA	NA	NA	NA	35	NA	NA	NA	0.74	NA	NA	NA	220	NA	NA	NA	NA	CM	37
phr1__LO_D_vs_NRC-1	NA	NA	NA	NA	NA	NA	NA	NA	NA	0	NA	NA	NA	0.72	NA	NA	NA	100	NA	NA	NA	NA	CM	37
phr1__LO_L_vs_NRC-1	NA	NA	NA	NA	NA	NA	NA	NA	NA	35	NA	NA	NA	0.75	NA	NA	NA	100	NA	NA	NA	NA	CM	37
phoR__HO_D_vs_NRC-1	NA	NA	NA	NA	NA	NA	NA	NA	NA	0	NA	NA	NA	0.56	NA	NA	NA	220	NA	NA	NA	NA	CM	37
phoR__HO_L_vs_NRC-1	NA	NA	NA	NA	NA	NA	NA	NA	NA	35	NA	NA	NA	0.54	NA	NA	NA	220	NA	NA	NA	NA	CM	37
phoR__LO_D_vs_NRC-1	NA	NA	NA	NA	NA	NA	NA	NA	NA	0	NA	NA	NA	0.53	NA	NA	NA	100	NA	NA	NA	NA	CM	37
phoR__LO_L_vs_NRC-1	NA	NA	NA	NA	NA	NA	NA	NA	NA	35	NA	NA	NA	0.53	NA	NA	NA	100	NA	NA	NA	NA	CM	37
cspD1_-0001_L_H_vs_NRC1d.sig	NA	NA	NA	NA	NA	NA	NA	NA	NA	NA	NA	NA	NA	0.58	NA	-0.7	NA	250	NA	-1	NA	NA	CM	37
cspD1_0005_H_vs_NRC1d.sig	NA	NA	NA	NA	NA	NA	NA	NA	NA	NA	NA	NA	NA	0.55	NA	57.6	NA	1100	NA	5	NA	NA	CM	37
cspD1_0010_H_vs_NRC1d.sig	NA	NA	NA	NA	NA	NA	NA	NA	NA	NA	NA	NA	NA	0.54	NA	58.1	NA	1100	NA	10	NA	NA	CM	37
cspD1_0020_H_vs_NRC1d.sig	NA	NA	NA	NA	NA	NA	NA	NA	NA	NA	NA	NA	NA	0.54	NA	57	NA	1100	NA	20	NA	NA	CM	37
cspD1_0045_H_vs_NRC1d.sig	NA	NA	NA	NA	NA	NA	NA	NA	NA	NA	NA	NA	NA	0.52	NA	100	NA	1100	NA	45	NA	NA	CM	37
cspD1_0180_H_vs	NA	NA	NA	NA	NA	NA	NA	NA	NA	NA	NA	NA	NA	0.5	NA	114	NA	110	NA	180	NA	NA	CM	37

_NRC1d.sig														7				0						
NRC1e_vs_NRC1f.sig	NA	NA	NA	NA	NA	NA	NA	NA	NA	NA	NA	NA	NA	0.68	NA	NA	NA	225	NA	NA	NA	NA	CM	37
NRC-1__HO_D_vs_NRC-1	NA	NA	NA	NA	NA	NA	NA	NA	NA	0	NA	NA	NA	0.88	NA	NA	NA	220	NA	NA	NA	NA	CM	37
NRC-1__HO_L_vs_NRC-1	NA	NA	NA	NA	NA	NA	NA	NA	NA	35	NA	NA	NA	0.82	NA	NA	NA	220	NA	NA	NA	NA	CM	37
NRC-1__LO_D_vs_NRC-1	NA	NA	NA	NA	NA	NA	NA	NA	NA	0	NA	NA	NA	0.85	NA	NA	NA	100	NA	NA	NA	NA	CM	37
NRC-1__LO_L_vs_NRC-1	NA	NA	NA	NA	NA	NA	NA	NA	NA	35	NA	NA	NA	0.88	NA	NA	NA	100	NA	NA	NA	NA	CM	37
kinA2_II__HO_D_vs_NRC-1c	NA	NA	NA	NA	NA	NA	NA	NA	NA	0	NA	NA	NA	0.72	NA	NA	NA	220	NA	NA	NA	NA	CM	37
kinA2_II__HO_L_vs_NRC-1c	NA	NA	NA	NA	NA	NA	NA	NA	NA	35	NA	NA	NA	0.77	NA	NA	NA	220	NA	NA	NA	NA	CM	37
kinA2_II__LO_D_vs_NRC-1c	NA	NA	NA	NA	NA	NA	NA	NA	NA	0	NA	NA	NA	0.65	NA	NA	NA	100	NA	NA	NA	NA	CM	37
kinA2_II__LO_L_vs_NRC-1c	NA	NA	NA	NA	NA	NA	NA	NA	NA	35	NA	NA	NA	0.66	NA	NA	NA	100	NA	NA	NA	NA	CM	37
kinA2_I__HO_D_vs_NRC-1	NA	NA	NA	NA	NA	NA	NA	NA	NA	0	NA	NA	NA	0.78	NA	NA	NA	220	NA	NA	NA	NA	CM	37
kinA2_I__HO_L_vs_NRC-1	NA	NA	NA	NA	NA	NA	NA	NA	NA	35	NA	NA	NA	0.68	NA	NA	NA	220	NA	NA	NA	NA	CM	37
kinA2_I__LO_D_vs_NRC-1	NA	NA	NA	NA	NA	NA	NA	NA	NA	0	NA	NA	NA	0.67	NA	NA	NA	100	NA	NA	NA	NA	CM	37
kinA2_I__LO_L_vs_NRC-1	NA	NA	NA	NA	NA	NA	NA	NA	NA	35	NA	NA	NA	0.69	NA	NA	NA	100	NA	NA	NA	NA	CM	37
htr8__HO_D_vs_NRC-1	NA	NA	NA	NA	NA	NA	NA	NA	NA	0	NA	NA	NA	0.77	NA	NA	NA	220	NA	NA	NA	NA	CM	37
htr8__HO_L_vs_NRC-1	NA	NA	NA	NA	NA	NA	NA	NA	NA	35	NA	NA	NA	0.74	NA	NA	NA	220	NA	NA	NA	NA	CM	37
htr8__LO_D_vs_NRC-1	NA	NA	NA	NA	NA	NA	NA	NA	NA	0	NA	NA	NA	0.72	NA	NA	NA	100	NA	NA	NA	NA	CM	37
htr8__LO_L_vs_NRC-1	NA	NA	NA	NA	NA	NA	NA	NA	NA	35	NA	NA	NA	0.73	NA	NA	NA	100	NA	NA	NA	NA	CM	37
htr2__HO_D_vs_NRC-1	NA	NA	NA	NA	NA	NA	NA	NA	NA	0	NA	NA	NA	0.75	NA	NA	NA	220	NA	NA	NA	NA	CM	37
htr2__HO_L_vs_NRC-1	NA	NA	NA	NA	NA	NA	NA	NA	NA	35	NA	NA	NA	0.69	NA	NA	NA	220	NA	NA	NA	NA	CM	37
htr2__LO_D_vs_NRC-1	NA	NA	NA	NA	NA	NA	NA	NA	NA	0	NA	NA	NA	0.65	NA	NA	NA	100	NA	NA	NA	NA	CM	37
htr2__LO_L_vs_NRC-1	NA	NA	NA	NA	NA	NA	NA	NA	NA	35	NA	NA	NA	0.68	NA	NA	NA	100	NA	NA	NA	NA	CM	37
htr1__HO_D_vs_N	NA	NA	NA	NA	NA	NA	NA	NA	NA	0	NA	NA	NA	0.7	NA	NA	NA	220	NA	NA	NA	NA	CM	37

RC-1														9										
htr1__HO_L_vs_NRC-1	NA	NA	NA	NA	NA	NA	NA	NA	NA	35	NA	NA	NA	0.67	NA	NA	NA	220	NA	NA	NA	NA	CM	37
htr1__LO_D_vs_NRC-1	NA	NA	NA	NA	NA	NA	NA	NA	NA	0	NA	NA	NA	0.66	NA	NA	NA	100	NA	NA	NA	NA	CM	37
htr1__LO_L_vs_NRC-1	NA	NA	NA	NA	NA	NA	NA	NA	NA	35	NA	NA	NA	0.71	NA	NA	NA	100	NA	NA	NA	NA	CM	37
htlD__HO_D_vs_NRC-1	NA	NA	NA	NA	NA	NA	NA	NA	NA	0	NA	NA	NA	0.8	NA	NA	NA	220	NA	NA	NA	NA	CM	37
htlD__HO_L_vs_NRC-1	NA	NA	NA	NA	NA	NA	NA	NA	NA	35	NA	NA	NA	0.81	NA	NA	NA	220	NA	NA	NA	NA	CM	37
htlD__LO_D_vs_NRC-1	NA	NA	NA	NA	NA	NA	NA	NA	NA	0	NA	NA	NA	0.78	NA	NA	NA	100	NA	NA	NA	NA	CM	37
htlD__LO_L_vs_NRC-1	NA	NA	NA	NA	NA	NA	NA	NA	NA	35	NA	NA	NA	0.79	NA	NA	NA	100	NA	NA	NA	NA	CM	37
gap__HO_D_vs_NRC-1c	NA	NA	NA	NA	NA	NA	NA	NA	NA	0	NA	NA	NA	0.95	NA	NA	NA	220	NA	NA	NA	NA	CM	37
gap__HO_L_vs_NRC-1c	NA	NA	NA	NA	NA	NA	NA	NA	NA	35	NA	NA	NA	0.92	NA	NA	NA	220	NA	NA	NA	NA	CM	37
gap__LO_D_vs_NRC-1c	NA	NA	NA	NA	NA	NA	NA	NA	NA	0	NA	NA	NA	0.79	NA	NA	NA	100	NA	NA	NA	NA	CM	37
gap__LO_L_vs_NRC-1c	NA	NA	NA	NA	NA	NA	NA	NA	NA	35	NA	NA	NA	0.82	NA	NA	NA	100	NA	NA	NA	NA	CM	37
gamma4__0000gy-000min	NA	NA	NA	NA	NA	NA	0	NA	NA	NA	NA	NA	NA	NA	NA	NA	NA	225	NA	0	NA	NA	CM	42
gamma4__0000gy-010min	NA	NA	NA	NA	NA	NA	0	NA	NA	NA	NA	NA	NA	NA	NA	NA	NA	225	NA	10	NA	NA	CM	42
gamma4__0000gy-020min	NA	NA	NA	NA	NA	NA	0	NA	NA	NA	NA	NA	NA	NA	NA	NA	NA	225	NA	20	NA	NA	CM	42
gamma4__0000gy-030min	NA	NA	NA	NA	NA	NA	0	NA	NA	NA	NA	NA	NA	NA	NA	NA	NA	225	NA	30	NA	NA	CM	42
gamma4__0000gy-040min	NA	NA	NA	NA	NA	NA	0	NA	NA	NA	NA	NA	NA	NA	NA	NA	NA	225	NA	40	NA	NA	CM	42
gamma4__0000gy-050min	NA	NA	NA	NA	NA	NA	0	NA	NA	NA	NA	NA	NA	NA	NA	NA	NA	225	NA	50	NA	NA	CM	42
gamma4__0000gy-060min	NA	NA	NA	NA	NA	NA	0	NA	NA	NA	NA	NA	NA	NA	NA	NA	NA	225	NA	60	NA	NA	CM	42
gamma4__0000gy-120min	NA	NA	NA	NA	NA	NA	0	NA	NA	NA	NA	NA	NA	NA	NA	NA	NA	225	NA	120	NA	NA	CM	42
gamma4__0000gy-240min	NA	NA	NA	NA	NA	NA	0	NA	NA	NA	NA	NA	NA	NA	NA	NA	NA	225	NA	240	NA	NA	CM	42
gamma__0000gy-0000m	NA	NA	NA	NA	NA	NA	0	NA	NA	NA	NA	NA	NA	NA	NA	NA	NA	225	NA	0	NA	NA	CM	42
gamma__0000gy-0010m	NA	NA	NA	NA	NA	NA	0	NA	NA	NA	NA	NA	NA	NA	NA	NA	NA	225	NA	10	NA	NA	CM	42
gamma__0000gy-0030m	NA	NA	NA	NA	NA	NA	0	NA	NA	NA	NA	NA	NA	NA	NA	NA	NA	225	NA	30	NA	NA	CM	42
gamma__0000gy-	NA	NA	NA	NA	NA	NA	0	NA	NA	NA	NA	NA	NA	NA	NA	NA	NA	225	NA	60	NA	NA	CM	42

0060m																								
gamma__0000gy-0240m	NA	NA	NA	NA	NA	NA	0	NA	NA	NA	NA	NA	NA	NA	NA	NA	NA	225	NA	240	NA	NA	CM	42
gamma__0000gy-0960m	NA	NA	NA	NA	NA	NA	0	NA	NA	NA	NA	NA	NA	NA	NA	NA	NA	225	NA	960	NA	NA	CM	42
EMS_Treated__000uM-000	NA	NA	NA	NA	0	NA	NA	NA	NA	NA	NA	NA	NA	0.28	NA	NA	NA	225	NA	0	NA	NA	CM	37
EMS_Treated__000uM-010	NA	NA	NA	NA	0	NA	NA	NA	NA	NA	NA	NA	NA	0.3	NA	NA	NA	225	NA	10	NA	NA	CM	37
EMS_Treated__000uM-020	NA	NA	NA	NA	0	NA	NA	NA	NA	NA	NA	NA	NA	0.34	NA	NA	NA	225	NA	20	NA	NA	CM	37
EMS_Treated__000uM-030	NA	NA	NA	NA	0	NA	NA	NA	NA	NA	NA	NA	NA	0.33	NA	NA	NA	225	NA	30	NA	NA	CM	37
EMS_Treated__000uM-040	NA	NA	NA	NA	0	NA	NA	NA	NA	NA	NA	NA	NA	0.35	NA	NA	NA	225	NA	40	NA	NA	CM	37
EMS_Treated__000uM-050	NA	NA	NA	NA	0	NA	NA	NA	NA	NA	NA	NA	NA	0.35	NA	NA	NA	225	NA	50	NA	NA	CM	37
EMS_Treated__000uM-060	NA	NA	NA	NA	0	NA	NA	NA	NA	NA	NA	NA	NA	0.32	NA	NA	NA	225	NA	60	NA	NA	CM	37
EMS_Treated__000uM-120	NA	NA	NA	NA	0	NA	NA	NA	NA	NA	NA	NA	NA	0.36	NA	NA	NA	225	NA	120	NA	NA	CM	37
circadian__dark_cycling_125w/m2_42C_1440min_vs_NRC-1d.sig	NA	NA	NA	NA	NA	NA	NA	NA	NA	150	NA	NA	NA	0.37	NA	NA	NA	125	NA	1440	NA	NA	CM	42
circadian__dark_cycling_125w/m2_42C_1615min_vs_NRC-1d.sig	NA	NA	NA	NA	NA	NA	NA	NA	NA	150	NA	NA	NA	0.41	NA	NA	NA	125	NA	1615	NA	NA	CM	42
circadian__dark_cycling_125w/m2_42C_1800min_vs_NRC-1d.sig	NA	NA	NA	NA	NA	NA	NA	NA	NA	150	NA	NA	NA	0.47	NA	NA	NA	125	NA	1800	NA	NA	CM	42
circadian__dark_cycling_125w/m2_42C_1985min_vs_NRC-1d.sig	NA	NA	NA	NA	NA	NA	NA	NA	NA	150	NA	NA	NA	0.42	NA	NA	NA	125	NA	1985	NA	NA	CM	42
circadian__dark_cycling_125w/m2_42C_2160min_vs_NRC-1d.sig	NA	NA	NA	NA	NA	NA	NA	NA	NA	0	NA	NA	NA	0.5	NA	NA	NA	125	NA	2160	NA	NA	CM	42
circadian__dark_cycling_125w/m2_42C_2340min_vs_NRC-1d.sig	NA	NA	NA	NA	NA	NA	NA	NA	NA	0	NA	NA	NA	0.56	NA	NA	NA	125	NA	2340	NA	NA	CM	42
circadian__dark_cycling_125w/m2_42C_2515min_vs_NRC-1d.sig	NA	NA	NA	NA	NA	NA	NA	NA	NA	0	NA	NA	NA	0.57	NA	NA	NA	125	NA	2515	NA	NA	CM	42

circadian__dark_cycling_125w/m2_42C_2705min_vs_NRC-1d.sig	NA	NA	NA	NA	NA	NA	NA	NA	NA	0	NA	NA	NA	0.75	NA	NA	NA	125	NA	2705	NA	NA	CM	42
circadian__dark_cycling_125w/m2_42C_2880min_vs_NRC-1d.sig	NA	NA	NA	NA	NA	NA	NA	NA	NA	150	NA	NA	NA	0.86	NA	NA	NA	125	NA	2880	NA	NA	CM	42
NRC-1b_vs_NRC-1a.sig	NA	NA	NA	NA	NA	NA	NA	NA	NA	NA	NA	NA	NA	0.85	NA	NA	NA	225	NA	NA	NA	NA	CM	37
NRC-1_vs_NRC-1c.sig	NA	NA	NA	NA	NA	NA	NA	NA	NA	NA	NA	NA	NA	0.84	NA	NA	NA	225	NA	NA	NA	NA	CM	37
NRC-1c_vs_NRC-1d.sig	NA	NA	NA	NA	NA	NA	NA	NA	NA	NA	NA	NA	NA	0.73	NA	NA	NA	225	NA	NA	NA	NA	CM	37
bop__HO_D_vs_NRC-1	NA	NA	NA	NA	NA	NA	NA	NA	NA	0	NA	NA	NA	0.8	NA	NA	NA	220	NA	NA	NA	NA	CM	37
bop__HO_L_vs_NRC-1	NA	NA	NA	NA	NA	NA	NA	NA	NA	35	NA	NA	NA	0.8	NA	NA	NA	220	NA	NA	NA	NA	CM	37
bop__LO_D_vs_NRC-1	NA	NA	NA	NA	NA	NA	NA	NA	NA	0	NA	NA	NA	0.76	NA	NA	NA	100	NA	NA	NA	NA	CM	37
bop__LO_L_vs_NRC-1	NA	NA	NA	NA	NA	NA	NA	NA	NA	35	NA	NA	NA	0.81	NA	NA	NA	100	NA	NA	NA	NA	CM	37
boa4__HO_D_vs_NRC-1	NA	NA	NA	NA	NA	NA	NA	NA	NA	0	NA	NA	NA	0.74	NA	NA	NA	220	NA	NA	NA	NA	CM	37
boa4__HO_L_vs_NRC-1	NA	NA	NA	NA	NA	NA	NA	NA	NA	35	NA	NA	NA	0.64	NA	NA	NA	220	NA	NA	NA	NA	CM	37
boa4__LO_D_vs_NRC-1	NA	NA	NA	NA	NA	NA	NA	NA	NA	0	NA	NA	NA	0.71	NA	NA	NA	100	NA	NA	NA	NA	CM	37
boa4__LO_L_vs_NRC-1	NA	NA	NA	NA	NA	NA	NA	NA	NA	35	NA	NA	NA	0.72	NA	NA	NA	100	NA	NA	NA	NA	CM	37
boa1__HO_D_vs_NRC-1	NA	NA	NA	NA	NA	NA	NA	NA	NA	0	NA	NA	NA	0.75	NA	NA	NA	220	NA	NA	NA	NA	CM	37
boa1__HO_L_vs_NRC-1	NA	NA	NA	NA	NA	NA	NA	NA	NA	35	NA	NA	NA	0.73	NA	NA	NA	220	NA	NA	NA	NA	CM	37
boa1__LO_D_vs_NRC-1	NA	NA	NA	NA	NA	NA	NA	NA	NA	0	NA	NA	NA	0.76	NA	NA	NA	100	NA	NA	NA	NA	CM	37
boa1__LO_L_vs_NRC-1	NA	NA	NA	NA	NA	NA	NA	NA	NA	35	NA	NA	NA	0.74	NA	NA	NA	100	NA	NA	NA	NA	CM	37
ark__HO_D_vs_NRC-1	NA	NA	NA	NA	NA	NA	NA	NA	NA	0	NA	NA	NA	0.69	NA	NA	NA	220	NA	NA	NA	NA	CM	37
ark__HO_L_vs_NRC-1	NA	NA	NA	NA	NA	NA	NA	NA	NA	35	NA	NA	NA	0.63	NA	NA	NA	220	NA	NA	NA	NA	CM	37
ark__LO_D_vs_NRC-1	NA	NA	NA	NA	NA	NA	NA	NA	NA	0	NA	NA	NA	0.65	NA	NA	NA	100	NA	NA	NA	NA	CM	37
ark__LO_L_vs_NRC-1	NA	NA	NA	NA	NA	NA	NA	NA	NA	35	NA	NA	NA	0.67	NA	NA	NA	100	NA	NA	NA	NA	CM	37
afsQ2__HO_D_vs_NRC-1	NA	NA	NA	NA	NA	NA	NA	NA	NA	0	NA	NA	NA	0.8	NA	NA	NA	220	NA	NA	NA	NA	CM	37

afsQ2__HO_L_vs_NRC-1	NA	NA	NA	NA	NA	NA	NA	NA	NA	35	NA	NA	NA	0.72	NA	NA	NA	220	NA	NA	NA	NA	CM	37
afsQ2__LO_D_vs_NRC-1	NA	NA	NA	NA	NA	NA	NA	NA	NA	0	NA	NA	NA	0.74	NA	NA	NA	100	NA	NA	NA	NA	CM	37
afsQ2__LO_L_vs_NRC-1	NA	NA	NA	NA	NA	NA	NA	NA	NA	35	NA	NA	NA	0.72	NA	NA	NA	100	NA	NA	NA	NA	CM	37
NRC1_H2O_0540_0.220_rep2_vs_NRC-1g.sig	NA	NA	NA	NA	NA	NA	NA	NA	NA	NA	NA	NA	NA	0.22	NA	NA	NA	225	NA	540	NA	NA	CM	37
NRC1_H2O_0890_0.468_rep2_vs_NRC-1g.sig	NA	NA	NA	NA	NA	NA	NA	NA	NA	NA	NA	NA	NA	0.47	NA	NA	NA	225	NA	890	NA	NA	CM	37
NRC1_H2O_1260_0.830_rep2_vs_NRC-1g.sig	NA	NA	NA	NA	NA	NA	NA	NA	NA	NA	NA	NA	NA	0.83	NA	NA	NA	225	NA	1260	NA	NA	CM	37
NRC1_H2O_1860_0.733_rep2_vs_NRC-1g.sig	NA	NA	NA	NA	NA	NA	NA	NA	NA	NA	NA	NA	NA	0.73	NA	NA	NA	225	NA	1860	NA	NA	CM	37
NRC1_H2O_2280_0.764_rep2_vs_NRC-1g.sig	NA	NA	NA	NA	NA	NA	NA	NA	NA	NA	NA	NA	NA	0.76	NA	NA	NA	225	NA	2280	NA	NA	CM	37
NRC1_H2O_2760_0.913_rep2_vs_NRC-1g.sig	NA	NA	NA	NA	NA	NA	NA	NA	NA	NA	NA	NA	NA	0.91	NA	NA	NA	225	NA	2760	NA	NA	CM	37
NRC1_H2O_3120_1.086_rep2_vs_NRC-1g.sig	NA	NA	NA	NA	NA	NA	NA	NA	NA	NA	NA	NA	NA	1.09	NA	NA	NA	225	NA	3120	NA	NA	CM	37
NRC1_H2O_0540_0.225_rep1_vs_NRC-1g.sig	NA	NA	NA	NA	NA	NA	NA	NA	NA	NA	NA	NA	NA	0.23	NA	NA	NA	225	NA	540	NA	NA	CM	37
NRC1_H2O_0890_0.496_rep1_vs_NRC-1g.sig	NA	NA	NA	NA	NA	NA	NA	NA	NA	NA	NA	NA	NA	0.5	NA	NA	NA	225	NA	890	NA	NA	CM	37
NRC1_H2O_1260_0.807_rep1_vs_NRC-1g.sig	NA	NA	NA	NA	NA	NA	NA	NA	NA	NA	NA	NA	NA	0.81	NA	NA	NA	225	NA	1260	NA	NA	CM	37
NRC1_H2O_1860_0.758_rep1_vs_NRC-1g.sig	NA	NA	NA	NA	NA	NA	NA	NA	NA	NA	NA	NA	NA	0.76	NA	NA	NA	225	NA	1860	NA	NA	CM	37
NRC1_H2O_2280_0.781_rep1_vs_NRC-1g.sig	NA	NA	NA	NA	NA	NA	NA	NA	NA	NA	NA	NA	NA	0.78	NA	NA	NA	225	NA	2280	NA	NA	CM	37
NRC1_H2O_2760_0.913_rep1_vs_NRC-1g.sig	NA	NA	NA	NA	NA	NA	NA	NA	NA	NA	NA	NA	NA	0.91	NA	NA	NA	225	NA	2760	NA	NA	CM	37
NRC1_H2O_3120_1.023_rep1_vs_NRC-1g.sig	NA	NA	NA	NA	NA	NA	NA	NA	NA	NA	NA	NA	NA	1.02	NA	NA	NA	225	NA	3120	NA	NA	CM	37

NRC1_Uracil_0540_0.205_rep2_vs_NRC-1g.sig	NA	NA	NA	NA	NA	NA	NA	NA	NA	NA	NA	NA	NA	0.21	NA	NA	NA	225	NA	540	NA	NA	CM	37
NRC1_Uracil_0890_0.420_rep2_vs_NRC-1g.sig	NA	NA	NA	NA	NA	NA	NA	NA	NA	NA	NA	NA	NA	0.42	NA	NA	NA	225	NA	890	NA	NA	CM	37
NRC1_Uracil_1260_0.812_rep2_vs_NRC-1g.sig	NA	NA	NA	NA	NA	NA	NA	NA	NA	NA	NA	NA	NA	0.81	NA	NA	NA	225	NA	1260	NA	NA	CM	37
NRC1_Uracil_1860_0.912_rep2_vs_NRC-1g.sig	NA	NA	NA	NA	NA	NA	NA	NA	NA	NA	NA	NA	NA	0.91	NA	NA	NA	225	NA	1860	NA	NA	CM	37
NRC1_Uracil_2280_0.881_rep2_vs_NRC-1g.sig	NA	NA	NA	NA	NA	NA	NA	NA	NA	NA	NA	NA	NA	0.88	NA	NA	NA	225	NA	2280	NA	NA	CM	37
NRC1_Uracil_2760_1.133_rep2_vs_NRC-1g.sig	NA	NA	NA	NA	NA	NA	NA	NA	NA	NA	NA	NA	NA	1.13	NA	NA	NA	225	NA	2760	NA	NA	CM	37
NRC1_Uracil_3120_1.296_rep2_vs_NRC-1g.sig	NA	NA	NA	NA	NA	NA	NA	NA	NA	NA	NA	NA	NA	1.3	NA	NA	NA	225	NA	3120	NA	NA	CM	37
NRC1_Uracil_0540_0.200_rep1_vs_NRC-1g.sig	NA	NA	NA	NA	NA	NA	NA	NA	NA	NA	NA	NA	NA	0.2	NA	NA	NA	225	NA	540	NA	NA	CM	37
NRC1_Uracil_0890_0.440_rep1_vs_NRC-1g.sig	NA	NA	NA	NA	NA	NA	NA	NA	NA	NA	NA	NA	NA	0.44	NA	NA	NA	225	NA	890	NA	NA	CM	37
NRC1_Uracil_1260_0.785_rep1_vs_NRC-1g.sig	NA	NA	NA	NA	NA	NA	NA	NA	NA	NA	NA	NA	NA	0.79	NA	NA	NA	225	NA	1260	NA	NA	CM	37
NRC1_Uracil_1860_0.882_rep1_vs_NRC-1g.sig	NA	NA	NA	NA	NA	NA	NA	NA	NA	NA	NA	NA	NA	0.88	NA	NA	NA	225	NA	1860	NA	NA	CM	37
NRC1_Uracil_2280_0.876_rep1_vs_NRC-1g.sig	NA	NA	NA	NA	NA	NA	NA	NA	NA	NA	NA	NA	NA	0.88	NA	NA	NA	225	NA	2280	NA	NA	CM	37
NRC1_Uracil_2760_1.039_rep1_vs_NRC-1g.sig	NA	NA	NA	NA	NA	NA	NA	NA	NA	NA	NA	NA	NA	1.04	NA	NA	NA	225	NA	2760	NA	NA	CM	37
NRC1_Uracil_3120_1.341_rep1_vs_NRC-1g.sig	NA	NA	NA	NA	NA	NA	NA	NA	NA	NA	NA	NA	NA	1.34	NA	NA	NA	225	NA	3120	NA	NA	CM	37
Dura3_Uracil_0690_0.200_rep2_vs_NRC-1g.sig	NA	NA	NA	NA	NA	NA	NA	NA	NA	NA	NA	NA	NA	0.2	NA	NA	NA	225	NA	690	NA	NA	CM	37
Dura3_Uracil_1200_0.467_rep2_vs_NRC-1g.sig	NA	NA	NA	NA	NA	NA	NA	NA	NA	NA	NA	NA	NA	0.47	NA	NA	NA	225	NA	1200	NA	NA	CM	37

Dura3_Uracil_1860_0.756_rep2_vs_NRC-1g.sig	NA	NA	NA	NA	NA	NA	NA	NA	NA	NA	NA	NA	NA	0.76	NA	NA	NA	225	NA	1860	NA	NA	CM	37
Dura3_Uracil_2280_0.830_rep2_vs_NRC-1g.sig	NA	NA	NA	NA	NA	NA	NA	NA	NA	NA	NA	NA	NA	0.83	NA	NA	NA	225	NA	2280	NA	NA	CM	37
Dura3_Uracil_2760_0.970_rep2_vs_NRC-1g.sig	NA	NA	NA	NA	NA	NA	NA	NA	NA	NA	NA	NA	NA	0.97	NA	NA	NA	225	NA	2760	NA	NA	CM	37
Dura3_Uracil_3120_1.147_rep2_vs_NRC-1g.sig	NA	NA	NA	NA	NA	NA	NA	NA	NA	NA	NA	NA	NA	1.15	NA	NA	NA	225	NA	3120	NA	NA	CM	37
Dura3_Uracil_0690_0.197_rep1_vs_NRC-1g.sig	NA	NA	NA	NA	NA	NA	NA	NA	NA	NA	NA	NA	NA	0.2	NA	NA	NA	225	NA	690	NA	NA	CM	37
Dura3_Uracil_1200_0.465_rep1_vs_NRC-1g.sig	NA	NA	NA	NA	NA	NA	NA	NA	NA	NA	NA	NA	NA	0.47	NA	NA	NA	225	NA	1200	NA	NA	CM	37
Dura3_Uracil_1860_0.755_rep1_vs_NRC-1g.sig	NA	NA	NA	NA	NA	NA	NA	NA	NA	NA	NA	NA	NA	0.76	NA	NA	NA	225	NA	1860	NA	NA	CM	37
Dura3_Uracil_2280_0.832_rep1_vs_NRC-1g.sig	NA	NA	NA	NA	NA	NA	NA	NA	NA	NA	NA	NA	NA	0.83	NA	NA	NA	225	NA	2280	NA	NA	CM	37
Dura3_Uracil_2760_0.975_rep1_vs_NRC-1g.sig	NA	NA	NA	NA	NA	NA	NA	NA	NA	NA	NA	NA	NA	0.98	NA	NA	NA	225	NA	2760	NA	NA	CM	37
Dura3_Uracil_3120_1.136_rep1_vs_NRC-1g.sig	NA	NA	NA	NA	NA	NA	NA	NA	NA	NA	NA	NA	NA	1.14	NA	NA	NA	225	NA	3120	NA	NA	CM	37
Dun_F2_000minb_vs_NRC-1g.sig	NA	NA	NA	NA	NA	NA	NA	NA	NA	120	NA	NA	NA	Get from Monica	NA	NA	NA	80	NA	0	NA	NA	MM1	30
Dun_F2_005minb_vs_NRC-1g.sig	NA	NA	NA	NA	NA	NA	NA	NA	NA	120	NA	NA	NA	Get from Monica	NA	NA	NA	80	NA	5	NA	NA	MM1	30
Dun_F2_010minb_vs_NRC-1g.sig	NA	NA	NA	NA	NA	NA	NA	NA	NA	120	NA	NA	NA	Get from Monica	NA	NA	NA	80	NA	10	NA	NA	MM1	30
Dun_F2_020minb_vs_NRC-1g.sig	NA	NA	NA	NA	NA	NA	NA	NA	NA	120	NA	NA	NA	Get from Mo	NA	NA	NA	80	NA	20	NA	NA	MM1	30

														nica										
Dun_F2_040minb_vs_NRC-1g.sig	NA	NA	NA	NA	NA	NA	NA	NA	NA	120	NA	NA	NA	Get from Monica	NA	NA	NA	80	NA	40	NA	NA	MM1	30
Dun_F2_080minb_vs_NRC-1g.sig	NA	NA	NA	NA	NA	NA	NA	NA	NA	120	NA	NA	NA	Get from Monica	NA	NA	NA	80	NA	80	NA	NA	MM1	30
Dun_F2_160minb_vs_NRC-1g.sig	NA	NA	NA	NA	NA	NA	NA	NA	NA	120	NA	NA	NA	Get from Monica	NA	NA	NA	80	NA	160	NA	NA	MM1	30
Dun_F2_320minb_vs_NRC-1g.sig	NA	NA	NA	NA	NA	NA	NA	NA	NA	120	NA	NA	NA	Get from Monica	NA	NA	NA	80	NA	320	NA	NA	MM1	30
NRC-1f_vs_NRC-1g.sig	NA	NA	NA	NA	NA	NA	NA	NA	NA	NA	NA	NA	NA	0.67	NA	NA	NA	225	NA	NA	NA	NA	CM	37
NRC1_03720_0.234_rep2_vs_NRC-1g.sig	NA	NA	NA	NA	NA	NA	NA	NA	NA	150	NA	NA	NA	0.23	NA	NA	NA	125	NA	3720	NA	NA	CM	37
NRC1_03960_0.409_rep2_vs_NRC-1g.sig	NA	NA	NA	NA	NA	NA	NA	NA	NA	150	NA	NA	NA	0.41	NA	NA	NA	125	NA	3960	NA	NA	CM	37
NRC1_04320_0.578_rep2_vs_NRC-1g.sig	NA	NA	NA	NA	NA	NA	NA	NA	NA	150	NA	NA	NA	0.58	NA	NA	NA	125	NA	4320	NA	NA	CM	37
NRC1_04476_0.715_rep2_vs_NRC-1g.sig	NA	NA	NA	NA	NA	NA	NA	NA	NA	150	NA	NA	NA	0.72	NA	NA	NA	125	NA	4476	NA	NA	CM	37
NRC1_05400_0.786_rep2_vs_NRC-1g.sig	NA	NA	NA	NA	NA	NA	NA	NA	NA	150	NA	NA	NA	0.79	NA	NA	NA	125	NA	5400	NA	NA	CM	37
NRC1_05778_0.722_rep2_vs_NRC-1g.sig	NA	NA	NA	NA	NA	NA	NA	NA	NA	150	NA	NA	NA	0.72	NA	NA	NA	125	NA	5778	NA	NA	CM	37
NRC1_07020_1.318_rep2_vs_NRC-1g.sig	NA	NA	NA	NA	NA	NA	NA	NA	NA	150	NA	NA	NA	1.32	NA	NA	NA	125	NA	7020	NA	NA	CM	37
NRC1_07740_2.681_rep2_vs_NRC-1g.sig	NA	NA	NA	NA	NA	NA	NA	NA	NA	150	NA	NA	NA	2.68	NA	NA	NA	125	NA	7740	NA	NA	CM	37

NRC1_08460_3.840_rep2_vs_NRC-1g.sig	NA	NA	NA	NA	NA	NA	NA	NA	NA	150	NA	NA	NA	3.84	NA	NA	NA	125	NA	8460	NA	NA	CM	37
NRC1_09540_4.690_rep2_vs_NRC-1g.sig	NA	NA	NA	NA	NA	NA	NA	NA	NA	150	NA	NA	NA	4.69	NA	NA	NA	125	NA	9540	NA	NA	CM	37
NRC1_10260_4.540_rep2_vs_NRC-1g.sig	NA	NA	NA	NA	NA	NA	NA	NA	NA	150	NA	NA	NA	4.54	NA	NA	NA	125	NA	###	NA	NA	CM	37
NRC1_10980_4.935_rep2_vs_NRC-1g.sig	NA	NA	NA	NA	NA	NA	NA	NA	NA	150	NA	NA	NA	4.94	NA	NA	NA	125	NA	###	NA	NA	CM	37
NRC1_11700_5.730_rep2_vs_NRC-1g.sig	NA	NA	NA	NA	NA	NA	NA	NA	NA	150	NA	NA	NA	5.73	NA	NA	NA	125	NA	###	NA	NA	CM	37
NRC1_03720_0.259_rep1_vs_NRC-1g.sig	NA	NA	NA	NA	NA	NA	NA	NA	NA	150	NA	NA	NA	0.26	NA	NA	NA	125	NA	3720	NA	NA	CM	37
NRC1_03960_0.364_rep1_vs_NRC-1g.sig	NA	NA	NA	NA	NA	NA	NA	NA	NA	150	NA	NA	NA	0.36	NA	NA	NA	125	NA	3960	NA	NA	CM	37
NRC1_04320_0.590_rep1_vs_NRC-1g.sig	NA	NA	NA	NA	NA	NA	NA	NA	NA	150	NA	NA	NA	0.59	NA	NA	NA	125	NA	4320	NA	NA	CM	37
NRC1_04476_0.762_rep1_vs_NRC-1g.sig	NA	NA	NA	NA	NA	NA	NA	NA	NA	150	NA	NA	NA	0.76	NA	NA	NA	125	NA	4476	NA	NA	CM	37
NRC1_05400_0.803_rep1_vs_NRC-1g.sig	NA	NA	NA	NA	NA	NA	NA	NA	NA	150	NA	NA	NA	0.8	NA	NA	NA	125	NA	5400	NA	NA	CM	37
NRC1_05778_0.710_rep1vs_NRC-1g.sig	NA	NA	NA	NA	NA	NA	NA	NA	NA	150	NA	NA	NA	0.71	NA	NA	NA	125	NA	5778	NA	NA	CM	37
NRC1_07020_1.329_rep1_vs_NRC-1g.sig	NA	NA	NA	NA	NA	NA	NA	NA	NA	150	NA	NA	NA	1.33	NA	NA	NA	125	NA	7020	NA	NA	CM	37
NRC1_07740_2.580_rep1_vs_NRC-1g.sig	NA	NA	NA	NA	NA	NA	NA	NA	NA	150	NA	NA	NA	2.58	NA	NA	NA	125	NA	7740	NA	NA	CM	37
NRC1_08460_3.510_rep1_vs_NRC-1g.sig	NA	NA	NA	NA	NA	NA	NA	NA	NA	150	NA	NA	NA	3.51	NA	NA	NA	125	NA	8460	NA	NA	CM	37
NRC1_09540_4.860_rep1_vs_NRC-1g.sig	NA	NA	NA	NA	NA	NA	NA	NA	NA	150	NA	NA	NA	4.86	NA	NA	NA	125	NA	9540	NA	NA	CM	37
NRC1_10260_4.860_rep1_vs_NRC-1g.sig	NA	NA	NA	NA	NA	NA	NA	NA	NA	150	NA	NA	NA	4.86	NA	NA	NA	125	NA	###	NA	NA	CM	37

NRC1_10980_5.130_rep1_vs_NRC-1g.sig	NA	NA	NA	NA	NA	NA	NA	NA	NA	150	NA	NA	NA	5.13	NA	NA	NA	125	NA	###	NA	NA	CM	37
NRC1_11700_5.640_rep1_vs_NRC-1g.sig	NA	NA	NA	NA	NA	NA	NA	NA	NA	150	NA	NA	NA	5.64	NA	NA	NA	125	NA	###	NA	NA	CM	37
H2O2_Recov._set_3_0mM_000min_vs_NRC-1f.sig	NA	NA	NA	NA	NA	NA	NA	NA	0	NA	NA	NA	NA	0.45	NA	NA	NA	225	NA	0	NA	NA	CM	42
H2O2_Recov._set_3_0mM_010min_vs_NRC-1f.sig	NA	NA	NA	NA	NA	NA	NA	NA	0	NA	NA	NA	NA	0.48	NA	NA	NA	225	NA	10	NA	NA	CM	42
H2O2_Recov._set_3_0mM_020min_vs_NRC-1f.sig	NA	NA	NA	NA	NA	NA	NA	NA	0	NA	NA	NA	NA	0.5	NA	NA	NA	225	NA	20	NA	NA	CM	42
H2O2_Recov._set_3_0mM_030min_vs_NRC-1f.sig	NA	NA	NA	NA	NA	NA	NA	NA	0	NA	NA	NA	NA	0.52	NA	NA	NA	225	NA	30	NA	NA	CM	42
H2O2_Recov._set_3_0mM_040min_vs_NRC-1f.sig	NA	NA	NA	NA	NA	NA	NA	NA	0	NA	NA	NA	NA	0.49	NA	NA	NA	225	NA	40	NA	NA	CM	42
H2O2_Recov._set_3_0mM_050min_vs_NRC-1f.sig	NA	NA	NA	NA	NA	NA	NA	NA	0	NA	NA	NA	NA	0.51	NA	NA	NA	225	NA	50	NA	NA	CM	42
H2O2_Recov._set_3_0mM_060min_vs_NRC-1f.sig	NA	NA	NA	NA	NA	NA	NA	NA	0	NA	NA	NA	NA	0.53	NA	NA	NA	225	NA	60	NA	NA	CM	42
H2O2_Recov._set_3_0mM_120min_vs_NRC-1f.sig	NA	NA	NA	NA	NA	NA	NA	NA	0	NA	NA	NA	NA	0.59	NA	NA	NA	225	NA	120	NA	NA	CM	42
H2O2_Recov._set_3_0mM_240min_vs_NRC-1f.sig	NA	NA	NA	NA	NA	NA	NA	NA	0	NA	NA	NA	NA	0.77	NA	NA	NA	225	NA	240	NA	NA	CM	42
H2O2_Const._set_2_0mM_000min_vs_NRC-1f.sig	NA	NA	NA	NA	NA	NA	NA	NA	0	NA	NA	NA	NA	0.55	NA	NA	NA	225	NA	0	NA	NA	CM	42
H2O2_Const._set_2_0mM_030min_vs_NRC-1f.sig	NA	NA	NA	NA	NA	NA	NA	NA	0	NA	NA	NA	NA	0.54	NA	NA	NA	225	NA	30	NA	NA	CM	42
H2O2_Const._set_2_0mM_060min_vs_NRC-1f.sig	NA	NA	NA	NA	NA	NA	NA	NA	0	NA	NA	NA	NA	0.56	NA	NA	NA	225	NA	60	NA	NA	CM	42
H2O2_Const._set_2_0mM_120min_vs_NRC-1f.sig	NA	NA	NA	NA	NA	NA	NA	NA	0	NA	NA	NA	NA	0.6	NA	NA	NA	225	NA	120	NA	NA	CM	42
H2O2_Const._set_2_0mM_240min_vs_NRC-1f.sig	NA	NA	NA	NA	NA	NA	NA	NA	0	NA	NA	NA	NA	0.65	NA	NA	NA	225	NA	240	NA	NA	CM	42

PQ_Recov._set_2_0mM_000min_vs_NRC-1f.sig	NA	NA	NA	NA	NA	NA	NA	NA	NA	NA	NA	NA	NA	0.43	NA	NA	0	225	NA	0	NA	NA	CM	42
PQ_Recov._set_2_0mM_010min_vs_NRC-1f.sig	NA	NA	NA	NA	NA	NA	NA	NA	NA	NA	NA	NA	NA	0.46	NA	NA	0	225	NA	10	NA	NA	CM	42
PQ_Recov._set_2_0mM_020min_vs_NRC-1f.sig	NA	NA	NA	NA	NA	NA	NA	NA	NA	NA	NA	NA	NA	0.47	NA	NA	0	225	NA	20	NA	NA	CM	42
PQ_Recov._set_2_0mM_030min_vs_NRC-1f.sig	NA	NA	NA	NA	NA	NA	NA	NA	NA	NA	NA	NA	NA	0.47	NA	NA	0	225	NA	30	NA	NA	CM	42
PQ_Recov._set_2_0mM_040min_vs_NRC-1f.sig	NA	NA	NA	NA	NA	NA	NA	NA	NA	NA	NA	NA	NA	0.46	NA	NA	0	225	NA	40	NA	NA	CM	42
PQ_Recov._set_2_0mM_050min_vs_NRC-1f.sig	NA	NA	NA	NA	NA	NA	NA	NA	NA	NA	NA	NA	NA	0.47	NA	NA	0	225	NA	50	NA	NA	CM	42
PQ_Recov._set_2_0mM_060min_vs_NRC-1f.sig	NA	NA	NA	NA	NA	NA	NA	NA	NA	NA	NA	NA	NA	0.48	NA	NA	0	225	NA	60	NA	NA	CM	42
PQ_Recov._set_2_0mM_120min_vs_NRC-1f.sig	NA	NA	NA	NA	NA	NA	NA	NA	NA	NA	NA	NA	NA	0.56	NA	NA	0	225	NA	120	NA	NA	CM	42
PQ_Recov._set_2_0mM_240min_vs_NRC-1f.sig	NA	NA	NA	NA	NA	NA	NA	NA	NA	NA	NA	NA	NA	0.71	NA	NA	0	225	NA	240	NA	NA	CM	42
PQ_Const._set_2_0mM_000min_vs_NRC-1f.sig	NA	NA	NA	NA	NA	NA	NA	NA	NA	NA	NA	NA	NA	0.53	NA	NA	0	225	NA	0	NA	NA	CM	42
PQ_Const._set_2_0mM_030min_vs_NRC-1f.sig	NA	NA	NA	NA	NA	NA	NA	NA	NA	NA	NA	NA	NA	0.55	NA	NA	0	225	NA	30	NA	NA	CM	42
PQ_Const._set_2_0mM_060min_vs_NRC-1f.sig	NA	NA	NA	NA	NA	NA	NA	NA	NA	NA	NA	NA	NA	0.58	NA	NA	0	225	NA	60	NA	NA	CM	42
PQ_Const._set_2_0mM_120min_vs_NRC-1f.sig	NA	NA	NA	NA	NA	NA	NA	NA	NA	NA	NA	NA	NA	0.63	NA	NA	0	225	NA	120	NA	NA	CM	42
PQ_Const._set_2_0mM_240min_vs_NRC-1f.sig	NA	NA	NA	NA	NA	NA	NA	NA	NA	NA	NA	NA	NA	0.71	NA	NA	0	225	NA	240	NA	NA	CM	42
H2O2_Recov._set_2_0mM_000min_vs_NRC-1f.sig	NA	NA	NA	NA	NA	NA	NA	NA	0	NA	NA	NA	NA	0.42	NA	NA	NA	225	NA	0	NA	NA	CM	42
H2O2_Recov._set_2_0mM_010min_vs_NRC-1f.sig	NA	NA	NA	NA	NA	NA	NA	NA	0	NA	NA	NA	NA	0.45	NA	NA	NA	225	NA	10	NA	NA	CM	42

H2O2_Recov._set_2_0mM_020min_vs_NRC-1f.sig	NA	NA	NA	NA	NA	NA	NA	NA	0	NA	NA	NA	NA	0.43	NA	NA	NA	225	NA	20	NA	NA	CM	42
H2O2_Recov._set_2_0mM_030min_vs_NRC-1f.sig	NA	NA	NA	NA	NA	NA	NA	NA	0	NA	NA	NA	NA	0.45	NA	NA	NA	225	NA	30	NA	NA	CM	42
H2O2_Recov._set_2_0mM_040min_vs_NRC-1f.sig	NA	NA	NA	NA	NA	NA	NA	NA	0	NA	NA	NA	NA	0.45	NA	NA	NA	225	NA	40	NA	NA	CM	42
H2O2_Recov._set_2_0mM_050min_vs_NRC-1f.sig	NA	NA	NA	NA	NA	NA	NA	NA	0	NA	NA	NA	NA	0.48	NA	NA	NA	225	NA	50	NA	NA	CM	42
H2O2_Recov._set_2_0mM_060min_vs_NRC-1f.sig	NA	NA	NA	NA	NA	NA	NA	NA	0	NA	NA	NA	NA	0.47	NA	NA	NA	225	NA	60	NA	NA	CM	42
H2O2_Recov._set_2_0mM_120min_vs_NRC-1f.sig	NA	NA	NA	NA	NA	NA	NA	NA	0	NA	NA	NA	NA	0.52	NA	NA	NA	225	NA	120	NA	NA	CM	42
H2O2_Recov._set_2_0mM_240min_vs_NRC-1f.sig	NA	NA	NA	NA	NA	NA	NA	NA	0	NA	NA	NA	NA	0.62	NA	NA	NA	225	NA	240	NA	NA	CM	42
H2O2_Const._set_1_0mM_000min_vs_NRC-1f.sig	NA	NA	NA	NA	NA	NA	NA	NA	0	NA	NA	NA	NA	0.54	NA	NA	NA	225	NA	0	NA	NA	CM	42
H2O2_Const._set_1_0mM_030min_vs_NRC-1f.sig	NA	NA	NA	NA	NA	NA	NA	NA	0	NA	NA	NA	NA	0.54	NA	NA	NA	225	NA	30	NA	NA	CM	42
H2O2_Const._set_1_0mM_060min_vs_NRC-1f.sig	NA	NA	NA	NA	NA	NA	NA	NA	0	NA	NA	NA	NA	0.56	NA	NA	NA	225	NA	60	NA	NA	CM	42
H2O2_Const._set_1_0mM_120min_vs_NRC-1f.sig	NA	NA	NA	NA	NA	NA	NA	NA	0	NA	NA	NA	NA	0.58	NA	NA	NA	225	NA	120	NA	NA	CM	42
H2O2_Const._set_1_0mM_240min_vs_NRC-1f.sig	NA	NA	NA	NA	NA	NA	NA	NA	0	NA	NA	NA	NA	0.62	NA	NA	NA	225	NA	240	NA	NA	CM	42
PQ_Recov._set_1_0mM_000min_vs_NRC-1f.sig	NA	NA	NA	NA	NA	NA	NA	NA	NA	NA	NA	NA	NA	0.49	NA	NA	0	225	NA	0	NA	NA	CM	42
PQ_Recov._set_1_0mM_010min_vs_NRC-1f.sig	NA	NA	NA	NA	NA	NA	NA	NA	NA	NA	NA	NA	NA	0.51	NA	NA	0	225	NA	10	NA	NA	CM	42
PQ_Recov._set_1_0mM_020min_vs_NRC-1f.sig	NA	NA	NA	NA	NA	NA	NA	NA	NA	NA	NA	NA	NA	0.51	NA	NA	0	225	NA	20	NA	NA	CM	42
PQ_Recov._set_1_0mM_030min_vs_NRC-1f.sig	NA	NA	NA	NA	NA	NA	NA	NA	NA	NA	NA	NA	NA	0.52	NA	NA	0	225	NA	30	NA	NA	CM	42

PQ_Recov._set_1_0mM_040min_vs_NRC-1f.sig	NA	NA	NA	NA	NA	NA	NA	NA	NA	NA	NA	NA	NA	0.51	NA	NA	0	225	NA	40	NA	NA	CM	42
PQ_Recov._set_1_0mM_050min_vs_NRC-1f.sig	NA	NA	NA	NA	NA	NA	NA	NA	NA	NA	NA	NA	NA	0.54	NA	NA	0	225	NA	50	NA	NA	CM	42
PQ_Recov._set_1_0mM_060min_vs_NRC-1f.sig	NA	NA	NA	NA	NA	NA	NA	NA	NA	NA	NA	NA	NA	0.54	NA	NA	0	225	NA	60	NA	NA	CM	42
PQ_Recov._set_1_0mM_120min_vs_NRC-1f.sig	NA	NA	NA	NA	NA	NA	NA	NA	NA	NA	NA	NA	NA	0.61	NA	NA	0	225	NA	120	NA	NA	CM	42
PQ_Recov._set_1_0mM_240min_vs_NRC-1f.sig	NA	NA	NA	NA	NA	NA	NA	NA	NA	NA	NA	NA	NA	0.76	NA	NA	0	225	NA	240	NA	NA	CM	42
PQ_Const._set_1_0mM_000min_vs_NRC-1f.sig	NA	NA	NA	NA	NA	NA	NA	NA	NA	NA	NA	NA	NA	0.53	NA	NA	0	225	NA	0	NA	NA	CM	42
PQ_Const._set_1_0mM_030min_vs_NRC-1f.sig	NA	NA	NA	NA	NA	NA	NA	NA	NA	NA	NA	NA	NA	0.54	NA	NA	0	225	NA	30	NA	NA	CM	42
PQ_Const._set_1_0mM_060min_vs_NRC-1f.sig	NA	NA	NA	NA	NA	NA	NA	NA	NA	NA	NA	NA	NA	0.57	NA	NA	0	225	NA	60	NA	NA	CM	42
PQ_Const._set_1_0mM_120min_vs_NRC-1f.sig	NA	NA	NA	NA	NA	NA	NA	NA	NA	NA	NA	NA	NA	0.62	NA	NA	0	225	NA	120	NA	NA	CM	42
PQ_Const._set_1_0mM_240min_vs_NRC-1f.sig	NA	NA	NA	NA	NA	NA	NA	NA	NA	NA	NA	NA	NA	0.7	NA	NA	0	225	NA	240	NA	NA	CM	42
MDM200gSalt_0.199_vs_NRC-1e.sig	NA	NA	NA	NA	NA	NA	NA	NA	NA	NA	NA	NA	NA	0.2	NA	NA	NA	225	NA	840	NA	NA	CM	37
MDM200gSalt_0.388_vs_NRC-1e.sig	NA	NA	NA	NA	NA	NA	NA	NA	NA	NA	NA	NA	NA	0.39	NA	NA	NA	225	NA	1560	NA	NA	CM	37
MDM200gSalt_0.466_vs_NRC-1e.sig	NA	NA	NA	NA	NA	NA	NA	NA	NA	NA	NA	NA	NA	0.47	NA	NA	NA	225	NA	2100	NA	NA	CM	37
MDM200gSalt_0.534_vs_NRC-1e.sig	NA	NA	NA	NA	NA	NA	NA	NA	NA	NA	NA	NA	NA	0.53	NA	NA	NA	225	NA	2700	NA	NA	CM	37
20060818_NRC1_rep2_0.194_vs_NRC-1e.sig	NA	NA	NA	NA	NA	NA	NA	NA	NA	NA	NA	NA	NA	0.19	NA	NA	NA	225	NA	330	NA	NA	CM	37
20060818_NRC1_rep2_0.424_vs_NRC-1e.sig	NA	NA	NA	NA	NA	NA	NA	NA	NA	NA	NA	NA	NA	0.42	NA	NA	NA	225	NA	630	NA	NA	CM	37
20060818_NRC1_rep2_0.821_vs_NRC-1e.sig	NA	NA	NA	NA	NA	NA	NA	NA	NA	NA	NA	NA	NA	0.82	NA	NA	NA	225	NA	1050	NA	NA	CM	37

20060818_NRC1_rep1_0.195_vs_NRC-1e.sig	NA	NA	NA	NA	NA	NA	NA	NA	NA	NA	NA	NA	NA	0.2	NA	NA	NA	225	NA	330	NA	NA	CM	37
20060818_NRC1_rep1_0.430_vs_NRC-1e.sig	NA	NA	NA	NA	NA	NA	NA	NA	NA	NA	NA	NA	NA	0.43	NA	NA	NA	225	NA	630	NA	NA	CM	37
20060818_NRC1_rep1_0.816_vs_NRC-1e.sig	NA	NA	NA	NA	NA	NA	NA	NA	NA	NA	NA	NA	NA	0.82	NA	NA	NA	225	NA	1050	NA	NA	CM	37
H2O2_Const._set_3_25mM_-001min_vs_NRC-1h1.sig	NA	NA	NA	NA	NA	NA	NA	NA	0	NA	NA	NA	NA	NA	NA	NA	NA	225	NA	-1	NA	NA	CM	37
H2O2_Const._set_3_25mM_005min_vs_NRC-1h1.sig	NA	NA	NA	NA	NA	NA	NA	NA	0.03	NA	NA	NA	NA	NA	NA	NA	NA	225	NA	5	NA	NA	CM	37
H2O2_Const._set_3_25mM_010min_vs_NRC-1h1.sig	NA	NA	NA	NA	NA	NA	NA	NA	0.03	NA	NA	NA	NA	NA	NA	NA	NA	225	NA	10	NA	NA	CM	37
H2O2_Const._set_3_25mM_020min_vs_NRC-1h1.sig	NA	NA	NA	NA	NA	NA	NA	NA	0.03	NA	NA	NA	NA	NA	NA	NA	NA	225	NA	20	NA	NA	CM	37
H2O2_Const._set_3_25mM_040min_vs_NRC-1h1.sig	NA	NA	NA	NA	NA	NA	NA	NA	0.03	NA	NA	NA	NA	NA	NA	NA	NA	225	NA	40	NA	NA	CM	37
H2O2_Const._set_3_25mM_080min_vs_NRC-1h1.sig	NA	NA	NA	NA	NA	NA	NA	NA	0.03	NA	NA	NA	NA	NA	NA	NA	NA	225	NA	80	NA	NA	CM	37
H2O2_Const._set_3_25mM_160min_vs_NRC-1h1.sig	NA	NA	NA	NA	NA	NA	NA	NA	0.03	NA	NA	NA	NA	NA	NA	NA	NA	225	NA	160	NA	NA	CM	37
H2O2_Const._set_4_25mM_-001min_vs_NRC-1h1.sig	NA	NA	NA	NA	NA	NA	NA	NA	0	NA	NA	NA	NA	NA	NA	NA	NA	225	NA	-1	NA	NA	CM	37
H2O2_Const._set_4_25mM_005min_vs_NRC-1h1.sig	NA	NA	NA	NA	NA	NA	NA	NA	0.03	NA	NA	NA	NA	NA	NA	NA	NA	225	NA	5	NA	NA	CM	37
H2O2_Const._set_4_25mM_010min_vs_NRC-1h1.sig	NA	NA	NA	NA	NA	NA	NA	NA	0.03	NA	NA	NA	NA	NA	NA	NA	NA	225	NA	10	NA	NA	CM	37
H2O2_Const._set_4_25mM_020min_vs_NRC-1h1.sig	NA	NA	NA	NA	NA	NA	NA	NA	0.03	NA	NA	NA	NA	NA	NA	NA	NA	225	NA	20	NA	NA	CM	37
H2O2_Const._set_4_25mM_040min_vs_NRC-1h1.sig	NA	NA	NA	NA	NA	NA	NA	NA	0.03	NA	NA	NA	NA	NA	NA	NA	NA	225	NA	40	NA	NA	CM	37
H2O2_Const._set_4_25mM_080min_v	NA	NA	NA	NA	NA	NA	NA	NA	0.03	NA	NA	NA	NA	NA	NA	NA	NA	225	NA	80	NA	NA	CM	37

s_NRC-1h1.sig																								
H2O2_Const._set_4_25mM_160min_vs_NRC-1h1.sig	NA	NA	NA	NA	NA	NA	NA	NA	0.03	NA	NA	NA	NA	NA	NA	NA	NA	225	NA	160	NA	NA	CM	37
PQ_Const._set_3_4mM_-001min_vs_NRC-1h1.sig	NA	NA	NA	NA	NA	NA	NA	NA	NA	NA	NA	NA	NA	NA	NA	NA	NA	0	225	NA	-1	NA	NA	CM	37
PQ_Const._set_3_4mM_005min_vs_NRC-1h1.sig	NA	NA	NA	NA	NA	NA	NA	NA	NA	NA	NA	NA	NA	NA	NA	NA	NA	0	225	NA	5	NA	NA	CM	37
PQ_Const._set_3_4mM_010min_vs_NRC-1h1.sig	NA	NA	NA	NA	NA	NA	NA	NA	NA	NA	NA	NA	NA	NA	NA	NA	NA	0	225	NA	10	NA	NA	CM	37
PQ_Const._set_3_4mM_020min_vs_NRC-1h1.sig	NA	NA	NA	NA	NA	NA	NA	NA	NA	NA	NA	NA	NA	NA	NA	NA	NA	0	225	NA	20	NA	NA	CM	37
PQ_Const._set_3_4mM_040min_vs_NRC-1h1.sig	NA	NA	NA	NA	NA	NA	NA	NA	NA	NA	NA	NA	NA	NA	NA	NA	NA	0	225	NA	40	NA	NA	CM	37
PQ_Const._set_3_4mM_080min_vs_NRC-1h1.sig	NA	NA	NA	NA	NA	NA	NA	NA	NA	NA	NA	NA	NA	NA	NA	NA	NA	0	225	NA	80	NA	NA	CM	37
PQ_Const._set_3_4mM_160min_vs_NRC-1h1.sig	NA	NA	NA	NA	NA	NA	NA	NA	NA	NA	NA	NA	NA	NA	NA	NA	NA	0	225	NA	160	NA	NA	CM	37
PQ_Const._set_4_4mM_-001min_vs_NRC-1h1.sig	NA	NA	NA	NA	NA	NA	NA	NA	NA	NA	NA	NA	NA	NA	NA	NA	NA	0	225	NA	-1	NA	NA	CM	37
PQ_Const._set_4_4mM_005min_vs_NRC-1h1.sig	NA	NA	NA	NA	NA	NA	NA	NA	NA	NA	NA	NA	NA	NA	NA	NA	NA	0	225	NA	5	NA	NA	CM	37
PQ_Const._set_4_4mM_010min_vs_NRC-1h1.sig	NA	NA	NA	NA	NA	NA	NA	NA	NA	NA	NA	NA	NA	NA	NA	NA	NA	0	225	NA	10	NA	NA	CM	37
PQ_Const._set_4_4mM_020min_vs_NRC-1h1.sig	NA	NA	NA	NA	NA	NA	NA	NA	NA	NA	NA	NA	NA	NA	NA	NA	NA	0	225	NA	20	NA	NA	CM	37
PQ_Const._set_4_4mM_040min_vs_NRC-1h1.sig	NA	NA	NA	NA	NA	NA	NA	NA	NA	NA	NA	NA	NA	NA	NA	NA	NA	0	225	NA	40	NA	NA	CM	37
PQ_Const._set_4_4mM_080min_vs_NRC-1h1.sig	NA	NA	NA	NA	NA	NA	NA	NA	NA	NA	NA	NA	NA	NA	NA	NA	NA	0	225	NA	80	NA	NA	CM	37
PQ_Const._set_4_4mM_160min_vs_NRC-1h1.sig	NA	NA	NA	NA	NA	NA	NA	NA	NA	NA	NA	NA	NA	NA	NA	NA	NA	0	225	NA	160	NA	NA	CM	37

KO_ura3.2_0.1716_vs_NRC-1_h1.sig	NA	NA	NA	NA	NA	NA	NA	NA	NA	NA	NA	NA	NA	0.17	NA	NA	NA	225	NA	915	NA	NA	FangYin's CDM	37
KO_ura3.2_0.3207_vs_NRC-1_h1.sig	NA	NA	NA	NA	NA	NA	NA	NA	NA	NA	NA	NA	NA	0.32	NA	NA	NA	225	NA	1587	NA	NA	FangYin's CDM	37
KO_ura3.2_0.4308_vs_NRC-1_h1.sig	NA	NA	NA	NA	NA	NA	NA	NA	NA	NA	NA	NA	NA	0.43	NA	NA	NA	225	NA	2640	NA	NA	FangYin's CDM	37
KO_ura3.2_0.5084_vs_NRC-1_h1.sig	NA	NA	NA	NA	NA	NA	NA	NA	NA	NA	NA	NA	NA	0.51	NA	NA	NA	225	NA	3817	NA	NA	FangYin's CDM	37
1451_growth_t1exp1_0.2OD_vs_NRC1e.sig	NA	NA	NA	NA	NA	NA	NA	NA	NA	NA	NA	NA	NA	0.19	NA	NA	NA	225	NA	NA	NA	NA	CM	37
1451_growth_t2exp1_0.3OD_vs_NRC1e.sig	NA	NA	NA	NA	NA	NA	NA	NA	NA	NA	NA	NA	NA	0.37	NA	NA	NA	225	NA	NA	NA	NA	CM	37
1451_growth_t3exp1_0.4OD_vs_NRC1e.sig	NA	NA	NA	NA	NA	NA	NA	NA	NA	NA	NA	NA	NA	0.42	NA	NA	NA	225	NA	NA	NA	NA	CM	37
ura3_growth_t2exp1_0.5OD_vs_NRC1e.sig	NA	NA	NA	NA	NA	NA	NA	NA	NA	NA	NA	NA	NA	0.5	NA	NA	NA	225	NA	NA	NA	NA	CM	37
ura3_growth_t3exp1_0.8OD_vs_NRC1e.sig	NA	NA	NA	NA	NA	NA	NA	NA	NA	NA	NA	NA	NA	0.82	NA	NA	NA	225	NA	NA	NA	NA	CM	37
1451_growth_t1_exp2_0.1OD_vs_NRC1f.sig	NA	NA	NA	NA	NA	NA	NA	NA	NA	NA	NA	NA	NA	0.13	NA	NA	NA	225	NA	NA	NA	NA	CM	37
1451_growth_t2_exp2_0.2OD_vs_NRC1f.sig	NA	NA	NA	NA	NA	NA	NA	NA	NA	NA	NA	NA	NA	0.23	NA	NA	NA	225	NA	NA	NA	NA	CM	37
1451_growth_t3_exp2_0.3OD_vs_NRC1f.sig	NA	NA	NA	NA	NA	NA	NA	NA	NA	NA	NA	NA	NA	0.3	NA	NA	NA	225	NA	NA	NA	NA	CM	37
ura3_growth_t1_exp2_0.3OD_vs_NRC1f.sig	NA	NA	NA	NA	NA	NA	NA	NA	NA	NA	NA	NA	NA	0.33	NA	NA	NA	225	NA	NA	NA	NA	CM	37
ura3_growth_t2_exp2_0.5OD_vs_NRC	NA	NA	NA	NA	NA	NA	NA	NA	NA	NA	NA	NA	NA	0.55	NA	NA	NA	225	NA	NA	NA	NA	CM	37

1f.sig																								
ura3_growth_t3_exp2_0.8OD_vs_NRC1f.sig	NA	NA	NA	NA	NA	NA	NA	NA	NA	NA	NA	NA	NA	0.79	NA	NA	NA	225	NA	NA	NA	NA	CM	37
NRC1e_vs_NRC1f_ctrl.sig	NA	NA	NA	NA	NA	NA	NA	NA	NA	NA	NA	NA	NA	NA	NA	NA	NA	225	NA	NA	NA	NA	CM	37
ura3_+glu_a_OD0.6_vs_NRC1e.sig	NA	NA	NA	NA	NA	NA	NA	7	NA	NA	NA	NA	NA	0.64	NA	NA	NA	225	NA	NA	NA	NA	Amy's CDM	37
ura3_-glu_a_OD0.6_vs_NRC1e.sig	NA	NA	NA	NA	NA	NA	NA	0	NA	NA	NA	NA	NA	0.64	NA	NA	NA	225	NA	NA	NA	NA	Amy's CDM	37
1451_+glu_a_OD0.6_vs_NRC1e.sig	NA	NA	NA	NA	NA	NA	NA	7	NA	NA	NA	NA	NA	0.3	NA	NA	NA	225	NA	NA	NA	NA	Amy's CDM	37
1451_-glu_a_OD0.6_vs_NRC1e.sig	NA	NA	NA	NA	NA	NA	NA	0	NA	NA	NA	NA	NA	0.1	NA	NA	NA	225	NA	NA	NA	NA	Amy's CDM	37
ura3_+glu_a_OD1.2_vs_NRC1e.sig	NA	NA	NA	NA	NA	NA	NA	7	NA	NA	NA	NA	NA	0.5	NA	NA	NA	225	NA	NA	NA	NA	Amy's CDM	37
ura3_-glu_a_OD1.2_vs_NRC1e.sig	NA	NA	NA	NA	NA	NA	NA	0	NA	NA	NA	NA	NA	1.47	NA	NA	NA	225	NA	NA	NA	NA	Amy's CDM	37
1451_growth_t4_exp2_0.5OD_vs_NRC1f.sig	NA	NA	NA	NA	NA	NA	NA	NA	NA	NA	NA	NA	NA	0.65	NA	NA	NA	225	NA	NA	NA	NA	Amy's CDM	37
1451_growth_t1_exp3_0.1OD_vs_NRC1f.sig	NA	NA	NA	NA	NA	NA	NA	NA	NA	NA	NA	NA	NA	0.14	NA	NA	NA	225	NA	NA	NA	NA	Amy's CDM	37
1451_growth_t2_exp3_0.2OD_vs_NRC1f.sig	NA	NA	NA	NA	NA	NA	NA	NA	NA	NA	NA	NA	NA	0.22	NA	NA	NA	225	NA	NA	NA	NA	Amy's CDM	37
1451_growth_t3_exp3_0.3OD_vs_NRC1f.sig	NA	NA	NA	NA	NA	NA	NA	NA	NA	NA	NA	NA	NA	0.31	NA	NA	NA	225	NA	NA	NA	NA	Amy's CDM	37

1451_growth_t4_exp3_0.6OD_vs_NRC1f.sig	NA	NA	NA	NA	NA	NA	NA	NA	NA	NA	NA	NA	NA	0.56	NA	NA	NA	225	NA	NA	NA	NA	Amy's CDM	37
ura3_growth_t4_exp2_1.2OD_vs_NRC1f.sig	NA	NA	NA	NA	NA	NA	NA	NA	NA	NA	NA	NA	NA	1.26	NA	NA	NA	225	NA	NA	NA	NA	Amy's CDM	37
ura3_growth_t1_exp3_0.3OD_vs_NRC1f.sig	NA	NA	NA	NA	NA	NA	NA	NA	NA	NA	NA	NA	NA	0.31	NA	NA	NA	225	NA	NA	NA	NA	Amy's CDM	37
ura3_growth_t2_exp3_0.5OD_vs_NRC1f.sig	NA	NA	NA	NA	NA	NA	NA	NA	NA	NA	NA	NA	NA	0.52	NA	NA	NA	225	NA	NA	NA	NA	Amy's CDM	37
ura3_growth_t3_exp3_0.8OD_vs_NRC1f.sig	NA	NA	NA	NA	NA	NA	NA	NA	NA	NA	NA	NA	NA	0.72	NA	NA	NA	225	NA	NA	NA	NA	Amy's CDM	37
ura3_growth_t4_exp3_1.2OD_vs_NRC1f.sig	NA	NA	NA	NA	NA	NA	NA	NA	NA	NA	NA	NA	NA	1.18	NA	NA	NA	225	NA	NA	NA	NA	Amy's CDM	37
1451_+glu_a_OD0.2_vs_NRC1e.sig	NA	NA	NA	NA	NA	NA	NA	7	NA	NA	NA	NA	NA	0.22	NA	NA	NA	225	NA	NA	NA	NA	Amy's CDM	37
1451_+glu_a_OD0.6repl_vs_NRC1e.sig	NA	NA	NA	NA	NA	NA	NA	7	NA	NA	NA	NA	NA	0.31	NA	NA	NA	225	NA	NA	NA	NA	Amy's CDM	37
1451_+glu_a_OD1.2repl_vs_NRC1e.sig	NA	NA	NA	NA	NA	NA	NA	7	NA	NA	NA	NA	NA	0.8	NA	NA	NA	225	NA	NA	NA	NA	Amy's CDM	37
1451_+glu_b_OD0.2_vs_NRC1g.sig	NA	NA	NA	NA	NA	NA	NA	7	NA	NA	NA	NA	NA	0.23	NA	NA	NA	225	NA	NA	NA	NA	Amy's CDM	37
1451_+glu_b_OD0.6repl_vs_NRC1g.sig	NA	NA	NA	NA	NA	NA	NA	7	NA	NA	NA	NA	NA	0.3	NA	NA	NA	225	NA	NA	NA	NA	Amy's CDM	37
1451_+glu_b_OD1.2repl_vs_NRC1g.sig	NA	NA	NA	NA	NA	NA	NA	7	NA	NA	NA	NA	NA	0.76	NA	NA	NA	225	NA	NA	NA	NA	Amy's CDM	37

1451_-glu_ab_OD0.2_vs_NRC1e.sig	NA	NA	NA	NA	NA	NA	NA	0	NA	NA	NA	NA	NA	0.04	NA	NA	NA	225	NA	NA	NA	NA	Amy's CDM	37
1451_-glu_a_OD0.6repl_vs_NRC1e.sig	NA	NA	NA	NA	NA	NA	NA	0	NA	NA	NA	NA	NA	0.1	NA	NA	NA	225	NA	NA	NA	NA	Amy's CDM	37
1451_-glu_a_OD1.2repl_vs_NRC1g.sig	NA	NA	NA	NA	NA	NA	NA	0	NA	NA	NA	NA	NA	0.15	NA	NA	NA	225	NA	NA	NA	NA	Amy's CDM	37
1451_-glu_b_OD0.6repl_vs_NRC1g.sig	NA	NA	NA	NA	NA	NA	NA	0	NA	NA	NA	NA	NA	0.11	NA	NA	NA	225	NA	NA	NA	NA	Amy's CDM	37
1451_-glu_b_OD1.2repl_vs_NRC1g.sig	NA	NA	NA	NA	NA	NA	NA	0	NA	NA	NA	NA	NA	0.1	NA	NA	NA	225	NA	NA	NA	NA	Amy's CDM	37
ura3_+glu_a_OD0.2_vs_NRC1e.sig	NA	NA	NA	NA	NA	NA	NA	7	NA	NA	NA	NA	NA	0.19	NA	NA	NA	225	NA	NA	NA	NA	Amy's CDM	37
ura3_+glu_a_OD0.6repl_vs_NRC1e.sig	NA	NA	NA	NA	NA	NA	NA	7	NA	NA	NA	NA	NA	0.3	NA	NA	NA	225	NA	NA	NA	NA	Amy's CDM	37
ura3_+glu_a_OD1.2repl_vs_NRC1e.sig	NA	NA	NA	NA	NA	NA	NA	7	NA	NA	NA	NA	NA	0.5	NA	NA	NA	225	NA	NA	NA	NA	Amy's CDM	37
ura3_+glu_b_OD0.2_vs_NRC1g.sig	NA	NA	NA	NA	NA	NA	NA	7	NA	NA	NA	NA	NA	0.18	NA	NA	NA	225	NA	NA	NA	NA	Amy's CDM	37
ura3_+glu_b_OD0.6repl_vs_NRC1g.sig	NA	NA	NA	NA	NA	NA	NA	7	NA	NA	NA	NA	NA	0.29	NA	NA	NA	225	NA	NA	NA	NA	Amy's CDM	37
ura3_+glu_b_OD1.2repl_vs_NRC1g.sig	NA	NA	NA	NA	NA	NA	NA	7	NA	NA	NA	NA	NA	0.53	NA	NA	NA	225	NA	NA	NA	NA	Amy's CDM	37
ura3_-glu_a_OD0.2_vs_NRC1e.sig	NA	NA	NA	NA	NA	NA	NA	0	NA	NA	NA	NA	NA	0.21	NA	NA	NA	225	NA	NA	NA	NA	Amy's CDM	37

ura3_-glu_a_OD0.6repl_vs_NRC1e.sig	NA	NA	NA	NA	NA	NA	NA	0	NA	NA	NA	NA	NA	0.64	NA	NA	NA	225	NA	NA	NA	NA	Amy's CDM	37
ura3_-glu_a_OD1.2repl_vs_NRC1e.sig	NA	NA	NA	NA	NA	NA	NA	0	NA	NA	NA	NA	NA	1.47	NA	NA	NA	225	NA	NA	NA	NA	Amy's CDM	37
ura3_-glu_b_OD0.2_vs_NRC1g.sig	NA	NA	NA	NA	NA	NA	NA	0	NA	NA	NA	NA	NA	0.21	NA	NA	NA	225	NA	NA	NA	NA	Amy's CDM	37
ura3_-glu_b_OD0.6repl_vs_NRC1g.sig	NA	NA	NA	NA	NA	NA	NA	0	NA	NA	NA	NA	NA	0.7	NA	NA	NA	225	NA	NA	NA	NA	Amy's CDM	37
ura3_-glu_b_OD1.2repl_vs_NRC1g.sig	NA	NA	NA	NA	NA	NA	NA	0	NA	NA	NA	NA	NA	1.6	NA	NA	NA	225	NA	NA	NA	NA	Amy's CDM	37
NRC-1_control_1week_vs_NRC-1h1.sig	NA	NA	NA	NA	NA	NA	NA	NA	NA	NA	NA	NA	NA	NA	NA	NA	NA	225	NA	NA	NA	NA	CM	NA
NRC-1_control_2days_vs_NRC-1h1.sig	NA	NA	NA	NA	NA	NA	NA	NA	NA	NA	NA	NA	NA	NA	NA	NA	NA	225	NA	NA	NA	NA	CM	NA
NRC-1_neg20C_1week_vs_NRC-1h1.sig	NA	NA	NA	NA	NA	NA	NA	NA	NA	NA	NA	NA	NA	NA	NA	NA	NA	225	NA	NA	NA	NA	CM	NA
EMS_Treated__100000uM-000	NA	NA	NA	NA	0.1	NA	NA	NA	NA	NA	NA	NA	NA	0.3	NA	NA	NA	225	NA	0	NA	NA	CM	42
EMS_Treated__100000uM-010	NA	NA	NA	NA	0.1	NA	NA	NA	NA	NA	NA	NA	NA	0.31	NA	NA	NA	225	NA	10	NA	NA	CM	42
EMS_Treated__100000uM-020	NA	NA	NA	NA	0.1	NA	NA	NA	NA	NA	NA	NA	NA	0.32	NA	NA	NA	225	NA	20	NA	NA	CM	42
EMS_Treated__100000uM-030	NA	NA	NA	NA	0.1	NA	NA	NA	NA	NA	NA	NA	NA	0.14	NA	NA	NA	225	NA	30	NA	NA	CM	42
EMS_Treated__100000uM-040	NA	NA	NA	NA	0.1	NA	NA	NA	NA	NA	NA	NA	NA	0.3	NA	NA	NA	225	NA	40	NA	NA	CM	42
EMS_Treated__100000uM-050	NA	NA	NA	NA	0.1	NA	NA	NA	NA	NA	NA	NA	NA	0.37	NA	NA	NA	225	NA	50	NA	NA	CM	42
EMS_Treated__100000uM-060	NA	NA	NA	NA	0.1	NA	NA	NA	NA	NA	NA	NA	NA	0.3	NA	NA	NA	225	NA	60	NA	NA	CM	42
EMS_Treated__100000uM-120	NA	NA	NA	NA	0.1	NA	NA	NA	NA	NA	NA	NA	NA	0.34	NA	NA	NA	225	NA	120	NA	NA	CM	42
MDM250gSalt_0.204_vs_NRC-1e.sig	NA	NA	NA	NA	NA	NA	NA	NA	NA	NA	NA	NA	NA	0.2	NA	NA	NA	225	NA	840	NA	NA	Amy's CD	37

																							M	
MDM250gSalt_0.396_vs_NRC-1e.sig	NA	NA	NA	NA	NA	NA	NA	NA	NA	NA	NA	NA	NA	0.4	NA	NA	NA	225	NA	1560	NA	NA	Amy's CDM	37
MDM250gSalt_0.481_vs_NRC-1e.sig	NA	NA	NA	NA	NA	NA	NA	NA	NA	NA	NA	NA	NA	0.48	NA	NA	NA	225	NA	2100	NA	NA	Amy's CDM	37
MDM250gSalt_0.49_vs_NRC-1e.sig	NA	NA	NA	NA	NA	NA	NA	NA	NA	NA	NA	NA	NA	0.49	NA	NA	NA	225	NA	2700	NA	NA	Amy's CDM	37
Dun_Supernat._000minb_vs_NRC-1g.sig	NA	NA	NA	NA	NA	NA	NA	NA	NA	NA	NA	NA	NA	NA	NA	NA	NA	80	NA	0	NA	NA	MM1	30
Dun_Supernat._005minb_vs_NRC-1g.sig	NA	NA	NA	NA	NA	NA	NA	NA	NA	NA	NA	NA	NA	NA	NA	NA	NA	80	NA	5	NA	NA	MM1	31
Dun_Supernat._010minb_vs_NRC-1g.sig	NA	NA	NA	NA	NA	NA	NA	NA	NA	NA	NA	NA	NA	NA	NA	NA	NA	80	NA	10	NA	NA	MM1	32
Dun_Supernat._020minb_vs_NRC-1g.sig	NA	NA	NA	NA	NA	NA	NA	NA	NA	NA	NA	NA	NA	NA	NA	NA	NA	80	NA	20	NA	NA	MM1	33
Dun_Supernat._040minb_vs_NRC-1g.sig	NA	NA	NA	NA	NA	NA	NA	NA	NA	NA	NA	NA	NA	NA	NA	NA	NA	80	NA	40	NA	NA	MM1	34
Dun_Supernat._080minb_vs_NRC-1g.sig	NA	NA	NA	NA	NA	NA	NA	NA	NA	NA	NA	NA	NA	NA	NA	NA	NA	80	NA	80	NA	NA	MM1	35
Dun_Supernat._160minb_vs_NRC-1g.sig	NA	NA	NA	NA	NA	NA	NA	NA	NA	NA	NA	NA	NA	NA	NA	NA	NA	80	NA	160	NA	NA	MM1	36
Dun_Supernat._320minb_vs_NRC-1g.sig	NA	NA	NA	NA	NA	NA	NA	NA	NA	NA	NA	NA	NA	NA	NA	NA	NA	80	NA	320	NA	NA	MM1	37
gamma4__2500gy-000min	NA	NA	NA	NA	NA	NA	2500	NA	NA	NA	NA	NA	NA	NA	NA	NA	NA	225	NA	0	NA	NA	CM	42
gamma4__2500gy-010min	NA	NA	NA	NA	NA	NA	2500	NA	NA	NA	NA	NA	NA	NA	NA	NA	NA	225	NA	10	NA	NA	CM	42
gamma4__2500gy-020min	NA	NA	NA	NA	NA	NA	2500	NA	NA	NA	NA	NA	NA	NA	NA	NA	NA	225	NA	20	NA	NA	CM	42
gamma4__2500gy-030min	NA	NA	NA	NA	NA	NA	2500	NA	NA	NA	NA	NA	NA	NA	NA	NA	NA	225	NA	30	NA	NA	CM	42
gamma4__2500gy-040min	NA	NA	NA	NA	NA	NA	2500	NA	NA	NA	NA	NA	NA	NA	NA	NA	NA	225	NA	40	NA	NA	CM	42

gamma4__2500gy-050min	NA	NA	NA	NA	NA	NA	2500	NA	NA	NA	NA	NA	NA	NA	NA	NA	NA	225	NA	50	NA	NA	CM	42
gamma4__2500gy-060min	NA	NA	NA	NA	NA	NA	2500	NA	NA	NA	NA	NA	NA	NA	NA	NA	NA	225	NA	60	NA	NA	CM	42
gamma4__2500gy-120min	NA	NA	NA	NA	NA	NA	2500	NA	NA	NA	NA	NA	NA	NA	NA	NA	NA	225	NA	120	NA	NA	CM	42
gamma4__2500gy-240min	NA	NA	NA	NA	NA	NA	2500	NA	NA	NA	NA	NA	NA	NA	NA	NA	NA	225	NA	240	NA	NA	CM	42
gamma__2500gy-0000m	NA	NA	NA	NA	NA	NA	2500	NA	NA	NA	NA	NA	NA	NA	NA	NA	NA	225	NA	0	NA	NA	CM	42
gamma__2500gy-0010m	NA	NA	NA	NA	NA	NA	2500	NA	NA	NA	NA	NA	NA	NA	NA	NA	NA	225	NA	10	NA	NA	CM	42
gamma__2500gy-0020m	NA	NA	NA	NA	NA	NA	2500	NA	NA	NA	NA	NA	NA	NA	NA	NA	NA	225	NA	20	NA	NA	CM	42
gamma__2500gy-0030m	NA	NA	NA	NA	NA	NA	2500	NA	NA	NA	NA	NA	NA	NA	NA	NA	NA	225	NA	30	NA	NA	CM	42
gamma__2500gy-0040m	NA	NA	NA	NA	NA	NA	2500	NA	NA	NA	NA	NA	NA	NA	NA	NA	NA	225	NA	40	NA	NA	CM	42
gamma__2500gy-0060m	NA	NA	NA	NA	NA	NA	2500	NA	NA	NA	NA	NA	NA	NA	NA	NA	NA	225	NA	60	NA	NA	CM	42
gamma__2500gy-0120m	NA	NA	NA	NA	NA	NA	2500	NA	NA	NA	NA	NA	NA	NA	NA	NA	NA	225	NA	120	NA	NA	CM	42
gamma__2500gy-0240m	NA	NA	NA	NA	NA	NA	2500	NA	NA	NA	NA	NA	NA	NA	NA	NA	NA	225	NA	240	NA	NA	CM	42
gamma__2500gy-0480m	NA	NA	NA	NA	NA	NA	2500	NA	NA	NA	NA	NA	NA	NA	NA	NA	NA	225	NA	480	NA	NA	CM	42
gamma__2500gy-0960m	NA	NA	NA	NA	NA	NA	2500	NA	NA	NA	NA	NA	NA	NA	NA	NA	NA	225	NA	960	NA	NA	CM	42
H2O2_Recov._set_3_25mM_000min_vs_NRC-1f.sig	NA	NA	NA	NA	NA	NA	NA	NA	0.03	NA	NA	NA	NA	0.43	NA	NA	NA	225	NA	0	NA	NA	CM	42
H2O2_Recov._set_3_25mM_010min_vs_NRC-1f.sig	NA	NA	NA	NA	NA	NA	NA	NA	0.03	NA	NA	NA	NA	0.49	NA	NA	NA	225	NA	10	NA	NA	CM	42
H2O2_Recov._set_3_25mM_020min_vs_NRC-1f.sig	NA	NA	NA	NA	NA	NA	NA	NA	0.03	NA	NA	NA	NA	0.45	NA	NA	NA	225	NA	20	NA	NA	CM	42
H2O2_Recov._set_3_25mM_030min_vs_NRC-1f.sig	NA	NA	NA	NA	NA	NA	NA	NA	0.03	NA	NA	NA	NA	0.48	NA	NA	NA	225	NA	30	NA	NA	CM	42
H2O2_Recov._set_3_25mM_040min_vs_NRC-1f.sig	NA	NA	NA	NA	NA	NA	NA	NA	0.03	NA	NA	NA	NA	0.46	NA	NA	NA	225	NA	40	NA	NA	CM	42
H2O2_Recov._set_3_25mM_050min_vs_NRC-1f.sig	NA	NA	NA	NA	NA	NA	NA	NA	0.03	NA	NA	NA	NA	0.47	NA	NA	NA	225	NA	50	NA	NA	CM	42
H2O2_Recov._set_3_25mM_060min_vs_NRC-1f.sig	NA	NA	NA	NA	NA	NA	NA	NA	0.03	NA	NA	NA	NA	0.45	NA	NA	NA	225	NA	60	NA	NA	CM	42

H2O2_Recov._set_3_25mM_120min_vs_NRC-1f.sig	NA	NA	NA	NA	NA	NA	NA	NA	0.03	NA	NA	NA	NA	0.51	NA	NA	NA	225	NA	120	NA	NA	CM	42
H2O2_Recov._set_3_25mM_240min_vs_NRC-1f.sig	NA	NA	NA	NA	NA	NA	NA	NA	0.03	NA	NA	NA	NA	0.6	NA	NA	NA	225	NA	240	NA	NA	CM	42
H2O2_Const._set_2_25mM_000min_vs_NRC-1f.sig	NA	NA	NA	NA	NA	NA	NA	NA	0.03	NA	NA	NA	NA	0.54	NA	NA	NA	225	NA	0	NA	NA	CM	42
H2O2_Const._set_2_25mM_030min_vs_NRC-1f.sig	NA	NA	NA	NA	NA	NA	NA	NA	0.03	NA	NA	NA	NA	0.55	NA	NA	NA	225	NA	30	NA	NA	CM	42
H2O2_Const._set_2_25mM_060min_vs_NRC-1f.sig	NA	NA	NA	NA	NA	NA	NA	NA	0.03	NA	NA	NA	NA	0.56	NA	NA	NA	225	NA	60	NA	NA	CM	42
H2O2_Const._set_2_25mM_120min_vs_NRC-1f.sig	NA	NA	NA	NA	NA	NA	NA	NA	0.03	NA	NA	NA	NA	0.58	NA	NA	NA	225	NA	120	NA	NA	CM	42
H2O2_Const._set_2_25mM_240min_vs_NRC-1f.sig	NA	NA	NA	NA	NA	NA	NA	NA	0.03	NA	NA	NA	NA	0.62	NA	NA	NA	225	NA	240	NA	NA	CM	42
PQ_Recov._set_2_4mM_000min_vs_NRC-1f.sig	NA	NA	NA	NA	NA	NA	NA	NA	NA	NA	NA	NA	NA	0.43	NA	NA	0	225	NA	0	NA	NA	CM	42
PQ_Recov._set_2_4mM_010min_vs_NRC-1f.sig	NA	NA	NA	NA	NA	NA	NA	NA	NA	NA	NA	NA	NA	0.46	NA	NA	0	225	NA	10	NA	NA	CM	42
PQ_Recov._set_2_4mM_020min_vs_NRC-1f.sig	NA	NA	NA	NA	NA	NA	NA	NA	NA	NA	NA	NA	NA	0.45	NA	NA	0	225	NA	20	NA	NA	CM	42
PQ_Recov._set_2_4mM_030min_vs_NRC-1f.sig	NA	NA	NA	NA	NA	NA	NA	NA	NA	NA	NA	NA	NA	0.48	NA	NA	0	225	NA	30	NA	NA	CM	42
PQ_Recov._set_2_4mM_040min_vs_NRC-1f.sig	NA	NA	NA	NA	NA	NA	NA	NA	NA	NA	NA	NA	NA	0.44	NA	NA	0	225	NA	40	NA	NA	CM	42
PQ_Recov._set_2_4mM_050min_vs_NRC-1f.sig	NA	NA	NA	NA	NA	NA	NA	NA	NA	NA	NA	NA	NA	0.46	NA	NA	0	225	NA	50	NA	NA	CM	42
PQ_Recov._set_2_4mM_060min_vs_NRC-1f.sig	NA	NA	NA	NA	NA	NA	NA	NA	NA	NA	NA	NA	NA	0.45	NA	NA	0	225	NA	60	NA	NA	CM	42
PQ_Recov._set_2_4mM_120min_vs_NRC-1f.sig	NA	NA	NA	NA	NA	NA	NA	NA	NA	NA	NA	NA	NA	0.5	NA	NA	0	225	NA	120	NA	NA	CM	42
PQ_Recov._set_2_4mM_240min_vs_NRC-1f.sig	NA	NA	NA	NA	NA	NA	NA	NA	NA	NA	NA	NA	NA	0.51	NA	NA	0	225	NA	240	NA	NA	CM	42

PQ_Const._set_2_4mM_000min_vs_NRC-1f.sig	NA	NA	NA	NA	NA	NA	NA	NA	NA	NA	NA	NA	NA	0.54	NA	NA	0	225	NA	0	NA	NA	CM	42
PQ_Const._set_2_4mM_030min_vs_NRC-1f.sig	NA	NA	NA	NA	NA	NA	NA	NA	NA	NA	NA	NA	NA	0.55	NA	NA	0	225	NA	30	NA	NA	CM	42
PQ_Const._set_2_4mM_060min_vs_NRC-1f.sig	NA	NA	NA	NA	NA	NA	NA	NA	NA	NA	NA	NA	NA	0.55	NA	NA	0	225	NA	60	NA	NA	CM	42
PQ_Const._set_2_4mM_120min_vs_NRC-1f.sig	NA	NA	NA	NA	NA	NA	NA	NA	NA	NA	NA	NA	NA	0.57	NA	NA	0	225	NA	120	NA	NA	CM	42
PQ_Const._set_2_4mM_240min_vs_NRC-1f.sig	NA	NA	NA	NA	NA	NA	NA	NA	NA	NA	NA	NA	NA	0.57	NA	NA	0	225	NA	240	NA	NA	CM	42
H2O2_Recov._set_2_25mM_000min_vs_NRC-1f.sig	NA	NA	NA	NA	NA	NA	NA	NA	0.03	NA	NA	NA	NA	0.34	NA	NA	NA	225	NA	0	NA	NA	CM	42
H2O2_Recov._set_2_25mM_010min_vs_NRC-1f.sig	NA	NA	NA	NA	NA	NA	NA	NA	0.03	NA	NA	NA	NA	0.36	NA	NA	NA	225	NA	10	NA	NA	CM	42
H2O2_Recov._set_2_25mM_020min_vs_NRC-1f.sig	NA	NA	NA	NA	NA	NA	NA	NA	0.03	NA	NA	NA	NA	0.35	NA	NA	NA	225	NA	20	NA	NA	CM	42
H2O2_Recov._set_2_25mM_030min_vs_NRC-1f.sig	NA	NA	NA	NA	NA	NA	NA	NA	0.03	NA	NA	NA	NA	0.36	NA	NA	NA	225	NA	30	NA	NA	CM	42
H2O2_Recov._set_2_25mM_040min_vs_NRC-1f.sig	NA	NA	NA	NA	NA	NA	NA	NA	0.03	NA	NA	NA	NA	0.36	NA	NA	NA	225	NA	40	NA	NA	CM	42
H2O2_Recov._set_2_25mM_050min_vs_NRC-1f.sig	NA	NA	NA	NA	NA	NA	NA	NA	0.03	NA	NA	NA	NA	0.36	NA	NA	NA	225	NA	50	NA	NA	CM	42
H2O2_Recov._set_2_25mM_060min_vs_NRC-1f.sig	NA	NA	NA	NA	NA	NA	NA	NA	0.03	NA	NA	NA	NA	0.35	NA	NA	NA	225	NA	60	NA	NA	CM	42
H2O2_Recov._set_2_25mM_120min_vs_NRC-1f.sig	NA	NA	NA	NA	NA	NA	NA	NA	0.03	NA	NA	NA	NA	0.36	NA	NA	NA	225	NA	120	NA	NA	CM	42
H2O2_Recov._set_2_25mM_240min_vs_NRC-1f.sig	NA	NA	NA	NA	NA	NA	NA	NA	0.03	NA	NA	NA	NA	0.38	NA	NA	NA	225	NA	240	NA	NA	CM	42
H2O2_Const._set_1_25mM_000min_vs_NRC-1f.sig	NA	NA	NA	NA	NA	NA	NA	NA	0.03	NA	NA	NA	NA	0.55	NA	NA	NA	225	NA	0	NA	NA	CM	42
H2O2_Const._set_1_25mM_030min_vs_NRC-1f.sig	NA	NA	NA	NA	NA	NA	NA	NA	0.03	NA	NA	NA	NA	0.56	NA	NA	NA	225	NA	30	NA	NA	CM	42

H2O2_Const._set_1_25mM_060min_vs_NRC-1f.sig	NA	NA	NA	NA	NA	NA	NA	NA	0.03	NA	NA	NA	NA	0.55	NA	NA	NA	225	NA	60	NA	NA	CM	42
H2O2_Const._set_1_25mM_120min_vs_NRC-1f.sig	NA	NA	NA	NA	NA	NA	NA	NA	0.03	NA	NA	NA	NA	0.58	NA	NA	NA	225	NA	120	NA	NA	CM	42
H2O2_Const._set_1_25mM_240min_vs_NRC-1f.sig	NA	NA	NA	NA	NA	NA	NA	NA	0.03	NA	NA	NA	NA	0.62	NA	NA	NA	225	NA	240	NA	NA	CM	42
PQ_Recov._set_1_4mM_000min_vs_NRC-1f.sig	NA	NA	NA	NA	NA	NA	NA	NA	NA	NA	NA	NA	NA	0.46	NA	NA	0	225	NA	0	NA	NA	CM	42
PQ_Recov._set_1_4mM_010min_vs_NRC-1f.sig	NA	NA	NA	NA	NA	NA	NA	NA	NA	NA	NA	NA	NA	0.51	NA	NA	0	225	NA	10	NA	NA	CM	42
PQ_Recov._set_1_4mM_020min_vs_NRC-1f.sig	NA	NA	NA	NA	NA	NA	NA	NA	NA	NA	NA	NA	NA	0.48	NA	NA	0	225	NA	20	NA	NA	CM	42
PQ_Recov._set_1_4mM_030min_vs_NRC-1f.sig	NA	NA	NA	NA	NA	NA	NA	NA	NA	NA	NA	NA	NA	0.51	NA	NA	0	225	NA	30	NA	NA	CM	42
PQ_Recov._set_1_4mM_040min_vs_NRC-1f.sig	NA	NA	NA	NA	NA	NA	NA	NA	NA	NA	NA	NA	NA	0.47	NA	NA	0	225	NA	40	NA	NA	CM	42
PQ_Recov._set_1_4mM_050min_vs_NRC-1f.sig	NA	NA	NA	NA	NA	NA	NA	NA	NA	NA	NA	NA	NA	0.49	NA	NA	0	225	NA	50	NA	NA	CM	42
PQ_Recov._set_1_4mM_060min_vs_NRC-1f.sig	NA	NA	NA	NA	NA	NA	NA	NA	NA	NA	NA	NA	NA	0.48	NA	NA	0	225	NA	60	NA	NA	CM	42
PQ_Recov._set_1_4mM_120min_vs_NRC-1f.sig	NA	NA	NA	NA	NA	NA	NA	NA	NA	NA	NA	NA	NA	0.53	NA	NA	0	225	NA	120	NA	NA	CM	42
PQ_Recov._set_1_4mM_240min_vs_NRC-1f.sig	NA	NA	NA	NA	NA	NA	NA	NA	NA	NA	NA	NA	NA	0.55	NA	NA	0	225	NA	240	NA	NA	CM	42
PQ_Const._set_1_4mM_000min_vs_NRC-1f.sig	NA	NA	NA	NA	NA	NA	NA	NA	NA	NA	NA	NA	NA	0.54	NA	NA	0	225	NA	0	NA	NA	CM	42
PQ_Const._set_1_4mM_030min_vs_NRC-1f.sig	NA	NA	NA	NA	NA	NA	NA	NA	NA	NA	NA	NA	NA	0.55	NA	NA	0	225	NA	30	NA	NA	CM	42
PQ_Const._set_1_4mM_060min_vs_NRC-1f.sig	NA	NA	NA	NA	NA	NA	NA	NA	NA	NA	NA	NA	NA	0.56	NA	NA	0	225	NA	60	NA	NA	CM	42
PQ_Const._set_1_4mM_120min_vs_NRC-1f.sig	NA	NA	NA	NA	NA	NA	NA	NA	NA	NA	NA	NA	NA	0.57	NA	NA	0	225	NA	120	NA	NA	CM	42

PQ_Const._set_1_4mM_240min_vs_NRC-1f.sig	NA	NA	NA	NA	NA	NA	NA	NA	NA	NA	NA	NA	NA	0.57	NA	NA	0	225	NA	240	NA	NA	CM	42
uv__200jm2_D_030m	NA	NA	NA	NA	NA	NA	NA	NA	NA	0	NA	NA	NA	NA	NA	50	NA	225	NA	30	200	NA	CM	42
uv__200jm2_D_060m	NA	NA	NA	NA	NA	NA	NA	NA	NA	0	NA	NA	NA	NA	NA	50	NA	225	NA	60	200	NA	CM	42
uv__200jm2_L_030m	NA	NA	NA	NA	NA	NA	NA	NA	NA	Light (JR lab)	NA	NA	NA	NA	NA	50	NA	225	NA	30	200	NA	CM	42
uv__200jm2_L_060m	NA	NA	NA	NA	NA	NA	NA	NA	NA	Light (JR lab)	NA	NA	NA	NA	NA	50	NA	225	NA	60	200	NA	CM	42
idr1-2_0min_-EDTA_CM_vs_NRC1-h1.sig	NA	NA	NA	0	NA	NA	NA	NA	NA	NA	NA	NA	NA	0.73	NA	NA	NA	225	NA	0	NA	NA	CM	37
idr1-2_20min_-EDTA_CM_vs_NRC1-h1.sig	NA	NA	NA	0	NA	NA	NA	NA	NA	NA	NA	NA	NA	0.73	NA	NA	NA	225	NA	20	NA	NA	CM	37
idr1-2_40min_-EDTA_CM_vs_NRC1-h1.sig	NA	NA	NA	0	NA	NA	NA	NA	NA	NA	NA	NA	NA	0.73	NA	NA	NA	225	NA	40	NA	NA	CM	37
idr1-2_60min_-EDTA_CM_vs_NRC1-h1.sig	NA	NA	NA	0	NA	NA	NA	NA	NA	NA	NA	NA	NA	0.73	NA	NA	NA	225	NA	60	NA	NA	CM	37
idr1_0min_-EDTA_CM_vs_NRC1-h1.sig	NA	NA	NA	0	NA	NA	NA	NA	NA	NA	NA	NA	NA	0.79	NA	NA	NA	225	NA	0	NA	NA	CM	37
idr1_20min_-EDTA_CM_vs_NRC1-h1.sig	NA	NA	NA	0	NA	NA	NA	NA	NA	NA	NA	NA	NA	0.79	NA	NA	NA	225	NA	20	NA	NA	CM	37
idr1_40min_-EDTA_CM_vs_NRC1-h1.sig	NA	NA	NA	0	NA	NA	NA	NA	NA	NA	NA	NA	NA	0.79	NA	NA	NA	225	NA	40	NA	NA	CM	37
idr1_60min_-EDTA_CM_vs_NRC1-h1.sig	NA	NA	NA	0	NA	NA	NA	NA	NA	NA	NA	NA	NA	0.79	NA	NA	NA	225	NA	60	NA	NA	CM	37
idr2_0min_-EDTA_CM_vs_NRC1-h1.sig	NA	NA	NA	0	NA	NA	NA	NA	NA	NA	NA	NA	NA	0.78	NA	NA	NA	225	NA	0	NA	NA	CM	37
idr2_20min_-EDTA_CM_vs_NRC1-h1.sig	NA	NA	NA	0	NA	NA	NA	NA	NA	NA	NA	NA	NA	0.78	NA	NA	NA	225	NA	20	NA	NA	CM	37
idr2_40min_-EDTA_CM_vs_NRC1-h1.sig	NA	NA	NA	0	NA	NA	NA	NA	NA	NA	NA	NA	NA	0.78	NA	NA	NA	225	NA	40	NA	NA	CM	37

idr2_60min_-EDTA_CM_vs_NRC1-h1.sig	NA	NA	NA	0	NA	NA	NA	NA	NA	NA	NA	NA	NA	0.78	NA	NA	NA	225	NA	60	NA	NA	CM	37
sirR_0min_-EDTA_CM_vs_NRC1-h1.sig	NA	NA	NA	0	NA	NA	NA	NA	NA	NA	NA	NA	NA	0.91	NA	NA	NA	225	NA	0	NA	NA	CM	37
sirR_20min_-EDTA_CM_vs_NRC1-h1.sig	NA	NA	NA	0	NA	NA	NA	NA	NA	NA	NA	NA	NA	0.91	NA	NA	NA	225	NA	20	NA	NA	CM	37
sirR_40min_-EDTA_CM_vs_NRC1-h1.sig	NA	NA	NA	0	NA	NA	NA	NA	NA	NA	NA	NA	NA	0.91	NA	NA	NA	225	NA	40	NA	NA	CM	37
sirR_60min_-EDTA_CM_vs_NRC1-h1.sig	NA	NA	NA	0	NA	NA	NA	NA	NA	NA	NA	NA	NA	0.91	NA	NA	NA	225	NA	60	NA	NA	CM	37
troR_0min_-EDTA_CM_vs_NRC1-h1.sig	NA	NA	NA	0	NA	NA	NA	NA	NA	NA	NA	NA	NA	0.76	NA	NA	NA	225	NA	0	NA	NA	CM	37
troR_20min_-EDTA_CM_vs_NRC1-h1.sig	NA	NA	NA	0	NA	NA	NA	NA	NA	NA	NA	NA	NA	0.76	NA	NA	NA	225	NA	20	NA	NA	CM	37
troR_40min_-EDTA_CM_vs_NRC1-h1.sig	NA	NA	NA	0	NA	NA	NA	NA	NA	NA	NA	NA	NA	0.76	NA	NA	NA	225	NA	40	NA	NA	CM	37
troR_60min_-EDTA_CM_vs_NRC1-h1.sig	NA	NA	NA	0	NA	NA	NA	NA	NA	NA	NA	NA	NA	0.76	NA	NA	NA	225	NA	60	NA	NA	CM	37
ura3_0min_-EDTA_CM_vs_NRC1-h1.sig	NA	NA	NA	0	NA	NA	NA	NA	NA	NA	NA	NA	NA	0.76	NA	NA	NA	225	NA	0	NA	NA	CM	37
ura3_20min_-EDTA_CM_vs_NRC1-h1.sig	NA	NA	NA	0	NA	NA	NA	NA	NA	NA	NA	NA	NA	0.76	NA	NA	NA	225	NA	20	NA	NA	CM	37
ura3_40min_-EDTA_CM_vs_NRC1-h1.sig	NA	NA	NA	0	NA	NA	NA	NA	NA	NA	NA	NA	NA	0.76	NA	NA	NA	225	NA	40	NA	NA	CM	37
ura3_60min_-EDTA_CM_vs_NRC1-h1.sig	NA	NA	NA	0	NA	NA	NA	NA	NA	NA	NA	NA	NA	0.76	NA	NA	NA	225	NA	60	NA	NA	CM	37
ura3_0min_1mM_EDTA_vs_NRC1-h1.sig	NA	NA	NA	0	NA	NA	NA	NA	NA	NA	NA	NA	NA	0.76	NA	NA	NA	225	NA	0	NA	NA	CM	37
ura3_20min_1mM_EDTA_vs_NRC1-h1.sig	NA	NA	NA	0	NA	NA	NA	NA	NA	NA	NA	NA	NA	0.76	NA	NA	NA	225	NA	20	NA	NA	CM	37
ura3_40min_1mM_EDTA_vs_NRC1-h1.sig	NA	NA	NA	0	NA	NA	NA	NA	NA	NA	NA	NA	NA	0.76	NA	NA	NA	225	NA	40	NA	NA	CM	37

ura3_60min_1mM_EDTA_vs_NRC1-h1.sig	NA	NA	NA	0	NA	NA	NA	NA	NA	NA	NA	NA	NA	0.76	NA	NA	NA	225	NA	60	NA	NA	CM	37
idr1-2_0min_1mM_EDTA_vs_NRC1-h1.sig	NA	NA	NA	0	NA	NA	NA	NA	NA	NA	NA	NA	NA	0.76	NA	NA	NA	225	NA	0	NA	NA	CM	37
idr1-2_20min_1mM_EDTA_vs_NRC1-h1.sig	NA	NA	NA	0	NA	NA	NA	NA	NA	NA	NA	NA	NA	0.76	NA	NA	NA	225	NA	20	NA	NA	CM	37
idr1-2_40min_1mM_EDTA_vs_NRC1-h1.sig	NA	NA	NA	0	NA	NA	NA	NA	NA	NA	NA	NA	NA	0.76	NA	NA	NA	225	NA	40	NA	NA	CM	37
idr1-2_60min_1mM_EDTA_vs_NRC1-h1.sig	NA	NA	NA	0	NA	NA	NA	NA	NA	NA	NA	NA	NA	0.76	NA	NA	NA	225	NA	60	NA	NA	CM	37
idr1_0min_1mM_EDTA_vs_NRC1-h1.sig	NA	NA	NA	0	NA	NA	NA	NA	NA	NA	NA	NA	NA	0.76	NA	NA	NA	225	NA	0	NA	NA	CM	37
idr1_20min_1mM_EDTA_vs_NRC1-h1.sig	NA	NA	NA	0	NA	NA	NA	NA	NA	NA	NA	NA	NA	0.76	NA	NA	NA	225	NA	20	NA	NA	CM	37
idr1_40min_1mM_EDTA_vs_NRC1-h1.sig	NA	NA	NA	0	NA	NA	NA	NA	NA	NA	NA	NA	NA	0.76	NA	NA	NA	225	NA	40	NA	NA	CM	37
idr1_60min_1mM_EDTA_vs_NRC1-h1.sig	NA	NA	NA	0	NA	NA	NA	NA	NA	NA	NA	NA	NA	0.76	NA	NA	NA	225	NA	60	NA	NA	CM	37
idr2_0min_1mM_EDTA_vs_NRC1-h1.sig	NA	NA	NA	0	NA	NA	NA	NA	NA	NA	NA	NA	NA	0.76	NA	NA	NA	225	NA	0	NA	NA	CM	37
idr2_20min_1mM_EDTA_vs_NRC1-h1.sig	NA	NA	NA	0	NA	NA	NA	NA	NA	NA	NA	NA	NA	0.76	NA	NA	NA	225	NA	20	NA	NA	CM	37
idr2_40min_1mM_EDTA_vs_NRC1-h1.sig	NA	NA	NA	0	NA	NA	NA	NA	NA	NA	NA	NA	NA	0.76	NA	NA	NA	225	NA	40	NA	NA	CM	37
idr2_60min_1mM_EDTA_vs_NRC1-h1.sig	NA	NA	NA	0	NA	NA	NA	NA	NA	NA	NA	NA	NA	0.76	NA	NA	NA	225	NA	60	NA	NA	CM	37
sirR_20min_1mM_EDTA_vs_NRC1-h1.sig	NA	NA	NA	0	NA	NA	NA	NA	NA	NA	NA	NA	NA	0.76	NA	NA	NA	225	NA	20	NA	NA	CM	37
sirR_40min_1mM_EDTA_vs_NRC1-h1.sig	NA	NA	NA	0	NA	NA	NA	NA	NA	NA	NA	NA	NA	0.76	NA	NA	NA	225	NA	40	NA	NA	CM	37

sirR_60min_1mM_EDTA_vs_NRC1-h1.sig	NA	NA	NA	0	NA	NA	NA	NA	NA	NA	NA	NA	NA	0.76	NA	NA	NA	225	NA	60	NA	NA	CM	37
troR_0min_1mM_EDTA_vs_NRC1-h1.sig	NA	NA	NA	0	NA	NA	NA	NA	NA	NA	NA	NA	NA	0.76	NA	NA	NA	225	NA	0	NA	NA	CM	37
troR_20min_1mM_EDTA_vs_NRC1-h1.sig	NA	NA	NA	0	NA	NA	NA	NA	NA	NA	NA	NA	NA	0.76	NA	NA	NA	225	NA	20	NA	NA	CM	37
troR_40min_1mM_EDTA_vs_NRC1-h1.sig	NA	NA	NA	0	NA	NA	NA	NA	NA	NA	NA	NA	NA	0.76	NA	NA	NA	225	NA	40	NA	NA	CM	37
troR_60min_1mM_EDTA_vs_NRC1-h1.sig	NA	NA	NA	0	NA	NA	NA	NA	NA	NA	NA	NA	NA	0.76	NA	NA	NA	225	NA	60	NA	NA	CM	37
KO_1179C.1_0.1694_vs_NRC-1_h1.sig	NA	NA	NA	NA	NA	NA	NA	NA	NA	NA	NA	NA	NA	0.17	NA	NA	NA	225	NA	1034	NA	NA	FangYin's CDM	37
KO_1179C.1_0.3684_vs_NRC-1_h1.sig	NA	NA	NA	NA	NA	NA	NA	NA	NA	NA	NA	NA	NA	0.37	NA	NA	NA	225	NA	2138	NA	NA	FangYin's CDM	37
KO_1179C.1_0.613_vs_NRC-1_h1.sig	NA	NA	NA	NA	NA	NA	NA	NA	NA	NA	NA	NA	NA	0.61	NA	NA	NA	225	NA	2832	NA	NA	FangYin's CDM	37
KO_1179C.1_1.1488_vs_NRC-1_h1.sig	NA	NA	NA	NA	NA	NA	NA	NA	NA	NA	NA	NA	NA	1.15	NA	NA	NA	225	NA	4095	NA	NA	FangYin's CDM	37
KO_trh6.1_0.1689_vs_NRC-1_h1.sig	NA	NA	NA	NA	NA	NA	NA	NA	NA	NA	NA	NA	NA	0.17	NA	NA	NA	225	NA	1034	NA	NA	FangYin's CDM	37
KO_trh6.1_0.3532_vs_NRC-1_h1.sig	NA	NA	NA	NA	NA	NA	NA	NA	NA	NA	NA	NA	NA	0.35	NA	NA	NA	225	NA	2138	NA	NA	FangYin's CDM	37
KO_trh6.1_0.4762_vs_NRC-1_h1.sig	NA	NA	NA	NA	NA	NA	NA	NA	NA	NA	NA	NA	NA	0.48	NA	NA	NA	225	NA	2832	NA	NA	FangYin's CD	37

																								M	
KO_trh6.1_0.7964_vs_NRC-1_h1.sig	NA	NA	NA	NA	NA	NA	NA	NA	NA	NA	NA	NA	NA	0.8	NA	NA	NA	225	NA	4095	NA	NA	FangYin's CDM	37
KO_1237C.1_0.2219_vs_NRC-1_h1.sig	NA	NA	NA	NA	NA	NA	NA	NA	NA	NA	NA	NA	NA	0.22	NA	NA	NA	225	NA	1034	NA	NA	FangYin's CDM	37
KO_1237C.1_0.3505_vs_NRC-1_h1.sig	NA	NA	NA	NA	NA	NA	NA	NA	NA	NA	NA	NA	NA	0.35	NA	NA	NA	225	NA	2138	NA	NA	FangYin's CDM	37
KO_1237C.1_0.4056_vs_NRC-1_h1.sig	NA	NA	NA	NA	NA	NA	NA	NA	NA	NA	NA	NA	NA	0.41	NA	NA	NA	225	NA	2832	NA	NA	FangYin's CDM	37
KO_1237C.1_0.4442_vs_NRC-1_h1.sig	NA	NA	NA	NA	NA	NA	NA	NA	NA	NA	NA	NA	NA	0.44	NA	NA	NA	225	NA	4095	NA	NA	FangYin's CDM	37
KO_1179C.2_0.1699_vs_NRC-1_h1.sig	NA	NA	NA	NA	NA	NA	NA	NA	NA	NA	NA	NA	NA	0.17	NA	NA	NA	225	NA	1034	NA	NA	FangYin's CDM	37
KO_1179C.2_0.3565_vs_NRC-1_h1.sig	NA	NA	NA	NA	NA	NA	NA	NA	NA	NA	NA	NA	NA	0.36	NA	NA	NA	225	NA	2138	NA	NA	FangYin's CDM	37
KO_1179C.2_0.6018_vs_NRC-1_h1.sig	NA	NA	NA	NA	NA	NA	NA	NA	NA	NA	NA	NA	NA	0.6	NA	NA	NA	225	NA	2832	NA	NA	FangYin's CDM	37
KO_1179C.2_1.1273_vs_NRC-1_h1.sig	NA	NA	NA	NA	NA	NA	NA	NA	NA	NA	NA	NA	NA	1.13	NA	NA	NA	225	NA	4095	NA	NA	FangYin's CDM	37
KO_ura3.3_0.1673_vs_NRC-1_h1.sig	NA	NA	NA	NA	NA	NA	NA	NA	NA	NA	NA	NA	NA	0.17	NA	NA	NA	225	NA	1034	NA	NA	FangYi	37

																						n's CDM	
KO_ura3.3_0.274_vs_NRC-1_h1.sig	NA	NA	NA	NA	NA	NA	NA	NA	NA	NA	NA	NA	NA	0.27	NA	NA	NA	225	NA	2138	NA	NA	FangYin's CDM	37
KO_ura3.3_0.4452_vs_NRC-1_h1.sig	NA	NA	NA	NA	NA	NA	NA	NA	NA	NA	NA	NA	NA	0.45	NA	NA	NA	225	NA	2832	NA	NA	FangYin's CDM	37
KO_ura3.3_0.8976_vs_NRC-1_h1.sig	NA	NA	NA	NA	NA	NA	NA	NA	NA	NA	NA	NA	NA	0.9	NA	NA	NA	225	NA	4095	NA	NA	FangYin's CDM	37
KO_trh6.2_0.1677_vs_NRC-1_h1.sig	NA	NA	NA	NA	NA	NA	NA	NA	NA	NA	NA	NA	NA	0.17	NA	NA	NA	225	NA	1034	NA	NA	FangYin's CDM	37
KO_trh6.2_0.3621_vs_NRC-1_h1.sig	NA	NA	NA	NA	NA	NA	NA	NA	NA	NA	NA	NA	NA	0.36	NA	NA	NA	225	NA	2138	NA	NA	FangYin's CDM	37
KO_trh6.2_0.5162_vs_NRC-1_h1.sig	NA	NA	NA	NA	NA	NA	NA	NA	NA	NA	NA	NA	NA	0.52	NA	NA	NA	225	NA	2832	NA	NA	FangYin's CDM	37
KO_trh6.2_0.838_vs_NRC-1_h1.sig	NA	NA	NA	NA	NA	NA	NA	NA	NA	NA	NA	NA	NA	0.84	NA	NA	NA	225	NA	4095	NA	NA	FangYin's CDM	37
KO_ura3.4_0.1642_vs_NRC-1_h1.sig	NA	NA	NA	NA	NA	NA	NA	NA	NA	NA	NA	NA	NA	0.16	NA	NA	NA	225	NA	1034	NA	NA	FangYin's CDM	37
KO_ura3.4_0.2812_vs_NRC-1_h1.sig	NA	NA	NA	NA	NA	NA	NA	NA	NA	NA	NA	NA	NA	0.28	NA	NA	NA	225	NA	2138	NA	NA	FangYin's CDM	37

KO_ura3.4_0.4645_vs_NRC-1_h1.sig	NA	NA	NA	NA	NA	NA	NA	NA	NA	NA	NA	NA	NA	0.46	NA	NA	NA	225	NA	2832	NA	NA	FangYin's CDM	37
KO_ura3.4_0.9128_vs_NRC-1_h1.sig	NA	NA	NA	NA	NA	NA	NA	NA	NA	NA	NA	NA	NA	0.91	NA	NA	NA	225	NA	4095	NA	NA	FangYin's CDM	37
KO_trh7.2_0.1446_vs_NRC-1_h1.sig	NA	NA	NA	NA	NA	NA	NA	NA	NA	NA	NA	NA	NA	0.14	NA	NA	NA	225	NA	1034	NA	NA	FangYin's CDM	37
KO_trh7.2_0.3424_vs_NRC-1_h1.sig	NA	NA	NA	NA	NA	NA	NA	NA	NA	NA	NA	NA	NA	0.34	NA	NA	NA	225	NA	2138	NA	NA	FangYin's CDM	37
KO_trh7.2_0.5404_vs_NRC-1_h1.sig	NA	NA	NA	NA	NA	NA	NA	NA	NA	NA	NA	NA	NA	0.54	NA	NA	NA	225	NA	2832	NA	NA	FangYin's CDM	37
KO_trh7.2_1.081_vs_NRC-1_h1.sig	NA	NA	NA	NA	NA	NA	NA	NA	NA	NA	NA	NA	NA	1.08	NA	NA	NA	225	NA	4095	NA	NA	FangYin's CDM	37
KO_1237.2_0.218_vs_NRC-1_h1.sig	NA	NA	NA	NA	NA	NA	NA	NA	NA	NA	NA	NA	NA	0.22	NA	NA	NA	225	NA	1034	NA	NA	FangYin's CDM	37
KO_1237.2_0.3619_vs_NRC-1_h1.sig	NA	NA	NA	NA	NA	NA	NA	NA	NA	NA	NA	NA	NA	0.36	NA	NA	NA	225	NA	2138	NA	NA	FangYin's CDM	37
KO_1237.2_0.3745_vs_NRC-1_h1.sig	NA	NA	NA	NA	NA	NA	NA	NA	NA	NA	NA	NA	NA	0.37	NA	NA	NA	225	NA	2832	NA	NA	FangYin's CDM	37
KO_1237.2_0.4319_vs_NRC-1_h1.sig	NA	NA	NA	NA	NA	NA	NA	NA	NA	NA	NA	NA	NA	0.43	NA	NA	NA	225	NA	4095	NA	NA	FangYin's CD	37

																							M	
KO_trh7.1_0.1442_vs_NRC-1_h1.sig	NA	NA	NA	NA	NA	NA	NA	NA	NA	NA	NA	NA	NA	0.14	NA	NA	NA	225	NA	1034	NA	NA	FangYin's CDM	37
KO_trh7.1_0.3293_vs_NRC-1_h1.sig	NA	NA	NA	NA	NA	NA	NA	NA	NA	NA	NA	NA	NA	0.33	NA	NA	NA	225	NA	2138	NA	NA	FangYin's CDM	37
KO_trh7.1_0.5217_vs_NRC-1_h1.sig	NA	NA	NA	NA	NA	NA	NA	NA	NA	NA	NA	NA	NA	0.52	NA	NA	NA	225	NA	2832	NA	NA	FangYin's CDM	37
O2_0258_-0001_L2H_vs_NRC1d.sig	NA	NA	NA	NA	NA	NA	NA	NA	NA	NA	NA	NA	NA	0.5	NA	0.8	NA	NA	NA	-1	NA	NA	CM	37
O2_0258_0005_H_vs_NRC1d.sig	NA	NA	NA	NA	NA	NA	NA	NA	NA	NA	NA	NA	NA	0.51	NA	52.4	NA	NA	NA	5	NA	NA	CM	37
O2_0258_0010_H_vs_NRC1d.sig	NA	NA	NA	NA	NA	NA	NA	NA	NA	NA	NA	NA	NA	0.51	NA	60.4	NA	NA	NA	10	NA	NA	CM	37
O2_0258_0020_H_vs_NRC1d.sig	NA	NA	NA	NA	NA	NA	NA	NA	NA	NA	NA	NA	NA	0.5	NA	66.4	NA	NA	NA	20	NA	NA	CM	37
O2_0258_0030_H_vs_NRC1d.sig	NA	NA	NA	NA	NA	NA	NA	NA	NA	NA	NA	NA	NA	0.5	NA	69.1	NA	NA	NA	30	NA	NA	CM	37
O2_0258_0045_H_vs_NRC1d.sig	NA	NA	NA	NA	NA	NA	NA	NA	NA	NA	NA	NA	NA	0.47	NA	71.8	NA	NA	NA	45	NA	NA	CM	37
O2_0258_0090_H_vs_NRC1d.sig	NA	NA	NA	NA	NA	NA	NA	NA	NA	NA	NA	NA	NA	0.48	NA	75.9	NA	NA	NA	90	NA	NA	CM	37
O2_0258_0180_H_vs_NRC1d.sig	NA	NA	NA	NA	NA	NA	NA	NA	NA	NA	NA	NA	NA	0.48	NA	79.5	NA	NA	NA	180	NA	NA	CM	37
o2_set1_-001m_L2H_005_vs_NRC-1c	NA	NA	NA	NA	NA	NA	NA	NA	NA	10	NA	NA	NA	0.55	NA	0.5	NA	1200	NA	-1	NA	NA	CM	37
o2_set1_0001m_L2H_500_vs_NRC-1c	NA	NA	NA	NA	NA	NA	NA	NA	NA	10	NA	NA	NA	0.57	NA	50	NA	1200	NA	1	NA	NA	CM	37
o2_set1_0005m_H_922_vs_NRC-1c	NA	NA	NA	NA	NA	NA	NA	NA	NA	10	NA	NA	NA	0.59	NA	92.2	NA	1200	NA	5	NA	NA	CM	37
o2_set1_0010m_H_947_vs_NRC-1c	NA	NA	NA	NA	NA	NA	NA	NA	NA	10	NA	NA	NA	0.53	NA	94.7	NA	1200	NA	10	NA	NA	CM	37
o2_set1_0020m_H_937_vs_NRC-1c	NA	NA	NA	NA	NA	NA	NA	NA	NA	10	NA	NA	NA	0.54	NA	93.7	NA	1200	NA	20	NA	NA	CM	37

o2_set1_0030m_H_931_vs_NRC-1c	NA	NA	NA	NA	NA	NA	NA	NA	NA	10	NA	NA	NA	0.51	NA	93.1	NA	1200	NA	30	NA	NA	CM	37
o2_set1_0045m_H_939_vs_NRC-1c	NA	NA	NA	NA	NA	NA	NA	NA	NA	10	NA	NA	NA	0.5	NA	93.9	NA	1200	NA	45	NA	NA	CM	37
o2_set1_0090m_H_941_vs_NRC-1c	NA	NA	NA	NA	NA	NA	NA	NA	NA	10	NA	NA	NA	0.5	NA	94.1	NA	1200	NA	90	NA	NA	CM	37
o2_set1_0180m_H_930_vs_NRC-1c	NA	NA	NA	NA	NA	NA	NA	NA	NA	10	NA	NA	NA	0.55	NA	93	NA	1200	NA	180	NA	NA	CM	37
o2_set1_0360m_H_903_vs_NRC-1c	NA	NA	NA	NA	NA	NA	NA	NA	NA	10	NA	NA	NA	0.64	NA	90.3	NA	1200	NA	360	NA	NA	CM	37
o2_set1_0362m_H2L_860_vs_NRC-1c	NA	NA	NA	NA	NA	NA	NA	NA	NA	10	NA	NA	NA	0.66	NA	86	NA	300	NA	362	NA	NA	CM	37
o2_set1_0367m_H2L_215_vs_NRC-1c	NA	NA	NA	NA	NA	NA	NA	NA	NA	10	NA	NA	NA	0.66	NA	21.5	NA	300	NA	367	NA	NA	CM	37
o2_set1_0372m_H2L_079_vs_NRC-1c	NA	NA	NA	NA	NA	NA	NA	NA	NA	10	NA	NA	NA	0.64	NA	7.9	NA	300	NA	372	NA	NA	CM	37
o2_set1_0382m_H2L_048_vs_NRC-1c	NA	NA	NA	NA	NA	NA	NA	NA	NA	10	NA	NA	NA	0.62	NA	4.8	NA	300	NA	382	NA	NA	CM	37
o2_set1_0387m_L_041_vs_NRC-1c	NA	NA	NA	NA	NA	NA	NA	NA	NA	10	NA	NA	NA	0.65	NA	4.1	NA	300	NA	387	NA	NA	CM	37
o2_set1_0392m_L_037_vs_NRC-1c	NA	NA	NA	NA	NA	NA	NA	NA	NA	10	NA	NA	NA	0.67	NA	3.7	NA	300	NA	392	NA	NA	CM	37
o2_set1_0397m_L_035_vs_NRC-1c	NA	NA	NA	NA	NA	NA	NA	NA	NA	10	NA	NA	NA	0.61	NA	3.5	NA	300	NA	397	NA	NA	CM	37
o2_set1_0407m_L_030_vs_NRC-1c	NA	NA	NA	NA	NA	NA	NA	NA	NA	10	NA	NA	NA	0.63	NA	3	NA	300	NA	407	NA	NA	CM	37
o2_set1_0417m_L_027_vs_NRC-1c	NA	NA	NA	NA	NA	NA	NA	NA	NA	10	NA	NA	NA	0.63	NA	2.7	NA	300	NA	417	NA	NA	CM	37
o2_set1_0432m_L_024_vs_NRC-1c	NA	NA	NA	NA	NA	NA	NA	NA	NA	10	NA	NA	NA	0.63	NA	2.4	NA	300	NA	432	NA	NA	CM	37
o2_set1_0477m_L_017_vs_NRC-1c	NA	NA	NA	NA	NA	NA	NA	NA	NA	10	NA	NA	NA	0.62	NA	1.7	NA	300	NA	477	NA	NA	CM	37
o2_set1_0567m_L_011_vs_NRC-1c	NA	NA	NA	NA	NA	NA	NA	NA	NA	10	NA	NA	NA	0.6	NA	1.1	NA	300	NA	567	NA	NA	CM	37
o2_set1_0747m_L_008_vs_NRC-1c	NA	NA	NA	NA	NA	NA	NA	NA	NA	10	NA	NA	NA	0.62	NA	0.8	NA	300	NA	747	NA	NA	CM	37
o2_set1_0750m_L2H_540_vs_NRC-1c	NA	NA	NA	NA	NA	NA	NA	NA	NA	10	NA	NA	NA	0.63	NA	54	NA	1200	NA	750	NA	NA	CM	37

o2_set1_0755m_L2H_825_vs_NRC-1c	NA	NA	NA	NA	NA	NA	NA	NA	NA	10	NA	NA	NA	0.64	NA	82.5	NA	1200	NA	755	NA	NA	CM	37
o2_set1_0760m_L2H_847_vs_NRC-1c	NA	NA	NA	NA	NA	NA	NA	NA	NA	10	NA	NA	NA	0.62	NA	84.7	NA	1200	NA	760	NA	NA	CM	37
o2_set1_0770m_L2H_852_vs_NRC-1c	NA	NA	NA	NA	NA	NA	NA	NA	NA	10	NA	NA	NA	0.61	NA	85.2	NA	1200	NA	770	NA	NA	CM	37
o2_set1_0780m_L2H_847_vs_NRC-1c	NA	NA	NA	NA	NA	NA	NA	NA	NA	10	NA	NA	NA	0.61	NA	84.7	NA	1200	NA	780	NA	NA	CM	37
o2_set2_H_L_000_vs_NRC-1d.sig	NA	NA	NA	NA	NA	NA	NA	NA	NA	NA	NA	NA	NA	0.6	NA	98.5	NA	250	NA	0	NA	NA	CM	37
o2_set2_H_L_005_vs_NRC-1d.sig	NA	NA	NA	NA	NA	NA	NA	NA	NA	NA	NA	NA	NA	0.6	NA	40.7	NA	250	NA	5	NA	NA	CM	37
o2_set2_H_L_010_vs_NRC-1d.sig	NA	NA	NA	NA	NA	NA	NA	NA	NA	NA	NA	NA	NA	0.62	NA	4.3	NA	250	NA	10	NA	NA	CM	37
o2_set2_H_L_020_vs_NRC-1d.sig	NA	NA	NA	NA	NA	NA	NA	NA	NA	NA	NA	NA	NA	0.61	NA	2.9	NA	250	NA	20	NA	NA	CM	37
o2_set2_L_000_vs_NRC-1d.sig	NA	NA	NA	NA	NA	NA	NA	NA	NA	NA	NA	NA	NA	0.62	NA	1.6	NA	250	NA	25	NA	NA	CM	37
o2_set2_L_005_vs_NRC-1d.sig	NA	NA	NA	NA	NA	NA	NA	NA	NA	NA	NA	NA	NA	0.6	NA	1.4	NA	250	NA	30	NA	NA	CM	37
o2_set2_L_010_vs_NRC-1d.sig	NA	NA	NA	NA	NA	NA	NA	NA	NA	NA	NA	NA	NA	0.61	NA	1.1	NA	250	NA	35	NA	NA	CM	37
o2_set2_L_020_vs_NRC-1d.sig	NA	NA	NA	NA	NA	NA	NA	NA	NA	NA	NA	NA	NA	0.59	NA	0.8	NA	250	NA	45	NA	NA	CM	37
o2_set2_L_030_vs_NRC-1d.sig	NA	NA	NA	NA	NA	NA	NA	NA	NA	NA	NA	NA	NA	0.57	NA	0.7	NA	250	NA	55	NA	NA	CM	37
o2_set2_L_045_vs_NRC-1d.sig	NA	NA	NA	NA	NA	NA	NA	NA	NA	NA	NA	NA	NA	0.56	NA	0.4	NA	250	NA	70	NA	NA	CM	37
o2_set2_L_090_vs_NRC-1d.sig	NA	NA	NA	NA	NA	NA	NA	NA	NA	NA	NA	NA	NA	0.59	NA	0.1	NA	250	NA	115	NA	NA	CM	37
o2_set2_L_135_vs_NRC-1d.sig	NA	NA	NA	NA	NA	NA	NA	NA	NA	NA	NA	NA	NA	0.57	NA	0	NA	250	NA	160	NA	NA	CM	37
o2_set2_L_180_vs_NRC-1d.sig	NA	NA	NA	NA	NA	NA	NA	NA	NA	NA	NA	NA	NA	0.56	NA	0	NA	250	NA	205	NA	NA	CM	37
o2_set2_L_270_vs_NRC-1d.sig	NA	NA	NA	NA	NA	NA	NA	NA	NA	NA	NA	NA	NA	0.55	NA	0	NA	250	NA	295	NA	NA	CM	37
o2_set2_L_360_vs_NRC-1d.sig	NA	NA	NA	NA	NA	NA	NA	NA	NA	NA	NA	NA	NA	0.57	NA	0	NA	250	NA	385	NA	NA	CM	37
o2_set3_-0005_min_LO2_vs_NRC1f.sig	0.56	NA	NA	NA	NA	NA	NA	NA	NA	NA	NA	NA	NA	0.38	NA	0	NA	250	NA	-5	NA	NA	CM	37
o2_set3_0000_min_L2HO2_vs_NRC1f.sig	0.8	NA	NA	NA	NA	NA	NA	NA	NA	NA	NA	NA	NA	0.36	NA	0	NA	1100	NA	0	NA	NA	CM	37

o2_set3_0005_min_HO2_vs_NRC1f.sig	0.59	NA	NA	NA	NA	NA	NA	NA	NA	NA	NA	NA	NA	0.36	NA	91.1	NA	1100	NA	5	NA	NA	CM	37
o2_set3_0010_min_HO2_vs_NRC1f.sig	0.7	NA	NA	NA	NA	NA	NA	NA	NA	NA	NA	NA	NA	0.41	NA	95.8	NA	1100	NA	10	NA	NA	CM	37
o2_set3_0020_min_HO2_vs_NRC1f.sig	0.75	NA	NA	NA	NA	NA	NA	NA	NA	NA	NA	NA	NA	0.41	NA	98.7	NA	1100	NA	20	NA	NA	CM	37
o2_set3_0030_min_HO2_vs_NRC1f.sig	0.77	NA	NA	NA	NA	NA	NA	NA	NA	NA	NA	NA	NA	0.4	NA	100	NA	1100	NA	30	NA	NA	CM	37
o2_set3_0045_min_HO2_vs_NRC1f.sig	0.9	NA	NA	NA	NA	NA	NA	NA	NA	NA	NA	NA	NA	0.41	NA	100	NA	1100	NA	45	NA	NA	CM	37
o2_set3_0060_min_HO2_vs_NRC1f.sig	1.1	NA	NA	NA	NA	NA	NA	NA	NA	NA	NA	NA	NA	0.4	NA	100	NA	1100	NA	60	NA	NA	CM	37
o2_set3_0090_min_HO2_vs_NRC1f.sig	0.88	NA	NA	NA	NA	NA	NA	NA	NA	NA	NA	NA	NA	0.4	NA	100	NA	1100	NA	90	NA	NA	CM	37
o2_set3_0120_min_HO2_vs_NRC1f.sig	1.23	NA	NA	NA	NA	NA	NA	NA	NA	NA	NA	NA	NA	0.41	NA	100	NA	1100	NA	120	NA	NA	CM	37
o2_set3_0180_min_HO2_vs_NRC1f.sig	1.29	NA	NA	NA	NA	NA	NA	NA	NA	NA	NA	NA	NA	0.42	NA	100	NA	1100	NA	180	NA	NA	CM	37
o2_set3_0240_min_HO2_vs_NRC1f.sig	1.36	NA	NA	NA	NA	NA	NA	NA	NA	NA	NA	NA	NA	0.4	NA	100	NA	1100	NA	240	NA	NA	CM	37
o2_set3_0300_min_HO2_vs_NRC1f.sig	1.4	NA	NA	NA	NA	NA	NA	NA	NA	NA	NA	NA	NA	0.4	NA	100	NA	1100	NA	300	NA	NA	CM	37
o2_set3_0360_min_HO2_vs_NRC1f.sig	1.76	NA	NA	NA	NA	NA	NA	NA	NA	NA	NA	NA	NA	0.39	NA	100	NA	1100	NA	360	NA	NA	CM	37
o2_set3_0420_min_HO2_vs_NRC1f.sig	1.19	NA	NA	NA	NA	NA	NA	NA	NA	NA	NA	NA	NA	0.4	NA	100	NA	1100	NA	420	NA	NA	CM	37
o2_set3_0540_min_HO2_vs_NRC1f.sig	1.51	NA	NA	NA	NA	NA	NA	NA	NA	NA	NA	NA	NA	0.44	NA	100	NA	1100	NA	540	NA	NA	CM	37
o2_set3_0600_min_HO2_vs_NRC1f.sig	1.86	NA	NA	NA	NA	NA	NA	NA	NA	NA	NA	NA	NA	0.43	NA	100	NA	1100	NA	600	NA	NA	CM	37
o2_set3_0660_min_HO2_vs_NRC1f.sig	1.83	NA	NA	NA	NA	NA	NA	NA	NA	NA	NA	NA	NA	0.43	NA	100	NA	1100	NA	660	NA	NA	CM	37
gamma3__0000gy-	NA	NA	NA	NA	NA	NA	0	NA	NA	NA	NA	NA	NA	NA	NA	NA	NA	225	NA	0	NA	NA	CM	42

0000m																								
gamma3__0000gy-0010m	NA	NA	NA	NA	NA	NA	0	NA	NA	NA	NA	NA	NA	NA	NA	NA	NA	225	NA	10	NA	NA	CM	42
gamma3__0000gy-0020m	NA	NA	NA	NA	NA	NA	0	NA	NA	NA	NA	NA	NA	NA	NA	NA	NA	225	NA	20	NA	NA	CM	42
gamma3__0000gy-0030m	NA	NA	NA	NA	NA	NA	0	NA	NA	NA	NA	NA	NA	NA	NA	NA	NA	225	NA	30	NA	NA	CM	42
gamma3__0000gy-0040m	NA	NA	NA	NA	NA	NA	0	NA	NA	NA	NA	NA	NA	NA	NA	NA	NA	225	NA	40	NA	NA	CM	42
gamma3__0000gy-0050m	NA	NA	NA	NA	NA	NA	0	NA	NA	NA	NA	NA	NA	NA	NA	NA	NA	225	NA	50	NA	NA	CM	42
gamma3__0000gy-0060m	NA	NA	NA	NA	NA	NA	0	NA	NA	NA	NA	NA	NA	NA	NA	NA	NA	225	NA	60	NA	NA	CM	42
gamma3__0000gy-0120m	NA	NA	NA	NA	NA	NA	0	NA	NA	NA	NA	NA	NA	NA	NA	NA	NA	225	NA	120	NA	NA	CM	42
gamma3__0000gy-0240m	NA	NA	NA	NA	NA	NA	0	NA	NA	NA	NA	NA	NA	NA	NA	NA	NA	225	NA	240	NA	NA	CM	42
gamma2__0000gy-0000m	NA	NA	NA	NA	NA	NA	0	NA	NA	NA	NA	NA	NA	NA	NA	NA	NA	225	NA	0	NA	NA	CM	42
gamma2__0000gy-0010m	NA	NA	NA	NA	NA	NA	0	NA	NA	NA	NA	NA	NA	NA	NA	NA	NA	225	NA	10	NA	NA	CM	42
gamma2__0000gy-0020m	NA	NA	NA	NA	NA	NA	0	NA	NA	NA	NA	NA	NA	NA	NA	NA	NA	225	NA	20	NA	NA	CM	42
gamma2__0000gy-0030m	NA	NA	NA	NA	NA	NA	0	NA	NA	NA	NA	NA	NA	NA	NA	NA	NA	225	NA	30	NA	NA	CM	42
gamma2__0000gy-0040m	NA	NA	NA	NA	NA	NA	0	NA	NA	NA	NA	NA	NA	NA	NA	NA	NA	225	NA	40	NA	NA	CM	42
gamma2__0000gy-0050m	NA	NA	NA	NA	NA	NA	0	NA	NA	NA	NA	NA	NA	NA	NA	NA	NA	225	NA	50	NA	NA	CM	42
gamma2__0000gy-0060m	NA	NA	NA	NA	NA	NA	0	NA	NA	NA	NA	NA	NA	NA	NA	NA	NA	225	NA	60	NA	NA	CM	42
gamma2__0000gy-0120m	NA	NA	NA	NA	NA	NA	0	NA	NA	NA	NA	NA	NA	NA	NA	NA	NA	225	NA	120	NA	NA	CM	42
gamma2__0000gy-0240m	NA	NA	NA	NA	NA	NA	0	NA	NA	NA	NA	NA	NA	NA	NA	NA	NA	225	NA	240	NA	NA	CM	42
PQ_Const._set_1_0.25mM_-001m_vs_NRC-1f.sig	NA	NA	NA	NA	NA	NA	NA	NA	NA	NA	NA	NA	NA	0.69	NA	34.4	0	225	NA	-1	NA	NA	CM	42
PQ_Const._set_1_0.25mM_000m_vs_NRC-1f.sig	NA	NA	NA	NA	NA	NA	NA	NA	NA	NA	NA	NA	NA	0.66	NA	35.8	0	225	NA	0	NA	NA	CM	42
PQ_Const._set_1_0.25mM_005m_vs_NRC-1f.sig	NA	NA	NA	NA	NA	NA	NA	NA	NA	NA	NA	NA	NA	0.68	NA	35.8	0	225	NA	5	NA	NA	CM	42
PQ_Const._set_1_0.25mM_010m_vs_NRC-1f.sig	NA	NA	NA	NA	NA	NA	NA	NA	NA	NA	NA	NA	NA	0.69	NA	35.4	0	225	NA	10	NA	NA	CM	42

PQ_Const._set_1_0.25mM_020m_vs_NRC-1f.sig	NA	NA	NA	NA	NA	NA	NA	NA	NA	NA	NA	NA	NA	0.68	NA	34	0	225	NA	20	NA	NA	CM	42
PQ_Const._set_1_0.25mM_040m_vs_NRC-1f.sig	NA	NA	NA	NA	NA	NA	NA	NA	NA	NA	NA	NA	NA	0.7	NA	31.8	0	225	NA	40	NA	NA	CM	42
PQ_Const._set_1_0.25mM_080m_vs_NRC-1f.sig	NA	NA	NA	NA	NA	NA	NA	NA	NA	NA	NA	NA	NA	0.65	NA	33.1	0	225	NA	80	NA	NA	CM	42
PQ_Const._set_1_0.25mM_160m_vs_NRC-1f.sig	NA	NA	NA	NA	NA	NA	NA	NA	NA	NA	NA	NA	NA	0.65	NA	36.1	0	225	NA	160	NA	NA	CM	42
PQ_Const._set_1_0.25mM_320m_vs_NRC-1f.sig	NA	NA	NA	NA	NA	NA	NA	NA	NA	NA	NA	NA	NA	0.54	NA	49.6	0	225	NA	320	NA	NA	CM	42
20061006_Cmyc_tfbE_rep2_0.169_vs_NRC-1e	NA	NA	NA	NA	NA	NA	NA	NA	NA	20	NA	NA	NA	0.17	tfbE	60	NA	220	cmyc	480	NA	NA	CM	37
20061006_Cmyc_tfbE_rep2_0.439_vs_NRC-1e	NA	NA	NA	NA	NA	NA	NA	NA	NA	20	NA	NA	NA	0.44	tfbE	60	NA	220	cmyc	870	NA	NA	CM	37
20061006_Cmyc_tfbE_rep2_0.877_vs_NRC-1e	NA	NA	NA	NA	NA	NA	NA	NA	NA	20	NA	NA	NA	0.88	tfbE	60	NA	220	cmyc	1410	NA	NA	CM	37
20061006_Cmyc_tfbE_rep1_0.170_vs_NRC-1e	NA	NA	NA	NA	NA	NA	NA	NA	NA	20	NA	NA	NA	0.17	tfbE	60	NA	220	cmyc	480	NA	NA	CM	37
20061006_Cmyc_tfbE_rep1_0.416_vs_NRC-1e	NA	NA	NA	NA	NA	NA	NA	NA	NA	20	NA	NA	NA	0.42	tfbE	60	NA	220	cmyc	870	NA	NA	CM	37
20061006_Cmyc_tfbE_rep1_0.835_vs_NRC-1e	NA	NA	NA	NA	NA	NA	NA	NA	NA	20	NA	NA	NA	0.84	tfbE	60	NA	220	cmyc	1410	NA	NA	CM	37
20061006_Cmyc_tfbD_rep2_0.176_vs_NRC-1e.sig	NA	NA	NA	NA	NA	NA	NA	NA	NA	20	NA	NA	NA	0.18	tfbD	60	NA	220	cmyc	480	NA	NA	CM	37
20061006_Cmyc_tfbD_rep2_0.416_vs_NRC-1e.sig	NA	NA	NA	NA	NA	NA	NA	NA	NA	20	NA	NA	NA	0.42	tfbD	60	NA	220	cmyc	960	NA	NA	CM	37
20061006_Cmyc_tfbD_rep2_0.851_vs_NRC-1e.sig	NA	NA	NA	NA	NA	NA	NA	NA	NA	20	NA	NA	NA	0.85	tfbD	60	NA	220	cmyc	1470	NA	NA	CM	37
20061006_Cmyc_tfbD_rep1_0.185_vs_NRC-1e.sig	NA	NA	NA	NA	NA	NA	NA	NA	NA	20	NA	NA	NA	0.19	tfbD	60	NA	220	cmyc	480	NA	NA	CM	37
20061006_Cmyc_tfbD_rep1_0.417_vs_NRC-1e.sig	NA	NA	NA	NA	NA	NA	NA	NA	NA	20	NA	NA	NA	0.42	tfbD	60	NA	220	cmyc	960	NA	NA	CM	37

20061006_Cmyc_tfbD_rep1_0.899_vs_NRC-1e.sig	NA	NA	NA	NA	NA	NA	NA	NA	NA	20	NA	NA	NA	0.9	tfbD	60	NA	220	cmyc	1470	NA	NA	CM	37
20061006_Cmyc_rep2_0.179_vs_NRC-1e.sig	NA	NA	NA	NA	NA	NA	NA	NA	NA	20	NA	NA	NA	0.18	NA	60	NA	220	cmyc	540	NA	NA	CM	37
20061006_Cmyc_rep2_0.399_vs_NRC-1e.sig	NA	NA	NA	NA	NA	NA	NA	NA	NA	20	NA	NA	NA	0.4	NA	60	NA	220	cmyc	870	NA	NA	CM	37
20061006_Cmyc_rep2_0.833_vs_NRC-1e.sig	NA	NA	NA	NA	NA	NA	NA	NA	NA	20	NA	NA	NA	0.83	NA	60	NA	220	cmyc	1470	NA	NA	CM	37
20061006_Cmyc_rep1_0.175_vs_NRC-1e.sig	NA	NA	NA	NA	NA	NA	NA	NA	NA	20	NA	NA	NA	0.18	NA	60	NA	220	cmyc	540	NA	NA	CM	37
20061006_Cmyc_rep1_0.417_vs_NRC-1e.sig	NA	NA	NA	NA	NA	NA	NA	NA	NA	20	NA	NA	NA	0.42	NA	60	NA	220	cmyc	870	NA	NA	CM	37
20061006_Cmyc_rep1_0.835_vs_NRC-1e.sig	NA	NA	NA	NA	NA	NA	NA	NA	NA	20	NA	NA	NA	0.84	NA	60	NA	220	cmyc	1470	NA	NA	CM	37
20060818_KO_ura3_rep2_0.189_vs_NRC-1e.sig	NA	NA	NA	NA	NA	NA	NA	NA	NA	20	NA	NA	NA	0.19	NA	60	NA	220	NA	330	NA	NA	CM	37
20060818_KO_ura3_rep2_0.376_vs_NRC-1e.sig	NA	NA	NA	NA	NA	NA	NA	NA	NA	20	NA	NA	NA	0.38	NA	60	NA	220	NA	690	NA	NA	CM	37
20060818_KO_ura3_rep2_0.828_vs_NRC-1e.sig	NA	NA	NA	NA	NA	NA	NA	NA	NA	20	NA	NA	NA	0.83	NA	60	NA	220	NA	1200	NA	NA	CM	37
20060818_KO_ura3_rep1_0.178_vs_NRC-1e.sig	NA	NA	NA	NA	NA	NA	NA	NA	NA	20	NA	NA	NA	0.18	NA	60	NA	220	NA	330	NA	NA	CM	37
20060818_KO_ura3_rep1_0.405_vs_NRC-1e.sig	NA	NA	NA	NA	NA	NA	NA	NA	NA	20	NA	NA	NA	0.41	NA	60	NA	220	NA	690	NA	NA	CM	37
20060818_KO_ura3_rep1_0.842_vs_NRC-1e.sig	NA	NA	NA	NA	NA	NA	NA	NA	NA	20	NA	NA	NA	0.84	NA	60	NA	220	NA	1200	NA	NA	CM	37
20060818_KO_tfbE_rep2_0.176_vs_NRC-1e.sig	NA	NA	NA	NA	NA	NA	NA	NA	NA	20	NA	NA	NA	0.18	NA	60	NA	220	NA	330	NA	NA	CM	37
20060818_KO_tfbE_rep2_0.410_vs_NRC-1e.sig	NA	NA	NA	NA	NA	NA	NA	NA	NA	20	NA	NA	NA	0.41	NA	60	NA	220	NA	690	NA	NA	CM	37
20060818_KO_tfbE_rep2_0.832_vs_NRC-1e.sig	NA	NA	NA	NA	NA	NA	NA	NA	NA	20	NA	NA	NA	0.83	NA	60	NA	220	NA	1140	NA	NA	CM	37

20060818_KO_tfbE_rep1_0.192_vs_NRC-1e.sig	NA	NA	NA	NA	NA	NA	NA	NA	NA	20	NA	NA	NA	0.19	NA	60	NA	220	NA	330	NA	NA	CM	37
20060818_KO_tfbE_rep1_0.432_vs_NRC-1e.sig	NA	NA	NA	NA	NA	NA	NA	NA	NA	20	NA	NA	NA	0.43	NA	60	NA	220	NA	690	NA	NA	CM	37
20060818_KO_tfbE_rep1_0.838_vs_NRC-1e.sig	NA	NA	NA	NA	NA	NA	NA	NA	NA	20	NA	NA	NA	0.84	NA	60	NA	220	NA	1140	NA	NA	CM	37
20060818_KO_tfbC_rep2_0.179_vs_NRC-1e.sig	NA	NA	NA	NA	NA	NA	NA	NA	NA	20	NA	NA	NA	0.18	NA	60	NA	220	NA	330	NA	NA	CM	37
20060818_KO_tfbC_rep2_0.435_vs_NRC-1e.sig	NA	NA	NA	NA	NA	NA	NA	NA	NA	20	NA	NA	NA	0.44	NA	60	NA	220	NA	690	NA	NA	CM	37
20060818_KO_tfbC_rep2_0.868_vs_NRC-1e.sig	NA	NA	NA	NA	NA	NA	NA	NA	NA	20	NA	NA	NA	0.87	NA	60	NA	220	NA	1200	NA	NA	CM	37
20060818_KO_tfbC_rep1_0.188_vs_NRC-1e.sig	NA	NA	NA	NA	NA	NA	NA	NA	NA	20	NA	NA	NA	0.19	NA	60	NA	220	NA	330	NA	NA	CM	37
20060818_KO_tfbC_rep1_0.412_vs_NRC-1e.sig	NA	NA	NA	NA	NA	NA	NA	NA	NA	20	NA	NA	NA	0.41	NA	60	NA	220	NA	690	NA	NA	CM	37
20060818_KO_tfbC_rep1_0.823_vs_NRC-1e.sig	NA	NA	NA	NA	NA	NA	NA	NA	NA	20	NA	NA	NA	0.82	NA	60	NA	220	NA	1200	NA	NA	CM	37
20060818_KO_tfbA_rep2_0.208_vs_NRC-1e.sig	NA	NA	NA	NA	NA	NA	NA	NA	NA	20	NA	NA	NA	0.21	NA	60	NA	220	NA	330	NA	NA	CM	37
20060818_KO_tfbA_rep2_0.425_vs_NRC-1e.sig	NA	NA	NA	NA	NA	NA	NA	NA	NA	20	NA	NA	NA	0.43	NA	60	NA	220	NA	690	NA	NA	CM	37
20060818_KO_tfbA_rep2_0.839_vs_NRC-1e.sig	NA	NA	NA	NA	NA	NA	NA	NA	NA	20	NA	NA	NA	0.84	NA	60	NA	220	NA	1260	NA	NA	CM	37
20060818_KO_tfbA_rep1_0.193_vs_NRC-1e.sig	NA	NA	NA	NA	NA	NA	NA	NA	NA	20	NA	NA	NA	0.19	NA	60	NA	220	NA	330	NA	NA	CM	37
20060818_KO_tfbA_rep1_0.399_vs_NRC-1e.sig	NA	NA	NA	NA	NA	NA	NA	NA	NA	20	NA	NA	NA	0.4	NA	60	NA	220	NA	690	NA	NA	CM	37
20060818_KO_tfbA_rep1_0.856_vs_NRC-1e.sig	NA	NA	NA	NA	NA	NA	NA	NA	NA	20	NA	NA	NA	0.86	NA	60	NA	220	NA	1260	NA	NA	CM	37
20060818_KO_hpyA_rep2_0.177_vs_NRC-1e.sig	NA	NA	NA	NA	NA	NA	NA	NA	NA	20	NA	NA	NA	0.18	NA	60	NA	220	NA	330	NA	NA	CM	37

20060818_KO_hpyA_rep2_0.406_vs_NRC-1e.sig	NA	NA	NA	NA	NA	NA	NA	NA	NA	20	NA	NA	NA	0.41	NA	60	NA	220	NA	750	NA	NA	CM	37
20060818_KO_hpyA_rep2_0.827_vs_NRC-1e.sig	NA	NA	NA	NA	NA	NA	NA	NA	NA	20	NA	NA	NA	0.83	NA	60	NA	220	NA	1260	NA	NA	CM	37
20060818_KO_hpyA_rep1_0.161_vs_NRC-1e.sig	NA	NA	NA	NA	NA	NA	NA	NA	NA	20	NA	NA	NA	0.16	NA	60	NA	220	NA	330	NA	NA	CM	37
20060818_KO_hpyA_rep1_0.421_vs_NRC-1e.sig	NA	NA	NA	NA	NA	NA	NA	NA	NA	20	NA	NA	NA	0.42	NA	60	NA	220	NA	750	NA	NA	CM	37
20060818_KO_hpyA_rep1_0.831_vs_NRC-1e.sig	NA	NA	NA	NA	NA	NA	NA	NA	NA	20	NA	NA	NA	0.83	NA	60	NA	220	NA	1260	NA	NA	CM	37
20060818_KO_bat_rep2_0.183_vs_NRC-1e.sig	NA	NA	NA	NA	NA	NA	NA	NA	NA	20	NA	NA	NA	0.18	NA	60	NA	220	NA	330	NA	NA	CM	37
20060818_KO_bat_rep2_0.416_vs_NRC-1e.sig	NA	NA	NA	NA	NA	NA	NA	NA	NA	20	NA	NA	NA	0.42	NA	60	NA	220	NA	690	NA	NA	CM	37
20060818_KO_bat_rep2_0.834_vs_NRC-1e.sig	NA	NA	NA	NA	NA	NA	NA	NA	NA	20	NA	NA	NA	0.83	NA	60	NA	220	NA	1260	NA	NA	CM	37
20060818_KO_bat_rep1_0.182_vs_NRC-1e.sig	NA	NA	NA	NA	NA	NA	NA	NA	NA	20	NA	NA	NA	0.18	NA	60	NA	220	NA	330	NA	NA	CM	37
20060818_KO_bat_rep1_0.391_vs_NRC-1e.sig	NA	NA	NA	NA	NA	NA	NA	NA	NA	20	NA	NA	NA	0.39	NA	60	NA	220	NA	690	NA	NA	CM	37
20060818_KO_bat_rep1_0.867_vs_NRC-1e.sig	NA	NA	NA	NA	NA	NA	NA	NA	NA	20	NA	NA	NA	0.87	NA	60	NA	220	NA	1260	NA	NA	CM	37
20060717_Cmyc_tbpF_rep2_0.219_vs_NRC-1d.sig	NA	NA	NA	NA	NA	NA	NA	NA	NA	20	NA	NA	NA	0.22	tbpF	60	NA	220	cmyc	540	NA	NA	CM	37
20060717_Cmyc_tbpF_rep2_0.393_vs_NRC-1d.sig	NA	NA	NA	NA	NA	NA	NA	NA	NA	20	NA	NA	NA	0.39	tbpF	60	NA	220	cmyc	840	NA	NA	CM	37
20060717_Cmyc_tbpF_rep2_0.801_vs_NRC-1d.sig	NA	NA	NA	NA	NA	NA	NA	NA	NA	20	NA	NA	NA	0.8	tbpF	60	NA	220	cmyc	1380	NA	NA	CM	37
20060717_Cmyc_tbpF_rep1_0.207_vs_NRC-1d.sig	NA	NA	NA	NA	NA	NA	NA	NA	NA	20	NA	NA	NA	0.21	tbpF	60	NA	220	cmyc	540	NA	NA	CM	37
20060717_Cmyc_tbpF_rep1_0.401_vs_NRC-1d.sig	NA	NA	NA	NA	NA	NA	NA	NA	NA	20	NA	NA	NA	0.4	tbpF	60	NA	220	cmyc	840	NA	NA	CM	37

20060717_Cmyc_tbpF_rep1_0.829_vs_NRC-1d.sig	NA	NA	NA	NA	NA	NA	NA	NA	NA	20	NA	NA	NA	0.83	tbpF	60	NA	220	cmyc	1380	NA	NA	CM	37
20060717_Cmyc_tbpE_rep2_0.192_vs_NRC-1d.sig	NA	NA	NA	NA	NA	NA	NA	NA	NA	20	NA	NA	NA	0.19	tbpE	60	NA	220	cmyc	540	NA	NA	CM	37
20060717_Cmyc_tbpE_rep2_0.453_vs_NRC-1d.sig	NA	NA	NA	NA	NA	NA	NA	NA	NA	20	NA	NA	NA	0.45	tbpE	60	NA	220	NA	960	NA	NA	CM	37
20060717_Cmyc_tbpE_rep2_0.899_vs_NRC-1d.sig	NA	NA	NA	NA	NA	NA	NA	NA	NA	20	NA	NA	NA	0.9	tbpE	60	NA	220	NA	1500	NA	NA	CM	37
20060717_Cmyc_tbpE_rep1_0.188_vs_NRC-1d.sig	NA	NA	NA	NA	NA	NA	NA	NA	NA	20	NA	NA	NA	0.19	tbpE	60	NA	220	cmyc	540	NA	NA	CM	37
20060717_Cmyc_tbpE_rep1_0.423_vs_NRC-1d.sig	NA	NA	NA	NA	NA	NA	NA	NA	NA	20	NA	NA	NA	0.42	tbpE	60	NA	220	cmyc	960	NA	NA	CM	37
20060717_Cmyc_tbpE_rep1_0.868_vs_NRC-1d.sig	NA	NA	NA	NA	NA	NA	NA	NA	NA	20	NA	NA	NA	0.87	tbpE	60	NA	220	cmyc	1500	NA	NA	CM	37
20060717_Cmyc_tbpD_rep2_0.185_vs_NRC-1d.sig	NA	NA	NA	NA	NA	NA	NA	NA	NA	20	NA	NA	NA	0.19	tbpD	60	NA	220	cmyc	540	NA	NA	CM	37
20060717_Cmyc_tbpD_rep2_0.413_vs_NRC-1d.sig	NA	NA	NA	NA	NA	NA	NA	NA	NA	20	NA	NA	NA	0.41	tbpD	60	NA	220	NA	1020	NA	NA	CM	37
20060717_Cmyc_tbpD_rep2_0.837_vs_NRC-1d.sig	NA	NA	NA	NA	NA	NA	NA	NA	NA	20	NA	NA	NA	0.84	tbpD	60	NA	220	NA	1620	NA	NA	CM	37
20060717_Cmyc_tbpD_rep1_0.179_vs_NRC-1d.sig	NA	NA	NA	NA	NA	NA	NA	NA	NA	20	NA	NA	NA	0.18	tbpD	60	NA	220	cmyc	540	NA	NA	CM	37
20060717_Cmyc_tbpD_rep1_0.416_vs_NRC-1d.sig	NA	NA	NA	NA	NA	NA	NA	NA	NA	20	NA	NA	NA	0.42	tbpD	60	NA	220	cmyc	1020	NA	NA	CM	37
20060717_Cmyc_tbpD_rep1_0.836_vs_NRC-1d.sig	NA	NA	NA	NA	NA	NA	NA	NA	NA	20	NA	NA	NA	0.84	tbpD	60	NA	220	cmyc	1620	NA	NA	CM	37
20060717_Cmyc_tbpC_rep2_0.21_vs_NRC-1d.sig	NA	NA	NA	NA	NA	NA	NA	NA	NA	20	NA	NA	NA	0.21	tbpC	60	NA	220	cmyc	540	NA	NA	CM	37
20060717_Cmyc_tbpC_rep2_0.428_vs_NRC-1d.sig	NA	NA	NA	NA	NA	NA	NA	NA	NA	20	NA	NA	NA	0.43	tbpC	60	NA	220	cmyc	900	NA	NA	CM	37
20060717_Cmyc_tbpC_rep2_0.868_vs_NRC-1d.sig	NA	NA	NA	NA	NA	NA	NA	NA	NA	20	NA	NA	NA	0.87	tbpC	60	NA	220	cmyc	1380	NA	NA	CM	37

20060717_Cmyc_tbpC_rep1_0.199_vs_NRC-1d.sig	NA	NA	NA	NA	NA	NA	NA	NA	NA	20	NA	NA	NA	0.21	tbpC	60	NA	220	cmyc	540	NA	NA	CM	37
20060717_Cmyc_tbpC_rep1_0.407_vs_NRC-1d.sig	NA	NA	NA	NA	NA	NA	NA	NA	NA	20	NA	NA	NA	0.41	tbpC	60	NA	220	cmyc	900	NA	NA	CM	37
20060717_Cmyc_tbpC_rep1_0.827_vs_NRC-1d.sig	NA	NA	NA	NA	NA	NA	NA	NA	NA	20	NA	NA	NA	0.83	tbpC	60	NA	220	cmyc	1380	NA	NA	CM	37
20060717_Cmyc_tbpB_rep2_0.225_vs_NRC-1e.sig	NA	NA	NA	NA	NA	NA	NA	NA	NA	20	NA	NA	NA	0.23	tbpB	60	NA	220	cmyc	540	NA	NA	CM	37
20060717_Cmyc_tbpB_rep2_0.446_vs_NRC-1e.sig	NA	NA	NA	NA	NA	NA	NA	NA	NA	20	NA	NA	NA	0.45	tbpB	60	NA	220	cmyc	900	NA	NA	CM	37
20060717_Cmyc_tbpB_rep2_0.865_vs_NRC-1e.sig	NA	NA	NA	NA	NA	NA	NA	NA	NA	20	NA	NA	NA	0.87	tbpB	60	NA	220	cmyc	1380	NA	NA	CM	37
20060717_Cmyc_tbpB_rep1_0.217_vs_NRC-1e.sig	NA	NA	NA	NA	NA	NA	NA	NA	NA	20	NA	NA	NA	0.22	tbpB	60	NA	220	cmyc	540	NA	NA	CM	37
20060717_Cmyc_tbpB_rep1_0.431_vs_NRC-1e.sig	NA	NA	NA	NA	NA	NA	NA	NA	NA	20	NA	NA	NA	0.43	tbpB	60	NA	220	cmyc	900	NA	NA	CM	37
20060717_Cmyc_tbpB_rep1_0.812_vs_NRC-1e.sig	NA	NA	NA	NA	NA	NA	NA	NA	NA	20	NA	NA	NA	0.81	tbpB	60	NA	220	cmyc	1380	NA	NA	CM	37
20060717_tbpA_Cmyc_rep2_0.211_vs_NRC-1e.sig	NA	NA	NA	NA	NA	NA	NA	NA	NA	20	NA	NA	NA	0.21	tbpA	60	NA	220	cmyc	540	NA	NA	CM	37
20060717_tbpA_Cmyc_rep2_0.447_vs_NRC-1e.sig	NA	NA	NA	NA	NA	NA	NA	NA	NA	20	NA	NA	NA	0.45	tbpA	60	NA	220	cmyc	840	NA	NA	CM	37
20060717_tbpA_Cmyc_rep2_0.922_vs_NRC-1e.sig	NA	NA	NA	NA	NA	NA	NA	NA	NA	20	NA	NA	NA	0.92	tbpA	60	NA	220	cmyc	1380	NA	NA	CM	37
20060717_tbpA_Cmyc_rep1_0.199_vs_NRC-1e.sig	NA	NA	NA	NA	NA	NA	NA	NA	NA	20	NA	NA	NA	0.2	tbpA	60	NA	220	cmyc	540	NA	NA	CM	37
20060717_tbpA_Cmyc_rep1_0.417_vs_NRC-1e.sig	NA	NA	NA	NA	NA	NA	NA	NA	NA	20	NA	NA	NA	0.42	tbpA	60	NA	220	cmyc	840	NA	NA	CM	37
20060717_tbpA_Cmyc_rep1_0.854_vs_NRC-1e.sig	NA	NA	NA	NA	NA	NA	NA	NA	NA	20	NA	NA	NA	0.85	tbpA	60	NA	220	cmyc	1380	NA	NA	CM	37
20060717_Cmyc_rep2_0.223_vs_NRC-1e.sig	NA	NA	NA	NA	NA	NA	NA	NA	NA	20	NA	NA	NA	0.22	NA	60	NA	220	cmyc	540	NA	NA	CM	37

20060717_Cmyc_rep2_0.407_vs_NRC-1e.sig	NA	NA	NA	NA	NA	NA	NA	NA	NA	20	NA	NA	NA	0.41	NA	60	NA	220	cmyc	840	NA	NA	CM	37
20060717_Cmyc_rep2_0.883_vs_NRC-1e.sig	NA	NA	NA	NA	NA	NA	NA	NA	NA	20	NA	NA	NA	0.88	NA	60	NA	220	cmyc	1380	NA	NA	CM	37
20060717_Cmyc_rep1_0.221_vs_NRC-1e.sig	NA	NA	NA	NA	NA	NA	NA	NA	NA	20	NA	NA	NA	0.22	NA	60	NA	220	cmyc	540	NA	NA	CM	37
20060717_Cmyc_rep1_0.402_vs_NRC-1e.sig	NA	NA	NA	NA	NA	NA	NA	NA	NA	20	NA	NA	NA	0.4	NA	60	NA	220	cmyc	840	NA	NA	CM	37
20060717_Cmyc_rep1_0.827_vs_NRC-1e.sig	NA	NA	NA	NA	NA	NA	NA	NA	NA	20	NA	NA	NA	0.83	NA	60	NA	220	cmyc	1380	NA	NA	CM	37
Overexpression_tfbD_Cmyc_0.821_vs_NRC-1e.sig	NA	NA	NA	NA	NA	NA	NA	NA	NA	20	NA	NA	NA	0.82	tfbD	50	NA	220	cmyc	NA	NA	NA	CM	37
NRC-1d_vs_NRC-1e.sig	NA	NA	NA	NA	NA	NA	NA	NA	NA	NA	NA	NA	NA	0.74	NA	NA	NA	225	NA	NA	NA	NA	CM	37
20060308_KO_ura3_0.189_vs_NRC-1e.sig	NA	NA	NA	NA	NA	NA	NA	NA	NA	20	NA	NA	NA	0.19	NA	NA	NA	220	NA	1080	NA	NA	CM	37
20060308_KO_ura3_0.448_vs_NRC-1e.sig	NA	NA	NA	NA	NA	NA	NA	NA	NA	20	NA	NA	NA	0.45	NA	NA	NA	220	NA	1500	NA	NA	CM	37
20060308_KO_ura3_0.853_vs_NRC-1e.sig	NA	NA	NA	NA	NA	NA	NA	NA	NA	20	NA	NA	NA	0.85	NA	NA	NA	220	NA	1860	NA	NA	CM	37
20060308_KO_tfbD_rep2_0.186_vs_NRC-1e.sig	NA	NA	NA	NA	NA	NA	NA	NA	NA	20	NA	NA	NA	0.19	NA	60	NA	220	NA	1080	NA	NA	CM	37
20060308_KO_tfbD_rep2_0.443_vs_NRC-1e.sig	NA	NA	NA	NA	NA	NA	NA	NA	NA	20	NA	NA	NA	0.44	NA	60	NA	220	NA	1440	NA	NA	CM	37
20060308_KO_tfbD_rep2_0.871_vs_NRC-1e.sig	NA	NA	NA	NA	NA	NA	NA	NA	NA	20	NA	NA	NA	0.87	NA	60	NA	220	NA	1860	NA	NA	CM	37
20060308_KO_tfbD_rep1_0.190_vs_NRC-1e.sig	NA	NA	NA	NA	NA	NA	NA	NA	NA	20	NA	NA	NA	0.19	NA	60	NA	220	NA	1080	NA	NA	CM	37
20060308_KO_tfbD_rep1_0.424_vs_NRC-1e.sig	NA	NA	NA	NA	NA	NA	NA	NA	NA	20	NA	NA	NA	0.42	NA	60	NA	220	NA	1440	NA	NA	CM	37
20060308_KO_tfbD_rep1_0.876_vs_NRC-1e.sig	NA	NA	NA	NA	NA	NA	NA	NA	NA	20	NA	NA	NA	0.88	NA	60	NA	220	NA	1860	NA	NA	CM	37
20060308_KO_tfbB_rep2_0.168_vs_N	NA	NA	NA	NA	NA	NA	NA	NA	NA	20	NA	NA	NA	0.17	NA	60	NA	220	NA	1080	NA	NA	CM	37

RC-1e.sig																								
20060308_KO_tfbB_rep2_0.441_vs_NRC-1e.sig	NA	NA	NA	NA	NA	NA	NA	NA	NA	20	NA	NA	NA	0.44	NA	60	NA	220	NA	1500	NA	NA	CM	37
20060308_KO_tfbB_rep2_0.934_vs_NRC-1e.sig	NA	NA	NA	NA	NA	NA	NA	NA	NA	20	NA	NA	NA	0.93	NA	60	NA	220	NA	1860	NA	NA	CM	37
20060308_KO_tfbB_rep1_0.165_vs_NRC-1e.sig	NA	NA	NA	NA	NA	NA	NA	NA	NA	20	NA	NA	NA	0.17	NA	60	NA	220	NA	1080	NA	NA	CM	37
20060308_KO_tfbB_rep1_0.442_vs_NRC-1e.sig	NA	NA	NA	NA	NA	NA	NA	NA	NA	20	NA	NA	NA	0.44	NA	60	NA	220	NA	1500	NA	NA	CM	37
20060308_KO_tfbB_rep1_0.792_vs_NRC-1e.sig	NA	NA	NA	NA	NA	NA	NA	NA	NA	20	NA	NA	NA	0.79	NA	60	NA	220	NA	1860	NA	NA	CM	37
20060308_KO_tbpD_rep2_0.183_vs_NRC-1e.sig	NA	NA	NA	NA	NA	NA	NA	NA	NA	20	NA	NA	NA	0.18	NA	60	NA	220	NA	1080	NA	NA	CM	37
20060308_KO_tbpD_rep2_0.434_vs_NRC-1e.sig	NA	NA	NA	NA	NA	NA	NA	NA	NA	20	NA	NA	NA	0.43	NA	60	NA	220	NA	1500	NA	NA	CM	37
20060308_KO_tbpD_rep2_0.841_vs_NRC-1e.sig	NA	NA	NA	NA	NA	NA	NA	NA	NA	20	NA	NA	NA	0.84	NA	60	NA	220	NA	1920	NA	NA	CM	37
20060308_KO_tbpD_rep1_0.160_vs_NRC-1e.sig	NA	NA	NA	NA	NA	NA	NA	NA	NA	20	NA	NA	NA	0.16	NA	60	NA	220	NA	1080	NA	NA	CM	37
20060308_KO_tbpD_rep1_0.443_vs_NRC-1e.sig	NA	NA	NA	NA	NA	NA	NA	NA	NA	20	NA	NA	NA	0.44	NA	60	NA	220	NA	1500	NA	NA	CM	37
20060308_KO_tbpD_rep1_0.895_vs_NRC-1e.sig	NA	NA	NA	NA	NA	NA	NA	NA	NA	20	NA	NA	NA	0.9	NA	60	NA	220	NA	1920	NA	NA	CM	37
20060308_KO_tbpC_rep2_0.181_vs_NRC-1e.sig	NA	NA	NA	NA	NA	NA	NA	NA	NA	20	NA	NA	NA	0.18	NA	60	NA	220	NA	1080	NA	NA	CM	37
20060308_KO_tbpC_rep2_0.419_vs_NRC-1e.sig	NA	NA	NA	NA	NA	NA	NA	NA	NA	20	NA	NA	NA	0.42	NA	60	NA	220	NA	1500	NA	NA	CM	37
20060308_KO_tbpC_rep2_0.783_vs_NRC-1e.sig	NA	NA	NA	NA	NA	NA	NA	NA	NA	20	NA	NA	NA	0.78	NA	60	NA	220	NA	1980	NA	NA	CM	37
20060308_KO_tbpC_rep1_0.162_vs_NRC-1e.sig	NA	NA	NA	NA	NA	NA	NA	NA	NA	20	NA	NA	NA	0.16	NA	60	NA	220	NA	1080	NA	NA	CM	37

20060308_KO_tbpC_rep1_0.387_vs_NRC-1e.sig	NA	NA	NA	NA	NA	NA	NA	NA	NA	20	NA	NA	NA	0.39	NA	60	NA	220	NA	1500	NA	NA	CM	37
20060308_KO_tbpC_rep1_0.749_vs_NRC-1e.sig	NA	NA	NA	NA	NA	NA	NA	NA	NA	20	NA	NA	NA	0.75	NA	60	NA	220	NA	1980	NA	NA	CM	37
20060308_KO_tbpA_rep2_0.212_vs_NRC-1e.sig	NA	NA	NA	NA	NA	NA	NA	NA	NA	20	NA	NA	NA	0.21	NA	60	NA	220	NA	1080	NA	NA	CM	37
20060308_KO_tbpA_rep2_0.405_vs_NRC-1e.sig	NA	NA	NA	NA	NA	NA	NA	NA	NA	20	NA	NA	NA	0.41	NA	60	NA	220	NA	1380	NA	NA	CM	37
20060308_KO_tbpA_rep2_0.785_vs_NRC-1e.sig	NA	NA	NA	NA	NA	NA	NA	NA	NA	20	NA	NA	NA	0.79	NA	60	NA	220	NA	1740	NA	NA	CM	37
20060308_KO_tbpA_rep1_0.196_vs_NRC-1e.sig	NA	NA	NA	NA	NA	NA	NA	NA	NA	20	NA	NA	NA	0.2	NA	60	NA	220	NA	1080	NA	NA	CM	37
20060308_KO_tbpA_rep1_0.398_vs_NRC-1e.sig	NA	NA	NA	NA	NA	NA	NA	NA	NA	20	NA	NA	NA	0.4	NA	60	NA	220	NA	1380	NA	NA	CM	37
20060308_KO_tbpA_rep1_0.813_vs_NRC-1e.sig	NA	NA	NA	NA	NA	NA	NA	NA	NA	20	NA	NA	NA	0.81	NA	60	NA	220	NA	1740	NA	NA	CM	37
Cmy_cspD2_1_hOD_vs_NRC-1d.sig	NA	NA	NA	NA	NA	NA	NA	NA	NA	20	NA	NA	NA	1	cspD2	50	NA	220	NA	NA	NA	NA	CM	37
Cmy_cspD2_1_mOD_vs_NRC-1d.sig	NA	NA	NA	NA	NA	NA	NA	NA	NA	20	NA	NA	NA	0.3	cspD2	50	NA	220	NA	NA	NA	NA	CM	37
Cmy_cspD2_2_hOD_vs_NRC-1d.sig	NA	NA	NA	NA	NA	NA	NA	NA	NA	20	NA	NA	NA	1	cspD2	50	NA	220	NA	NA	NA	NA	CM	37
Cmy_cspD2_2_mOD_vs_NRC-1d.sig	NA	NA	NA	NA	NA	NA	NA	NA	NA	20	NA	NA	NA	0.3	cspD2	50	NA	220	NA	NA	NA	NA	CM	37
Cmy_cspD1_1_hOD_vs_NRC-1d.sig	NA	NA	NA	NA	NA	NA	NA	NA	NA	20	NA	NA	NA	1	cspD1	50	NA	220	NA	NA	NA	NA	CM	37
Cmy_cspD1_1_mOD_vs_NRC-1d.sig	NA	NA	NA	NA	NA	NA	NA	NA	NA	20	NA	NA	NA	0.3	cspD1	50	NA	220	NA	NA	NA	NA	CM	37
Cmy_cspD1_2_hOD_vs_NRC-1d.sig	NA	NA	NA	NA	NA	NA	NA	NA	NA	20	NA	NA	NA	1	cspD1	50	NA	220	NA	NA	NA	NA	CM	37
Cmy_cspD1_2_mOD_vs_NRC-1d.sig	NA	NA	NA	NA	NA	NA	NA	NA	NA	20	NA	NA	NA	0.3	cspD1	50	NA	220	NA	NA	NA	NA	CM	37
20050726_Cmyc_tfbF_rep2_0.180_vs_NRC-1d.sig	NA	NA	NA	NA	NA	NA	NA	NA	NA	20	NA	NA	NA	0.18	tfbF	60	NA	220	cmyc	1200	NA	NA	CM	37
20050726_Cmyc_tfbF_rep2_0.470_vs_NRC-1d.sig	NA	NA	NA	NA	NA	NA	NA	NA	NA	20	NA	NA	NA	0.47	tfbF	60	NA	220	cmyc	1725	NA	NA	CM	37

20050726_Cmyc_tfbF_rep2_0.821_vs_NRC-1d.sig	NA	NA	NA	NA	NA	NA	NA	NA	NA	20	NA	NA	NA	0.82	tfbF	60	NA	220	cmyc	2580	NA	NA	CM	37
20050726_Cmyc_tfbF_rep2_0.918_vs_NRC-1d.sig	NA	NA	NA	NA	NA	NA	NA	NA	NA	20	NA	NA	NA	0.92	tfbF	60	NA	220	cmyc	3000	NA	NA	CM	37
20050726_Cmyc_tfbF_rep1_0.198_vs_NRC-1d.sig	NA	NA	NA	NA	NA	NA	NA	NA	NA	20	NA	NA	NA	0.2	tfbF	60	NA	220	cmyc	1200	NA	NA	CM	37
20050726_Cmyc_tfbF_rep1_0.490_vs_NRC-1d.sig	NA	NA	NA	NA	NA	NA	NA	NA	NA	20	NA	NA	NA	0.49	tfbF	60	NA	220	cmyc	1725	NA	NA	CM	37
20050726_Cmyc_tfbF_rep1_0.820_vs_NRC-1d.sig	NA	NA	NA	NA	NA	NA	NA	NA	NA	20	NA	NA	NA	0.82	tfbF	60	NA	220	cmyc	2580	NA	NA	CM	37
20050726_Cmyc_tfbF_rep1_0.946_vs_NRC-1d.sig	NA	NA	NA	NA	NA	NA	NA	NA	NA	20	NA	NA	NA	0.95	tfbF	60	NA	220	cmyc	3000	NA	NA	CM	37
20050726_Cmyc_tfbC_rep2_0.148_vs_NRC-1d.sig	NA	NA	NA	NA	NA	NA	NA	NA	NA	20	NA	NA	NA	0.15	tfbC	60	NA	220	cmyc	1200	NA	NA	CM	37
20050726_Cmyc_tfbC_rep2_0.430_vs_NRC-1d.sig	NA	NA	NA	NA	NA	NA	NA	NA	NA	20	NA	NA	NA	0.43	tfbC	60	NA	220	cmyc	1725	NA	NA	CM	37
20050726_Cmyc_tfbC_rep2_0.880_vs_NRC-1d.sig	NA	NA	NA	NA	NA	NA	NA	NA	NA	20	NA	NA	NA	0.88	tfbC	60	NA	220	cmyc	2580	NA	NA	CM	37
20050726_Cmyc_tfbC_rep2_1.114_vs_NRC-1d.sig	NA	NA	NA	NA	NA	NA	NA	NA	NA	20	NA	NA	NA	1.11	tfbC	60	NA	220	cmyc	3000	NA	NA	CM	37
20050726_Cmyc_tfbC_rep1_0.132_vs_NRC-1d.sig	NA	NA	NA	NA	NA	NA	NA	NA	NA	20	NA	NA	NA	0.12	tfbC	60	NA	220	cmyc	1200	NA	NA	CM	37
20050726_Cmyc_tfbC_rep1_0.394_vs_NRC-1d.sig	NA	NA	NA	NA	NA	NA	NA	NA	NA	20	NA	NA	NA	0.39	tfbC	60	NA	220	cmyc	1725	NA	NA	CM	37
20050726_Cmyc_tfbC_rep1_0.857_vs_NRC-1d.sig	NA	NA	NA	NA	NA	NA	NA	NA	NA	20	NA	NA	NA	0.86	tfbC	60	NA	220	cmyc	2580	NA	NA	CM	37
20050726_Cmyc_tfbC_rep1_1.080_vs_NRC-1d.sig	NA	NA	NA	NA	NA	NA	NA	NA	NA	20	NA	NA	NA	1.08	tfbC	60	NA	220	cmyc	3000	NA	NA	CM	37
20050726_Cmyc_tfbB_rep2_0.152_vs_NRC-1d.sig	NA	NA	NA	NA	NA	NA	NA	NA	NA	20	NA	NA	NA	0.15	tfbB	60	NA	220	cmyc	1200	NA	NA	CM	37
20050726_Cmyc_tfbB_rep2_0.496_vs_NRC-1d.sig	NA	NA	NA	NA	NA	NA	NA	NA	NA	20	NA	NA	NA	0.5	tfbB	60	NA	220	cmyc	1725	NA	NA	CM	37

20050726_Cmyc_tfbB_rep2_0.840_vs_NRC-1d.sig	NA	NA	NA	NA	NA	NA	NA	NA	NA	20	NA	NA	NA	0.84	tfbB	60	NA	220	cmyc	2580	NA	NA	CM	37
20050726_Cmyc_tfbB_rep2_1.041_vs_NRC-1d.sig	NA	NA	NA	NA	NA	NA	NA	NA	NA	20	NA	NA	NA	1.04	tfbB	60	NA	220	cmyc	3000	NA	NA	CM	37
20050726_Cmyc_tfbB_rep1_0.157_vs_NRC-1d.sig	NA	NA	NA	NA	NA	NA	NA	NA	NA	20	NA	NA	NA	0.16	tfbB	60	NA	220	cmyc	1200	NA	NA	CM	37
20050726_Cmyc_tfbB_rep1_0.448_vs_NRC-1d.sig	NA	NA	NA	NA	NA	NA	NA	NA	NA	20	NA	NA	NA	0.45	tfbB	60	NA	220	cmyc	1725	NA	NA	CM	37
20050726_Cmyc_tfbB_rep1_0.814_vs_NRC-1d.sig	NA	NA	NA	NA	NA	NA	NA	NA	NA	20	NA	NA	NA	0.81	tfbB	60	NA	220	cmyc	2580	NA	NA	CM	37
20050726_Cmyc_tfbB_rep1_0.872_vs_NRC-1d.sig	NA	NA	NA	NA	NA	NA	NA	NA	NA	20	NA	NA	NA	0.87	tfbB	60	NA	220	cmyc	3000	NA	NA	CM	37
20050726_Cmyc_tfbA_rep2_0.144_vs_NRC-1d.sig	NA	NA	NA	NA	NA	NA	NA	NA	NA	20	NA	NA	NA	0.14	tfbA	60	NA	220	cmyc	1200	NA	NA	CM	37
20050726_Cmyc_tfbA_rep2_0.399_vs_NRC-1d.sig	NA	NA	NA	NA	NA	NA	NA	NA	NA	20	NA	NA	NA	0.4	tfbA	60	NA	220	cmyc	1725	NA	NA	CM	37
20050726_Cmyc_tfbA_rep2_0.888_vs_NRC-1d.sig	NA	NA	NA	NA	NA	NA	NA	NA	NA	20	NA	NA	NA	0.89	tfbA	60	NA	220	cmyc	2580	NA	NA	CM	37
20050726_Cmyc_tfbA_rep2_0.976_vs_NRC-1d.sig	NA	NA	NA	NA	NA	NA	NA	NA	NA	20	NA	NA	NA	0.98	tfbA	60	NA	220	cmyc	3000	NA	NA	CM	37
20050726_Cmyc_tfbA_rep1_0.141_vs_NRC-1d.sig	NA	NA	NA	NA	NA	NA	NA	NA	NA	20	NA	NA	NA	0.14	tfbA	60	NA	220	cmyc	1200	NA	NA	CM	37
20050726_Cmyc_tfbA_rep1_0.412_vs_NRC-1d.sig	NA	NA	NA	NA	NA	NA	NA	NA	NA	20	NA	NA	NA	0.41	tfbA	60	NA	220	cmyc	1725	NA	NA	CM	37
20050726_Cmyc_tfbA_rep1_0.908_vs_NRC-1d.sig	NA	NA	NA	NA	NA	NA	NA	NA	NA	20	NA	NA	NA	0.91	tfbA	60	NA	220	cmyc	2580	NA	NA	CM	37
20050726_Cmyc_tfbA_rep1_0.983_vs_NRC-1d.sig	NA	NA	NA	NA	NA	NA	NA	NA	NA	20	NA	NA	NA	0.98	tfbA	60	NA	220	cmyc	3000	NA	NA	CM	37
20050620_NRC1_rep2_0.183_vs_NRC-1d.sig	NA	NA	NA	NA	NA	NA	NA	NA	NA	20	NA	NA	NA	0.18	NA	60	NA	220	NA	1260	NA	NA	CM	37
20050620_NRC1_rep2_0.505_vs_NRC-1d.sig	NA	NA	NA	NA	NA	NA	NA	NA	NA	20	NA	NA	NA	0.51	NA	60	NA	220	NA	1800	NA	NA	CM	37

20050620_NRC1_rep2_1.030_vs_NRC-1d.sig	NA	NA	NA	NA	NA	NA	NA	NA	NA	20	NA	NA	NA	1.03	NA	60	NA	220	NA	2520	NA	NA	CM	37
20050620_NRC1_rep1_0.173_vs_NRC-1d.sig	NA	NA	NA	NA	NA	NA	NA	NA	NA	20	NA	NA	NA	0.17	NA	60	NA	220	NA	1260	NA	NA	CM	37
20050620_NRC1_rep1_0.484_vs_NRC-1d.sig	NA	NA	NA	NA	NA	NA	NA	NA	NA	20	NA	NA	NA	0.48	NA	60	NA	220	NA	1800	NA	NA	CM	37
20050620_NRC1_rep1_1.276_vs_NRC-1d.sig	NA	NA	NA	NA	NA	NA	NA	NA	NA	20	NA	NA	NA	1.28	NA	60	NA	220	NA	2520	NA	NA	CM	37
20050620_Cmyc_tfbG_rep2_0.170_vs_NRC-1d.sig	NA	NA	NA	NA	NA	NA	NA	NA	NA	20	NA	NA	NA	0.17	tfbG	60	NA	220	cmyc	1260	NA	NA	CM	37
20050620_Cmyc_tfbG_rep2_0.433_vs_NRC-1d.sig	NA	NA	NA	NA	NA	NA	NA	NA	NA	20	NA	NA	NA	0.43	tfbG	60	NA	220	cmyc	1800	NA	NA	CM	37
20050620_Cmyc_tfbG_rep2_1.000_vs_NRC-1d.sig	NA	NA	NA	NA	NA	NA	NA	NA	NA	20	NA	NA	NA	1	tfbG	60	NA	220	cmyc	2520	NA	NA	CM	37
20050620_Cmyc_tfbG_rep1_0.180_vs_NRC-1d.sig	NA	NA	NA	NA	NA	NA	NA	NA	NA	20	NA	NA	NA	0.18	tfbG	60	NA	220	cmyc	1260	NA	NA	CM	37
20050620_Cmyc_tfbG_rep1_0.408_vs_NRC-1d.sig	NA	NA	NA	NA	NA	NA	NA	NA	NA	20	NA	NA	NA	0.41	tfbG	60	NA	220	cmyc	1800	NA	NA	CM	37
20050620_Cmyc_tfbG_rep1_1.080_vs_NRC-1d.sig	NA	NA	NA	NA	NA	NA	NA	NA	NA	20	NA	NA	NA	1.08	tfbG	60	NA	220	cmyc	2520	NA	NA	CM	37
20050620_Cmyc_tfbE_rep2_0.118_vs_NRC-1d.sig	NA	NA	NA	NA	NA	NA	NA	NA	NA	20	NA	NA	NA	0.12	tfbE	60	NA	220	cmyc	1260	NA	NA	CM	37
20050620_Cmyc_tfbE_rep2_0.383_vs_NRC-1d.sig	NA	NA	NA	NA	NA	NA	NA	NA	NA	20	NA	NA	NA	0.38	tfbE	60	NA	220	cmyc	1800	NA	NA	CM	37
20050620_Cmyc_tfbE_rep2_1.042_vs_NRC-1d.sig	NA	NA	NA	NA	NA	NA	NA	NA	NA	20	NA	NA	NA	1.04	tfbE	60	NA	220	cmyc	2520	NA	NA	CM	37
20050620_Cmyc_tfbE_rep1_0.113_vs_NRC-1d.sig	NA	NA	NA	NA	NA	NA	NA	NA	NA	20	NA	NA	NA	0.11	tfbE	60	NA	220	cmyc	1260	NA	NA	CM	37
20050620_Cmyc_tfbE_rep1_0.378_vs_NRC-1d.sig	NA	NA	NA	NA	NA	NA	NA	NA	NA	20	NA	NA	NA	0.38	tfbE	60	NA	220	cmyc	1800	NA	NA	CM	37
20050620_Cmyc_tfbE_rep1_1.142_vs_NRC-1d.sig	NA	NA	NA	NA	NA	NA	NA	NA	NA	20	NA	NA	NA	1.14	tfbE	60	NA	220	cmyc	2520	NA	NA	CM	37

20050620_Cmyc_tfbD_rep2_0.153_vs_NRC-1d.sig	NA	NA	NA	NA	NA	NA	NA	NA	NA	20	NA	NA	NA	0.15	tfbD	60	NA	220	cmyc	1260	NA	NA	CM	37
20050620_Cmyc_tfbD_rep2_0.334_vs_NRC-1d.sig	NA	NA	NA	NA	NA	NA	NA	NA	NA	20	NA	NA	NA	0.33	tfbD	60	NA	220	cmyc	1800	NA	NA	CM	37
20050620_Cmyc_tfbD_rep2_0.922_vs_NRC-1d.sig	NA	NA	NA	NA	NA	NA	NA	NA	NA	20	NA	NA	NA	0.92	tfbD	60	NA	220	cmyc	2520	NA	NA	CM	37
20050620_Cmyc_tfbD_rep1_0.156_vs_NRC-1d.sig	NA	NA	NA	NA	NA	NA	NA	NA	NA	20	NA	NA	NA	0.16	tfbD	60	NA	220	cmyc	1260	NA	NA	CM	37
20050620_Cmyc_tfbD_rep1_0.336_vs_NRC-1d.sig	NA	NA	NA	NA	NA	NA	NA	NA	NA	20	NA	NA	NA	0.34	tfbD	60	NA	220	cmyc	1800	NA	NA	CM	37
20050620_Cmyc_tfbD_rep1_0.944_vs_NRC-1d.sig	NA	NA	NA	NA	NA	NA	NA	NA	NA	20	NA	NA	NA	0.94	tfbD	60	NA	220	cmyc	2520	NA	NA	CM	37
20050620_Cmyc_rep2_0.177_vs_NRC-1d.sig	NA	NA	NA	NA	NA	NA	NA	NA	NA	20	NA	NA	NA	0.18	NA	60	NA	220	cmyc	1260	NA	NA	CM	37
20050620_Cmyc_rep2_0.457_vs_NRC-1d.sig	NA	NA	NA	NA	NA	NA	NA	NA	NA	20	NA	NA	NA	0.46	NA	60	NA	220	cmyc	1800	NA	NA	CM	37
20050620_Cmyc_rep2_1.072_vs_NRC-1d.sig	NA	NA	NA	NA	NA	NA	NA	NA	NA	20	NA	NA	NA	1.07	NA	60	NA	220	cmyc	2520	NA	NA	CM	37
20050620_Cmyc_rep1_0.207_vs_NRC-1d.sig	NA	NA	NA	NA	NA	NA	NA	NA	NA	20	NA	NA	NA	0.21	NA	60	NA	220	cmyc	1260	NA	NA	CM	37
20050620_Cmyc_rep1_0.474_vs_NRC-1d.sig	NA	NA	NA	NA	NA	NA	NA	NA	NA	20	NA	NA	NA	0.47	NA	60	NA	220	cmyc	1800	NA	NA	CM	37
20050620_Cmyc_rep1_1.052_vs_NRC-1d.sig	NA	NA	NA	NA	NA	NA	NA	NA	NA	20	NA	NA	NA	1.05	NA	60	NA	220	cmyc	2520	NA	NA	CM	37
NRC-1e_vs_NRC-1h1.sig	NA	NA	NA	NA	NA	NA	NA	NA	NA	NA	NA	NA	NA	0.48	NA	NA	NA	225	NA	NA	NA	NA	CM	37
H2O2_Recov._set_1_0mM_000min_vs_NRC-1d.sig	NA	NA	NA	NA	NA	NA	NA	NA	0	NA	NA	NA	NA	0.26	NA	NA	NA	225	NA	0	NA	NA	CM	42
H2O2_Recov._set_1_0mM_010min_vs_NRC-1d.sig	NA	NA	NA	NA	NA	NA	NA	NA	0	NA	NA	NA	NA	0.27	NA	NA	NA	225	NA	10	NA	NA	CM	42
H2O2_Recov._set_1_0mM_020min_vs_NRC-1d.sig	NA	NA	NA	NA	NA	NA	NA	NA	0	NA	NA	NA	NA	0.27	NA	NA	NA	225	NA	20	NA	NA	CM	42
H2O2_Recov._set_1_0mM_030min_vs	NA	NA	NA	NA	NA	NA	NA	NA	0	NA	NA	NA	NA	0.26	NA	NA	NA	225	NA	30	NA	NA	CM	42

_NRC-1d.sig																								
H2O2_Recov._set_1_0mM_040min_vs_NRC-1d.sig	NA	NA	NA	NA	NA	NA	NA	NA	0	NA	NA	NA	NA	0.27	NA	NA	NA	225	NA	40	NA	NA	CM	42
H2O2_Recov._set_1_0mM_050min_vs_NRC-1d.sig	NA	NA	NA	NA	NA	NA	NA	NA	0	NA	NA	NA	NA	0.28	NA	NA	NA	225	NA	50	NA	NA	CM	42
H2O2_Recov._set_1_0mM_060min_vs_NRC-1d.sig	NA	NA	NA	NA	NA	NA	NA	NA	0	NA	NA	NA	NA	0.28	NA	NA	NA	225	NA	60	NA	NA	CM	42
H2O2_Recov._set_1_0mM_120min_vs_NRC-1d.sig	NA	NA	NA	NA	NA	NA	NA	NA	0	NA	NA	NA	NA	0.31	NA	NA	NA	225	NA	120	NA	NA	CM	42
KO_asnC.2_0.1825_vs_NRC-1_h1.sig	NA	NA	NA	NA	NA	NA	NA	NA	NA	NA	NA	NA	NA	0.18	NA	NA	NA	225	NA	915	NA	NA	FangYin's CDM	37
KO_asnC.2_0.2809_vs_NRC-1_h1.sig	NA	NA	NA	NA	NA	NA	NA	NA	NA	NA	NA	NA	NA	0.28	NA	NA	NA	225	NA	1587	NA	NA	FangYin's CDM	37
KO_asnC.2_0.6128_vs_NRC-1_h1.sig	NA	NA	NA	NA	NA	NA	NA	NA	NA	NA	NA	NA	NA	0.61	NA	NA	NA	225	NA	2640	NA	NA	FangYin's CDM	37
KO_asnC.2_1.3133_vs_NRC-1_h1.sig	NA	NA	NA	NA	NA	NA	NA	NA	NA	NA	NA	NA	NA	1.31	NA	NA	NA	225	NA	3817	NA	NA	FangYin's CDM	37
KO_trh2.2_0.1864_vs_NRC-1_h1.sig	NA	NA	NA	NA	NA	NA	NA	NA	NA	NA	NA	NA	NA	0.19	NA	NA	NA	225	NA	915	NA	NA	FangYin's CDM	37
KO_trh2.2_0.3121_vs_NRC-1_h1.sig	NA	NA	NA	NA	NA	NA	NA	NA	NA	NA	NA	NA	NA	0.31	NA	NA	NA	225	NA	1587	NA	NA	FangYin's CDM	37
KO_trh2.2_0.5883_vs_NRC-1_h1.sig	NA	NA	NA	NA	NA	NA	NA	NA	NA	NA	NA	NA	NA	0.59	NA	NA	NA	225	NA	2640	NA	NA	FangYin's CDM	37

KO_trh2.2_1.1865_vs_NRC-1_h1.sig	NA	NA	NA	NA	NA	NA	NA	NA	NA	NA	NA	NA	NA	1.19	NA	NA	NA	225	NA	3817	NA	NA	FangYin's CDM	37
KO_trh4.1_0.1572_vs_NRC-1_h1.sig	NA	NA	NA	NA	NA	NA	NA	NA	NA	NA	NA	NA	NA	0.16	NA	NA	NA	225	NA	915	NA	NA	FangYin's CDM	37
KO_trh4.1_0.2633_vs_NRC-1_h1.sig	NA	NA	NA	NA	NA	NA	NA	NA	NA	NA	NA	NA	NA	0.26	NA	NA	NA	225	NA	1587	NA	NA	FangYin's CDM	37
KO_trh4.1_0.4315_vs_NRC-1_h1.sig	NA	NA	NA	NA	NA	NA	NA	NA	NA	NA	NA	NA	NA	0.43	NA	NA	NA	225	NA	2640	NA	NA	FangYin's CDM	37
KO_trh4.1_0.5223_vs_NRC-1_h1.sig	NA	NA	NA	NA	NA	NA	NA	NA	NA	NA	NA	NA	NA	0.52	NA	NA	NA	225	NA	3817	NA	NA	FangYin's CDM	37
KO_asnC_0.1774_vs_NRC-1h1.sig	NA	NA	NA	NA	NA	NA	NA	NA	NA	NA	NA	NA	NA	0.18	NA	NA	NA	225	NA	915	NA	NA	FangYin's CDM	37
KO_asnC_0.2829_vs_NRC-1h1.sig	NA	NA	NA	NA	NA	NA	NA	NA	NA	NA	NA	NA	NA	0.28	NA	NA	NA	225	NA	1587	NA	NA	FangYin's CDM	37
KO_asnC_0.6051_vs_NRC-1h1.sig	NA	NA	NA	NA	NA	NA	NA	NA	NA	NA	NA	NA	NA	0.61	NA	NA	NA	225	NA	2640	NA	NA	FangYin's CDM	37
KO_asnC_1.3076_vs_NRC-1h1.sig	NA	NA	NA	NA	NA	NA	NA	NA	NA	NA	NA	NA	NA	1.31	NA	NA	NA	225	NA	3817	NA	NA	FangYin's CDM	37
KO_trh2.1_0.1814_vs_NRC-1_h1.sig	NA	NA	NA	NA	NA	NA	NA	NA	NA	NA	NA	NA	NA	0.18	NA	NA	NA	225	NA	915	NA	NA	FangYin's CD	37

																							M	
KO_trh2.1_0.3088_vs_NRC-1_h1.sig	NA	NA	NA	NA	NA	NA	NA	NA	NA	NA	NA	NA	NA	0.31	NA	NA	NA	225	NA	1587	NA	NA	FangYin's CDM	37
KO_trh2.1_0.5662_vs_NRC-1_h1.sig	NA	NA	NA	NA	NA	NA	NA	NA	NA	NA	NA	NA	NA	0.57	NA	NA	NA	225	NA	2640	NA	NA	FangYin's CDM	37
KO_trh2.1_1.2145_vs_NRC-1_h1.sig	NA	NA	NA	NA	NA	NA	NA	NA	NA	NA	NA	NA	NA	1.21	NA	NA	NA	225	NA	3817	NA	NA	FangYin's CDM	37
NRC-1.2_0.1684_vs_NRC-1_h1.sig	NA	NA	NA	NA	NA	NA	NA	NA	NA	NA	NA	NA	NA	0.17	NA	NA	NA	225	NA	915	NA	NA	FangYin's CDM	37
NRC-1.2_0.3063_vs_NRC-1_h1.sig	NA	NA	NA	NA	NA	NA	NA	NA	NA	NA	NA	NA	NA	0.31	NA	NA	NA	225	NA	1587	NA	NA	FangYin's CDM	37
NRC-1.2_0.3895_vs_NRC-1_h1.sig	NA	NA	NA	NA	NA	NA	NA	NA	NA	NA	NA	NA	NA	0.39	NA	NA	NA	225	NA	2640	NA	NA	FangYin's CDM	37
NRC-1.2_1.1065_vs_NRC-1_h1.sig	NA	NA	NA	NA	NA	NA	NA	NA	NA	NA	NA	NA	NA	1.11	NA	NA	NA	225	NA	3817	NA	NA	FangYin's CDM	37
KO_trh3_0.1968_vs_NRC-1_h1.sig	NA	NA	NA	NA	NA	NA	NA	NA	NA	NA	NA	NA	NA	0.2	NA	NA	NA	225	NA	915	NA	NA	FangYin's CDM	37
KO_trh3_0.2946_vs_NRC-1_h1.sig	NA	NA	NA	NA	NA	NA	NA	NA	NA	NA	NA	NA	NA	0.29	NA	NA	NA	225	NA	1587	NA	NA	FangYin's CDM	37
KO_trh3_0.5791_vs_NRC-1_h1.sig	NA	NA	NA	NA	NA	NA	NA	NA	NA	NA	NA	NA	NA	0.58	NA	NA	NA	225	NA	2640	NA	NA	FangYi	37

																						n's CDM	
KO_trh3_1.3116_vs_NRC-1_h1.sig	NA	NA	NA	NA	NA	NA	NA	NA	NA	NA	NA	NA	NA	1.31	NA	NA	NA	225	NA	3817	NA	NA	FangYin's CDM	37
KO_trh4.2_0.1729_vs_NRC-1_h1.sig	NA	NA	NA	NA	NA	NA	NA	NA	NA	NA	NA	NA	NA	0.17	NA	NA	NA	225	NA	915	NA	NA	FangYin's CDM	37
KO_trh4.2_0.279_vs_NRC-1_h1.sig	NA	NA	NA	NA	NA	NA	NA	NA	NA	NA	NA	NA	NA	0.28	NA	NA	NA	225	NA	1587	NA	NA	FangYin's CDM	37
KO_trh4.2_0.4373_vs_NRC-1_h1.sig	NA	NA	NA	NA	NA	NA	NA	NA	NA	NA	NA	NA	NA	0.44	NA	NA	NA	225	NA	2640	NA	NA	FangYin's CDM	37
KO_trh4.2_0.5434_vs_NRC-1_h1.sig	NA	NA	NA	NA	NA	NA	NA	NA	NA	NA	NA	NA	NA	0.54	NA	NA	NA	225	NA	3817	NA	NA	FangYin's CDM	37
KO_ura3.1_0.1857_vs_NRC-1_h1.sig	NA	NA	NA	NA	NA	NA	NA	NA	NA	NA	NA	NA	NA	0.19	NA	NA	NA	225	NA	915	NA	NA	FangYin's CDM	37
KO_ura3.1_0.3501_vs_NRC-1_h1.sig	NA	NA	NA	NA	NA	NA	NA	NA	NA	NA	NA	NA	NA	0.35	NA	NA	NA	225	NA	1587	NA	NA	FangYin's CDM	37
KO_ura3.1_0.4424_vs_NRC-1_h1.sig	NA	NA	NA	NA	NA	NA	NA	NA	NA	NA	NA	NA	NA	0.44	NA	NA	NA	225	NA	2640	NA	NA	FangYin's CDM	37
KO_ura3.1_0.525_vs_NRC-1_h1.sig	NA	NA	NA	NA	NA	NA	NA	NA	NA	NA	NA	NA	NA	0.53	NA	NA	NA	225	NA	3817	NA	NA	FangYin's CDM	37

KO_trh3.2_0.1949_vs_NRC-1_h1.sig	NA	NA	NA	NA	NA	NA	NA	NA	NA	NA	NA	NA	NA	0.19	NA	NA	NA	225	NA	915	NA	NA	FangYin's CDM	37
KO_trh3.2_0.295_vs_NRC-1_h1.sig	NA	NA	NA	NA	NA	NA	NA	NA	NA	NA	NA	NA	NA	0.3	NA	NA	NA	225	NA	1587	NA	NA	FangYin's CDM	37
KO_trh3.2_0.5673_vs_NRC-1_h1.sig	NA	NA	NA	NA	NA	NA	NA	NA	NA	NA	NA	NA	NA	0.57	NA	NA	NA	225	NA	2640	NA	NA	FangYin's CDM	37
KO_trh3.2_1.3887_vs_NRC-1_h1.sig	NA	NA	NA	NA	NA	NA	NA	NA	NA	NA	NA	NA	NA	1.39	NA	NA	NA	225	NA	3817	NA	NA	FangYin's CDM	37
NRC-1_0.1779_vs_NRC-1_h1.sig	NA	NA	NA	NA	NA	NA	NA	NA	NA	NA	NA	NA	NA	0.18	NA	NA	NA	225	NA	915	NA	NA	FangYin's CDM	37
NRC-1_0.3279_vs_NRC-1_h1.sig	NA	NA	NA	NA	NA	NA	NA	NA	NA	NA	NA	NA	NA	0.33	NA	NA	NA	225	NA	1587	NA	NA	FangYin's CDM	37
NRC-1_0.3882_vs_NRC-1_h1.sig	NA	NA	NA	NA	NA	NA	NA	NA	NA	NA	NA	NA	NA	0.39	NA	NA	NA	225	NA	2640	NA	NA	FangYin's CDM	37
NRC-1_1.0338_vs_NRC-1_h1.sig	NA	NA	NA	NA	NA	NA	NA	NA	NA	NA	NA	NA	NA	1.03	NA	NA	NA	225	NA	3817	NA	NA	FangYin's CDM	37
H2O2_Recov._set_1_50mM_000min_vs_NRC-1d.sig	NA	NA	NA	NA	NA	NA	NA	NA	0.05	NA	NA	NA	NA	0.27	NA	NA	NA	225	NA	0	NA	NA	CM	42
H2O2_Recov._set_1_50mM_010min_vs_NRC-1d.sig	NA	NA	NA	NA	NA	NA	NA	NA	0.05	NA	NA	NA	NA	0.28	NA	NA	NA	225	NA	10	NA	NA	CM	42
H2O2_Recov._set_1_50mM_020min_vs_NRC-1d.sig	NA	NA	NA	NA	NA	NA	NA	NA	0.05	NA	NA	NA	NA	0.28	NA	NA	NA	225	NA	20	NA	NA	CM	42

H2O2_Recov._set_1_50mM_030min_vs_NRC-1d.sig	NA	NA	NA	NA	NA	NA	NA	NA	0.05	NA	NA	NA	NA	0.25	NA	NA	NA	225	NA	30	NA	NA	CM	42
H2O2_Recov._set_1_50mM_040min_vs_NRC-1d.sig	NA	NA	NA	NA	NA	NA	NA	NA	0.05	NA	NA	NA	NA	0.25	NA	NA	NA	225	NA	40	NA	NA	CM	42
H2O2_Recov._set_1_50mM_050min_vs_NRC-1d.sig	NA	NA	NA	NA	NA	NA	NA	NA	0.05	NA	NA	NA	NA	0.27	NA	NA	NA	225	NA	50	NA	NA	CM	42
H2O2_Recov._set_1_50mM_060min_vs_NRC-1d.sig	NA	NA	NA	NA	NA	NA	NA	NA	0.05	NA	NA	NA	NA	0.27	NA	NA	NA	225	NA	60	NA	NA	CM	42
H2O2_Recov._set_1_50mM_120min_vs_NRC-1d.sig	NA	NA	NA	NA	NA	NA	NA	NA	0.05	NA	NA	NA	NA	0.28	NA	NA	NA	225	NA	120	NA	NA	CM	42
gamma3__2500gy-0000m	NA	NA	NA	NA	NA	NA	2500	NA	NA	NA	NA	NA	NA	NA	NA	NA	NA	225	NA	0	NA	NA	CM	42
gamma3__2500gy-0010m	NA	NA	NA	NA	NA	NA	2500	NA	NA	NA	NA	NA	NA	NA	NA	NA	NA	225	NA	10	NA	NA	CM	42
gamma3__2500gy-0020m	NA	NA	NA	NA	NA	NA	2500	NA	NA	NA	NA	NA	NA	NA	NA	NA	NA	225	NA	20	NA	NA	CM	42
gamma3__2500gy-0030m	NA	NA	NA	NA	NA	NA	2500	NA	NA	NA	NA	NA	NA	NA	NA	NA	NA	225	NA	30	NA	NA	CM	42
gamma3__2500gy-0040m	NA	NA	NA	NA	NA	NA	2500	NA	NA	NA	NA	NA	NA	NA	NA	NA	NA	225	NA	40	NA	NA	CM	42
gamma3__2500gy-0050m	NA	NA	NA	NA	NA	NA	2500	NA	NA	NA	NA	NA	NA	NA	NA	NA	NA	225	NA	50	NA	NA	CM	42
gamma3__2500gy-0060m	NA	NA	NA	NA	NA	NA	2500	NA	NA	NA	NA	NA	NA	NA	NA	NA	NA	225	NA	60	NA	NA	CM	42
gamma3__2500gy-0120m	NA	NA	NA	NA	NA	NA	2500	NA	NA	NA	NA	NA	NA	NA	NA	NA	NA	225	NA	120	NA	NA	CM	42
gamma3__2500gy-0240m	NA	NA	NA	NA	NA	NA	2500	NA	NA	NA	NA	NA	NA	NA	NA	NA	NA	225	NA	240	NA	NA	CM	42
gamma2__2500gy-0000m	NA	NA	NA	NA	NA	NA	2500	NA	NA	NA	NA	NA	NA	NA	NA	NA	NA	225	NA	0	NA	NA	CM	42
gamma2__2500gy-0010m	NA	NA	NA	NA	NA	NA	2500	NA	NA	NA	NA	NA	NA	NA	NA	NA	NA	225	NA	10	NA	NA	CM	42
gamma2__2500gy-0020m	NA	NA	NA	NA	NA	NA	2500	NA	NA	NA	NA	NA	NA	NA	NA	NA	NA	225	NA	20	NA	NA	CM	42
gamma2__2500gy-0030m	NA	NA	NA	NA	NA	NA	2500	NA	NA	NA	NA	NA	NA	NA	NA	NA	NA	225	NA	30	NA	NA	CM	42
gamma2__2500gy-0040m	NA	NA	NA	NA	NA	NA	2500	NA	NA	NA	NA	NA	NA	NA	NA	NA	NA	225	NA	40	NA	NA	CM	42
gamma2__2500gy-0050m	NA	NA	NA	NA	NA	NA	2500	NA	NA	NA	NA	NA	NA	NA	NA	NA	NA	225	NA	50	NA	NA	CM	42
gamma2__2500gy-0060m	NA	NA	NA	NA	NA	NA	2500	NA	NA	NA	NA	NA	NA	NA	NA	NA	NA	225	NA	60	NA	NA	CM	42
gamma2__2500gy-	NA	NA	NA	NA	NA	NA	250	NA	NA	NA	NA	NA	NA	NA	NA	NA	NA	225	NA	120	NA	NA	CM	42

0120m							0																	
gamma2__2500gy-0240m	NA	NA	NA	NA	NA	NA	2500	NA	NA	NA	NA	NA	NA	NA	NA	NA	NA	225	NA	240	NA	NA	CM	42
sDura3D1179_pCu_d0.100mM_t+015m_vs_NRC-1h1.sig	NA	NA	0	NA	NA	NA	NA	NA	NA	5	NA	NA	NA	NA	NA	NA	NA	225	NA	15	NA	NA	CM	37
sDura3D1179_pCu_d0.100mM_t+030m_vs_NRC-1h1.sig	NA	NA	0	NA	NA	NA	NA	NA	NA	5	NA	NA	NA	NA	NA	NA	NA	225	NA	30	NA	NA	CM	37
sDura3D1179_pCu_d0.100mM_t+060m_vs_NRC-1h1.sig	NA	NA	0	NA	NA	NA	NA	NA	NA	5	NA	NA	NA	NA	NA	NA	NA	225	NA	60	NA	NA	CM	37
sDura3D1179_pCu_d0.100mM_t+180m_vs_NRC-1h1.sig	NA	NA	0	NA	NA	NA	NA	NA	NA	5	NA	NA	NA	NA	NA	NA	NA	225	NA	180	NA	NA	CM	37
sDura3D1179_pCu_d0.100mM_t-015m_vs_NRC-1h1.sig	NA	NA	0	NA	NA	NA	NA	NA	NA	5	NA	NA	NA	NA	NA	NA	NA	225	NA	-15	NA	NA	CM	37
sDura3D1179_pCu_d0.700mM_t+015m_vs_NRC-1h1.sig	NA	NA	0	NA	NA	NA	NA	NA	NA	5	NA	NA	NA	NA	NA	NA	NA	225	NA	15	NA	NA	CM	37
sDura3D1179_pCu_d0.700mM_t+030m_vs_NRC-1h1.sig	NA	NA	0	NA	NA	NA	NA	NA	NA	5	NA	NA	NA	NA	NA	NA	NA	225	NA	30	NA	NA	CM	37
sDura3D1179_pCu_d0.700mM_t+060m_vs_NRC-1h1.sig	NA	NA	0	NA	NA	NA	NA	NA	NA	5	NA	NA	NA	NA	NA	NA	NA	225	NA	60	NA	NA	CM	37
sDura3D1179_pCu_d0.700mM_t+180m_vs_NRC-1h1.sig	NA	NA	0	NA	NA	NA	NA	NA	NA	5	NA	NA	NA	NA	NA	NA	NA	225	NA	180	NA	NA	CM	37
sDura3D1179_pCu_d0.700mM_t-015m_vs_NRC-1h1.sig	NA	NA	0	NA	NA	NA	NA	NA	NA	5	NA	NA	NA	NA	NA	NA	NA	225	NA	-15	NA	NA	CM	37
sDura3D1179_pCu_d1.000mM_t+015m_vs_NRC-1h1.sig	NA	NA	0	NA	NA	NA	NA	NA	NA	5	NA	NA	NA	NA	NA	NA	NA	225	NA	15	NA	NA	CM	37
sDura3D1179_pCu_d1.000mM_t+030m_vs_NRC-1h1.sig	NA	NA	0	NA	NA	NA	NA	NA	NA	5	NA	NA	NA	NA	NA	NA	NA	225	NA	30	NA	NA	CM	37
sDura3D1179_pCu_d1.000mM_t+060m_vs_NRC-1h1.sig	NA	NA	0	NA	NA	NA	NA	NA	NA	5	NA	NA	NA	NA	NA	NA	NA	225	NA	60	NA	NA	CM	37
sDura3D1179_pCu_d1.000mM_t+180m_vs_NRC-1h1.sig	NA	NA	0	NA	NA	NA	NA	NA	NA	5	NA	NA	NA	NA	NA	NA	NA	225	NA	180	NA	NA	CM	37

sDura3D1179_pCu_d1.000mM_t-015m_vs_NRC-1h1.sig	NA	NA	0	NA	NA	NA	NA	NA	NA	5	NA	NA	NA	NA	NA	NA	NA	225	NA	-15	NA	NA	CM	37
sDura3D1179_pNULL_d0.000mM_t+015m_vs_NRC-1h1.sig	NA	NA	NA	NA	NA	NA	NA	NA	NA	5	NA	NA	NA	NA	NA	NA	NA	225	NA	15	NA	NA	CM	37
sDura3D1179_pNULL_d0.000mM_t+030m_vs_NRC-1h1.sig	NA	NA	NA	NA	NA	NA	NA	NA	NA	5	NA	NA	NA	NA	NA	NA	NA	225	NA	30	NA	NA	CM	37
sDura3D1179_pNULL_d0.000mM_t+060m_vs_NRC-1h1.sig	NA	NA	NA	NA	NA	NA	NA	NA	NA	5	NA	NA	NA	NA	NA	NA	NA	225	NA	60	NA	NA	CM	37
sDura3D1179_pNULL_d0.000mM_t+180m_vs_NRC-1h1.sig	NA	NA	NA	NA	NA	NA	NA	NA	NA	5	NA	NA	NA	NA	NA	NA	NA	225	NA	180	NA	NA	CM	37
sDura3D1179_pNULL_d0.000mM_t-015m_vs_NRC-1h1.sig	NA	NA	NA	NA	NA	NA	NA	NA	NA	5	NA	NA	NA	NA	NA	NA	NA	225	NA	-15	NA	NA	CM	37
sDura3D1179_pZn_d0.005mM_t+015m_vs_NRC-1h1.sig	NA	NA	NA	NA	NA	NA	NA	NA	NA	5	NA	NA	NA	NA	NA	NA	NA	225	NA	15	NA	0	CM	37
sDura3D1179_pZn_d0.005mM_t+030m_vs_NRC-1h1.sig	NA	NA	NA	NA	NA	NA	NA	NA	NA	5	NA	NA	NA	NA	NA	NA	NA	225	NA	30	NA	0	CM	37
sDura3D1179_pZn_d0.005mM_t+060m_vs_NRC-1h1.sig	NA	NA	NA	NA	NA	NA	NA	NA	NA	5	NA	NA	NA	NA	NA	NA	NA	225	NA	60	NA	0	CM	37
sDura3D1179_pZn_d0.005mM_t+180m_vs_NRC-1h1.sig	NA	NA	NA	NA	NA	NA	NA	NA	NA	5	NA	NA	NA	NA	NA	NA	NA	225	NA	180	NA	0	CM	37
sDura3D1179_pZn_d0.005mM_t-015m_vs_NRC-1h1.sig	NA	NA	NA	NA	NA	NA	NA	NA	NA	5	NA	NA	NA	NA	NA	NA	NA	225	NA	-15	NA	0	CM	37
sDura3D1179_pZn_d0.020mM_t+015m_vs_NRC-1h1.sig	NA	NA	NA	NA	NA	NA	NA	NA	NA	5	NA	NA	NA	NA	NA	NA	NA	225	NA	15	NA	0	CM	37
sDura3D1179_pZn_d0.020mM_t+030m_vs_NRC-1h1.sig	NA	NA	NA	NA	NA	NA	NA	NA	NA	5	NA	NA	NA	NA	NA	NA	NA	225	NA	30	NA	0	CM	37
sDura3D1179_pZn_d0.020mM_t+060m_vs_NRC-1h1.sig	NA	NA	NA	NA	NA	NA	NA	NA	NA	5	NA	NA	NA	NA	NA	NA	NA	225	NA	60	NA	0	CM	37

sDura3D1179_pZn_d0.020mM_t+180m_vs_NRC-1h1.sig	NA	NA	NA	NA	NA	NA	NA	NA	NA	5	NA	NA	NA	NA	NA	NA	NA	225	NA	180	NA	0	CM	37
sDura3D1179_pZn_d0.020mM_t-015m_vs_NRC-1h1.sig	NA	NA	NA	NA	NA	NA	NA	NA	NA	5	NA	NA	NA	NA	NA	NA	NA	225	NA	-15	NA	0	CM	37
sDura3D1179_pZn_d0.050mM_t+015m_vs_NRC-1h1.sig	NA	NA	NA	NA	NA	NA	NA	NA	NA	5	NA	NA	NA	NA	NA	NA	NA	225	NA	15	NA	0	CM	37
sDura3D1179_pZn_d0.050mM_t+030m_vs_NRC-1h1.sig	NA	NA	NA	NA	NA	NA	NA	NA	NA	5	NA	NA	NA	NA	NA	NA	NA	225	NA	30	NA	0	CM	37
sDura3D1179_pZn_d0.050mM_t+060m_vs_NRC-1h1.sig	NA	NA	NA	NA	NA	NA	NA	NA	NA	5	NA	NA	NA	NA	NA	NA	NA	225	NA	60	NA	0	CM	37
sDura3D1179_pZn_d0.050mM_t+180m_vs_NRC-1h1.sig	NA	NA	NA	NA	NA	NA	NA	NA	NA	5	NA	NA	NA	NA	NA	NA	NA	225	NA	180	NA	0	CM	37
sDura3D1179_pZn_d0.050mM_t-015m_vs_NRC-1h1.sig	NA	NA	NA	NA	NA	NA	NA	NA	NA	5	NA	NA	NA	NA	NA	NA	NA	225	NA	-15	NA	0	CM	37
sDura3_pCu_d0.100mM_t+015m_vs_NRC-1h1.sig	NA	NA	0	NA	NA	NA	NA	NA	NA	5	NA	NA	NA	NA	NA	NA	NA	225	NA	15	NA	NA	CM	37
sDura3_pCu_d0.100mM_t+030m_vs_NRC-1h1.sig	NA	NA	0	NA	NA	NA	NA	NA	NA	5	NA	NA	NA	NA	NA	NA	NA	225	NA	30	NA	NA	CM	37
sDura3_pCu_d0.100mM_t+060m_vs_NRC-1h1.sig	NA	NA	0	NA	NA	NA	NA	NA	NA	5	NA	NA	NA	NA	NA	NA	NA	225	NA	60	NA	NA	CM	37
sDura3_pCu_d0.100mM_t+180m_vs_NRC-1h1.sig	NA	NA	0	NA	NA	NA	NA	NA	NA	5	NA	NA	NA	NA	NA	NA	NA	225	NA	180	NA	NA	CM	37
sDura3_pCu_d0.100mM_t-015m_vs_NRC-1h1.sig	NA	NA	0	NA	NA	NA	NA	NA	NA	5	NA	NA	NA	NA	NA	NA	NA	225	NA	-15	NA	NA	CM	37
sDura3_pCu_d0.700mM_t+015m_vs_NRC-1h1.sig	NA	NA	0	NA	NA	NA	NA	NA	NA	5	NA	NA	NA	NA	NA	NA	NA	225	NA	15	NA	NA	CM	37
sDura3_pCu_d0.700mM_t+030m_vs_NRC-1h1.sig	NA	NA	0	NA	NA	NA	NA	NA	NA	5	NA	NA	NA	NA	NA	NA	NA	225	NA	30	NA	NA	CM	37
sDura3_pCu_d0.700mM_t+060m_vs_NRC-1h1.sig	NA	NA	0	NA	NA	NA	NA	NA	NA	5	NA	NA	NA	NA	NA	NA	NA	225	NA	60	NA	NA	CM	37

sDura3_pCu_d0.700mM_t+180m_vs_NRC-1h1.sig	NA	NA	0	NA	NA	NA	NA	NA	NA	5	NA	NA	NA	NA	NA	NA	NA	225	NA	180	NA	NA	CM	37
sDura3_pCu_d0.700mM_t-015m_vs_NRC-1h1.sig	NA	NA	0	NA	NA	NA	NA	NA	NA	5	NA	NA	NA	NA	NA	NA	NA	225	NA	-15	NA	NA	CM	37
sDura3_pCu_d1.000mM_t+015m_vs_NRC-1h1.sig	NA	NA	0	NA	NA	NA	NA	NA	NA	5	NA	NA	NA	NA	NA	NA	NA	225	NA	15	NA	NA	CM	37
sDura3_pCu_d1.000mM_t+030m_vs_NRC-1h1.sig	NA	NA	0	NA	NA	NA	NA	NA	NA	5	NA	NA	NA	NA	NA	NA	NA	225	NA	30	NA	NA	CM	37
sDura3_pCu_d1.000mM_t+060m_vs_NRC-1h1.sig	NA	NA	0	NA	NA	NA	NA	NA	NA	5	NA	NA	NA	NA	NA	NA	NA	225	NA	60	NA	NA	CM	37
sDura3_pCu_d1.000mM_t+180m_vs_NRC-1h1.sig	NA	NA	0	NA	NA	NA	NA	NA	NA	5	NA	NA	NA	NA	NA	NA	NA	225	NA	180	NA	NA	CM	37
sDura3_pCu_d1.000mM_t-015m_vs_NRC-1h1.sig	NA	NA	0	NA	NA	NA	NA	NA	NA	5	NA	NA	NA	NA	NA	NA	NA	225	NA	-15	NA	NA	CM	37
sDura3_pNULL_d0.000mM_t+015m_vs_NRC-1h1.sig	NA	NA	NA	NA	NA	NA	NA	NA	NA	5	NA	NA	NA	NA	NA	NA	NA	225	NA	15	NA	NA	CM	37
sDura3_pNULL_d0.000mM_t+030m_vs_NRC-1h1.sig	NA	NA	NA	NA	NA	NA	NA	NA	NA	5	NA	NA	NA	NA	NA	NA	NA	225	NA	30	NA	NA	CM	37
sDura3_pNULL_d0.000mM_t+060m_vs_NRC-1h1.sig	NA	NA	NA	NA	NA	NA	NA	NA	NA	5	NA	NA	NA	NA	NA	NA	NA	225	NA	60	NA	NA	CM	37
sDura3_pNULL_d0.000mM_t+180m_vs_NRC-1h1.sig	NA	NA	NA	NA	NA	NA	NA	NA	NA	5	NA	NA	NA	NA	NA	NA	NA	225	NA	180	NA	NA	CM	37
sDura3_pNULL_d0.000mM_t-015m_vs_NRC-1h1.sig	NA	NA	NA	NA	NA	NA	NA	NA	NA	5	NA	NA	NA	NA	NA	NA	NA	225	NA	-15	NA	NA	CM	37
sDura3_pZn_d0.005mM_t+015m_vs_NRC-1h1.sig	NA	NA	NA	NA	NA	NA	NA	NA	NA	5	NA	NA	NA	NA	NA	NA	NA	225	NA	15	NA	0	CM	37
sDura3_pZn_d0.005mM_t+030m_vs_NRC-1h1.sig	NA	NA	NA	NA	NA	NA	NA	NA	NA	5	NA	NA	NA	NA	NA	NA	NA	225	NA	30	NA	0	CM	37
sDura3_pZn_d0.005mM_t+060m_vs_NRC-1h1.sig	NA	NA	NA	NA	NA	NA	NA	NA	NA	5	NA	NA	NA	NA	NA	NA	NA	225	NA	60	NA	0	CM	37

sDura3_pZn_d0.005mM_t+180m_vs_NRC-1h1.sig	NA	NA	NA	NA	NA	NA	NA	NA	NA	5	NA	NA	NA	NA	NA	NA	NA	225	NA	180	NA	0	CM	37
sDura3_pZn_d0.005mM_t-015m_vs_NRC-1h1.sig	NA	NA	NA	NA	NA	NA	NA	NA	NA	5	NA	NA	NA	NA	NA	NA	NA	225	NA	-15	NA	0	CM	37
sDura3_pZn_d0.020mM_t+015m_vs_NRC-1h1.sig	NA	NA	NA	NA	NA	NA	NA	NA	NA	5	NA	NA	NA	NA	NA	NA	NA	225	NA	15	NA	0	CM	37
sDura3_pZn_d0.020mM_t+030m_vs_NRC-1h1.sig	NA	NA	NA	NA	NA	NA	NA	NA	NA	5	NA	NA	NA	NA	NA	NA	NA	225	NA	30	NA	0	CM	37
sDura3_pZn_d0.020mM_t+060m_vs_NRC-1h1.sig	NA	NA	NA	NA	NA	NA	NA	NA	NA	5	NA	NA	NA	NA	NA	NA	NA	225	NA	60	NA	0	CM	37
sDura3_pZn_d0.020mM_t+180m_vs_NRC-1h1.sig	NA	NA	NA	NA	NA	NA	NA	NA	NA	5	NA	NA	NA	NA	NA	NA	NA	225	NA	180	NA	0	CM	37
sDura3_pZn_d0.020mM_t-015m_vs_NRC-1h1.sig	NA	NA	NA	NA	NA	NA	NA	NA	NA	5	NA	NA	NA	NA	NA	NA	NA	225	NA	-15	NA	0	CM	37
sDura3_pZn_d0.050mM_t+015m_vs_NRC-1h1.sig	NA	NA	NA	NA	NA	NA	NA	NA	NA	5	NA	NA	NA	NA	NA	NA	NA	225	NA	15	NA	0	CM	37
sDura3_pZn_d0.050mM_t+030m_vs_NRC-1h1.sig	NA	NA	NA	NA	NA	NA	NA	NA	NA	5	NA	NA	NA	NA	NA	NA	NA	225	NA	30	NA	0	CM	37
sDura3_pZn_d0.050mM_t+060m_vs_NRC-1h1.sig	NA	NA	NA	NA	NA	NA	NA	NA	NA	5	NA	NA	NA	NA	NA	NA	NA	225	NA	60	NA	0	CM	37
sDura3_pZn_d0.050mM_t+180m_vs_NRC-1h1.sig	NA	NA	NA	NA	NA	NA	NA	NA	NA	5	NA	NA	NA	NA	NA	NA	NA	225	NA	180	NA	0	CM	37
sDura3_pZn_d0.050mM_t-015m_vs_NRC-1h1.sig	NA	NA	NA	NA	NA	NA	NA	NA	NA	5	NA	NA	NA	NA	NA	NA	NA	225	NA	-15	NA	0	CM	37

Appendix S. List of Lrp binding targets whose expression correlated with the Lrp

Positive Correlation			
Lrp	**condition**	**canonical_Name**	**gene_Name**
AsnC	high paraquat constant	*VNG0405C*	*VNG0405C*
AsnC	high paraquat constant	*VNG0421C*	*VNG0421C*
AsnC	high paraquat constant	*VNG0865C*	*VNG0865C*
AsnC	high paraquat constant	*VNG0867G*	*asnA*
AsnC	high paraquat constant	*VNG1069C*	*VNG1069C*
AsnC	high paraquat constant	*VNG1297C*	*VNG1297C*
AsnC	high paraquat constant	*VNG1323C*	*VNG1323C*
AsnC	high paraquat constant	*VNG1608C*	*VNG1608C*
AsnC	high paraquat constant	*VNG1688C*	*VNG1688C*
AsnC	high paraquat constant	*VNG1689G*	*rpl13p*
AsnC	high paraquat constant	*VNG1690G*	*rpl4e*
AsnC	high paraquat constant	*VNG1691G*	*rpl23p*
AsnC	high paraquat constant	*VNG1692G*	*rpl2p*
AsnC	high paraquat constant	*VNG1693G*	*rps19p*
AsnC	high paraquat constant	*VNG1695G*	*rpl22p*
AsnC	high paraquat constant	*VNG1697G*	*rps3p*
AsnC	high paraquat constant	*VNG1698G*	*rpl29p*
AsnC	high paraquat constant	*VNG1699C*	*VNG1699C*
AsnC	high paraquat constant	*VNG1700G*	*rps17p*
AsnC	high paraquat constant	*VNG1701G*	*rpl14p*
AsnC	high paraquat constant	*VNG1702G*	*rpl24p*
AsnC	high paraquat constant	*VNG1703G*	*rps4e*
AsnC	high paraquat constant	*VNG1705G*	*rpl5p*
AsnC	high paraquat constant	*VNG1706G*	*rps14p*
AsnC	high paraquat constant	*VNG1707G*	*rps8p*
AsnC	high paraquat constant	*VNG1709G*	*rpl6p*
AsnC	high paraquat constant	*VNG1711G*	*rpl32e*
AsnC	high paraquat constant	*VNG1713G*	*rpl19e*
AsnC	high paraquat constant	*VNG1714G*	*rpl18p*
AsnC	high paraquat constant	*VNG1715G*	*rps5p*
AsnC	high paraquat constant	*VNG1716G*	*rpl30p*
AsnC	high paraquat constant	*VNG1718G*	*rpl15p*
AsnC	high paraquat constant	*VNG1719G*	*secY*
AsnC	high paraquat constant	*VNG1735C*	*VNG1735C*
AsnC	high paraquat constant	*VNG1779C*	*VNG1779C*
AsnC	high paraquat constant	*VNG1941C*	*VNG1941C*
AsnC	high paraquat constant	*VNG2307C*	*VNG2307C*

AsnC	high paraquat constant	*VNG2474C*	*VNG2474C*
AsnC	high paraquat constant	*VNG0124C*	*VNG0124C*
AsnC	high paraquat constant	*VNG1874C*	*VNG1874C*
AsnC	high paraquat constant	*VNG2555C*	*VNG2555C*
AsnC	high paraquat constant	*VNG0002G*	*yvrO*
AsnC	high paraquat constant	*VNG0003C*	*VNG0003C*
AsnC	high paraquat constant	*VNG0133G*	*rpa*
AsnC	high paraquat constant	*VNG0134G*	*hpyA*
AsnC	high paraquat constant	*VNG0647G*	*nuoM*
AsnC	high paraquat constant	*VNG0648G*	*ndhG3*
AsnC	high paraquat constant	*VNG1143G*	*rps2p*
AsnC	high paraquat constant	*VNG1145G*	*mvk*
AsnC	high paraquat constant	*VNG1150G*	*idsA*
AsnC	high paraquat constant	*VNG1553G*	*cbiF*
AsnC	high paraquat constant	*VNG1554G*	*cbiG*
AsnC	high paraquat constant	*VNG1555G*	*cobH*
AsnC	high paraquat constant	*VNG1557G*	*cbiH*
AsnC	high paraquat constant	*VNG1568G*	*cbiJ*
AsnC	high paraquat constant	*VNG1816G*	*trh3*
AsnC	high paraquat constant	*VNG1939G*	*purC*
AsnC	high paraquat constant	*VNG2150G*	*etfB*
AsnC	high paraquat constant	*VNG2151G*	*etfA*
AsnC	high paraquat constant	*VNG2220G*	*lpdA*
AsnC	high paraquat constant	*VNG2397G*	*cysA*
AsnC	high paraquat constant	*VNG0386G*	*trpG2*
AsnC	high paraquat constant	*VNG1433G*	*rps17e*
AsnC	high paraquat constant	*VNG0146H*	*VNG0146H*
AsnC	high paraquat constant	*VNG0184H*	*VNG0184H*
AsnC	high paraquat constant	*VNG0217H*	*VNG0217H*
AsnC	high paraquat constant	*VNG1787H*	*VNG1787H*
AsnC	high paraquat constant	*VNG1910H*	*VNG1910H*
AsnC	high paraquat constant	*VNG2149H*	*VNG2149H*
AsnC	high paraquat constant	*VNG1487H*	*VNG1487H*
AsnC	high paraquat constant	*VNG1244C*	*VNG1244C*
AsnC	high paraquat constant	*VNG0537C*	*VNG0537C*
AsnC	high paraquat constant	*VNG0983C*	*VNG0983C*
AsnC	high paraquat constant	*VNG1287C*	*VNG1287C*
AsnC	high paraquat constant	*VNG0013C*	*VNG0013C*
AsnC	high paraquat constant	*VNG0035C*	*VNG0035C*
AsnC	high paraquat constant	*VNG0598C*	*VNG0598C*
AsnC	high paraquat constant	*VNG0925C*	*VNG0925C*
AsnC	high paraquat constant	*VNG2172C*	*VNG2172C*

AsnC	high paraquat constant	*VNG0006G*	*glmS*
AsnC	high paraquat constant	*VNG0137G*	*cca*
AsnC	high paraquat constant	*VNG0163G*	*mutS1*
AsnC	high paraquat constant	*VNG0630G*	*ribE*
AsnC	high paraquat constant	*VNG0862G*	*hisF*
AsnC	high paraquat constant	*VNG0864G*	*purL*
AsnC	high paraquat constant	*VNG0920H*	*VNG0920H*
AsnC	high paraquat constant	*VNG0921G*	*potA1*
AsnC	high paraquat constant	*VNG1079G*	*menB*
AsnC	high paraquat constant	*VNG1294G*	*slyD*
AsnC	high paraquat constant	*VNG1359G*	*rad2*
AsnC	high paraquat constant	*VNG1369G*	*hemV1*
AsnC	high paraquat constant	*VNG1773G*	*cad*
AsnC	high paraquat constant	*VNG2051G*	*rpoE''*
AsnC	high paraquat constant	*VNG2053G*	*rpoE'*
AsnC	high paraquat constant	*VNG2054H*	*VNG2054H*
AsnC	high paraquat constant	*VNG2056G*	*eif2g*
AsnC	high paraquat constant	*VNG2138G*	*atpB*
AsnC	high paraquat constant	*VNG2139G*	*atpA*
AsnC	high paraquat constant	*VNG2140G*	*atpF*
AsnC	high paraquat constant	*VNG2141G*	*atpC*
AsnC	high paraquat constant	*VNG2462G*	*dpa*
AsnC	high paraquat constant	*VNG2654G*	*eef2*
AsnC	high paraquat constant	*VNG2657G*	*rps7p*
AsnC	high paraquat constant	*VNG0546C*	*VNG0546C*
AsnC	high paraquat constant	*VNG0548C*	*VNG0548C*
AsnC	high paraquat constant	*VNG0549G*	*eif2a*
AsnC	high paraquat constant	*VNG0550G*	*rps27e*
AsnC	high paraquat constant	*VNG0551G*	*rpl44e*
AsnC	high paraquat constant	*VNG1376H*	*VNG1376H*
AsnC	high paraquat constant	*VNG2177H*	*VNG2177H*
AsnC	high paraquat constant	*VNG0408H*	*VNG0408H*
AsnC	high paraquat constant	*VNG1410H*	*VNG1410H*
AsnC	high paraquat constant	*VNG1642H*	*VNG1642H*
AsnC	high paraquat constant	*VNG1777H*	*VNG1777H*
AsnC	high paraquat constant	*VNG2525H*	*VNG2525H*
AsnC	high paraquat constant	*VNG2554H*	*VNG2554H*
AsnC	high paraquat constant	*VNG5022G*	*gvpJ1*
AsnC	high paraquat constant	*VNG6347H*	*VNG6347H*
AsnC	high paraquat	*VNG0255C*	*VNG0255C*
AsnC	high paraquat	*VNG0256H*	*VNG0256H*
AsnC	high paraquat	*VNG0363G*	*nfi*

AsnC	high paraquat	*VNG0405C*	*VNG0405C*
AsnC	high paraquat	*VNG0421C*	*VNG0421C*
AsnC	high paraquat	*VNG0631C*	*VNG0631C*
AsnC	high paraquat	*VNG0865C*	*VNG0865C*
AsnC	high paraquat	*VNG0867G*	*asnA*
AsnC	high paraquat	*VNG1069C*	*VNG1069C*
AsnC	high paraquat	*VNG1297C*	*VNG1297C*
AsnC	high paraquat	*VNG1323C*	*VNG1323C*
AsnC	high paraquat	*VNG1608C*	*VNG1608C*
AsnC	high paraquat	*VNG1688C*	*VNG1688C*
AsnC	high paraquat	*VNG1689G*	*rpl13p*
AsnC	high paraquat	*VNG1690G*	*rpl4e*
AsnC	high paraquat	*VNG1691G*	*rpl23p*
AsnC	high paraquat	*VNG1692G*	*rpl2p*
AsnC	high paraquat	*VNG1693G*	*rps19p*
AsnC	high paraquat	*VNG1695G*	*rpl22p*
AsnC	high paraquat	*VNG1697G*	*rps3p*
AsnC	high paraquat	*VNG1698G*	*rpl29p*
AsnC	high paraquat	*VNG1699C*	*VNG1699C*
AsnC	high paraquat	*VNG1700G*	*rps17p*
AsnC	high paraquat	*VNG1701G*	*rpl14p*
AsnC	high paraquat	*VNG1702G*	*rpl24p*
AsnC	high paraquat	*VNG1703G*	*rps4e*
AsnC	high paraquat	*VNG1705G*	*rpl5p*
AsnC	high paraquat	*VNG1706G*	*rps14p*
AsnC	high paraquat	*VNG1707G*	*rps8p*
AsnC	high paraquat	*VNG1709G*	*rpl6p*
AsnC	high paraquat	*VNG1711G*	*rpl32e*
AsnC	high paraquat	*VNG1713G*	*rpl19e*
AsnC	high paraquat	*VNG1714G*	*rpl18p*
AsnC	high paraquat	*VNG1715G*	*rps5p*
AsnC	high paraquat	*VNG1716G*	*rpl30p*
AsnC	high paraquat	*VNG1718G*	*rpl15p*
AsnC	high paraquat	*VNG1719G*	*secY*
AsnC	high paraquat	*VNG1735C*	*VNG1735C*
AsnC	high paraquat	*VNG1779C*	*VNG1779C*
AsnC	high paraquat	*VNG1941C*	*VNG1941C*
AsnC	high paraquat	*VNG2307C*	*VNG2307C*
AsnC	high paraquat	*VNG2369C*	*VNG2369C*
AsnC	high paraquat	*VNG2474C*	*VNG2474C*
AsnC	high paraquat	*VNG0045C*	*VNG0045C*
AsnC	high paraquat	*VNG1874C*	*VNG1874C*

AsnC	high paraquat	*VNG2555C*	*VNG2555C*
AsnC	high paraquat	*VNG0002G*	*yvrO*
AsnC	high paraquat	*VNG0003C*	*VNG0003C*
AsnC	high paraquat	*VNG0133G*	*rpa*
AsnC	high paraquat	*VNG0134G*	*hpyA*
AsnC	high paraquat	*VNG0136G*	*aup*
AsnC	high paraquat	*VNG0307G*	*trpB*
AsnC	high paraquat	*VNG0647G*	*nuoM*
AsnC	high paraquat	*VNG0648G*	*ndhG3*
AsnC	high paraquat	*VNG1143G*	*rps2p*
AsnC	high paraquat	*VNG1145G*	*mvk*
AsnC	high paraquat	*VNG1148G*	*argB*
AsnC	high paraquat	*VNG1150G*	*idsA*
AsnC	high paraquat	*VNG1553G*	*cbiF*
AsnC	high paraquat	*VNG1554G*	*cbiG*
AsnC	high paraquat	*VNG1555G*	*cobH*
AsnC	high paraquat	*VNG1557G*	*cbiH*
AsnC	high paraquat	*VNG1568G*	*cbiJ*
AsnC	high paraquat	*VNG1816G*	*trh3*
AsnC	high paraquat	*VNG1939G*	*purC*
AsnC	high paraquat	*VNG1992G*	*pgi*
AsnC	high paraquat	*VNG1993H*	*VNG1993H*
AsnC	high paraquat	*VNG2150G*	*etfB*
AsnC	high paraquat	*VNG2151G*	*etfA*
AsnC	high paraquat	*VNG2220G*	*lpdA*
AsnC	high paraquat	*VNG2397G*	*cysA*
AsnC	high paraquat	*VNG2526G*	*dppF*
AsnC	high paraquat	*VNG2527G*	*dppD*
AsnC	high paraquat	*VNG2529G*	*dppB2*
AsnC	high paraquat	*VNG2531G*	*dppC1*
AsnC	high paraquat	*VNG1433G*	*rps17e*
AsnC	high paraquat	*VNG0146H*	*VNG0146H*
AsnC	high paraquat	*VNG0184H*	*VNG0184H*
AsnC	high paraquat	*VNG0217H*	*VNG0217H*
AsnC	high paraquat	*VNG0219H*	*VNG0219H*
AsnC	high paraquat	*VNG1910H*	*VNG1910H*
AsnC	high paraquat	*VNG2149H*	*VNG2149H*
AsnC	high paraquat	*VNG1487H*	*VNG1487H*
AsnC	high paraquat	*VNG0132C*	*VNG0132C*
AsnC	high paraquat	*VNG1244C*	*VNG1244C*
AsnC	high paraquat	*VNG0147C*	*VNG0147C*
AsnC	high paraquat	*VNG0537C*	*VNG0537C*

AsnC	high paraquat	*VNG0539C*	*VNG0539C*
AsnC	high paraquat	*VNG0555C*	*VNG0555C*
AsnC	high paraquat	*VNG0615C*	*VNG0615C*
AsnC	high paraquat	*VNG0983C*	*VNG0983C*
AsnC	high paraquat	*VNG2518C*	*VNG2518C*
AsnC	high paraquat	*VNG0013C*	*VNG0013C*
AsnC	high paraquat	*VNG0035C*	*VNG0035C*
AsnC	high paraquat	*VNG0598C*	*VNG0598C*
AsnC	high paraquat	*VNG0925C*	*VNG0925C*
AsnC	high paraquat	*VNG2172C*	*VNG2172C*
AsnC	high paraquat	*VNG0006G*	*glmS*
AsnC	high paraquat	*VNG0137G*	*cca*
AsnC	high paraquat	*VNG0163G*	*mutS1*
AsnC	high paraquat	*VNG0172G*	*mutS2*
AsnC	high paraquat	*VNG0494G*	*grpE*
AsnC	high paraquat	*VNG0610G*	*hhoA*
AsnC	high paraquat	*VNG0862G*	*hisF*
AsnC	high paraquat	*VNG0864G*	*purL*
AsnC	high paraquat	*VNG0920H*	*VNG0920H*
AsnC	high paraquat	*VNG0921G*	*potA1*
AsnC	high paraquat	*VNG0966G*	*cheR*
AsnC	high paraquat	*VNG1294G*	*slyD*
AsnC	high paraquat	*VNG1359G*	*rad2*
AsnC	high paraquat	*VNG1369G*	*hemV1*
AsnC	high paraquat	*VNG1773G*	*cad*
AsnC	high paraquat	*VNG2051G*	*rpoE''*
AsnC	high paraquat	*VNG2053G*	*rpoE'*
AsnC	high paraquat	*VNG2054H*	*VNG2054H*
AsnC	high paraquat	*VNG2056G*	*eif2g*
AsnC	high paraquat	*VNG2060G*	*phnP*
AsnC	high paraquat	*VNG2138G*	*atpB*
AsnC	high paraquat	*VNG2139G*	*atpA*
AsnC	high paraquat	*VNG2140G*	*atpF*
AsnC	high paraquat	*VNG2141G*	*atpC*
AsnC	high paraquat	*VNG2462G*	*dpa*
AsnC	high paraquat	*VNG2482G*	*pstB1*
AsnC	high paraquat	*VNG2484G*	*pstC1*
AsnC	high paraquat	*VNG2654G*	*eef2*
AsnC	high paraquat	*VNG2657G*	*rps7p*
AsnC	high paraquat	*VNG0546C*	*VNG0546C*
AsnC	high paraquat	*VNG0548C*	*VNG0548C*
AsnC	high paraquat	*VNG0549G*	*eif2a*

AsnC	high paraquat	*VNG0550G*	*rps27e*
AsnC	high paraquat	*VNG1376H*	*VNG1376H*
AsnC	high paraquat	*VNG1832H*	*VNG1832H*
AsnC	high paraquat	*VNG2177H*	*VNG2177H*
AsnC	high paraquat	*VNG0408H*	*VNG0408H*
AsnC	high paraquat	*VNG0420H*	*VNG0420H*
AsnC	high paraquat	*VNG0430H*	*VNG0430H*
AsnC	high paraquat	*VNG1410H*	*VNG1410H*
AsnC	high paraquat	*VNG1777H*	*VNG1777H*
AsnC	high paraquat	*VNG1921H*	*VNG1921H*
AsnC	high paraquat	*VNG2525H*	*VNG2525H*
AsnC	high paraquat	*VNG2554H*	*VNG2554H*
AsnC	high paraquat	*VNG5074C*	*VNG5074C*
AsnC	high paraquat	*VNG5022G*	*gvpJ1*
AsnC	high paraquat	*VNG6347H*	*VNG6347H*
AsnC	high paraquat	*VNG6212G*	*iucA*
AsnC	high paraquat	*VNG6214G*	*hxyA*
AsnC	high paraquat	*VNG6377H*	*VNG6377H*
AsnC	low h202 constant	*VNG0110C*	*VNG0110C*
AsnC	low h202 constant	*VNG0255C*	*VNG0255C*
AsnC	low h202 constant	*VNG0256H*	*VNG0256H*
AsnC	low h202 constant	*VNG0363G*	*nfi*
AsnC	low h202 constant	*VNG0405C*	*VNG0405C*
AsnC	low h202 constant	*VNG0421C*	*VNG0421C*
AsnC	low h202 constant	*VNG0631C*	*VNG0631C*
AsnC	low h202 constant	*VNG1069C*	*VNG1069C*
AsnC	low h202 constant	*VNG1297C*	*VNG1297C*
AsnC	low h202 constant	*VNG1323C*	*VNG1323C*
AsnC	low h202 constant	*VNG1608C*	*VNG1608C*
AsnC	low h202 constant	*VNG1688C*	*VNG1688C*
AsnC	low h202 constant	*VNG1689G*	*rpl13p*
AsnC	low h202 constant	*VNG1690G*	*rpl4e*
AsnC	low h202 constant	*VNG1691G*	*rpl23p*
AsnC	low h202 constant	*VNG1692G*	*rpl2p*
AsnC	low h202 constant	*VNG1693G*	*rps19p*
AsnC	low h202 constant	*VNG1695G*	*rpl22p*
AsnC	low h202 constant	*VNG1697G*	*rps3p*
AsnC	low h202 constant	*VNG1698G*	*rpl29p*
AsnC	low h202 constant	*VNG1699C*	*VNG1699C*
AsnC	low h202 constant	*VNG1700G*	*rps17p*
AsnC	low h202 constant	*VNG1701G*	*rpl14p*
AsnC	low h202 constant	*VNG1702G*	*rpl24p*

AsnC	low h202 constant	*VNG1703G*	*rps4e*
AsnC	low h202 constant	*VNG1705G*	*rpl5p*
AsnC	low h202 constant	*VNG1706G*	*rps14p*
AsnC	low h202 constant	*VNG1707G*	*rps8p*
AsnC	low h202 constant	*VNG1709G*	*rpl6p*
AsnC	low h202 constant	*VNG1711G*	*rpl32e*
AsnC	low h202 constant	*VNG1713G*	*rpl19e*
AsnC	low h202 constant	*VNG1714G*	*rpl18p*
AsnC	low h202 constant	*VNG1715G*	*rps5p*
AsnC	low h202 constant	*VNG1716G*	*rpl30p*
AsnC	low h202 constant	*VNG1718G*	*rpl15p*
AsnC	low h202 constant	*VNG1719G*	*secY*
AsnC	low h202 constant	*VNG1735C*	*VNG1735C*
AsnC	low h202 constant	*VNG1779C*	*VNG1779C*
AsnC	low h202 constant	*VNG1941C*	*VNG1941C*
AsnC	low h202 constant	*VNG2369C*	*VNG2369C*
AsnC	low h202 constant	*VNG2466C*	*VNG2466C*
AsnC	low h202 constant	*VNG2475C*	*VNG2475C*
AsnC	low h202 constant	*VNG0045C*	*VNG0045C*
AsnC	low h202 constant	*VNG0505C*	*VNG0505C*
AsnC	low h202 constant	*VNG1874C*	*VNG1874C*
AsnC	low h202 constant	*VNG0003C*	*VNG0003C*
AsnC	low h202 constant	*VNG0133G*	*rpa*
AsnC	low h202 constant	*VNG0136G*	*aup*
AsnC	low h202 constant	*VNG0307G*	*trpB*
AsnC	low h202 constant	*VNG0364G*	*yusZ3*
AsnC	low h202 constant	*VNG0387G*	*ilvE1*
AsnC	low h202 constant	*VNG0647G*	*nuoM*
AsnC	low h202 constant	*VNG0648G*	*ndhG3*
AsnC	low h202 constant	*VNG1143G*	*rps2p*
AsnC	low h202 constant	*VNG1145G*	*mvk*
AsnC	low h202 constant	*VNG1150G*	*idsA*
AsnC	low h202 constant	*VNG1160G*	*ndk*
AsnC	low h202 constant	*VNG1341G*	*fabG*
AsnC	low h202 constant	*VNG1435G*	*asd*
AsnC	low h202 constant	*VNG1528G*	*nac*
AsnC	low h202 constant	*VNG1553G*	*cbiF*
AsnC	low h202 constant	*VNG1554G*	*cbiG*
AsnC	low h202 constant	*VNG1555G*	*cobH*
AsnC	low h202 constant	*VNG1557G*	*cbiH*
AsnC	low h202 constant	*VNG1568G*	*cbiJ*
AsnC	low h202 constant	*VNG1816G*	*trh3*

AsnC	low h202 constant	*VNG1818G*	*idi*
AsnC	low h202 constant	*VNG1992G*	*pgi*
AsnC	low h202 constant	*VNG1993H*	*VNG1993H*
AsnC	low h202 constant	*VNG2094G*	*trh4*
AsnC	low h202 constant	*VNG2220G*	*lpdA*
AsnC	low h202 constant	*VNG2397G*	*cysA*
AsnC	low h202 constant	*VNG2526G*	*dppF*
AsnC	low h202 constant	*VNG2604G*	*thi1*
AsnC	low h202 constant	*VNG2606G*	*thiD*
AsnC	low h202 constant	*VNG0386G*	*trpG2*
AsnC	low h202 constant	*VNG1159G*	*rpl24e*
AsnC	low h202 constant	*VNG1433G*	*rps17e*
AsnC	low h202 constant	*VNG0022H*	*VNG0022H*
AsnC	low h202 constant	*VNG0055H*	*VNG0055H*
AsnC	low h202 constant	*VNG0138H*	*VNG0138H*
AsnC	low h202 constant	*VNG0146H*	*VNG0146H*
AsnC	low h202 constant	*VNG0184H*	*VNG0184H*
AsnC	low h202 constant	*VNG0217H*	*VNG0217H*
AsnC	low h202 constant	*VNG0244H*	*VNG0244H*
AsnC	low h202 constant	*VNG0296H*	*VNG0296H*
AsnC	low h202 constant	*VNG0717H*	*VNG0717H*
AsnC	low h202 constant	*VNG0861H*	*VNG0861H*
AsnC	low h202 constant	*VNG1002H*	*VNG1002H*
AsnC	low h202 constant	*VNG1115H*	*VNG1115H*
AsnC	low h202 constant	*VNG1229H*	*VNG1229H*
AsnC	low h202 constant	*VNG1891H*	*VNG1891H*
AsnC	low h202 constant	*VNG1910H*	*VNG1910H*
AsnC	low h202 constant	*VNG1956H*	*VNG1956H*
AsnC	low h202 constant	*VNG1487H*	*VNG1487H*
AsnC	low h202 constant	*VNG2581H*	*VNG2581H*
AsnC	low h202 constant	*VNG1244C*	*VNG1244C*
AsnC	low h202 constant	*VNG1388H*	*VNG1388H*
AsnC	low h202 constant	*VNG1389C*	*VNG1389C*
AsnC	low h202 constant	*VNG0147C*	*VNG0147C*
AsnC	low h202 constant	*VNG0537C*	*VNG0537C*
AsnC	low h202 constant	*VNG0539C*	*VNG0539C*
AsnC	low h202 constant	*VNG0555C*	*VNG0555C*
AsnC	low h202 constant	*VNG0615C*	*VNG0615C*
AsnC	low h202 constant	*VNG1165G*	*ksgA*
AsnC	low h202 constant	*VNG1168C*	*VNG1168C*
AsnC	low h202 constant	*VNG1198C*	*VNG1198C*
AsnC	low h202 constant	*VNG1228C*	*VNG1228C*

AsnC	low h202 constant	*VNG1681C*	*VNG1681C*
AsnC	low h202 constant	*VNG1687C*	*VNG1687C*
AsnC	low h202 constant	*VNG2518C*	*VNG2518C*
AsnC	low h202 constant	*VNG0013C*	*VNG0013C*
AsnC	low h202 constant	*VNG0035C*	*VNG0035C*
AsnC	low h202 constant	*VNG0470G*	*trp3*
AsnC	low h202 constant	*VNG0598C*	*VNG0598C*
AsnC	low h202 constant	*VNG0925C*	*VNG0925C*
AsnC	low h202 constant	*VNG2172C*	*VNG2172C*
AsnC	low h202 constant	*VNG0006G*	*glmS*
AsnC	low h202 constant	*VNG0163G*	*mutS1*
AsnC	low h202 constant	*VNG0164G*	*hef*
AsnC	low h202 constant	*VNG0172G*	*mutS2*
AsnC	low h202 constant	*VNG0180G*	*hop*
AsnC	low h202 constant	*VNG0223G*	*moxR*
AsnC	low h202 constant	*VNG0610G*	*hhoA*
AsnC	low h202 constant	*VNG0806G*	*htr4*
AsnC	low h202 constant	*VNG0862G*	*hisF*
AsnC	low h202 constant	*VNG0869G*	*tfbD*
AsnC	low h202 constant	*VNG0920H*	*VNG0920H*
AsnC	low h202 constant	*VNG0921G*	*potA1*
AsnC	low h202 constant	*VNG1079G*	*menB*
AsnC	low h202 constant	*VNG1284G*	*trkH1*
AsnC	low h202 constant	*VNG1294G*	*slyD*
AsnC	low h202 constant	*VNG1520G*	*mutY*
AsnC	low h202 constant	*VNG1815G*	*carA*
AsnC	low h202 constant	*VNG1929G*	*tmk*
AsnC	low h202 constant	*VNG1987G*	*secD*
AsnC	low h202 constant	*VNG2051G*	*rpoE''*
AsnC	low h202 constant	*VNG2053G*	*rpoE'*
AsnC	low h202 constant	*VNG2054H*	*VNG2054H*
AsnC	low h202 constant	*VNG2056G*	*eif2g*
AsnC	low h202 constant	*VNG2060G*	*phnP*
AsnC	low h202 constant	*VNG2138G*	*atpB*
AsnC	low h202 constant	*VNG2139G*	*atpA*
AsnC	low h202 constant	*VNG2140G*	*atpF*
AsnC	low h202 constant	*VNG2141G*	*atpC*
AsnC	low h202 constant	*VNG2142G*	*atpE*
AsnC	low h202 constant	*VNG2482G*	*pstB1*
AsnC	low h202 constant	*VNG2483G*	*pstA1*
AsnC	low h202 constant	*VNG2484G*	*pstC1*
AsnC	low h202 constant	*VNG2486G*	*yqgG*

AsnC	low h202 constant	*VNG2654G*	*eef2*
AsnC	low h202 constant	*VNG2657G*	*rps7p*
AsnC	low h202 constant	*VNG0546C*	*VNG0546C*
AsnC	low h202 constant	*VNG0548C*	*VNG0548C*
AsnC	low h202 constant	*VNG0549G*	*eif2a*
AsnC	low h202 constant	*VNG0550G*	*rps27e*
AsnC	low h202 constant	*VNG0626G*	*maoC2*
AsnC	low h202 constant	*VNG0323H*	*VNG0323H*
AsnC	low h202 constant	*VNG1376H*	*VNG1376H*
AsnC	low h202 constant	*VNG1630H*	*VNG1630H*
AsnC	low h202 constant	*VNG1832H*	*VNG1832H*
AsnC	low h202 constant	*VNG1989H*	*VNG1989H*
AsnC	low h202 constant	*VNG1991H*	*VNG1991H*
AsnC	low h202 constant	*VNG2177H*	*VNG2177H*
AsnC	low h202 constant	*VNG0054H*	*VNG0054H*
AsnC	low h202 constant	*VNG0198H*	*VNG0198H*
AsnC	low h202 constant	*VNG0204H*	*VNG0204H*
AsnC	low h202 constant	*VNG0408H*	*VNG0408H*
AsnC	low h202 constant	*VNG0430H*	*VNG0430H*
AsnC	low h202 constant	*VNG0612H*	*VNG0612H*
AsnC	low h202 constant	*VNG1410H*	*VNG1410H*
AsnC	low h202 constant	*VNG1919H*	*VNG1919H*
AsnC	low h202 constant	*VNG1921H*	*VNG1921H*
AsnC	low h202 constant	*VNG2014H*	*VNG2014H*
AsnC	low h202 constant	*VNG2148H*	*VNG2148H*
AsnC	low h202 constant	*VNG2403H*	*VNG2403H*
AsnC	low h202 constant	*VNG2525H*	*VNG2525H*
AsnC	low h202 constant	*VNG2562H*	*VNG2562H*
AsnC	low h202 constant	*VNG5074C*	*VNG5074C*
AsnC	low h202 constant	*VNG5124H*	*VNG5124H*
AsnC	low h202 constant	*VNG5022G*	*gvpJ1*
AsnC	low h202 constant	*VNG6334H*	*VNG6334H*
AsnC	low h202 constant	*VNG6378H*	*VNG6378H*
AsnC	low h202 constant	*VNG6432H*	*VNG6432H*
AsnC	low h202 constant	*VNG6212G*	*iucA*
AsnC	low h202 constant	*VNG6213G*	*iucB*
AsnC	low h202 constant	*VNG6214G*	*hxyA*
AsnC	low h202 constant	*VNG6216G*	*iucC*
AsnC	low h202 constant	*VNG6142C*	*VNG6142C*
AsnC	low h202 constant	*VNG6377H*	*VNG6377H*
AsnC	low h202 constant	*VNG6145H*	*VNG6145H*
AsnC	low h202 constant	*VNG6346H*	*VNG6346H*

AsnC	low h202 constant	*VNG6404H*	*VNG6404H*
AsnC	low h202 constant	*VNG6431H*	*VNG6431H*
AsnC	ros constant	*VNG0255C*	*VNG0255C*
AsnC	ros constant	*VNG0256H*	*VNG0256H*
AsnC	ros constant	*VNG0363G*	*nfi*
AsnC	ros constant	*VNG0405C*	*VNG0405C*
AsnC	ros constant	*VNG0421C*	*VNG0421C*
AsnC	ros constant	*VNG0631C*	*VNG0631C*
AsnC	ros constant	*VNG0865C*	*VNG0865C*
AsnC	ros constant	*VNG0867G*	*asnA*
AsnC	ros constant	*VNG1069C*	*VNG1069C*
AsnC	ros constant	*VNG1297C*	*VNG1297C*
AsnC	ros constant	*VNG1323C*	*VNG1323C*
AsnC	ros constant	*VNG1608C*	*VNG1608C*
AsnC	ros constant	*VNG1688C*	*VNG1688C*
AsnC	ros constant	*VNG1689G*	*rpl13p*
AsnC	ros constant	*VNG1690G*	*rpl4e*
AsnC	ros constant	*VNG1691G*	*rpl23p*
AsnC	ros constant	*VNG1692G*	*rpl2p*
AsnC	ros constant	*VNG1693G*	*rps19p*
AsnC	ros constant	*VNG1695G*	*rpl22p*
AsnC	ros constant	*VNG1697G*	*rps3p*
AsnC	ros constant	*VNG1698G*	*rpl29p*
AsnC	ros constant	*VNG1699C*	*VNG1699C*
AsnC	ros constant	*VNG1700G*	*rps17p*
AsnC	ros constant	*VNG1701G*	*rpl14p*
AsnC	ros constant	*VNG1702G*	*rpl24p*
AsnC	ros constant	*VNG1703G*	*rps4e*
AsnC	ros constant	*VNG1705G*	*rpl5p*
AsnC	ros constant	*VNG1706G*	*rps14p*
AsnC	ros constant	*VNG1707G*	*rps8p*
AsnC	ros constant	*VNG1709G*	*rpl6p*
AsnC	ros constant	*VNG1711G*	*rpl32e*
AsnC	ros constant	*VNG1713G*	*rpl19e*
AsnC	ros constant	*VNG1714G*	*rpl18p*
AsnC	ros constant	*VNG1715G*	*rps5p*
AsnC	ros constant	*VNG1716G*	*rpl30p*
AsnC	ros constant	*VNG1718G*	*rpl15p*
AsnC	ros constant	*VNG1719G*	*secY*
AsnC	ros constant	*VNG1735C*	*VNG1735C*
AsnC	ros constant	*VNG1779C*	*VNG1779C*
AsnC	ros constant	*VNG1941C*	*VNG1941C*

AsnC	ros constant	*VNG2307C*	*VNG2307C*
AsnC	ros constant	*VNG2369C*	*VNG2369C*
AsnC	ros constant	*VNG2474C*	*VNG2474C*
AsnC	ros constant	*VNG0045C*	*VNG0045C*
AsnC	ros constant	*VNG0124C*	*VNG0124C*
AsnC	ros constant	*VNG1874C*	*VNG1874C*
AsnC	ros constant	*VNG0002G*	*yvrO*
AsnC	ros constant	*VNG0003C*	*VNG0003C*
AsnC	ros constant	*VNG0133G*	*rpa*
AsnC	ros constant	*VNG0134G*	*hpyA*
AsnC	ros constant	*VNG0136G*	*aup*
AsnC	ros constant	*VNG0307G*	*trpB*
AsnC	ros constant	*VNG0647G*	*nuoM*
AsnC	ros constant	*VNG0648G*	*ndhG3*
AsnC	ros constant	*VNG0674C*	*VNG0674C*
AsnC	ros constant	*VNG1143G*	*rps2p*
AsnC	ros constant	*VNG1145G*	*mvk*
AsnC	ros constant	*VNG1148G*	*argB*
AsnC	ros constant	*VNG1150G*	*idsA*
AsnC	ros constant	*VNG1435G*	*asd*
AsnC	ros constant	*VNG1553G*	*cbiF*
AsnC	ros constant	*VNG1554G*	*cbiG*
AsnC	ros constant	*VNG1555G*	*cobH*
AsnC	ros constant	*VNG1557G*	*cbiH*
AsnC	ros constant	*VNG1568G*	*cbiJ*
AsnC	ros constant	*VNG1816G*	*trh3*
AsnC	ros constant	*VNG1818G*	*idi*
AsnC	ros constant	*VNG1939G*	*purC*
AsnC	ros constant	*VNG1992G*	*pgi*
AsnC	ros constant	*VNG1993H*	*VNG1993H*
AsnC	ros constant	*VNG2150G*	*etfB*
AsnC	ros constant	*VNG2151G*	*etfA*
AsnC	ros constant	*VNG2220G*	*lpdA*
AsnC	ros constant	*VNG2295G*	*hisB*
AsnC	ros constant	*VNG2397G*	*cysA*
AsnC	ros constant	*VNG0386G*	*trpG2*
AsnC	ros constant	*VNG1159G*	*rpl24e*
AsnC	ros constant	*VNG1433G*	*rps17e*
AsnC	ros constant	*VNG0146H*	*VNG0146H*
AsnC	ros constant	*VNG0184H*	*VNG0184H*
AsnC	ros constant	*VNG0217H*	*VNG0217H*
AsnC	ros constant	*VNG1787H*	*VNG1787H*

AsnC	ros constant	*VNG1910H*	*VNG1910H*
AsnC	ros constant	*VNG2149H*	*VNG2149H*
AsnC	ros constant	*VNG1487H*	*VNG1487H*
AsnC	ros constant	*VNG1244C*	*VNG1244C*
AsnC	ros constant	*VNG1388H*	*VNG1388H*
AsnC	ros constant	*VNG0537C*	*VNG0537C*
AsnC	ros constant	*VNG0539C*	*VNG0539C*
AsnC	ros constant	*VNG0555C*	*VNG0555C*
AsnC	ros constant	*VNG0615C*	*VNG0615C*
AsnC	ros constant	*VNG0983C*	*VNG0983C*
AsnC	ros constant	*VNG1198C*	*VNG1198C*
AsnC	ros constant	*VNG1287C*	*VNG1287C*
AsnC	ros constant	*VNG2518C*	*VNG2518C*
AsnC	ros constant	*VNG0013C*	*VNG0013C*
AsnC	ros constant	*VNG0035C*	*VNG0035C*
AsnC	ros constant	*VNG0598C*	*VNG0598C*
AsnC	ros constant	*VNG0925C*	*VNG0925C*
AsnC	ros constant	*VNG2172C*	*VNG2172C*
AsnC	ros constant	*VNG0006G*	*glmS*
AsnC	ros constant	*VNG0137G*	*cca*
AsnC	ros constant	*VNG0163G*	*mutS1*
AsnC	ros constant	*VNG0172G*	*mutS2*
AsnC	ros constant	*VNG0630G*	*ribE*
AsnC	ros constant	*VNG0806G*	*htr4*
AsnC	ros constant	*VNG0862G*	*hisF*
AsnC	ros constant	*VNG0864G*	*purL*
AsnC	ros constant	*VNG0920H*	*VNG0920H*
AsnC	ros constant	*VNG0921G*	*potA1*
AsnC	ros constant	*VNG1079G*	*menB*
AsnC	ros constant	*VNG1284G*	*trkH1*
AsnC	ros constant	*VNG1294G*	*slyD*
AsnC	ros constant	*VNG1359G*	*rad2*
AsnC	ros constant	*VNG1369G*	*hemV1*
AsnC	ros constant	*VNG1773G*	*cad*
AsnC	ros constant	*VNG1987G*	*secD*
AsnC	ros constant	*VNG2051G*	*rpoE''*
AsnC	ros constant	*VNG2053G*	*rpoE'*
AsnC	ros constant	*VNG2054H*	*VNG2054H*
AsnC	ros constant	*VNG2056G*	*eif2g*
AsnC	ros constant	*VNG2060G*	*phnP*
AsnC	ros constant	*VNG2138G*	*atpB*
AsnC	ros constant	*VNG2139G*	*atpA*

AsnC	ros constant	*VNG2140G*	*atpF*
AsnC	ros constant	*VNG2141G*	*atpC*
AsnC	ros constant	*VNG2462G*	*dpa*
AsnC	ros constant	*VNG2484G*	*pstC1*
AsnC	ros constant	*VNG2654G*	*eef2*
AsnC	ros constant	*VNG2657G*	*rps7p*
AsnC	ros constant	*VNG0546C*	*VNG0546C*
AsnC	ros constant	*VNG0548C*	*VNG0548C*
AsnC	ros constant	*VNG0549G*	*eif2a*
AsnC	ros constant	*VNG0550G*	*rps27e*
AsnC	ros constant	*VNG0551G*	*rpl44e*
AsnC	ros constant	*VNG1376H*	*VNG1376H*
AsnC	ros constant	*VNG1832H*	*VNG1832H*
AsnC	ros constant	*VNG2177H*	*VNG2177H*
AsnC	ros constant	*VNG0408H*	*VNG0408H*
AsnC	ros constant	*VNG0430H*	*VNG0430H*
AsnC	ros constant	*VNG1410H*	*VNG1410H*
AsnC	ros constant	*VNG1777H*	*VNG1777H*
AsnC	ros constant	*VNG1921H*	*VNG1921H*
AsnC	ros constant	*VNG2525H*	*VNG2525H*
AsnC	ros constant	*VNG2562H*	*VNG2562H*
AsnC	ros constant	*VNG5022G*	*gvpJ1*
AsnC	ros constant	*VNG6347H*	*VNG6347H*
AsnC	ros constant	*VNG6432H*	*VNG6432H*
AsnC	ros constant	*VNG6212G*	*iucA*
AsnC	ros constant	*VNG6213G*	*iucB*
AsnC	ros constant	*VNG6377H*	*VNG6377H*
Trh3	high paraquat	*VNG1557G*	*cbiH*
Trh3	high paraquat	*VNG1568G*	*cbiJ*
Trh3	high paraquat	*VNG1700G*	*rps17p*
Trh3	high paraquat	*VNG1701G*	*rpl14p*
Trh3	high paraquat	*VNG1702G*	*rpl24p*
Trh3	high paraquat	*VNG1703G*	*rps4e*
Trh3	high paraquat	*VNG1705G*	*rpl5p*
Trh3	high paraquat	*VNG1706G*	*rps14p*
Trh3	high paraquat	*VNG1707G*	*rps8p*
Trh3	high paraquat	*VNG1709G*	*rpl6p*
Trh3	high paraquat	*VNG1711G*	*rpl32e*
Trh3	high paraquat	*VNG1713G*	*rpl19e*
Trh3	high paraquat	*VNG1714G*	*rpl18p*
Trh3	high paraquat	*VNG1715G*	*rps5p*
Trh3	high paraquat	*VNG1716G*	*rpl30p*

Trh3	high paraquat	*VNG1718G*	*rpl15p*
Trh3	high paraquat	*VNG1719G*	*secY*
Trh3	high paraquat	*VNG1814G*	*carB*
Trh3	high paraquat	*VNG2151G*	*etfA*
Trh3	high paraquat	*VNG0488H*	*VNG0488H*
Trh3	high paraquat	*VNG2204H*	*VNG2204H*
Trh3	low h202 constant	*VNG1557G*	*cbiH*
Trh3	low h202 constant	*VNG1568G*	*cbiJ*
Trh3	low h202 constant	*VNG1700G*	*rps17p*
Trh3	low h202 constant	*VNG1701G*	*rpl14p*
Trh3	low h202 constant	*VNG1702G*	*rpl24p*
Trh3	low h202 constant	*VNG1703G*	*rps4e*
Trh3	low h202 constant	*VNG1705G*	*rpl5p*
Trh3	low h202 constant	*VNG1706G*	*rps14p*
Trh3	low h202 constant	*VNG1707G*	*rps8p*
Trh3	low h202 constant	*VNG1709G*	*rpl6p*
Trh3	low h202 constant	*VNG1711G*	*rpl32e*
Trh3	low h202 constant	*VNG1713G*	*rpl19e*
Trh3	low h202 constant	*VNG1714G*	*rpl18p*
Trh3	low h202 constant	*VNG1715G*	*rps5p*
Trh3	low h202 constant	*VNG1716G*	*rpl30p*
Trh3	low h202 constant	*VNG1718G*	*rpl15p*
Trh3	low h202 constant	*VNG1719G*	*secY*
Trh3	low h202 constant	*VNG1814G*	*carB*
Trh3	low h202 constant	*VNG1079G*	*menB*
Trh3	low h202 constant	*VNG2204H*	*VNG2204H*
Negative Correlation			
Lrp	**condition**	**canonical_Name**	**gene_Name**
Trh4	copper	*VNG0405C*	*VNG0405C*
Trh4	copper	*VNG0421C*	*VNG0421C*
Trh4	copper	*VNG1069C*	*VNG1069C*
Trh4	copper	*VNG1297C*	*VNG1297C*
Trh4	copper	*VNG1779C*	*VNG1779C*
Trh4	copper	*VNG1845C*	*VNG1845C*
Trh4	copper	*VNG2470C*	*VNG2470C*
Trh4	copper	*VNG0166G*	*psmA2*
Trh4	copper	*VNG0174G*	*cat1*
Trh4	copper	*VNG0403G*	*proS*
Trh4	copper	*VNG0666G*	*ctaB*
Trh4	copper	*VNG0667G*	*trp4*
Trh4	copper	*VNG0872G*	*gatA*
Trh4	copper	*VNG1097G*	*cysS*

Trh4	copper	*VNG1432G*	*dhs*
Trh4	copper	*VNG1550G*	*cbiT*
Trh4	copper	*VNG1551G*	*cbiL*
Trh4	copper	*VNG1553G*	*cbiF*
Trh4	copper	*VNG1554G*	*cbiG*
Trh4	copper	*VNG1555G*	*cobH*
Trh4	copper	*VNG1557G*	*cbiH*
Trh4	copper	*VNG1816G*	*trh3*
Trh4	copper	*VNG1818G*	*idi*
Trh4	copper	*VNG2150G*	*etfB*
Trh4	copper	*VNG2151G*	*etfA*
Trh4	copper	*VNG1693G*	*rps19p*
Trh4	copper	*VNG1695G*	*rpl22p*
Trh4	copper	*VNG1697G*	*rps3p*
Trh4	copper	*VNG1698G*	*rpl29p*
Trh4	copper	*VNG1699C*	*VNG1699C*
Trh4	copper	*VNG1700G*	*rps17p*
Trh4	copper	*VNG1701G*	*rpl14p*
Trh4	copper	*VNG1702G*	*rpl24p*
Trh4	copper	*VNG1703G*	*rps4e*
Trh4	copper	*VNG1705G*	*rpl5p*
Trh4	copper	*VNG1706G*	*rps14p*
Trh4	copper	*VNG1707G*	*rps8p*
Trh4	copper	*VNG1709G*	*rpl6p*
Trh4	copper	*VNG1711G*	*rpl32e*
Trh4	copper	*VNG1713G*	*rpl19e*
Trh4	copper	*VNG1714G*	*rpl18p*
Trh4	copper	*VNG1715G*	*rps5p*
Trh4	copper	*VNG1716G*	*rpl30p*
Trh4	copper	*VNG1718G*	*rpl15p*
Trh4	copper	*VNG1719G*	*secY*
Trh4	copper	*VNG2076G*	*rpl40e*
Trh4	copper	*VNG0184H*	*VNG0184H*
Trh4	copper	*VNG0780H*	*VNG0780H*
Trh4	copper	*VNG1034H*	*VNG1034H*
Trh4	copper	*VNG1487H*	*VNG1487H*
Trh4	copper	*VNG1558H*	*VNG1558H*
Trh4	copper	*VNG1559H*	*VNG1559H*
Trh4	copper	*VNG1561C*	*VNG1561C*
Trh4	copper	*VNG1562H*	*VNG1562H*
Trh4	copper	*VNG1807H*	*VNG1807H*
Trh4	copper	*VNG0147C*	*VNG0147C*

Trh4	copper	*VNG1483C*	*VNG1483C*
Trh4	copper	*VNG0172G*	*mutS2*
Trh4	copper	*VNG0610G*	*hhoA*
Trh4	copper	*VNG0665G*	*coxB1*
Trh4	copper	*VNG0862G*	*hisF*
Trh4	copper	*VNG0873G*	*ykhA*
Trh4	copper	*VNG0920H*	*VNG0920H*
Trh4	copper	*VNG0921G*	*potA1*
Trh4	copper	*VNG1294G*	*slyD*
Trh4	copper	*VNG1815G*	*carA*
Trh4	copper	*VNG1887G*	*gpm*
Trh4	copper	*VNG1987G*	*secD*
Trh4	copper	*VNG2138G*	*atpB*
Trh4	copper	*VNG2139G*	*atpA*
Trh4	copper	*VNG2140G*	*atpF*
Trh4	copper	*VNG2141G*	*atpC*
Trh4	copper	*VNG2203G*	*prsA*
Trh4	copper	*VNG2648G*	*rps10p*
Trh4	copper	*VNG2649G*	*eef1a*
Trh4	copper	*VNG2060G*	*phnP*
Trh4	copper	*VNG2062G*	*atp*
Trh4	copper	*VNG1376H*	*VNG1376H*
Trh4	copper	*VNG0370H*	*VNG0370H*
Trh4	copper	*VNG0420H*	*VNG0420H*
Trh4	copper	*VNG1777H*	*VNG1777H*
Trh4	copper	*VNG6316G*	*arcC*
Trh4	high copper	*VNG0405C*	*VNG0405C*
Trh4	high copper	*VNG0421C*	*VNG0421C*
Trh4	high copper	*VNG1069C*	*VNG1069C*
Trh4	high copper	*VNG1297C*	*VNG1297C*
Trh4	high copper	*VNG1779C*	*VNG1779C*
Trh4	high copper	*VNG1845C*	*VNG1845C*
Trh4	high copper	*VNG2470C*	*VNG2470C*
Trh4	high copper	*VNG0166G*	*psmA2*
Trh4	high copper	*VNG0174G*	*cat1*
Trh4	high copper	*VNG0403G*	*proS*
Trh4	high copper	*VNG0666G*	*ctaB*
Trh4	high copper	*VNG0667G*	*trp4*
Trh4	high copper	*VNG0872G*	*gatA*
Trh4	high copper	*VNG1097G*	*cysS*
Trh4	high copper	*VNG1432G*	*dhs*
Trh4	high copper	*VNG1550G*	*cbiT*

Trh4	high copper	*VNG1551G*	*cbiL*
Trh4	high copper	*VNG1553G*	*cbiF*
Trh4	high copper	*VNG1554G*	*cbiG*
Trh4	high copper	*VNG1555G*	*cobH*
Trh4	high copper	*VNG1557G*	*cbiH*
Trh4	high copper	*VNG1816G*	*trh3*
Trh4	high copper	*VNG1818G*	*idi*
Trh4	high copper	*VNG1693G*	*rps19p*
Trh4	high copper	*VNG1695G*	*rpl22p*
Trh4	high copper	*VNG1697G*	*rps3p*
Trh4	high copper	*VNG1698G*	*rpl29p*
Trh4	high copper	*VNG1699C*	*VNG1699C*
Trh4	high copper	*VNG1700G*	*rps17p*
Trh4	high copper	*VNG1701G*	*rpl14p*
Trh4	high copper	*VNG1702G*	*rpl24p*
Trh4	high copper	*VNG1703G*	*rps4e*
Trh4	high copper	*VNG1705G*	*rpl5p*
Trh4	high copper	*VNG1706G*	*rps14p*
Trh4	high copper	*VNG1707G*	*rps8p*
Trh4	high copper	*VNG1709G*	*rpl6p*
Trh4	high copper	*VNG1711G*	*rpl32e*
Trh4	high copper	*VNG1713G*	*rpl19e*
Trh4	high copper	*VNG1714G*	*rpl18p*
Trh4	high copper	*VNG1715G*	*rps5p*
Trh4	high copper	*VNG1716G*	*rpl30p*
Trh4	high copper	*VNG1718G*	*rpl15p*
Trh4	high copper	*VNG1719G*	*secY*
Trh4	high copper	*VNG2076G*	*rpl40e*
Trh4	high copper	*VNG0184H*	*VNG0184H*
Trh4	high copper	*VNG0780H*	*VNG0780H*
Trh4	high copper	*VNG1034H*	*VNG1034H*
Trh4	high copper	*VNG1487H*	*VNG1487H*
Trh4	high copper	*VNG1558H*	*VNG1558H*
Trh4	high copper	*VNG1559H*	*VNG1559H*
Trh4	high copper	*VNG1561C*	*VNG1561C*
Trh4	high copper	*VNG1562H*	*VNG1562H*
Trh4	high copper	*VNG1807H*	*VNG1807H*
Trh4	high copper	*VNG0147C*	*VNG0147C*
Trh4	high copper	*VNG1483C*	*VNG1483C*
Trh4	high copper	*VNG0172G*	*mutS2*
Trh4	high copper	*VNG0610G*	*hhoA*
Trh4	high copper	*VNG0665G*	*coxB1*

Trh4	high copper	*VNG0862G*	*hisF*
Trh4	high copper	*VNG0873G*	*ykhA*
Trh4	high copper	*VNG0920H*	*VNG0920H*
Trh4	high copper	*VNG0921G*	*potA1*
Trh4	high copper	*VNG1294G*	*slyD*
Trh4	high copper	*VNG1887G*	*gpm*
Trh4	high copper	*VNG1987G*	*secD*
Trh4	high copper	*VNG2138G*	*atpB*
Trh4	high copper	*VNG2139G*	*atpA*
Trh4	high copper	*VNG2140G*	*atpF*
Trh4	high copper	*VNG2141G*	*atpC*
Trh4	high copper	*VNG2203G*	*prsA*
Trh4	high copper	*VNG2648G*	*rps10p*
Trh4	high copper	*VNG2649G*	*eef1a*
Trh4	high copper	*VNG2060G*	*phnP*
Trh4	high copper	*VNG1376H*	*VNG1376H*
Trh4	high copper	*VNG0370H*	*VNG0370H*
Trh4	high copper	*VNG0420H*	*VNG0420H*
Trh4	high copper	*VNG1777H*	*VNG1777H*
Trh4	high copper	*VNG6316G*	*Arc*

Appendix T. List of genes whose expression correlated with the Lrp, and were also dysregulated in Lrp knockout strains

Positive Correlation			
Lrp	**condition**	**canonical_Name**	**gene_Name**
AsnC	high paraquat constant	*VNG0374G*	*nusG*
AsnC	high paraquat constant	*VNG0399H*	*VNG0399H*
AsnC	high paraquat constant	*VNG0435H*	*VNG0435H*
AsnC	high paraquat constant	*VNG0559G*	*apt*
AsnC	high paraquat constant	*VNG0660H*	*VNG0660H*
AsnC	high paraquat constant	*VNG0681G*	*hbd1*
AsnC	high paraquat constant	*VNG0767H*	*VNG0767H*
AsnC	high paraquat constant	*VNG0782H*	*VNG0782H*
AsnC	high paraquat constant	*VNG0860G*	*rpoL*
AsnC	high paraquat constant	*VNG0863H*	*VNG0863H*
AsnC	high paraquat constant	*VNG0891G*	*yjlD*
AsnC	high paraquat constant	*VNG0893G*	*udp2*
AsnC	high paraquat constant	*VNG0896G*	*cda*
AsnC	high paraquat constant	*VNG0897G*	*rbsC1*
AsnC	high paraquat constant	*VNG0901G*	*rbsA*
AsnC	high paraquat constant	*VNG0905G*	*pmu2*
AsnC	high paraquat constant	*VNG0921G*	*potA1*
AsnC	high paraquat constant	*VNG0982C*	*VNG0982C*
AsnC	high paraquat constant	*VNG0983C*	*VNG0983C*
AsnC	high paraquat constant	*VNG0987H*	*VNG0987H*
AsnC	high paraquat constant	*VNG1112H*	*VNG1112H*
AsnC	high paraquat constant	*VNG1224G*	*orc8*
AsnC	high paraquat constant	*VNG1578H*	*VNG1578H*
AsnC	high paraquat constant	*VNG1879G*	*thb*
AsnC	high paraquat constant	*VNG2045G*	*gcp*
AsnC	high paraquat constant	*VNG2067H*	*VNG2067H*
AsnC	high paraquat constant	*VNG2106G*	*sdh*
AsnC	high paraquat constant	*VNG2222G*	*pheA*
AsnC	high paraquat constant	*VNG2276G*	*pmm*
AsnC	high paraquat constant	*VNG2299H*	*VNG2299H*
AsnC	high paraquat constant	*VNG2341H*	*VNG2341H*
AsnC	high paraquat constant	*VNG2451H*	*VNG2451H*
AsnC	high paraquat constant	*VNG2646C*	*VNG2646C*
AsnC	high paraquat constant	*VNG5019G*	*gvpM1*
AsnC	high paraquat constant	*VNG5020G*	*gvpL1*
AsnC	high paraquat constant	*VNG5022G*	*gvpJ1*
AsnC	high paraquat constant	*VNG5025G*	*gvpH1*

AsnC	high paraquat constant	*VNG5027G*	*gvpF1*
AsnC	high paraquat constant	*VNG5137H*	*VNG5137H*
AsnC	high paraquat constant	*VNG5173H*	*VNG5173H*
AsnC	high paraquat constant	*VNG5183G*	*arsC*
AsnC	high paraquat constant	*VNG6135C*	*VNG6135C*
AsnC	high paraquat constant	*VNG6181H*	*VNG6181H*
AsnC	high paraquat constant	*VNG6182H*	*VNG6182H*
AsnC	high paraquat constant	*VNG6194H*	*VNG6194H*
AsnC	high paraquat constant	*VNG6205C*	*VNG6205C*
AsnC	high paraquat constant	*VNG6256G*	*lipB*
AsnC	high paraquat constant	*VNG6299G*	*hypE*
AsnC	high paraquat constant	*VNG6308G*	*gltP*
AsnC	high paraquat constant	*VNG6311G*	*pyrI*
AsnC	high paraquat constant	*VNG6332H*	*VNG6332H*
AsnC	high paraquat constant	*VNG6347H*	*VNG6347H*
AsnC	high paraquat constant	*VNG6379C*	*VNG6379C*
AsnC	high paraquat	*VNG0053H*	*VNG0053H*
AsnC	high paraquat	*VNG0374G*	*nusG*
AsnC	high paraquat	*VNG0399H*	*VNG0399H*
AsnC	high paraquat	*VNG0435H*	*VNG0435H*
AsnC	high paraquat	*VNG0438G*	*ferA3*
AsnC	high paraquat	*VNG0559G*	*apt*
AsnC	high paraquat	*VNG0660H*	*VNG0660H*
AsnC	high paraquat	*VNG0681G*	*hbd1*
AsnC	high paraquat	*VNG0684G*	*fbp*
AsnC	high paraquat	*VNG0741H*	*VNG0741H*
AsnC	high paraquat	*VNG0767H*	*VNG0767H*
AsnC	high paraquat	*VNG0782H*	*VNG0782H*
AsnC	high paraquat	*VNG0821C*	*VNG0821C*
AsnC	high paraquat	*VNG0860G*	*rpoL*
AsnC	high paraquat	*VNG0863H*	*VNG0863H*
AsnC	high paraquat	*VNG0891G*	*yjlD*
AsnC	high paraquat	*VNG0893G*	*udp2*
AsnC	high paraquat	*VNG0896G*	*cda*
AsnC	high paraquat	*VNG0897G*	*rbsC1*
AsnC	high paraquat	*VNG0898G*	*rbsC2*
AsnC	high paraquat	*VNG0901G*	*rbsA*
AsnC	high paraquat	*VNG0905G*	*pmu2*
AsnC	high paraquat	*VNG0921G*	*potA1*
AsnC	high paraquat	*VNG0966G*	*cheR*
AsnC	high paraquat	*VNG0983C*	*VNG0983C*
AsnC	high paraquat	*VNG0987H*	*VNG0987H*

AsnC	high paraquat	*VNG1112H*	*VNG1112H*
AsnC	high paraquat	*VNG1224G*	*orc8*
AsnC	high paraquat	*VNG1578H*	*VNG1578H*
AsnC	high paraquat	*VNG1617H*	*VNG1617H*
AsnC	high paraquat	*VNG1879G*	*thb*
AsnC	high paraquat	*VNG2032G*	*fad1*
AsnC	high paraquat	*VNG2045G*	*gcp*
AsnC	high paraquat	*VNG2067H*	*VNG2067H*
AsnC	high paraquat	*VNG2106G*	*sdh*
AsnC	high paraquat	*VNG2222G*	*pheA*
AsnC	high paraquat	*VNG2276G*	*pmm*
AsnC	high paraquat	*VNG2299H*	*VNG2299H*
AsnC	high paraquat	*VNG2341H*	*VNG2341H*
AsnC	high paraquat	*VNG2451H*	*VNG2451H*
AsnC	high paraquat	*VNG2646C*	*VNG2646C*
AsnC	high paraquat	*VNG5019G*	*gvpM1*
AsnC	high paraquat	*VNG5020G*	*gvpL1*
AsnC	high paraquat	*VNG5022G*	*gvpJ1*
AsnC	high paraquat	*VNG5025G*	*gvpH1*
AsnC	high paraquat	*VNG5027G*	*gvpF1*
AsnC	high paraquat	*VNG5034G*	*gvpO1*
AsnC	high paraquat	*VNG5038H*	*VNG5038H*
AsnC	high paraquat	*VNG5081H*	*VNG5081H*
AsnC	high paraquat	*VNG5137H*	*VNG5137H*
AsnC	high paraquat	*VNG5173H*	*VNG5173H*
AsnC	high paraquat	*VNG5183G*	*arsC*
AsnC	high paraquat	*VNG6135C*	*VNG6135C*
AsnC	high paraquat	*VNG6171H*	*VNG6171H*
AsnC	high paraquat	*VNG6175G*	*trkA2*
AsnC	high paraquat	*VNG6181H*	*VNG6181H*
AsnC	high paraquat	*VNG6182H*	*VNG6182H*
AsnC	high paraquat	*VNG6194H*	*VNG6194H*
AsnC	high paraquat	*VNG6205C*	*VNG6205C*
AsnC	high paraquat	*VNG6210G*	*gabT*
AsnC	high paraquat	*VNG6211G*	*bdb*
AsnC	high paraquat	*VNG6212G*	*iucA*
AsnC	high paraquat	*VNG6214G*	*hxyA*
AsnC	high paraquat	*VNG6250G*	*phoT3*
AsnC	high paraquat	*VNG6299G*	*hypE*
AsnC	high paraquat	*VNG6308G*	*gltP*
AsnC	high paraquat	*VNG6311G*	*pyrI*
AsnC	high paraquat	*VNG6329H*	*VNG6329H*

AsnC	high paraquat	*VNG6332H*	*VNG6332H*
AsnC	high paraquat	*VNG6335H*	*VNG6335H*
AsnC	high paraquat	*VNG6347H*	*VNG6347H*
AsnC	low h202 constant	*VNG0053H*	*VNG0053H*
AsnC	low h202 constant	*VNG0374G*	*nusG*
AsnC	low h202 constant	*VNG0438G*	*ferA3*
AsnC	low h202 constant	*VNG0709C*	*VNG0709C*
AsnC	low h202 constant	*VNG0741H*	*VNG0741H*
AsnC	low h202 constant	*VNG0793G*	*htr6*
AsnC	low h202 constant	*VNG0821C*	*VNG0821C*
AsnC	low h202 constant	*VNG0834C*	*VNG0834C*
AsnC	low h202 constant	*VNG0847H*	*VNG0847H*
AsnC	low h202 constant	*VNG0863H*	*VNG0863H*
AsnC	low h202 constant	*VNG0891G*	*yjlD*
AsnC	low h202 constant	*VNG0893G*	*udp2*
AsnC	low h202 constant	*VNG0896G*	*cda*
AsnC	low h202 constant	*VNG0897G*	*rbsC1*
AsnC	low h202 constant	*VNG0898G*	*rbsC2*
AsnC	low h202 constant	*VNG0901G*	*rbsA*
AsnC	low h202 constant	*VNG0905G*	*pmu2*
AsnC	low h202 constant	*VNG0921G*	*potA1*
AsnC	low h202 constant	*VNG0941C*	*VNG0941C*
AsnC	low h202 constant	*VNG0969H*	*VNG0969H*
AsnC	low h202 constant	*VNG0982C*	*VNG0982C*
AsnC	low h202 constant	*VNG0987H*	*VNG0987H*
AsnC	low h202 constant	*VNG0989C*	*VNG0989C*
AsnC	low h202 constant	*VNG1036H*	*VNG1036H*
AsnC	low h202 constant	*VNG1112H*	*VNG1112H*
AsnC	low h202 constant	*VNG1426H*	*VNG1426H*
AsnC	low h202 constant	*VNG1578H*	*VNG1578H*
AsnC	low h202 constant	*VNG1617H*	*VNG1617H*
AsnC	low h202 constant	*VNG1654G*	*cdc48e*
AsnC	low h202 constant	*VNG1879G*	*thb*
AsnC	low h202 constant	*VNG2032G*	*fad1*
AsnC	low h202 constant	*VNG2045G*	*gcp*
AsnC	low h202 constant	*VNG2067H*	*VNG2067H*
AsnC	low h202 constant	*VNG2222G*	*pheA*
AsnC	low h202 constant	*VNG2244H*	*VNG2244H*
AsnC	low h202 constant	*VNG2276G*	*pmm*
AsnC	low h202 constant	*VNG2299H*	*VNG2299H*
AsnC	low h202 constant	*VNG2399H*	*VNG2399H*
AsnC	low h202 constant	*VNG2451H*	*VNG2451H*

AsnC	low h202 constant	*VNG2452C*	*VNG2452C*
AsnC	low h202 constant	*VNG2563H*	*VNG2563H*
AsnC	low h202 constant	*VNG5019G*	*gvpM1*
AsnC	low h202 constant	*VNG5020G*	*gvpL1*
AsnC	low h202 constant	*VNG5022G*	*gvpJ1*
AsnC	low h202 constant	*VNG5025G*	*gvpH1*
AsnC	low h202 constant	*VNG5027G*	*gvpF1*
AsnC	low h202 constant	*VNG5034G*	*gvpO1*
AsnC	low h202 constant	*VNG5081H*	*VNG5081H*
AsnC	low h202 constant	*VNG5173H*	*VNG5173H*
AsnC	low h202 constant	*VNG6171H*	*VNG6171H*
AsnC	low h202 constant	*VNG6175G*	*trkA2*
AsnC	low h202 constant	*VNG6179G*	*cat3*
AsnC	low h202 constant	*VNG6205C*	*VNG6205C*
AsnC	low h202 constant	*VNG6210G*	*gabT*
AsnC	low h202 constant	*VNG6211G*	*bdb*
AsnC	low h202 constant	*VNG6212G*	*iucA*
AsnC	low h202 constant	*VNG6214G*	*hxyA*
AsnC	low h202 constant	*VNG6216G*	*iucC*
AsnC	low h202 constant	*VNG6250G*	*phoT3*
AsnC	low h202 constant	*VNG6270G*	*gldA*
AsnC	low h202 constant	*VNG6275H*	*VNG6275H*
AsnC	low h202 constant	*VNG6287H*	*VNG6287H*
AsnC	low h202 constant	*VNG6299G*	*hypE*
AsnC	low h202 constant	*VNG6308G*	*gltP*
AsnC	low h202 constant	*VNG6311G*	*pyrI*
AsnC	low h202 constant	*VNG6326G*	*trp6*
AsnC	low h202 constant	*VNG6329H*	*VNG6329H*
AsnC	low h202 constant	*VNG6334H*	*VNG6334H*
AsnC	low h202 constant	*VNG6335H*	*VNG6335H*
AsnC	low h202 constant	*VNG6348H*	*VNG6348H*
AsnC	low h202 constant	*VNG6351G*	*tfbC*
AsnC	low h202 constant	*VNG6363G*	*orc4*
AsnC	low h202 constant	*VNG6372H*	*VNG6372H*
AsnC	low h202 constant	*VNG6375H*	*VNG6375H*
AsnC	low h202 constant	*VNG6379C*	*VNG6379C*
AsnC	low h202 constant	*VNG6381H*	*VNG6381H*
AsnC	low h202 constant	*VNG6384H*	*VNG6384H*
AsnC	ros constant	*VNG0053H*	*VNG0053H*
AsnC	ros constant	*VNG0374G*	*nusG*
AsnC	ros constant	*VNG0399H*	*VNG0399H*
AsnC	ros constant	*VNG0435H*	*VNG0435H*

AsnC	ros constant	*VNG0438G*	*ferA3*
AsnC	ros constant	*VNG0559G*	*apt*
AsnC	ros constant	*VNG0587H*	*VNG0587H*
AsnC	ros constant	*VNG0681G*	*hbd1*
AsnC	ros constant	*VNG0741H*	*VNG0741H*
AsnC	ros constant	*VNG0782H*	*VNG0782H*
AsnC	ros constant	*VNG0821C*	*VNG0821C*
AsnC	ros constant	*VNG0834C*	*VNG0834C*
AsnC	ros constant	*VNG0860G*	*rpoL*
AsnC	ros constant	*VNG0863H*	*VNG0863H*
AsnC	ros constant	*VNG0891G*	*yjlD*
AsnC	ros constant	*VNG0893G*	*udp2*
AsnC	ros constant	*VNG0896G*	*cda*
AsnC	ros constant	*VNG0897G*	*rbsC1*
AsnC	ros constant	*VNG0898G*	*rbsC2*
AsnC	ros constant	*VNG0901G*	*rbsA*
AsnC	ros constant	*VNG0905G*	*pmu2*
AsnC	ros constant	*VNG0921G*	*potA1*
AsnC	ros constant	*VNG0982C*	*VNG0982C*
AsnC	ros constant	*VNG0983C*	*VNG0983C*
AsnC	ros constant	*VNG0987H*	*VNG0987H*
AsnC	ros constant	*VNG0989C*	*VNG0989C*
AsnC	ros constant	*VNG1112H*	*VNG1112H*
AsnC	ros constant	*VNG1224G*	*orc8*
AsnC	ros constant	*VNG1426H*	*VNG1426H*
AsnC	ros constant	*VNG1578H*	*VNG1578H*
AsnC	ros constant	*VNG1617H*	*VNG1617H*
AsnC	ros constant	*VNG1654G*	*cdc48e*
AsnC	ros constant	*VNG1879G*	*thb*
AsnC	ros constant	*VNG2045G*	*gcp*
AsnC	ros constant	*VNG2067H*	*VNG2067H*
AsnC	ros constant	*VNG2222G*	*pheA*
AsnC	ros constant	*VNG2244H*	*VNG2244H*
AsnC	ros constant	*VNG2276G*	*pmm*
AsnC	ros constant	*VNG2299H*	*VNG2299H*
AsnC	ros constant	*VNG2341H*	*VNG2341H*
AsnC	ros constant	*VNG2399H*	*VNG2399H*
AsnC	ros constant	*VNG2451H*	*VNG2451H*
AsnC	ros constant	*VNG2563H*	*VNG2563H*
AsnC	ros constant	*VNG5019G*	*gvpM1*
AsnC	ros constant	*VNG5020G*	*gvpL1*
AsnC	ros constant	*VNG5022G*	*gvpJ1*

AsnC	ros constant	*VNG5025G*	*gvpH1*
AsnC	ros constant	*VNG5027G*	*gvpF1*
AsnC	ros constant	*VNG5081H*	*VNG5081H*
AsnC	ros constant	*VNG5137H*	*VNG5137H*
AsnC	ros constant	*VNG5173H*	*VNG5173H*
AsnC	ros constant	*VNG5183G*	*arsC*
AsnC	ros constant	*VNG6135C*	*VNG6135C*
AsnC	ros constant	*VNG6171H*	*VNG6171H*
AsnC	ros constant	*VNG6181H*	*VNG6181H*
AsnC	ros constant	*VNG6194H*	*VNG6194H*
AsnC	ros constant	*VNG6205C*	*VNG6205C*
AsnC	ros constant	*VNG6210G*	*gabT*
AsnC	ros constant	*VNG6211G*	*bdb*
AsnC	ros constant	*VNG6212G*	*iucA*
AsnC	ros constant	*VNG6287H*	*VNG6287H*
AsnC	ros constant	*VNG6299G*	*hypE*
AsnC	ros constant	*VNG6308G*	*gltP*
AsnC	ros constant	*VNG6311G*	*pyrI*
AsnC	ros constant	*VNG6332H*	*VNG6332H*
AsnC	ros constant	*VNG6335H*	*VNG6335H*
AsnC	ros constant	*VNG6347H*	*VNG6347H*
AsnC	ros constant	*VNG6379C*	*VNG6379C*
AsnC	ros constant	*VNG6384H*	*VNG6384H*
Trh3	high paraquat	*VNG0373H*	*VNG0373H*
Trh3	high paraquat	*VNG0403G*	*proS*
Trh3	high paraquat	*VNG0439C*	*VNG0439C*
Trh3	high paraquat	*VNG0453G*	*pstA2*
Trh3	high paraquat	*VNG0536G*	*sirR*
Trh3	high paraquat	*VNG0617H*	*VNG0617H*
Trh3	high paraquat	*VNG0683C*	*VNG0683C*
Trh3	high paraquat	*VNG0686C*	*VNG0686C*
Trh3	high paraquat	*VNG0762H*	*VNG0762H*
Trh3	high paraquat	*VNG0767H*	*VNG0767H*
Trh3	high paraquat	*VNG0860G*	*rpoL*
Trh3	high paraquat	*VNG0867G*	*asnA*
Trh3	high paraquat	*VNG0879C*	*VNG0879C*
Trh3	high paraquat	*VNG0898G*	*rbsC2*
Trh3	high paraquat	*VNG0901G*	*rbsA*
Trh3	high paraquat	*VNG0905G*	*pmu2*
Trh3	high paraquat	*VNG0921G*	*potA1*
Trh3	high paraquat	*VNG0923G*	*sfuB*
Trh3	high paraquat	*VNG0983C*	*VNG0983C*

Trh3	high paraquat	*VNG1574G*	*cobI*
Trh3	high paraquat	*VNG1626C*	*VNG1626C*
Trh3	high paraquat	*VNG1814G*	*carB*
Trh3	high paraquat	*VNG1818G*	*idi*
Trh3	high paraquat	*VNG1875G*	*mvaA*
Trh3	high paraquat	*VNG2059H*	*VNG2059H*
Trh3	high paraquat	*VNG2076G*	*rpl40e*
Trh3	high paraquat	*VNG2299H*	*VNG2299H*
Trh3	high paraquat	*VNG2451H*	*VNG2451H*
Trh3	high paraquat	*VNG2599H*	*VNG2599H*
Trh3	high paraquat	*VNG2622H*	*VNG2622H*
Trh3	high paraquat	*VNG5011H*	*VNG5011H*
Trh3	high paraquat	*VNG5012H*	*VNG5012H*
Trh3	high paraquat	*VNG5019G*	*gvpM1*
Trh3	high paraquat	*VNG5020G*	*gvpL1*
Trh3	high paraquat	*VNG5022G*	*gvpJ1*
Trh3	high paraquat	*VNG5025G*	*gvpH1*
Trh3	high paraquat	*VNG5027G*	*gvpF1*
Trh3	high paraquat	*VNG5038H*	*VNG5038H*
Trh3	high paraquat	*VNG5088H*	*VNG5088H*
Trh3	high paraquat	*VNG5139C*	*VNG5139C*
Trh3	high paraquat	*VNG5148H*	*VNG5148H*
Trh3	high paraquat	*VNG5169H*	*VNG5169H*
Trh3	high paraquat	*VNG5173H*	*VNG5173H*
Trh3	high paraquat	*VNG6133H*	*VNG6133H*
Trh3	high paraquat	*VNG6159H*	*VNG6159H*
Trh3	high paraquat	*VNG6181H*	*VNG6181H*
Trh3	high paraquat	*VNG6210G*	*gabT*
Trh3	high paraquat	*VNG6212G*	*iucA*
Trh3	high paraquat	*VNG6299G*	*hypE*
Trh3	high paraquat	*VNG6335H*	*VNG6335H*
Trh3	high paraquat	*VNG6337G*	*sojE*
Trh3	high paraquat	*VNG6365H*	*VNG6365H*
Trh3	low h202 constant	*VNG0403G*	*proS*
Trh3	low h202 constant	*VNG0563G*	*ndhG2*
Trh3	low h202 constant	*VNG0565C*	*VNG0565C*
Trh3	low h202 constant	*VNG0578H*	*VNG0578H*
Trh3	low h202 constant	*VNG0617H*	*VNG0617H*
Trh3	low h202 constant	*VNG0633G*	*purE*
Trh3	low h202 constant	*VNG0641C*	*VNG0641C*
Trh3	low h202 constant	*VNG0703H*	*VNG0703H*
Trh3	low h202 constant	*VNG0741H*	*VNG0741H*

Trh3	low h202 constant	*VNG0879C*	*VNG0879C*
Trh3	low h202 constant	*VNG0891G*	*yjlD*
Trh3	low h202 constant	*VNG0898G*	*rbsC2*
Trh3	low h202 constant	*VNG0901G*	*rbsA*
Trh3	low h202 constant	*VNG0905G*	*pmu2*
Trh3	low h202 constant	*VNG0941C*	*VNG0941C*
Trh3	low h202 constant	*VNG1268H*	*VNG1268H*
Trh3	low h202 constant	*VNG1574G*	*cobI*
Trh3	low h202 constant	*VNG1626C*	*VNG1626C*
Trh3	low h202 constant	*VNG1632G*	*cbiQ*
Trh3	low h202 constant	*VNG1814G*	*carB*
Trh3	low h202 constant	*VNG1818G*	*idi*
Trh3	low h202 constant	*VNG1875G*	*mvaA*
Trh3	low h202 constant	*VNG2076G*	*rpl40e*
Trh3	low h202 constant	*VNG2094G*	*trh4*
Trh3	low h202 constant	*VNG2299H*	*VNG2299H*
Trh3	low h202 constant	*VNG2370C*	*VNG2370C*
Trh3	low h202 constant	*VNG2599H*	*VNG2599H*
Trh3	low h202 constant	*VNG2622H*	*VNG2622H*
Trh3	low h202 constant	*VNG5012H*	*VNG5012H*
Trh3	low h202 constant	*VNG5019G*	*gvpM1*
Trh3	low h202 constant	*VNG5020G*	*gvpL1*
Trh3	low h202 constant	*VNG5022G*	*gvpJ1*
Trh3	low h202 constant	*VNG5025G*	*gvpH1*
Trh3	low h202 constant	*VNG5027G*	*gvpF1*
Trh3	low h202 constant	*VNG5088H*	*VNG5088H*
Trh3	low h202 constant	*VNG5139C*	*VNG5139C*
Trh3	low h202 constant	*VNG5169H*	*VNG5169H*
Trh3	low h202 constant	*VNG5173H*	*VNG5173H*
Trh3	low h202 constant	*VNG6159H*	*VNG6159H*
Trh3	low h202 constant	*VNG6177G*	*kdpB*
Trh3	low h202 constant	*VNG6210G*	*gabT*
Trh3	low h202 constant	*VNG6212G*	*iucA*
Trh3	low h202 constant	*VNG6216G*	*iucC*
Trh3	low h202 constant	*VNG6270G*	*gldA*
Trh3	low h202 constant	*VNG6299G*	*hypE*
Trh3	low h202 constant	*VNG6335H*	*VNG6335H*
Trh3	low h202 constant	*VNG6365H*	*VNG6365H*
Trh3	low h202 constant	*VNG6379C*	*VNG6379C*
Negative Correlation			
Lrp	**condition**	**canonical_Name**	**gene_Name**
Trh4	copper	*VNG0376G*	*ftsZ1*

Trh4	copper	*VNG0420H*	*VNG0420H*
Trh4	copper	*VNG0424C*	*VNG0424C*
Trh4	copper	*VNG0438G*	*ferA3*
Trh4	copper	*VNG0473G*	*porB*
Trh4	copper	*VNG0630G*	*ribE*
Trh4	copper	*VNG0660H*	*VNG0660H*
Trh4	copper	*VNG0702H*	*VNG0702H*
Trh4	copper	*VNG0738H*	*VNG0738H*
Trh4	copper	*VNG0777G*	*taqD*
Trh4	copper	*VNG0879C*	*VNG0879C*
Trh4	copper	*VNG0905G*	*pmu2*
Trh4	copper	*VNG0914H*	*VNG0914H*
Trh4	copper	*VNG0920H*	*VNG0920H*
Trh4	copper	*VNG0943C*	*VNG0943C*
Trh4	copper	*VNG0983C*	*VNG0983C*
Trh4	copper	*VNG1438H*	*VNG1438H*
Trh4	copper	*VNG1861C*	*VNG1861C*
Trh4	copper	*VNG6181H*	*VNG6181H*
Trh4	copper	*VNG6420H*	*VNG6420H*
Trh4	high copper	*VNG0376G*	*ftsZ1*
Trh4	high copper	*VNG0420H*	*VNG0420H*
Trh4	high copper	*VNG0424C*	*VNG0424C*
Trh4	high copper	*VNG0436G*	*nhaC1*
Trh4	high copper	*VNG0473G*	*porB*
Trh4	high copper	*VNG0630G*	*ribE*
Trh4	high copper	*VNG0660H*	*VNG0660H*
Trh4	high copper	*VNG0702H*	*VNG0702H*
Trh4	high copper	*VNG0777G*	*taqD*
Trh4	high copper	*VNG0905G*	*pmu2*
Trh4	high copper	*VNG0914H*	*VNG0914H*
Trh4	high copper	*VNG0920H*	*VNG0920H*
Trh4	high copper	*VNG0943C*	*VNG0943C*
Trh4	high copper	*VNG0983C*	*VNG0983C*
Trh4	high copper	*VNG1438H*	*VNG1438H*
Trh4	high copper	*VNG1861C*	*VNG1861C*
Trh4	high copper	*VNG5012H*	*VNG5012H*
Trh4	high copper	*VNG6181H*	*VNG6181H*
Trh4	high copper	*VNG6182H*	*VNG6182H*
Trh4	high copper	*VNG6420H*	*VNG6420H*

Appendix U. List of Lrp binding targets whose expression correlated with the Lrp and were dyregulated upon the deletion of Lrp

Positive Correlation			
Lrp	**condition**	**canonical_Name**	**gene_Name**
AsnC	high paraquat constant	*VNG0983C*	*VNG0983C*
AsnC	high paraquat constant	*VNG0921G*	*potA1*
AsnC	high paraquat constant	*VNG5022G*	*gvpJ1*
AsnC	high paraquat constant	*VNG6347H*	*VNG6347H*
AsnC	high paraquat	*VNG0983C*	*VNG0983C*
AsnC	high paraquat	*VNG0921G*	*potA1*
AsnC	high paraquat	*VNG0966G*	*cheR*
AsnC	high paraquat	*VNG5022G*	*gvpJ1*
AsnC	high paraquat	*VNG6347H*	*VNG6347H*
AsnC	high paraquat	*VNG6212G*	*iucA*
AsnC	high paraquat	*VNG6214G*	*hxyA*
AsnC	low h202 constant	*VNG0921G*	*potA1*
AsnC	low h202 constant	*VNG5022G*	*gvpJ1*
AsnC	low h202 constant	*VNG6334H*	*VNG6334H*
AsnC	low h202 constant	*VNG6212G*	*iucA*
AsnC	low h202 constant	*VNG6214G*	*hxyA*
AsnC	low h202 constant	*VNG6216G*	*iucC*
AsnC	ros constant	*VNG0983C*	*VNG0983C*
AsnC	ros constant	*VNG0921G*	*potA1*
AsnC	ros constant	*VNG5022G*	*gvpJ1*
AsnC	ros constant	*VNG6347H*	*VNG6347H*
AsnC	ros constant	*VNG6212G*	*iucA*
Trh3	high paraquat	*VNG1814G*	*carB*
Trh3	low h202 constant	*VNG1814G*	*carB*
Negative Correlation			
Lrp	**condition**	**canonical_Name**	**gene_Name**
Trh4	copper	*VNG0920H*	*VNG0920H*
Trh4	copper	*VNG0420H*	*VNG0420H*
Trh4	high copper	*VNG0920H*	*VNG0920H*
Trh4	high copper	*VNG0420H*	*VNG0420H*

Appendix V. Condition sets tested for each Lrp

AsnC	VNG1179C	VNG1237C	Trh2
circadian	circadian	circadian	circadian
cobalt	cobalt	cobalt	cobalt
copper	copper	copper	copper
dark	dark	dark	dark
early-exponential phase	early-exponential phase	early-exponential phase	early-exponential phase
edta	edta	edta	edta
ems	ems	ems	ems
expects dark	expects dark	expects dark	expects dark
expects high light	expects high light	expects high light	expects high light
expects low light	expects low light	expects low light	expects low light
exponential phase	exponential phase	exponential phase	exponential phase
gamma	gamma	gamma	gamma
glucose perturbation	glucose perturbation	h202 recovery	glucose perturbation
h202 recovery	h202 recovery	h202	h202 recovery
h202	h202	high copper	h202
high atp level	high copper	high h202 recovery	high copper
high copper	high h202 recovery	high iron	high h202 recovery
high h202 recovery	high iron	high light	high iron
high iron	high light	high oxygen	high light
high light	high oxygen	high oxygen shift	high oxygen
high oxygen	high oxygen shift	high paraquat constant	high oxygen shift
high oxygen shift	high paraquat constant	high paraquat recovery	high paraquat constant
high paraquat constant	high paraquat recovery	high paraquat	high paraquat recovery
high paraquat recovery	high paraquat	high temperature	high paraquat
high paraquat	high temperature	iron	high temperature
high temperature	high zinc	irradiation	high2low
high zinc	iron	low atp level	iron
high2low	irradiation	low h202 constant	irradiation
iron	low atp level	low h202 recovery	low atp level
irradiation	low copper	low h202	low h202 constant
lag phase	low h202 constant	low iron	low h202 recovery
low atp level	low h202 recovery	low light	low h202
low h202 constant	low h202	low oxygen	low iron
low h202 recovery	low iron	low oxygen shift	low light
low h202	low light	low salt	low oxygen
low iron	low oxygen	low temperature	low oxygen shift
low light	low oxygen shift	low zinc	low salt
low oxygen	low paraquat constant	low2high	low temperature
low oxygen shift	low salt	manganese	low zinc

low paraquat constant	low temperature	medium atp level	low2high
low salt	low zinc	medium copper	manganese
low temperature	low2high	medium zinc	medium atp level
low zinc	manganese	medium-high oxygen	medium copper
low2high	medium atp level	medium-low oxygen	medium zinc
manganese	medium copper	metal chelation	medium-high oxygen
medium atp level	medium zinc	mid-exponential phase	medium-low oxygen
medium copper	medium-high oxygen	nickel	metal chelation
medium zinc	medium-low oxygen	oxygen shift	mid-exponential phase
medium-high oxygen	metal chelation	paraquat constant	oxygen shift
medium-low oxygen	mid-exponential phase	paraquat	paraquat constant
metal chelation	nickel	ros constant	paraquat
mid-exponential phase	oxygen shift	ros recovery	ros constant
nickel	paraquat constant	ros	ros recovery
oxygen shift	paraquat	saturation phase	ros
paraquat constant	ros constant	uv	saturation phase
paraquat	ros recovery	zinc	zinc
ros constant	ros		
ros recovery	saturation phase		
ros	uv		
saturation phase	zinc		
zinc			
Trh3	**Trh4**	**Trh6**	**Trh7**
circadian	circadian	circadian	circadian
cobalt	cobalt	cobalt	copper
copper	copper	copper	dark
dark	dark	dark	early-exponential phase
early-exponential phase	early-exponential phase	early-exponential phase	edta
edta	edta	edta	ems
ems	ems	ems	expects dark
expects dark	expects dark	expects dark	expects high light
expects high light	expects high light	expects high light	expects low light
expects low light	expects low light	expects low light	exponential phase
exponential phase	exponential phase	exponential phase	gamma
gamma	gamma	gamma	glucose perturbation
glucose perturbation	glucose perturbation	glucose perturbation	h202 recovery
h202 recovery	h202 recovery	h202 recovery	h202
h202	h202	h202	high copper
high atp level	high copper	high atp level	high h202 recovery
high copper	high h202 recovery	high copper	high iron
high h202 recovery	high iron	high h202 recovery	high light
high iron	high light	high iron	high oxygen

high light	high oxygen	high light	high oxygen shift
high oxygen	high paraquat constant	high oxygen	high paraquat constant
high oxygen shift	high paraquat recovery	high oxygen shift	high paraquat recovery
high paraquat constant	high paraquat	high paraquat constant	high paraquat
high paraquat recovery	high temperature	high paraquat recovery	high temperature
high paraquat	iron	high paraquat	high zinc
high temperature	irradiation	high temperature	iron
iron	low copper	high zinc	irradiation
irradiation	low h202 constant	iron	lag phase
low atp level	low h202 recovery	irradiation	low atp level
low h202 constant	low h202	low atp level	low h202 constant
low h202 recovery	low iron	low copper	low h202 recovery
low h202	low light	low h202 constant	low h202
low iron	low oxygen	low h202 recovery	low iron
low light	low oxygen shift	low h202	low light
low oxygen	low paraquat constant	low iron	low oxygen
low paraquat constant	low salt	low light	low oxygen shift
low salt	low temperature	low oxygen	low paraquat constant
low temperature	low2high	low oxygen shift	low salt
low zinc	manganese	low paraquat constant	low temperature
low2high	medium zinc	low salt	low zinc
manganese	medium-high oxygen	low temperature	low2high
medium zinc	medium-low oxygen	low zinc	medium copper
medium-high oxygen	metal chelation	low2high	medium zinc
medium-low oxygen	mid-exponential phase	manganese	medium-high oxygen
metal chelation	oxygen shift	medium atp level	medium-low oxygen
mid-exponential phase	paraquat constant	medium copper	metal chelation
nickel	paraquat	medium zinc	mid-exponential phase
oxygen shift	ros constant	medium-high oxygen	nickel
paraquat constant	ros recovery	medium-low oxygen	oxygen shift
paraquat	ros	metal chelation	paraquat constant
ros constant	saturation phase	mid-exponential phase	paraquat
ros recovery	uv	nickel	ros constant
ros	zinc	oxygen shift	ros recovery
saturation phase		paraquat constant	ros
zinc		paraquat	saturation phase
		ros constant	uv
		ros recovery	zinc
		ros	
		saturation phase	
		uv	
		zinc	

Appendix W. List of sequences for phylogenetic analysis

RefSeq accesion	organism	RefSeq accesion	organism
NP_280631.1	Halobacterium sp. NRC-1	YP_004763044.1	Thermococcus sp. 4557
NP_280074.1	Halobacterium sp. NRC-1	YP_004762655.1	Thermococcus sp. 4557
NP_615877.1	Methanosarcina acetivorans C2A	YP_004762508.1	Thermococcus sp. 4557
YP_659303.1	Haloquadratum walsbyi DSM 16790	YP_004762137.1	Thermococcus sp. 4557
YP_659040.1	Haloquadratum walsbyi DSM 16790	YP_004762085.1	Thermococcus sp. 4557
YP_658761.1	Haloquadratum walsbyi DSM 16790	YP_004624591.1	Pyrococcus yayanosii CH1
YP_658336.1	Haloquadratum walsbyi DSM 16790	YP_004624449.1	Pyrococcus yayanosii CH1
YP_656903.1	Haloquadratum walsbyi DSM 16790	YP_004624435.1	Pyrococcus yayanosii CH1
YP_001689882.1	Halobacterium salinarum R1	YP_004624271.1	Pyrococcus yayanosii CH1
YP_004891789.1	Thermoproteus tenax Kra 1	YP_004623895.1	Pyrococcus yayanosii CH1
YP_135900.1	Haloarcula marismortui ATCC 43049	YP_004623870.1	Pyrococcus yayanosii CH1
YP_004796433.1	Haloarcula hispanica ATCC 33960	YP_004623722.1	Pyrococcus yayanosii CH1
YP_658485.1	Haloquadratum walsbyi DSM 16790	YP_004623451.1	Pyrococcus yayanosii CH1
YP_657576.1	Haloquadratum walsbyi DSM 16790	YP_004623302.1	Pyrococcus yayanosii CH1
YP_003535316.1	Haloferax volcanii DS2	YP_004623196.1	Pyrococcus yayanosii CH1
YP_004891855.1	Thermoproteus tenax Kra 1	YP_004459316.1	Acidianus hospitalis W1
NP_070451.1	Archaeoglobus fulgidus DSM 4304	YP_004458069.1	Acidianus hospitalis W1
NP_577979.1	Pyrococcus furiosus DSM 3638	YP_004457616.1	Acidianus hospitalis W1
YP_023292.1	Picrophilus torridus DSM 9790	YP_003131622.1	Halorhabdus utahensis DSM 12940
NP_148115.1	Aeropyrum pernix K1	YP_003130186.1	Halorhabdus utahensis DSM 12940
YP_002960263.1	Thermococcus gammatolerans EJ3	YP_003130184.1	Halorhabdus utahensis DSM 12940
YP_002960311.1	Thermococcus gammatolerans EJ3	YP_003129216.1	Halorhabdus utahensis DSM 12940
YP_002959437.1	Thermococcus gammatolerans EJ3	YP_001040961.1	Staphylothermus marinus F1
YP_002959358.1	Thermococcus gammatolerans EJ3	YP_001040420.1	Staphylothermus marinus F1
YP_002958833.1	Thermococcus gammatolerans EJ3	YP_001040226.1	Staphylothermus marinus F1
YP_002958533.1	Thermococcus gammatolerans EJ3	YP_001046793.1	Methanoculleus marisnigri JR1
YP_002959476.1	Thermococcus gammatolerans EJ3	YP_001029447.1	Methanocorpusculum labreanum Z
YP_003400173.1	Archaeoglobus profundus DSM	YP_256629.1	Sulfolobus acidocaldarius DSM 639

	5631		
YP_001581846.1	Nitrosopumilus maritimus SCM1	YP_255421.1	Sulfolobus acidocaldarius DSM 639
YP_002958756.1	Thermococcus gammatolerans EJ3	YP_657093.1	Haloquadratum walsbyi DSM 16790
YP_003177982.1	Halomicrobium mukohataei DSM 12286	YP_004176659.1	Desulfurococcus mucosus DSM 2162
YP_003177376.1	Halomicrobium mukohataei DSM 12286	YP_004176616.1	Desulfurococcus mucosus DSM 2162
YP_003176757.1	Halomicrobium mukohataei DSM 12286	YP_004175968.1	Desulfurococcus mucosus DSM 2162
YP_003176546.1	Halomicrobium mukohataei DSM 12286	YP_004003964.1	Methanothermus fervidus DSM 2088
YP_001190896.1	Metallosphaera sedula DSM 5348	YP_003901746.1	Vulcanisaeta distributa DSM 14429
YP_001737200.1	Candidatus Korarchaeum cryptofilum OPF8	YP_003901375.1	Vulcanisaeta distributa DSM 14429
YP_003400366.1	Archaeoglobus profundus DSM 5631	YP_003738399.1	Halalkalicoccus jeotgali B3
YP_003400290.1	Archaeoglobus profundus DSM 5631	YP_003738222.1	Halalkalicoccus jeotgali B3
YP_003400241.1	Archaeoglobus profundus DSM 5631	YP_003725952.1	Methanohalobium evestigatum Z-7303
YP_003131740.1	Halorhabdus utahensis DSM 12940	YP_003725920.1	Methanohalobium evestigatum Z-7303
YP_003130446.1	Halorhabdus utahensis DSM 12940	YP_003649748.1	Thermosphaera aggregans DSM 11486
YP_003130267.1	Halorhabdus utahensis DSM 12940	YP_003405570.1	Haloterrigena turkmenica DSM 5511
YP_003130264.1	Halorhabdus utahensis DSM 12940	YP_002466962.1	Methanosphaerula palustris E1-9c
YP_003130119.1	Halorhabdus utahensis DSM 12940	YP_001794343.1	Thermoproteus neutrophilus V24Sta
YP_003129338.1	Halorhabdus utahensis DSM 12940	YP_001794230.1	Thermoproteus neutrophilus V24Sta
YP_001325059.1	Methanococcus aeolicus Nankai-3	YP_001794004.1	Thermoproteus neutrophilus V24Sta
YP_001583049.1	Nitrosopumilus maritimus SCM1	YP_001689667.1	Halobacterium salinarum R1
YP_919563.1	Thermofilum pendens Hrk 5	YP_001689637.1	Halobacterium salinarum R1
YP_001329608.1	Methanococcus maripaludis C7	YP_001689334.1	Halobacterium salinarum R1
YP_001322978.1	Methanococcus vannielii SB	YP_001689314.1	Halobacterium salinarum R1
YP_001096978.1	Methanococcus maripaludis C5	YP_001689265.1	Halobacterium salinarum R1
YP_004338808.1	Thermoproteus uzoniensis 768-20	YP_001689227.1	Halobacterium salinarum R1
YP_004244227.1	Vulcanisaeta moutnovskia 768-28	YP_001689137.1	Halobacterium salinarum R1
YP_003815551.1	Acidilobus saccharovorans 345-15	YP_001583096.1	Nitrosopumilus maritimus SCM1
YP_136322.1	Haloarcula marismortui ATCC	YP_001582921.1	Nitrosopumilus maritimus SCM1

	43049		
NP_377581.1	Sulfolobus tokodaii str. 7	YP_001582858.1	Nitrosopumilus maritimus SCM1
NP_377555.1	Sulfolobus tokodaii str. 7	YP_001582819.1	Nitrosopumilus maritimus SCM1
NP_341795.1	Sulfolobus solfataricus P2	YP_001582531.1	Nitrosopumilus maritimus SCM1
NP_280622.1	Halobacterium sp. NRC-1	YP_001582517.1	Nitrosopumilus maritimus SCM1
NP_247708.1	Methanocaldococcus jannaschii DSM 2661	YP_001582335.1	Nitrosopumilus maritimus SCM1
YP_003177970.1	Halomicrobium mukohataei DSM 12286	YP_001582188.1	Nitrosopumilus maritimus SCM1
YP_003176764.1	Halomicrobium mukohataei DSM 12286	YP_001582044.1	Nitrosopumilus maritimus SCM1
YP_003176583.1	Halomicrobium mukohataei DSM 12286	YP_001581717.1	Nitrosopumilus maritimus SCM1
YP_004616442.1	Methanosalsum zhilinae DSM 4017	YP_001435832.1	Ignicoccus hospitalis KIN4/I
YP_004342350.1	Archaeoglobus veneficus SNP6	YP_001435795.1	Ignicoccus hospitalis KIN4/I
YP_004035700.1	Halogeometricum borinquense DSM 11551	YP_001435613.1	Ignicoccus hospitalis KIN4/I
YP_002308337.1	Thermococcus onnurineus NA1	YP_001435295.1	Ignicoccus hospitalis KIN4/I
YP_002308002.1	Thermococcus onnurineus NA1	YP_001434898.1	Ignicoccus hospitalis KIN4/I
YP_002307897.1	Thermococcus onnurineus NA1	YP_001434817.1	Ignicoccus hospitalis KIN4/I
YP_002307669.1	Thermococcus onnurineus NA1	YP_001434713.1	Ignicoccus hospitalis KIN4/I
YP_002307365.1	Thermococcus onnurineus NA1	YP_003536868.1	Haloferax volcanii DS2
YP_002306907.1	Thermococcus onnurineus NA1	YP_003536540.1	Haloferax volcanii DS2
YP_002306865.1	Thermococcus onnurineus NA1	YP_003536525.1	Haloferax volcanii DS2
YP_001192020.1	Metallosphaera sedula DSM 5348	YP_003536435.1	Haloferax volcanii DS2
YP_001191294.1	Metallosphaera sedula DSM 5348	YP_003536338.1	Haloferax volcanii DS2
YP_001191287.1	Metallosphaera sedula DSM 5348	YP_003536055.1	Haloferax volcanii DS2
YP_001190787.1	Metallosphaera sedula DSM 5348	YP_003535829.1	Haloferax volcanii DS2
YP_001190267.1	Metallosphaera sedula DSM 5348	YP_003535790.1	Haloferax volcanii DS2
YP_001190114.1	Metallosphaera sedula DSM 5348	YP_003535355.1	Haloferax volcanii DS2
YP_001737982.1	Candidatus Korarchaeum cryptofilum OPF8	YP_003534317.1	Haloferax volcanii DS2
YP_001737669.1	Candidatus Korarchaeum cryptofilum OPF8	YP_931134.1	Pyrobaculum islandicum DSM 4184
YP_001737072.1	Candidatus Korarchaeum cryptofilum OPF8	YP_931087.1	Pyrobaculum islandicum DSM 4184
YP_001737020.1	Candidatus Korarchaeum cryptofilum OPF8	YP_930513.1	Pyrobaculum islandicum DSM 4184
YP_001154444.1	Pyrobaculum arsenaticum DSM 13514	YP_929571.1	Pyrobaculum islandicum DSM 4184

YP_001154323.1	Pyrobaculum arsenaticum DSM 13514	YP_004410493.1	Metallosphaera cuprina Ar-4
YP_001154056.1	Pyrobaculum arsenaticum DSM 13514	YP_004409993.1	Metallosphaera cuprina Ar-4
YP_001056591.1	Pyrobaculum calidifontis JCM 11548	YP_002960315.1	Thermococcus gammatolerans EJ3
YP_001056074.1	Pyrobaculum calidifontis JCM 11548	YP_002959243.1	Thermococcus gammatolerans EJ3
YP_001055503.1	Pyrobaculum calidifontis JCM 11548	YP_002958483.1	Thermococcus gammatolerans EJ3
YP_003400663.1	Archaeoglobus profundus DSM 5631	ZP_09042980.1	Methanolinea tarda NOBI-1
YP_001405150.1	Methanoregula boonei 6A8	ZP_09030407.1	Halobacterium sp. DL1
YP_001404118.1	Methanoregula boonei 6A8	ZP_09030252.1	Halobacterium sp. DL1
YP_001404117.1	Methanoregula boonei 6A8	ZP_09030225.1	Halobacterium sp. DL1
YP_001403169.1	Methanoregula boonei 6A8	ZP_09030095.1	Halobacterium sp. DL1
YP_004781461.1	Pyrolobus fumarii 1A	ZP_09029032.1	Halobacterium sp. DL1
YP_004796821.1	Haloarcula hispanica ATCC 33960	ZP_09028822.1	Halobacterium sp. DL1
YP_003131751.1	Halorhabdus utahensis DSM 12940	ZP_09028745.1	Halobacterium sp. DL1
YP_003130658.1	Halorhabdus utahensis DSM 12940	ZP_09028374.1	Halobacterium sp. DL1
YP_001040205.1	Staphylothermus marinus F1	ZP_09027328.1	Halobacterium sp. DL1
YP_001040069.1	Staphylothermus marinus F1	ZP_09026876.1	Desulfurococcus fermentans DSM 16532
YP_001047138.1	Methanoculleus marisnigri JR1	ZP_09026647.1	Desulfurococcus fermentans DSM 16532
YP_001046792.1	Methanoculleus marisnigri JR1	YP_004385029.1	Methanosaeta concilii GP6
YP_001045919.1	Methanoculleus marisnigri JR1	YP_004383975.1	Methanosaeta concilii GP6
YP_659023.1	Haloquadratum walsbyi DSM 16790	YP_004383390.1	Methanosaeta concilii GP6
YP_658818.1	Haloquadratum walsbyi DSM 16790	YP_004382874.1	Methanosaeta concilii GP6
YP_003902531.1	Vulcanisaeta distributa DSM 14429	YP_004893205.1	Thermoproteus tenax Kra 1
YP_003649813.1	Thermosphaera aggregans DSM 11486	YP_004892872.1	Thermoproteus tenax Kra 1
YP_002467619.1	Methanosphaerula palustris E1-9c	ZP_08969421.1	Natronobacterium gregoryi SP2
YP_002467618.1	Methanosphaerula palustris E1-9c	ZP_08969337.1	Natronobacterium gregoryi SP2
YP_002465121.1	Methanosphaerula palustris E1-9c	ZP_08968147.1	Natronobacterium gregoryi SP2
YP_001794232.1	Thermoproteus neutrophilus V24Sta	ZP_08967924.1	Natronobacterium gregoryi SP2
YP_001794049.1	Thermoproteus neutrophilus V24Sta	ZP_08966224.1	Natronobacterium gregoryi SP2
YP_001689744.1	Halobacterium salinarum R1	ZP_08965149.1	Natrinema pellirubrum DSM 15624

YP_001583029.1	Nitrosopumilus maritimus SCM1	ZP_08964818.1	Natrinema pellirubrum DSM 15624
YP_001582626.1	Nitrosopumilus maritimus SCM1	ZP_08964326.1	Natrinema pellirubrum DSM 15624
YP_001582481.1	Nitrosopumilus maritimus SCM1	ZP_08963785.1	Natrinema pellirubrum DSM 15624
YP_001582072.1	Nitrosopumilus maritimus SCM1	ZP_08963729.1	Natrinema pellirubrum DSM 15624
YP_001435428.1	Ignicoccus hospitalis KIN4/I	ZP_08963669.1	Natrinema pellirubrum DSM 15624
YP_001435084.1	Ignicoccus hospitalis KIN4/I	ZP_08963537.1	Natrinema pellirubrum DSM 15624
YP_003536251.1	Haloferax volcanii DS2	ZP_08963436.1	Natrinema pellirubrum DSM 15624
YP_930515.1	Pyrobaculum islandicum DSM 4184	ZP_08963206.1	Natrinema pellirubrum DSM 15624
YP_004408608.1	Metallosphaera cuprina Ar-4	ZP_08962509.1	Natrinema pellirubrum DSM 15624
YP_002960132.1	Thermococcus gammatolerans EJ3	ZP_08962311.1	Natrinema pellirubrum DSM 15624
ZP_09028241.1	Halobacterium sp. DL1	ZP_08961897.1	Natrinema pellirubrum DSM 15624
ZP_08965365.1	Natrinema pellirubrum DSM 15624	YP_004424495.1	Pyrococcus sp. NA2
YP_003482775.1	Aciduliprofundum boonei T469	YP_004424487.1	Pyrococcus sp. NA2
YP_003479365.1	Natrialba magadii ATCC 43099	YP_004424456.1	Pyrococcus sp. NA2
YP_003435041.1	Ferroglobus placidus DSM 10642	YP_004424415.1	Pyrococcus sp. NA2
YP_003420138.1	Sulfolobus islandicus L.D.8.5	YP_004423810.1	Pyrococcus sp. NA2
YP_002915172.1	Sulfolobus islandicus M.16.4	YP_004423807.1	Pyrococcus sp. NA2
YP_002843887.1	Sulfolobus islandicus M.16.27	YP_004423635.1	Pyrococcus sp. NA2
YP_002839981.1	Sulfolobus islandicus Y.N.15.51	YP_004423588.1	Pyrococcus sp. NA2
YP_002567018.1	Halorubrum lacusprofundi ATCC 49239	YP_004423517.1	Pyrococcus sp. NA2
YP_002566777.1	Halorubrum lacusprofundi ATCC 49239	YP_004423491.1	Pyrococcus sp. NA2
YP_002566129.1	Halorubrum lacusprofundi ATCC 49239	YP_004423406.1	Pyrococcus sp. NA2
YP_002565982.1	Halorubrum lacusprofundi ATCC 49239	YP_004423207.1	Pyrococcus sp. NA2
YP_002565843.1	Halorubrum lacusprofundi ATCC 49239	YP_004423099.1	Pyrococcus sp. NA2
YP_002564762.1	Halorubrum lacusprofundi ATCC 49239	YP_004423028.1	Pyrococcus sp. NA2
YP_002564488.1	Halorubrum lacusprofundi ATCC 49239	YP_003483243.1	Aciduliprofundum boonei T469
YP_002838148.1	Sulfolobus islandicus Y.G.57.14	YP_003483036.1	Aciduliprofundum boonei T469
YP_002832643.1	Sulfolobus islandicus L.S.2.15	YP_003482395.1	Aciduliprofundum boonei T469
YP_002829936.1	Sulfolobus islandicus M.14.25	YP_003482040.1	Natrialba magadii ATCC 43099
YP_876228.1	Cenarchaeum symbiosum A	YP_003481856.1	Natrialba magadii ATCC 43099
ZP_08667514.1	Candidatus Nitrosoarchaeum koreensis MY1	YP_003481640.1	Natrialba magadii ATCC 43099
YP_001540653.1	Caldivirga maquilingensis IC-167	YP_003481194.1	Natrialba magadii ATCC 43099
YP_001540054.1	Caldivirga maquilingensis IC-167	YP_003481009.1	Natrialba magadii ATCC 43099
YP_001539990.1	Caldivirga maquilingensis IC-167	YP_003480847.1	Natrialba magadii ATCC 43099
YP_919987.1	Thermofilum pendens Hrk 5	YP_003480652.1	Natrialba magadii ATCC 43099
YP_919431.1	Thermofilum pendens Hrk 5	YP_003480502.1	Natrialba magadii ATCC 43099
YP_001549576.1	Methanococcus maripaludis C6	YP_003479931.1	Natrialba magadii ATCC 43099

ZP_08256316.1	Candidatus Nitrosoarchaeum limnia SFB1	YP_003479600.1	Natrialba magadii ATCC 43099
YP_842490.1	Methanosaeta thermophila PT	YP_003479447.1	Natrialba magadii ATCC 43099
ZP_06388404.1	Sulfolobus solfataricus 98/2	YP_003479179.1	Natrialba magadii ATCC 43099
YP_004337755.1	Thermoproteus uzoniensis 768-20	YP_003479053.1	Natrialba magadii ATCC 43099
YP_004245835.1	Vulcanisaeta moutnovskia 768-28	YP_003478847.1	Natrialba magadii ATCC 43099
YP_004245485.1	Vulcanisaeta moutnovskia 768-28	YP_003458859.1	Methanocaldococcus sp. FS406-22
YP_004244120.1	Vulcanisaeta moutnovskia 768-28	YP_003436893.1	Ferroglobus placidus DSM 10642
YP_003816754.1	Acidilobus saccharovorans 345-15	YP_003436180.1	Ferroglobus placidus DSM 10642
NP_148695.2	Aeropyrum pernix K1	YP_003436135.1	Ferroglobus placidus DSM 10642
NP_147981.2	Aeropyrum pernix K1	YP_003435609.1	Ferroglobus placidus DSM 10642
YP_874895.1	Aeropyrum pernix K1	YP_003435431.1	Ferroglobus placidus DSM 10642
YP_566724.1	Methanococcoides burtonii DSM 6242	YP_003434606.1	Ferroglobus placidus DSM 10642
YP_565903.1	Methanococcoides burtonii DSM 6242	YP_003434478.1	Ferroglobus placidus DSM 10642
YP_306917.1	Methanosarcina barkeri str. Fusaro	YP_003424703.1	Methanobrevibacter ruminantium M1
YP_304997.1	Methanosarcina barkeri str. Fusaro	YP_003420788.1	Sulfolobus islandicus L.D.8.5
YP_184547.1	Thermococcus kodakarensis KOD1	YP_003420260.1	Sulfolobus islandicus L.D.8.5
YP_184523.1	Thermococcus kodakarensis KOD1	YP_003419765.1	Sulfolobus islandicus L.D.8.5
YP_184368.1	Thermococcus kodakarensis KOD1	YP_003418510.1	Sulfolobus islandicus L.D.8.5
YP_183904.1	Thermococcus kodakarensis KOD1	YP_003418318.1	Sulfolobus islandicus L.D.8.5
YP_183698.1	Thermococcus kodakarensis KOD1	YP_003406077.1	Haloterrigena turkmenica DSM 5511
YP_183672.1	Thermococcus kodakarensis KOD1	YP_003357605.1	Methanocella paludicola SANAE
YP_183623.1	Thermococcus kodakarensis KOD1	YP_003357604.1	Methanocella paludicola SANAE
YP_183247.1	Thermococcus kodakarensis KOD1	YP_003356398.1	Methanocella paludicola SANAE
YP_182980.1	Thermococcus kodakarensis KOD1	YP_003355667.1	Methanocella paludicola SANAE
YP_182921.1	Thermococcus kodakarensis KOD1	YP_003355545.1	Methanocella paludicola SANAE
YP_137759.1	Haloarcula marismortui ATCC 43049	YP_003355510.1	Methanocella paludicola SANAE
YP_137704.1	Haloarcula marismortui ATCC	YP_002915260.1	Sulfolobus islandicus M.16.4

	43049		
YP_137243.1	Haloarcula marismortui ATCC 43049	YP_002914792.1	Sulfolobus islandicus M.16.4
YP_137113.1	Haloarcula marismortui ATCC 43049	YP_002913661.1	Sulfolobus islandicus M.16.4
YP_135916.1	Haloarcula marismortui ATCC 43049	YP_002913465.1	Sulfolobus islandicus M.16.4
YP_135231.1	Haloarcula marismortui ATCC 43049	YP_002843972.1	Sulfolobus islandicus M.16.27
YP_023833.1	Picrophilus torridus DSM 9790	YP_002843566.1	Sulfolobus islandicus M.16.27
YP_023669.1	Picrophilus torridus DSM 9790	YP_002842557.1	Sulfolobus islandicus M.16.27
YP_023206.1	Picrophilus torridus DSM 9790	YP_002842406.1	Sulfolobus islandicus M.16.27
YP_023154.1	Picrophilus torridus DSM 9790	YP_002842219.1	Sulfolobus islandicus M.16.27
NP_988257.1	Methanococcus maripaludis S2	YP_002841573.1	Sulfolobus islandicus Y.N.15.51
NP_577976.2	Pyrococcus furiosus DSM 3638	YP_002841543.1	Sulfolobus islandicus Y.N.15.51
NP_634064.1	Methanosarcina mazei Go1	YP_002840323.1	Sulfolobus islandicus Y.N.15.51
NP_633763.1	Methanosarcina mazei Go1	YP_002839860.1	Sulfolobus islandicus Y.N.15.51
NP_633752.1	Methanosarcina mazei Go1	YP_002839359.1	Sulfolobus islandicus Y.N.15.51
NP_615539.1	Methanosarcina acetivorans C2A	YP_002567638.1	Halorubrum lacusprofundi ATCC 49239
NP_579782.1	Pyrococcus furiosus DSM 3638	YP_002567001.1	Halorubrum lacusprofundi ATCC 49239
NP_579463.1	Pyrococcus furiosus DSM 3638	YP_002566972.1	Halorubrum lacusprofundi ATCC 49239
NP_579330.1	Pyrococcus furiosus DSM 3638	YP_002566400.1	Halorubrum lacusprofundi ATCC 49239
NP_578960.1	Pyrococcus furiosus DSM 3638	YP_002565690.1	Halorubrum lacusprofundi ATCC 49239
NP_577842.1	Pyrococcus furiosus DSM 3638	YP_002565557.1	Halorubrum lacusprofundi ATCC 49239
NP_577783.1	Pyrococcus furiosus DSM 3638	YP_002564895.1	Halorubrum lacusprofundi ATCC 49239
NP_560759.1	Pyrobaculum aerophilum str. IM2	YP_002564820.1	Halorubrum lacusprofundi ATCC 49239
NP_444208.1	Halobacterium sp. NRC-1	YP_002838806.1	Sulfolobus islandicus Y.G.57.14
NP_394674.1	Thermoplasma acidophilum DSM 1728	YP_002838279.1	Sulfolobus islandicus Y.G.57.14
NP_394441.1	Thermoplasma acidophilum DSM 1728	YP_002837714.1	Sulfolobus islandicus Y.G.57.14
NP_394081.1	Thermoplasma acidophilum DSM 1728	YP_002836578.1	Sulfolobus islandicus Y.G.57.14
NP_393737.1	Thermoplasma acidophilum DSM 1728	YP_002836363.1	Sulfolobus islandicus Y.G.57.14
NP_377434.1	Sulfolobus tokodaii str. 7	YP_002832780.1	Sulfolobus islandicus L.S.2.15
NP_377039.1	Sulfolobus tokodaii str. 7	YP_002832283.1	Sulfolobus islandicus L.S.2.15
NP_376938.1	Sulfolobus tokodaii str. 7	YP_002831154.1	Sulfolobus islandicus L.S.2.15
NP_376154.1	Sulfolobus tokodaii str. 7	YP_002830975.1	Sulfolobus islandicus L.S.2.15
NP_376041.1	Sulfolobus tokodaii str. 7	YP_002830512.1	Sulfolobus islandicus M.14.25

NP_343760.1	Sulfolobus solfataricus P2	YP_002830022.1	Sulfolobus islandicus M.14.25
NP_343708.1	Sulfolobus solfataricus P2	YP_002829573.1	Sulfolobus islandicus M.14.25
NP_343520.1	Sulfolobus solfataricus P2	YP_002828520.1	Sulfolobus islandicus M.14.25
NP_343274.1	Sulfolobus solfataricus P2	YP_002828333.1	Sulfolobus islandicus M.14.25
NP_342127.1	Sulfolobus solfataricus P2	YP_876900.1	Cenarchaeum symbiosum A
NP_341713.1	Sulfolobus solfataricus P2	YP_876727.1	Cenarchaeum symbiosum A
NP_280759.1	Halobacterium sp. NRC-1	YP_875285.1	Cenarchaeum symbiosum A
NP_280549.1	Halobacterium sp. NRC-1	YP_003894197.1	Methanoplanus petrolearius DSM 11571
NP_280520.1	Halobacterium sp. NRC-1	YP_003893221.1	Methanoplanus petrolearius DSM 11571
NP_280224.1	Halobacterium sp. NRC-1	YP_004810193.1	halophilic archaeon DL31
NP_280204.1	Halobacterium sp. NRC-1	YP_004809973.1	halophilic archaeon DL31
NP_280156.1	Halobacterium sp. NRC-1	YP_004809972.1	halophilic archaeon DL31
NP_280119.1	Halobacterium sp. NRC-1	YP_004809384.1	halophilic archaeon DL31
NP_247119.1	Methanocaldococcus jannaschii DSM 2661	YP_004809172.1	halophilic archaeon DL31
NP_143748.1	Pyrococcus horikoshii OT3	YP_004809115.1	halophilic archaeon DL31
NP_143745.1	Pyrococcus horikoshii OT3	YP_004808803.1	halophilic archaeon DL31
NP_143534.1	Pyrococcus horikoshii OT3	YP_004808638.1	halophilic archaeon DL31
NP_143448.1	Pyrococcus horikoshii OT3	YP_004807939.1	halophilic archaeon DL31
NP_143380.1	Pyrococcus horikoshii OT3	NP_071273.2	Archaeoglobus fulgidus DSM 4304
NP_142954.1	Pyrococcus horikoshii OT3	NP_071274.1	Archaeoglobus fulgidus DSM 4304
NP_142925.1	Pyrococcus horikoshii OT3	NP_070571.1	Archaeoglobus fulgidus DSM 4304
NP_142197.1	Pyrococcus horikoshii OT3	NP_070551.1	Archaeoglobus fulgidus DSM 4304
NP_142146.1	Pyrococcus horikoshii OT3	NP_070277.1	Archaeoglobus fulgidus DSM 4304
NP_142078.1	Pyrococcus horikoshii OT3	NP_069977.1	Archaeoglobus fulgidus DSM 4304
NP_142064.1	Pyrococcus horikoshii OT3	NP_069950.1	Archaeoglobus fulgidus DSM 4304
NP_127367.1	Pyrococcus abyssi GE5	NP_069418.1	Archaeoglobus fulgidus DSM 4304
NP_126646.1	Pyrococcus abyssi GE5	NP_069275.1	Archaeoglobus fulgidus DSM 4304
NP_126331.1	Pyrococcus abyssi GE5	ZP_08668723.1	Candidatus Nitrosoarchaeum koreensis MY1
NP_126261.1	Pyrococcus abyssi GE5	ZP_08668470.1	Candidatus Nitrosoarchaeum koreensis MY1
NP_126173.1	Pyrococcus abyssi GE5	ZP_08668148.1	Candidatus Nitrosoarchaeum koreensis MY1
NP_125878.1	Pyrococcus abyssi GE5	ZP_08667822.1	Candidatus Nitrosoarchaeum koreensis MY1
NP_125830.1	Pyrococcus abyssi GE5	ZP_08667529.1	Candidatus Nitrosoarchaeum koreensis MY1
NP_125761.1	Pyrococcus abyssi GE5	YP_001540051.1	Caldivirga maquilingensis IC-167
NP_125747.1	Pyrococcus abyssi GE5	YP_004585840.1	Halopiger xanaduensis SH-6
NP_111856.1	Thermoplasma volcanium GSS1	ZP_08562002.1	Halorhabdus tiamatea SARL4B
NP_111646.1	Thermoplasma volcanium GSS1	ZP_08561947.1	Halorhabdus tiamatea SARL4B
NP_111177.1	Thermoplasma volcanium GSS1	ZP_08561888.1	Halorhabdus tiamatea SARL4B
NP_110896.1	Thermoplasma volcanium GSS1	ZP_08560034.1	Halorhabdus tiamatea SARL4B
YP_004742913.1	Methanococcus maripaludis X1	ZP_08559561.1	Halorhabdus tiamatea SARL4B
YP_003859067.1	Ignisphaera aggregans DSM	ZP_08559445.1	Halorhabdus tiamatea SARL4B

	17230		
YP_003178506.1	Halomicrobium mukohataei DSM 12286	ZP_08559008.1	Halorhabdus tiamatea SARL4B
YP_003178353.1	Halomicrobium mukohataei DSM 12286	ZP_08558955.1	Halorhabdus tiamatea SARL4B
YP_003177435.1	Halomicrobium mukohataei DSM 12286	YP_003668783.1	Staphylothermus hellenicus DSM 12710
YP_003177422.1	Halomicrobium mukohataei DSM 12286	YP_920273.1	Thermofilum pendens Hrk 5
YP_003177406.1	Halomicrobium mukohataei DSM 12286	YP_920073.1	Thermofilum pendens Hrk 5
YP_003177236.1	Halomicrobium mukohataei DSM 12286	YP_919985.1	Thermofilum pendens Hrk 5
YP_002995258.1	Thermococcus sibiricus MM 739	YP_919778.1	Thermofilum pendens Hrk 5
YP_002994829.1	Thermococcus sibiricus MM 739	YP_003737647.1	Halalkalicoccus jeotgali B3
YP_002994668.1	Thermococcus sibiricus MM 739	YP_003736438.1	Halalkalicoccus jeotgali B3
YP_002994644.1	Thermococcus sibiricus MM 739	YP_003736407.1	Halalkalicoccus jeotgali B3
YP_002994391.1	Thermococcus sibiricus MM 739	YP_003735922.1	Halalkalicoccus jeotgali B3
YP_002994234.1	Thermococcus sibiricus MM 739	YP_003735902.1	Halalkalicoccus jeotgali B3
YP_002994125.1	Thermococcus sibiricus MM 739	YP_327726.1	Natronomonas pharaonis DSM 2160
YP_002994041.1	Thermococcus sibiricus MM 739	YP_327683.1	Natronomonas pharaonis DSM 2160
YP_002993922.1	Thermococcus sibiricus MM 739	ZP_05570595.1	Ferroplasma acidarmanus fer1
YP_002993864.1	Thermococcus sibiricus MM 739	ZP_05570514.1	Ferroplasma acidarmanus fer1
YP_448566.1	Methanosphaera stadtmanae DSM 3091	ZP_05570368.1	Ferroplasma acidarmanus fer1
YP_447346.1	Methanosphaera stadtmanae DSM 3091	YP_002428124.1	Desulfurococcus kamchatkensis 1221n
YP_004616550.1	Methanosalsum zhilinae DSM 4017	YP_134294.1	Haloarcula marismortui ATCC 43049
YP_004616549.1	Methanosalsum zhilinae DSM 4017	YP_003616762.1	methanocaldococcus infernus ME
YP_004597843.1	Halopiger xanaduensis SH-6	YP_003707018.1	Methanococcus voltae A3
YP_004597748.1	Halopiger xanaduensis SH-6	YP_003542599.1	Methanohalophilus mahii DSM 5219
YP_004597313.1	Halopiger xanaduensis SH-6	YP_003541468.1	Methanohalophilus mahii DSM 5219
YP_004596669.1	Halopiger xanaduensis SH-6	YP_004072201.1	Thermococcus barophilus MP
YP_004596535.1	Halopiger xanaduensis SH-6	YP_004072148.1	Thermococcus barophilus MP
YP_004596136.1	Halopiger xanaduensis SH-6	YP_004071967.1	Thermococcus barophilus MP
YP_004595281.1	Halopiger xanaduensis SH-6	YP_004071576.1	Thermococcus barophilus MP
YP_004576378.1	Methanothermococcus okinawensis IH1	YP_004071182.1	Thermococcus barophilus MP
YP_004521104.1	Methanobacterium sp. SWAN-1	YP_004071101.1	Thermococcus barophilus MP
YP_004520894.1	Methanobacterium sp. SWAN-1	YP_004070521.1	Thermococcus barophilus MP
YP_004483735.1	Methanotorris igneus Kol 5	YP_004070465.1	Thermococcus barophilus MP
YP_004341155.1	Archaeoglobus veneficus SNP6	ZP_08257913.1	Candidatus Nitrosoarchaeum limnia SFB1
YP_004340804.1	Archaeoglobus veneficus SNP6	ZP_08257249.1	Candidatus Nitrosoarchaeum limnia SFB1

YP_004037934.1	Halogeometricum borinquense DSM 11551	ZP_08256570.1	Candidatus Nitrosoarchaeum limnia SFB1
YP_004036977.1	Halogeometricum borinquense DSM 11551	ZP_05571454.1	Ferroplasma acidarmanus fer1
YP_004036934.1	Halogeometricum borinquense DSM 11551	ZP_05571355.1	Ferroplasma acidarmanus fer1
YP_004036541.1	Halogeometricum borinquense DSM 11551	YP_684455.1	uncultured methanogenic archaeon RC-I
YP_004036396.1	Halogeometricum borinquense DSM 11551	YP_684931.1	uncultured methanogenic archaeon RC-I
YP_004035765.1	Halogeometricum borinquense DSM 11551	YP_684932.1	uncultured methanogenic archaeon RC-I
YP_004035478.1	Halogeometricum borinquense DSM 11551	YP_684933.1	uncultured methanogenic archaeon RC-I
YP_004035403.1	Halogeometricum borinquense DSM 11551	YP_686097.1	uncultured methanogenic archaeon RC-I
YP_002307729.1	Thermococcus onnurineus NA1	YP_686276.1	uncultured methanogenic archaeon RC-I
YP_002307046.1	Thermococcus onnurineus NA1	YP_686689.1	uncultured methanogenic archaeon RC-I
YP_002306500.1	Thermococcus onnurineus NA1	YP_687156.1	uncultured methanogenic archaeon RC-I
YP_001192356.1	Metallosphaera sedula DSM 5348	YP_687304.1	uncultured methanogenic archaeon RC-I
YP_001190931.1	Metallosphaera sedula DSM 5348	YP_001012320.1	Hyperthermus butylicus DSM 5456
YP_001190718.1	Metallosphaera sedula DSM 5348	YP_331249.1	Natronomonas pharaonis DSM 2160
YP_003247308.1	Methanocaldococcus vulcanius M7	YP_331139.1	Natronomonas pharaonis DSM 2160
YP_003246974.1	Methanocaldococcus vulcanius M7	YP_330977.1	Natronomonas pharaonis DSM 2160
YP_003128380.1	Methanocaldococcus fervens AG86	YP_330742.1	Natronomonas pharaonis DSM 2160
YP_001737562.1	Candidatus Korarchaeum cryptofilum OPF8	YP_327026.1	Natronomonas pharaonis DSM 2160
YP_001737300.1	Candidatus Korarchaeum cryptofilum OPF8	YP_326389.1	Natronomonas pharaonis DSM 2160
YP_001736931.1	Candidatus Korarchaeum cryptofilum OPF8	YP_325702.1	Natronomonas pharaonis DSM 2160
YP_001736687.1	Candidatus Korarchaeum cryptofilum OPF8	ZP_08045557.1	Haladaptatus paucihalophilus DX253
YP_001154058.1	Pyrobaculum arsenaticum DSM 13514	ZP_08045554.1	Haladaptatus paucihalophilus DX253
YP_001152870.1	Pyrobaculum arsenaticum DSM 13514	ZP_08045479.1	Haladaptatus paucihalophilus DX253
YP_001056076.1	Pyrobaculum calidifontis JCM 11548	ZP_08044737.1	Haladaptatus paucihalophilus DX253
YP_001055714.1	Pyrobaculum calidifontis JCM	ZP_08044544.1	Haladaptatus paucihalophilus DX253

	11548		
YP_003533835.1	Haloferax volcanii DS2	ZP_08044419.1	Haladaptatus paucihalophilus DX253
YP_003533764.1	Haloferax volcanii DS2	ZP_08044112.1	Haladaptatus paucihalophilus DX253
YP_003533154.1	Haloferax volcanii DS2	ZP_08043830.1	Haladaptatus paucihalophilus DX253
YP_003533147.1	Haloferax volcanii DS2	ZP_08043457.1	Haladaptatus paucihalophilus DX253
YP_503891.1	Methanospirillum hungatei JF-1	ZP_08043099.1	Haladaptatus paucihalophilus DX253
YP_004289555.1	Methanobacterium sp. AL-21	ZP_08042985.1	Haladaptatus paucihalophilus DX253
YP_004289409.1	Methanobacterium sp. AL-21	ZP_08042809.1	Haladaptatus paucihalophilus DX253
YP_003404785.1	Haloterrigena turkmenica DSM 5511	ZP_05571621.1	Ferroplasma acidarmanus fer1
YP_003404699.1	Haloterrigena turkmenica DSM 5511	YP_843557.1	Methanosaeta thermophila PT
YP_003404557.1	Haloterrigena turkmenica DSM 5511	YP_843307.1	Methanosaeta thermophila PT
YP_003404442.1	Haloterrigena turkmenica DSM 5511	YP_843029.1	Methanosaeta thermophila PT
YP_003403850.1	Haloterrigena turkmenica DSM 5511	YP_842934.1	Methanosaeta thermophila PT
YP_003403836.1	Haloterrigena turkmenica DSM 5511	YP_842538.1	Methanosaeta thermophila PT
YP_003403396.1	Haloterrigena turkmenica DSM 5511	ZP_06389802.1	Sulfolobus solfataricus 98/2
YP_003403091.1	Haloterrigena turkmenica DSM 5511	ZP_06388811.1	Sulfolobus solfataricus 98/2
YP_003403007.1	Haloterrigena turkmenica DSM 5511	ZP_06388318.1	Sulfolobus solfataricus 98/2
YP_003402287.1	Haloterrigena turkmenica DSM 5511	ZP_06387751.1	Sulfolobus solfataricus 98/2
YP_003401873.1	Haloterrigena turkmenica DSM 5511	ZP_06387003.1	Sulfolobus solfataricus 98/2
YP_003401006.1	Archaeoglobus profundus DSM 5631	ZP_05975527.1	Methanobrevibacter smithii DSM 2374
YP_003399765.1	Archaeoglobus profundus DSM 5631	YP_004044527.1	Halogeometricum borinquense DSM 11551
YP_004780362.1	Pyrolobus fumarii 1A	YP_004038370.1	Halogeometricum borinquense DSM 11551
YP_004797601.1	Haloarcula hispanica ATCC 33960	YP_004044229.1	Halogeometricum borinquense DSM 11551
YP_004796450.1	Haloarcula hispanica ATCC 33960	ZP_03607844.1	Methanobrevibacter smithii DSM 2375
YP_004796070.1	Haloarcula hispanica ATCC 33960	ZP_04875821.1	Aciduliprofundum boonei T469
YP_004795741.1	Haloarcula hispanica ATCC 33960	ZP_04875316.1	Aciduliprofundum boonei T469
YP_004795214.1	Haloarcula hispanica ATCC 33960	ZP_04874179.1	Aciduliprofundum boonei T469
YP_004795156.1	Haloarcula hispanica ATCC 33960	ZP_04873728.1	Aciduliprofundum boonei T469
YP_004794685.1	Haloarcula hispanica ATCC 33960	ZP_04873462.1	Aciduliprofundum boonei T469
YP_004786233.1	Haloarcula hispanica ATCC 33960	ZP_04873412.1	Aciduliprofundum boonei T469
YP_004786103.1	Haloarcula hispanica ATCC 33960	YP_001273605.1	Methanobrevibacter smithii ATCC 35061

YP_004763685.1	Thermococcus sp. 4557	YP_003738675.1	Halalkalicoccus jeotgali B3
YP_004763354.1	Thermococcus sp. 4557	YP_003738946.1	Halalkalicoccus jeotgali B3
YP_004763157.1	Thermococcus sp. 4557	NP_149165.1	Pyrococcus sp. JT1